

Jens Hagen
Industrial Catalysis

Related Titles

I. Chorkendorff, J. W. Niemantsverdriet

Concepts of Modern Catalysis and Kinetics

2003

ISBN 3-527-30574-2

J. M. Thomas, W. J. Thomas

Principles and Practice of Heterogeneous Catalysis

1996

ISBN 3-527-29288-8

J. G. Sanchez Marcano, T. T. Tsotsis

Catalytic Membranes and Membrane Reactors

2002

ISBN 3-527-30277-8

J. W. Niemantsverdriet

Spectroscopy in Catalysis An Introduction

2000

ISBN 3-527-30200-X

B. Cornils, W. A. Herrmann, R. Schlögl,
C.-H. Wong

Catalysis from A to Z A Concise Encyclopedia

2nd Edition

2003

ISBN 3-527-30373-1

R. I. Wijnngaarden, K. R. Westerterp,
A. Kronberg

Industrial Catalysis Optimizing Catalysts and Processes

1998

ISBN 3-527-28581-4

Jens Hagen

Industrial Catalysis

A Practical Approach

Second, Completely Revised and Extended Edition



**WILEY-
VCH**

WILEY-VCH Verlag GmbH & Co. KGaA

Author

Prof. Dr. Jens Hagen
University of Applied Sciences Mannheim
Windeckstrasse 110
68163 Mannheim
Germany

■ All books published by Wiley-VCH are carefully produced. Nevertheless, authors, editors, and publisher do not warrant the information contained in these books, including this book, to be free of errors. Readers are advised to keep in mind that statements, data, illustrations, procedural details or other items may inadvertently be inaccurate.

Library of Congress Card No.:

applied for

British Library Cataloguing-in-Publication Data

A catalogue record for this book is available from the British Library

Bibliographic information published by**Die Deutsche Bibliothek**

Die Deutsche Bibliothek lists this publication in the Deutsche Nationalbibliografie; detailed bibliographic data is available in the Internet at <<http://dnb.ddb.de>>

© 2006 WILEY-VCH Verlag GmbH & Co. KGaA,
Weinheim, Germany

All rights reserved (including those of translation into other languages). No part of this book may be reproduced in any form – by photoprinting, microfilm, or any other means – nor transmitted or translated into a machine language without written permission from the publishers. Registered names, trademarks, etc. used in this book, even when not specifically marked as such, are not to be considered unprotected by law.

Cover illustration SCHULZ Grafik-Design,
Fußgönheim

Typesetting Prosatz Unger, Weinheim

Printing betz-druck GmbH, Darmstadt

Binding J. Schäffer GmbH, Grünstadt

Printed in the Federal Republic of Germany

Printed on acid-free paper

ISBN-13: 978-3-527-31144-6

ISBN-10: 3-527-31144-0

Contents

Preface to the Second Edition *XI*

Preface to the First Edition *XIII*

Abbreviations *XV*

1 Introduction *1*

- 1.1 The Phenomenon Catalysis *1*
- 1.2 Mode of Action of Catalysts *4*
 - 1.2.1 Activity *4*
 - 1.2.1.1 Turnover Frequency TOF *7*
 - 1.2.1.2 Turnover Number TON [T 46] *7*
 - 1.2.2 Selectivity *8*
 - 1.2.3 Stability *9*
- 1.3 Classification of Catalysts *9*
- 1.4 Comparison of Homogeneous and Heterogeneous Catalysis *10*
Exercises for Chapter 1 *14*

2 Homogeneous Catalysis with Transition Metal Catalysts *15*

- 2.1 Key Reactions in Homogeneous Catalysis *16*
 - 2.1.1 Coordination and Exchange of Ligands *16*
 - 2.1.2 Complex Formation *19*
 - 2.1.3 Acid–Base Reactions *21*
 - 2.1.4 Redox Reactions: Oxidative Addition and Reductive Elimination *24*
 - 2.1.5 Insertion and Elimination Reactions *30*
 - 2.1.6 Reactions at Coordinated Ligands *34*
Exercises for Section 2.1 *37*
 - 2.2 Catalyst Concepts in Homogeneous Catalysis *40*
 - 2.2.1 The 16/18-Electron Rule *40*
 - 2.2.2 Catalytic Cycles *41*
 - 2.2.3 Hard and Soft Catalysis *42*
 - 2.2.3.1 Hard Catalysis with Transition Metal Compounds *44*
 - 2.2.3.2 Soft Catalysis with Transition Metal Compounds *45*
- Exercises for Section 2.2 *51*

| | | |
|----------|--|-----------|
| 2.3 | Characterization of Homogeneous Catalysts | 52 |
| | Exercises for Section 2.3 | 58 |
| 3 | Homogeneously Catalyzed Industrial Processes | 59 |
| 3.1 | Overview | 59 |
| 3.2 | Examples of Industrial Processes | 62 |
| 3.2.1 | Oxo Synthesis | 62 |
| 3.2.2 | Production of Acetic Acid by Carbonylation of Methanol | 65 |
| 3.2.3 | Selective Ethylene Oxidation by the Wacker Process | 67 |
| 3.2.4 | Oxidation of Cyclohexane | 69 |
| 3.2.5 | Suzuki Coupling | 70 |
| 3.2.6 | Oligomerization of Ethylene (SHOP Process) | 71 |
| 3.2.7 | Metallocene-based Olefin Polymerization | 73 |
| 3.3 | Asymmetric Catalysis | 75 |
| 3.3.1 | Introduction | 75 |
| 3.3.2 | Catalysts | 75 |
| 3.3.3 | Commercial Applications | 76 |
| 3.3.3.1 | Asymmetric Hydrogenation | 77 |
| 3.3.3.2 | Enantioselective Isomerization: L-Menthol | 78 |
| 3.3.3.3 | Asymmetric Epoxidation | 79 |
| | Exercises for Chapter 3 | 80 |
| 4 | Biocatalysis | 83 |
| 4.1 | Introduction | 83 |
| 4.2 | Kinetics of Enzyme-catalyzed Reactions | 87 |
| 4.3 | Industrial Processes with Biocatalysts | 92 |
| 4.3.1 | Acrylamide from Acrylonitrile | 93 |
| 4.3.2 | Aspartame through Enzymatic Peptide Synthesis | 94 |
| 4.3.3 | L-Amino Acids by Aminoacylase Process | 95 |
| 4.3.4 | 4-Hydroxyphenoxypropionic Acid as Herbicide Intermediate | 96 |
| | Exercises for Chapter 4 | 97 |
| 5 | Heterogeneous Catalysis: Fundamentals | 99 |
| 5.1 | Individual Steps in Heterogeneous Catalysis | 99 |
| 5.2 | Kinetics and Mechanisms of Heterogeneously Catalyzed Reactions | 102 |
| 5.2.1 | The Importance of Adsorption in Heterogeneous Catalysis | 102 |
| 5.2.2 | Kinetic Treatment | 107 |
| 5.2.3 | Mechanisms of Heterogeneously Catalyzed Gas-Phase Reactions | 109 |
| 5.2.3.1 | Langmuir–Hinshelwood Mechanism (1921) | 109 |
| 5.2.3.2 | Eley–Rideal Mechanism (1943) | 111 |
| | Exercises for Section 5.2 | 114 |
| 5.3 | Catalyst Concepts in Heterogeneous Catalysis | 116 |
| 5.3.1 | Energetic Aspects of Catalytic Activity | 116 |
| | Exercises for Section 5.3.1 | 130 |

| | | |
|----------|--|------------|
| 5.3.2 | Steric Effects | 131 |
| | Exercises for Section 5.3.2 | 142 |
| 5.3.3 | Electronic Factors | 143 |
| 5.3.3.1 | Metals | 145 |
| 5.3.3.2 | Bimetallic Catalysts | 151 |
| 5.3.3.3 | Semiconductors | 155 |
| 5.3.3.4 | Isolators: Acidic and Basic Catalysts | 169 |
| | Exercises for Section 5.3.3 | 177 |
| 5.4 | Catalyst Performance | 179 |
| 5.4.1 | Factors which Affect the Catalyst Performance | 179 |
| 5.4.2 | Supported Catalysts | 180 |
| 5.4.3 | Promoters | 189 |
| 5.4.4 | Inhibitors | 194 |
| | Exercises for Section 5.4 | 195 |
| 5.5 | Catalyst Deactivation and Regeneration | 195 |
| 5.5.1 | Catalyst Poisoning | 197 |
| 5.5.2 | Poisoning of Metals | 199 |
| 5.5.3 | Poisoning of Semiconductor Oxides | 200 |
| 5.5.4 | Poisoning of Solid Acids | 200 |
| 5.5.5 | Deposits on the Catalyst Surface | 201 |
| 5.5.6 | Thermal Processes and Sintering | 203 |
| 5.5.7 | Catalyst Losses via the Gas Phase | 204 |
| | Exercises for Section 5.5 | 207 |
| 5.6 | Characterization of Heterogeneous Catalysts | 207 |
| 5.6.1 | Physical Characterization | 208 |
| 5.6.2 | Chemical Characterization and Surface Analysis | 214 |
| | Exercises for Section 5.6 | 221 |
| 6 | Catalyst Shapes and Production of Heterogeneous Catalysts | 223 |
| 6.1 | Catalyst Production | 223 |
| 6.2 | Immobilization of Homogeneous Catalysts | 231 |
| 6.2.1 | Highly Dispersed Supported Metal Catalysts | 235 |
| 6.2.2 | SSP Catalysts | 235 |
| 6.2.3 | SLP Catalysts | 236 |
| | Exercises for Chapter 6 | 237 |
| 7 | Shape-Selective Catalysis: Zeolites | 239 |
| 7.1 | Composition and Structure of Zeolites | 239 |
| 7.2 | Production of Zeolites | 242 |
| 7.3 | Catalytic Properties of the Zeolites | 243 |
| 7.3.1 | Shape Selectivity | 243 |
| 7.3.1.1 | Reactant Selectivity | 245 |
| 7.3.1.2 | Product Selectivity | 247 |
| 7.3.1.3 | Restricted Transition State Selectivity | 247 |
| 7.3.2 | Acidity of Zeolites | 248 |

| | | |
|----------|---|------------|
| 7.4 | Isomorphic Substitution of Zeolites | 252 |
| 7.5 | Metal-Doped Zeolites | 253 |
| 7.6 | Applications of Zeolites | 255 |
| | Exercises for Chapter 7 | 258 |
| 8 | Heterogeneously Catalyzed Processes in Industry | 261 |
| 8.1 | Overview | 261 |
| 8.1.1 | Production of Inorganic Chemicals | 261 |
| 8.1.2 | Production of Organic Chemicals | 261 |
| 8.1.3 | Refinery Processes | 262 |
| 8.1.4 | Catalysts in Environmental Protection | 264 |
| 8.2 | Examples of Industrial Processes – Bulk Chemicals | 266 |
| 8.2.1 | Ammonia Synthesis | 266 |
| 8.2.2 | Hydrogenation | 267 |
| 8.2.3 | Methanol Synthesis | 270 |
| 8.2.4 | Selective Oxidation of Propene | 272 |
| 8.2.5 | Olefin Polymerization | 276 |
| | Exercises for Section 8.1 and 8.2 | 278 |
| 8.3 | Fine Chemicals Manufacture | 281 |
| 8.3.1 | Fine Chemicals and their Synthesis | 281 |
| 8.3.2 | Selected Examples of Industrial Processes | 285 |
| 8.3.2.1 | Hydrogenation | 285 |
| 8.3.2.2 | Oxidation | 288 |
| 8.3.2.3 | Catalytic C–C-linkage | 289 |
| 8.3.2.4 | Acid/Base Catalysis | 291 |
| | Exercises for Section 8.3 | 292 |
| 9 | Electrocatalysis | 295 |
| 9.1 | Comparison Between Electrocatalysis and Heterogeneous Catalysis | 295 |
| 9.2 | Electrochemical Reactions and Electrode Kinetics | 296 |
| 9.2.1 | Hydrogen Electrode Reaction | 296 |
| 9.2.2 | Oxygen Electrode Reaction | 298 |
| 9.3 | Electrocatalytic Processes | 302 |
| 9.3.1 | Electrocatalytic Hydrogenation | 302 |
| 9.3.2 | Electrocatalytic Oxidation | 304 |
| 9.3.3 | Electrochemical Addition | 305 |
| 9.3.4 | Electrocatalytic Oxidation of Methanol | 306 |
| 9.4 | Electrocatalysis in Fuel Cells | 307 |
| 9.4.1 | Basic Principles | 307 |
| 9.4.2 | Types of Fuel Cell and Catalyst | 308 |
| 9.4.3 | Important Reactions in Fuel Cell Technology | 311 |
| 9.4.3.1 | The Anodic Reaction | 311 |
| 9.4.3.2 | The Cathodic Reaction | 312 |
| 9.4.3.3 | Methanol Oxidation | 313 |
| | Exercises for Chapter 9 | 315 |

| | | |
|-----------|---|------------|
| 10 | Environmental Catalysis and Green Chemistry | 317 |
| 10.1 | Automotive Exhaust Catalysis | 317 |
| 10.2 | NO _x Removal Systems | 318 |
| 10.2.1 | Selective Catalytic Reduction of Nitrogen Oxides | 318 |
| 10.2.2 | NO _x Storage-Reduction Catalyst for Lean-Burning Engines | 320 |
| 10.3 | Catalytic Afterburning | 322 |
| 10.4 | Green Chemistry and Catalysis | 324 |
| 10.4.1 | Examples of Catalytical Processes | 325 |
| 10.4.1.1 | Aldol Condensation | 325 |
| 10.4.1.2 | Diels-Alder Reaction | 326 |
| 10.4.1.3 | Hydrogenation | 327 |
| 10.4.1.4 | Cyclization in Water | 327 |
| 10.4.1.5 | Use of Ionic Liquids | 327 |
| | Exercises for Chapter 10 | 328 |
| 11 | Photocatalysis | 331 |
| 11.1 | Basic Principles | 331 |
| 11.2 | Photoreduction and Oxidation of Water | 333 |
| 11.2.1 | Water Reduction | 334 |
| 11.2.2 | Water Oxidation | 335 |
| 11.3 | Photocleavage of Water | 336 |
| 11.4 | Other Reactions | 337 |
| | Exercises for Chapter 11 | 338 |
| 12 | Phase-Transfer Catalysis | 339 |
| 12.1 | Definition | 339 |
| 12.2 | Catalysts for PTC | 339 |
| 12.3 | Mechanism and Benefits of PTC | 340 |
| 12.4 | PTC Reactions | 341 |
| 12.5 | Selected Industrial Processes with PTC | 342 |
| | Exercises for Chapter 12 | 345 |
| 13 | Planning, Development, and Testing of Catalysts | 347 |
| 13.1 | Stages of Catalyst Development | 347 |
| 13.2 | An Example of Catalyst Planning: Conversion of Olefins to Aromatics | 350 |
| 13.3 | Selection and Testing of Catalysts in Practice | 355 |
| 13.3.1 | Catalyst Screening | 356 |
| 13.3.2 | Catalyst Test Reactors and Kinetic Modeling | 358 |
| 13.3.3 | Statistical Test Planning and Optimization [6, 21] | 369 |
| 13.3.3.1 | Factorial Test Plans | 370 |
| 13.3.3.2 | Plackett–Burman Plan | 375 |
| 13.3.3.3 | Experimental Optimization by the Simplex Method | 376 |
| 13.3.3.4 | Statistical Test Planning with a Computer Program | 379 |
| 13.3.4 | Kinetic Modeling and Simulation | 383 |

| | | |
|-----------|--|------------|
| 13.3.5 | Modeling and Simulation with POLYMATH | 396 |
| 13.3.6 | Catalyst Discovery via High-Throughput Experimentation | 397 |
| | Exercises for Chapter 13 | 400 |
| 14 | Catalysis Reactors | 403 |
| 14.1 | Two-Phase Reactors | 410 |
| 14.2 | Three-Phase Reactors | 413 |
| 14.2.1 | Fixed-Bed Reactors | 414 |
| 14.2.2 | Suspension Reactors | 416 |
| 14.3 | Reactors for Homogeneously Catalyzed Reactions | 420 |
| | Exercises for Chapter 14 | 422 |
| 15 | Economic Importance of Catalysts | 425 |
| 16 | Future Development of Catalysis | 429 |
| 16.1 | Homogeneous Catalysis | 429 |
| 16.2 | Heterogeneous Catalysis | 431 |
| 16.2.1 | Use of Other, Cheaper Raw Materials | 433 |
| 16.2.2 | Catalysts for Energy Generation | 434 |
| 16.2.3 | Better Strategies for Catalyst Development | 435 |
| | Solutions to the Exercises | 439 |
| | References | 483 |
| | Subject Index | 493 |

Preface to the Second Edition

During the last years catalysis has made a rapid progress, there can be observed many new applications of catalysts. For obvious reasons catalysis is the key to the success in developing new processes for various fields in industry. The use of suitable catalysts for new processes requires a basic knowledge of catalytic principles.

In this book, my main objective is to present an overview on catalysis, so that both the student and the experienced practitioner can see the broad picture. It was the intention to compile a text of about 500 pages surveying the whole area of catalysis, that means homogeneous catalysis, heterogeneous catalysis, biocatalysis and special topics of applied catalysis. It is felt that sufficient information is given here for a rational approach to be applied in a basic understanding of the phenomenon catalysis.

In the present edition some space is dedicated to special topics such as electrocatalysis, photocatalysis, asymmetric catalysis, phase-transfer catalysis, environmental catalysis, and fine chemicals manufacture. On the basis of fundamental reaction engineering equations, examples for calculation and modeling of catalysis reactors are given with the easy-to-learn PC program POLYMATH. Well over 170 exercises help the reader to test and consolidate the gained knowledge.

The book is based on my own lecture course for chemical engineers at the University of Applied Sciences Mannheim and several vocational training seminars for chemists and engineers in industry. I hope this book will be useful both to students who have studied chemistry or chemical engineering and to graduates and chemists who work in or are interested in the chemical industry.

Grateful appreciation is given to the following companies which provided photographic material: Degussa AG, Hanau and Marl, HTE AG, Heidelberg, and Süd-Chemie AG, Heufeld. I am particular grateful to Prof. V. M. Schmidt, Mannheim, for his valuable advice in electrocatalysis and additional material. I also want to thank the numerous students who followed my courses in Mannheim.

I thank the publishers, for their kind and competent support. I gratefully acknowledge the help of Dr. Romy Kirsten, who directed the project, Claudia Grössl for production, and Dr. Melanie Rohn for copy-editing. Special thanks and appreciation to my wife Julia for her patience, understanding and the encouragement to stay with this project to its completion.

Mannheim, October 2005

Jens Hagen

Preface to the First Edition

Catalysts have been used in the chemical industry for hundreds of years, and many large-scale industrial processes can only be carried out with the aid of catalysis. However, it is only since the 1970s that catalysis has become familiar to the general public, mainly because of developments in environmental protection, an example being the well known and widely used catalytic converter for automobiles.

Catalysis is a multidisciplinary area of chemistry, in particular, industrial chemistry. Anyone who is involved with chemical reactions will eventually have something to do with catalysts.

In spite of years of experience with catalysts and the vast number of publications concerning catalytic processes, there is still no fundamental theory of catalysis. As is often the case in chemistry, empirical concepts are used to explain experimental results or to make predictions about new reactions, with greater or lesser degrees of success.

To date there has been no standard book that deals equally with both heterogeneous and homogeneous catalysis, as well as industrial aspects thereof. The books published up to now generally describe a particular area or special aspects of catalysis and are therefore less suitable for teaching or studying on one's own. For this reason, it is not easy for those commencing their careers to become familiar with the complex field of catalysis.

This book is based on my own lecture course for chemical engineers at the Fachhochschule Mannheim (Mannheim University of Applied Sciences M.U.A.S) and is intended for students of chemistry, industrial chemistry, and process engineering, as well as chemists, engineers, and technicians in industry who are involved with catalysts. Largely dispensing with complex theoretical and mathematical treatments, the book describes the fundamental principles of catalysis in an easy to understand fashion. Numerous examples and exercises with solutions serve to consolidate the understanding of the material. The book is particularly well suited to studying on one's own.

It is assumed that the reader has a basic knowledge of chemistry, in particular, of reaction kinetics and organometallic chemistry. Homogeneous transition metal catalysis and heterogeneous catalysis are treated on the basis of the most important catalyst concepts, and the applications of catalysts are discussed with many examples. The book aids practically oriented readers in becoming familiar with the processes

of catalyst development and testing and therefore deals with aspects of test planning, optimization, and reactor simulation. Restricting the coverage to fundamental aspects made it necessary to treat certain areas that would be of interest to specialists in concise form or to omit them completely.

I wish to thank all those who supported me in producing this book. Special thanks are due to Dr. R. Eis for all the hard work and care he invested in preparing the figures and for his helpful contributions and suggestions. I am grateful to the following companies for providing photographic material: BASF, Ludwigshafen, Germany; Degussa, Hanau, Germany; Hoffmann-LaRoche, Kaiseraugst, Switzerland; Döduco, Sinsheim, Germany; and VINCI Technologies, Rueil-Malmaison, France. Interesting examples of catalyst development were taken from the Diploma theses of Fachhochschule graduates, of whom K. Kromm and T. Zwick are especially worthy of mention.

I was pleased to accept the publisher's offer to produce an English version of the book. The introduction of international study courses leading to a Bachelor's or Master's degree in Germany and other countries makes it necessary to provide students with books in English. I am particularly grateful to Dr. S. Hawkins for his competent translation of the German text with valuable advice and additional material.

I thank the publishers, Wiley-VCH Weinheim, for their kind support. Thanks are due to Dr. B. Böck, who directed the project, C. Grössl for production, and S. Pauker for the cover graphics.

Mannheim, January 1999

Jens Hagen

Abbreviations

| | |
|-----------------|--|
| A | area [m^2] |
| A^* | adsorbed (activated) molecules of component A |
| a | catalyst activity |
| a_s | area per mass [m^2/kg] |
| A | electron acceptor |
| ADH | alcohol dehydrogenase enzyme |
| ads | adsorbed (subscript) |
| AES | Auger electron spectroscopy |
| aq | aqueous solution (subscript) |
| bcc | body-centered cubic |
| bipy | 2,2'-bipyridine |
| Bu | butyl C_4H_9 - |
| c_i | concentration of component i [mol/L] |
| CB | conduction band |
| C.I. | constraint index |
| Cp | cyclopentadienyl C_5H_5 - |
| CSTR | continuous stirred tank reactor |
| D | diffusion coefficient [m^2/s] |
| d | deactivation (subscript) |
| D | electron donor |
| DMFC | direct methanol fuel cell |
| E | E factor, rate of waste [kg] per product unit [kg] |
| E_a | activation energy [J/mol] |
| E_{bg} | bandgap energy [eV] |
| E_{F} | Fermi level |
| E | enzyme |
| e.e. | enantiomeric excess [%] |
| eff | effective (subscript) |
| E_i | ionisation energy |
| E_r | redox potential [V] |
| Et | ethyl C_2H_5 - |
| ESCA | electron spectroscopy for chemical analysis |
| ESR | electron spin resonance spectroscopy |

| | |
|-----------------------------|--|
| e | electrons |
| F | Faraday constant [96 485 C/mol] |
| fcc | face-centered cubic |
| ΔG | Gibb's free energy [J/mol] |
| G | gas (subscript, too) |
| GHSV | gas hourly space velocity [h^{-1}] |
| H | Henry's law constant |
| H_{ex} | external holdup |
| ΔH_{ads} | adsorption enthalpy [J/mol] |
| ΔH_{f} | enthalpy change of formation [J/mol] |
| H_{m} | modified Henry's law constant |
| ΔH_{R} | reaction enthalpy [J/mol] |
| H_0 | Hammett acidity function |
| HC | hydrocarbon |
| HSAB | hard and soft acids and bases |
| h | hard |
| hcp | hexagonal close packing |
| I | inhibitor |
| IL | ionic liquid |
| ISS | ion scattering spectroscopy |
| j | current density [A/m^2] |
| K | equilibrium constant |
| K_{i} | adsorption equilibrium constant of component i |
| K_{i} | inhibition constant |
| K_{M} | Michaelis constant |
| k | reaction rate constant |
| k_0 | pre-exponential factor |
| $k_{\text{L}} a_{\text{L}}$ | gas-liquid mass transfer coefficient |
| $k_{\text{S}} a_{\text{S}}$ | liquid-solid mass transfer coefficient |
| k_{tot} | global mass transfer coefficient |
| L | liquid (subscript) |
| L | ligand |
| LEED | low-energy electron diffraction |
| LF | liquid flow [L/min] |
| M | metal |
| m | mass [kg] |
| $m_{\text{cat.}}$ | mass of catalyst [kg] |
| MAO | methylaluminoxane |
| Med | mediator, redox catalyst |
| n | number of moles [mol] |
| n | order of reaction |
| \dot{n} | flow rate [mol/s] |
| $\dot{n}_{\text{A},0}$ | feed flow rate of starting material A [mol/s] |
| NAD | nicotinamide adenine dinucleotide cofactor |
| NHE | normal hydrogen electrode |

| | |
|------------------------|--|
| NSR | NO _x storage-reduction |
| ODE | ordinary differential equation |
| Oxad | oxidative addition |
| <i>P</i> | total pressure [bar] |
| PEG | polyethylene glycol |
| PEMFC | proton exchange membrane fuel cell |
| Ph | phenyl C ₆ H ₅ - |
| PPh ₃ | triphenylphosphine |
| PTC | phase-transfer catalysis |
| <i>p</i> | pressure [bar] |
| <i>p_i</i> | partial pressure of component <i>i</i> [bar] |
| py | pyridine |
| <i>R</i> | ideal gas law constant [J mol ⁻¹ K ⁻¹] |
| <i>R</i> | recycle ratio |
| R | alkyl |
| <i>r</i> | reaction rate [mol L ⁻¹ h ⁻¹] |
| <i>r_{eff}</i> | effective reaction rate per unit mass of catalyst [mol kg ⁻¹ h ⁻¹] |
| rel | relative (subscript) |
| <i>r_d</i> | deactivation rate |
| <i>S</i> | Tafel slope (electrocatalysis) |
| <i>S</i> | surface area [m ² /kg] |
| Δ <i>S</i> | entropy change [J mol ⁻¹ K ⁻¹] |
| <i>S_p</i> | selectivity [mol/mol] or [%] |
| S | solid (subscript, too) |
| SCR | selective catalytic reduction |
| SIMS | secondary-ion mass spectroscopy |
| SLPC | supported liquid phase catalysts |
| SMSI | strong metal-support interaction |
| SSPC | supported solid phase catalysts |
| s | soft |
| <i>s</i> | sample standard deviation |
| <i>s</i> ² | experimental error variance |
| <i>S</i> ⁻¹ | mass index, ratio of all the materials [kg] to the product [kg] |
| S | substrate |
| sc | supercritical |
| STY | space time yield [mol L ⁻¹ h ⁻¹ , kg L ⁻¹ h ⁻¹] |
| <i>T</i> | temperature [K] |
| TEM | transmission electron microscopy |
| <i>TF</i> | time-factor [<i>m_{cat}</i> / <i>n_{A,0}</i>] |
| <i>TOF</i> | turnover frequency [s ⁻¹] |
| <i>TON</i> | turnover number [mol mol ⁻¹ s ⁻¹] |
| <i>t</i> | time [s, h] |
| TPD | temperature-programmed desorption |
| TPR | temperature-programmed reduction |
| TS 1 | titanium(IV) silicalite zeolite catalyst |

| | |
|----------------------|--|
| U | cell voltage [V] |
| V | volume [m^3] |
| \dot{V} | volumetric flow-rate |
| V_R | reaction volume [m^3] |
| VB | valence band |
| VOC | volatile organic compound |
| X | conversion [mol/mol] or [%] |
| \bar{x} | mean value of measurements |
| \vec{x} | positional vector (simplex method) |
| z | tube length [m] |
| δ | percentage d-band occupancy |
| ϵ | excitation energy of semiconductors [eV] |
| ϵ_P | void fraction of particle |
| η | catalyst effectiveness factor |
| η | overpotential [V] |
| θ_i | degree of coverage of the surface of component i |
| ν | stretching frequencies (IR) [cm^{-1}] |
| ν_i | stoichiometric coefficient |
| ρ | density [g/mL] |
| $\rho_{\text{cat.}}$ | pellet density of the catalyst [g/mL] |
| τ | tortuosity |
| σ | interfacial tension |
| ϕ_0 | work function [eV] |
| * | active centers on the catalyst surface |

1

Introduction

1.1 The Phenomenon Catalysis

Catalysis is the key to chemical transformations. Most industrial syntheses and nearly all biological reactions require catalysts. Furthermore, catalysis is the most important technology in environmental protection, i. e., the prevention of emissions. A well-known example is the catalytic converter for automobiles.

Catalytic reactions were already used in antiquity, although the underlying principle of catalysis was not recognized at the time. For example, the fermentation of sugar to ethanol and the conversion of ethanol to acetic acid are catalyzed by enzymes (biocatalysts). However, the systematic scientific development of catalysis only began about 200 years ago, and its importance has grown up to the present day [2].

The term “catalysis” was introduced as early as 1836 by Berzelius in order to explain various decomposition and transformation reactions. He assumed that catalysts possess special powers that can influence the affinity of chemical substances.

A definition that is still valid today is due to Ostwald (1895): “a catalyst accelerates a chemical reaction without affecting the position of the equilibrium.” Ostwald recognized catalysis as a ubiquitous phenomenon that was to be explained in terms of the laws of physical chemistry.

While it was formerly assumed that the catalyst remained unchanged in the course of the reaction, it is now known that the catalyst is involved in chemical bonding with the reactants during the catalytic process. Thus catalysis is a cyclic process: the reactants are bound to one form of the catalyst, and the products are released from another, regenerating the initial state.

In simple terms, the catalytic cycle can be described as shown in Figure 1-1 [T9]. The intermediate catalyst complexes are in most cases highly reactive and difficult to detect.

In theory, an ideal catalyst would not be consumed, but this is not the case in practice. Owing to competing reactions, the catalyst undergoes chemical changes, and its activity becomes lower (catalyst deactivation). Thus catalysts must be regenerated or eventually replaced.

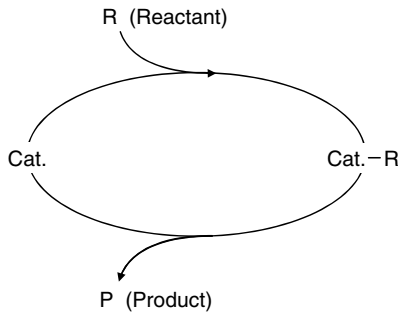


Fig. 1-1 Catalytic cycle

Apart from accelerating reactions, catalysts have another important property: they can influence the selectivity of chemical reactions. This means that completely different products can be obtained from a given starting material by using different catalyst systems. Industrially, this targeted reaction control is often even more important than the catalytic activity [6].

Catalysts can be gases, liquids, or solids. Most industrial catalysts are liquids or solids, whereby the latter react only via their surface. The importance of catalysis in the chemical industry is shown by the fact that 75 % of all chemicals are produced with the aid of catalysts; in newly developed processes, the figure is over 90 %. Numerous organic intermediate products, required for the production of plastics, synthetic fibers, pharmaceuticals, dyes, crop-protection agents, resins, and pigments, can only be produced by catalytic processes.

Most of the processes involved in crude-oil processing and petrochemistry, such as purification stages, refining, and chemical transformations, require catalysts. Environmental protection measures such as automobile exhaust control and purification of off-gases from power stations and industrial plant would be inconceivable without catalysts [5].

Catalysts have been successfully used in the chemical industry for more than 100 years, examples being the synthesis of sulfuric acid, the conversion of ammonia to nitric acid, and catalytic hydrogenation. Later developments include new highly selective multicomponent oxide and metallic catalysts, zeolites, and the introduction of homogeneous transition metal complexes in the chemical industry. This was supplemented by new high-performance techniques for probing catalysts and elucidating the mechanisms of heterogeneous and homogeneous catalysis.

The brief historical survey given in Table 1-1 shows just how closely the development of catalysis is linked to the history of industrial chemistry [4].

Table 1-1 History of the catalysis of industrial processes [4]

| Catalytic reaction | Catalyst | Discoverer or company/year |
|--|--------------------------------------|---|
| Sulfuric acid (lead-chamber process) | NO_x | Désormes, Clement, 1806 |
| Chlorine production by HCl oxidation | CuSO_4 | Deacon, 1867 |
| Sulfuric acid (contact process) | Pt, V_2O_5 | Winkler, 1875; Knietzsch, 1888 (BASF) |
| Nitric acid by NH_3 oxidation | Pt/Rh nets | Ostwald, 1906 |
| Fat hardening | Ni | Normann, 1907 |
| Ammonia synthesis from N_2 , H_2 | Fe | Mittasch, Haber, Bosch, 1908; Production, 1913 (BASF) |
| Hydrogenation of coal to hydrocarbons | Fe, Mo, Sn | Bergius, 1913; Pier, 1927 |
| Oxidation of benzene, naphthalene to MSA or PSA | V_2O_5 | Weiss, Downs, 1920 |
| Methanol synthesis from CO/H_2 | $\text{ZnO}/\text{Cr}_2\text{O}_3$ | Mittasch, 1923 |
| Hydrocarbons from CO/H_2 (motor fuels) | Fe, Co, Ni | Fischer, Tropsch, 1925 |
| Oxidation of ethylene to ethylene oxide | Ag | Lefort, 1930 |
| Alkylation of olefins with isobutane to gasoline | AlCl_3 | Ipatieff, Pines, 1932 |
| Cracking of hydrocarbons | $\text{Al}_2\text{O}_3/\text{SiO}_2$ | Houdry, 1937 |
| Hydroformylation of ethylene to propanal | Co | Roelen, 1938 (Ruh Chemie) |
| Cracking in a fluidized bed | aluminosilicates | Lewis, Gilliland, 1939 (Standard Oil) |
| Ethylene polymerization, low-pressure | Ti compounds | Ziegler, Natta, 1954 |
| Oxidation of ethylene to acetaldehyde | Pd/Cu chlorides | Hafner, Smidt (Wacker) |
| Ammonoxidation of propene to acrylonitrile | Bi/Mo | Idol, 1959 (SOHIO process) |
| Olefin metathesis | Re, W, Mo | Banks, Bailey, 1964 |
| Hydrogenation, isomerization, hydroformylation | Rh-, Ru complexes | Wilkinson, 1964 |
| Asymmetric hydrogenation | Rh/chiral phosphine | Knowles, 1974; L-Dopa (Monsanto) |
| Three-way catalyst | Pt, Rh/monolith | General Motors, Ford, 1974 |
| Methanol conversion to hydrocarbons | Zeolites | Mobil Chemical Co., 1975 |
| α -olefins from ethylene | Ni/chelate phosphine | Shell (SHOP process) 1977 |

Table 1-1 (continued)

| Catalytic reaction | Catalyst | Discoverer or company/year |
|---|------------------------------|--------------------------------------|
| Sharpless oxidation, epoxidation | Ti/ROOH/tartrate | May & Baker, Upjohn, ARCO, 1981 |
| Selective oxidations with H ₂ O ₂ | titanium zeolite (TS-1) | Enichem, 1983 |
| Hydroformylation | Rh/phosphine/ aqueous | Rhône-Poulenc/Ruhrchemie, 1984 |
| Polymerization of olefines | zirconocene/MAO | Sinn, Kaminsky, 1985 |
| Selective catalytic reduction SCR (power plants) | V, W, Ti oxides/ monolith | ~1986 |
| Acetic acid | Ir/I ⁻ /Ru | „Cativa“-process, BP Chemicals, 1996 |

1.2

Mode of Action of Catalysts

The suitability of a catalyst for an industrial process depends mainly on the following three properties:

- Activity
- Selectivity
- Stability (deactivation behavior)

The question which of these functions is the most important is generally difficult to answer because the demands made on the catalyst are different for each process. First, let us define the above terms [6, 7].

1.2.1

Activity

Activity is a measure of how fast one or more reactions proceed in the presence of the catalyst. Activity can be defined in terms of kinetics or from a more practically oriented viewpoint. In a formal kinetic treatment, it is appropriate to measure reaction rates in the temperature and concentration ranges that will be present in the reactor.

The reaction rate r is calculated as the rate of change of the amount of substance n_A of reactant A with time relative to the reaction volume or the mass of catalyst:

$$r = \frac{\text{converted amount of substance of a reactant}}{\text{volume or catalyst mass} \cdot \text{time}} \quad (\text{mol L}^{-1} \text{ h}^{-1} \text{ or mol kg}^{-1} \text{ h}^{-1}) \quad (1-1)$$

Kinetic activities are derived from the fundamental rate laws, for example, that for a simple irreversible reaction $A \rightarrow P$:

$$\frac{dn_A}{dt} = kVf(c_A) \quad (1-2)$$

k = rate constant

$f(c_A)$ is a concentration term that can exhibit a first- or higher order dependence on adsorption equilibria (see Section 5.2).

The temperature dependence of rate constants is given by the Arrhenius equation:

$$k = k_0 e^{-(E_a/RT)} \quad (1-3)$$

E_a = activation energy of the reaction

k_0 = pre-exponential factor

R = gas constant

As Equations 1-2 and 1-3 show, there are three possibilities for expressing catalyst activity, i. e., as:

- Reaction rate
- Rate constant k
- Activation energy E_a

Empirical rate equations are obtained by measuring reaction rates at various concentrations and temperatures. If, however, different catalysts are to be compared for a given reaction, the use of constant concentration and temperature conditions is often difficult because each catalyst requires its own optimal conditions. In this case it is appropriate to use the initial reaction rates r_0 obtained by extrapolation to the start of the reaction.

Another measure of catalyst activity is the turnover number TON, which originates from the field of enzymatic catalysis.

In the case of homogeneous catalysis, in which well-defined catalyst molecules are generally present in solution, the TON can be directly determined. For heterogeneous catalysts, this is generally difficult, because the activity depends on the size of the catalyst surface, which, however, does not have a uniform structure. For example, the activity of a supported metal catalyst is due to active metal atoms dispersed over the surface.

The number of active centers per unit mass or volume of catalyst can be determined indirectly by means of chemisorption experiments, but such measurements require great care, and the results are often not applicable to process conditions. Although the TON appears attractive due to its molecular simplicity, it should be used prudently in special cases.

In practice, readily determined measures of activity are often sufficient. For comparative measurements, such as catalyst screening, determination of process para-

meters, optimization of catalyst production conditions, and deactivation studies, the following activity measures can be used:

- Conversion under constant reaction conditions
- Space velocity for a given, constant conversion
- Space–time yield
- Temperature required for a given conversion

Catalysts are often investigated in continuously operated test reactors, in which the conversions attained at constant space velocity are compared [6]

The space velocity is the volume flow rate \dot{V}_0 , relative to the catalyst mass m_{cat} :

$$\text{Space velocity} = \frac{\dot{V}_0}{m_{\text{cat}}} \quad (\text{m}^3 \text{ kg}^{-1} \text{ s}^{-1}) \quad (1-4)$$

The conversion X_A is the ratio of the amount of reactant A that has reacted to the amount that was introduced into the reactor. For a batch reactor:

$$X_A = \frac{n_{A,0} - n_A}{n_{A,0}} \quad (\text{mol/mol or \%}) \quad (1-5)$$

If we replace the catalyst mass in Equation 1-4 with the catalyst volume, then we see that the space velocity is proportional to the reciprocal of the residence time.

Figure 1-2 compares two catalysts of differing activity with one another, and shows that for a given space velocity, catalyst A is better than catalyst B.

Of course, such measurements must be made under constant conditions of starting material ratio, temperature, and pressure.

Often the performance of a reactor is given relative to the catalyst mass or volume, so that reactors of different size or construction can be compared with one another. This quantity is known as the space–time yield *STY*:

$$STY = \frac{\text{Desired product quantity}}{\text{Catalyst volume} \cdot \text{time}} \quad (\text{mol L}^{-1} \text{ h}^{-1}) \quad (1-6)$$

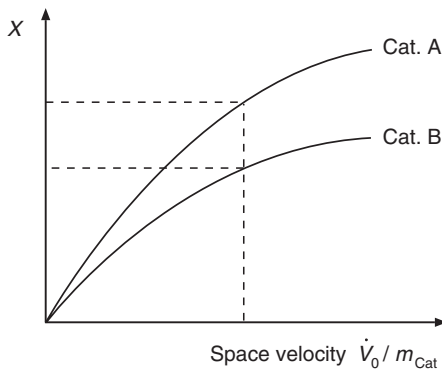


Fig. 1-2 Comparison of catalyst activities

Determination of the temperature required for a given conversion is another method of comparing catalysts. The best catalyst is the one that gives the desired conversion at a lower temperature. This method can not, however, be recommended since the kinetics are often different at higher temperature, making misinterpretations likely. This method is better suited to carrying out deactivation measurements on catalysts in pilot plants.

1.2.1.1 Turnover Frequency TOF

The turnover frequency TOF (the term was borrowed from enzyme catalysis) quantifies the specific activity of a catalytic center for a special reaction under defined reaction conditions by the number of molecular reactions or catalytic cycles occurring at the center per unit time. For heterogeneous catalysts the number of active centers is derived usually from sorption methods (Eq. 1-7).

$$\text{TOF} = \frac{\text{volumetric rate of reaction}}{\text{number of centers/volume}} = \frac{\text{moles}}{\text{volume} \cdot \text{time}} \frac{\text{volume}}{\text{moles}} = \text{time}^{-1} \quad (1-7)$$

For most relevant industrial applications the TOF is in the range 10^{-2} – 10^2 s^{-1} (enzymes 10^3 – 10^7 s^{-1}).

Examples:

TOF values for the hydrogenation of cyclohexene at 25 °C and 1 bar (supported catalysts, structure insensitive reaction; Table 1-2):

Table 1-2 TOF values for the hydrogenation of cyclohexene [T 46]

| Metal | TOF (s^{-1}) | |
|-------|-------------------------|--------------|
| | Gas phase | Liquid phase |
| Ni | 2.0 | 0.45 |
| Rh | 6.1 | 1.3 |
| Pd | 3.2 | 1.5 |
| Pt | 2.8 | 0.6 |

1.2.1.2 Turnover Number TON [T 46]

The turnover number specifies the maximum use that can be made of a catalyst for a special reaction under defined conditions by a number of molecular reactions or reaction cycles occurring at the reactive center up to the decay of activity. The relationship between TOF and TON is (Eq. 1-8):

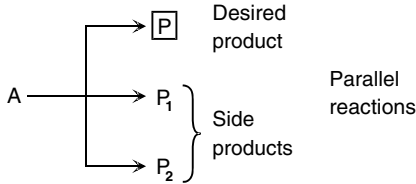
$$\text{TON} = \text{TOF} [\text{time}^{-1}] \cdot \text{lifetime of the catalyst} [\text{time}] [-] \quad (1-8)$$

For industrial applications the TON is in the range 10^6 – 10^7 .

1.2.2

Selectivity

The selectivity S_p of a reaction is the fraction of the starting material that is converted to the desired product P. It is expressed by the ratio of the amount of desired product to the reacted quantity of a reaction partner A and therefore gives information about the course of the reaction. In addition to the desired reaction, parallel and sequential reactions can also occur (Scheme 1-1).



Sequential
reaction

Scheme 1-1 Parallel and sequential reactions

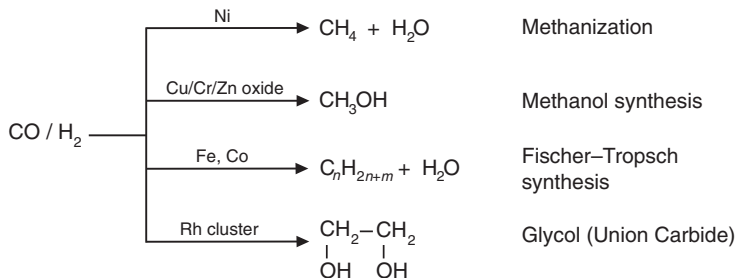
Since this quantity compares starting materials and products, the stoichiometric coefficients v_i of the reactants must be taken into account, which gives rise to the following equation [6]:

$$S_p = \frac{n_p / \nu_p}{(n_{A,0} - n_A) / |\nu_A|} = \frac{n_p |\nu_A|}{(n_{A,0} - n_A) \nu_p} \quad (\text{mol/mol or \%}) \quad (1-9)$$

In comparative selectivity studies, the reaction conditions of temperature and conversion or space velocity must, of course, be kept constant.

If the reaction is independent of the stoichiometry, then the selectivity $S_p = 1$. The selectivity is of great importance in industrial catalysis, as demonstrated by the example of synthesis gas chemistry, in which, depending on the catalyst used, completely different reaction products are obtained (Scheme 1-2) [2].

Selectivity problems are of particular relevance to oxidation reactions.



Scheme 1-2 Reactions of synthesis gas

1.2.3

Stability

The chemical, thermal, and mechanical stability of a catalyst determines its lifetime in industrial reactors. Catalyst stability is influenced by numerous factors, including decomposition, coking, and poisoning. Catalyst deactivation can be followed by measuring activity or selectivity as a function of time.

Catalysts that lose activity during a process can often be regenerated before they ultimately have to be replaced. The total catalyst lifetime is of crucial importance for the economics of a process.

Today the efficient use of raw materials and energy is of major importance, and it is preferable to optimize existing processes than to develop new ones. For various reasons, the target quantities should be given the following order of priority:

Selectivity > Stability > Activity

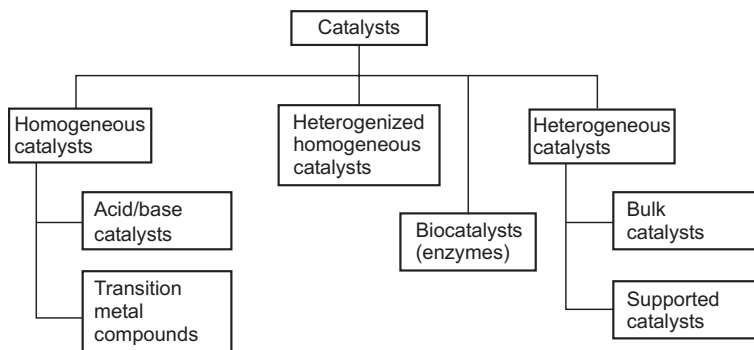
1.3

Classification of Catalysts

The numerous catalysts known today can be classified according to various criteria: structure, composition, area of application, or state of aggregation.

Here we shall classify the catalysts according to the state of aggregation in which they act. There are two large groups: heterogeneous catalysts (solid-state catalysts) and homogeneous catalysts (Scheme 1-3). There are also intermediate forms such as homogeneous catalysts attached to solids (supported catalysts), also known as immobilized catalysts [4].

In supported catalysts the catalytically active substance is applied to a support material that has a large surface area and is usually porous. By far the most important catalysts are the heterogeneous catalysts. The market share of homogeneous catalysts is estimated to be only ca. 10–15 % [5, 6]. In the following, we shall briefly discuss the individual groups of catalysts.



Scheme 1-3 Classification of catalysts

Catalytic processes that take place in a uniform gas or liquid phase are classified as homogeneous catalysis. Homogeneous catalysts are generally well-defined chemical compounds or coordination complexes, which, together with the reactants, are molecularly dispersed in the reaction medium. Examples of homogeneous catalysts include mineral acids and transition metal compounds (e.g., rhodium carbonyl complexes in oxo synthesis).

Heterogeneous catalysis takes place between several phases. Generally the catalyst is a solid, and the reactants are gases or liquids. Examples of heterogeneous catalysts are Pt/Rh nets for the oxidation of ammonia to nitrous gases (Ostwald process), supported catalysts such as nickel on kieselguhr for fat hardening [1], and amorphous or crystalline aluminosilicates for cracking petroleum fractions.

Of increasing importance are the so-called biocatalysts (enzymes). Enzymes are protein molecules of colloidal size [e.g., poly(amino acids)]. Some of them act in dissolved form in cells, while others are chemically bound to cell membranes or on surfaces. Enzymes can be classified somewhere between molecular homogeneous catalysts and macroscopic heterogeneous catalysts.

Enzymes are the driving force for biological reactions [4]. They exhibit remarkable activities and selectivities. For example, the enzyme catalase decomposes hydrogen peroxide 10^9 times faster than inorganic catalysts. The enzymes are organic molecules that almost always have a metal as the active center. Often the only difference to the industrial homogeneous catalysts is that the metal center is ligated by one or more proteins, resulting in a relatively high molecular mass.

Apart from high selectivity, the major advantage of enzymes is that they function under mild conditions, generally at room temperature in aqueous solution at pH values near 7. Their disadvantage is that they are sensitive, unstable molecules which are destroyed by extreme reaction conditions. They generally function well only at physiological pH values in very dilute solutions of the substrate.

Enzymes are expensive and difficult to obtain in pure form. Only recently have enzymes, often in immobilized form, been increasingly used for reactions of non-biological substances. With the increasing importance of biotechnological processes, enzymes will also grow in importance.

It would seem reasonable to treat homogeneous catalysis, heterogeneous catalysis, and enzymatic catalysis as separate disciplines.

1.4

Comparison of Homogeneous and Heterogeneous Catalysis

Whereas for heterogeneous catalysts, phase boundaries are always present between the catalyst and the reactants, in homogeneous catalysis, catalyst, starting materials, and products are present in the same phase. Homogeneous catalysts have a higher degree of dispersion than heterogeneous catalysts since in theory each individual atom can be catalytically active. In heterogeneous catalysts only the surface atoms are active [3].

Due to their high degree of dispersion, homogeneous catalysts exhibit a higher activity per unit mass of metal than heterogeneous catalysts. The high mobility of the

molecules in the reaction mixture results in more collisions with substrate molecules. The reactants can approach the catalytically active center from any direction, and a reaction at an active center does not block the neighboring centers. This allows the use of lower catalyst concentrations and milder reaction conditions.

The most prominent feature of homogeneous transition metal catalysts are the high selectivities that can be achieved. Homogeneously catalyzed reactions are controlled mainly by kinetics and less by material transport, because diffusion of the reactants to the catalyst can occur more readily. Due to the well-defined reaction site, the mechanism of homogeneous catalysis is relatively well understood. Mechanistic investigations can readily be carried out under reaction conditions by means of spectroscopic methods (Fig. 1-3). In contrast, processes occurring in heterogeneous catalysis are often obscure.

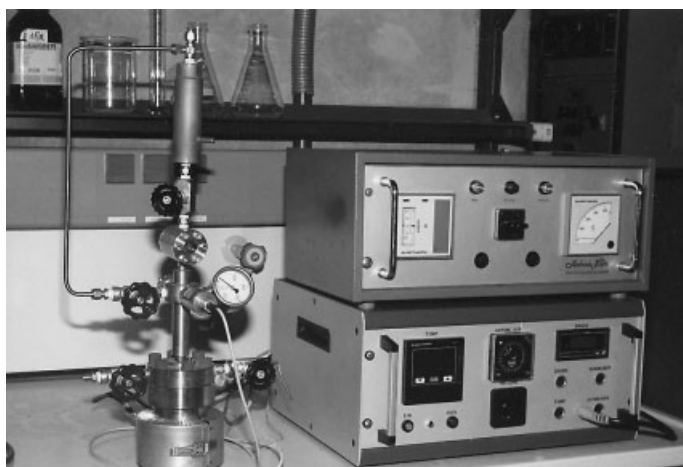


Fig. 1-3 Laboratory autoclave with dropping funnel, viewing window, and magnetic stirrer for the investigation of homogeneously catalyzed processes (high-pressure laboratory, FH Mannheim)

Owing to the thermal stability of organometallic complexes in the liquid phase, industrially realizable homogeneous catalysis is limited to temperatures below 200 °C. In this temperature range, homogeneous catalysts can readily be stabilized or modified by addition of ligands; considerable solvent effects also occur.

In industrial use, both types of catalyst are subject to deactivation as a result of chemical or physical processes. Table 1-3 summarizes the advantages and disadvantages of the two classes of catalyst.

The major disadvantage of homogeneous transition metal catalysts is the difficulty of separating the catalyst from the product. Heterogeneous catalysts are either automatically removed in the process (e.g., gas-phase reactions in fixed-bed reactors), or they can be separated by simple methods such as filtration or centrifugation. In the case of homogeneous catalysts, more complicated processes such as distillation, liquid-liquid extraction, and ion exchange must often be used [3].

Table 1-3 Comparison of homogeneous and heterogeneous catalysts

| | Homogeneous | Heterogeneous |
|----------------------------|--|--|
| <i>Effectivity</i> | | |
| Active centers | all metal atoms | only surface atoms |
| Concentration | low | high |
| Selectivity | high | lower |
| Diffusion problems | practically absent | present (mass-transfer-controlled reaction) |
| Reaction conditions | mild (50–200 °C) | severe (often >250 °C) |
| Applicability | limited | wide |
| Activity loss | irreversible reaction with products (cluster formation); poisoning | sintering of the metal crystallites; poisoning |
| <i>Catalyst properties</i> | | |
| Structure/stoichiometry | defined | undefined |
| Modification possibilities | high | low |
| Thermal stability | low | high |
| <i>Catalyst separation</i> | | |
| Catalyst recycling | sometimes laborious (chemical decomposition, distillation, extraction) | fixed-bed: unnecessary suspension: filtration |
| Cost of catalyst losses | high | low |

The separability of homogeneous catalysts has been improved in the last few years by using organometallic complexes that are soluble in both organic and aqueous phases. These can readily be removed from the product stream at the reactor outlet by transferring them to the aqueous phase. This two-phase method has already been used successfully in large-scale industrial processes, for example:

- the Shell higher olefin process (SHOP), with nickel complex catalysts
- the Ruhrchemie/Rhône-Poulenc oxo synthesis with soluble rhodium catalysts (see Section 3.2)

There are of course also parallels between homogeneous and heterogeneous transition metal catalysts. Many reaction mechanisms of homogeneous and heterogeneous catalysts exhibit similarities with regard to the intermediates and the product distribution.

Table 1-4 Comparison of the key reactions of homogeneous and heterogeneous transition metal catalysis [10]

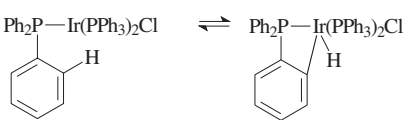
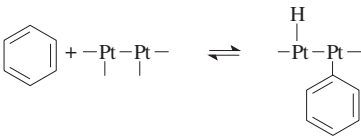
| Homogeneous phase Oxid reactions | Heterogeneous phase dissociative chemisorption |
|--|---|
| $\text{Ir}(\text{PPh}_3)_3\text{Cl} + \text{H}_2 \rightleftharpoons \begin{array}{c} \text{H} \quad \text{H} \\ \diagdown \quad / \\ \text{Ir}(\text{PPh}_3)_3\text{Cl} \end{array}$ | $\text{H}_2 + \begin{array}{c} -\text{Pt}-\text{Pt}- \\ \quad \end{array} \rightleftharpoons \begin{array}{c} \text{H} \quad \text{H} \\ \quad \\ -\text{Pt}-\text{Pt}- \end{array}$ |
| $\text{Pt}(\text{PPh}_3)_2 + \text{HC} \equiv \text{CR} \rightleftharpoons \text{Pt}(\text{H})(\text{C} \equiv \text{CR})(\text{PPh}_3)_2$ | $\text{R}-\text{C} \equiv \text{CH} + \begin{array}{c} -\text{M}-\text{M}- \\ \quad \end{array} \rightleftharpoons \begin{array}{c} \text{H} \quad \text{C} \equiv \text{C}-\text{R} \\ \quad \\ -\text{M}-\text{M}- \end{array}$ |
| $\begin{array}{c} \text{Ph}_2\text{P}-\text{Ir}(\text{PPh}_3)_2\text{Cl} \\ \\ \text{H} \end{array} \rightleftharpoons \begin{array}{c} \text{Ph}_2\text{P}-\text{Ir}(\text{PPh}_3)_2\text{Cl} \\ \\ \text{H} \end{array}$  | $\text{C}_6\text{H}_6 + \begin{array}{c} -\text{Pt}-\text{Pt}- \\ \quad \end{array} \rightleftharpoons \begin{array}{c} \text{H} \\ \\ -\text{Pt}-\text{Pt}- \\ \\ \text{C}_6\text{H}_5 \end{array}$  |

Table 1-4 shows in more detail that the key reactions of homogeneous catalysis, such as hydride elimination and oxidative addition, correspond to dissociative chemisorption in heterogeneous catalysis (see Section 2.1).

The hope of increasing the separability of homogeneous catalysts by, for example, fixing them on solid supports has not yet been realized. The aim of many research projects is to maintain the high selectivity of homogeneous catalysts while at the same time exploiting the advantages of easier catalyst separation. The main problems are still catalyst “bleeding” and the relatively low stability and high sensitivity to poisoning of the heterogenized complexes.

An interesting intermediate between homogeneous and heterogeneous catalysts are the metal cluster catalysts. In many reactions that require several active centers of the catalyst, it is found that heterogeneous catalysts are active, while homogeneous catalysts give zero conversion. The reason is that crystallites on a metal surface exhibit several active centers, while conventional soluble catalysts generally contain only one metal center.

In contrast, metal clusters have several active centers or can form multi-electron systems. Metal clusters such as $\text{Rh}_6(\text{CO})_{16}$, $\text{Rh}_4(\text{CO})_{12}$, $\text{Ir}_4(\text{CO})_{12}$, $\text{Ru}_3(\text{CO})_{12}$, and more complex structures have been successfully tested in carbonylation reactions. Rhodium clusters catalyze the conversion of synthesis gas to ethylene glycol, albeit at very high pressures up to now.

With increasing size, the clusters become less soluble, and the precipitation of extremely small particles from solution is possible, that is, a transition from homogeneous to heterogeneous catalysis.

In conclusion, it can be stated that homogeneous and heterogeneous catalysts should be used to complement one another and not regarded as competitors, since each group has its special characteristics and properties.

► Exercises for Chapter 1

Exercise 1.1

Classify the following reactions as homogeneous or heterogeneous catalysis and justify your answer:

- The higher reaction rate for the oxidation of SO_2 with O_2 in the presence of NO .
- The hydrogenation of liquid vegetable oil in the presence of a finely divided Ni catalyst.
- The transformation of an aqueous solution of D-glucose into a mixture of the D and L forms, catalyzed by aqueous HCl .

Exercise 1.2

Compare homogeneous and heterogeneous catalysis according to the following criteria:

| | Heterogeneous catalysts | Homogeneous catalysts |
|---------------------|-------------------------|-----------------------|
| Active center | | |
| Concentration | | |
| Diffusion problems | | |
| Modifiability | | |
| Catalyst separation | | |

Exercise 1.3

Give four reasons why heterogeneous catalysts are preferred in industrial processes.

Exercise 1.4

- Explain the difference between the activity and the selectivity of a catalyst.
- Name three methods for measuring the activity of catalysts.

Exercise 1.5

Compare the key activation steps in the hydrogenation of alkenes with homogeneous and heterogeneous transition metal catalysts. What are the names of these steps?

| | Homogeneous catalysis | Heterogeneous catalysis |
|----------------------------|-----------------------|-------------------------|
| Activation of H_2 | | |
| Activation of the olefin | | |

2

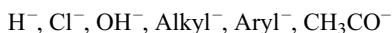
Homogeneous Catalysis with Transition Metal Catalysts

Most advances in industrial homogeneous catalysis are based on the development of organometallic catalysts. Thousands of organometallic complexes (i.e., compounds with metal–carbon bonds) have become known in the last few decades, and the rapid development of the organic chemistry of the transition metals has been driven by their potential applications as industrial catalysts [12].

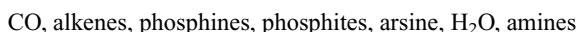
The chemistry of organo transition metal catalysis is explained in terms of the reactivity of organic ligands bound to the metal center. The d orbitals of the transition metals allow ligands such as H (hydride), CO, and alkenes to be bound in such a way that they are activated towards further reactions.

The most important reactions in catalytic cycles are those involving ligands located in the coordination sphere of the same metal center. The molecular transformations generally require a loose coordination of the reactants to the central atom and facile release of the products from the coordination sphere. Both processes must proceed with an activation energy that is as low as possible, and thus extremely labile metal complexes are required. Such complexes have a vacant coordination site or at least one weakly bound ligand.

Reasons for the binding power of transition metals are that they can exist in various oxidation states and that they can exhibit a range of coordination numbers. The coordination complexes can be classified by dividing the ligands into two groups: ionic and neutral ligands [T11]. Ionic ligands include:



and examples of neutral ligands are:



This distinction is useful for assigning oxidation states and in describing the course of reactions. However, it must be emphasized that this description is of a largely formal nature and sometimes does not describe the true bonding situation. Thus, although it is true that hydrogen ligands mostly react as H^- and alkyl groups as R^- , it is also possible that, for example, methyl groups react as CH_2^- or CH_3^+ .

Rather than discussing the fundamentals of organometallic chemistry, this chapter is intended to give a survey of the most important types of reaction, a knowledge of which is sufficient for understanding the reaction cycles of homogeneous transition metal catalysis.

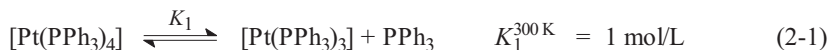
2.1

Key Reactions in Homogeneous Catalysis [9]

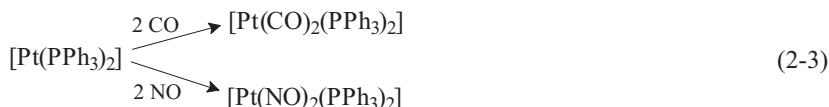
2.1.1

Coordination and Exchange of Ligands [18]

In many transition metal complexes, the coordination number is variable. Especially in solution or as the result of thermal dissociation, ligands can be released from the complex or undergo exchange, or free coordination sites can be occupied by solvent molecules. Therefore, most complexes do not react in their coordinatively saturated form, but via an intermediate of lower coordination number with which they are in equilibrium. For example, triphenylphosphine platinum complexes are involved in the following equilibrium reactions [T12]:



In aromatic solvents, the first equilibrium constant K_1 indicates rapid dissociation, but the second equilibrium constant is very small. However, the extremely high reactivity of $[\text{Pt}(\text{PPh}_3)_2]$ compensates for this concentration effect, and complete reaction occurs with π -acidic molecules such as CO and NO:



The rapid dissociation of many complexes is explained in terms of steric hindrance of the ligands. With increasing space requirements of the phosphine or phosphite ligands, the rate of dissociation increases. A semi-quantitative measure for steric demand is the cone angle of the ligand (Table 2-1), as introduced by Tolman [20].

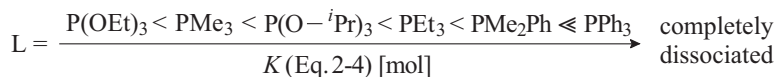
Accordingly, the sterically most demanding ligands should exhibit the fastest dissociation. This is demonstrated by the dissociation constants for complexes of nickel. For the reaction



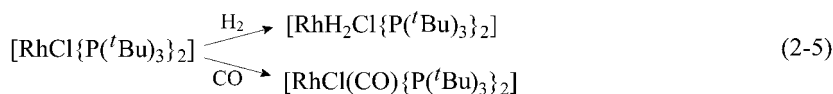
Table 2-1 Typical cone angles for trivalent phosphorus ligands [20]

| Ligand | Cone angle [°] |
|---|----------------|
| PH ₃ | 87 |
| P(OMe) ₃ | 107 |
| P(OEt) ₃ | 109 |
| PMe ₃ | 118 |
| P(OPh) ₃ | 121 |
| P(O- ^{<i>i</i>} Pr) ₃ | 130 |
| PEt ₃ | 132 |
| PMe ₂ Ph | 136 |
| PPh ₃ | 145 |
| P(^{<i>i</i>} Pr) ₃ | 160 |
| P(cyclohexyl) ₃ | 170 |
| P(^{<i>t</i>} Bu) ₃ | 182 |

the following sequence, which correlates with the cone angles listed in Table 2-1, was found:



However, care should be taken before making general statements, since the cone angles refer to a constant metal–phosphorus bond length and therefore do not reflect the true space filling in the coordinated state. Even complexes containing voluminous ligands can undergo addition of one or two small molecules:

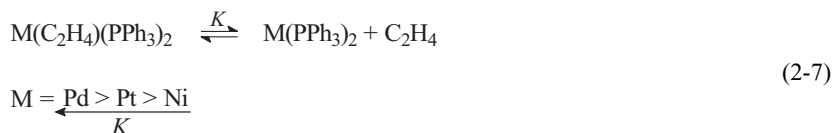


For ligand dissociation/association processes, Tolman introduced the 16/18-electron rule [19] (see Section 2.2.1). For each covalently bonded ligand, two electrons are added to the number of d electrons of the central transition metal atom (corresponding to its formal oxidation state) to give a total valence electron count. An example for a complex involved in a thermal dissociative equilibrium is the well-known Wilkinson's catalyst:



The active form of the catalyst is generated by loss of PPh₃ ligands in solution (Eq. 2-6). An important step in the catalytic reactions of alkenes is the complexation of the substrate at the transition metal center to give a so-called π complex [18].

The differing tendency of metals to bind alkenes is illustrated by the following trend (given isostructural complexes):

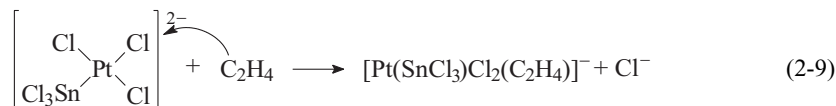


The tendency of ethylene complexes to dissociate (Eq. 2-7) can be explained in terms of the strength of the backbonding from the metal to the alkene $\text{M} \rightarrow \text{C}_2\text{H}_4$ ($\text{M} = \text{Ni} > \text{Pt} > \text{Pd}$; $\text{Co} > \text{Ir} > \text{Rh}$; $\text{Fe} > \text{Os} > \text{Ru}$). Care must be taken, however, in predicting the coordination equilibria of labile metal olefin or similar complexes since steric and electronic factors also play a role.

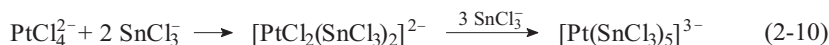
The coordination of certain ligands to a transition metal center can be facilitated by exploiting the *trans* effect. For example, the reaction



is slow, but can be accelerated by adding SnCl_2 . This leads to formation of a SnCl_3^- group, whose strong *trans* effect labilizes the chloro ligand in the *trans* position (Eq. 2-9).



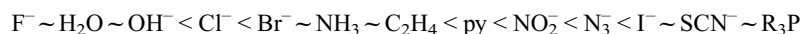
The trichlorotin(II) ion SnCl_3^- can replace the ligands Cl^- , CO , and PF_3 in nucleophilic ligand-exchange reactions (e. g., Eq. 2-10).



Ligand-substitution reactions, particularly those involving readily accessible square-planar Pd^{II} or Pt^{II} complexes are often used as model reactions for ranking ligands in order of their nucleophilicity (Eq. 2-11).

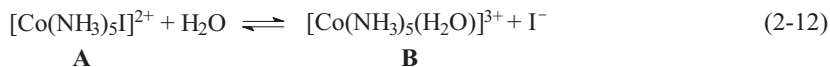


The reactions, which proceed by an $\text{S}_{\text{N}}2$ mechanism, give the following series [14] for the nucleophilicity of the incoming ligand Y:



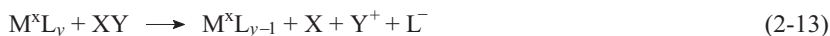
The Pt^{II} complex of Equation 2-11 has a soft, electrophilic center. Therefore, according to the HSAB (hard and soft acids and bases) concept, fast substitution reactions should occur with soft reagents such as phosphines, thiosulfate, iodide, and

olefins. Ligand-exchange processes can often be explained in terms of the higher stability of the product complex:



The HSAB concept is helpful here, too: each soft or hard fragment strives for stabilization on a corresponding center (symbiotic effect). Complex **A** exhibits a hard/soft dissymmetry (NH_3 is hard, I^- soft), whereas in complex **B** the hard Co^{3+} center is stabilized exclusively by hard ligands.

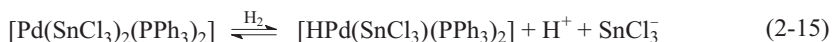
The final example of ligand-exchange processes to be treated in this chapter is the heterolytic addition of reagents [T11]. Here a substrate XY undergoes addition to the metal center without changing the formal oxidation state or coordination number of the metal center. The molecular fragments X or Y are bound to the metal center as shown schematically in Equation 2-13.



Often, one anionic ligand is replaced by another, as in the addition of hydrogen to ruthenium(II) complexes:



The activation of molecular hydrogen by Pt^{II} , Ru^{III} , and Pd/Sn catalyst systems can be explained analogously (Eq. 2-15).



In each case, hydrido metal compounds are formed as catalytically active complexes. Finally, it should be mentioned that in practice heterolytic addition can often not be distinguished from oxidative addition followed by reductive elimination, which is discussed later in this book.

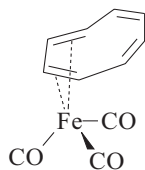
2.1.2

Complex Formation [7]

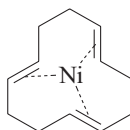
An important step in the catalytic reactions of alkenes is the complexation of the substrate at the transition metal center. Differences in ability of olefins to coordinate can influence the selectivity of a catalytic process to such an extent that, for example, in a positionally isomeric olefins, the terminal olefins react preferentially to give the desired product.

In alkene complexes, the transition metal can have oxidation state 0 or higher. The olefin ligands are bound to the transition metal through one or more double bonds, the exact number depending on the number of free sites in the electron shell of the metal atom. Generally sufficient olefins or other Lewis bases are added to

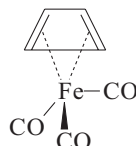
give the transition metal the electron configuration of the next higher noble gas, for example [T1]:



Cyclooctatetraene
iron tricarbonyl.
Formal Fe charge: 0.
Number of π electrons
involved: 4

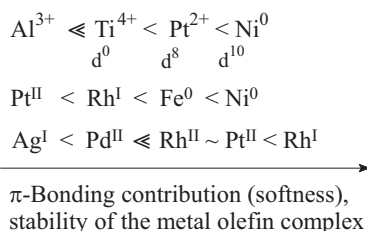


1,5,9-Cyclododecatriene
nickel.
Formal Ni charge: 0.
Number of π electrons
involved: 6



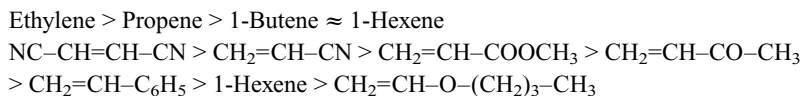
Cyclobutadiene
iron tricarbonyl.
Formal Fe charge: 0.
Number of π electrons
involved: 4

In olefin–metal bonding, a distinction is made between σ and π bonding contributions. The π bonding contribution for several metals increases as follows:

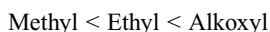


Metal–olefin backbonding is particularly strong for soft metals that are rich in d electrons, but negligible at low d electron densities. For silver and palladium complexes, with their dominant σ contributions, the metal–olefin bond strength can be increased by donor substituents on the olefin, while in the case of the soft platinum complexes, it is increased by electron-withdrawing groups on the olefin. For a given metal ion, the σ -acceptor property becomes stronger with increasing positive charge. Thus Rh^{II} (d^7) is a stronger σ acceptor than Rh^{I} (d^8).

The coordination ability of olefins can also be compared. The following series, obtained for a nickel(0) complex, illustrates the importance of electronic effects in the olefin:



The strength of the nickel–olefin bond is increased by electron-withdrawing substituents such as cyano and carboxyl groups, and decreased by electron-donating groups. Donor ability increase in the series

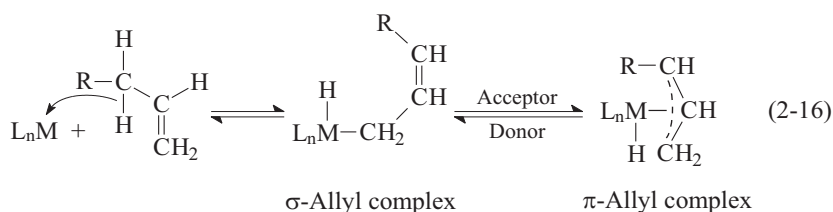


This behavior shows that for soft metal centers like Ni^0 (d^{10}), backbonding of electrons from filled d orbitals of the metal into empty olefin π^* orbitals (i.e., π bonding) dominates.

However, even relatively hard metal centers such as Ti^{III} , V^{III} , V^{II} , and Cr^{III} form unstable olefin complexes that are important intermediates in catalytic reactions.

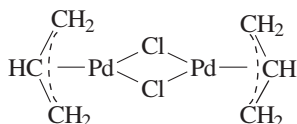
With their delocalized π -electron system, allyl ligands can bond to metals in a manner similar to olefins. Allyl complexes have been detected as intermediates in catalytic processes involving propene or higher olefins and dienes. Examples include the cyclooligomerization of butadiene and the codimerization of butadiene with ethylene.

The abstraction of a hydrogen atom from an alkyl group next to a double bond (1,3 hydride shift) leads to formation of hydrido metal π -allyl complexes via intermediate σ -allyl compounds:



This reaction occurs mainly in metal complexes of low oxidation state.

Typical examples of this class of compounds are $[\text{Mn}(\eta^3\text{-C}_3\text{H}_5)(\text{CO})_4]$ and the dimer $[\{\text{Pd}(\eta^3\text{-C}_3\text{H}_5)\text{Cl}\}_2]$ with the structure:

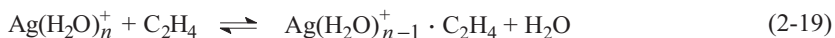
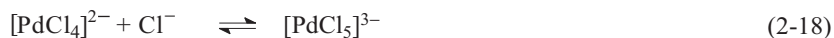
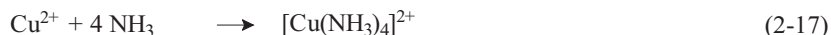


The equilibrium between σ - and π -allyl complexes can be influenced by the ligands. Thus strongly basic alkyl phosphine ligands favor the σ structure, as has been shown for allyl metal halide complexes of Pt^{II} and Ni^{II} . Soft π -acceptor ligands such as CO favor the formation of π -allyl complexes.

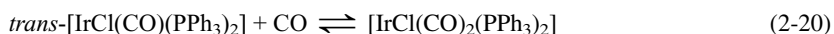
2.1.3

Acid–Base Reactions

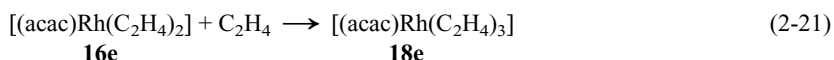
According to the general acid–base concepts of Brønsted and Lewis, metal cations are generally regarded as acids. Therefore, transition metal cations or coordinatively unsaturated compounds can undergo addition of neutral or anionic nucleophiles to give cationic (Eq. 2-17), anionic (Eq. 2-18), and π -acceptor complexes (Eq. 2-19).



Another example of Lewis acid behavior is shown in Equation 2-20, in which an iridium complex takes up a CO ligand to form a dicarbonyl complex.



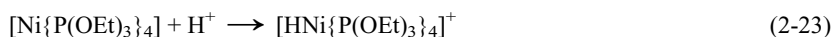
In the reverse of dissociation, 16-electron species can add a ligand to give 18-electron complexes [19]:



The Brønsted theory states that the acid/base character of a compound depends on its reaction partner and is therefore not an absolute. An indication that transition metal compounds can act as bases is provided by the long-known protonation reactions of transition metal complexes, generally of low oxidation state. An example is cobalt carbonyl hydride, the true catalyst in many carbonylation reactions:



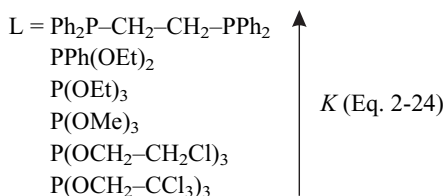
Metal basicity is also exhibited by phosphine and phosphite complexes of nickel(0), which can be protonated by acids of various strengths:



The hydride formation constant K for the general reaction of Equation 2-24



can be strongly influenced by the donor character of the phosphine ligand L:

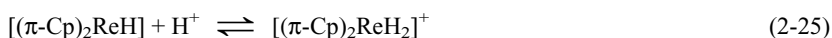


With very good σ donors like diphosphines, nickel(0) becomes a strong metal base, and the corresponding hydride is highly stable. Phosphine ligands that remove

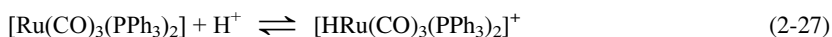
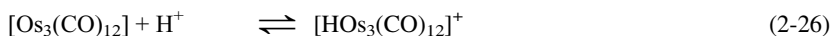
electron density from the metal center lower the complex-formation constant. Thus trialkylphosphine ligands, which primarily act as σ donors, increase the electron density at nickel atom and give rise to strong metal bases.

For example, $[\text{Ni}(\text{PEt}_3)_4]$ can be protonated with weak acids such as ethanol. An intermediate basicity is obtained with triarylphosphines and -phosphites, and protonation of the corresponding nickel complexes requires strong mineral acids. In contrast, PF_3 complexes exhibit negligible basicity because PF_3 is a strong electron acceptor, like CO.

Some transition metal hydrides are also strong bases; $[\pi\text{-Cp}_2\text{ReH}]$ (Eq. 2-25) has a basicity comparable to that of ammonia.

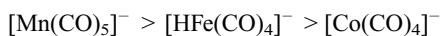


Many neutral carbonyl complexes can also be protonated; examples are given in Equations 2-26 and 2-27.

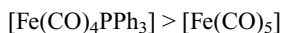


Shriver has presented extensive data on transition metal basicity and described trends according to the position of the metal in the periodic table [15]. On the basis of IR spectroscopic data, the following rules can be drawn up:

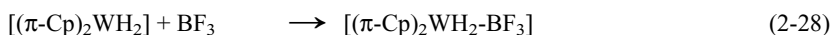
- 1) Low oxidation states, especially negative ones or metal(0) complexes, increase the metal basicity. With increasing oxidation state, metals become more acidic.
- 2) Transition metal basicity increases from right to left in a period, and from top to bottom in a group; for example:



- 3) Electron-donor ligands such as phosphines increase the metal basicity:

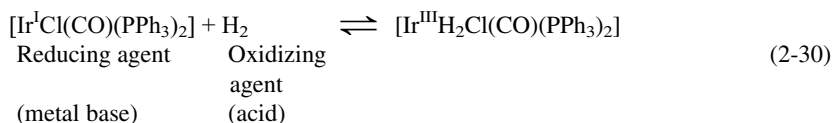


Another possibility for classifying transition metal basicity is complex formation with various Lewis acids. Numerous stable adducts can be regarded as the result of acid–base reactions of transition metal complexes (Eqs. 2-28 and 2-29).



The tendency of σ donors to increase basicity is also observed in complex formation. Thus the iron complexes $[\text{Fe}(\text{CO})_3(\text{EPh}_3)_2]$ ($\text{E} = \text{P}, \text{As}, \text{Sb}$) form stable 1 : 1 adducts with HgCl_2 and HgBr_2 . Adducts with the unsubstituted $[\text{Fe}(\text{CO})_5]$ are less stable.

The oxidative addition reactions treated in the next section can in principle be interpreted as acid–base reactions. In the oxidative addition of hydrogen to a square-planar d^8 iridium complex (Eq. 2-30), the transition metal complex acts as an electron-providing metal base, and the substance undergoing addition can be regarded as an acid [10]:



2.1.4

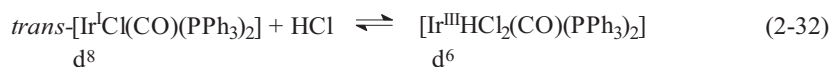
Redox Reactions: Oxidative Addition and Reductive Elimination

Coordinatively unsaturated transition metal complexes can in general add neutral or anionic nucleophiles. Oxidative addition to coordinatively unsaturated transition metal compounds has opened up undreamt of synthetic possibilities [18]. This reaction and its reverse – reductive elimination – are formally described by the following equilibrium:

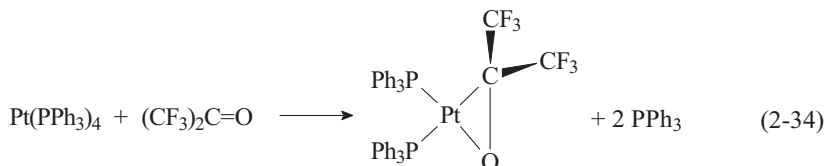
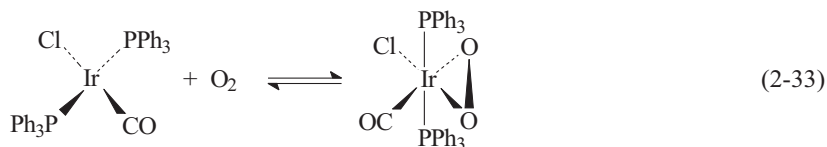


In general, the bonds of small covalent molecules XY ($\text{H}-\text{X}$, $\text{C}-\text{X}$, $\text{H}-\text{H}$, $\text{C}-\text{H}$, $\text{C}-\text{C}$, etc.) add to a low oxidation state transition metal, whose oxidation state then increases by two units. The reaction is mainly observed with complexes of d^8 and d^{10} transition metals (e. g., Fe^0 , Ru^0 , Os^0 , Rh^1 , Ir^1 , Ni^0 , Pd^0 , Pt^0 , Pd^{II} , Pt^{II}). The reaction can take two possible courses:

- 1) The molecules being added split into two η^1 ligands, which are both formally anionically bound to the metal center. One of the most thoroughly investigated compounds is a square-planar iridium complex whose central atom gives up two electrons and is oxidized to Ir^{III} (Eq. 2-32).



- 2) The molecules being added contain multiple bonds and are bound as η^2 ligands, without bond cleavage. The resulting complexes contain three-membered rings, as shown in Equations 2-33 and 2-34.



The most important molecules for oxidative addition reactions are listed in Table 2-2.

Some illustrative examples of the possible types of reaction follow [17]:



Equation 2-35 describes the addition and simultaneous activation of molecular hydrogen, an important step in homogeneous hydrogenation reactions.

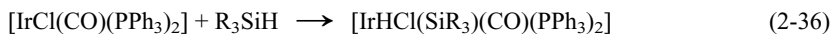


Table 2-2 Oxidative addition reactions on transition metal complexes; classification of the adding compounds

| Bond cleavage (Addends dissociate) | No bond cleavage (Addends stay associated) |
|---|---|
| H ₂ | O ₂ |
| X ₂ | SO ₂ |
| HX (X = Hal, CN, RCOO, ClO ₄) | CS ₂ |
| H ₂ S | CF ₂ =CF ₂ |
| C ₆ H ₅ SH | (NC) ₂ C=C(CN) ₂ |
| RX | R-C≡C-R' |
| RCOX | (CF ₃) ₂ CO |
| RSO ₂ X | RNCO |
| R ₃ SnX | R ₂ C=C=O |
| R ₃ SiX | |
| HgX ₂ | |
| CH ₃ HgX | |
| SiCl ₄ | |
| C ₆ H ₆ | |

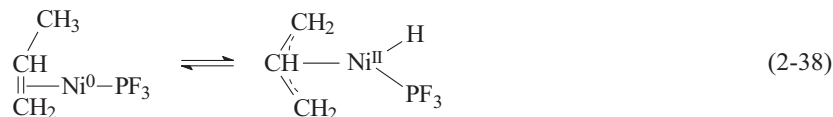
R = alkyl, aryl, CF₃ etc.
X = Hal

Equation 2-36 can be regarded as a model reaction for the first step of hydro-silylation.

Anionic Rh^{I} complexes readily undergo addition of alkyl halides (Eq. 2-37).

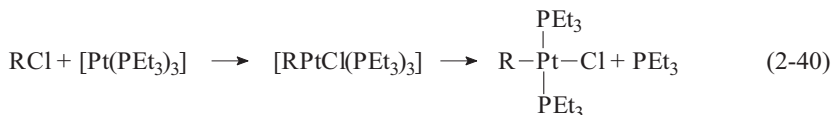
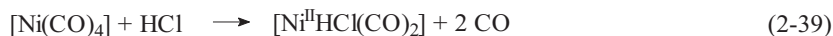


The formation of η^3 -allyl complexes can also be regarded as an oxidative addition reaction. Proton abstraction from an olefin leads to the formally anionic allyl group (Eq. 2-38).



Nickel, palladium, and platinum d^{10} complexes preferentially add polar reagents (acids; alkyl, acyl, and metal halides), whereby a ligand must dissociate to give a free coordination site (Eq. 2-39).

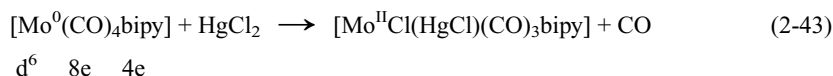
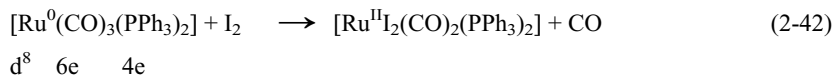
In Equation 2-40, addition of alkyl halide occurs first and is followed by dissociation of a phosphine ligand.



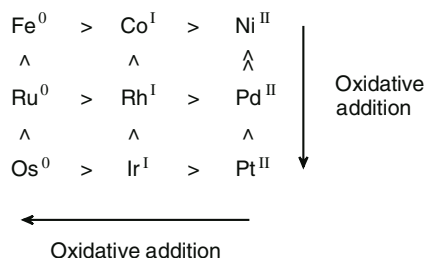
With Brønsted acids the reaction can proceed via an ionic intermediate (Eq. 2-41).



Other oxidative addition reactions that involve simultaneous ligand dissociation can be explained by applying the 18-electron rule [19]. These usually involve coordinatively saturated 18-electron complexes (d electrons + electron lone pairs of the ligands), which must first lose a ligand to provide a vacant coordination site for oxidative addition (Eqs. 2-42 and 2-43).



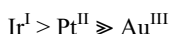
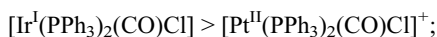
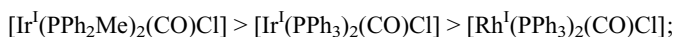
The mechanisms of oxidative addition reactions, which in some cases are complicated, will not be discussed further here. What is of interest, however, is the general reactivity



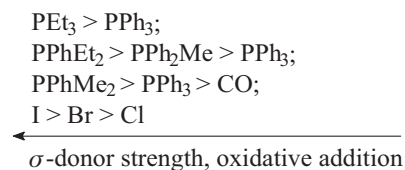
Scheme 2-1 Tendency to undergo oxidative addition for the metals of groups 8–10

of the transition metals. For the metals of group VIII, the trend shown in Scheme 2-1 was found for oxidative addition reactions of the type $d^8 \rightarrow d^6$, given the same ligands.

The tendency to undergo oxidative addition increases from top to bottom in a group and from right to left in a period, as does the metal basicity. This is shown by numerous empirical orders of reactivity [10]:

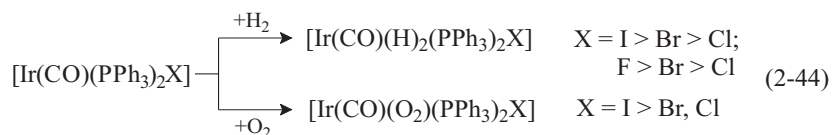


Ligand effects are of major importance in oxidative addition reactions. Increasing donor character of a ligand increases the electron density at the metal center and favors oxidative addition. This means that electron-releasing (basic) ligands make the metal base stronger, while electron-withdrawing ligands weaken it. Some examples for ligand influences are given in the following:



Alkylphosphines, which are good σ donors, facilitate oxidative addition, while π -acceptor ligands make it more difficult. However, steric effects must also be considered. For instance, a low reaction rate is observed for the strongly basic, bulky ligand tri-*tert*-butylphosphine.

For the square-planar iridium complex $[\text{Ir}(\text{CO})(\text{PPh}_3)_2\text{X}]$, the ligand effects shown in Equation 2-44 were found.



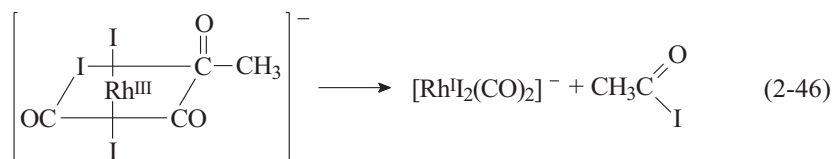
Although the fluoro ligand lowers the σ basicity, it is also a good π donor that increases the π basicity of the metal, and it is the latter effect that predominates in the oxidative addition of hydrogen (Eq. 2-44).

The complex $[\text{Ir}(\text{CO})(\text{PPh}_3)_2\text{Cl}]$ reacts with hydrogen at room temperature to give a dihydride complex, but the analogous rhodium complex $[\text{Rh}(\text{CO})(\text{PPh}_3)_2\text{Cl}]$ does not; only the chloro complex $[\text{Rh}(\text{PPh}_3)_3\text{Cl}]$ forms a hydrogen adduct. The comparison once again demonstrates the effect of the metal basicity ($\text{Ir} > \text{Rh}$), but also the influence of the ligands: donor ligands (PPh_3) increase the reactivity, and the stronger π acid CO lowers it. The even stronger π acid N_2 behaves in a similar manner compared to CO : the dinitrogen complex $[\text{IrCl}(\text{PPh}_3)_2\text{N}_2]$ does not undergo addition of hydrogen. If σ -donor and π -acceptor ligands are approximately in balance, as in the complex $[\text{Ni}(\text{CO})_2(\text{PPh}_3)_2]$, then the compound is relatively stable and unreactive towards oxidative addition. Dissociation of ligands is also more difficult.

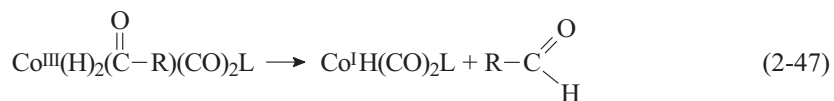
As would be expected, reductive elimination, the reverse of oxidative addition, is favored by ligands that lower the electron density at the metal center. The last step of a catalytic cycle is often an irreversible reductive elimination in which the product is released. Equation 2-45 shows the formation of an alkane from a alkyl hydride complex.



In the rhodium-catalyzed carbonylation of methanol via methyl iodide, acetyl iodide is formed by reductive elimination from an anionic rhodium^{III} acyl complex [T14]:



In the same manner, aldehydes are formed as the final products of cobalt-catalyzed hydroformylation:

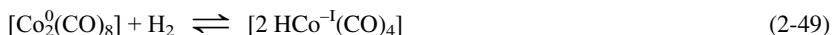


Reductive elimination is generally not the rate-determining step in a catalytic process.

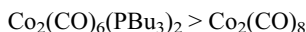
Besides oxidative addition, there is also another type of homolytic addition in transition metal chemistry [11]. By definition, in this type of reaction, a substrate XY adds to two metal centers in such a way that the formal oxidation state of each metal increases or decreases by one unit (Eq. 2-48).



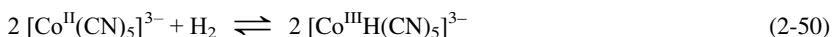
An industrially important example is the activation of $[\text{Co}_2(\text{CO})_8]$ with hydrogen (Eq. 2-49), the resulting complex being the active catalyst in carbonylation reactions.



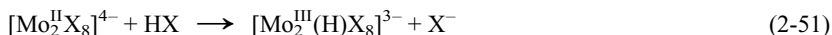
In this case, the metal is assigned a formal negative oxidation state since the product behaves as a strong acid and should therefore be regarded as a hydro compound. As with oxidative addition, electron-donating ligands such as trialkylphosphines increase the rate of reaction. For hydrogen addition:



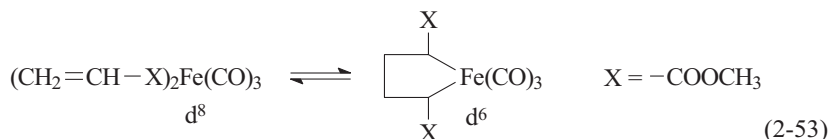
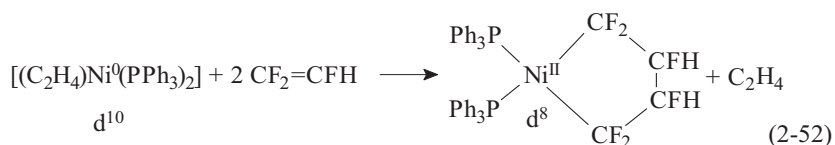
When hydrogen is passed into an aqueous cobalt cyanide solution, hydridopentacyanocobalt ions are formed (Eq. 2-50) and can be used for the reduction of organic and inorganic substrates:



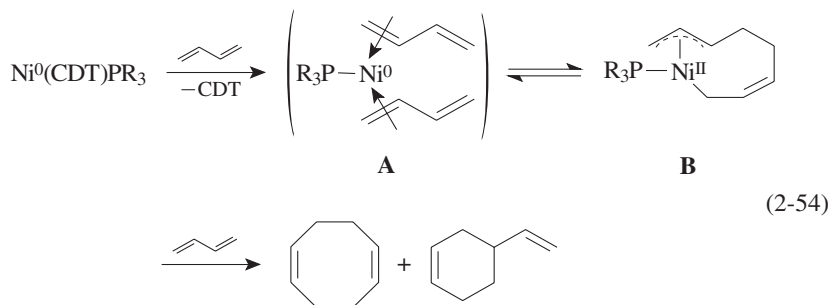
Another example is the addition of hydrogen halides to metal-metal bonds, as in, for example, $[\text{Mo}_2^{\text{II}}\text{X}_8]^{4-}$ (Eq. 2-51; X = Cl, Br). This type of reaction could be of interest for catalysis with clusters.



Oxidative coupling, as defined by Tolman, is a reaction in which the oxidation state of the metal increases by two units and the coordination number remains unchanged [19]. Hence it is a special case of oxidative addition. Many C-C coupling reactions proceed according to this scheme, in which an unsaturated ligand accepts two electrons from the transition metal. The resulting dicarbanion is bound to the metal center in a chelating fashion (Eqs. 2-52 and 2-53).



In the above two examples, oxidative coupling of two olefin molecules occurs. It is likely that the catalysis of numerous cyclooligomerization reactions of unsaturated hydrocarbons proceeds in this manner, as shown for the example of butadiene in Equation 2-54.



First, a ligand displacement reaction with butadiene gives a nickel(0) π complex **A**, which undergoes oxidative coupling to give the metal-containing ring **B**, a π -allyl σ -alkyl complex. Finally, reductive elimination gives the main products 1,5-cyclooctadiene and 4-vinylcyclohexene.

2.1.5

Insertion and Elimination Reactions

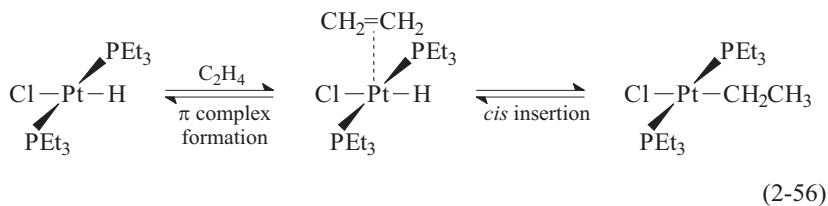
Insertion reactions play an important role in the catalysis of C–C and C–H coupling [1]. Insertion of CO and olefins into metal–alkyl and metal–hydride bonds are of major importance in industrial chemistry. Insertion reactions take place according to the following scheme:



X = H, C, N, O, Cl, metal

YZ = CO, olefin, diene, alkyne, nitrile, etc.

Initially, a molecule XY is inserted into an M–X bond without changing the formal oxidation state of the metal M. A simple example is the insertion of an olefin into a Pt–H bond to give an alkyl complex (Eq. 2-56).

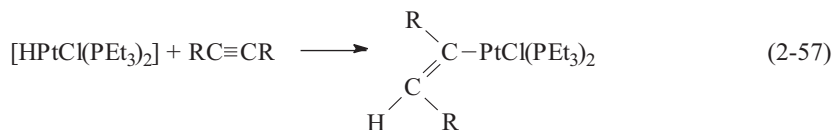


Formally speaking, the above insertion reaction is a nucleophilic attack of a base (hydride ion) on a positively polarized olefin (coordination of the olefin lowers its electron density and thus facilitates nucleophilic attack).

Olefin insertion is particularly facile in the case of the complexes $[\text{PtH}(\text{SnCl}_3)(\text{PR}_3)_2]$. The soft π -acceptor ligand $[\text{SnCl}_3]^-$ stabilizes the metal–hydride bond (symbiosis of soft ligands) and hence catalyzes the insertion reaction as

a preliminary step of hydrogenation. Pt/Sn systems are known to be good hydrogenation catalysts.

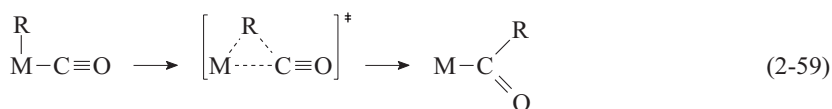
Equation 2-57 describes the insertion of acetylene into a Pt–H bond to give a vinylplatinum complex.



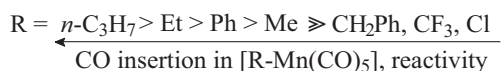
An important step in industrial carbonylation reactions is the insertion of CO into metal–carbon bonds (Eq. 2-58) [3, 4], which was described as early as 1957.



Formally, CO inserts into the polarized metal–carbon bond to give an acyl metal complex. However, it has been shown that in fact an alkyl group migration to a CO group coordinated in the *cis* position occurs. This migration probably occurs via a three-center transition state (Eq. 2-59).



For the carbonylation of manganese complexes of the type $[\text{RMn}(\text{CO})_5]$, the following influence of the substituents has been found:

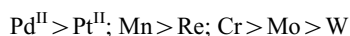


The trend can be explained as follows: the electron-releasing alkyl groups cause a stronger polarization of the metal–carbon bond, but more electronegative electron-withdrawing ligands lower the reaction rate. This σ effect has been confirmed by model calculations [1].

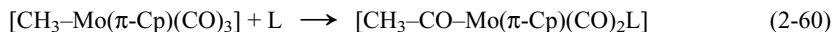
If the stability and reactivity of the metal complexes in a triad of the periodic table are compared, two counteropposing trends become apparent [3]:



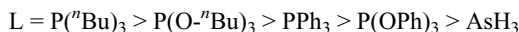
The harder metals at the top of the groups are more reactive towards carbonyl insertion. Thus iridium carbonyl complexes are less reactive than the rhodium and cobalt homologues. The following also applies:



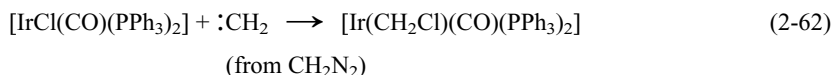
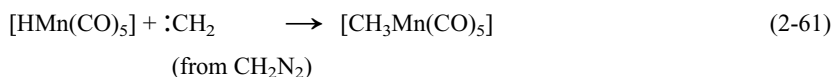
The influence of nucleophilic ligands on the CO insertion reaction has been investigated for molybdenum complexes (Eq. 2-60).



In the nonpolar solvent toluene, the reaction rate decreases in the sequence:

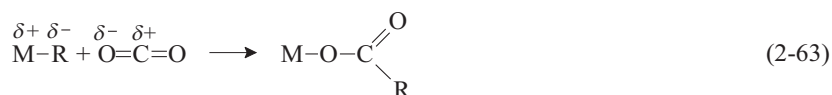


As expected, the alkylphosphines of higher σ basicity activate the CO insertion reaction, as do polar solvents such as ether, which can increase the reaction rate by a factor of 10^3 to 10^4 . Examples of very fast insertions are the reactions of carbenes with M-H, M-C, and M-Cl bonds (Eqs. 2-61 and 2-62).

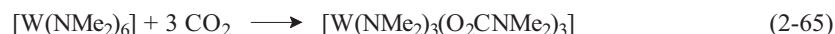
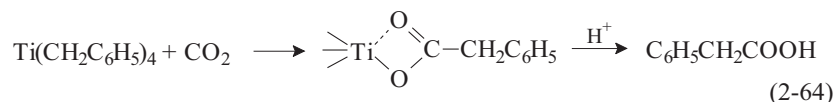


The insertion reactions discussed below can be explained well by using the HSAB concept [7].

Carboxylation reactions with the hard Lewis acid CO_2 are of potential interest for future industrial syntheses. Understandably, the hardest alkyl metal compounds are required to facilitate reactions of the type:

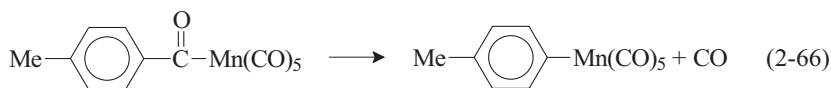


This is shown by the following reactions:

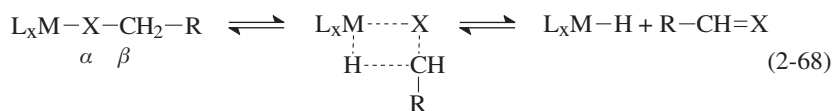


The benzyl complex of titanium is a very hard starting material (Eq. 2-64), as is the tungsten dialkylamide (Eq. 2-65).

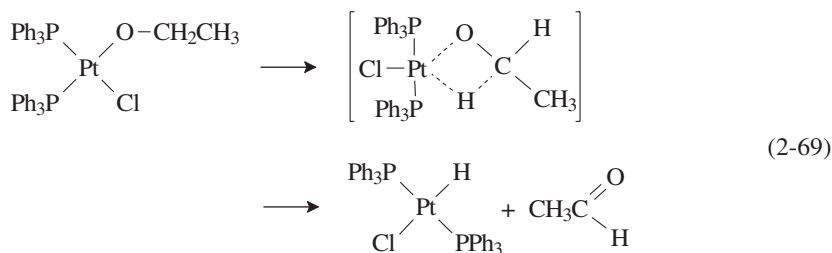
Elimination reactions can proceed as the direct reverse of insertion reactions. Thus the elimination of CO from acyl complexes (Eq. 2-66) and of CO_2 from carboxylates (Eq. 2-67) can result in the formation of metal-aryl bonds. Such eliminations occur under the influence of heat and light.



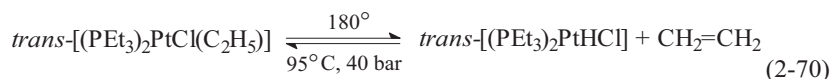
Decomposition reactions can proceed by another mechanism, namely, β elimination. In particular, β -hydride elimination is an important mechanism for the decomposition of σ -organyl complexes (Eq. 2-68).



The products of this intramolecular rearrangement are a metal hydride complex and a stable unsaturated compound. Formally, it can be regarded as a competitive reaction between the metal center and the the unsaturated ligand fragment or the soft base H^- . Generally, such elimination reactions are favored by high reaction temperatures and low oxidation states of the transition metal. The HSAB concept predicts that β -hydride elimination is favored when the metal center is made softer and the unsaturated product harder. For example, acetaldehyde is more readily eliminated than ethylene (Eq. 2-69).



Alkoxy complexes of transition metals are generally less stable because of the presence of a hard(OR)/soft(M) dissymmetry. The elimination of alkene from the more stable alkyl metal complexes generally requires drastic conditions (Eq. 2-70).



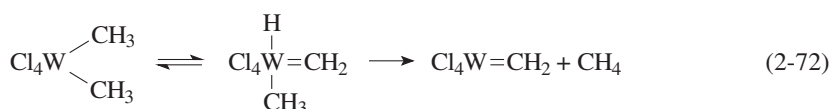
This can be explained in terms of the softness of the R^- group, which stabilizes the complex.

β -Hydride elimination is favored by a free coordination site at the metal center, as exemplified by the complex $[\text{Bu}_2\text{Pt}(\text{PPh}_3)_2]$, thermal decomposition of which is inhibited by the presence of an excess of triphenylphosphine. This shows that dissociation of a PPh_3 ligand is required for the elimination reaction to occur.

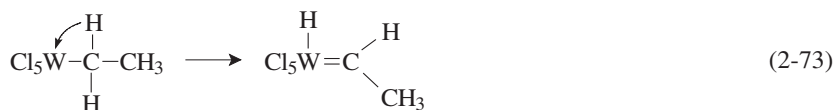
Understandably, metal complexes containing alkyl groups that have no hydrogen atoms in the β position, such as methyl, benzyl, and neopentyl, are more stable than other alkyl derivatives. The decomposition of metal alkyls — the reverse of olefin insertion — is of importance in the transition metal catalyzed isomerization of olefins and as a chain-termination reaction in olefin polymerization. The α elimination reaction should also be mentioned here. It is mainly of importance in W and Mo complexes [T11]. Extraction of an α hydrogen atom from methyl compounds leads to intermediate alkylidene species:



The decomposition of methyltungsten compounds with formation of methane is believed to involve such hydrido carbene intermediates:



In ethyltungsten complexes, for which β elimination of alkene would be expected, the α elimination according to Equation 2-73 is favored.

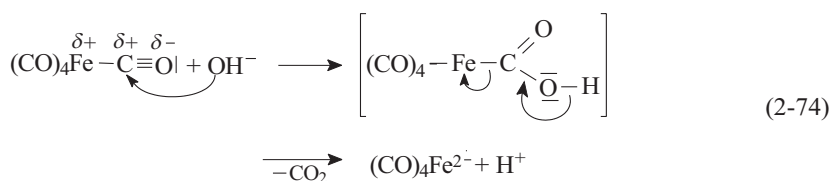


Metal carbene complexes are discussed as intermediates in metathesis reactions (olefin disproportionation).

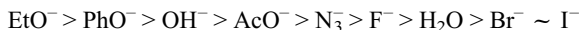
2.1.6

Reactions at Coordinated Ligands

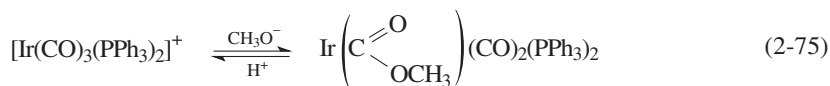
Nucleophilic attack on coordinated ligands is a widely encountered type of reaction. For example, carbonyl complexes are readily attacked by various nucleophiles, including OH^- , OR^- , NR_3 , NR_2^- , H^- , and CH_3^- . A well-known example is the base reaction of carbonyl complexes (Eq. 2-74).



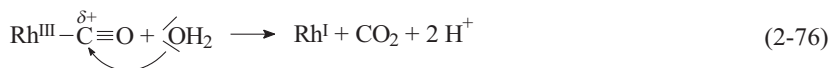
The carbonyl carbon atom of carbonyl complexes is an electrophilic center that according to the HSAB concept can be regarded as a hard acid (similar to H^+). The attack of the hard base OH^- initially gives a hydroxycarbonyl species, which, however, is unstable and loses CO_2 , forming a carbonyl metallate anion. The effectiveness of nucleophiles with respect to the carbonyl carbon atom decreases in the following sequence [T12]:



Thus the hard oxygen bases react more readily with metal carbonyls than the softer bases. Alkoxide ions attack coordinated carbon monoxide to form alkoxy carbonyl complexes. This reaction (Eq. 2-75) has been observed for many complexes of the metals Mn, Re, Fe, Ru, Os, Co, Rh, Ir, Pd, Pt, and Hg.



As a final example of ligand reactions of carbonyls, the rhodium-catalyzed CO conversion reaction will be mentioned. Anionic rhodium complexes such as $[Rh(CO)_2I_2]^-$ undergo nucleophilic attack by water with formation of CO_2 (Eq. 2-76).



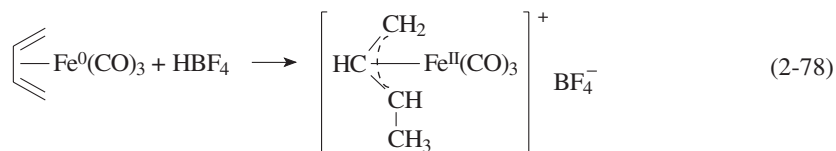
The resulting rhodium^I carbonyl complex can be oxidized back to rhodium^{III} by protons (Eq. 2-77); the final products are CO_2 and H_2 .



Electrophilic attack on a ligand is often observed for complexes of olefins and aromatic compounds. The electrophilic or nucleophilic behavior of these π ligands can be predicted on the basis of the σ/π bonding model. The olefin reacts not only as a σ donor but also as a π acceptor.

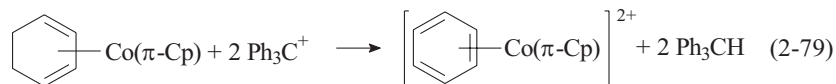
When π backbonding from the metal to the olefin predominates, electrons flow from the metal to the olefin, which then exhibits carbanion behavior. In this case, electrophilic attack readily occurs [21]. Low metal oxidation states (0, +1) and anionic complexes favor electrophilic attack on coordinated ligands. Of course, substituent effects also play a role: electron-withdrawing groups can inhibit electrophilic attack.

The reactivity of ligands towards nucleophiles increases for higher oxidation states of the metal (+2, +3) and for cationic complexes. The following examples illustrate this rule:

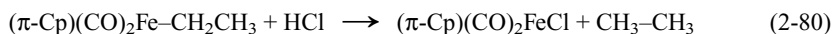


In Equation 2-78 a proton attacks a diene ligand to give an π -allyl complex.

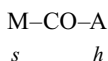
In the following reaction hydride ions are removed from a diene complex to give an arene complex (Eq. 2-79)



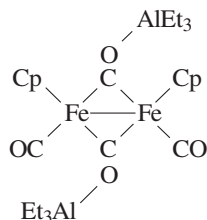
The final example (Eq. 2-80) shows that alkyl complexes can undergo irreversible cleavage of alkane on reaction with acids.



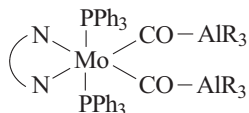
The dual activation of ligands is also of interest for catalytic reactions. Carbon monoxide is classified according to the HSAB concept as a very soft Lewis base. Thus activation occurs by coordination of the C atom to soft transition metals. The CO ligand can, however, react as a hard Lewis base via the oxygen atom. Sufficiently hard Lewis acids A can therefore coordinate to the oxygen atom and further weaken the C–O bond [16]:



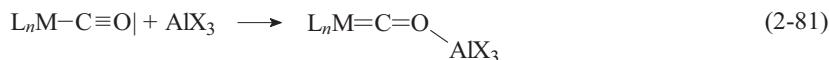
Hard Lewis acids (A = AlCl₃, AlR₃, BCl₃) preferentially attack bridging CO ligands:



But examples are also known for the coordination of Lewis acids to terminal CO ligands:

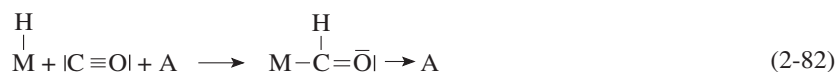


Bifunctional activation of CO leads to carbene-like resonance structures of the type shown in Equation 2-81.



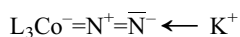
The attack of the electrophile is particularly facile in the case of anionic and other electron-rich complexes. The dual activation of CO ligands weakens the C–O bond and lowers the C–O stretching frequency in the IR spectrum.

It has been found that the presence of Lewis acids or protons can accelerate carbonyl insertion reactions, providing another possibility of modifying catalysts. Mixtures of transition metal carbonyls and Lewis acids could in future be of interest as catalysts for CO hydrogenation, for example, in Fischer–Tropsch reactions (Eq. 2-82) [T11].



The hard electron acceptor A lowers the electron density in the CO moiety, facilitating attack of the hydride on the carbonyl carbon atom.

In dinitrogen complexes, polarization of the N₂ ligand occurs with an electron-rich metal center on one side and a strongly polarizing, hard cation on the other [13]. As an example, the following resonance structure can be given for the cobalt complex [$\{KCo(N_2)(PMe_3)_3\}_6$]:



This ligand polarization favors electrophilic attack on the terminal nitrogen atom. Reactions that activate dinitrogen are of interest as the basis for the fixation of nitrogen as ammonia.

► Exercises for Section 2.1

Exercise 2.1

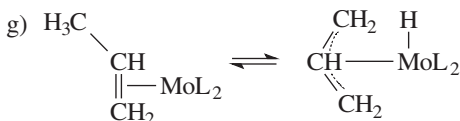
What is the oxidation state of the transition metal in the following complexes?

- | | |
|---------------------------|---------------------------|
| a) $[V(CO)_6]^-$ | f) $[H_2Fe(CO)_4]$ |
| b) $[Mn(NO)_3CO]$ | g) $[Ni_4(CO)_9]^{2-}$ |
| c) $[Pt(SnCl_3)_5]^{3-}$ | h) $[Fe(CO)_3(SbCl_3)_2]$ |
| d) $[RhCl(H_2O)_5]^{2+}$ | i) $O_2[PtF_6]$ |
| e) $[(\pi-C_5H_5)_2Co]^+$ | j) $[HRh(CO)(PPh_3)_3]$ |

Exercise 2.2

What type of reaction is occurring in the following:

- a) $\text{trans-}[\text{PtCl}_2(\text{PEt}_3)_2] + \text{HCl} \rightarrow [\text{PtCl}_3\text{H}(\text{PEt}_3)_2]$
 b) $[\text{W}(\text{CH}_3)_6] \rightarrow 3 \text{CH}_4 + \text{W}(\text{CH}_2)_3$
 c) $[\text{Co}(\text{H})_2\{\text{P}(\text{OMe})_3\}_4]^+ \rightleftharpoons [\text{Co}\{\text{P}(\text{OMe})_3\}_4]^+ + \text{H}_2$
 d) $[(\pi\text{-C}_5\text{H}_5)\text{W}(\text{CO})_3]\text{Na} + \text{CH}_3\text{I} \rightarrow [(\pi\text{-C}_5\text{H}_5)\text{W}(\text{CO})_3\text{Me}] + \text{NaI}$
 e) $[\text{IrCl}(\text{CO})(\text{PPh}_3)_2] + \text{Me}_3\text{O}^+\text{BF}_4^- \rightarrow [\text{IrMeCl}(\text{CO})(\text{PPh}_3)_2]^+\text{BF}_4^- + \text{Me}_2\text{O}$
 f) $[(\pi\text{-C}_5\text{H}_5)\text{Mn}(\text{CO})_3] + \text{C}_2\text{F}_4 \rightarrow [(\pi\text{-C}_5\text{H}_5)\text{Mn}(\text{CO})_2\text{C}_2\text{F}_4] + \text{CO}$



- h) $[(\pi\text{-C}_5\text{H}_5)_2\text{ReH}] + \text{BF}_3 \rightleftharpoons [(\pi\text{-C}_5\text{H}_5)_2\text{ReHBF}_3]$

Exercise 2.3

Classify the following reactions by means of the oxidation states:

- a) $\text{CoCO}_3 + 2 \text{H}_2 + 8 \text{CO} \rightarrow [\text{Co}_2(\text{CO})_8] + 2 \text{CO}_2 + 2 \text{H}_2\text{O}$
 b) $2 [\text{Fe}(\text{CO})_2(\text{NO})_2] + \text{I}_2 \rightarrow [\text{FeI}(\text{NO})_2]_2 + 4 \text{CO}$
 c) $[\text{Pt}(\text{PPh}_3)_3] + \text{CH}_3\text{I} \rightarrow [\text{CH}_3\text{PtI}(\text{PPh}_3)_2] + \text{PPh}_3$
 d) $[\text{Mn}(\text{CO})_5\text{Cl}] + \text{AlCl}_3 + \text{CO} \rightarrow [\text{Mn}(\text{CO})_6]^+[\text{AlCl}_4]^-$
 e) $[\text{PtCl}_2(\text{PR}_3)_2] + 2 \text{N}_2\text{H}_4 \rightarrow [\text{PtHCl}(\text{PR}_3)_2] + \text{N}_2 + \text{NH}_3 + \text{NH}_4\text{Cl}$

Exercise 2.4

Interpret the following ligand-exchange reactions and explain how they differ from one another:

- a) $[\text{W}(\text{CO})_6] + \text{Si}_2\text{Br}_6 \rightarrow [\text{W}(\text{CO})_5\text{SiBr}_2] + \text{SiBr}_4 + \text{CO}$
 b) $[\text{Pt}(\text{PPh}_3)_4] + \text{Si}_2\text{Cl}_6 \rightarrow [\text{Pt}(\text{PPh}_3)_2(\text{SiCl}_3)_2] + 2 \text{PPh}_3$
 c) $[\text{Fe}(\text{CO})_5] + \text{PEt}_3 \rightarrow [(\text{PEt}_3)\text{Fe}(\text{CO})_4] + \text{CO}$

Exercise 2.5

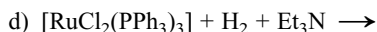
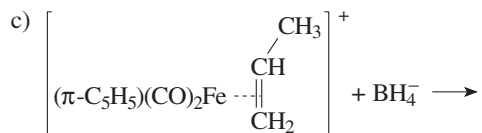
Rhodium complexes react with ethylene according to Equations (a) and (b). Comment on the two reactions.

- a) $[\text{Rh}(\text{NH}_3)_5\text{H}]^{2+} + \text{CH}_2=\text{CH}_2 \rightarrow [\text{Rh}(\text{NH}_3)_5\text{C}_2\text{H}_5]^{2+}$
 b) $[\text{RhCl}(\text{PPh}_3)_3] + \text{CH}_2=\text{CH}_2 \rightleftharpoons [\text{RhCl}(\text{C}_2\text{H}_4)(\text{PPh}_3)_2] + \text{PPh}_3$

Exercise 2.6

Complete the following equations and name the type of reaction involved in each case.

- a) $[\text{IrCl}(\text{CO})(\text{PR}_3)_2] + \text{SnCl}_4 \rightarrow$
 b) $[(\pi\text{-C}_5\text{H}_5)_2(\text{CO})_3\text{WH}] + \text{CH}_2\text{N}_2 \rightarrow$

**Exercise 2.7**

Define the term oxidative addition. What conditions are required for reactions of this type? What is the reverse reaction called?

Exercise 2.8

Define the term “insertion reaction” and give an example.

Exercise 2.9

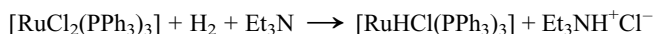
What reaction occurs when the platinum hydride complex $[\text{PtH}(\text{SnCl}_3)(\text{CO})(\text{PPh}_3)]$ is treated with hydrogen under pressure in an autoclave?

Exercise 2.10

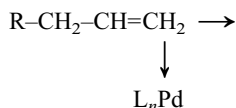
Transition metal complexes can readily catalyze olefin isomerization. This can occur without cocatalysts via π -allyl complexes. Formulate such a reaction between the coordinatively unsaturated complex $\square\text{-ML}_m$ and the olefin $\text{RCH}_2\text{CH}=\text{CH}_2$.

Exercise 2.11

- a) Many d^8 transition metal complexes react with molecular hydrogen under nonpolar conditions. This is surprising given the high intramolecular bond energy of H–H (ca. 450 kJ/mol). Give an explanation.
- b) Explain the following H_2 activation reaction:

**Exercise 2.12**

α -Olefins readily undergo addition to Pd complexes. Which reactions can subsequently occur?

**Exercise 2.13**

Why is no 2-butene formed in the nickel-catalyzed dimerization of ethylene?

Exercise 2.14

Addition of PPh_3 to Wilkinson's catalyst $[\text{RhCl}(\text{PPh}_3)_3]$ lowers the turnover rate in the hydrogenation of propene. Give a plausible mechanistic explanation for this observation.

2.2**Catalyst Concepts in Homogeneous Catalysis**

A catalytic process can be depicted as a reaction cycle in which substrates are converted to products with regeneration of the catalytically active species. At the end of the process, the catalyst is present in its original form. The cyclic depiction of catalytic processes is particularly clear and is also helpful in developing new processes.

2.2.1**The 16/18-Electron Rule**

As we have already seen, transition metal catalyzed reactions proceed stepwise according to fixed rules regarding the oxidation state and coordination number of the metal center.

Particularly useful is the 16/18-electron rule proposed by Tolman [19], which has been successfully employed to specify preferred reaction paths in homogeneous catalysis.

The rule is based on the observation that the well-characterized diamagnetic complexes of the transition metals in particular have 16 or 18 valence electrons. All ligands bound covalently to the metal center contribute two electrons to the valence shell, and the metal atom provides all the d electrons, corresponding to its formal oxidation state.

Examples:

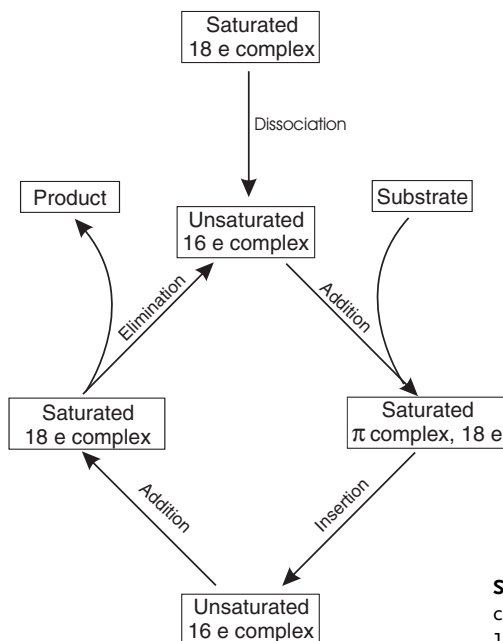
$[\text{Rh}^{\text{I}}\text{Cl}(\text{PPh}_3)_3]$ has $8 + (4 \times 2) = 16$ valence electrons
8 e

$[\text{CH}_3\text{Mn}^{\text{I}}(\text{CO})_5]$ has $6 + (6 \times 2) = 18$ valence electrons
6 e

Tolman specified the following rules for organometallic complexes and their reactions:

- 1) Under normal conditions, diamagnetic organometallic complexes of the transition metals exist in measurable concentrations only as 16- or 18-electron complexes.
- 2) Organometallic reactions, including catalytic processes, proceed by elemental steps involving intermediates with 16 or 18 valence electrons.

The second rule can be depicted schematically for the key reactions of homogeneous catalysis as shown in Scheme 2-2.



Scheme 2-2 Course of a homogeneously catalyzed reaction according to the 16/18-electron rule

2.2.2

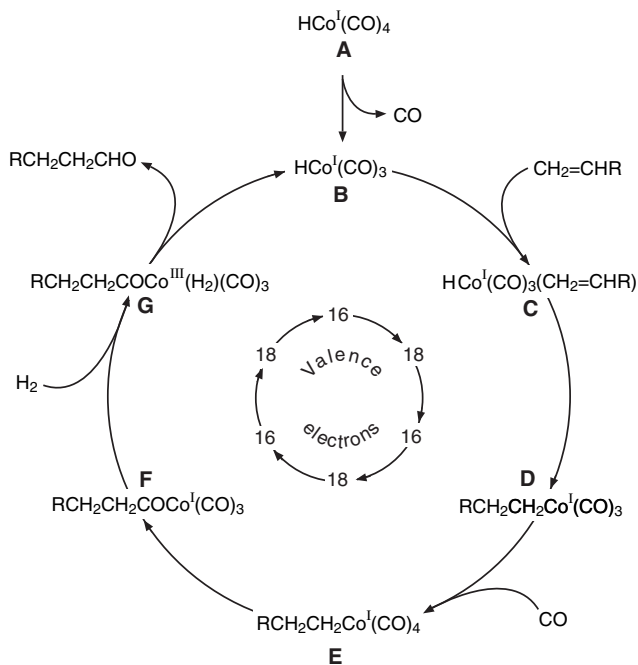
Catalytic Cycles

With a knowledge of the key reactions of homogeneous catalysis and the 16/18-electron rule, homogeneously catalyzed processes can be depicted as cyclic processes. This way of describing catalytic mechanisms was also introduced by Tolman.

We will now discuss the industrially important hydroformylation of a terminal alkene in terms of a cyclic process (Scheme 2-3) [T11].

The catalyst precursor is the 18-electron hydrido cobalt tetracarbonyl complex **A**, which dissociates a CO ligand to give the 16-electron active catalyst **B**. The next step is the coordination of alkene to give the 18-electron π complex **C**. This is followed by rapid insertion of the alkene into the metal–hydrogen bond by hydride migration to form the cobalt^I alkyl complex **D**. The next step is addition of CO from the gas phase to afford the 18-electron tetracarbonyl complex **E**, which undergoes CO insertion to give the 16-electron acyl complex **F**. This is followed by oxidative addition of H₂ to the Co^I acyl complex to form the 18-electron Co^{III} dihydrido complex **G**.

The final, rate-determining step of the catalytic cycle is the hydrogenolysis of the acyl complex to aldehyde, which is reductively eliminated from the complex, reforming the active catalyst **B**, which can then start a new cycle. Thus the cycle consists of a series of 16/18-electron processes, as shown in the inner circle of Scheme 2-3.



Scheme 2-3 Cobalt-catalyzed hydroformylation of a terminal alkene in terms of the 16/18-electron rule

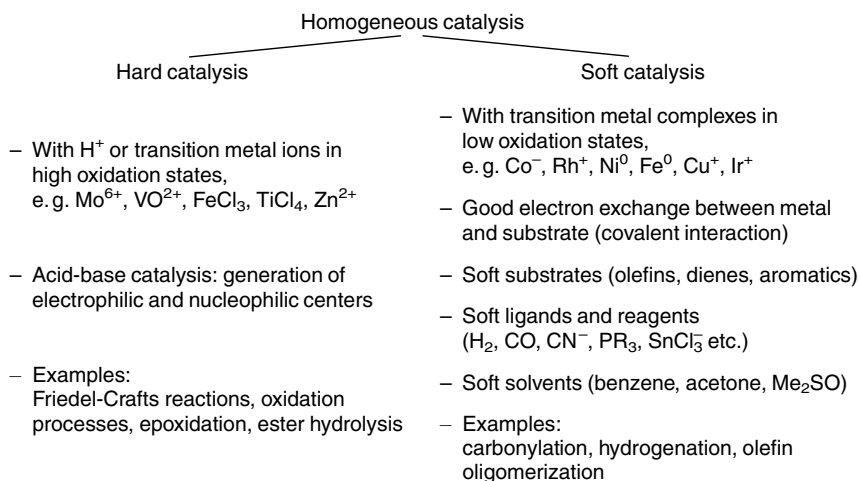
As we have seen in this example of an industrial reaction, the cobalt passes through a series of intermediates, each of which promotes a particular step of the total reaction. Thus there is not a single catalyst, but various catalyst species that take part in the entire process. This is typical of homogeneous catalysis. Generally, the complex that is introduced into the system is referred to as the catalyst, although strictly speaking this is incorrect.

In contrast to heterogeneous catalysts, the compounds used in homogeneous transition metal catalysis have well-defined structures, as can be shown directly by analytical methods. Often, however, it is difficult to identify the species that is truly catalytically active because of the numerous closely interrelated reactions, which can often not be independently investigated. However, detailed knowledge of the reaction mechanism of homogeneous catalysis is a prerequisite for making optimal use of the reactions.

2.2.3

Hard and Soft Catalysis

As we have already seen, catalytic processes generally consist of complicated series of reactions, whereby the activation of individual steps can place different demands on the catalyst. Ugo has classified the homogeneous catalysis of organic reactions on the basis of the HSAB concept [21].



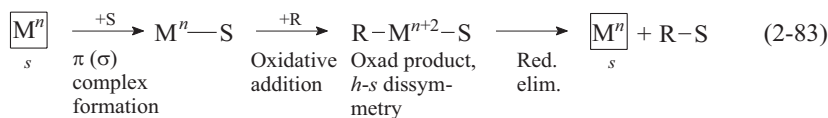
Scheme 2-4 Hard and soft catalysis with transition metal compounds

If the first step of a reaction cycle is regarded as an acid–base reaction between the catalyst and the organic substrate, then a distinction can be made between “hard” and “soft” catalysis, providing a simple basis for understanding transition metal catalyzed processes (Scheme 2-4).

Petrochemical catalytic reactions are predominantly soft; hard catalysis with transition metal ions is less important.

A second possibility for classifying homogeneous catalysis with transition metal complexes is the redox mechanism of such reactions [T16]. During the sequence of reactions, the transition metal formally changes its oxidation state by two units. The catalytic cycle begins, for example, with a coordinatively unsaturated soft metal complex, passes through an oxidation state two units higher as the result of an oxidative addition reaction with the reagent, and re-forms the starting complex by reductive elimination of the product.

In the intermediate of higher oxidation state, the metal is harder, and a hard–soft dissymmetry of the ligands favors the irreversible elimination of the product. In this way the key role of oxidative addition and its reverse reaction in the homogeneous catalysis of C–C and C–H coupling reactions can be understood: in the simplest case, the interplay of oxidative addition and reductive elimination can be represented by a redox reaction (Eq. 2-83).



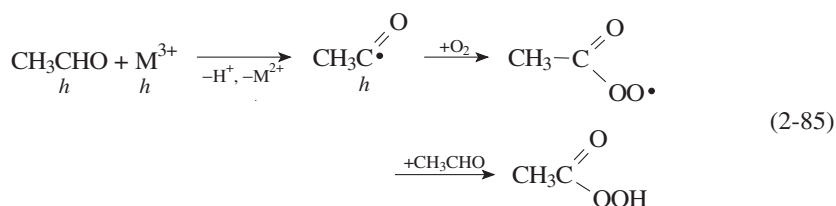
S = substrate, R = reagent

2.2.3.1 Hard Catalysis with Transition Metal Compounds

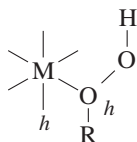
An example of hard catalysis is the oxidation of aldehydes with Co^{III} or Mn^{III} salts (Eq. 2-84).



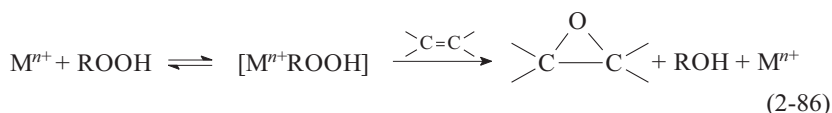
Initially, acetaldehyde is oxidized to peracetic acid via hard acetyl radical intermediates (Eq. 2-85). The peracetic acid then oxidizes acetaldehyde to acetic acid.



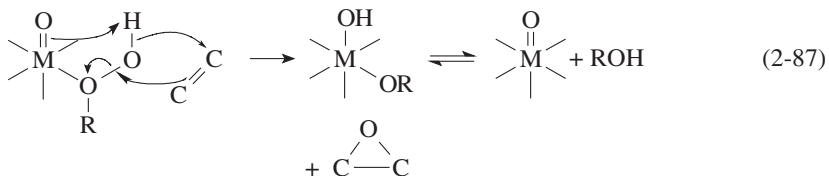
Oxidation catalysts often have a large proportion of ionic bonding, mostly with simple σ bonding of hard ligands (H_2O , ROH , RNH_2 , OH^- , COO^-) to the metal ion. An example is the selective epoxidation of olefins with organic hydroperoxides (Eq. 2-86). The key step of this process is the nondissociative coordination of the hydroperoxide molecule by a hard-hard interaction of the type:



The metal center lowers the electron density on the peroxide oxygen atom, activating it towards nucleophilic attack of the olefin. Typical catalysts are Mo^{VI} , W^{VI} , and Ti^{IV} compounds.



If the metal complex contains $\text{M}=\text{O}$ groups (e.g., oxo complexes of molybdenum or vanadium), oxygen transfer from the metal hydroperoxide complex to the alkene proceeds via a cyclic transition state (Eq. 2-87).



As expected the catalytic effectivity increases with increasing Lewis acidity of the complex: $\text{MoO}_3 > \text{WO}_3$; electron-withdrawing ligands also increase the activity: $[\text{MoO}_2(\text{acac})_2] > [\text{MoO}_2(\text{diol})_2]$.

The oxirane process for the epoxidation of propene is of industrial importance. In this process, isobutane is oxidized with air to *tert*-butyl hydroperoxide, preferably with hard Mo^{V} and Mo^{VI} salts as catalysts. The hydroperoxide then oxidizes the propene.

Now let us turn our attention to hydrogenation reactions. Certain hydrogenation catalysts are highly substrate specific. While a combination of CoCl_2 and AlR_3 (hard) hydrogenates both α -olefins and dienes, in the presence of phosphine or phosphite, the diene is preferentially hydrogenated in the mixture (soft–soft interaction).

As a hard reagent, an aqueous hydrochloric acid solution of RuCl_2 catalyzes the hydrogenation of α,β -unsaturated carboxylic acids and amides, but not that of simple soft olefins.

Hard transition metal catalysts are also used in olefin polymerization. A prerequisite for polymerization is a rapid insertion reaction, which in turn requires high polarity of the metal–alkyl bond and positive polarization of the olefin. Therefore, in particular electropositive transition metals with low numbers of d electrons, such as Ti^{IV} , Ti^{III} , V^{III} , V^{II} , Cr^{II} , Zr^{IV} , are used as relatively hard catalysts here. In contrast, softer, electron-rich nickel^{II} complexes only lead to olefin dimerization or oligomerization. The reason is presumably the more facile β -hydride elimination reaction, which results in early chain termination.

2.2.3.2 Soft Catalysis with Transition Metal Compounds

Typical catalysts for the isomerization, hydrogenation, oligomerization, and carbonylation of olefins are characterized by a low oxidation state of the central atom, which is stabilized by σ – π interactions with soft ligands such as H^- , CO , PR_3 , and X^- [7].

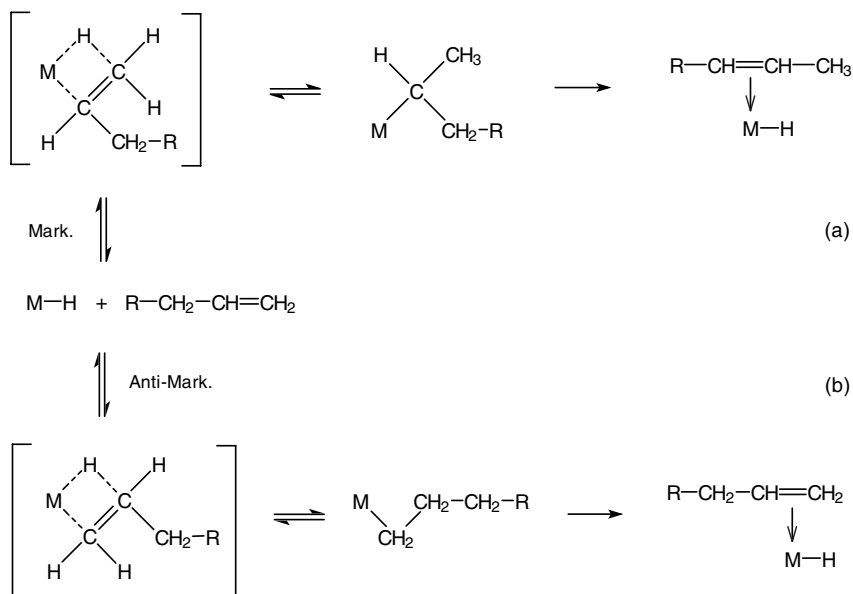
Numerous metal hydrides, such as $[\text{HCo}(\text{CO})_4]$ and $[\text{HRh}(\text{CO})(\text{PPh}_3)_3]$, or combinations of a metal complex and a hydride source (e.g., $[\text{Co}_2(\text{CO})_8]/\text{H}_2$, $[\text{Ni}\{\text{P}(\text{OEt}_3)\}_4]/\text{H}_2\text{SO}_4$) catalyze the isomerization of 1-alkenes to 2-alkenes. In the industrial carbonylation of α -olefins, this double-bond isomerization is undesirable since the linear end products are of greater industrial importance.

Two mechanisms are discussed for the double-bond isomerization of olefins:

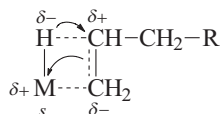
- The metal alkyl mechanism
- The metal allyl mechanism

The following examples illustrate the application of the HSAB concept to the above-mentioned possibilities. The addition of M-H to the double bond (Scheme 2-5) can proceed by a Markownikov (a) or anti-Markownikov route (b). Only after Markownikov addition is the 2-olefin formed by β -elimination.

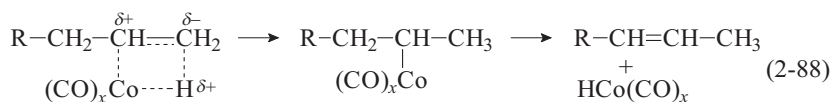
Therefore, the isomerization depends crucially on the hydride character of the hydrogen atom. The hydride ligands of soft complexes such as $[\text{HRh}(\text{CO})(\text{PPh}_3)_3]$ preferably undergo anti-Markownikow addition with the following polarization:



Scheme 2-5 Isomerization of α -olefins by the metal alkyl mechanism



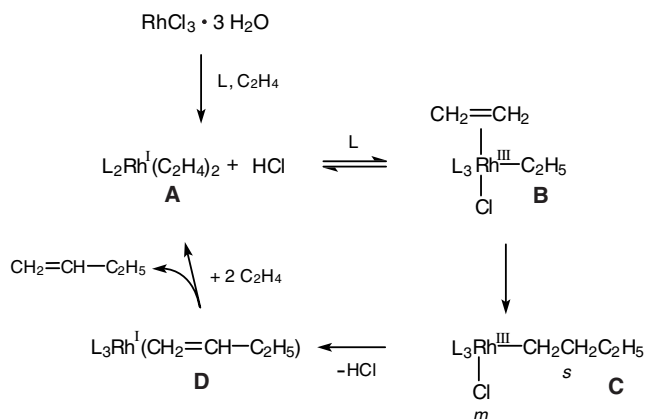
With harder compounds such as $[\text{HCo}(\text{CO})_4]$, in which the hydrogen atom has more protic than hydridic character, Markownikow addition is followed by isomerization (Eq. 2-88).



Thus the harder cobalt carbonyl compounds are more strongly isomerizing than the softer rhodium species. Furthermore, bulky, soft ligands like PPh_3 also favor anti-Markownikow addition for steric reasons.

An alternative reaction path for olefin isomerization involves metal alkyl intermediates (see also Section 2.1.2).

As the next example of soft catalysis, we shall discuss the dimerization of ethylene to 1-butene, which is catalyzed by rhodium complexes in a redox cycle (Scheme 2-6). The active Rh^{I} catalyst **A** undergoes oxidative addition of HCl and insertion of ethylene into the $\text{Rh}-\text{H}$ bond to give the Rh^{III} alkyl complex **B**. The following ethylene insertion reaction is the rate-determining step and is favored by the medium-hard Rh^{III} center. The resulting Rh^{III} butyl complex **C** has a hard-soft dis-

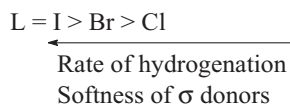


Scheme 2-6 Dimerization of ethylene to 1-butene with a rhodium catalyst (m = medium hard; s = soft)

symmetry, and the system is stabilized by reductive elimination of HCl to give the soft Rh^{I} butene complex **D**, from which the desired product 1-butene is released in a displacement reaction with ethylene.

The homogeneously catalyzed hydrogenation of olefins and dienes has also been thoroughly investigated [12]. The advantage of the homogeneous reactions are the high selectivities that can be achieved in many cases. For example, with the weak catalysts $[\text{RhCl}(\text{PPh}_3)_3]$, $[\text{RuCl}_2(\text{PPh}_3)_3]$, and $[\text{RhH}(\text{CO})(\text{PPh}_3)_3]$, only alkene and alkyne groups are attacked, while other, harder unsaturated groups such as CHO, COOH, CN, and NO_2 remain unchanged [T11]. Wilkinson's catalyst $[\text{RhCl}(\text{PPh}_3)_3]$ allows the hydrogenation of alkenes and alkynes to be carried out at 25°C and 1 bar hydrogen pressure.

The rate-determining step in catalytic hydrogenation is believed to be the olefin-hydride migration (insertion reaction) to form a metal alkyl complex. This insertion reaction can be regarded as the nucleophilic attack of a hydride ligand on an activated double bond. This explains why groups that increase the electron density on the hydrido group or lower the electron density in the olefinic double bond generally increase the reaction rate. In the hydrogenation of cyclohexene with $[\text{RhClL}_3]$, the following ligand influence has been found:

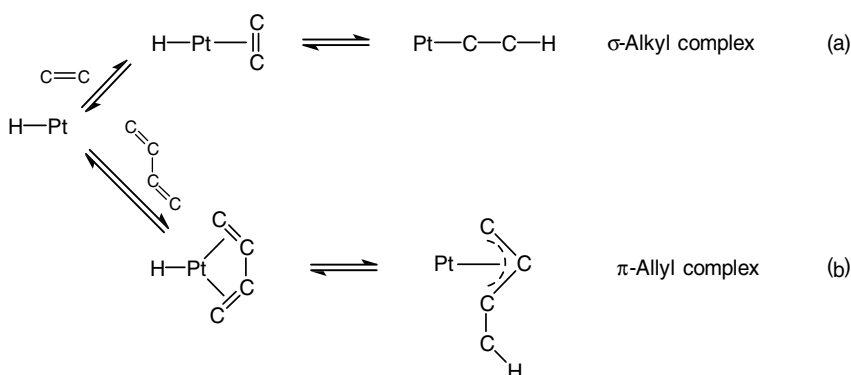


As an example of substrate effects, acrylonitrile and allyl acetate are more rapidly hydrogenated than unsubstituted 1-hexene.

As expected, soft catalyst systems such as $[\text{HCo}(\text{CN})_5]^-/\text{CN}^-$ are particularly effective in hydrogenating soft substrates like conjugated dienes. In the case of butadiene, the CN^- concentration can be used to control the selectivity for the

end products 1-butene and 2-butene. Other soft homogeneous catalysts such as $[\text{Fe}(\text{CO})_5]$, $[\eta^5\text{-CpM}(\text{CO})_3\text{H}]$ ($\text{M} = \text{Cr}, \text{Mo}, \text{W}$), $[\text{Ru}(\text{H})\text{Cl}(\text{PPh}_3)_3]$, and *trans*- $[\text{Pt}(\text{SnCl}_3)\text{H}(\text{PPh}_3)_2]$ also reduce conjugated dienes selectively to mono-enes.

The selectivity for the hydrogenation of dienes in the presence of mono-olefins depends on the stability of the π -allyl intermediates formed. For a hydrogenation mixture of diene, mono-olefin, and Pt/Sn catalyst, the competing reactions shown in Scheme 2-7 can be envisaged [T14].

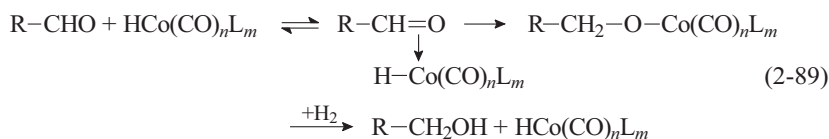


Scheme 2-7 Hydrogenation of dienes and monoolefins with Pt/Sn catalysts

Reaction route (b), in which the softer π -allyl complex is formed, is preferentially followed by soft catalyst systems. This is the case when excess ligand R_3P , CO, or $[\text{SnCl}_3]^-$ is present.

The reduction of harder substrates such as phenol requires harder catalysts (e.g., combinations with Lewis acids). The catalyst combination $\text{Co}(\text{2-ethyl hexanoate})_2/\text{AlEt}_3$ allows the reduction of phenol to cyclohexanol to be carried out under mild conditions with over 90 % selectivity [T11].

The most important homogeneously catalyzed industrial syntheses are the carbonylation reactions [T5]. Whereas hydroformylation of olefins with soft rhodium catalysts gives exclusively aldehydes as oxo products, with the harder cobalt catalysts alcohols can also be obtained. The initially formed aldehydes, which can be regarded as relatively hard, are better able to form complexes with the hard cobalt center (Eq. 2-89).



The Reppe alcohol synthesis from olefins and $\text{CO}/\text{H}_2\text{O}$ with hard iron/amine catalysts can be explained analogously: the end products are almost exclusively alco-

hols; the catalyst has a much higher hydrogenation activity than cobalt phosphine complexes.

The HSAB concept can also be applied to the related hydrocarboxylation reaction, in which carboxylic acids are produced from olefins, CO, water, and small amounts of hydrogen. With hard cobalt/*tert*-amine catalysts, the products are the hard carboxylic acids, whereas rhodium catalysts give mainly aldehydes. Rhodium makes the intermediate acyl complexes softer, and in the subsequent elimination step H₂, which is softer than H₂O, gives aldehyde as product.

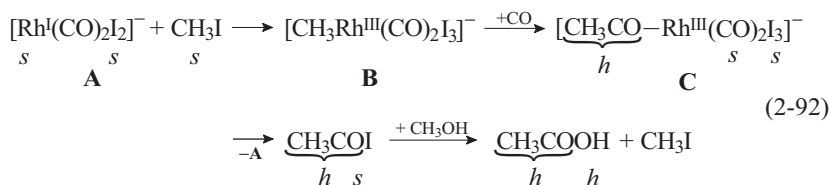
Another carbonylation reaction of major industrial importance is the reaction of methanol with CO to give acetic acid, catalyzed by carbonyls of Fe, Co, and especially Rh in the presence of halides (Eq. 2-90).



As in the case of hydroformylation, rhodium catalysts allow the process to be carried out at low temperatures and pressures (ca. 180 °C, 35 bar, Monsanto process). At the beginning of the reaction, iodide promoters convert the hard substrate methanol to the soft methyl iodide (Eq. 2-91).



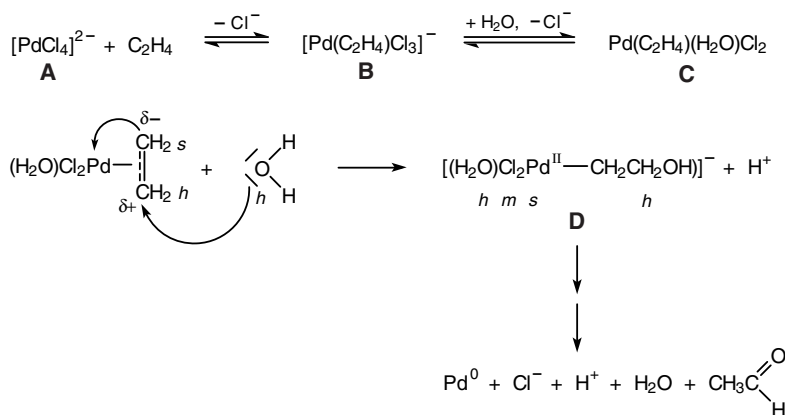
Rhodium(III) halide is used as catalyst precursor. Under the reaction conditions, it is reductively carbonylated to the active catalyst species, the anionic rhodium(I) complex [Rh(CO)₂I₂]⁻. The reaction then proceeds as shown in Equation 2-92.



The soft Rh^I complex anion **A** readily undergoes oxidative addition of methyl iodide. Insertion of CO into the Rh–C bond of the resulting complex **B** then gives the acetyl rhodium complex **C**. Owing to a hard–soft dissymmetry, rapid elimination of acetyl iodide occurs. This initial product of the reaction is immediately solvolyzed by methanol to give acetic acid. The rate-determining step is believed to be the oxidative addition of methyl iodide to the Rh^I complex.

The experimental finding that bromide and chloride promoters are far less effective is explained by the fact that the rate of oxidative addition of RX to rhodium complexes decreases in the order I > Br > Cl, that is, with decreasing donor strength (softness) of the halide ligand.

The selective oxidation of ethylene to acetaldehyde with Pd^{II}/Cu^{II} chloride solutions has attained major industrial importance (Wacker process). This reaction can be regarded as an oxidative olefin substitution (oxypalladation). Once again the in-



Scheme 2-8 Palladium-catalyzed oxidation of ethylene to acetaldehyde

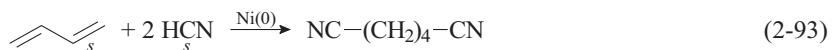
dividual steps can be explained by applying the HSAB concept. The reaction mechanism in the presence of chloride has been studied in detail. The steps of interest here are shown in Scheme 2-8.

After coordination of the ethylene to the tetrachloropalladate **A**, the strong *trans* effect of the ethylene ligand in complex **B** facilitates ligand substitution to give the aquo complex **C**. The function of this neutral aquo complex is possibly that it exhibits less π backbonding from the metal to the olefin than the anionic complex, and the olefin therefore more readily undergoes nucleophilic attack in the former.

Newer investigations have shown that the complex undergoes nucleophilic attack by the hard reagent water [T18], whereas formerly insertion of ethylene into a palladium hydroxo species in an intramolecular step was assumed. The soft palladium(II) center in the hydroxyalkyl complex **D** is coordinated by several hard ligands, which explains the strong tendency towards elimination with release of the final product.

With the hard base water, oxidative olefin substitution leads to acetaldehyde; with acetic acid, vinyl acetate is formed. Finally, the metallic palladium is oxidized by atmospheric oxygen in the presence of Cu^{2+} , re-forming the starting complex.

The final example of a typical soft catalysis to be discussed here is the hydrocyanation of butadiene to adiponitrile (Eq. 2-93). Since both the substrate and the reagent HCN are very soft, soft Ni^0 complexes such as $[\text{Ni}\{\text{P(OAr)}_3\}_4]$ are preferred as catalysts.



All the examples discussed here show that the selectivity of a homogeneously catalyzed reaction is decisively influenced by the central atom of the catalyst. Fine tuning can be made by modification of the ligands. The HSAB concept can be helpful in selecting catalysts, ligands, and solvents, as well as in planning test reactions.

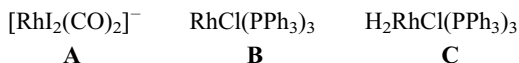
► Exercises for Section 2.2

Exercise 2.15

The acetylacetonate complex $[(\text{acac})\text{Rh}(\text{C}_2\text{H}_4)_2]$ undergoes rapid ethylene exchange, as has been shown by NMR spectroscopy. In contrast, $[(\eta^5\text{-C}_5\text{H}_5)\text{Rh}(\text{C}_2\text{H}_4)_2]$ is inert. Explain these findings.

Exercise 2.16

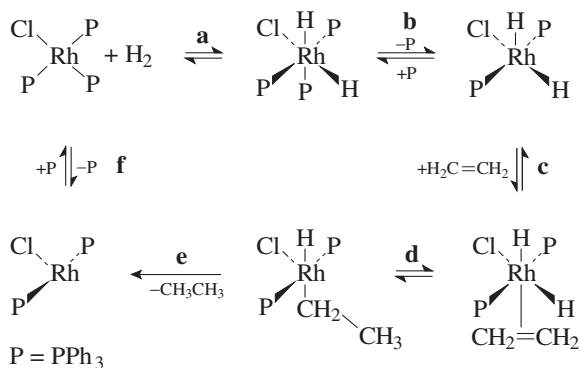
The following rhodium complexes are important catalyst intermediates:



- What is the oxidation state of the metal in complexes **A**, **B**, and **C**?
- Which of the complexes are coordinatively saturated?

Exercise 2.17

In the literature, the mechanism of the catalytic hydrogenation of ethylene with Wilkinson's catalyst $[\text{RhCl}(\text{PPh}_3)_3]$ is given as follows:



Discuss the individual steps (a–f) of the reaction cycle.

Exercise 2.18

The thermodynamic stability of the complexes $[\text{PtX}_4]^{2-}$ increases in the series $\text{X} = \text{Cl} < \text{Br} < \text{I} < \text{CN}$. Explain these experimental findings.

Exercise 2.19

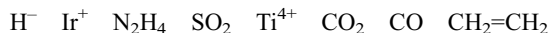
Certain carbonylation reactions can be carried out under mild conditions with the catalyst $[\text{PdCl}_2(\text{PPh}_3)_2]$. Addition of SnCl_2 in the presence of hydrogen gives even more stable and more active catalysts. Explain this in terms of the HSAB concept.

Exercise 2.20

Catalyst poisons for transition metal catalysts are often bases with P, As, Sb, Se, or Te in low oxidation states. Strong O and N bases such as amines and oxy anions are, however, not poisons. Give an explanation for this.

Exercise 2.21

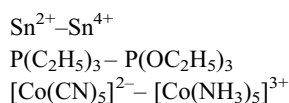
a) Classify the following compounds according to the HSAB concept (acid, base; hard, soft, medium):



b) Apart from CO, which of the following fragments occur preferentially in carbonyl complexes?



c) Which of the following pairs of compounds is harder (with reason)?

**2.3****Characterization of Homogeneous Catalysts**

In homogeneous catalysis, stoichiometric model reactions with well-defined transition metal complexes can be used to elucidate individual steps of the catalytic cycle. Other methods for testing the validity of an assumed reaction mechanism are the use of labelled compounds and the spectroscopic identification of intermediates [13]. An advantage of such investigations is that they can generally be carried out under mild conditions, for example, standard pressure and low temperatures.

Investigations of catalytically active systems is much more difficult. Complications here are the low catalyst concentration, the high reaction temperatures, and often also high pressures. Nevertheless, in some cases active catalysts can be isolated and analytically characterized. For example, catalytic processes can be terminated (“frozen”), or individual steps can be blocked by deliberate poisoning.

In the early years of homogeneous catalysis, it was thought that in-situ spectroscopy (IR, NMR, ESR, Raman, etc.) would make a major contribution to the understanding of catalysis. However, experience has shown that this expectation has only partially been fulfilled. Infrared spectroscopy has proved useful in studying carbonyl complexes [5].

First of all, the postulated mechanism must be consistent with the kinetic measurements. Initially the rate law for the total process is of interest, but the rate laws for the individual steps of the reaction are also important. The influence of using different ligands in the catalyst and other substituents on the reactants, as well as solvent effects, provides further information.

Isotopic labelling allows element-transfer steps to be identified, and stereochemical studies provided support for certain reaction mechanisms.

The possible investigation methods are summarized in the following:

- 1) Deduction of reaction mechanisms
 - fundamental steps (key reactions, 16/18-electron rule)
 - electronic structure and stereochemistry of metal centers
- 2) Modelling of reaction steps
 - stoichiometric reactions
 - complex-formation equilibria of the metal complex
 - use of labelled compounds
 - spectroscopic methods
 - rate laws of the individual steps
- 3) Investigations performed on the catalytically active system
 - isolation of the catalyst
 - in-situ spectroscopy (IR, NMR, UV)
 - kinetics of the total reaction (e. g., gas consumption)
 - selectivity and stereospecificity
- 4) Special methods
 - influence of ligands
 - solvent effects
 - influence of substituents of the reactants

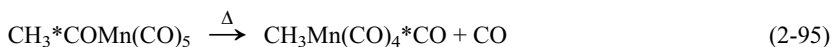
Here we will not deal with the individual analytical steps in detail, but instead give examples for the applicability of individual methods.

In the hydrogenation of olefins catalyzed by $[\text{RhCl}(\text{PPh}_3)_3]$, the metal complexes have mostly been characterized by ^1H and ^{31}P NMR spectroscopy. Electronic and steric effects in ligand-exchange reactions involving phosphine ligands can also be studied by ^{31}P NMR spectroscopy. Infrared spectroscopy was used to identify metal carbonyl clusters in the rhodium-catalyzed production of ethylene glycol from synthesis gas [T11]. There are numerous examples for the use of IR spectroscopy in the literature, including high-pressure applications.

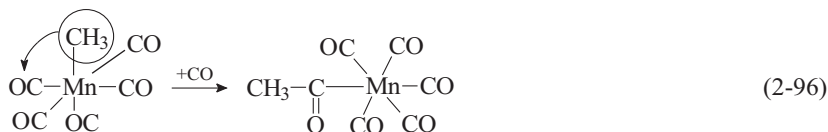
An example of the use of isotopically labelled compounds is the elucidation of the mechanism of the insertion of CO into σ -alkyl complexes to give acyl complexes. Such carbonylation reactions are often reversible. The carbonylation of methylmanganese pentacarbonyl with ^{14}C CO was used as model reaction. None of the ^{14}C label was found in the acetyl group (Eq. 2-94).



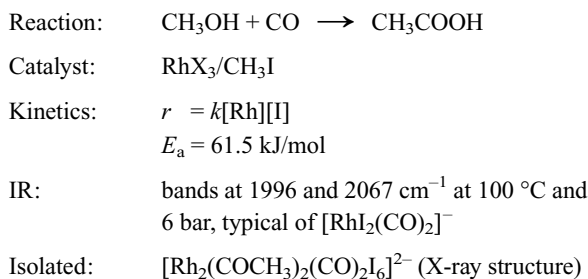
The reverse reaction (Eq. 2-95) shows that the labelled CO is incorporated as a ligand; no radioactivity was detectable in the gas phase.



These experiments, together with kinetic and IR investigations, lead to the conclusion that carbonylation and decarbonylation are intramolecular processes. It was shown that instead of a carbonyl insertion into the metal–carbon bond, a methyl-group migration occurs (Eq. 2-96).



Extensive investigations have been carried out on the Rh/iodide-catalyzed carbonylation of methanol to acetic acid. The most important results are summarized in the following:



Model reactions on Rh and Ir complexes.

A further example of practical catalyst development is the hydroformylation of long-chain α -olefins with various copper(I) complex catalysts [6]. Modification of the catalysts with tertiary phosphines and amines led to aldehydes as products in varying yields, with alcohols and alkanes as byproducts. It was found that defined copper complexes have only a low catalytic activity. Only after the introduction of tertiary amines as solvents and catalyst components were better results obtained.

Since apart from the catalyst components, their stoichiometry and the reaction conditions can be varied, there is a wide range of possibilities for optimization experiments. The course of the reaction was followed by a simple high-pressure IR system. Sample spectra are shown in Figure 2-1.

Immediately after application of synthesis gas pressure, a band (1) is observed for dissolved CO at 2130 cm^{-1} . The peak at 2060 cm^{-1} indicates a mononuclear copper carbonyl complex. The complex of type $[\text{Cu}(\text{CO})\text{L}]$ (L = ligand), formed in situ, is the active catalyst. After a reaction time of 140 min, an aldehyde band appears at 1720 cm^{-1} (3), while the sharp olefin peak at 1640 cm^{-1} (4) continually decreases in intensity. The catalyst is only effective in the temperature range 160 – 180°C and rapidly decomposes above 180°C .

The high-pressure IR system is shown schematically in Figure 2-2 [8]. The autoclave is equipped with a magnetic piston stirrer that also acts as a displacement pump with a teflon ball valve. The reaction solution is pumped through the steel ca-

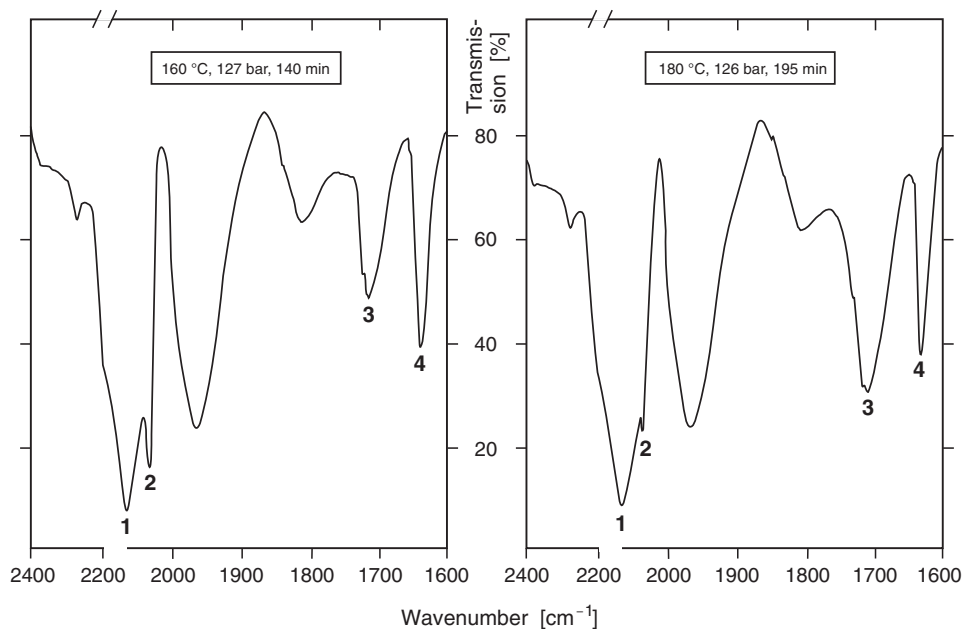


Fig. 2-1 Carbonylation of 1-decene in a high-pressure IR apparatus; catalyst $[(PPh_3)_3CuCl]/$ tetramethylethylenediamine, solvent THF.

- Bands: 1) 2130 cm^{-1} , dissolved CO
 2) 2060 cm^{-1} , Cu(CO) complex
 3) $1710\text{--}1720\text{ cm}^{-1}$, aldehyde
 4) 1640 cm^{-1} , 1-decene

pillary, a microfilter, a nonreturn valve, and finally the high-pressure cell with 15 mm thick salt windows ($NaCl$ or CaF_2). The solution is then returned to the autoclave. Figure 2-3 shows the complete mobile IR unit.

An IR unit of this type offers the following possibilities:

- Detection of intermediates and reaction products under test conditions [5]
- Performing kinetic measurements as a prerequisite for reactor design
- Investigation and characterization of catalyst species for optimization of the test conditions

In the final example, we shall consider kinetics and ligand effects in the cobalt-catalyzed hydroformylation of olefins. The unmodified cobalt catalyst in this case is $[HCo(CO)_4]$, which dissociates with loss of CO in an equilibrium reaction (Eq. 2-97).



The product is formed in the rate-determining step by hydrogenolysis of the metal acyl complex, which plays a key role in this reaction.

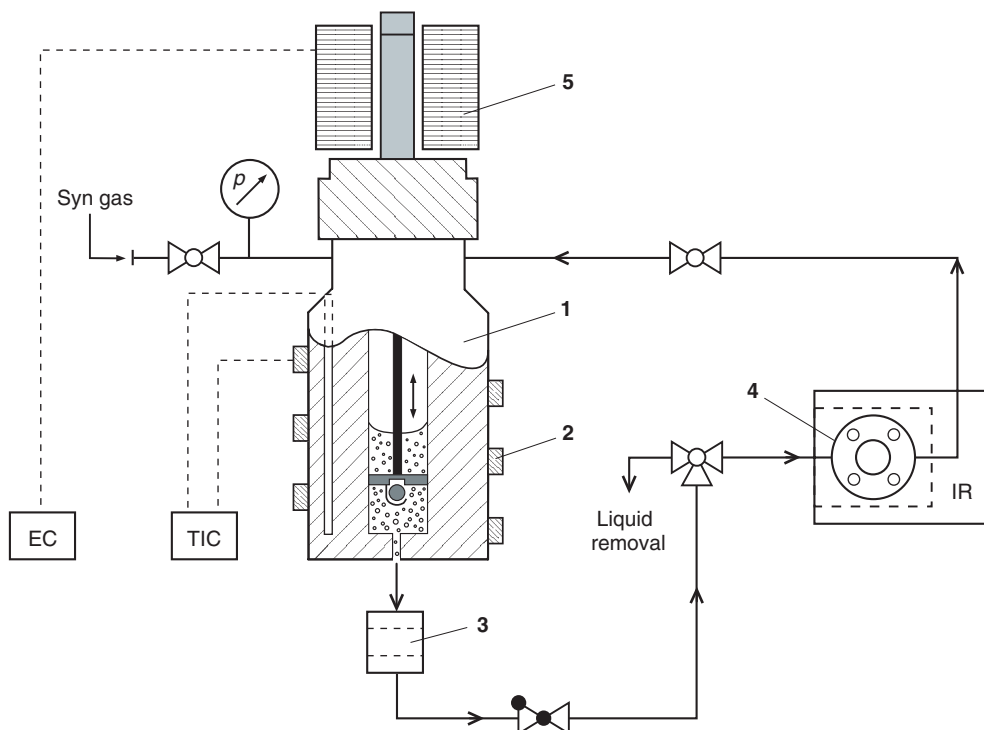


Fig. 2-2 Schematic of the high-pressure IR apparatus (FH Mannheim)
 1) Magnetic-piston autoclave with recirculating pump; 2) Heating strip;
 3) Microfilter; 4) High-pressure IR cuvette; 5) Magnetic coil

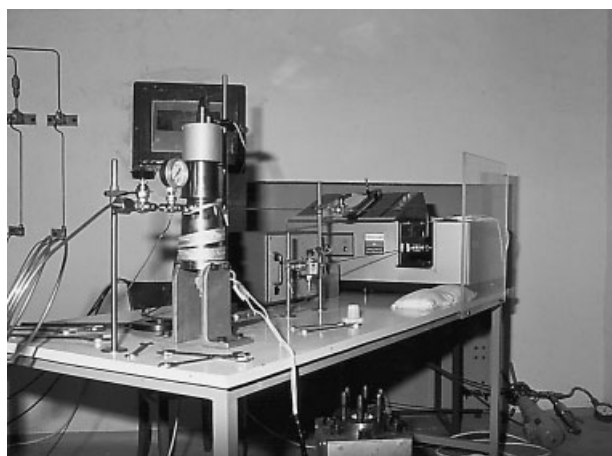


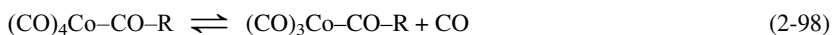
Fig. 2-3 IR high-pressure plant for homogeneous catalysis
 (high-pressure laboratory, FH Mannheim)

Kinetics: $r = k[\text{olefin}][\text{Co}] p_{\text{H}_2} (p_{\text{CO}})^{-1}$

Increasing partial pressure of CO: higher selectivity for linear aldehydes

IR: $[(\text{CO})_4\text{Co}-\text{CO}-\text{CH}_2\text{CH}_2\text{R}]$ in a cobalt/1-octene system at 150 °C and 250 bar

The higher content of linear aldehydes in the reaction mixture is explained by the lower steric hindrance of the CO insertion reaction for a linear acyl complex compared to the branched isomer. However, kinetic measurements showed that the reaction rate is inversely proportional to the CO partial pressure, which can be explained by the equilibrium reactions (2-97) and (2-98), the latter preceding oxidative addition of hydrogen.



In both cases the tetracarbonyl species are inactive, and their formation is favored by high CO pressure.

Under normal oxo synthesis conditions, a small fraction of the aldehyde product is hydrogenated to alcohol (Eq. 2-99).

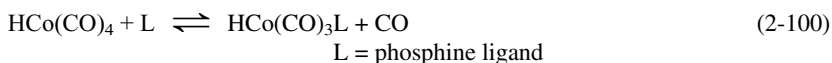


In this reaction, too, the active catalyst is the hydrido tricarbonyl complex $[\text{HCo}(\text{CO})_3]$. This cobalt-catalyzed hydrogenation of aldehydes is even more strongly inhibited by CO [T11].

Kinetics: $r = k[\text{RCHO}][\text{Co}] p_{\text{H}_2} (p_{\text{CO}})^{-2}$

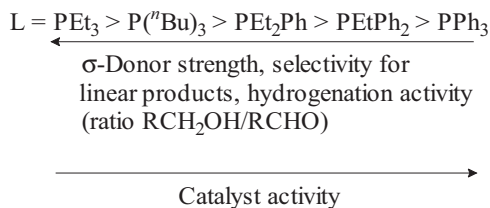
This explains the low hydrogenation activity under hydroformylation conditions where CO partial pressures can exceed 100 bar.

In the case of phosphine-modified cobalt catalysts, ligand effects have been thoroughly investigated. The influence of ligand basicity can be represented by the following equilibrium reaction (Eq. 2-100).



With donors such as triphenylphosphine the equilibrium lies well to the left; with increasing ligand basicity it is displaced to the right. In the more stable catalysts $[\text{HCo}(\text{CO})_3\text{L}]$, strongly basic trialkylphosphine ligands increase the electron density at the metal center and thus on the hydride ligand. This facilitates the migration of the hydride ligand to the acyl carbon atom and promotes the oxidative addition of hydrogen. Complexes containing tertiary phosphines also have higher hydrogenation activity. The following catalyst properties are influenced by the σ -donor strength:

Ligand influences in hydroformylation with $\text{HCo}(\text{CO})_3\text{L}$

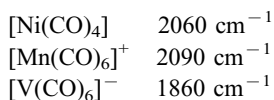


Such *tert*-phosphine-modified catalysts are used industrially in the Shell hydroformylation process. This is one of many examples of the influence of auxiliary ligands (cocatalysts) on homogeneous catalysis.

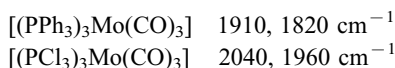
► Exercises for Section 2.3

Exercise 2.22

a) Discuss the CO stretching frequencies of the following transition metal complexes:



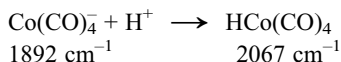
b) For molybdenum carbonyl complexes, the following CO bands are found in the IR:



Explain the position of the CO bands.

Exercise 2.23

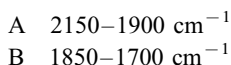
In many carbonylation reactions, cobalt carbonyl hydride is regarded as the active catalyst. The following CO stretching frequencies were measured:



Explain this finding.

Exercise 2.24

For the catalyst octacarbonyldicobalt different CO stretching frequencies were measured in the regions A and B:



Which structure can be deduced for the complex?

3

Homogeneously Catalyzed Industrial Processes

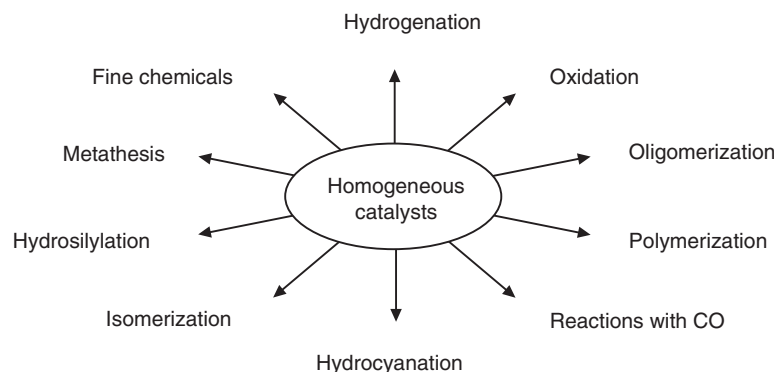
3.1

Overview

In the last three decades homogeneous catalysis has undergone major growth. Many new processes with transition metal catalysts have been developed, and many new products have become available. Although heterogeneous catalysis is still of much greater economic importance in industrial processes, homogeneous catalysis is continually increasing in importance. The share of homogeneous transition metal catalysis in catalytic processes is currently estimated at 10–15 % [8]. Economic data on homogeneous catalysis are difficult to obtain. Homogeneous catalysts are often used internally in a company without this fact being made public. In many cases the catalysts are prepared in situ from metal compounds.

Homogeneous transition metal catalyzed reactions are now used in nearly all areas of the chemical industry, as shown in Scheme 3-1 [10].

Homogeneous hydrogenation is used in polymer synthesis, the hydrogenation of aldehydes to alcohols (oxo process), in asymmetric hydrogenation (L-dopa, Monsanto), and for the hydrogenation of benzene to cyclohexane (Procatalyse).



Scheme 3-1 Homogeneous transition metal catalyzed reactions carried out industrially [10]

The most important industrial application of homogeneous catalysts is the oxidation of hydrocarbons with oxygen or peroxides. Mechanistically, a distinction is made between:

- Homolytic processes: the transition metals react with formation of radicals, and the oxidation or reduction steps are one-electron processes
- Heterolytic processes: normal two-electron steps of coordination chemistry

Oligomerization reactions involve mono-olefins and dienes; polymerization reactions are mechanistically similar. Polymerization or copolymerization with soluble or insoluble transition metal catalysts is used to produce:

- Polyethylene and polypropylene (Ti- and Zr-based metallocene catalysts)
- Ethylene–butadiene rubber
- Poly(*cis*-1,4-butadiene)
- Poly(*cis*-1,4-isoprene)

Polymers prepared with transition metal complexes have different physical properties to those prepared by radical polymerization.

Reactions with CO are one of the most important areas of application of homogeneous catalysis [T5]. They belong to the earliest industrial processes and are associated with the names Walter Reppe (BASF, Ludwigshafen) and Otto Roelen (Ruh Chemie, Oberhausen).

The hydrocyanation of butadiene with two moles of HCN in the presence of nickel complexes to give adiponitrile with high regioselectivity has been developed to industrial scale by DuPont.

Isomerization processes involving homogeneous catalysts are mostly intermediate steps in industrial processes. For example, in the Shell oxo process, inner olefins are converted to primary alcohols. The isomerization occurs prior to CO insertion. The key step in the above mentioned DuPont process is the isomerization of 2-methyl-3-butenitrile to a linear nitrile. A further example is the Cu_2Cl_2 catalyzed isomerization of dichlorobutenes [10].

Metathesis of mono- and diolefins can be performed with both homogeneous and heterogeneous catalysis. The most important processes involving metathesis steps, the SHOP process and the Phillips triolefin process, are based on heterogeneous catalysts. Homogeneous catalysts are used in the ring opening metathesis of norbornene (Norsorex, CDF-Chemie) and cyclooctene (Vestenamer, Hüls) [7].

Homogeneous catalysis is also used in the manufacture of low-scale but high-value products such as pharmaceuticals and agrochemicals. A rapidly growing area is the synthesis of fine chemicals [16]. Table 3-1 summarizes the most important industrial processes involving homogeneous catalysts [8]. Production data of selected processes are listed in Table 3-2, where the wide range from commodities to specialty chemicals can be seen.

Table 3-1 Industrial processes with homogeneous transition metal catalysis [8]

| Unit operation | Process/products |
|----------------------------|---|
| Dimerization of olefins | dimerization of monoolefins (Dimersol process); synthesis of 1,4-hexadiene from butadiene and ethylene (DuPont) |
| Oligomerization of olefins | trimerization of butadiene to cyclododecatriene (Hüls); oligomerization of ethylene to α -olefins (SHOP, Shell) |
| Polymerization | polymers from olefins and dienes (Ziegler-Natta-catalysis) |
| CO reactions | carbonylations (hydroformylation, hydrocarboxylation, Reppe reactions); carbonylation of methanol to acetic acid (Monsanto); carbonylation of methyl acetate |
| Hydrocyanation | adiponitrile from butadiene and HCN (DuPont) |
| Oxidation | cyclohexane oxidation; production of carboxylic acids (adipic and terephthalic acid); epoxides (propylene oxide, Halcon process); epoxyalcohols; acetaldehyde (Wacker-Hoechst) |
| Isomerization | isomerization of double bonds; conversion of 1,4-dichloro-2-butene to 3,4-dichloro-1-butene (DuPont) |
| Metathesis | octenenamer from cyclooctene (Hüls) |
| Hydrogenation | asymmetric hydrogenation (L-dopa, Monsanto); benzene to cyclohexane (Procatalyse); L-menthol (Takasago) |

Table 3-2 Production of selected chemicals by homogeneous catalysis

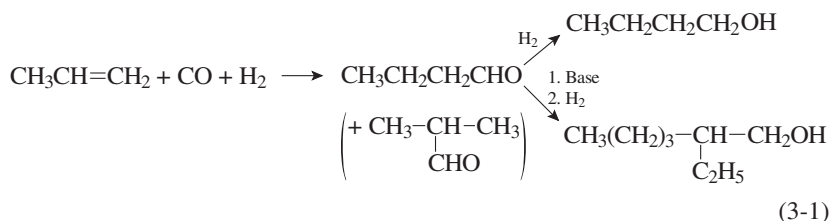
| Process | Catalyst | Capacity (1000 t/a) |
|--|--|------------------------|
| Hydroformylation | HRh(CO) _n (PR ₃) _m HCo(CO) _n (PR ₃) _m | 3700 2500 |
| Hydrocyanation (DuPont) | Ni[(P(OR ₃)] ₄ | ~1000 |
| Ethene-oligomerization (SHOP) | Ni(P [^] O)-chelate complex | 870 |
| Acetic acid (Eastman Kodak) | HRhI ₂ (CO) ₂ /HI/CH ₃ I | 1200 |
| Acetic acid anhydride (Tennessee-Eastman) | HRhI ₂ (CO) ₂ /HI/CH ₃ I | 230 |
| Metolachlor (Novartis) | [Ir(ferrocenyldiphosphine)]I/ H ₂ SO ₄ | 10 |
| Citronellal (Takasago) | [Rh(binap)(COD)]BF ₄ | 1.5 |
| Indenoxide (Merck) | chiral Mn(salen)-complex | 600 kg scale |
| Glycidol (ARCO, SIPSY) | Ti(O ⁱ Pr) ₄ /diethyl tartrate | several tons |

3.2 Examples of Industrial Processes

In this chapter, we will take a closer look at some large-scale industrial processes that involve homogeneous transition metal catalysts [3, 6].

3.2.1 Oxo Synthesis

Oxo synthesis, or more formally hydroformylation, is an olefin/CO coupling reaction which in the presence of hydrogen leads to the next higher aldehyde. The process was discovered in 1938 by Otto Roelen at Ruhrchemie, where it was first commercialized [4]. This reaction is the most important industrial homogeneous catalysis in terms of both scale and value. The most important olefin starting material is propene, which is mainly converted to 1-butanol and 2-ethylhexanol via the initial product butyraldehyde (Eq. 3-1).



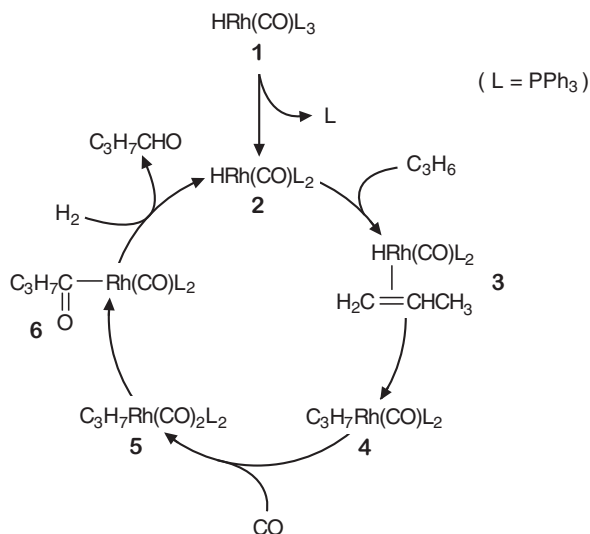
The most important location for this reaction is Germany, with the plants of Hoechst (Ruhrchemie works in Oberhausen) and BASF in Ludwigshafen. Approximately 50 % of world capacity is located in Europe and about 30 % in the USA. Numerous industrial variants of oxo synthesis are known. Cobalt and rhodium catalysts are used, the latter now being preferred [3].

The original catalyst was $[\text{Co}_2(\text{CO})_8]$, which was modified with phosphines to increase the yield of the industrially more important linear aldehydes. A breakthrough was achieved in 1976 at Union Carbide with the introduction of rhodium catalysts such as $[\text{HRh}(\text{CO})(\text{PPh}_3)_3]$. The rhodium-catalyzed process operates at ca. 100 °C and 10–25 bar and gives a high ratio of linear to branched products.

The low pressure allows the synthesis gas to be used directly under its normal production conditions, so that investments for compressors and high-pressure reactors can be saved. However, the economic advantages are strongly dependent on the lifetime of the expensive catalysts, and loss-free catalyst recovery is of crucial importance [14].

The mechanisms of hydroformylation with rhodium and cobalt catalysts have been studied in detail and are very similar. We have already learnt that for cobalt the active catalyst precursor is $[\text{HCo}(\text{CO})_4]$; in the case of the modified rhodium catalyst it is the complex $[\text{HRh}(\text{CO})(\text{PPh}_3)_3]$.

The catalytic cycle for the rhodium system in the presence of excess triphenylphosphine as co-catalyst is shown in Scheme 3-2 [T14].



Scheme 3-2 Mechanism of the hydroformylation of propene with $[\text{HRh}(\text{CO})(\text{PPh}_3)_3]$

Dissociation of a phosphine ligand leads to a coordinatively unsaturated complex **2**, to which the olefin coordinates. This is followed by the familiar steps of olefin insertion, CO insertion to give the Rh acyl complex **6**, and hydrogenolysis of the acyl complex with liberation of the aldehyde, which completes the cycle.

The Shell process is a variant of the cobalt-catalyzed process in which phosphine-modified catalysts of the type $[\text{HCo}(\text{CO})_3(\text{PR}_3)]$ are used. Such catalysts, which are stable at low pressures, favor the hydrogenation of the initially formed aldehydes, so that the main products are oxo alcohols. However, a disadvantage is the lower catalyst activity and increased extent of side reactions, especially the hydrogenation of the olefin starting material. The superiority of the low-pressure rhodium process can be seen from the process data listed in Table 3-3.

Table 3-3 Industrial propene hydroformylation processes [14]

| | Catalysts | | |
|--------------------------------|-----------------------------|---|--|
| | Co | Co/phosphine | Rh/phosphine |
| Reaction pressure (bar) | 200–300 | 50–100 | 7–25 |
| Reaction temperature (°C) | 140–180 | 180–200 | 90–125 |
| Selectivity C ₄ (%) | 82–85 | >85 | >90 |
| <i>n</i> /iso-Aldehyde | 80/20 | up to 90/10 | up to 95/5 |
| Catalyst | $[\text{HCo}(\text{CO})_4]$ | $[\text{HCo}(\text{CO})_3(\text{PBu}_3)]$ | $[\text{HRh}(\text{CO})(\text{PPh}_3)_3]/$ PPh_3 up to 1 : 500 |
| Main products | aldehydes | alcohols | aldehydes |
| Hydrogenation to alkane (%) | 1 | 15 | 0.9 |

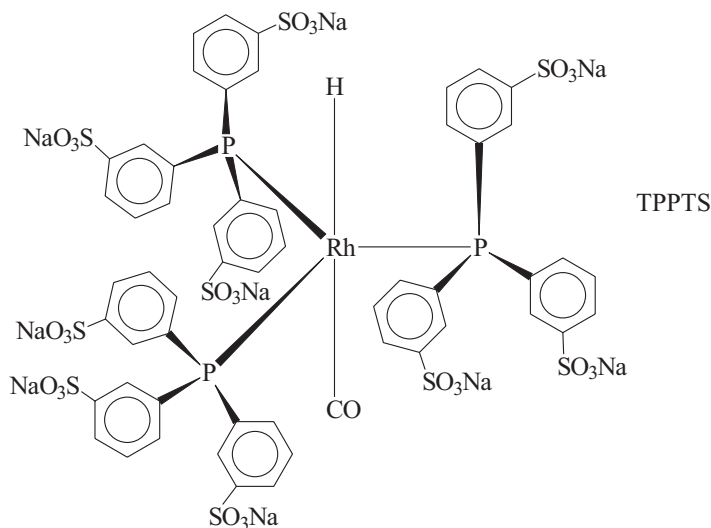
The advantages of the rhodium catalysis can be summarized as follows:

- 1) Rhodium is about 1000 times more active than cobalt as a hydroformylation catalyst.
- 2) The large excess of PPh_3 allows high aldehyde selectivity and a high fraction of linear product to be achieved and at the same time inhibits hydrogenation reactions.
- 3) The presence of PPh_3 dramatically increases the stability of the catalyst and prolongs its life. The low volatility of the catalyst allows the product to be distilled from the reactor with minimal rhodium losses (<1 ppm).
- 4) Efficient purification of the reactants avoids catalyst poisons and prolongs catalyst life [14].

The costs of the rhodium process are, however, higher owing to the required work up, catalyst recycling, and corrosion problems. Therefore, intensive research is being carried out to develop heterogeneous rhodium catalysts. However, this has so far been thwarted by the low stability of the catalysts.

A recent breakthrough has been the use of two-phase technology, commercialized in the Ruhrchemie/Rhône Poulenc process, which uses a new water-soluble rhodium complex with polar SO_3Na groups on the phenyl rings of the phosphine (TPPTS) [1].

The Ruhrchemie works in Oberhausen produces over 300 000 t/a of butyraldehyde using a two-phase water/organic phase system. The process gives improved product selectivity (n/i ratio $>95/5$), and the separation of the catalyst and its recycling are straightforward. Figure 3-1 shows a flowsheet of the process. Such two-phase processes in which the reaction occurs at the phase boundary are expected to be of major future importance in industrial chemistry [16].



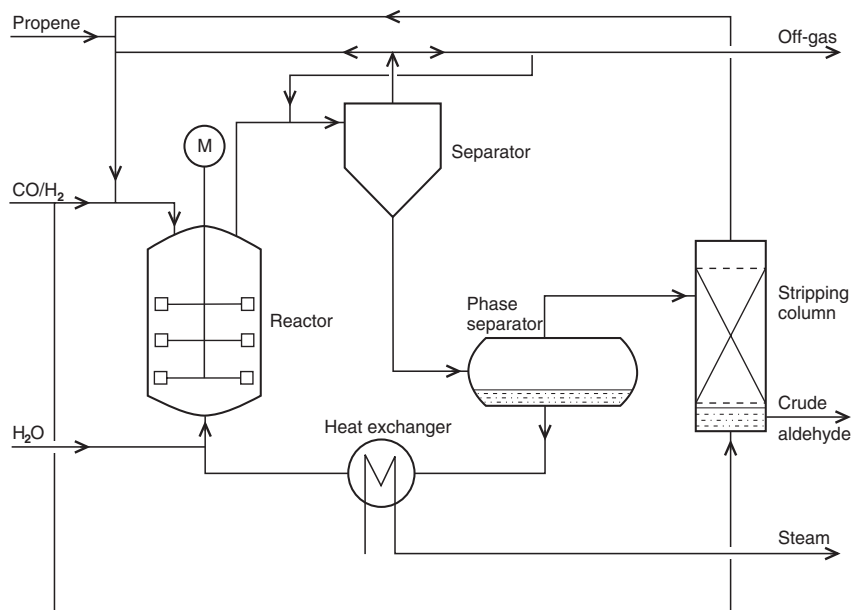


Fig. 3-1 Ruhrchemie/Rhône-Poulenc process for the hydroformylation of propene

3.2.2

Production of Acetic Acid by Carbonylation of Methanol

Another industrially important process with soluble rhodium catalysts is the direct carbonylation of methanol to acetic acid (Eq. 3-2) [T5].



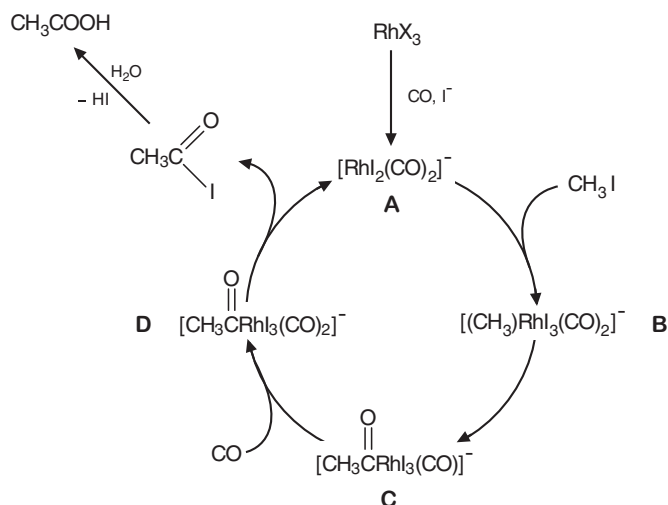
The process was commercialized by Monsanto and has replaced the original high-pressure cobalt-catalyzed BASF process. The catalytic cycle of the Monsanto process is shown in Scheme 3-3 [T18].

The rate-determining step is oxidative addition of methyl iodide to the four-coordinate 16-electron complex $[\text{RhI}_2(\text{CO})_2]^-$ **A** to give the six-coordinate 18-electron complex **B**. This is followed by CO insertion to give the 16-electron acyl complex **C**. Further coordination of CO to the metal center leads to the 18-electron complex **D**, which undergoes reductive elimination of acetyl iodide, re-forming the active catalyst **A**. The acetyl iodide is then hydrolyzed by water to acetic acid and HI (Eq. 3-3).



The strong acid HI converts the methanol starting material to methyl iodide (Eq. 3-4).





Scheme 3-3 Carbonylation of methanol to produce acetic acid (Monsanto process)

This reaction mechanism is supported by model studies. Particularly advantageous are the mild reaction conditions (30–40 bar, 150–200 °C) and the high selectivity with respect to methanol (99 %) and CO (> 90 %) compared to the older cobalt process. Methanol carbonylation is one of the few industrially important catalytic reactions whose kinetics are known in full [7].

Since the reaction is zero order with respect to the reactants, stirred tank reactors have no disadvantages relative to tubular reactors. In fact, stirred vessels allow better heat and material transfer in the gas–liquid reaction. Since the intermediates are anionic, the reaction is carried out in polar solvents.

Industrially, processes in which the products are separated by distillation predominate. Numerous columns are necessary because the boiling point of acetic acid lies between those of the low-boiling components (unchanged CO, CH_3I , and the by-product dimethyl ether) and that of the higher boiling rhodium complex.

The economics of the process depend on loss-free rhodium recycling, which is now readily achievable. A disadvantage is the corrosivity of the iodide, which requires the use of expensive stainless steels for all plant components. Up to now, alternatives such as replacement of the halogen or immobilization of the catalyst have not proved feasible.

Today, methanol carbonylation is carried out mostly in plants using the Monsanto process, which has been licensed worldwide.

A remarkable step change to existing technology has been 1996 the introduction of the “Cativa” technology by BP Chemicals (now BP Amoco). This process incorporated the first commercial use of iridium (promoted by iodine, Ru-salt etc.), rather than rhodium, as a catalyst for methanol carbonylation. The main improvements of the process are much higher reactivity ($45 \text{ mol L}^{-1} \text{ h}^{-1}$, Rh $10\text{--}15 \text{ mol L}^{-1} \text{ h}^{-1}$) coupled with low by-product formation and lower energy requirements for the purification of the product acid.

Ir catalysts are considerably more stable than Rh under the preferred „low water“ operation conditions (0.5%) and are also more active. The technology has been incorporated worldwide in high capacity plants up to 500,000 t/a.

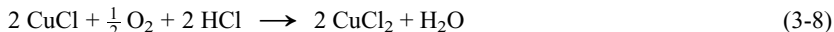
3.2.3

Selective Ethylene Oxidation by the Wacker Process

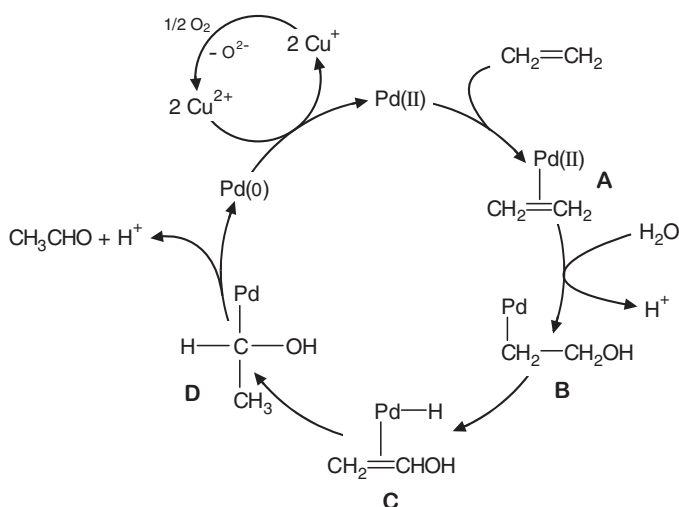
The Wacker process was the first organometallic catalytic oxidation [15, 16]. It was developed 1959 by Smidt and co-workers at the Wacker Consortium for Industrial Electrochemistry in Munich and is mainly used for the production of acetaldehyde from ethylene and oxygen (Eq. 3-5)



The process proceeds by homogeneous catalysis on PdCl_2 . It had been known much earlier that solutions of Pd^{II} complexes stoichiometrically oxidize ethylene to acetaldehyde, but the crucial discovery was the exploitation of this reaction in a catalytic cycle. A closed-cycle process was developed in which an excess of the oxidizing agent Cu^{2+} re-oxidizes the palladium formed in the process without its depositing on the reactor walls. The Cu^+ formed in the redox process is re-oxidized to Cu^{2+} by oxygen. The reaction steps are described by Equations 3-6 to 3-8.



The complete catalytic process is depicted in Scheme 3-4.



Scheme 3-4 Mechanism for the oxidation of ethylene to acetaldehyde in the Wacker process (chloride ligands omitted)

A mechanistic study of the Wacker process involving detailed stereochemical investigations showed that CO bond formation occurs with *trans* stereochemistry; that is, the ethylene molecule is not attacked intramolecularly by a coordinated water molecule. Instead, an additional, uncomplexed water molecule attacks the double bond.

The formation of **B** by addition of water is followed by two further steps in which the coordinated alcohol is isomerized. First, a β -hydride elimination gives **C**, and then an insertion reaction forms **D**. The elimination of the product acetaldehyde and H^+ gives Pd^0 , which is oxidized back to Pd^{2+} by Cu^{2+}/O_2 . With the exception of this last step, the oxidation state of palladium in all steps of the cycle is +2 [7].

In industry, bubble column reactors are used to react the gaseous starting materials ethylene and air (or oxygen) with the aqueous hydrochloric acid solution of the catalyst. Two process variants compete with one another.

In the one-step process, reaction and regeneration with oxygen are carried out simultaneously, while in the two-step process they are carried out separately. In the latter case, air can be used for regeneration, and complete ethylene conversion is achieved. A disadvantage is the higher energy requirement for catalyst circulation compared to the gas circulation used in the one-stage process. In addition, the double reactor design for higher pressures and the use of corrosion-resistant materials lead to higher investment costs.

The two-step process operates at 100–110 °C and 10 bar; catalyst regeneration is carried out at 100 °C/10 bar. Selectivities of 94 % are attained. Side products, such as acetic acid and crotonaldehyde, and chlorinated compounds are removed by two-stage distillation, and the crude aldehyde is concentrated (Fig. 3-2). This process accounts for about 85 % of total acetaldehyde production.

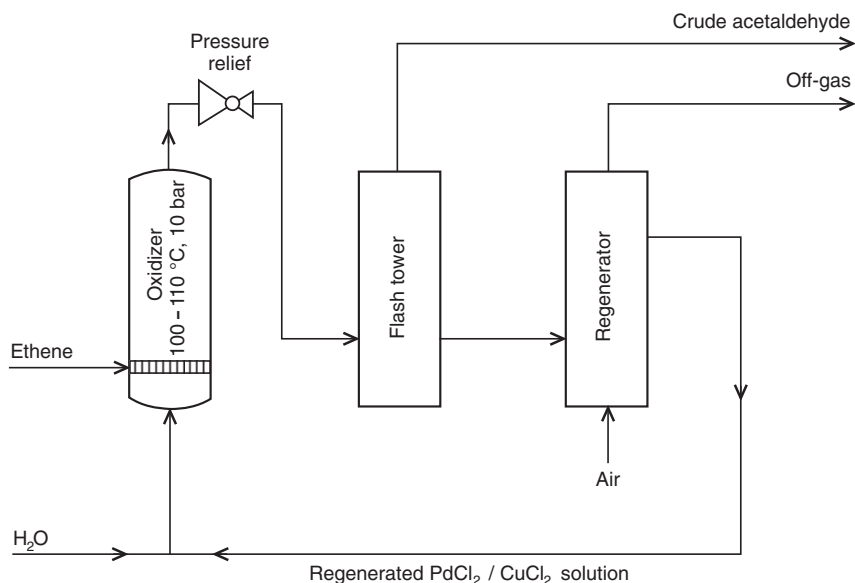


Fig. 3-2 Acetaldehyde production in the two-stage Wacker–Hoechst process

In analogous processes, the oxidation of ethylene in the presence of acetic acid produces vinyl acetate, and in the presence of alcohols, vinyl ethers. In this case heterogeneous catalysts are mainly used.

3.2.4

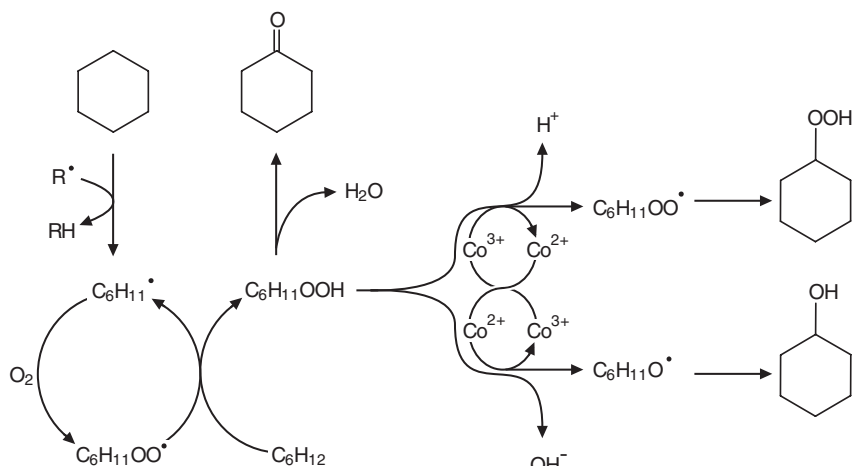
Oxidation of Cyclohexane

The chemistry of the Wacker process is atypical for an oxidation reaction. Normally, catalytic oxidations proceed by chain reactions initiated by radical intermediates. Well-known products of such reactions are hydroperoxides, which themselves often undergo further reaction to give other products.

Radical reactions are characterized by complex product distributions since oxygen exhibits high reactivity towards organic reactants, metal centers, and many ligands. Metals play an important role as initiators for radical chain reactions. Radicals are often generated by metal-catalyzed decomposition of organic hydroperoxides [15].

An industrially important example of such a process is the oxidation of cyclohexane to cyclohexanone and cyclohexanol. Cobalt salts are used as multifunctional catalysts. Cyclohexane is generally oxidized in the presence of about 20 ppm of a soluble cobalt salt such as cobalt naphthenate in the liquid phase at 125–165 °C and 8–15 bar up to a conversion of 10–12 %.

Higher conversions are undesirable as the selectivity decreases because the products are more reactive than cyclohexane. Sometimes boric acid is added to stabilize the oxidation mixture. The selectivities with respect to cyclohexanone and cyclohexanol are 80–85 %. Unreacted cyclohexane is removed by distillation and recycled. The high-boiling components, mainly cyclohexanone and cyclohexanol, are purified by distillation [12]. The most important intermediate in cyclohexane oxidation is cyclohexyl hydroperoxide; a proposed mechanism is shown in Scheme 3-5.



Scheme 3-5 Proposed mechanism for the oxidation of cyclohexane via free radicals.

The radical process begins with the radical-transfer agents R^\bullet and ROO^\bullet ($R = C_6H_{11}$). Cobalt acts as an electron-transfer catalyst and redox initiator in the process. In a one-electron step, the oxidation state of the metal varies between +2 and +3, and radicals are released from the cyclohexane hydroperoxide. Since the cobalt is also involved in a cyclic process, its function is purely catalytic, and thus only small amounts of catalyst are required. Other metals such as V, Cr, Mo, Mn can also be used. Industrial variants of the process have been developed by companies such as BASF, Bayer, DuPont, ICI, Inventa, Scientific Design, and Vickers-Zimmer [T9].

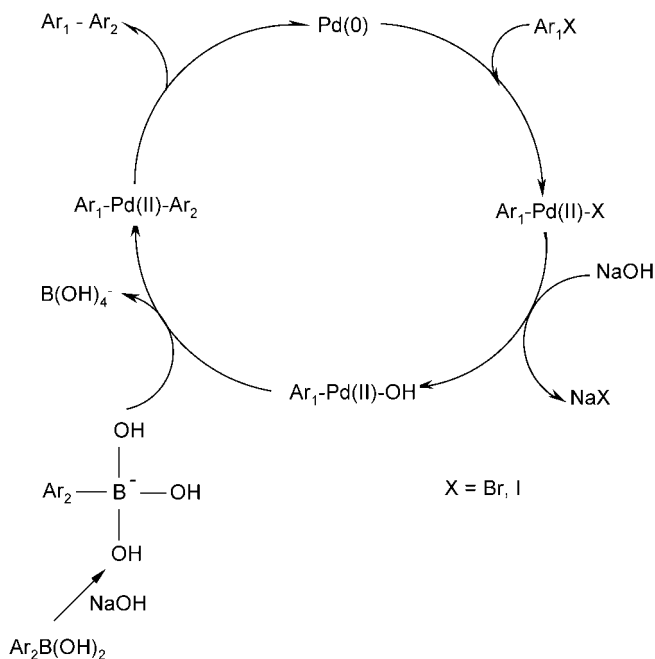
The mixture of cyclohexanone and cyclohexanol can be converted to adipic acid in a second step by oxidation with nitric acid in the presence of metal compounds such as Cu^{II} or V^V salts as homogeneous catalysts.

3.2.5

Suzuki Coupling [19, 24]

The Suzuki coupling is a palladium-catalyzed cross coupling between organoboronic acid and halides. The following sequence of elementary steps is generally accepted to explain the reaction mechanism (Scheme 3-6):

In the first step proceeds an oxidative addition of the aryl halide to a low-coordination $Pd(0)$ species, usually a $Pd(0)$ diphosphine complex. The halide in the σ -aryl $Pd(II)$ species is substituted by the aryl group of the organoborane reagent by trans-



Scheme 3-6 Proposed mechanism for the palladium-catalyzed Suzuki coupling [24]

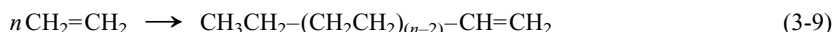
metallation. Aryl-aryl reductive elimination leads to the biaryl product and the catalytic active Pd(0) complex, which can be recycled.

The boronic acid must be activated, for example with base. This activation of the boron atom enhances the polarisation of the organic ligand, and facilitates transmetallation. If starting materials are substituted with base labile groups (for example esters), powdered KF effects this activation while leaving base labile groups unaffected. Recent catalyst and methods developments have broadened the possible applications enormously, so that the scope of the reaction partners is not restricted to aryls, but includes alkyls, alkenyls and alkynyls. Potassium trifluoroborates and organoboranes or boronate esters may be used in place of boronic acids. Suzuki coupling of aryl chlorides have also been described. In these cases Ni can also be used as catalyst. In part due to the stability, ease of preparation and low toxicity of the boronic acid compounds, there is currently widespread interest in applications of the Suzuki coupling, especially in fine chemicals area.

3.2.6

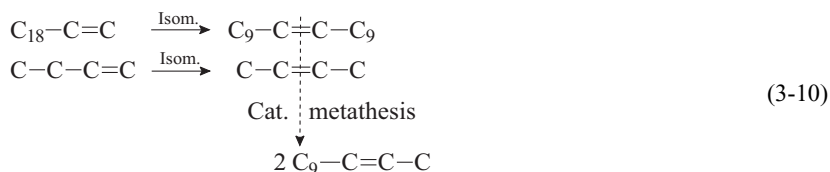
Oligomerization of Ethylene (SHOP Process)

Long-chain α -olefins are of major industrial importance in the production of detergents, plasticizers, and lubricants. Today such α -olefins are mainly produced by oligomerization of ethylene (Eq. 3-9). Numerous homogeneous transition metal catalyst on the basis of Co, Ti, and Ni have been described for this reaction.

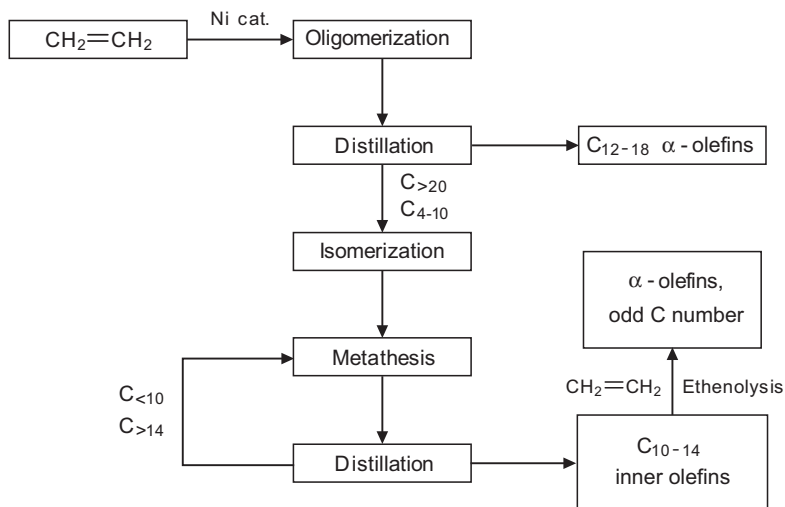


The nickel-catalyzed Shell higher olefin process (SHOP) is of major industrial importance [9,11]. Ethylene is converted to α -olefins with a statistical distribution in which the lower oligomers are favored (so-called Schulz-Flory distribution). This is carried out at 80–120 °C and 70–140 bar in the presence of a nickel catalyst with phosphine ligands such as $\text{Ph}_2\text{PCH}_2\text{COOK}$. The product mixture is separated into C_{4-10} , C_{12-18} , and C_{20+} fractions by distillation.

The C_{12-18} fraction contains α -olefins with the desired chain length for the detergent industry. The top and bottom olefins are subjected to a combination of double-bond isomerization and metathesis. Isomerization gives a mixture of inner olefins with a statistical distribution of the double bond, metathesis of which gives a new mixture of inner olefins from which the C_{10-14} olefins can be separated by distillation. The process is depicted schematically in Equation 3-10.



If, however, the inner olefins are cleaved with ethylene over heterogeneous catalysts (e. g., $\text{Re}_2\text{O}_7/\text{Sn}(\text{CH}_3)_4/\text{Al}_2\text{O}_3$), a mixture of unbranched terminal olefins is ob-

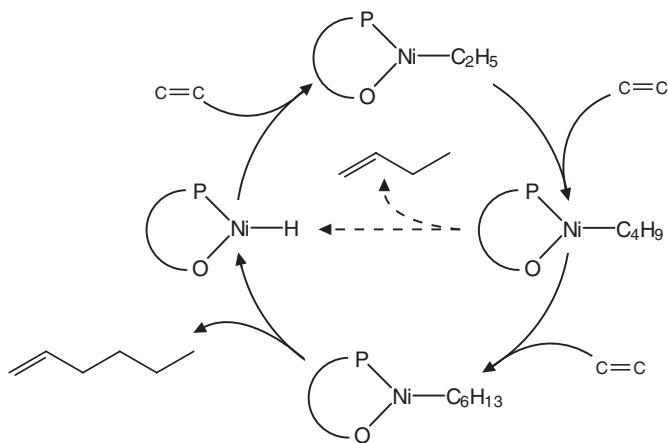


Scheme 3-7 Block schematic of the SHOP process

tained. Undesired higher and lower olefins are recycled. The products consist of 94–97% *n*, α -olefins and >99.5% monoolefins. A schematic of the SHOP process is shown in Scheme 3-7.

The combination of isomerization and metathesis with distillation and recycling offers a unique technology for obtaining a desired carbon-number distribution [7].

Mechanistic investigations with special nickel complex catalysts have shown that nickel hydrides with chelating P–O groups are the catalytically active species. The metal hydride reacts with ethylene to give alkylnickel intermediates, which can grow further by ethylene insertion or eliminate the corresponding α -olefins. A simplified mechanism is shown in Scheme 3-8 [9].



Scheme 3-8 Schematic of ethylene oligomerization with nickel complex catalysts [9]

The SHOP process first came on-stream in Geismar (USA) in 1979 and has since reached a capacity of 600 000 t/a. Further plants were built in the UK, the Netherlands, and France. The major advantage of the process is the ability to adjust the α -olefin products in response to market demands.

The products 1-hexene and 1-octene are copolymerized with ethylene to give high tensile strength polyethylenes for use in packaging materials. 1-Decene is used for producing high-temperature motor oils, and the higher olefins are converted to ten-sides.

Prior to introduction of the SHOP process α -olefins were produced by pyrolysis of waxes above 500 °C (e.g., Chevron process) or by olefin oligomerization with triethylaluminium (Gulf process). However, both produce olefins that are less suited to market requirements [17].

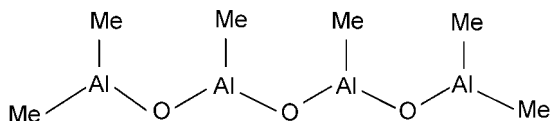
3.2.7

Metallocene-based Olefin Polymerization [22, 25]

The main industrial use for organometallic derived catalysts is in the manufacture of high molecular weight polyolefins. Usually there are employed heterogeneous catalysts which are highly efficient in olefin polymerization. Many questions remain unanswered concerning the intimate details of reaction mechanisms for the majority of the classical polymerization catalysts. Therefore, a great number of nominally homogeneous Ziegler-Natta catalysts have been studied particularly in the past in order to attempt to understand the elementary steps of polymerization.

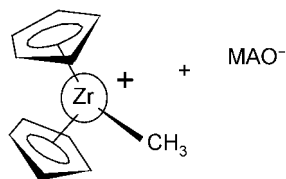
The so-called metallocenes, a group of organometallic materials was discovered in the early 1950s. The metallocenes build a large family of „sandwich compounds“ involving metals held between different ring systems. In 1977, a new generation of so-called „single-site“ homogeneous catalysts, based on combinations of metallocenes, particularly derivatives of Cp_2ZrCl_2 activated with methylaluminoxanes (MAO) were discovered. The zirconium compounds have proved more active than their Ti or Hf analogues. The activator MAO with the approximate composition $[\text{MeAlO}]_n$, is formed by the controlled hydrolysis of AlMe_3 . Both metallocene and MAO, as well as the active complex, are hydrocarbon soluble and the catalysts are up to 100 times more active than common heterogeneous counterparts. Thus, using Cp_2ZrCl_2 and MAO, polyethylene may be produced at rates of up to $40\,000 \text{ kg g}^{-1} \text{ Zr h}^{-1}$ under mild reaction conditions (for example, 2.5 bar C_2H_4 , 30 °C, metallocene concentration $6.25 \times 10^{-6} \text{ M}$ in toluene, MAO/metallocene ratio 250 : 1).

We will discuss briefly the mechanism of metallocene catalysis and the role of methylaluminoxanes, as follows. The methylaluminoxanes are formed by the controlled reaction of AlMe_3 and water, with elimination of CH_4 , and have the approximate composition $[\text{MeAlO}]_n$ with a molecular mass in the range 1000–1500 g/mol. They contain linear, cyclic and cross-linked compounds. The following formula shows a simplified picture of the MAO structure:



Excess of MAO is normally required, typical Al: metallocene ratios ranging between 50–100 for supported systems and 400–20 000 in solution. The optimum ratio depends on the metallocene used and the experimental conditions.

The metallocene reacts with the MAO, and methyl groups replace chlorine on the metallocene. MAO then acts as a Lewis acid taking one of the methyl groups from the Zr to give the active catalyst:



For Ti, Zr, and Hf, the resulting catalytically active species is therefore a 14-electron cationic alkylmetallocenium ion formed by dissociation of the metallocene aluminosiloxane complex. The [aluminosiloxane-Me]⁻ anion is considered to be weakly coordinated or even non-coordinating. The positive Zr ion is stabilised by sharing electrons from a C-H bond.

The reaction mechanism is believed to involve successive additions and insertions of ethylene at each Zr centre comprising the „single-site“ catalyst. Due to this special structure, these highly active catalysts produce uniform homo- and co-polymers with narrow molecular mass distributions. Furthermore, the polymer structure may be controlled by the symmetry of the catalyst precursors.

Using metallocene catalysts it has proved possible to tailor the microstructure of the polymers by fine-tuning of the ligands. Besides polyethylene, it is possible to co-polymerize ethylene with α -olefins such as propylene, but-1-ene, pent-1-ene, hex-1-ene, and oct-1-ene, in order to produce LLDPE. In addition, many kinds of co-polymers and elastomers, and new structures of polypropylenes, polymers and co-polymers of cyclic olefins can be obtained. Furthermore, catalysts with chiral centers can be beneficial in stereospecific polymerization to build the desired isotactic products.

3.3 Asymmetric Catalysis

3.3.1

Introduction [18, 21, 23]

Synthesis of optically pure compounds via transition metal mediated chiral catalysis is very useful from an industrial point of view. There can be produced large amounts of chiral compounds with the use of very small quantities of a chiral source. Compared to the substrate to be refined, the chiral catalyst is present in substoichiometric quantities. Therefore, asymmetric catalysis results in an economical multiplication of the chiral information contained in a small amount of catalysts. Multiplication factors up to millions are possible.

Today, pharmaceuticals and vitamins, agrochemicals, flavors and fragrances, but also functional materials are increasingly produced as enantiomerically pure compounds. The reason for this is the often superior performance of the pure enantiomers. For some purposes the production and application of pure enantiomers are required by law. The enantioselectivity (expressed as e.e. %) of a catalyst should be >99% for pharmaceuticals if no purification is possible; e.e. >80% are often acceptable for agrochemicals or if further enrichment is easy.

The catalyst productivity, given as turnover number or as substrate/catalyst ratio (s/c), determines catalyst costs. For hydrogenation reactions TONs ought to be > 1000 for high value products and > 50 000 for large scale or less expensive products. Catalyst re-use increases the productivity. The catalyst activity given as average turnover frequency (TOF) affects the production capacity. For hydrogenations, TOFs ought to be > 500 h⁻¹ for small and > 10 000 h⁻¹ for large scale products.

3.3.2

Catalysts [19, 22]

Three types of enantioselective catalysts have proven to be synthetically useful. The most versatile are homogeneous metal complexes with chiral ligands. The advantage of transition metal catalyzed asymmetric transformation is that there is a possibility of improving the catalysts by modification of the ligands. The most common ligands are bidentate, i.e. have chiral backbone with two coordinating heteroatoms. For noble metals, especially Rh, Pd, Ru and Ir, these are usually tertiary P or N atoms, for the early transition metals such as Ti, B or Zn, ligands with O or N coordinating atoms are preferred.

Also useful for synthetic application are heterogeneous metallic catalysts, modified with chiral auxiliaries and finally chiral soluble organic bases or acids. Less easy to apply are chiral polymeric and gel-type materials, phase-transfer catalysts or immobilized complexes.

The essential feature for a selective synthesis of one optical isomer of a chiral substance is an asymmetric site that will bind a prochiral olefin preferentially in one conformation. The recognition of the preferred conformation can be accomplished

by the use of a chiral ligand coordinated to the metal, the ligand creating what is effectively a chiral hole within the coordination sphere. An important factor in the successful application of homogeneous asymmetric catalysts has been the design and development of a range of chiral, usually bidentate, phosphine ligands, especially those having C_2 symmetry, for use with different metal centers. Some of the most successful examples are illustrated as follows:

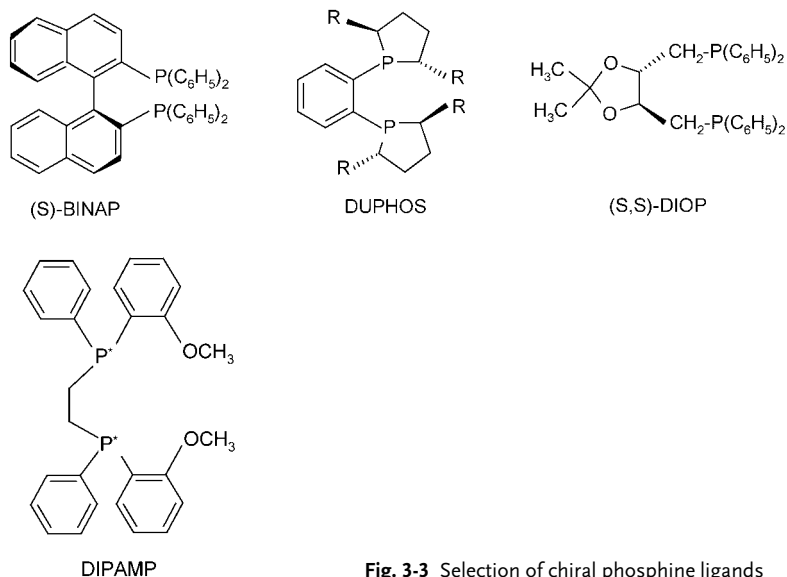


Fig. 3-3 Selection of chiral phosphine ligands

3.3.3

Commercial Applications [18, 20]

Relatively few enantioselective catalytic reactions are used on an industrial scale today. A major reason for this fact is that the application of enantioselective catalysts on a technical scale presents some very special challenges and problems.

Chiral ligands and many metal precursors are expensive and/or not easily available. Typical costs for chiral diphosphines are US \$ 100–500/g for laboratory quantities and US \$ 5000 to >20 000/kg on a large scale.

In addition, many other aspects have to be considered when developing an enantioselective catalytic reaction for industrial use:

- Catalyst separation, stability and poisoning
- Handling problems
- Recycling/regeneration of the catalyst
- Space time yield
- Process sensitivity
- Toxicity of metals and reagent
- Safety aspects as well as the need for high pressure equipment

As follows some processes have been selected to illustrate both the range of catalytic reactions and their importance in key enabling reaction steps in the manufacture of specific products.

3.3.3.1 Asymmetric Hydrogenation

Monsanto L-Dopa Process

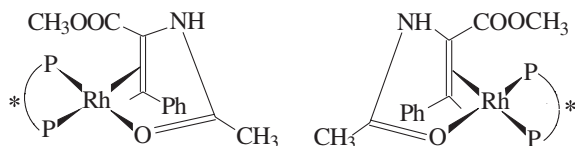
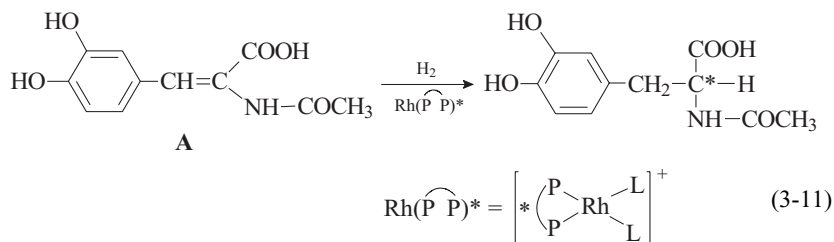
As we have seen, rhodium(I) phosphine complexes are particularly active hydrogenation catalysts. The most intensively investigated catalysts are $[\text{RhCl}(\text{PPh}_3)_3]$ (Wilkinson's catalyst) and $[\text{HRh}(\text{CO})(\text{PPh}_3)_3]$, both of which have long been commercially available.

Wilkinson's catalyst is very sensitive to the nature of the phosphine ligand and the alkene substrate. It is used for laboratory-scale organic syntheses and for the production of fine chemicals.

One of the most elegant applications of homogeneous catalytic hydrogenation is the Monsanto process for the synthesis of L-dopa, a chiral amino acid used in the treatment of Parkinson's disease.

For the synthesis of such optically active products in enantioselective reactions, rhodium(I) catalysts similar to Wilkinson's catalyst but with optically active phosphine ligands were developed. A requirement is that the alkenes to be hydrogenated must be prochiral, that is, they must have a structure that on complexation to the metal center leads to (*R*) or (*S*) chirality [2].

In the Monsanto process, the acetamidocinnamic acid derivative **A** is asymmetrically hydrogenated to give a levorotatory precursor of L-dopa (3,4-dihydroxyphenylalanine). L-Dopa is formed by removing the acetyl protecting group from the nitrogen atom (Eq. 3-11). The asymmetry is introduced by a cationic rhodium complex containing optically active phosphine ligands. Asymmetric chelate ligands are particularly effective in forming an asymmetric coordination center for the complexation of an olefin. The resulting complex can exist in two diastereomeric forms that differ in the way the alkene is coordinated [T18].



Diastereomeric complexes generally have different thermodynamic and kinetic stabilities, and in favorable cases one of these effects can lead to enantioselective product formation.

Variation of the ligands in the rhodium complex eventually led to the chiral phosphine DIPAMP.

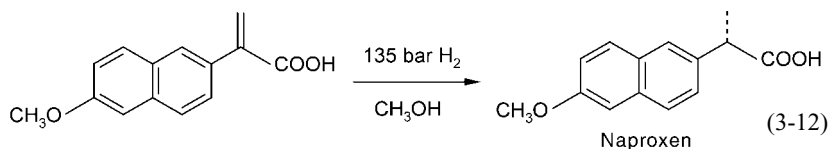
Rhodium catalysts with the DIPAMP ligand (see Fig. 3-3) can hydrogenate amino acid precursors to give optically active amino acids with enantiomeric excesses up to 96 % (enantiomer ratio of 98 : 2).

Particularly interesting in this process is that the diastereomer that is present in lower concentration leads to the desired product. This is explained by its lower activation energy, which makes a higher turnover rate possible.

Asymmetric hydrogenation is a good example of the tailoring of catalysts by modification of the ligands [16].

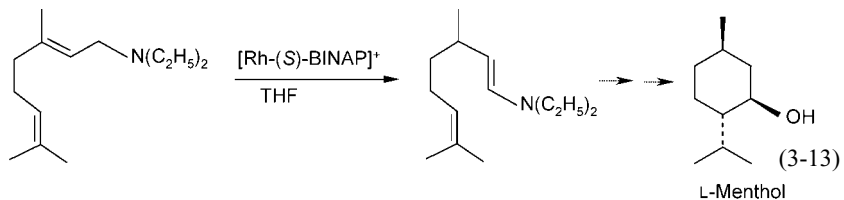
S-Naproxen [22]

The drug naproxen is a member of the class of 2-arylpropionic acids. (*S*)-naproxen, is one of the world's largest-selling prescription drugs. It is sold as the pure (*S*)-isomer because the (*R*)-isomer is a liver toxin. The desired isomer may be obtained by conventional optical resolution of the racemate. Many alternative routes have been explored, but the most favoured one employs asymmetric hydrogenation. α -naphthylacrylic acid provides the substrate for enantioselective hydrogenation using an (*S*)-BINAP Ru(II) chloride complex. The reaction is carried out at 135 bar H₂ in the presence of excess triethylamine to give the required product in optical yields of 96–98 % (Eq. 3-12):



3.3.3.2 Enantioselective Isomerization: L-Menthol [21, 22]

An elegant example of a highly efficient catalytic asymmetric synthesis is the Takasago process for the manufacture of L-menthol, an important product in the flavours and fragrances industry. The key step is a Rh-BINAP catalyzed isomerization of a prochiral enamine to a chiral amine (Eq. 3-13). The product is obtained in 99 % e.e. using a substrate/catalyst ratio of 8000–10 000 : 1 and recycling of the catalyst affords TONs of up to 400 000 after 15 h at 100 °C. The Takasago process currently accounts for about half of the world production (ca. 4500 t/a) of L-menthol.



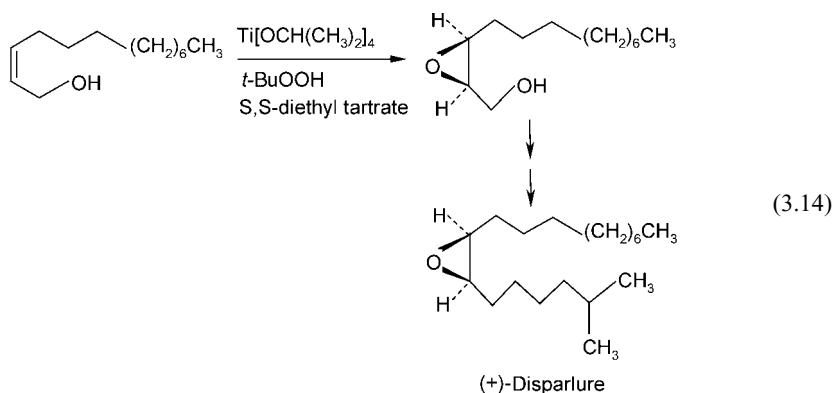
The „handedness“ of the product depends on the chirality of the BINAP ligand present in the catalytic Rh precursor $[\text{Rh}(\pm)(\text{BINAP})(\text{COD})]\text{ClO}_4$. The product is distilled directly from the reaction mixture at low pressure and the active catalytic residue can be re-used directly.

The menthol synthesis is all the more remarkable because three chiral centers are created, all of which are necessary to produce the characteristic menthol odour and local anaesthetic action.

3.3.3.3 Asymmetric Epoxidation

(+)-Disparlure [21]

Together with hydrogenation and isomerization, epoxidation completes the trio of commercially significant applications of enantioselective homogeneously catalyzed reactions. Stereospecific olefin epoxidation is distinctive in that it creates two chiral centers simultaneously. The enantioselective epoxidation method developed by Sharpless and co-workers is an important asymmetric transformation known today. This method involves the epoxidation of allylic alcohols with *tert.*-butyl hydroperoxide and titanium isopropoxide in the presence of optically active pure tartrate esters (Eq. 3-14).

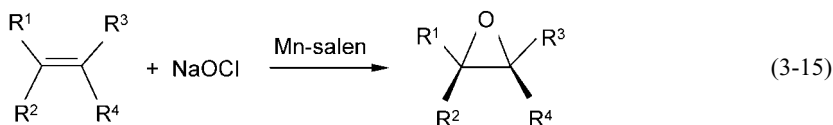


This synthesis of a chiral epoxide as an intermediate to (+)-disparlure, the pheromone for the gypsy moth, was commercialized in 1981. The resulting epoxyalcohol (see Eq. 3-14) is formed in 80% yield and 90–95% enantiomeric purity before recrystallization. It was found that the use of molecular sieves greatly improves this process by removing minute amounts of water present in the reaction medium. Water was found to deactivate the catalyst. Further conversion to (+)-disparlure requires three subsequent conventional reaction steps via an intermediate aldehyde.

The introduction of this asymmetric epoxidation route on the multi-kilogram scale reduced the price of disparlure by an order of magnitude. The very high activity of the substance used for insect control suggests that a production capacity of only a few kg/a is required to satisfy demand.

Jacobsen Epoxidation [22]

A more recent alternative approach, developed by Jacobsen and co-workers, concerns the catalytic asymmetric epoxidation of unfunctionalized olefins using cheap NaOCl as oxidant in the presence of Mn complexes of chiral Schiff bases as catalysts, the so-called „salen“ (Fig. 3-4). Values of 97% e.e. have been achieved using cis-disubstituted or trisubstituted alkenes. Equation 3-15 describes the Jacobsen epoxidation of olefins schematically.



Salen ligands can be obtained from salicylaldehyde and diamines. In principle, the Jacobsen route provides greater flexibility than Sharpless epoxidation procedure. Potential problems to full-scale commercialization include the availability of the olefins and the Schiff base (salen) ligands on a large scale, and the activity and stability of the catalyst.

It seems likely that the principal reactions discussed before, namely asymmetric hydrogenation, isomerization, and epoxidation, will ultimately find extensive use in the production of pharmaceuticals, given the regulatory trend towards the treatment of enantiomers of the same compound as distinct therapeutic agents. The complex chemistry in this area comprises a relatively young discipline, but there can be no doubt that commercial applications of enantioselective homogeneous catalysis are set to increase rapidly.

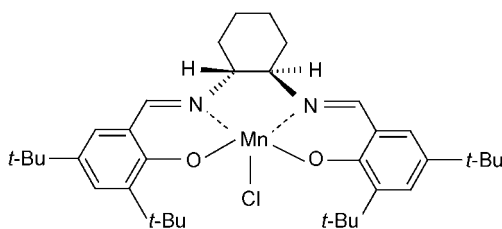


Fig. 3-4 Mn-salen (Jacobsen complex)

► Exercises for Chapter 3

Exercise 3.1

The homogeneous catalytic hydrogenation of 1,3-butadiene with dihydrido platinum complexes gives a mixture of 1-butene, *cis*-2-butene, and *trans*-2-butene. Which intermediates are involved in the process?

Exercise 3.2

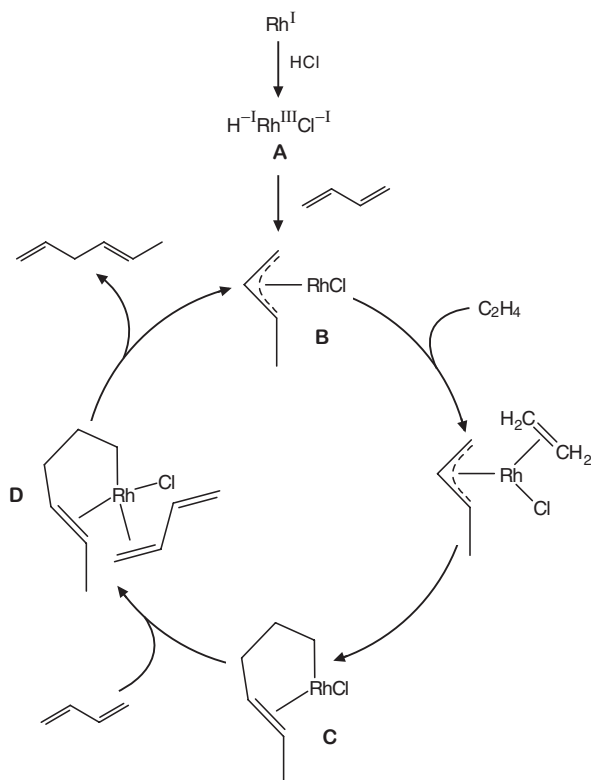
How is heptanal produced industrially?

Exercise 3.3

Acetic acid can be produced by two homogeneous catalytic processes. Name the two routes and the catalysts involved.

Exercise 3.4

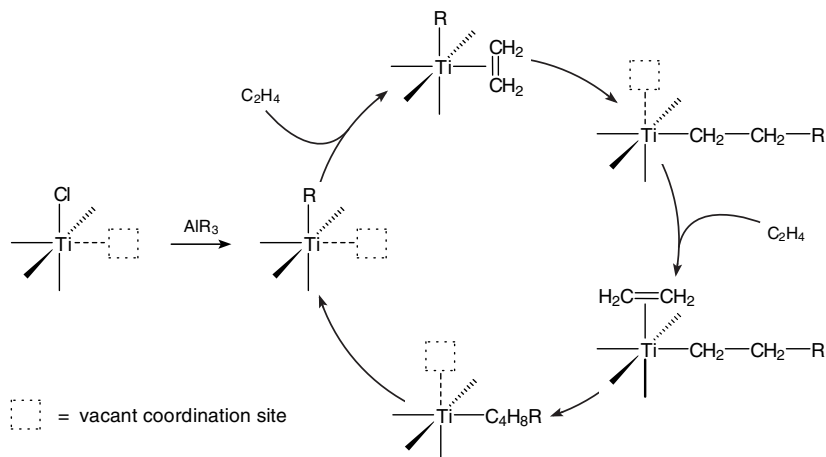
The stereoselective coupling of butadiene with ethylene to give *trans*-1,4-hexadiene is described by the cyclic process shown in Scheme 3-8. Discuss the catalytic cycle and the individual intermediates **A** to **D**.



Scheme 3-8 Rhodium-catalyzed coupling of ethylene and butadiene

Exercise 3.5

The low-pressure polymerization of ethylene with Ziegler catalysts (Ti^{III} compounds/ Al alkyls) is depicted in Scheme 3-9. Explain the mechanism of the polymerization.



Scheme 3-9 Ziegler polymerization of ethylene with Ti/Al catalysts

Exercise 3.6

Why is it not to be expected that modification of the surface of heterogeneous catalysts with optically active substances will lead to asymmetric hydrogenations with high optical yields?

Exercise 3.7

Explain the term „enantioselective synthesis”.

Exercise 3.8

What is the meaning of ee (enantiomeric excess)?

Exercise 3.9

How do chiral hydrogenation catalysts work?

Exercise 3.10

Explain why natural L-asparagine is bitter, whereas artificial D-asparagine is sweet.

Exercise 3.11

Sharpless coined the term “ligand-accelerated catalysis”. What does that mean?

Exercise 3.12

Identify the chiral centre in the compound 3-methylhexane and draw the products as mirror image form.

Exercise 3.13

Find out how the catalyst efficiency of the Takasago synthesis of menthol was developed.

4 Biocatalysis

4.1 Introduction [1]

Biocatalysis covers a broad range of scientific and technical disciplines with the aim to develop biocatalysts and biocatalytic processes for practical purposes. Biocatalysts are based on diverse natural sources, they include whole cells of microbial, plant or animal origin, as well as cell-free extracts and enzymes. Currently, only a very small fraction of the known biocatalysts are being applied on a commercial scale. For example, of the approximately 4000 known enzymes, about 400 are available commercially, but only about 40 are actually used for industrial processes. Biocatalysts are generally much more efficient than chemical catalysts. Typically, enzymes can show turnover numbers of $>100\,000\text{ s}^{-1}$ compared with the values of $0.01\text{--}1\text{ s}^{-1}$ usually observed for heterogeneous and homogeneous catalysts.

Enzymes can operate under relatively mild conditions and usually exhibit a very high degree of substrate-, chemo-, regio-, and enantioselectivity. In this chapter we cannot cover the whole area of biocatalysis. We will give preference to biocatalysts used in industrial production processes.

Subsequently, selected applications of biocatalysts will be examined, used as either isolated enzymes or enzymes that operate in immobilized or permeabilized cells. Synthesis routes in which one or all of the steps are biocatalytic have advanced dramatically in recent years. Increasingly, biocatalysts are combined with chemical catalysts or utilized in a network of reactions in a whole cell. It can be pointed out, that biocatalysts do not operate by different scientific principles from usual catalysts. All enzyme actions can be explained by rational chemical and physical principles. However, enzymes can create unusual and superior reaction conditions such as extremely low $\text{p}K_{\text{a}}$ values or a high positive potential for a redox metal ion.

Biocatalysis is an interdisciplinary area. For a successful practice of biocatalysis three disciplines are needed: biochemistry and organic chemistry from chemistry, molecular biology, enzymology, and protein chemistry from biology, and catalysis, transport phenomena, and reaction engineering from chemical engineering. The most important areas of application are the pharmaceuticals, food, fine chemicals, basic chemicals, pulp and paper, agriculture, medicine, energy production, and mining industries (Fig. 4-1).

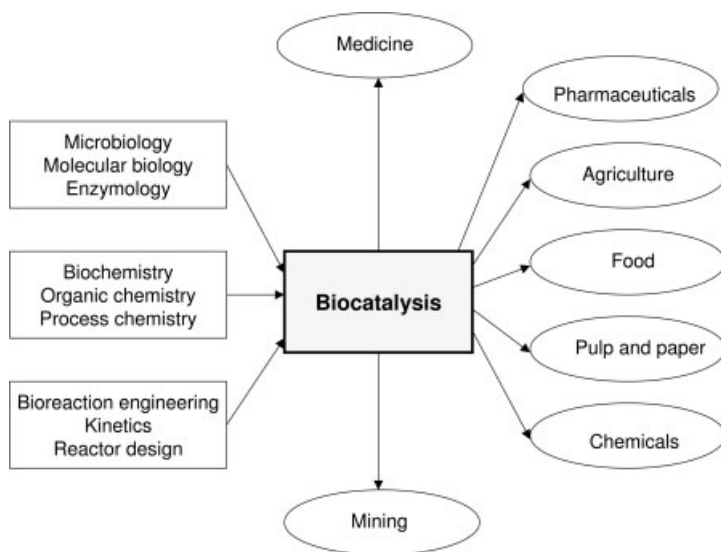


Fig. 4-1 Biocatalysis as an interdisciplinary area

Enzymes show some advantages and disadvantages with other kinds of catalysts (Table 4-1). Whereas enzymes often exhibit great advantages in terms of selectivity, their stability is often insufficient. Furthermore, long development times of new biocatalysts remain a problem and a challenge.

Table 4-1 Advantages and disadvantages of biocatalysts and enzymes [1]

| Advantages | Disadvantages |
|--|---|
| Very high enantioselectivity | often low specific activity |
| Very high regioselectivity | instability at extremes of temperature and pH |
| Transformation under mild conditions | availability for selected reactions only |
| Solvent often water | long development times for new enzymes and processes |
| Sustainable development, green chemistry | enzymes often require complicated co-substrates such as cofactors |

The greatest advantage of enzymes is their often unsurpassed selectivity, especially in the differentiation between enantiomeric substrates when a pair of substrates has Gibbs free enthalpy differences ΔG_{RS} between the *R*- and the *S*-enantiomer of around 1–3 kJ/mol. With enzymes sometimes enantioselectivities of >99% e.e. can sometimes be achieved.

There are recognized six classes of enzyme-catalyzed reaction in systematic nomenclature. Their names and the type of chemical reaction catalyzed by each are presented in Table 4-2.

Table 4-2 The six categories of enzymes according to the type of reaction [4]

| Name | Reaction catalyzed |
|-------------------|---|
| 1. Oxidoreductase | oxidation-reduction reactions |
| 2. Transferases | transfer of chemical group from one substrate to another or from one part of substrate to another |
| 3. Hydrolases | hydrolysis reactions |
| 4. Lyases | elimination of groups from adjacent atoms or addition of groups to double bonds |
| 5. Isomerases | rearrangements (isomerizations) |
| 6. Ligases | formation of bonds to groups with hydrolysis of ATP, etc. |

We will briefly illustrate how enzymatic reactions are controlled by familiar chemical principles of structure and reactivity.

Active Sites

Substrates bind at a specific site on the enzyme, which presumably contains the functional groups that interact directly with the substrate during catalysis. Therefore, the enzymes form stoichiometric enzyme-substrate (E-S) complexes. These active sites are only a small part of the overall enzyme molecule. Most enzymes consist of >100 amino acids and are roughly globular proteins with diameters >25 Å. But the substrate binding to the active site is relatively weak. The equilibrium constant for the complex formation with the substrate or a product is typically only in the range 10^{-2} to 10^{-8} M, corresponding to a value of $\Delta G = -12$ to -50 kJ/mol. An enzyme must be able to release its product readily, therefore, the E-S complex must not be too stable. The specificity of an enzyme depends on complementary structures of substrate and active site. This is called the simple lock and key model (Fig. 4-2). In practice, however, a so-called induced-fit model is more realistic. The implication of this model is that less rigid active sites fold around the substrate during complex formation.

Enzymes exhibit a multi-point contact with the substrate, that means a structural flexibility to facilitate catalysis of a reaction. These distinctive features differ from those of the active sites employed by soluble transition metal complexes and solid state catalysis. Further important factors in enzymatic catalysis are simultaneous acid and base catalysis and hydrophobic/hydrophilic interactions at the same time.

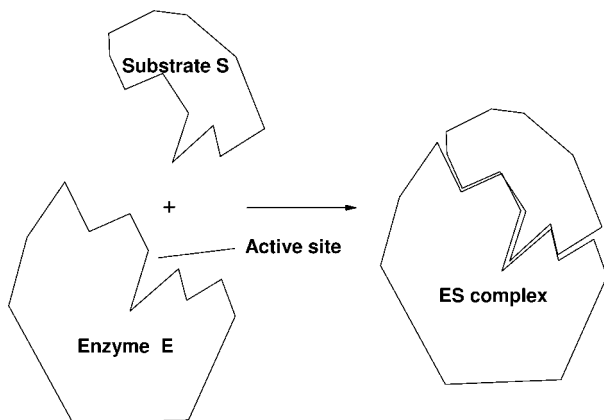


Fig. 4-2 Lock and key model for enzyme-substrate interaction

Coenzymes

In many enzymatic reactions, and in particular biological reactions, a second substrate must be introduced to activate the enzyme. This substrate, which is referred to as a cofactor or coenzyme even though it is not an enzyme as such, attaches to the enzyme and is most often either reduced or oxidized during the course of the reaction. Many enzymatic reactions require coenzymes, especially to provide the oxidizing/reducing equivalents for oxidations/reductions. An example of the type of system in which a cofactor is used is the formation of ethanol from acetaldehyde in the presence of the enzyme alcohol dehydrogenase (ADH) and the cofactor nicotinamide adenine dinucleotide (NAD):

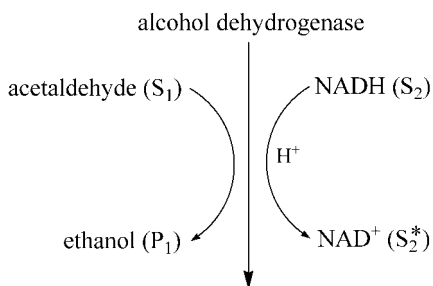


Fig. 4-3 Effect of coenzyme during acetaldehyde reduction

The problem of cofactor regeneration is an important limitation in the use of many biocatalysts, and hence requires specific consideration.

4.2

Kinetics of Enzyme-catalyzed Reactions [2, 3]

What we have seen is, that enzymes are highly specific catalysts in biological systems. Enzymes are catalytic proteins, they represent the most efficient class of catalysts. Their active site can, for example, be a carboxylic or an amino group, embedded in a specific geometry. Several weak interactions (electrostatic, H-bonds, van der Waals) help in establishing the highly specific manner in which a substrate molecule binds to the active site.

The kinetics of enzyme-catalyzed reactions resemble those of the heterogeneous reactions. However, because in practice there are a few characteristic differences in how the equations are handled, we will treat the enzymatic case as follows.

The enzyme, E, acts by forming a complex with the reactant, S, (commonly referred to as substrate), to give a product, P, according to the following scheme (Eqs. 4-1 and 4-2):



Although we can easily measure the total concentration of enzyme $[E]_{\text{tot}}$, it is difficult to measure the concentration of free enzyme $[E]$. Because enzyme, substrate and product are all in the same medium we can conveniently work with concentrations. With the total enzyme concentration $[E]_{\text{tot}}$ the conservation of active species requires that

$$[E] + [ES] = [E]_{\text{tot}} \quad (4-3)$$

The rate of product formation (Eq. 4-4) follows from the reaction equation (Eq. 4-2):

$$\frac{d[P]}{dt} = k_2[ES] \quad (4-4)$$

All relevant rates are in concentration per unit of time. The unknown concentration of the unoccupied enzymes follows by assuming that the reaction is at steady state (Eq. 4-5).

$$\frac{d[ES]}{dt} = k_1[E][S] - (k_{-1} + k_2)[ES] = 0 \quad (4-5)$$

which leads with Equation 4-3 to Equation 4-6

$$k_1[E]_{\text{tot}}[S] - k_1[ES][S] - (k_{-1} + k_2)[ES] = 0 \quad (4-6)$$

or Equation 4-7:

$$[\text{ES}] = \frac{k_1[\text{E}]_{\text{tot}}[\text{S}]}{(k_{-1} + k_2) + k_1[\text{S}]} \quad (4-7)$$

Substituting into Equation (4-4) and introducing the Michaelis constant K_M we obtain Equation 4-8:

$$r = \frac{d[\text{P}]}{dt} = \frac{k_2[\text{E}]_{\text{tot}}[\text{S}]}{K_M + [\text{S}]} \quad (4-8)$$

Equation 4-8 is the Michaelis-Menten expression for the rate of an enzymatic reaction. Compared with a gas phase molecule that reacts in a monomolecular reaction on a solid catalyst, the reciprocal of the Michaelis constant takes the place of the equilibrium constant of adsorption in the Langmuir-Hinshelwood equations. In case of very high substrate concentrations, the rate reaches its maximum (Eq. 4-9).

$$r_{\text{max}} = k_2[\text{E}]_{\text{tot}} \quad \text{for} \quad [\text{S}] \gg K_M \quad (4-9)$$

and there results a very high efficiency. Because k_2 equals $r_{\text{max}}/[\text{E}]_{\text{tot}}$, it is often referred to as the turnover frequency and hence it is also often referred to as k_{cat} . On the other hand, if the substrate concentration is much smaller than K_M , the rate is given by Equation 4-10:

$$r = \frac{k_2}{K_M}[\text{E}]_{\text{tot}}[\text{S}] \quad \text{for} \quad [\text{S}] \ll K_M \quad (4-10)$$

and most of the enzyme is free. The ratio k_2/K_M , the so-called specificity constant, is appropriate for comparing the enzymes' specificity for different substrates. There exists a practical upper limit to the value of k_2/K_M of about $10^9 \text{ mol L}^{-1} \text{ s}^{-1}$, due to the rate of diffusion of substrate molecules to the enzyme through the solution. Hence enzymatic reactions approaching this upper limit are nearly perfect. For example, the enzyme catalase, which catalyzes the decomposition of H_2O_2 to H_2O and O_2 at a turnover number of $k_{\text{cat}} = 10^7 \text{ s}^{-1}$ and a high specificity constant of $k_{\text{cat}}/K_M = 4 \cdot 10^8 \text{ mol L}^{-1} \text{ s}^{-1}$. Such activities are orders of magnitude higher than those of heterogeneous catalysts.

The rate for an enzyme-catalyzed reaction can be normalized as been shown in Figure 4-4.

Figure 4-4 shows the possibility of controlling the enzyme-catalyzed reaction depending on the substrate concentration. The rate of product formation can be optimally controlled in the low substrate concentration regime. When the enzymes are almost saturated by substrate the rate hardly changes with $[\text{S}]$. Therefore, in cases where substrate control of the rate is important, the reaction should ideally run in the region of substrate concentration between 5 and 10 K_M .

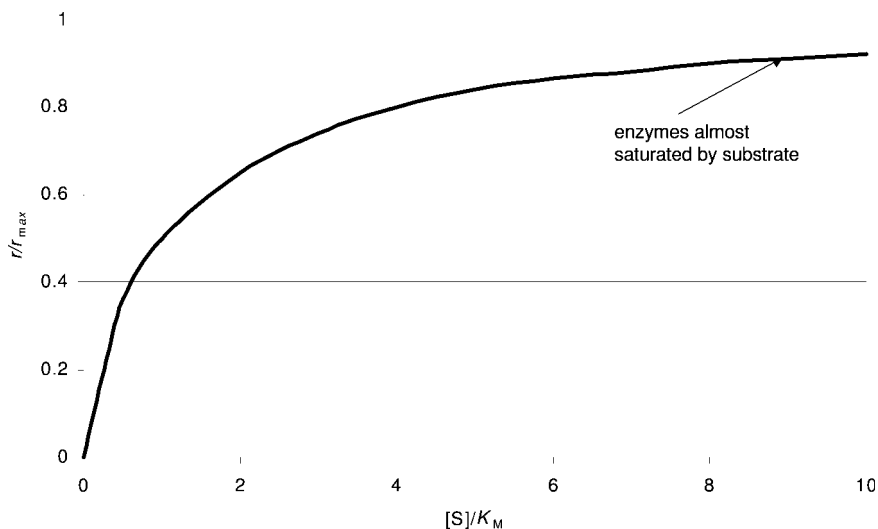


Fig. 4-4 Normalized rate for an enzyme-catalyzed reaction

For practical purposes, it is convenient to rearrange the Michaelis-Menten rate expression to Equation 4-11:

$$\frac{1}{r} = \frac{1}{k_2[E]_{\text{tot}}} + \frac{K_M}{k_2[E]_{\text{tot}}[S]} = \frac{1}{r_{\max}} + \frac{K_M}{k_2[E]_{\text{tot}}[S]} \quad (4-11)$$

Making use of Equation 4-11 a plot of $1/r$ versus $1/[S]$ is linear with a slope $K_M/k_2[E]_{\text{tot}}$ and an intercept $1/r_{\max}$. Such a graph is a so-called Lineweaver-Burk plot, as be shown in Figure 4-5:

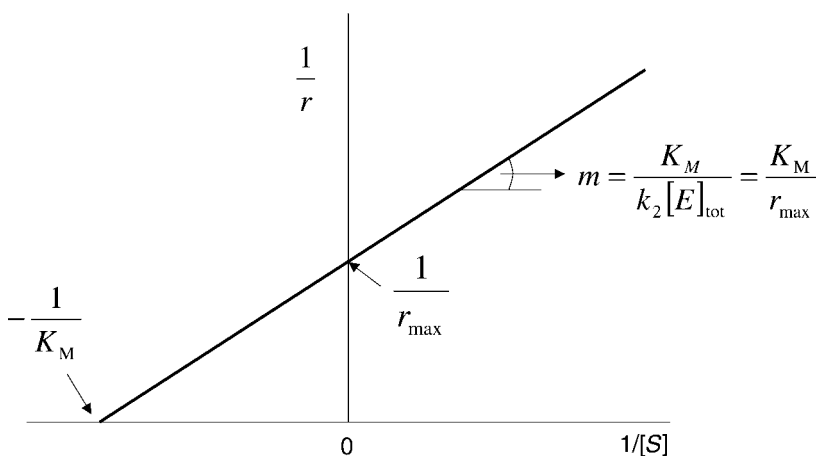


Fig 4-5 Lineweaver-Burk plot [2]

Another factor that greatly influences the rate of enzyme-catalyzed reactions in addition to pH and temperature is the presence of an inhibitor. As follows, we need to mention the effect that different inhibitors have on the rate. The three most common types of reversible inhibition occurring in enzymatic reactions are competitive, uncompetitive, and noncompetitive [3]. The enzyme molecule is analogous to the heterogeneous catalytic surface in that it contains active sites. When competitive inhibition occurs, the substrate and inhibitor are usually similar molecules that compete for the same site on the enzyme. The resulting inhibitor-enzyme complex is inactive. The reactions can be developed as follows (Eq. 4-1 and Eqs. 4-12 to 4-3).



From these reactions the rate law for *competitive inhibition* can be obtained as

$$r = \frac{r_{\max}[S]}{[S] + K_M(1 + [I]/K_i)} \quad (4-14)$$

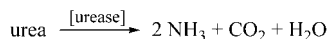
with I = inhibitor and K_i = inhibition constant.

Competitive inhibition is important in biological control mechanisms; for instance, if the product acts as an inhibitor. For instance, the enzyme invertase catalyzes the hydrolysis of sucrose into glucose and fructose. As glucose is a competitive inhibitor, it ensures that the reaction does not to proceed too far.

Uncompetitive inhibition occurs when the inhibitor deactivates the enzyme-substrate complex, usually by attaching itself to both the substrate and enzyme molecules of the complex. *Noncompetitive inhibition* occurs with enzymes containing at least two different types of sites. The inhibitor attaches to only one type of site and the substrate only to the other [3].

Example: Determination of an Enzyme-catalyzed Reaction [3]

Determine the Michaelis-Menten parameters r_{\max} and K_M for the enzyme-catalyzed reaction



The rate of reaction is given as a function of urea (substrate S) concentration in the following table:

| | | | | | |
|---|------|------|------|-------|-------|
| [S] (kmol/m ³) | 0.2 | 0.02 | 0.01 | 0.005 | 0.002 |
| r (kmol m ⁻³ s ⁻¹) | 1.08 | 0.55 | 0.38 | 0.2 | 0.09 |

Solution:

Inverting Equation 4-8 $r = \frac{r_{\max} [S]}{K_M + [S]}$ gives us Equations 4-15 and 4-16:

$$\frac{1}{r} = \frac{1}{r_{\max}} + \frac{K_M}{r_{\max}} \frac{1}{[S]} \quad (4-15)$$

(y) (x)

$$y = a + b x \quad (4-16)$$

A plot of the reciprocal reaction rate versus the reciprocal urea concentration should be a straight line with an intercept $1/r_{\max}$ and slope K_M/r_{\max} (Lineweaver-Burk plot). We can solve this equation either graphically or numerically using the POLYMATH nonlinear regression program. The following table can be set up:

| [S] (kmol/m ³) | <i>r</i> (kmol m ⁻³ s ⁻¹) | 1/[S] (m ³ /kmol) | 1/ <i>r</i> (m ³ s kmol ⁻¹) |
|-------------------------------|---|---------------------------------|---|
| 0.20 | 1.08 | 5.0 | 0.93 |
| 0.02 | 0.55 | 50.0 | 1.82 |
| 0.01 | 0.38 | 100.0 | 2.63 |
| 0.005 | 0.20 | 200.0 | 5.00 |
| 0.002 | 0.09 | 500.0 | 11.11 |

Solving Equation 4-16 numerically yields

$$a = 0.755$$

$$b = 0.0207$$

So, $a = 1/r_{\max} = 0.755$ and $r_{\max} = 1.325$

$$b = 0.0207 = K_M/r_{\max}$$

$$K_M = 0.0207 r_{\max} = 0.0207 \cdot 1.325 = 0.027.$$

Substituting K_M and r_{\max} into Equation (4-8) yields

$$r = \frac{r_{\max} [S]}{K_M + [S]} = \frac{1.325 [S]}{0.027 + [S]}$$

Figure 4-6 shows the Lineweaver-Burk plot corresponding to the example.

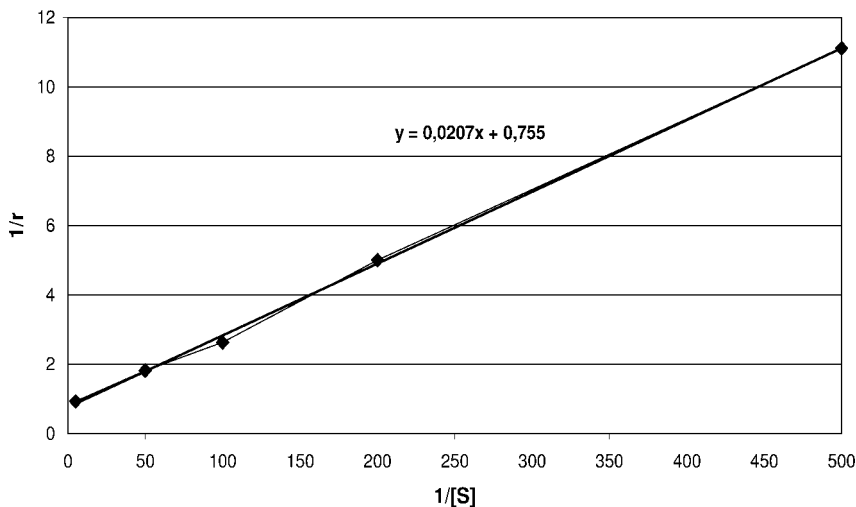


Fig. 4-6 Lineweaver-Burk plot for the urea reaction

4.3

Industrial Processes with Biocatalysts [1, 4]

Biocatalytic processes and technologies are penetrating increasingly in all branches of the chemical process industries. In basic chemicals, nitrile hydratase and nitrilases have been most successful. For example, acrylamide from acrylonitrile is now a 30,000 t/a process. In fine chemicals, enantiomerically pure amino acids are produced by several different companies.

The food industry is also a large area for biocatalysis applications: high-fructose corn syrup (HFCS) from glucose with glucose isomerase, the thermolysin-catalyzed synthesis of the artificial sweetener Aspartame[®], and synthesis of nutraceuticals such as L-carnitine can serve as examples.

Enzymatic processes are important in the areas of crop protection and pharma intermediates too. Technical improvements can result directly from immobilization (e.g. increased product purity and/or yield, reduced waste production) but also indirectly. Immobilization of cells or enzymes enables the use of continuous rather than batch operation, thus simplifying process control and reducing labor costs. Of course, this is only advantageous for large-scale processes, whereas most bioproducts are only produced on a small scale.

Immobilized enzymes are mainly used in the production of fine chemicals and pharmaceuticals, because currently they cannot compete economically with conventional catalysts in the bulk chemical industry. Here, we will focus only on some examples from the following areas: basic chemicals, fine chemicals, food industry and crop protection intermediates.

4.3.1

Acrylamide from Acrylonitrile [1, 4, 5]

Acrylamide is the first bulk chemical manufactured using an industrial biotransformation. Acrylamide which is produced 200 000 t/a is an important industrial chemical that is mainly processed into water-soluble polymers and copolymers, which find applications as flocculants, paper-making aids, thickening agents, surface coatings, and additives for enhanced oil recovery. The chemical manufacture of acrylamide has been established for a long time, it is based on Cu-catalysis. The production of acrylamide using immobilized whole cells of *Rhodococcus rhodochrous* is a remarkable example of a lyase-catalyzed commercial process. The enzyme responsible for water addition to the double bond of acrylonitrile is nitrile hydratase (Eq. 4-17):



Both the conventional and bio-processes involve the same reaction.

In Table 4-3 are given some details of each process for comparison:

Table 4-3 Acrylamide by chemical process and by biotransformation [5]

| Conventional Process | | Biotransformation |
|------------------------------------|---|--|
| <i>Catalyst</i> | A copper salt | the enzyme nitrile hydratase in whole cells of <i>Rhodococcus rhodochrous</i> , immobilized on poly(propenamide) gel |
| | The rate of acrylamide formation is slower than the rate of acrylic acid formation | the immobilized cells can be used repeatedly |
| <i>Conditions</i> | High energy input | pH 7.5, 5 °C; yield >99,99% |
| <i>Separation and purification</i> | Copper ions need to be removed from product; difficult to separate and purify the acrylamide; large quantities of toxic waste | no need to recover unreacted acrylonitrile because the yield is so high; polyacrylamide of higher molecular weight |

The biocatalytic acrylamide process is carried out by Nitto Chemical Corp., now part of the Mitsubishi Rayon Corp., on a scale of 30 000 t/a, in fed batch mode up to 25–40% acrylamide at 0–10 °C to complete conversion with a significant cost advantage with respect to the conventional chemical process.

4.3.2

Aspartame through Enzymatic Peptide Synthesis [1]

Aspartame is a dipeptide ester, α -L-aspartyl-L-phenylalanine-OMe, 200 times as sweet as sucrose. Aspartame is utilized by now as a low-calorie sweetener in soft drinks, salad dressings, ready-made meals, table-top sweeteners, and pharmaceuticals, and had reached a market volume of 12 000–15 000 t/a. One of the most successful and interesting syntheses is the Toyo Soda enzymatic process which runs on an industrial scale in a joint venture with DSM (Dutch State Mines, Geleen, NL).

Formation of the peptide bond is catalyzed by thermolysin, a neutral zinc protease (Fig. 4-7). The enzyme employed was found in the bacterial strain *Bacillus proteoliticus/thermoproteolyticus* in the Rokko Hot Spring in Japan. The enzyme is stable up to temperatures of 60 °C. It is extracted and used in a form soluble in water. In this process the amino acids phenylalanine and aspartic acid are coupled by the enzyme. The process, including the main steps, is shown schematically in Fig. 4-7.

The reaction is limited by the equilibrium position, and so products have to be removed from the mixture in order to achieve high yields. In excess of phenylalanine methyl ester the protected aspartame forms a poorly soluble carboxylate anion which precipitates from the reaction mixture. This makes it easy to remove by filtration. The last step of the process is the removal of protecting group by conventional

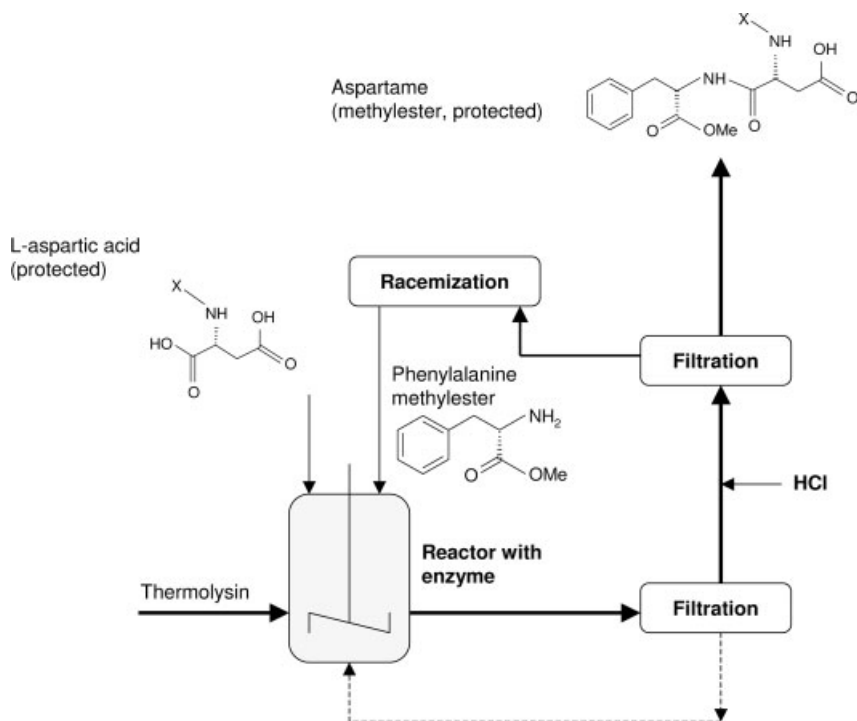


Fig. 4-7 Biosynthetic route to aspartame [5]

hydrogenation. More than 99.99% of the aspartame produced by this enzyme-catalyzed process is the required sweet isomer. It is hard to imagine any method other than enzyme catalysis giving such a high selectivity [5].

The advantages of this process are:

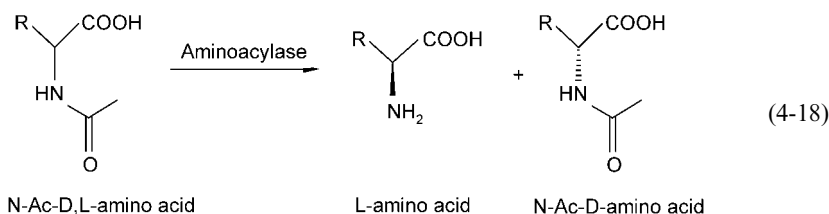
- The enzyme is completely stereo selective, this means that it is possible to use either a racemic mixture or the L-isomer of the substrate.
- None of the bitter isomer of aspartame is produced.
- The reaction takes place under mild conditions (pH 7.0–7.5, temperature 50 °C, in aqueous solution).
- After the enzyme reaction there is further chemical processing to remove protecting groups, and to convert the methyl ester to aspartame itself.

4.3.3

L-Amino Acids by Aminoacylase Process [1]

The demand for L-amino acids for food and medical applications is growing fast. Both chemical and microbial processes can be used for their production. However, the chemical routes lack stereoselectivity, thus leading to lower productivity. In Japan the immobilized enzyme aminoacylase has been used for the production of L-amino acids, of which methionine is the most important, since 1996.

The best-established method for the enzymatic production of L-amino acids is the separation of racemates of *N*-acetyl-DL-amino acids by aminoacylase. *N*-Acetyl-L-amino acid is cleaved and yields L-amino acids whereas the D-amino acid compound does not react (Eq. 4-18).



The L-amino acid is separated by ion exchange or by crystallization, in the following step the remaining *N*-acetyl-D-amino acid is recycled by thermal racemization under drastic conditions or by a racemase to achieve an overall yield of about 45%. The aminoacylase process was commercialized by Tanabe Seiyaku (Japan) in 1969 using the very first immobilized enzyme reactor system at all whereas the process has been run in batch mode since 1954. Especially for the continuous process, enzyme from *Aspergillus oryzae* fungus was immobilized. Degussa (Frankfurt, Germany) introduced 1982 the enzyme membrane reactor applying soluble enantioselective L-aminoacylase from the strain mentioned above. Currently, several hundred tons per year of L-methionine are produced by this enzymatic conversion technology. Figure 4-8 shows a scheme of the Degussa enzyme membrane reactor.

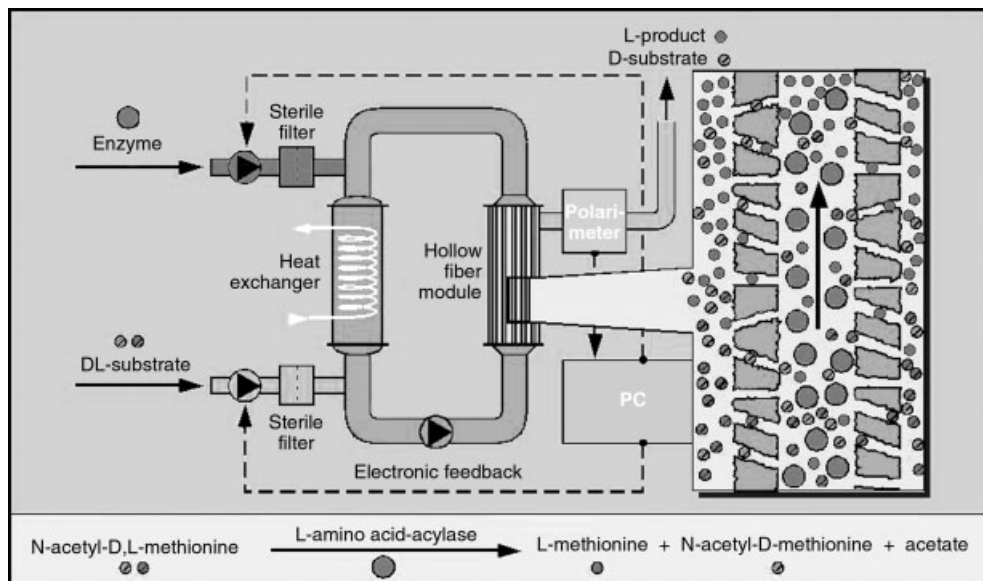
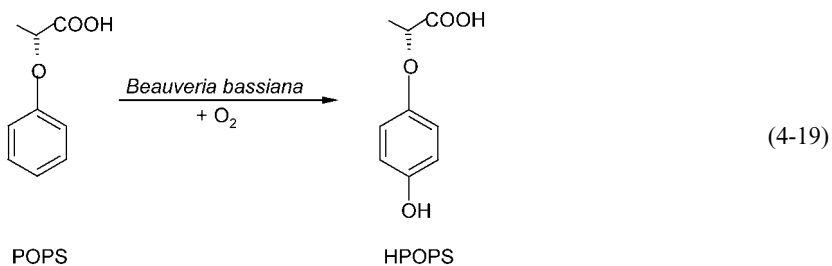


Fig. 4-8. Pilot scale enzyme membrane reactor for the production of L-amino acids (Degussa AG)

4.3.4

4-Hydroxyphenoxypropionic Acid as Herbicide Intermediate [1]

The hydroxylation of aromatics serves as an example for a successful industrial production of intermediates in a technical scale. BASF Ludwigshafen produces isomerically pure (*R*)-2-(4-hydroxyphenoxy)-propionic acid (HPOPS) from (*R*)-2-phenoxypropionic acid (POPS) in a 100 m³ fermenter for use as a herbicide intermediate (Eq. 4-19).



Despite the good product properties (chemical composition >99%, e.e. >98%) the best strain from a huge collection had to be further developed. Starting with classical mutation techniques, the space time yield could be improved from 0.5 g L⁻¹ d⁻¹ to 7.0 g L⁻¹ d⁻¹ and the substrate/product tolerance could be increased to 100 g/L. It took several years to increase the product titer from 1–5 g/L to 120 g/L after muta-

tion of the parent strain. Today this hydroxylation of aromatics runs on a scale of >100 t/a.

Finally, we can draw the following conclusions from this chapter:

- Biocatalysis includes both enzyme catalysis and biotransformation using whole microorganisms.
- Biocatalysis is a dynamic area of research providing many chances for innovation.
- Major chemical companies have built up groups and have arrived successfully at products.
- The quest for sustainable production (chemicals and energy) favors biocatalysis.
- Chiral intermediates made through biocatalysis are a growing business.

► Exercises for Chapter 4

Exercise 4.1

Make a table comparing advantages and disadvantages of enzymes with conventional homogeneous and heterogeneous catalysts. Include comparisons of catalyst activity, selectivity, stability, sensitivity to reaction environment and cost.

Exercise 4.2

Compare the advantages and disadvantages of using enzymes in either their natural cell environment or in immobilized form.

Exercise 4.3

Kinetics of enzyme-catalyzed reactions may often be reported as a turnover frequency. Explain this term.

Exercise 4.4

The form of kinetics describing the typical enzyme-catalyzed reaction is the following (the Michaelis–Menten equation):

$$r = \frac{k_{\text{cat}} [E]_{\text{tot}} [S]}{K_M + [S]}$$

Interpret the terms k_{cat} and K_M (the Michaelis constant) and show that the form of the kinetics is equivalent to Langmuir–Hinshelwood kinetics.

Exercise 4.5

What are cofactors, what do you know about their mode of operation?

Exercise 4.6

Explain why very tight binding of a substrate to an enzyme is not desirable for enzyme catalysis, whereas tight binding of the transition state is.

Exercise 4.7

Compare competitive inhibition and uncompetitive inhibition in enzyme catalysis.

Exercise 4.8

Explain the distinction between enzyme fermentations and microbial fermentations.

5 Heterogeneous Catalysis: Fundamentals

5.1 Individual Steps in Heterogeneous Catalysis

Heterogeneously catalyzed reactions are composed of purely chemical and purely physical reaction steps. For the catalytic process to take place, the starting materials must be transported to the catalyst. Thus, apart from the actual chemical reaction, diffusion, adsorption, and desorption processes are of importance for the progress of the overall reaction.

We will now consider the simplest case of a catalytic gas reaction on a porous catalyst. The following reaction steps can be expected (Fig. 5-1) [T20, T26]:

- 1) Diffusion of the starting materials through the boundary layer to the catalyst surface.
- 2) Diffusion of the starting materials into the pores (pore diffusion).
- 3) Adsorption of the reactants on the inner surface of the pores.
- 4) Chemical reaction on the catalyst surface.
- 5) Desorption of the products from the catalyst surface.
- 6) Diffusion of the products out of the pores.
- 7) Diffusion of the products away from the catalyst through the boundary layer and into the gas phase.

In heterogeneous catalysis chemisorption of the reactants and products on the catalyst surface is of central importance, so that the actual chemical reaction (step 4) can not be considered independently from steps 3 and 5. Therefore, these steps must be included in the microkinetics of the reaction. In cases where the other transport processes discussed above play a role, the term macrokinetics is used.

The measured reaction rate, known as the effective reaction rate, is determined by the most strongly inhibited and therefore slowest step of the reaction sequence. This rate-determining step also determines the reaction order.

The effective reaction rate r_{eff} is influenced by many parameters, including the nature of the phase boundary, the bulk density of the catalyst, the pore structure, and the transport rate in the diffusion boundary layer. If the physical reaction steps are rate determining, then the catalyst capacity is not fully exploited.

If one wishes to determine the mechanism and to describe it exactly in terms of rate equations, then one must ensure that only steps 3–5 are rate determining.

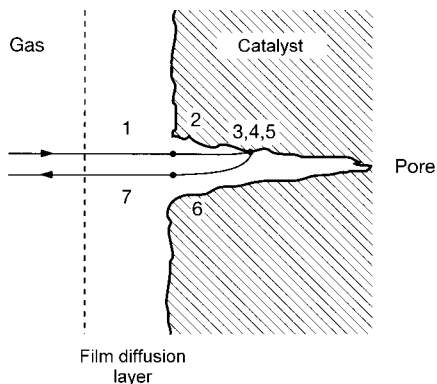


Fig. 5-1 Individual steps of a heterogeneously catalyzed gas-phase reaction

For example, the film diffusion resistance can be suppressed by increasing the gas velocity in the reactor. If pore diffusion is of decisive influence, then the ratio of the outer to the inner surface area is too small. In this case, lowering the particle size of the catalyst shortens the diffusion path, and the reaction rate increases until it is no longer dependent on pore diffusion.

Plotting concentration against position in the pore provides information about the ratio of the reaction rate to the transport rate. First we shall discuss this qualitatively. As shown in Figure 5-2, the following regions can be distinguished:

- Film diffusion region: the reaction is fast compared to diffusion in the film layer and to diffusion in the pores.
- Pore diffusion region: the reaction is fast compared to diffusion in the pores, but slow compared to film diffusion.
- Kinetic region: the reaction is slow compared to diffusion in the pores and through the gas film.

Changing the temperature changes the ratio of reaction to transport rate (Fig. 5-3). In the kinetic region, the reaction rate increases rapidly with increasing temperature, as in a homogeneous reaction obeying the Arrhenius law. In the pore diffusion region, the reaction rate also increases according to the Arrhenius law, but at the same time the con-

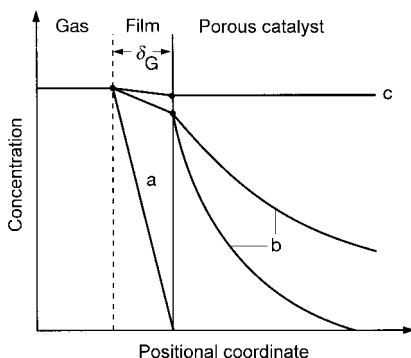


Fig. 5-2 Concentration–position curves in the film diffusion region (a), the pore diffusion region (b), and the kinetic region (c)

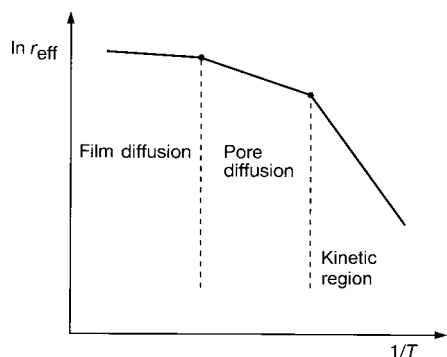


Fig. 5-3 Dependence of effective reaction rate on temperature

centration profile becomes steeper, so that an ever decreasing fraction of the catalyst is active. This results in a less rapid increase of the reaction rate than in the kinetic region.

In the film diffusion region, r_{eff} increases slowly with increasing temperature because the diffusion has only a slight temperature dependence. There is practically no reaction resistance, and the gas already undergoes complete conversion on the outer surface of the catalyst.

Mathematical treatment of the total catalytic process is complicated by strong coupling of the physical and chemical reaction steps, and by the heat of reaction of the chemical reactions. This leads to temperature and pressure gradients that are difficult to solve mathematically.

Basic homogeneous and heterogeneous reactions are compared in Table 5-1. It can be seen again that there are some similarities between both areas of catalysis.

Table 5-1 Comparison of homogeneous and heterogeneous catalytic reactions

| Homogeneous | Heterogeneous |
|---|--|
| – | Diffusion of the reactants to the catalyst surface active centers at the surface |
| Coordinatively unsaturated centers – generation of vacant sites | |
| Molecular coordination of small molecules such as H_2 | physical adsorption (physisorption) |
| Oxidative addition with formation of chemical bonds | chemical adsorption (chemisorption) |
| Insertion reaction; formation and conversion of metallacyclic compounds; nucleophilic or electrophilic attack | reactions on the catalyst surface |
| Reductive elimination; β -elimination | desorption of the products, diffusion of the products away from the catalyst |

5.2

Kinetics and Mechanisms of Heterogeneously Catalyzed Reactions [T20, T32]

Knowledge concerning the kinetic parameters of a catalytic reaction is of major practical importance:

- 1) Knowledge of the reaction order with respect to the reactants and products is a prerequisite for studying the mechanism of the reaction. A precise reaction mechanism allows the catalyst to be optimized on a scientific basis.
- 2) The design of the reactor, including the size and shape of the catalyst particles, depends directly on the reaction order of the reactants and the thermodynamic conditions (see also Chapter 14).
- 3) The influence of temperature on the reaction rate can give helpful indications as to which is the slowest step of the total catalytic process.

As we have already seen in the preceding chapter, the adsorption steps that precede and follow the chemical reaction are part of the microkinetics. For this reason we shall now deal with the phenomenon of adsorption in more detail.

5.2.1

The Importance of Adsorption in Heterogeneous Catalysis [T42, T43]

First we must distinguish between physical adsorption (physisorption) and chemical adsorption (chemisorption).

Physisorption is the result of van der Waals forces, and the accompanying heat of adsorption is comparable in magnitude to the heat of evaporation of the adsorbate. In chemisorption, chemical bonds are formed between the catalyst and the starting material. The resulting surface molecules are much more reactive than free adsorbate molecules, and the heats of adsorption are comparable in magnitude to heats of chemical reaction. This is demonstrated by the following example: the heat of adsorption of oxygen on carbon is ca. 330 kJ/mol, which is almost as high as the heat of combustion of carbon (394 kJ/mol).

One might be tempted to believe that highly effective adsorbents are also good catalysts, but in reality the situation is not so simple, because catalytic reactions proceed highly specifically. Today it is known that adsorption is a necessary but not sufficient prerequisite for molecules to react with one another under the influence of a solid surface. Furthermore, it is important that a distinction be made between the amount of adsorbed substance and the rate of adsorption.

Since both types of adsorption are exothermic, raising the temperature generally decreases the equilibrium quantity of adsorbate. Physisorption is fast, and equilibrium is rapidly reached, even at low temperature. Chemisorption generally requires high activation energies. The rate of adsorption is low at low temperatures, but the process can be rapid at higher temperatures.

The rate of both types of adsorption is strongly dependent on pressure. Chemisorption leads only to a monolayer, whereas in physisorption multilayers can form. Table 5-2 compares the two types of adsorption.

Table 5-2 Comparison of physisorption and chemisorption

| | Physisorption | Chemisorption |
|--------------------|---|--|
| Cause | van der Waals forces, no electron transfer | covalent/electrostatic forces, electron transfer |
| Adsorbents | all solids | some solids |
| Adsorbates | all gases below the critical point, intact molecules | some chemically reactive gases, dissociation into atoms, ions, radicals |
| Temperature range | low temperatures | generally high temperatures |
| Heat of adsorption | low, \approx heat of fusion (ca. 10 kJ/mol), always exothermic | high, \approx heat of reaction (80–200 (600) kJ/mol), usually exothermic |
| Rate | very fast | strongly temperature dependent |
| Activation energy | low | generally high (unactivated: low) |
| Surface coverage | multilayers | monolayer |
| Reversibility | highly reversible | often reversible |
| Applications | determination of surface area and pore size | determination of surface concen- trations and kinetics, rates of adsorption and desorption, deter- mination of active centers |

The surface also has a major influence on adsorption. Whereas in physisorption only the magnitude of the surface area is important, chemisorption is highly specific. For example, hydrogen is chemisorbed by nickel but not by alumina, and oxygen by carbon but not by MgO. Some examples of chemisorption processes are given in Table 5-3.

The type of surface also has considerable influence on chemisorption, with surface irregularities such as corners, edges, and lattice defects playing a major role. In particular, raised areas, generally atoms with free valences, are referred to as active centers. The number of active centers is shown by the example of cumene cracking,

Table 5-3 Examples of chemisorption processes

| System | Heat of chemisorption [kJ/mol] | Activation energy [kJ/mol] |
|---|-----------------------------------|-------------------------------|
| H ₂ on graphite | 189 | 25 |
| CO on Cr ₂ O ₃ | 38–63 | 0.8–3 |
| N ₂ on Fe (with promoters Al ₂ O ₃ , K ₂ O) | 147 | 67 |
| CO on Pd | 72–76 | 9.6–38.0 |
| H ₂ on W powder | 84–315 | 42–105 |

in which the active-center concentration is $3.6 \times 10^{19}/\text{g}$ catalyst or $1.2 \times 10^{17}/\text{m}^2$ catalyst surface.

Finally, let us summarize the most important factors influencing the reaction kinetics:

- 1) Adsorption is a necessary step preceding the actual chemical reaction on solid catalyst surfaces.
- 2) Heterogeneous catalysis involves chemisorption, which has the characteristics of a chemical reaction in that the molecules of the starting material react with the surface atoms of the catalyst.
- 3) Catalyst surfaces have heterogeneous structures, and chemisorption takes place preferentially at active sites on the surface.

In the following we shall consider the fundamental laws of adsorption, which provide the basis for the rate expressions of heterogeneously catalyzed reactions [15, T32].

Adsorption equilibria are normally described empirically. The Freundlich equation (Eq. 5-1) describes general practical cases of adsorption.

$$c_A = a p_A^n \quad (5-1)$$

c_A = concentration of the adsorbed gas

p_A = partial pressure of the adsorbed gas under equilibrium conditions

a = empirical constant

n = fraction between 0 and 1

Experimentally it is found that the amount of gas adsorbed by a solid increases with increasing total pressure P . Langmuir expressed the concentration of the adsorbed gas as a function of the partial pressure p_A and two constants (Eq. 5-2).

$$c_A = \frac{a b p_A}{(1 + b p_A)} \quad a, b = \text{empirical constants} \quad (5-2)$$

The adsorption isotherm rises up to a quantity of adsorbed substance corresponding to mononuclear coverage of the boundary layer (Fig. 5-4).

Consideration of the boundary conditions shows that for large values of b or p_A , $c_A = a$, an expression identical to the Freundlich equation with $n = 0$. At very low partial pressure p_A or very small values of b , Equation 5-2 becomes the Freundlich equation with $n = 1$ (Eq. 5-3).

$$c_A = a b p_A \quad (5-3)$$

The intermediate pressure range can therefore be described by the Freundlich equation with $n = 0-1$.

For a better understanding of catalysis we shall now derive the Langmuir equation on the basis of chemisorption on the active centers of the catalyst. Langmuir assumed the simple case of an energetically homogeneous catalyst surface, so that the adsorption enthalpy is independent of the degree of coverage of the surface θ_A .

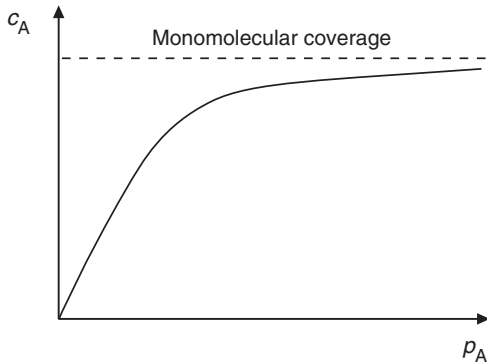


Fig. 5-4 Langmuir isotherm

For the reaction of a molecule A from the gas phase with a free site of the catalyst surface F:



the law of mass action is

$$K_A = \frac{c_{AF}}{c_F p_A} \quad (5-5)$$

c_{AF} = effective concentration of chemisorbed A per unit mass of catalyst

c_F = effective concentration of active centers on the surface of the catalyst per unit mass of adsorbent

Introducing the degree of coverage of the surface we obtain

$$c_{AF} = \theta_A \quad \theta_A = \text{Degree of coverage of starting material A}$$

$$c_F = (1 - \theta_A)$$

and Equation 5-5 becomes Equation 5-6

$$K_A = \frac{\theta_A}{(1 - \theta_A) p_A} \quad (5-6)$$

which can be rearranged in terms of the degree of coverage θ_A (Eq. 5-7)

$$\theta_A = \frac{K_A p_A}{1 + K_A p_A} \quad (5-7)$$

The Langmuir isotherms derived therefrom provide the basis for the formulation of rate equations.

Consider a mononuclear gas-phase reaction $A \rightarrow C$ in which A is adsorbed without dissociation and the product C is not adsorbed. The reaction rate with respect to A thus depends only on the concentration of adsorbed A, that is, on its degree of coverage (Eq. 5-8).

$$-\frac{dp_A}{dt} = k\theta_A = \frac{kK_A p_A}{1 + K_A p_A} \quad (5-8)$$

Considering the boundary conditions shows that:

- 1) If K_A or p_A becomes so small that the product $K_A p_A \ll 1$, then $\theta_A \approx K_A p_A$ and the reaction is first order in A. Under these conditions the degree of coverage is low.
- 2) If K_A or p_A becomes so large that the product $K_A p_A \gg 1$, then θ_A becomes independent of p_A and the reaction is zero order in A. This is the case when the degree of coverage is near unity.

If neither of these approximations applies, the reaction order in A must lie between 0 and 1. If it is possible to follow the reaction order of such a reaction over a wide pressure range, then at low pressure a reaction order of unity would be observed, which at higher pressures eventually drops to zero.

Let us now consider another widely occurring situation: mixed adsorption. In this case two gases A and B compete for free sites on the catalyst surface. The number of free sites is now $1 - \theta_A - \theta_B$, and Equations 5-9 and 5-10 are obtained for the degrees of coverage of the two starting materials.

$$\theta_A = \frac{K_A p_A}{1 + K_A p_A + K_B p_B} \quad (5-9)$$

$$\theta_B = \frac{K_B p_B}{1 + K_A p_A + K_B p_B} \quad (5-10)$$

Some molecules undergo dissociative chemisorption on the surface, as we shall see below. For the reaction:



we obtain the expression

$$\theta_A = \frac{K_A \sqrt{p_A}}{1 + K_A \sqrt{p_A}} \quad (5-12)$$

Other possibilities for the adsorption of gas molecules can be discussed in an analogous manner, and the derived relationships serve as the basis for rate equations and for understanding the mechanisms of heterogeneously catalyzed reactions [2].

5.2.2

Kinetic Treatment [8, T26]

A prerequisite for the design and operation of chemical reactors is knowledge of the dependence of the reaction rate r on the process parameters. It has proved useful to make a distinction between micro- and macrokinetics. Whereas the true reaction rate (microkinetics) depends only on the concentration of the reactants, the temperature, and the catalyst, the macrokinetics in industrial systems are additionally influenced by mass- and heat-transfer processes in the reactor.

According to Equation 1-2, the reaction rate can depend on the concentration of all the reactants, but also on the concentration of the catalyst. It should be noted that a rate equation as a time law, the so-called formal reaction kinetics, does not describe the reaction mechanism of a chemical conversion. A strict distinction must be made between molecularity (i.e., the number of molecules involved in an elementary step) and reaction order.

As we have already seen, there are reactions for which a constant reaction order can not be given, that is, the reaction rate can not be expressed in terms of a power of the concentration. This is often the case for heterogeneous reactions.

In the case of heterogeneous reactions the reaction rate can be expressed relative to the specific surface area S of the catalyst (m^2/kg) instead of the reaction volume in Equation 1-2 (Eq. 5-13).

$$r_{A,S} = -\frac{1}{S} \frac{dn_A}{dt} = k f(c_A) \text{ kmol kg m}^{-2} \text{ s}^{-1} \quad (5-13)$$

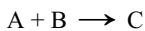
The most practical approach, however, is to express the reaction rate relative to the mass of catalyst m_{cat} to give an expression for the effective reaction rate $r_{A,\text{eff}}$ (Eq. 5-14).

$$r_{A,\text{eff}} = -\frac{1}{m_{\text{cat}}} \frac{dn_A}{dt} = k f(c_A) \text{ kmol kg}^{-1} \text{ s}^{-1} \quad (5-14)$$

It should again be emphasized that the effective reaction rate in heterogeneous reactions depends not only on the temperature and the concentration of the reactants, but also on macrokinetic parameters such as phase boundary, bulk density, and particle size of the catalyst; pore structure; and rate of diffusion.

In the following we will deal with setting up rate equations for simple heterogeneously catalyzed gas-phase reactions [T20, T26].

Consider the gas-phase reaction



The dependence of the reaction rate on the partial pressure of the components can in general form be expressed as a power law of the type

$$r = k p_A^a p_B^b p_C^c \quad (5-15)$$

where r is the effective reaction rate per unit mass of catalyst and k is the rate coefficient, the dimensions of which depend on the values of the exponents a , b , and c . The exponents are generally not equal to unity. It is noteworthy that in homogeneous reactions the product does not normally appear in the rate equation (i.e., c is generally zero). In heterogeneous reactions the product can remain adsorbed on the surface and thus influence the reaction rate.

The applicability of such formal approaches is limited by the fact that the exponents are not always constants and may be dependent on temperature and pressure. Such treatments are generally restricted to narrow pressure ranges and are therefore not particularly meaningful.

A better basis for developing rate equations can often be obtained by modelling the adsorption and desorption of the reaction partners on active centers. The rate equations then contain the partial pressures of the components of the reaction mixture. The effective reaction rate can be expressed as the ratio of the product of the kinetic term and the driving force (or distance from equilibrium) to the resistance term (Eq. 5-16).

$$r_{\text{eff}} = \frac{(\text{kinetic term}) \cdot (\text{driving force})}{(\text{resistance term})^n} \quad (5-16)$$

The exponent n usually has the value 1 or 2 and depends on the number of catalytically active centers of the catalyst surface that are involved in the rate-determining step. The resistance term can also be referred to as the chemisorption term.

The terms in Equation 5-16 contain the relative adsorptivity of the catalyst for the individual components of the reaction mixture. For a complete derivation of the kinetics of a catalytic reaction, that is, the functional relationship between r and the variables concentration, temperature, and pressure, the reaction mechanism must be known. It is often sufficient to formulate the kinetic equation in terms of the slowest, rate-determining elementary step [2]. In this way, multiparameter equations can often be replaced by equivalent rate expressions that describe the influence of the most important experimental variables with sufficient accuracy. For irreversible reactions in which the rate of mass transport is decisive, simple expressions of the type shown in Equation 5-17 are often sufficient.

$$r_{\text{eff}} = k p_A^n \quad (5-17)$$

or, for the reaction $A + B \longrightarrow R + S$

$$r_{\text{eff}} = \frac{k p_A p_B}{(1 + K_A p_A + K_R p_R)^n} \quad (5-18)$$

Rate expressions such as those of Equations 5-17 and 5-18 are based on the theory of active centers.

The methods for determining reliable rate equations that describe the mechanisms of heterogeneously catalyzed reactions, some of which are quite laborious, will not

be described in further detail here. Chemical engineers are interested in the kinetics of a reaction in so far as they can be used in reactor design.

5.2.3

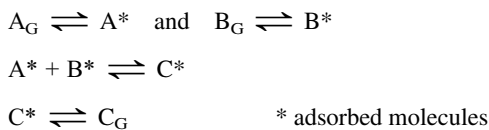
Mechanisms of Heterogeneously Catalyzed Gas-Phase Reactions [15, 34, T35]

In this chapter we shall deal with bimolecular gas-phase reactions, which occur widely in heterogeneous catalysis. Two mechanisms are often discussed for reactions of the type:



5.2.3.1 Langmuir–Hinshelwood Mechanism (1921)

This mechanism is based on the following assumption: both reaction partners are adsorbed without dissociation at different free sites on the catalyst surface. This is then followed by the actual surface reaction between neighboring chemisorbed molecules to give the product C, adsorbed on the surface. In the final step the product is desorbed. The reaction sequence is thus:



The Langmuir–Hinshelwood mechanism can be depicted as shown in Figure 5-5.

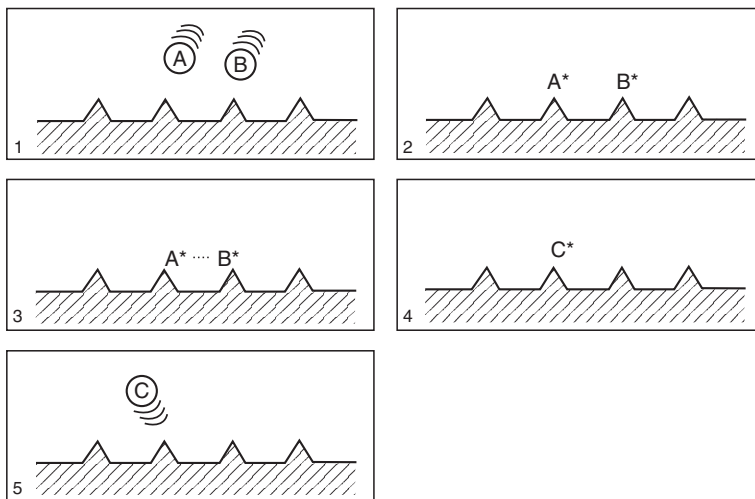


Fig. 5-5 Langmuir–Hinshelwood mechanism (schematic)

Each of the above-mentioned steps can be rate determining, but here we shall only discuss the case in which the surface reaction between the two adsorbed molecules is the rate-determining step. On the basis of the relationship for mixed adsorption, the following rate equation can be formulated (Eq. 5-20).

$$r_{\text{eff}} = \frac{dp_C}{dt} = k \theta_A \theta_B = \frac{k K_A p_A K_B p_B}{(1 + K_A p_A + K_B p_B)^2} \quad (5-20)$$

Of the numerous boundary conditions that are possible, we will consider only two in more detail here:

- 1) When both starting materials are only weakly adsorbed, then both K_A and $K_B \ll 1$ and the rate equation becomes $r_{\text{eff}} = k' p_A p_B$ and $k' = k K_A K_B$. The reaction is first order in both reactants and second order overall.
- 2) When A is weakly and B strongly adsorbed, $K_A \ll 1 \ll K_B$ and the rate equation reduces to

$$r_{\text{eff}} = \frac{k'' p_A}{p_B} \quad \text{where} \quad k'' = k \frac{K_A}{K_B}$$

The reaction order is one with respect to A and minus one with respect to B.

Let us consider the reaction rate as a function of the partial pressure of component A, that is, at constant partial pressure p_B :

- 1) At low partial pressure p_A , the product $K_A p_A$ in the denominator of Equation 5-20 is negligible compared to $(1 + K_B p_B)$ and it follows that

$$r_{\text{eff}} \approx k K_A p_A \frac{K_B p_B}{1 + K_B p_B} \approx k' p_A$$

Thus the reaction rate in this case is proportional to p_A .

- 2) The reaction rate reaches a maximum when $\theta_A = \theta_B$ or $K_A p_A = K_B p_B$.
- 3) At high partial pressure p_A , the term $(1 + K_B p_B)$ in the denominator of Equation 5-20 is negligible compared to $K_A p_A$ and it follows that

$$r_{\text{eff}} \approx \frac{k''}{K_A p_A} \approx \frac{1}{p_A}$$

Hence the reaction order with respect to component A is -1 .

Figure 5-6 depicts the three cases qualitatively [15].

At low partial pressure of component A, the degree of coverage θ_A is low, and all the chemisorbed molecules can react with component B. The reaction rate increases to a maximum where the surface is covered to an equal extent with A and B (i.e., $\theta_A = \theta_B$). With increasing partial pressure of component A, the surface becomes increasingly occupied by A, and the probability of reaction with chemisorbed B decreases. Thus it could be said that the surface is blocked by A.

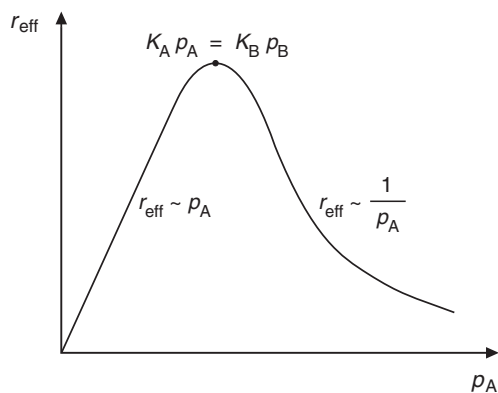
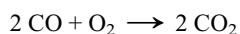


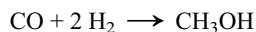
Fig. 5-6 Limiting cases of a bimolecular gas-phase reaction according to the Langmuir–Hinshelwood mechanism

The Langmuir–Hinshelwood mechanism has been proven for many reactions, including some carried out on an industrial scale, for example:

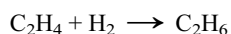
- 1) Oxidation of CO on Pt catalysts



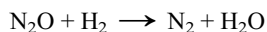
- 2) Methanol synthesis on ZnO catalysts



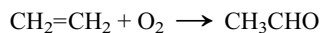
- 3) Hydrogenation of ethylene on Cu catalysts



- 4) Reduction of N_2O with H_2 on Pt or Au catalysts

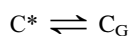
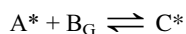
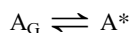


- 5) Oxidation of ethylene to acetaldehyde on Pd catalysts



5.2.3.2 Eley–Rideal Mechanism (1943)

In this mechanism only one of the gaseous reaction partners (e.g., A) is chemisorbed. Component A then reacts in this activated state with starting material B from the gas phase to give the chemisorbed product C. In the final step the product is desorbed from the catalyst surface. The reaction sequence is thus:



In this case only the degree of coverage of the gas A is decisive for the reaction kinetics, and on the basis of the Langmuir isotherm (Eq. 5-7), the following rate equation can be formulated:

$$r_{\text{eff}} = k \theta_A p_B = k \frac{K_A p_A}{(1 + K_A p_A)} p_B \quad (5-21)$$

The Eley–Rideal mechanism is depicted schematically in Figure 5-7.

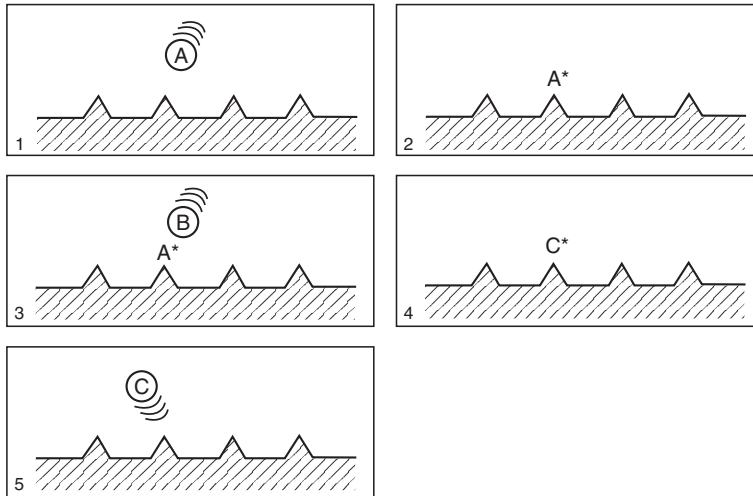
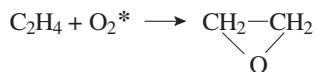


Fig. 5-7 Eley–Rideal mechanism (schematic)

If we observe the reaction rate as a function of the partial pressure of component A at constant p_B , we see that it follows the isotherm for p_A and eventually reaches a constant final value (Fig. 5-8).

Several examples of reactions that follow the Eley–Rideal mechanism can be given:

1) Oxidation of ethylene to ethylene oxide:



In this industrially important oxidation reaction, it has been shown that in the initial stages molecularly adsorbed oxygen reacts with ethylene from the gas phase to give ethylene oxide. However, at the same time O_2 is dissociatively adsorbed as highly reactive atomic oxygen, which in an undesired side reaction gives rise to the combustion products CO_2 and H_2O .

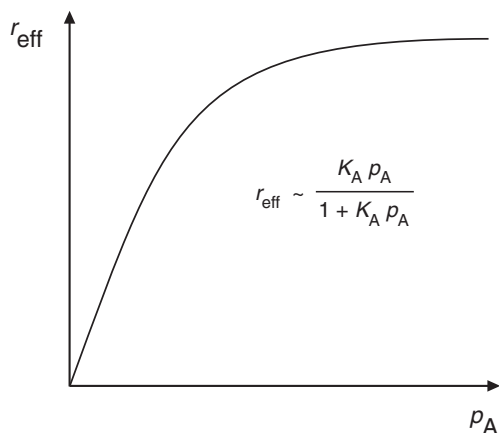
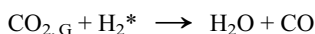
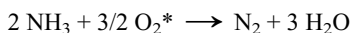


Fig. 5-8. Bimolecular gas-phase reaction with the Eley–Rideal mechanism

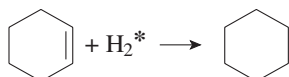
2) Reduction of CO_2 with H_2 :



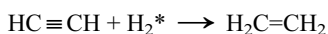
3) Oxidation of ammonia on Pt catalysts:



4) Hydrogenation of cyclohexene:



5) Selective hydrogenation of acetylene on Ni or Fe catalysts:



The two above-mentioned mechanisms are relatively straightforward. In the literature, however, up to a hundred different mechanisms and their rate equations are described. Knowledge of the mechanism of a heterogeneously catalyzed reaction is a prerequisite for obtaining functional relationships between the reaction rate and the variables on which it depends.

For practical reactor calculations, however, it is generally sufficient to use a kinetic approach based on the rate-determining elementary step. In many cases, an empirical rate equation that describes the influence of the most important variables with sufficient accuracy in the chosen operating range is adequate.

Mathematical modelling of the reaction kinetics on the basis of statistical methods allows one to choose between different models and to obtain the best possible rate expression, but the effort required is considerable.

► Exercises for Section 5.2

Exercise 5.1

The adsorption of CO on activated carbon was followed experimentally at 0°C. At the given pressures, the following quantities of adsorbed gas were measured (corrected to a standard pressure of 1 bar):

| | | | | | | | |
|------------------------|------|------|------|------|------|------|------|
| p [mbar] | 133 | 267 | 400 | 533 | 667 | 800 | 933 |
| V [cm ³] | 10.3 | 19.3 | 27.3 | 34.1 | 40.0 | 45.5 | 48.0 |

Determine whether the measurements conform to the Langmuir isotherm and calculate

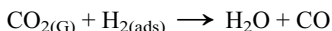
- the constant K_A and
- the volume corresponding to complete coverage

Exercise 5.2

The decomposition of phosphine PH₃ on tungsten catalysts is first order at low pressures but zero order at high pressures. Interpret these findings.

Exercise 5.3

The reduction of CO₂ with H₂ on Pt catalysts is described by the equation:



- According to which well-known mechanism does this hydrogenation proceed (with explanation)?
- What is the name of a general kinetic treatment for such reactions, based on adsorption theory?

Exercise 5.4

The kinetics of isobutene oligomerization on macroporous polystyrene sulfonic acid is described as follows:

At low concentrations of isobutene (IB)

$$r = k_1 c_{\text{IB}}^2,$$

and at high concentrations

$$r = k_2 c_{\text{IB}}$$

Which simple model can be used to explain this?

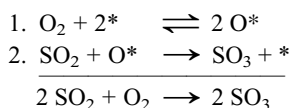
Exercise 5.5 [T24]

When organosulfur compounds react with H₂ in the presence of a sulfur-containing Ni-Mo/ γ -Al₂O₃ supported catalyst, the reaction is much faster than that of organonitrogen compounds under the same conditions. However, when a mixture of the same

sulfur and nitrogen compounds is hydrogenated, then the nitrogen compounds react faster, regardless of the concentration ratio. Explain these observations with the aid of a kinetic model.

Exercise 5.6

The oxidation of SO_2 on Pt catalysts proceeds in two steps:



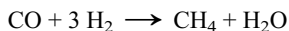
Explain these reaction steps. What mechanism is involved?

Exercise 5.7

In carrying out heterogeneously catalyzed reactions, a distinction is made between microkinetics and macrokinetics. Which steps have to be taken into account in the case of microkinetics?

Exercise 5.8

A methanation reaction was investigated on a commercial supported catalyst 0.5 % Rh/ γ - Al_2O_3 :



The degree of dispersion D of the the catalyst was found to be 42 % by means of chemisorption measurements with H_2 . At 10 bar and 300°C a catalyst turnover number of 0.16 s^{-1} was determined for methane. Calculate the rate of formation of methane r'_{CH_4} in $\text{mol s}^{-1}\text{g}(\text{cat.})^{-1}$ (metal + support).

Exercise 5.9

Distinguish between chemisorption and physisorption according to the following criteria:

| | Chemisorption | Physisorption |
|-----------------------------|---------------|---------------|
| Cause | | |
| Adsorption heat (magnitude) | | |
| Temperature range | | |
| Number of adsorbed layers | | |

5.3 Catalyst Concepts in Heterogeneous Catalysis

5.3.1 Energetic Aspects of Catalytic Activity [8, T38]

If a molecule is to enter a reactive state, it must undergo activated adsorption on the catalyst surface. Hence the catalyst must chemisorb at least one of the reaction partners, as we have already seen.

The strength of adsorption of the molecules is decisive for effective catalysis: neither too strong nor too weak binding of the reactants can induce the required reactivity; a certain medium binding strength is optimum.

Thus chemisorption and the associated energetic aspects play a crucial role in understanding heterogeneous catalysis [10]. The active centers on the catalyst surface are probably the result of free valences or electron defects, which weaken the bonds in the adsorbed molecules to such an extent that a reaction can readily occur. The course of a heterogeneously catalyzed reaction is compared to that of an uncatalyzed reaction in Figure 5-9.

In Figure 5-9 the three elementary steps on the catalyst surface are depicted qualitatively together with the corresponding energies. For the catalyzed reaction a distinction should be made between the apparent activation energy, starting from the ground state of the gaseous molecule, and the true activation energy, relative to the

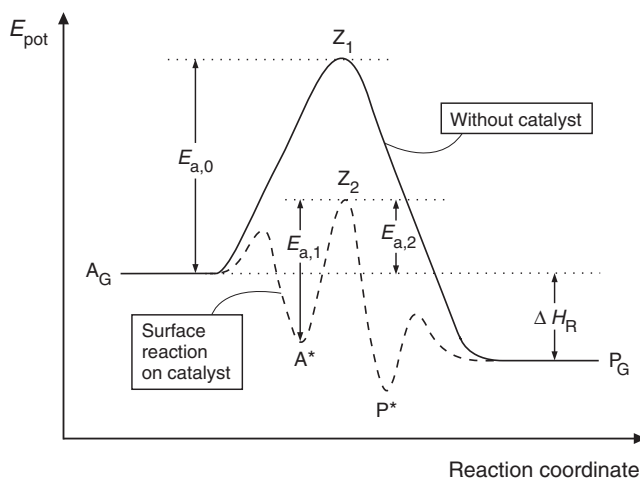


Fig. 5-9 Course of a heterogeneously catalyzed gas-phase reaction $A_G \rightarrow P_G$
 $E_{a,0}$ = activation energy of the homogeneous uncatalyzed gas-phase reaction
 $E_{a,1}$ = true activation energy
 $E_{a,2}$ = apparent activation energy of the catalyzed reaction
 Z_1 = transition state of the gas-phase reaction
 Z_2 = transition state of the surface reaction
 ΔH_R = reaction enthalpy

chemisorbed state. The latter, also known as catalytic activation energy, is more important.

Sometimes the product or transition state being formed may be so strongly bound on the surface that its desorption or further reaction is hindered. In this case the catalyst is poisoned by the product and becomes inactive.

For a deeper understanding of the catalytic reaction mechanism, knowledge regarding the structure and stability of the adsorbed intermediates is particularly important. In many cases a simple qualitative view of the chemisorption is sufficient.

The chemisorption of gases on metals has been the subject of particularly intensive investigations, and the available data allow the catalytic properties of metals to be explained well. Experimentally determined, qualitative orders of catalytic effectiveness are often found in the literature. For example, for the adsorption of hydrocarbons:

acetylenes > dienes > alkenes > alkanes
polar substances > nonpolar substances

For the strength of chemisorption on many metals, the following sequence is given:

$O_2 > C_2H_2 > C_2H_4 > CO > H_2 > CO_2 > N_2$

The following explanation can be given: the reactivity of metal surfaces towards the above gases differs widely, depending on the chemical structure of the metal. As early as the 1950s, the metals were classified according to their chemisorption capabilities [T20]. Table 5-4 lists the metals in groups A to E in order of decreasing activity. The highest activity is found for the transition metals, although there are a few exceptions. In general the activity first increases along a transition metal period and then declines again at the end. The metals of group A chemisorb all seven gases, including nitrogen, which is generally the most difficult to activate.

Table 5-4 Classification of the metals according to their chemisorption properties [T20]

| Metal groups | Gases | | | | | | |
|--|----------------|-------------------------------|-------------------------------|----|----------------|-----------------|----------------|
| | O ₂ | C ₂ H ₂ | C ₂ H ₄ | CO | H ₂ | CO ₂ | N ₂ |
| (A) Ti, Zr, Hf, V, Nb, Ta, Cr, Mo, W, Fe, Ru, Os | + | + | + | + | + | + | + |
| (B ₁) Ni, Co | + | + | + | + | + | + | - |
| (B ₂) Rh, Pd, Pt, Ir | + | + | + | + | + | - | - |
| (B ₃) Mn, Cu | + | + | + | + | ± | - | - |
| (C) Al, Au | + | + | + | + | - | - | - |
| (D) Li, Na, K | + | + | - | - | - | - | - |
| (E) Mg, Ag, Zn, Cd, In, Si, Ge, Sn, Pb, As, Sb, Bi | + | - | - | - | - | - | - |

+ strong chemisorption; ± weak chemisorption; - no chemisorption

The elements of lowest activity chemisorb only oxygen, which is the most easily activated. In between are the metals of medium activity, which activate only molecules from O₂ to CO or H₂. Metals that adsorb several gases can be classified according to various criteria:

- The adsorption coefficient, which reflects the strength of adsorption
- Exchange of one bound gas with another
- The heat of adsorption

A criterium for adsorption is whether it is volumetrically measurable at 10⁻³ bar at room temperature. In some cases the precise classification of a metal depends on its purity or its physical state. For example, technical-grade copper weakly adsorbs hydrogen, but pure copper not at all.

Let us now attempt to explain the above classification of the metals in terms of their atomic structure. The metals of class A belong to groups 4–8 of the periodic table, class B₁ contains the nonnoble metals of groups 9 and 10, and class B₂ the noble metals of these groups. Class B₃ contains manganese and copper, two metals of the first transition metal period with anomalous behavior. All other metals of classes C, D, and E precede or follow the transition metals in the periodic table.

Thus the electronic structure of the metals is decisive for their catalytic activity. The transition metals, with their partially filled d orbitals, are particularly good catalysts. These orbitals are responsible for the covalent binding of gases on metal surfaces in chemisorption and catalysis. Whereas transition metals have one or more unpaired d electrons in the outer electron shell, the weakly chemisorbing main group elements have only s or p electrons. It is postulated that unpaired d electrons are necessary to hold the chemisorbed molecules in a weakly bound state, from which they can then be transferred into a strongly bound state.

The existence of such a transition state lowers the activation energy in general. For reactive molecules such as CO and O₂, such transition states are not absolutely necessary and they are therefore adsorbed by most metals.

Next we shall consider the binding of chemical species to the metal surface in more detail, starting with simple thermodynamic considerations. Adsorption is an exothermic process in which strong binding forces arise between the adsorbed molecules and the surface atoms of the catalyst. At the same time the degree of freedom of the molecules decreases when they leave the gas phase and are adsorbed on the catalyst. Therefore, the entropy *S* is negative. For a thermodynamically feasible adsorption process, the Gibbs free energy should be negative:

$$\Delta G = \Delta H - T \Delta S \quad (5-22)$$

Since it can be expected that the reaction entropy values will not vary greatly from reactant to reactant, the adsorption enthalpy ΔH will depend, as a first approximation, mainly on the strength of chemical bonding between the gas molecules and the catalyst. Two fundamental types of chemisorption processes can be distinguished [T35]:

- Molecular or associative chemisorption, in which all bonds of the adsorbate molecule are retained
- Dissociative chemisorption, in which the bonds of the adsorbate molecule are cleaved and molecular fragments are adsorbed on the catalyst surface

Molecular chemisorption occurs with molecules having multiple bonds or free electron pairs. For example, on platinum surfaces, ethylene gives up two π electrons of its double bond and forms two σ bonds with Pt atoms. The resulting sp^3 hybridization results in a tetrahedral arrangement of bonds (Fig. 5-10).

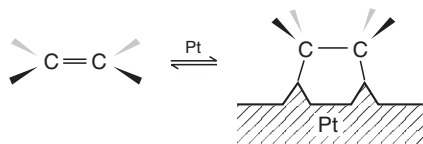


Fig. 5-10 Molecular chemisorption of ethylene on a Pt surface

Further examples of molecular chemisorption are:



Dissociative chemisorption occurs mainly with molecules containing single bonds, for example, the adsorption of H_2 on nickel, in which the hydrogen is adsorbed in atomic form on the surface. The potential diagram (Fig. 5-11) [10, T43] consists of two intersecting curves, the flatter of which (curve 1) corresponds to the physisorption of molecular hydrogen. Via the state of physisorption with only low heat of adsorption, molecular hydrogen passes through the point of intersection A with the potential curve of atomic hydrogen (curve 2). At this point dissociation begins, initially reaching a state in which the H–H bond is weakened and the new Ni–H bond is forming.

The chemisorbed hydrogen has the lowest potential energy and the shortest distance to the catalyst surface (point B). For the reaction according to



the binding strength is given by the reaction enthalpy of -46 kJ/mol. Note that two Ni–H bonds are formed from the single chemical bond in the H_2 molecule. Dissociative chemisorption always increases the number of chemical bonds, and this ensures that the total process is exothermic.

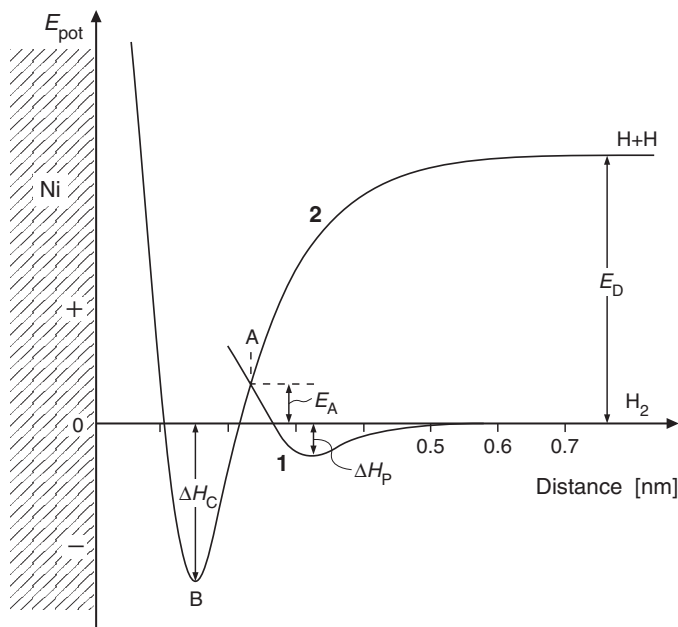


Fig. 5-11 Potential energy and interatomic distances in the adsorption of hydrogen on nickel
 Curve 1: physisorption (0.32 nm, $\Delta H_P = -4$ kJ/mol)
 Curve 2: chemisorption (0.16 nm, $\Delta H_C = -46$ kJ/mol)
 E_D = dissociation energy of H_2 (218 kJ/mol)
 E_A = activation energy for adsorption

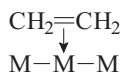
The entropy change for the chemisorption of H_2 on nickel is ca. $-68 \text{ J} (\text{mol H})^{-1} \text{ K}^{-1}$ [T22]. Thus the Gibb's free energy of reaction at 300 K can be calculated according to Equation 5-22 as:

$$\Delta G = -46 + (300 \times 0.068) = -25.6 \text{ kJ/mol}$$

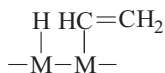
The probability of reaction is thus extremely high. The diagram also shows that the idea that the H_2 molecule dissociates and is then chemisorbed on the Ni surface is purely hypothetical, and that in fact physisorption precedes chemisorption. The total process can be described schematically as shown in Figure 5-12.

For both types of chemisorption there are numerous examples that exhibit parallels to organometallic chemistry and therefore homogeneous catalysis.

In the chemisorption of alkenes, other surface complexes can occur, for example, π complexes with a donor-acceptor bond and dissociatively bound complexes:



Metal π complex



Dissociatively chemisorbed ethylene

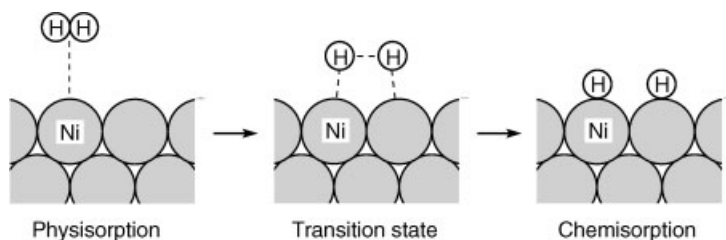
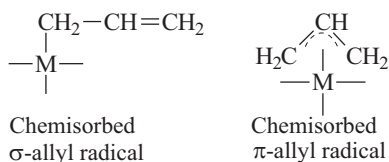
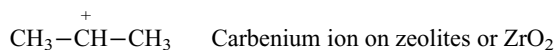


Fig. 5-12 Dissociative adsorption of hydrogen on nickel surfaces

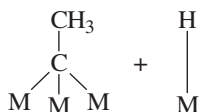
Dissociative chemisorption occurs preferably with alkenes in which the allylic methyl group is highly activated (e. g., propene). Hydrogen abstraction gives an allyl radical, which can be bound as follows:



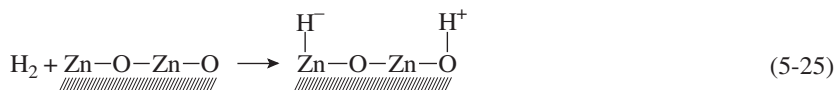
Other species can occur on certain metal oxides:



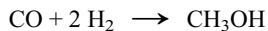
The molecular chemisorption of ethylene is observed below room temperature, but at higher temperatures the alkene can be cleaved with formation of ethyldiyne complexes of the type:



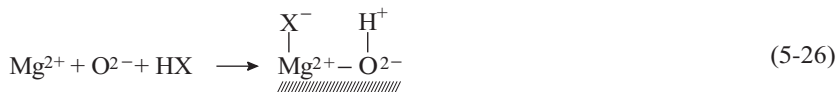
Another example of dissociative chemisorption is the heterolytic cleavage of hydrogen on metal oxide surfaces. The reaction of hydrogen with a zinc oxide surface produces a zinc-hydride bond and a proton bound to an oxygen center (Eq. 5-25) [T39].



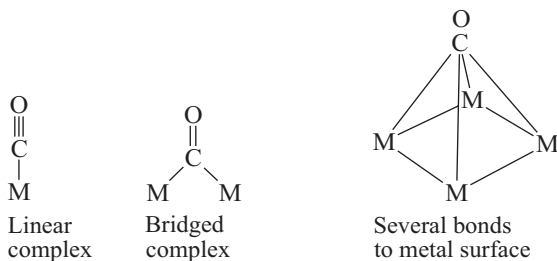
It is assumed that this reaction is an important step in the catalytic hydrogenation of CO to methanol:



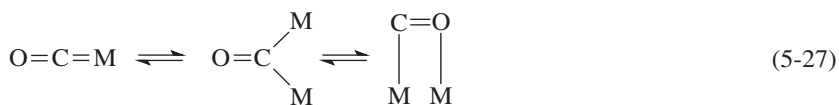
Heterolytic chemisorption can also take place on Brønsted acids, as has been shown for MgO (Eq. 5-26) [35].



Numerous different adsorption complexes have been observed for CO, which can form linear, bridging, and multicenter bonds with metal atoms:



The stoichiometry depends on the adsorbing metal and the degree of coverage of the surface by the adsorbate, smooth transitions between the structures being possible (Eq. 5-27).



The chemisorption of CO is molecular on some transition metals and dissociative on others, depending on the electronic structure of the metal (Table 5-5).

Table 5-5 Chemisorption of CO on transition metals [T20]

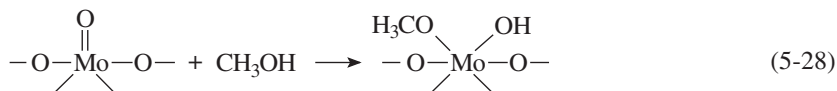
| Dissociative chemisorption of CO | Boundary region | Molecular chemisorption of CO |
|----------------------------------|--------------------|-------------------------------|
| Fe 3d ⁶ | Ni 3d ⁸ | Cu 3d ¹⁰ |
| Mo 4d ⁴ | Ru 4d ⁶ | 50–60 kJ/mol |
| Ti, Mn, Cr | Re 5d ⁵ | Pd 4d ⁸ |
| ≈ 400 kJ/mol | | 140–170 kJ/mol |
| | | Pt 5d ⁸ |

It should be emphasized once again that the surface state of a solid does not necessarily correspond to the conditions within the solid. For example, it was found that not all copper(II) oxide preparations adsorb CO from the gas phase, and that Cu^{2+} does not react with CO. The active oxides have Cu^+ ions on the surface which can bind CO as a ligand.

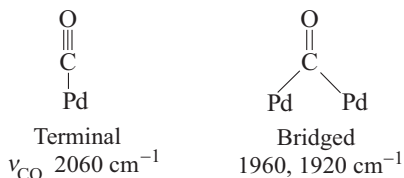
Thus predictions of possible bond formation can not be made solely on basis of chemical relationships; geometrical effects must also be considered. For example, CO is adsorbed molecularly on smooth Ni surfaces but dissociatively at steps. The probability of dissociative chemisorption is generally higher at surface defects such as steps and edges.

Nitrogen, which is isoelectronic with CO, is also chemisorbed on metal surfaces. Orbital theory can be used to explain the metal–nitrogen binding strength. Electron density flows to the metal from the bonding π orbitals of the nitrogen molecule, and backdonation occurs from the metal into the antibonding π^* N_2 orbitals, weakening the N–N bond. This is of importance in ammonia synthesis. It is assumed that the nitrogen is first molecularly chemisorbed and that the subsequent dissociative chemisorption of the nitrogen molecule is the decisive step of the catalytic cycle.

Oxygen-containing compounds such as alcohols also undergo dissociative chemisorption, an example being the adsorption of gaseous methanol on molybdenum oxide catalysts (Eq. 5-28). Such metal oxides, and in particular mixed metal oxides, act as redox catalysts, as we shall see in Section 5.3.3.



The nature of the ligands on metal surfaces is often deduced by comparing their IR spectra with those of comparable inorganic or organometallic complexes [28]. Terminal and bridging CO complexes have been detected on metal surfaces by IR spectroscopy. For the adsorption of CO on Pd surfaces, several readily assignable bands were found:



Support materials can also strongly influence the spectra of adsorbed CO. For Pt catalysts it was found that the ratio of bridging to terminal ligands was much higher on an SiO_2 support than on Al_2O_3 . Thus the strength of adsorption also depends on the nature of the support. For example, an SiO_2 support has only a minor influence on Ni catalysts, whereas Al_2O_3 and TiO_2 have major effects. The CO chemisorption complexes found on supported Ni catalysts are listed in Table 5-6 [T37].

Table 5-6 IR bands of surface CO complexes on supported Ni catalysts

| Bands [cm^{-1}] | Intensity | Structure |
|----------------------------|-----------|-----------|
| 1915 | strong | |
| 2035 | strong | |
| 1963 | medium | |
| 2057 | medium | |
| 2082 | weak | |

The IR spectra of many hydrocarbon ligands on metal surfaces also resemble those of discrete organometallic species, as shown by the example of ethylene complexes (Table 5-7). Weakening of the double bond is evident both in the supported catalyst and in the isolated complex (for comparison: gaseous ethylene has an IR band at 1640 cm^{-1}).

In the case of nitrogen, coordination to metal surfaces was observed by IR spectroscopy before dinitrogen complexes had been synthesized and characterized.

IR spectroscopy was also helpful in elucidating the mechanism of the decomposition of formic acid, a well-known model reaction in heterogeneous catalysis. On me-

Table 5-7 IR bands of ethylene complexes

| | Supported catalyst Pd/SiO ₂ | Comparison π complex Pd(C ₂ H ₄) |
|--|---|--|
| ν_{CH_2} [cm^{-1}] | 2980 | 2952 |
| $\nu_{\text{C}=\text{C}}$ [cm^{-1}] | 1510 | 1502 |

Method: matrix isolation

Pd in C₂H₄/Xe = 1 : 100 matrix at 15 K, ultrahigh vacuum

tal surfaces formic acid decomposes to hydrogen and carbon dioxide (Eq. 5-29), and it was shown that the reaction proceeds via chemisorbed metal formates.

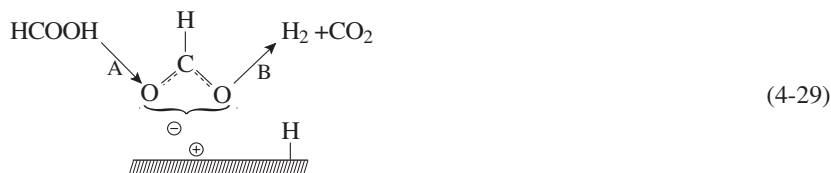


Figure 5-13 shows the relative activity of various metal catalysts for the decomposition of formic acid [T20]. The y -axis gives the temperature required to achieve a particular catalytic activity: the lower the temperature, the higher the activity of the catalyst. On the x -axis the heats of formation of the corresponding metal formates are plotted. This so-called volcano plot shows a very good correlation between the strength of adsorption of the formic acid as a metal formate and the heat of formation of the individual compounds.

How can this typical shape of the curve be explained? Left of the maximum are the metals with too weak adsorption (e.g., Ag, Au), and those to the right (Ni, Co, Fe, W) are also poor catalysts since the adsorption complexes are too stable. The most effective catalysts, in the middle, have the appropriate medium binding strength.

Instead of the heat of formation, other thermodynamic quantities can be used, such as the heats of adsorption and desorption. Numerous examples of such volcano plots can be found in the literature.

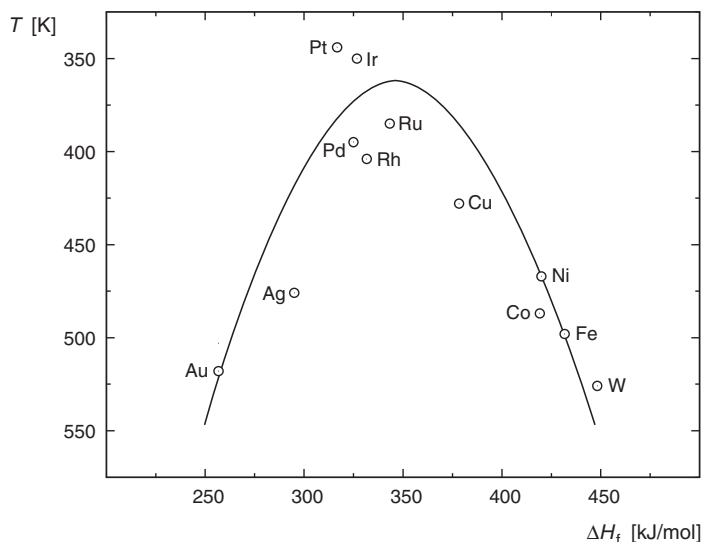


Fig. 5-13 Relative activity of metals for the decomposition of formic acid as a function of the heat of formation of the metal formates (volcano plot)

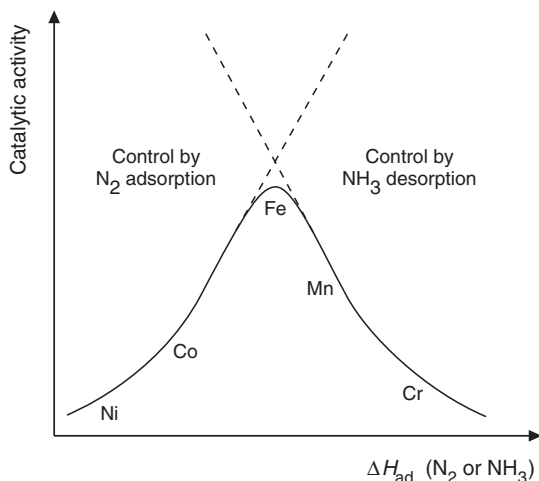


Fig. 5-14 Volcano plot for ammonia synthesis

Another example shows the importance of adsorption strength in ammonia synthesis. In this case the activity of the first transition metal row was measured (Fig. 5-14).

Metals on the left bind N_2 too strongly, and those on the right, too weakly. Exactly the right binding strength was found for iron, the classical ammonia catalyst.

The influence of the electronic structure of the metal and hence its position in the periodic table is also demonstrated by other reactions (Table 5-8).

Table 5-8 Relative reaction rates on transition metal catalysts [T22]

| Row | Reaction | Metals and relative reaction rates | | | | | |
|-----|--|------------------------------------|-------|--|--|-----|-----|
| 1 | Hydrogenation of ethylene (metal catalysts) | Cr | Fe | Co | Ni | Cu | |
| | | 0.95 | 15 | 100 | 36 | 1.2 | |
| 2 | Hydrodesulfurization of dibenzothiophene (metal sulfide catalysts) | Nb | Mo | Tc | Ru | Rh | Pd |
| | | 0.5 | 2 | 13 | 100 | 26 | 3 |
| 3 | Hydrogenolysis of CH_3NH_2 to methane (metal catalysts) | | Re | Os | Ir | Pt | Au |
| | | | 0.008 | 0.9 | 100 | 11 | 0.5 |

Maximum reaction rates are found for metals with six to eight d electrons, a fact which can be explained in terms of electronic effects. The reactants must be rapidly adsorbed on the surface, and the chemisorptive bonding must be strong to attain high adsorbate concentrations. However, these bonds must subsequently be broken so that reaction with other reactants can occur; that is, a compromise is necessary. A general trend, apparent in Table 5-8, is that the bonding strength of chemisorption decreases along a transition metal row. At the beginning of a row, the chemisorption bonds are so strong that they can not be subsequently broken. At the end of a row, the chemisorption bonds are too weak, so that high degrees of coverage of the catalyst surface, and therefore high reaction rates, can not be attained.

To explain the catalytic activity, thermodynamic correlations, often involving the heats of adsorption of the reactants or of related simpler molecules, are widely used. However, the heats of adsorption are often not known, in which case the following quantities are used:

- Heat of desorption
- Heat of formation of intermediates
- IR frequencies of metal–adsorbate bonds, etc.

Such correspondence of the surface chemistry with the physicochemical data of the solid is not always found, since, as we have seen, the surface of a solid rarely corresponds to its interior.

Figure 5-15 describes the adsorption of hydrogen. The chemisorption enthalpy increases from group 4 to 6, then decreases. In groups 8–10 it remains almost constant [T20].

An anomaly occurs at manganese, which is attributed to the half-filled d shell.

Interestingly the heat of formation of ZrH_2 of -163 kJ/mol corresponds exactly to the heat of adsorption of H_2 on Zr. Similar dependences of the adsorption enthalpies as a function of the position of the metal in the periodic table have also been found for N_2 , CO, and CO_2 .

Finally, let us discuss some industrial reactions with the aid of the concept introduced above. The hydrogenation of unsaturated hydrocarbons is one of the most important catalytic reactions in organic chemistry. In particular the hydrogenation of ethylene was long studied as a model reaction for testing the activity of metal catalysts [22]. Today's models for the catalytic hydrogenation of unsaturated compounds are largely based on the general theory of catalytic hydrogenation developed by Balandin and by Horiuti and Polanyi [30].

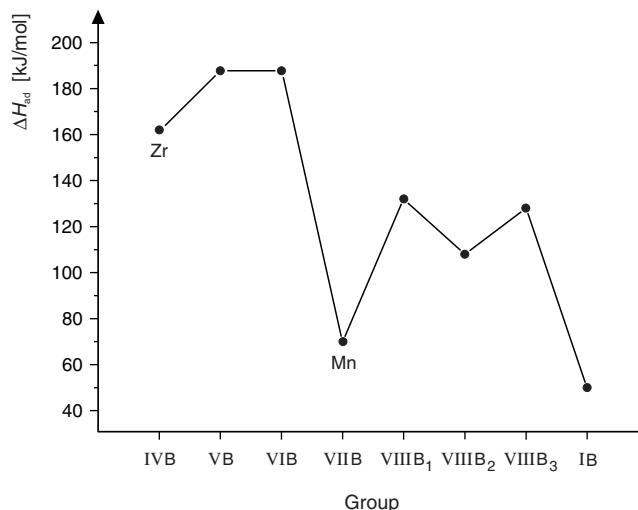
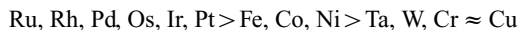
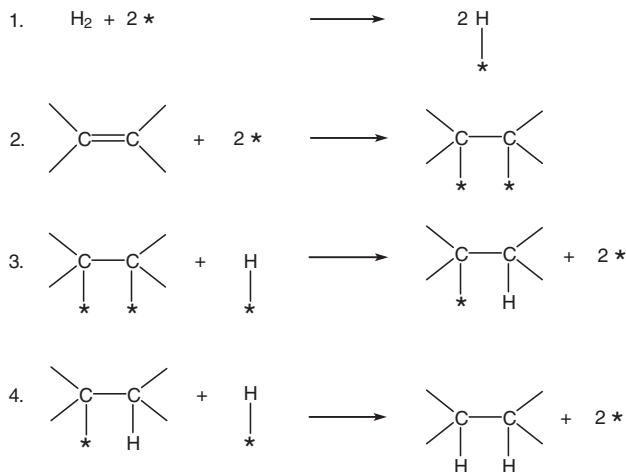


Fig. 5-15 Mean chemisorption enthalpies of hydrogen as a function of the position of the elements in the periodic table [T20]

In general transition metal catalysts are used, and they can be roughly ordered according to their catalytic activity as follows:



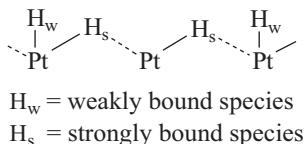
For the hydrogenation of olefinic double bonds, both the alkene and hydrogen must be activated. Various mechanisms have been proposed for alkene hydrogenation, one of which we will discuss in more detail here (Scheme 5-1) [32].



Scheme 5-1 Mechanism for the hydrogenation of an alkene [32]

The chemisorbed alkene reacts stepwise with atomically adsorbed hydrogen. In step 3, a hemihydrogenated product is formed; in the case of ethylene this is an ethyl radical, which in the final step is hydrogenated to ethane, desorption of which frees the active center for further reaction.

Analytical methods such as adsorption measurements with H_2 , H_2/D_2 exchange reactions, and IR spectroscopy have shown that H_2 can be adsorbed on the surface in different forms, as shown here for the example of Pt:



The singly bonded H atoms perpendicular to the surface can be distinguished from the H atoms more strongly bonded between two Pt centers by IR spectroscopy. In addition, molecular adsorption of hydrogen at a surface site also occurs. An analogy to

hydride complexes can be seen, for which mono- and dihydrido species are also known, as demonstrated by the example of the Ir complexes $[\text{IrHCl}_2(\text{PR}_3)_3]$ and $[\text{IrH}_2\text{Cl}(\text{PR}_3)_3]$.

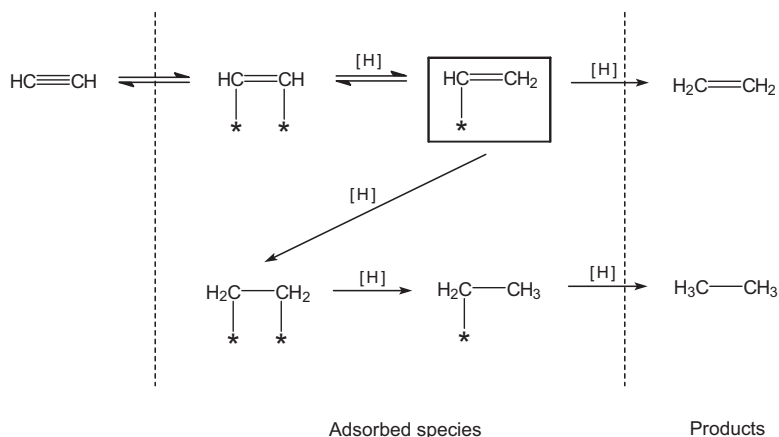
We have already dealt with such complexes as important intermediates in homogeneous catalysis. Hydrogen is homolytically cleaved at the metal center in an oxidative addition reaction to give a dihydrido complex, which can transfer hydrogen stepwise to the coordinated olefin. Hence the similarity between heterogeneous and homogeneous catalysis is not surprising, and industrial reactions can often be catalyzed both heterogeneously and homogeneously by the same metal. For example, $[\text{RhCl}(\text{PPh}_3)_3]$ and Rh/activated carbon are both active hydrogenation catalysts.

Palladium catalysts are very important in selective hydrogenation reactions. In the industrial production of alkenes, acetylenes and other compounds must be removed prior to work up. Let us consider the proposed mechanism in more detail. According to Scheme 5-2, the hemihydrogenated intermediate is the vinyl radical, which can react further to give ethylene or ethane. The selectivity of the reaction depends strongly on the catalyst and the reaction conditions. Selectivity generally decreases with increasing hydrogen pressure and decreasing temperature. Palladium usually exhibits complete selectivity for the hydrogenation of acetylene and related compounds. The high selectivity can be attributed to the fact that it adsorbs H atoms dissociatively on the surface in relatively low concentration.

Another standard reaction in which the dissociative adsorption of hydrogen is the rate-determining step is H_2/D_2 exchange in hydrocarbons. The following activity series was found:



This is one of the best methods for determining the nature and reactivity of adsorbed intermediates on the catalyst surface. Model reactants include CH_4 , for which the role of adsorbed CH_2 groups was proved, and ethane, for which alkyl/alkene interconversion on the metal surface was investigated.

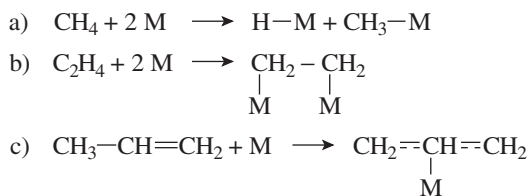


Scheme 5-2 Mechanism for the hydrogenation of acetylene [T20]

► Exercises for Section 5.3.1

Exercise 5.10

The activation of methane, ethylene, and propylene on metal surfaces is described as follows:



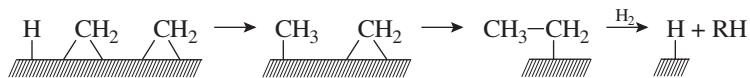
Compare the three processes.

Exercise 5.11

Modern investigations of the Fischer–Tropsch synthesis by X-ray and UV photoelectron spectroscopy have shown the presence of surface carbides and oxygen atoms in the adsorption of CO on various metals.

- W and Mo dissociate CO below 170 K
- Fe and Ni dissociate CO between 300 and 420 K, whereby Ni reacts faster, forming thermally unstable carbides
- Platinum group metals bind CO mainly nondissociatively

The following mechanism has been proposed: adsorbed hydrogen removes the oxygen as water, which is desorbed, and converts the C fragments to CH and CH₂ groups, which then polymerize:



Which catalytic properties are to be expected for the above-mentioned metals?

Exercise 5.12

At high temperature finely divided titanium reacts with N₂ to give a stable nitride. The rate-determining step in ammonia synthesis with iron catalysts is cleavage of the N≡N bond. Why is titanium inactive and iron active as a catalyst for ammonia synthesis?

Exercise 5.13

The effectiveness of Pt in catalyzing the reaction $2\text{H}_{(\text{aq})}^+ + 2\text{e}^- \rightarrow \text{H}_{2(\text{g})}$ is lowered by the presence of CO. Give an explanation.

Exercise 5.14

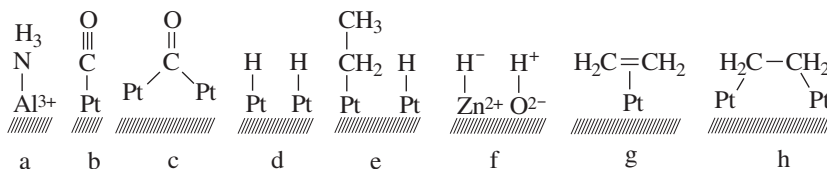
The activation energy of a catalytic reaction is 110 kJ/mol. On using catalyst pellets, an activation energy of only 50 kJ/mol is measured. Give an explanation for this finding.

Exercise 5.15

For the adsorption of CO on W surfaces, two values of the activation energy for desorption are given in the literature: 120 and 300 kJ/mol. What could the reason for this be?

Exercise 5.16

The following examples of surface complexes of molecules are depicted in a publication:



Discuss these examples.

Exercise 5.17

What is the preferred mode of bonding of H₂S on a catalyst surface?

5.3.2

Steric Effects [T22, T37]

Apart from energetic and electronic effects, steric (geometric) effects also play an important role in chemisorption and heterogeneous catalysis [32]. The porosity and the surface of solids must therefore also be taken into account. A steric factor means that a molecule has to be adsorbed on the catalyst in such a manner that it fits properly on the surface atoms. Only then can it be readily activated.

As early as 1929 Balandin introduced the multiplet theory, which is based on purely structural and geometric considerations, into the field of catalysis. If we assume that the molecule to be adsorbed is large and therefore is not adsorbed at a single active center (single-point adsorption), but at two or more centers (multipoint adsorption), then it becomes clear that the steric conditions and topology of the surface are of crucial importance for the activation of the reactants. Balandin referred to the principle of “geometric correspondence” between the reactant molecules and the surface atoms of the catalyst.

In enzymatic catalysis this “key/keyhole” mechanism is so pronounced that the reactant molecule must fit exactly to the geometry of the catalyst for reaction to occur. Such reactions, which normally occur with 100 % selectivity, are of course not found in heterogeneous catalysis.

Extension of the model then led to the concept of active centers on the catalyst surface, presumably attributable to free valences or electron defects (see Section 5.3.3). Therefore, methods for characterizing catalyst surfaces are of great importance, and they play a key role in understanding catalysis.

It is tempting to use summed parameters such as lattice type and interatomic distances in the lattice to explain particular reactions [T40]. However, this is rarely successful, and one should not expect too much of this concept.

One of the first predictions made on the basis of steric effects was that the ease of chemisorption of diatomic molecules should strongly depend on the lattice dimensions of the metallic catalysts. The reasoning was that for large interatomic distances, diatomic molecules would have to dissociate to be completely chemisorbed, while for closely packed lattices, repulsion effects would hinder chemisorption. This is exemplified by our first example, the dehydrogenation of cyclohexane.

It was shown that only elements with interatomic distances between 0.248 and 0.277 nm catalyze the dehydrogenation of cyclohexane. Table 5-9 lists the lattice distances and lattice types for several metallic catalysts.

Table 5-9 Structure and lattice spacings (distance to next-nearest neighbor in nm) of metals [T40]

| Lattice type | | | | | |
|---------------------------|-------|---------------------------|-------|-------------------------------|-------|
| Body-centered cubic (bcc) | | Face-centered cubic (fcc) | | Hexagonal close packing (hcp) | |
| Ta | 0.286 | Ce | 0.366 | Mg | 0.320 |
| W | 0.272 | Ag | 0.288 | Zr | 0.312 |
| Mo | 0.272 | Au | 0.288 | Cd | 0.298 |
| V | 0.260 | Al | 0.286 | Ti | 0.292 |
| α -Cr | 0.246 | Pt* | 0.276 | Os* | 0.270 |
| α -Fe | 0.248 | Pd* | 0.274 | Zn* | 0.266 |
| | | Ir* | 0.270 | Ru* | 0.266 |
| | | Rh* | 0.268 | β -Co* | 0.252 |
| | | Cu* | 0.256 | Be | 0.224 |
| | | α -Co* | 0.252 | | |
| | | Ni* | 0.248 | | |

* Metals that catalyze the dehydrogenation of cyclohexane

It can be seen that only metals with close packed structures, that is the highest surface-atom density, catalyze this reaction:

fcc, from Pt to Ni
hcp, from Os to Co

Apparently, many of the best metal catalysts have the fcc lattice structure. A prerequisite for fundamental investigations of heterogeneous catalysis is that the surface structure of the metal be exactly known and that no impurities are present. Single crystals are preferred for such investigations. Since metals are crystalline, the atoms at the surface form regular two-dimensional arrangements.

A widely used system for describing the lattice planes of a crystalline structure are the Miller indices. These indicate which and how many crystallographic axes of a unit cell are intercepted by a lattice plane. The indices give the relative axis sections a , b , and c in reciprocal whole-number form (Fig. 5-16).

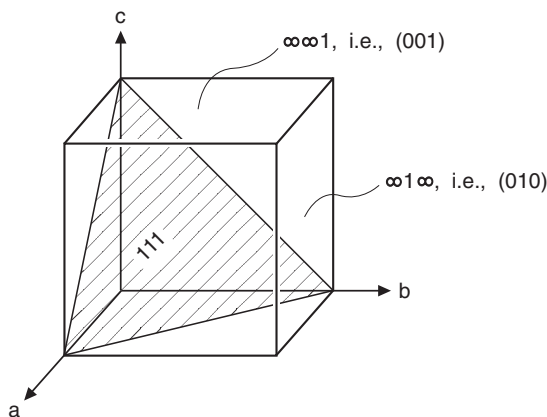


Fig. 5-16 Lattice planes in a cubic lattice with Miller indices

The surface of a cube intersects only one axis and therefore has the designation (100). The surface of a prism intersects two axes of the cubic system, i.e., (110). An octahedron surface is designated (111) since it intersects all three axes at equal distances.

Many catalysts have the fcc structure. The arrangement of the atoms in the above-mentioned surfaces is depicted in Figure 5-17. Also shown is the number of neighboring atoms and free valences of the surface atoms for the example of the nickel lattice [T33]. The highest number of free valences, namely five, occurs for the prismatic faces.

Single crystals a few centimeters in size can be grown for many transition metals and cut so that a specific surface is exposed. Such single-crystal surfaces have the advantage that they can be precisely characterized by modern methods of surface analysis, and molecules adsorbed on the surface, such as CO, N₂O, O₂, and hydrocarbons, can be detected and their bonding modes determined.

Single-crystal surfaces are of course of no importance as practical catalysts, but they provide interesting information about the processes that can take place on real polycrystalline surfaces [18]. Industrial catalysts consist of numerous small crystallites that are randomly oriented and whose surfaces present many crystallographic planes to the reactants. In addition they exhibit steps and lattice defects. The dispersity of a catalyst (particles/cm³) and the surface of a catalyst are closely interrelated.

Figure 5-18 shows schematically the stepped surface of a catalyst with lattice defects, protruding atoms, which may also be adsorbed species, and kinks.

In addition to terraces of surfaces with high density such as (111) and (110), there are also steps of monoatomic height. For example, the (557) surface of platinum consists of terraces of (111) surfaces linked by monoatomic (001) surfaces. Such stepped surfaces

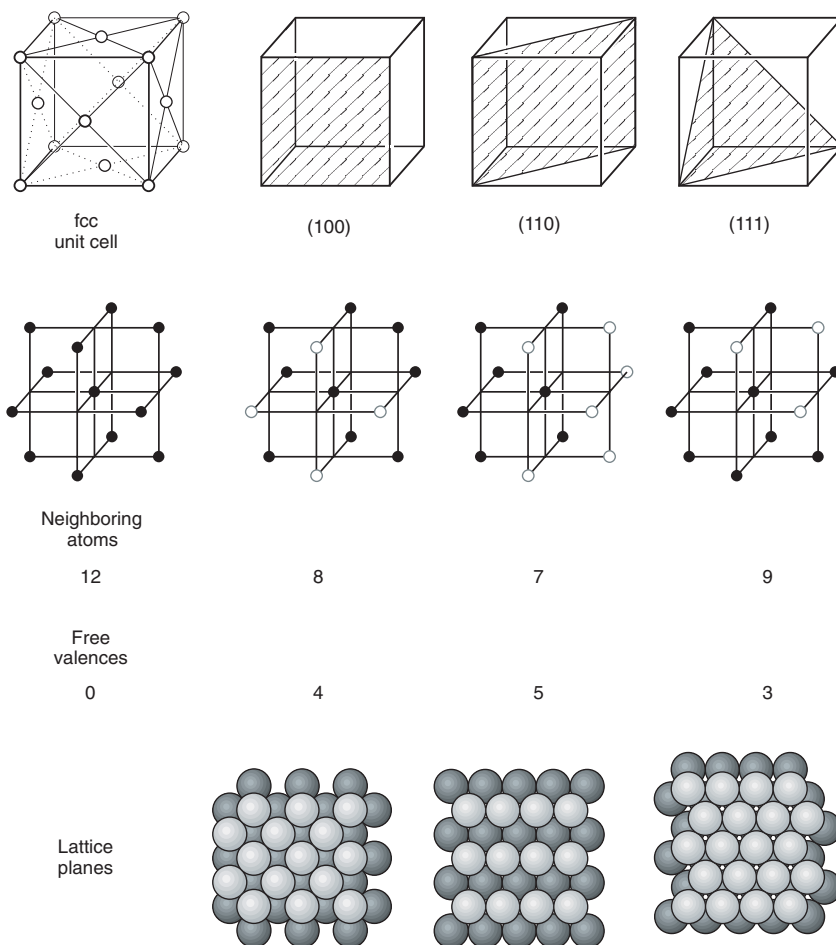


Fig. 5-17 Neighboring atoms and free valences of nickel surfaces in the face-centered cubic (fcc) lattice

can also be characterized by the methods of surface science. Interestingly, these stepped surfaces are remarkably stable under various reaction conditions [32].

Especially crystallites of greater than 10 nm in diameter can exhibit high-index crystal surfaces, and the kinks can even be seen in scanning electron micrographs.

The species actually responsible for the catalytic activity are atoms or groups of atoms (active centers) in the catalyst surface whose chemisorption properties depend strongly on the degree of dispersion of the solid. Thus the catalyst turnover number TON is used as a measure of atomic regions of the catalyst surface (see also Section 1.2) [26].

Since steric factors are not important in all heterogeneously catalyzed reactions, a distinction can be made between structure-sensitive reactions, which react to changes in the surface structure, and structure-insensitive reactions. Numerous

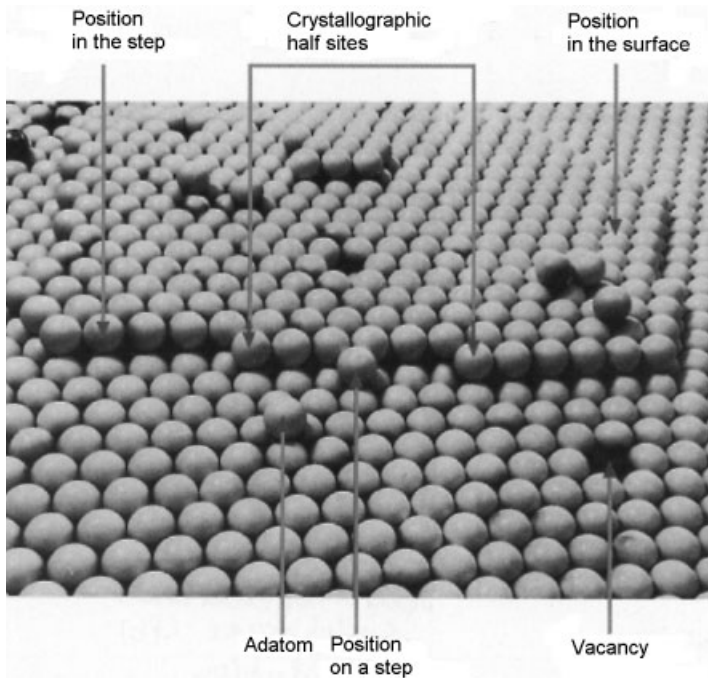


Fig. 5-18 Model of a single-crystal surface (BASF, Ludwigshafen, Germany)

examples exist for both types of reaction, and we shall distinguish between them on the basis of the parameters that influence them (Table 5-10).

Table 5-11 lists industrial examples of both types of reaction.

Complete separation according to reaction type is, however, not possible, as will be shown in the following examples. Whereas the hydrogenation of ethylene on nickel catalysts is structure-sensitive, it proceeds on platinum crystals, foils, and supported catalysts with almost constant rate and activation energy. The reaction on rhodium is also

Table 5-10 Classification of metal-catalyzed reactions [T24]

| Reactions | Effects and their influences | | | | |
|-----------------------|------------------------------|-----------------|----------------|---------------|------------------------------------|
| | Structure | Alloy formation | Cat. poisoning | Type of metal | Multiplicity of the active centers |
| Structure insensitive | — | low | moderate | moderate | 1 or 2 atoms |
| Structure sensitive | moderate | large | large | very large | multiple centers |

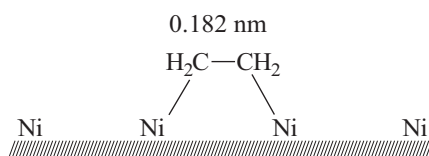
Table 5-11 Steric effects in chemical reactions

| Structure-sensitive reactions | Structure-insensitive reactions |
|--|---|
| <i>Hydrogenolysis:</i> Ethane (Ni) Methylcyclopentane (Pt) Cyclohexane (Pt) | Ring opening: cyclopropane (Pt) Hydrogenation: benzene (Pt) ketones Dehydrogenation: cyclohexane (Pt) CO oxidation Oxidation of ethylene to ethylene oxide (Ag) |
| <i>Hydrogenation:</i> Benzene (Ni) Ethylene (Ni) | |
| <i>Isomerization:</i> Isobutane, hexane (Pt) | |
| <i>Cyclization:</i> Hexane, heptane (Pt) Ammonia synthesis (Fe) | |
| <i>Methanization</i> | |

structure-insensitive. At normal pressure, the Pt(111) and Rh(111) surfaces are both covered by a monolayer of strongly chemisorbed ethylidyne C_2H_3 .

Hydrodesulfurization is structure-insensitive over Mo catalysts but structure-sensitive on Re catalysts. Ethylene oxidation on Ag catalysts is classified as structure-insensitive. Probably the oxygen modifies the surface such that each surface reacts the same.

Let us consider the hydrogenation of ethylene on Ni catalysts in more detail. The adsorption of ethylene on nickel is associative, especially in the presence of hydrogen. Spectroscopic investigations have shown that the ethylene double bond opens, forming two σ bonds to neighboring Ni atoms and giving the ethane structure.



The bond should, however, not be too strong, so that further reaction is possible. For the nickel surfaces with low Miller indices, two Ni–Ni bond lengths were found: 0.25 and 0.35 nm. The results of LEED investigations are summarized in Table 5-12 [T19, T23].

Table 5-12 Adsorption and hydrogenation of ethylene on nickel surfaces [T23]

| Ni – Ni distance | Surfaces | Ni – C – C angle | Binding | Catalytic effect |
|------------------|--------------|------------------|----------------|------------------|
| 0.25 nm | (111) | 105° | stable, strong | low |
| 0.35 nm | (100), (110) | 123° | weaker | high |

The following explanation can be given for the experimental findings. For the bond length of 0.25 nm, an Ni–C–C bond angle of 105° can be calculated for two-point adsorption. Since this is close to the tetrahedral angle of 109° , stable chemisorption of ethylene on the (111) face can be assumed. For the longer Ni–Ni distance of 0.35 nm, the geometrical situation is less favorable, and chemisorption is therefore weaker. The ethylene molecule is strained and thus can more readily be hydrogenated.

These considerations can also be applied to other metals. Thus the (100) planes of metals with larger atomic spacings than nickel (e.g., Pd, Pt, and Fe) should exhibit weaker chemisorption, and the same should also be true of metals with shorter interatomic distances such as tantalum. Figure 5-19 shows the rate of ethylene hydrogenation as function of metal–metal distance (volcano plot).

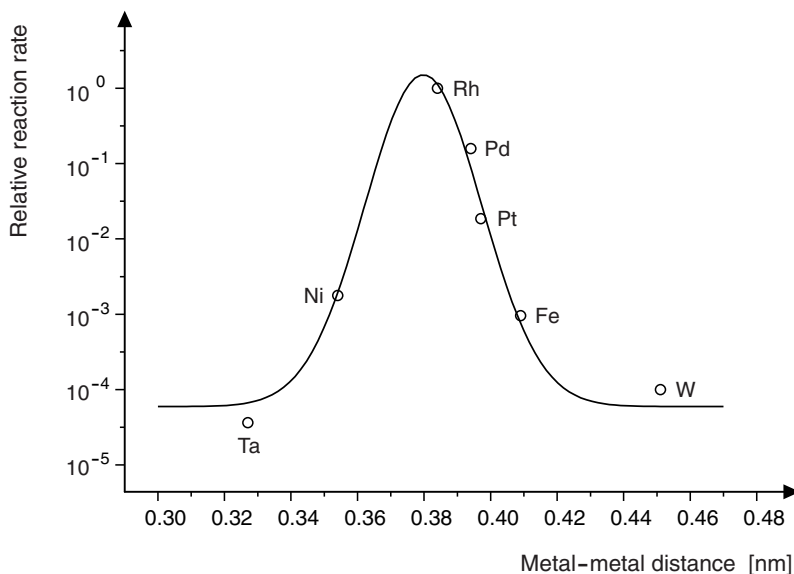


Fig. 5-19 Ethylene hydrogenation as a function of the metal–metal distance in the lattice [T35]

Since two-point adsorption is no longer possible if the metal–metal distance is too large, the optimal catalyst for ethylene hydrogenation should have a certain medium interatomic distance. This is the case for rhodium with 0.375 nm, but since energetic aspects (adsorption enthalpies) must also be taken into account, it can not be said that this is solely the result of steric effects.

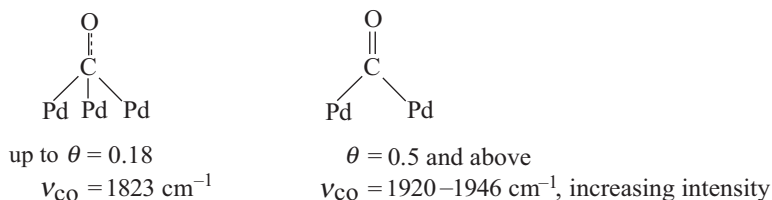
It is found in many reactions that a particular surface is favored. For example the (111) surface is particularly active in fcc and hcp metals. A strong dependence is found for ammonia synthesis on iron catalysts (Table 5-13) [T35]. Ammonia synthesis is one of the most structurally sensitive reactions. The opposite order was found for the decomposition of ammonia on copper, i. e., $(111) > (100)$. In the decomposition of formic acid, the (111) surface is three times more active than (110) or (100).

Table 5-13 Activity of surfaces in ammonia synthesis [T35]

| Surface | Relative activity |
|---------|-------------------|
| 110 | 1 |
| 100 | 21 |
| 111 | 440 |

In the hydrogenation of benzene and the dehydrogenation of cyclohexane, sixpoint adsorption of the molecule on the catalyst has been found. The double bonds open, and chemisorption occurs by formation of σ bonds. Here, too, the (111) surface is clearly favored.

In the next example we will consider the catalytic oxidation of CO [4]. LEED studies have shown that in CO adsorption, the Pd surface is covered by an ordered monolayer. The CO molecules are undissociatively adsorbed by at least two surface sites. The IR spectra of CO adsorbed on Pd (111) surfaces showed bands whose position depends on the degree of coverage of the surface. At low degrees of coverage up to $\theta = 0.18$, a weak $\nu(\text{CO})$ band is observed at 1823 cm^{-1} . It was concluded that the CO molecule is bound to three Pd atoms, which are present in excess, weakening the C–O bond:



At higher degrees of coverage, fewer free Pd atoms are present on the surface, and a bridging structure with a stronger C–O bond is formed. This structure is retained up to the formation of a monomolecular layer. Thus the CO molecules are bound not by single metal atoms but by an ensemble of several metal atoms.

In the oxidation of CO, the reaction partner oxygen must also be considered. There are two possibilities for the adsorption of two gases on solid surfaces:

- Cooperative adsorption: the two partners form an common ordered surface structure
- Competitive adsorption: the two gases hinder one another in adsorption and form two independent surface structures

Our example is a case of competitive adsorption. If the catalyst is first exposed to O_2 , then atomic adsorption of oxygen on the surface occurs. If CO is then introduced at room temperature, the reaction proceeds rapidly by the Eley–Rideal mechanism (Eq. 5-30).



If CO is first adsorbed and then oxygen is introduced then no reaction occurs (Eq. 5-31).



Finally, if a Pd surface partially covered with CO is allowed to react with O_2 , then the latter is adsorbed at the free sites, and ordered surface structures are formed. Only at the boundary layers of the two adsorbed reactants is reaction then possible, and this proceeds slowly according to the Langmuir–Hinshelwood mechanism (Eq. 5-32).



Hence the oxidation process depends on the fastest reaction (Eq. 5-30), and this is also the case when mixtures of CO and O_2 react. At low temperatures CO blocks the surface and the reaction is slow. With increasing temperature, above ca. 100°C , CO is partially desorbed, and O_2 is chemisorbed on the surface. The reaction rate passes through a maximum around 200°C , after which it falls again. The reaction is structure-insensitive over a wide range, as has been shown on various Pd surfaces [32].

A similar course of reaction was found on Pt surfaces [T36]. Again, CO undergoes molecular adsorption, and the degree of coverage decreases rapidly with increasing temperature (Fig. 5-20a). This is shown by the residence times on the surface:

| | |
|---------------------|-----------------|
| Room temperature | ∞ |
| 150°C | ca. 1 s |
| 400°C | ca. 10^{-4} s |

The O_2 is initially adsorbed in molecular form as a peroxide-like compound, which rapidly dissociates with release of energy (Fig. 5-20b). Since the oxygen atoms require several free centers for adsorption, saturation coverage with oxygen is rapidly reached.

The low degree of coverage allows adsorption of CO between the oxygen atoms, and the reaction proceeds by the Langmuir–Hinshelwood mechanism. The CO_2 product is only weakly bound on the surface and is rapidly desorbed into the surround-

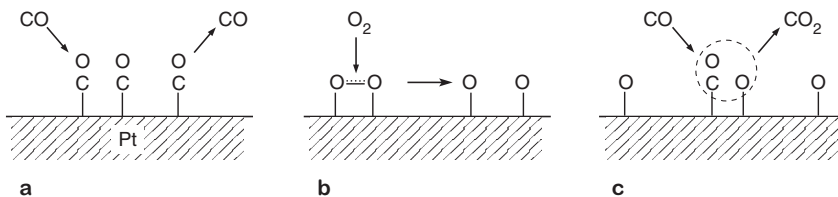


Fig. 5-20 Oxidation of CO on platinum surfaces

ing gas phase (Fig. 5-20c). As in the case of Pd catalysts, no reaction is observed between chemisorbed CO and O₂ from the gas phase.

Platinum catalysts are of major importance for the activation of hydrogen and in reactions of hydrocarbons (e. g., hydrogenation, dehydrogenation, hydrogenolysis). In many cases steps and kinks on the surface have a major influence on the catalytic activity.

Modern surface analysis methods such as LEED allow the number of step and kink atoms to be determined. For example, 2.5×10^{14} step atoms per square centimeter were found for a ($\bar{5}57$) surface of platinum, and 2.3×10^{14} step atoms and 7×10^{13} kink atoms per square centimeter for a ($\bar{6}79$) surface [32].

It was found that oxygen and hydrogen are not adsorbed on smooth (100) and (111) surfaces of Pt but on surfaces with an ordered step structure. The (111) surface is also inactive in the dehydrogenation of cyclohexane. A particularly strong dependence of the activity on the density of step and kink atoms was observed in the hydrogenolysis of cyclohexane to *n*-hexane. Here the Pt atoms at kinks are an order of magnitude more active than the step atoms. On the basis of strength of coordination and catalytic activity, three types of Pt atoms can be distinguished:

- Largely coordinatively saturated surface atoms: low activity
- Step atoms: more active, catalyze the cleavage of C–H and H–H bonds
- Highly coordinatively unsaturated kink atoms: preferably catalyze the cleavage of C–C bonds

The step and kink atoms responsible for C–H and C–C bond cleavage do not become covered by carbon and therefore are not subject to deactivation by surface coking. It is assumed that any carbon layer forming here is immediately removed by hydrogenation.

Similar investigations have been carried out on ethylene and CO. Here, too, the reactivity of steps was found to be much higher than that of smooth surfaces. The following chemisorption complexes of CO on Pt were detected by IR spectroscopy:

- $\nu(\text{CO})$ on steps: 2066 cm^{-1} , low coverage, weaker CO bond
- $\nu(\text{CO})$ on terraces: 2090 cm^{-1} , high coverage

Another good example for the function of stepped surfaces is the adsorption and decomposition of acetonitrile on Ni surfaces (Fig. 5-21) [11].

It was shown that on smooth (111) surfaces, the binding of acetonitrile is weak and reversible. At 90 °C the molecules are desorbed, with only 1–2 % undergoing cleavage with loss of hydrogen to leave C and N fragments on the surface. On (110) surfaces, which have a higher density of steps, 90 % of the molecules are decomposed at 110 °C. This experimental finding is explained by the fact that the CN group is perpendicular to the surface in both cases. On smooth surfaces there is no interaction of the CH₃ group with the catalyst surface (Fig. 5-21 a), and the molecule remains largely intact. In contrast, molecules that are adsorbed on or next to steps can be readily decomposed (Fig. 5-21 b, c).

As the above examples have shown, the atomic surface structure of a catalyst can have a considerable influence on the catalyst activity and the selectivity of heterogeneously catalyzed reactions. The surface structure of a catalyst metal particle is

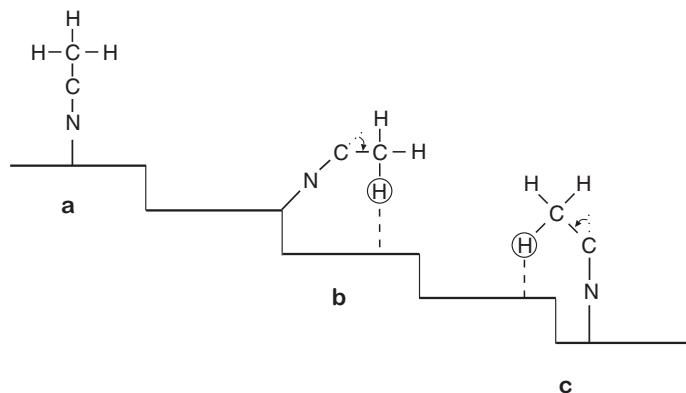


Fig. 5-21 Adsorption and cleavage of acetonitrile on Ni surfaces [11]

characterized by the nature of the surface and the ratio of surface, step, and corner atoms. While the characterization of a single particle is relatively simple, it is practically impossible for a real catalyst or supported catalyst due to the distribution of particle sizes and shapes [20].

Measurement of the metal dispersion (ratio of metal surface to total metal content) allows qualitative assignments to be made. In the case of noble metals it is generally determined by adsorption measurements with H_2 or CO. Corner atoms dominate for small highly dispersed metal particles, the maximum number of step atoms occurs at medium dispersity, and, as would be expected, terrace atoms are predominant at low degrees of dispersion.

The following were measured for a uniformly dispersed supported Pd catalyst:

| | |
|---------------------------|-----------------------|
| Pd particle size | 4–10 nm |
| Pd specific surface area | 9.5 m ² /g |
| Dispersion | 21% |
| BET specific surface area | 500 m ² /g |

At the usual commercial metal concentrations of 0.1–1%, the dispersion can range from 40 to nearly 100%, with particle sizes of 1–4 nm [T41].

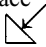
In general, catalyst activity increases with increasing size of the catalyst surface. However, since many reaction rates are strongly dependent on the surface structure, a linear correlation between catalyst activity and surface area can not be expected. In some reactions the selectivity of the catalyst decreases with increasing surface area.

The surface of the support is also important. Catalytic transformations such as hydrogenation, hydrodesulfurization, and hydrodenitrogenation are favored by large support surface areas, whereas selective oxidations such as olefin epoxidation do not require a support surface to suppress problematic side reactions.

Modern methods of surface characterization allow relationships to be found between catalyst structure and catalyst behavior, even for highly complex industrial catalysts. A goal of catalyst research is to use such methods to optimize catalyst production.

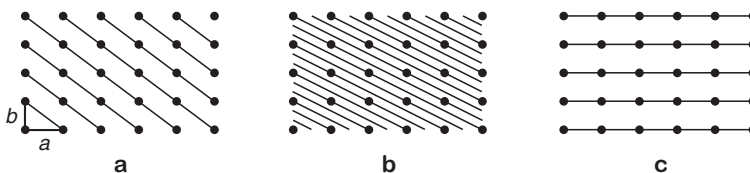
► Exercises for Section 5.3.2

Exercise 5.18

- a) Assign the lattice planes (100), (110), and (111) to the following surfaces:
- Cube surface
 - Octahedron surface
 - Prism surface 
- b) What significance do these surfaces have in heterogeneous catalysis?

Exercise 5.19

A three-dimensional right-angled lattice is formed by a unit cell with sides of length a , b , and c . The following figure shows a view with the a - and b -axes. What are the Miller indices of the three planes?

**Exercise 5.20**

It is reported in the literature that in the aromatization of hydrocarbons the reaction rate on Pt(111) is an order of magnitude higher than on Pt(100).

- a) What is the meaning of the numbers in parentheses?
 b) Discuss the findings.

Exercise 5.21

The hydrogenation of ethylene on Pt crystallites, films, foils, and supported catalysts proceeds with practically the same activation energy of 45 kJ/mol. Explain this finding.

Exercise 5.22

In automobile catalytic converters, why is the Pt/Rh catalyst present as a fine dispersion on a ceramic surface rather than as a foil?

5.3.3

Electronic Factors [29, L33]

The concept of electronic factors in catalysis deals with the relationship between the electronic structure of solids, which depends on their physical properties, and the reactivity of adsorbed intermediates.

The key question was: how does the catalytic activity of a solid depend on its geometrical and electronic properties?

In the 1960s extensive searches for electronic effects were undertaken, but although much data and many understandings were obtained, a generally valid catalyst concept could not be developed. Nevertheless, the concept is useful for explaining many experimental findings and in classifying catalysts. For solids, two classes of catalysts can be distinguished:

Redox Catalysts [T34]

This group of catalysts comprises solids exhibiting electrical conductivity, that is, having mobile electrons (metals and semiconductors). Many reactions proceed by the redox mechanism, for example:

- Hydrogenation of alkenes, aromatics, and other compounds with double bonds
- Hydrogenation of CO and CO₂ to methane
- Ammonia synthesis
- Synthesis of hydrocarbons and alcohols from synthesis gas
- Oxidation of hydrocarbons, SO₂, NH₃, etc.
- Dehydrogenation of organic compounds
- Decomposition of formic acid
- Polymerization of hydrocarbons

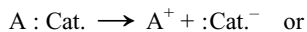
These are all homolytic processes in which chemical bonds are broken with the aid of the catalyst (Eq. 5-33). This leads to formation of radicals, followed by electron transfer between the reaction partners.



Typical redox catalysts are metals, semiconductors (e. g., metal oxides in various oxidation states), and special metal complexes. Metals that form an oxide layer on the surface under oxidizing conditions can also be regarded as semiconductors.

Acid/Base Catalysts (Ionic Catalysts)

These catalysts have no mobile charge carriers and thus behave as insulators. With increasing temperature the insulator property is partially lost. Ionic catalysts do not cleave electron pairs in the reactants. Charge is carried by ions, mainly protons. Such heterolytic reactions with the catalyst can be formulated as shown in Equation 5-34).



Heterolytic cleavage is energetically less favorable than homolytic cleavage. Such catalytic processes include:

- Hydrolysis
- Hydration and dehydration
- Polymerization and polycondensation
- Cracking reactions
- Alkylation
- Isomerization
- Disproportionation

These reactions require ionic intermediates and are catalyzed by acidic or basic solids like Al_2O_3 or CaO and especially mixed oxides such as $\text{Al}_2\text{O}_3/\text{SiO}_2$ and MgO/SiO_2 . Electronic effects can also successfully explain the phenomena of catalyst promotion and catalyst poisoning. Solid-state catalysts can be classified according to their electrical conductivity and electron-transfer properties as shown in Table 5-14.

Having discussed the electronic properties of the catalyst, let us now turn our attention to electron transfer between substrate and catalyst. The following classification is relative to the substrate:

- Acceptor reactions: electrons flow from catalyst to substrate; the adsorbate acts as an acceptor (examples: starting materials with high electron affinity; reactions in which oxygen is mobilized)
- Donor reactions: electrons flow from substrate to catalyst (examples: substrates that readily release electrons, i.e., reducing agents with low ionization energies; reactions in which H_2 or CO is mobilized)

This classification is shown schematically in Figure 5-22.

Table 5-14 Classification of solid-state catalysts

| | Conductors | Semiconductors | Insulators |
|---|--|---|---|
| Conductivity range, $\Omega^{-1} \text{ cm}^{-1}$ | $10^6 - 10^4$ | $10^3 - 10^{-9}$, increases with increasing temperature | $10^{-9} - 10^{-20}$ |
| Electron transfer | electron exchange metal/adsorbate | electron transfer at high temperatures | – |
| Examples | numerous metals, mostly transition metals and alloys | metalloids (Si, Ge, etc.); nonstoichiometric oxides and sulfides (ZnO, Cu_2O , NiO, ZnS, Ni_2S_3 , etc.) | stoichiometric oxides (Al_2O_3 , SiO_2 , B_2O_3 , MgO, SiO_2/MgO , $\text{SiO}_2/\text{Al}_2\text{O}_3$, etc.), salts, solid acids |

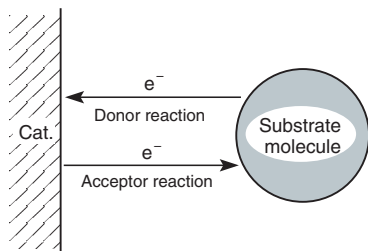


Fig. 5-22 Electron transfer between catalyst and substrate

5.3.3.1 Metals [T27, T35]

For metals and metal alloys in particular, relationships have been sought between collective properties and catalytic behavior. The metallic state was generally described by the simple band model or the Pauling valence structure theory.

In metals the valence shell is formed by the s or d band. The main-group elements with their s bands are typical electron donors and form strong bonds with electron acceptors such as sulfur or oxygen; stable sulfides and oxides are formed. These metals are therefore not suitable as catalysts. In contrast the transition metals with their d bands are excellent catalysts. It is noteworthy that both hydrogenations and oxidations can be carried out with d-block elements.

Let us now describe the electronic structure of the transition metals with the aid of the band model. According to this model the metal is a collective source of electrons and electron holes (Fig. 5-23). In a row of the periodic table, the metals on the left have fewer d electrons to fill the bands. There are two regions of energetic states, namely, the valence band and the conduction band with mobile electrons or positive holes. The potential energy of the electrons is characterized by the Fermi level, which corresponds to the electrochemical potential of the electrons and electron holes.

The position of the Fermi level also indicates the number density of electrons in the band model. The energy required to transport an electron from the edge of the Fermi level into vacuum corresponds to the work function ϕ_0 (Fig. 5-24a). For the d-block metals, the work function is around 4 eV and therefore in the UV range.

A certain number of free levels or d-holes are available for bonding with adsorbates. The lower the Fermi level, the stronger the adsorption. How do donors and acceptors function in the band model? In the surface layer, the free electrons or holes allow molecules to be bound to the surface, whereby the strength of binding depends on the position of the Fermi level. An acceptor (e.g., O_2) removes electron density from the conduction band of the metal, as a result of which the Fermi level drops to E_F and the work function $\phi_A > \phi_0$ (Fig. 5-24b). A donor (e.g., H_2 , CO , C_2H_4) donates electrons to the conduction band of the metal, and the work function becomes corresponding lower: $\phi_A < \phi_0$ (Fig. 5-24c).

Metals normally have a narrow d band. The catalytic properties are strongly influenced by the occupational density of the electrons in this band. In many cases a direct relationship has been found between the catalytic activity of transition metals

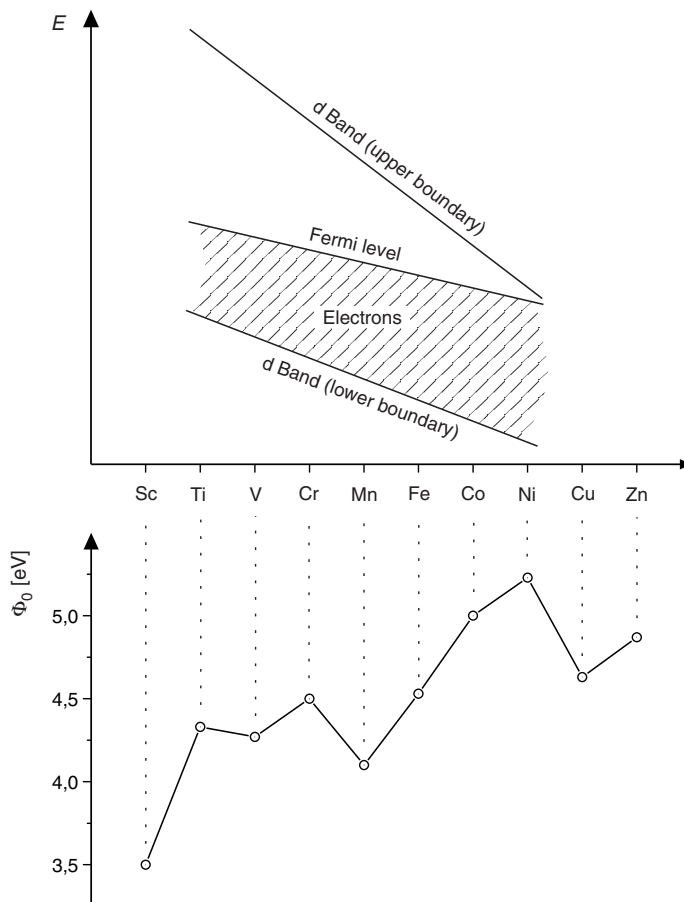


Fig. 5-23 Electron density of the 3 d band and work function ϕ_0 of the transition metals of the fourth period

and the electronic properties of the unfilled d bands. This is shown by the general trend of the rate of adsorption along the transition metal rows. For atomic species strong binding is observed on the left-hand side of a row. For molecular species it was found that the rate of dissociative adsorption on the noble metals increases from right to left as a function of the d-band occupation.

In the following example we shall examine the hydrogenation of CO on various metal catalysts. A clear dependence of reaction rate on d-band filling is observed (Fig. 5-25). Thus the familiar volcano plots can also be explained by an electronic factor [38].

Besides the electron occupation of the d bands, another description can be used for obtaining correlations, namely, the valence bond theory of metals. The bonding in a transition metal is partially due to unpaired electrons in bonding d orbitals. The contribution of these d electrons to the valence bonding was termed “percentage d

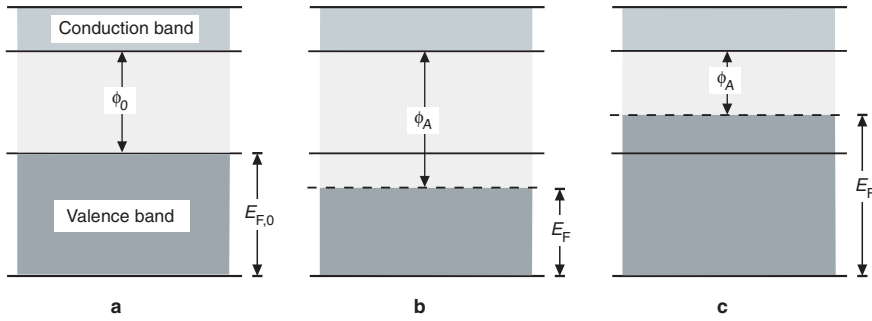


Fig. 5-24 Acceptor and donor function according to the band model:

a) no adsorption; b) acceptor; c) donor

$E_{F,0}$ = Fermi level; E_F = Fermi energy

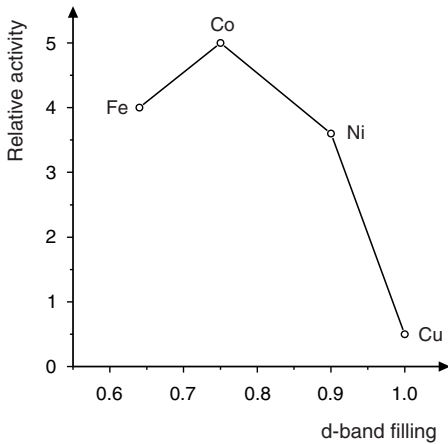


Fig. 5-25 Hydrogenation of CO to methane on various metal catalysts

character” of the metallic bonding by Pauling, who made a distinction between three types of d orbitals in transition metals:

- Bonding d orbitals involved in covalent dsp hybrid bonds
- Metallic (free) d orbitals
- Atomic d orbitals

The percentage d character δ can be calculated by using Equation 5-35.

$$\delta = \frac{\text{number of bonding d electrons} \times 100}{\text{bonding electrons} + \text{metallic orbitals}} \quad (5-35)$$

For nickel a δ value of 40 % has been calculated, and the highest values are found for Ru and Rh (50 %).

Relationships have indeed been found between the percentage d character and the catalytic activity, as we shall see for the hydrogenation of ethylene [T20]. However,

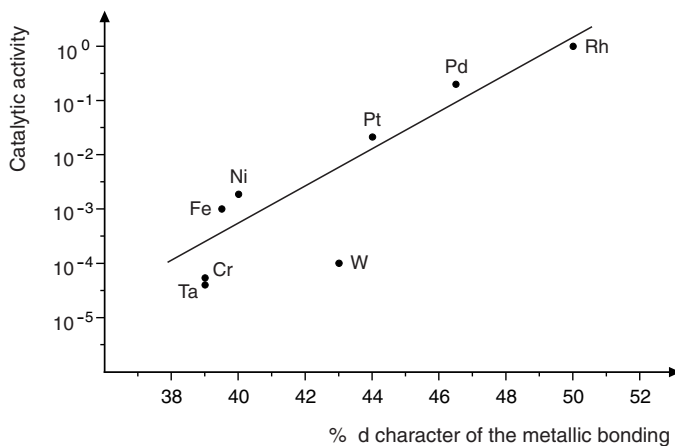


Fig. 5-26 Dependence of the catalytic activity of transition metals in the hydrogenation of ethylene on the percentual d character of the metallic bonding

the results (Fig. 5-26) can not be attributed exclusively to electronic effects. According to Pauling, the d character of the metallic bonding increases with decreasing lattice constants. Therefore, it is possible that geometric factors play the crucial role.

The degree to which the d band is filled with electrons has considerable influence on the chemisorption capability of metals. Alloying an active metal with another active or even inactive metal can increase or decrease the activity. This is shown by the example of the metals of groups 8–10 of the periodic table, which are particularly active in hydrogenation and dehydrogenation.

Alloying of these metals with the hydrogenation-inactive group 11 metals Cu, Ag, and Au leads to d-band filling of the base metal and lowers the hydrogenation activity. On investigating such bimetallic alloys, enrichment of copper on the surface was found, indicating that phase separation occurred during production of the alloy. This was determined by H₂ adsorption measurements. Hydrogenation of ethylene was investigated on Cu/Ni, Cu/Pt, and Cu/Pd alloys. Increasing the copper content raised the Fermi level and thus led to a lower reaction rate. In contrast, the activity of Ni is increased on alloying with Fe.

Similar effects are observed in other donor reactions, namely, the decomposition of formic acid and the decomposition of methanol. The opposite effect occurred in the decomposition of hydrogen peroxide. Here raising the Fermi level by adding copper accelerates the reaction. It is believed that an acceptor reaction is the rate-determining step, probably formation of O⁻ or OH⁻ ions.

In the case of Cu/Ni alloys it was found that the surface is primarily covered with copper over a wide range of compositions (18–95 % Ni). This can be shown by adsorption measurements with hydrogen (Fig. 5-27).

These Ni/Cu alloys exhibit special selectivity effects, which has been demonstrated in the hydrogenolysis of ethane to methane (Eq. 5-36) and the dehydrogenation of cyclohexane to benzene (Eq. 5-37).

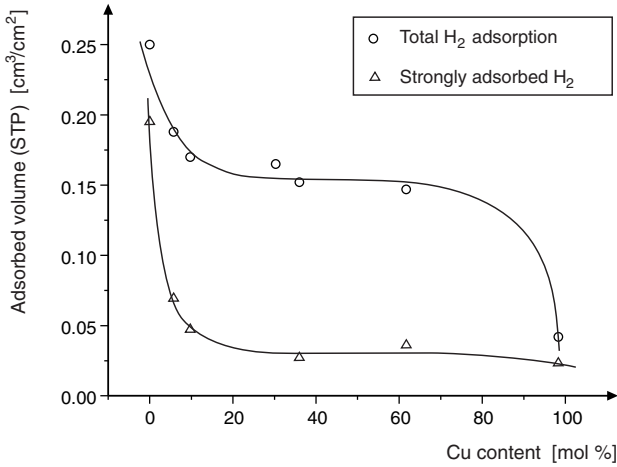
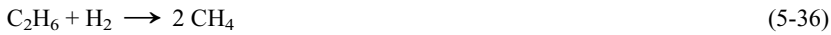


Fig. 5-27 Adsorption of hydrogen on copper–nickel alloys



As shown in Figure 5-28 the rate of hydrogenolysis of ethane decreases by three orders of magnitude on addition of 5 % Cu. It was found that at least two neighboring Ni sites are required to take up carbon fragments during the cleavage reaction. Increasing the content of copper, which is enriched on the surface, drastically reduces the number of mutually adjacent Ni sites.

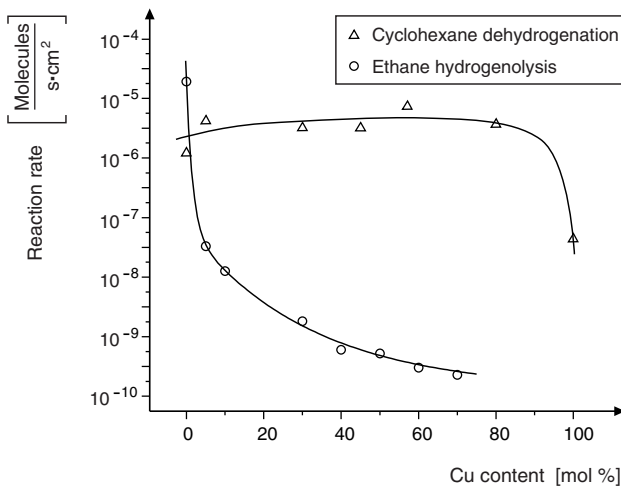


Fig. 5-28. Specific activity of copper–nickel alloys for the dehydrogenation of cyclohexane and the hydrogenolysis of ethane to methane at 316 °C

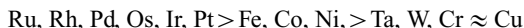
In contrast, the rate of cyclohexane dehydrogenation increases slightly for small contents of Cu in the alloy, then remains constant over a wide range, and only decreases at high Cu contents. Such effects are also noticeable for other alloys in cyclohexane dehydrogenation. For example, Pd/Ni, Pd/Ru, and Pd/Pt alloys have higher activities than Pd alone.

This effect has some industrial relevance. Thus the hydrogenolysis activity of supported Ru/Os reforming catalysts can be reduced by adding small amounts of copper, so that more alkenes are formed. These high surface area catalysts (ca. 300 m²/g) contain the metal in the form of mixed crystals, often less than 5 nm in diameter (“bimetallic clusters”). Here, too, the Cu is found exclusively on the surface of the noble metal Ru.

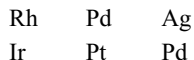
According to the current state of knowledge, the band model of metals has several shortcomings. As a simple physical model, it fails to take into account the various types of bonding and surface states. For example, chemisorption processes, which can not cause a change in conductivity, are not considered. Problems occur in particular in explaining the behavior of alloys. The electronic interactions between metal and adsorbate may be masked by steric effects, and experimental results are often not readily interpretable.

For these reasons we shall look at the suitability of metal catalysts in a more empirical manner, giving a few general rules [T40]:

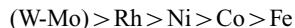
- 1) Metals are used as catalysts for hydrogenation, isomerization, and oxidation.
- 2) For reactions involving hydrogen (alone or in combination with hydrocarbons), the following activity series holds:



- 3) Pd is an excellent catalyst that is often active and selective. Pd enables selective hydrogenation of double bonds to be carried out in the presence of other functional groups.
- 4) Activities sometimes correlate with the percentage d character of the metallic bonding, but there are many exceptions.
- 5) Activities sometimes correlate with the lattice parameters of the metal.
- 6) The following metals are particularly stable towards oxygen and sulfur:



- 7) The activity of metals decreases in the order:



Numerous relative activity series for particular reactions can be found in the literature (Table 5-15). They differ widely and are often contradictory. Therefore, care must be taken in transferring them to other reactions and reaction conditions.

Table 5-15 Relative catalytic activity of metals [T33, T40, T41]

| | |
|--------------------------------------|--|
| Hydrogenation of olefins | Rh > Ru > Pd > Pt > Ir \approx Ni > Co > Fe > Re \geq Cu |
| Hydrogenation of ethylene | Rh, Ru > Pd > Pt > Ni > Co, Ir > Fe > Cu |
| Hydrogenolysis | Rh \geq Ni \geq Co \geq Fe > Pd > Pt |
| Hydrogenation of acetylenes | Pd > Pt > Ni, Rh > Fe, Cu, Co, Ir, Ru > Os |
| Hydrogenation of aromatics | Pt > Rh > Ru > Ni > Pd > Co > Fe |
| Dehydrogenation | Rh > Pt > Pd > Ni > Co \geq Fe |
| Double bond isomerization of alkenes | Fe \approx Ni \approx Rh > Pd > Ru > Os > Pt > Ir \approx Cu |
| Hydration | Pt > Rh > Pd \geq Ni \geq W \geq Fe |

5.3.3.2 Bimetallic Catalysts

There are many examples for bimetallic catalysts which are applied in industrial processes (Table 5-16).

Table 5-16. Bimetallic catalysts in industrial processes

| Catalyst | Process |
|--|---|
| Ni/Cu-SiO ₂ | hydrogenation of aromatics and long-chain olefins in the solvent industry |
| Pd/Fe-SiO ₂ | hydrogenation of 2,4-dinitrotoluene to 2,4-diaminotoluene (through 2-nitro-4-aminotoluene and 2-amino-4-nitrotoluene) |
| Rh, Ru, Ni + Sn | hydrogenation of esters to acids or alcohols |
| Rh/Mo-SiO ₂ or Al ₂ O ₃ | hydrogenation of CO and CO ₂ to methanol and dimethylether |
| Ni/Sn; Rh/Sn | hydrogenation of ethyl acetate to ethanol |
| Pt/Sn | dehydrogenation and cracking of alkanes |

We will discuss some special reactions with bimetallic catalysts in more detail. For example, the hydrogenation of ethyl acetate to ethanol has been studied with Rh/Sn-SiO₂ catalysts (Table 5-17). With increasing Sn content the following results were described [40].

The experimental results have been explained by following assumptions:

- Isolation of Rh atoms by Sn atoms at the catalyst surface
- The chemisorption ability of the bimetallic particles for CO and H₂ is drastically reduced
- IR: Rh/Sn-SiO₂ shows only terminal carbonyl groups at 2000 cm⁻¹
- E_a: Rh/SiO₂ 75.2 kJ/mol; Rh/Sn-SiO₂ 46 kJ/mol
- Electronic effect of Sn increases the electron density of Rh

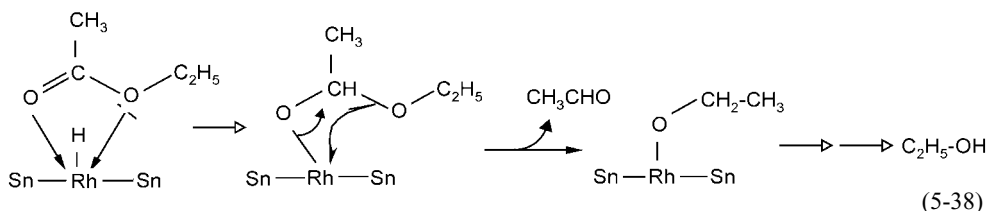
The reaction sequence on the catalyst surface is given in Equation 5-38.

Table 5-17 Hydrogenation of ethyl acetate to ethanol with Rh/Sn-SiO₂ catalysts [40]

| Catalyst Sn/Rh ratio | Conversion (%) | r (x 10 ³) (mol h ⁻¹ g ⁻¹) | Selectivity (%) | | |
|-------------------------|-------------------|--|--------------------|-------------------------------|----------------------|
| | | | EtOH | C ₂ H ₆ | CH ₄ + CO |
| 0/1 | 1.32 | 6.0 | 57.2 | 9.7 | 33.1 |
| 0.2/1 | 0.11 | 0.5 | 66.0 | 14.2 | 19.8 |
| 0.7/1 | 1.12 | 5.1 | 94.9 | 3.9 | 1.2 |
| 1.0/1 | 2.42 | 11.0 | 95.2 | 4.0 | 0.8 |
| 1.4/1 | 3.76 | 17.1 | 95.6 | 3.7 | 0.7 |
| 1.7/1 | 4.66 | 21.1 | 97.2 | 2.5 | 0.3 |
| 1.7/1* | 50 | 21 | 85.0 | 9.0 | 1.2 |
| 1.7/1* | 85 | 21 | 80.0 | 12.2 | 1.8 |

543 K, H₂/ethyl acetate = 9 : 1, 50 bar, differential flow reactor

* Long reaction times, also formation of diethylether and acetaldehyde



The selective gas-phase hydrogenation of crotonaldehyde has been investigated with supported bimetallic Pt catalysts. The results are given in Table 5-18.

Table 5-18 Hydrogenation of crotonaldehyde with bimetallic catalysts [42]

| Catalyst Pt content (mol-%) | TOF (mol/H _{ads} s) | C ₄ H ₁₀ | Selectivities (mol-%) | | |
|-----------------------------------|---------------------------------|--------------------------------|-----------------------|---------|--------------------|
| | | | Butanal | Butanol | Crotyl- alcohol |
| Pt/SiO ₂ (100) | 0.03 | 0.2 | 98.3 | 1.5 | 0 |
| Pt/Ni-SiO ₂ (70) | 0.45 | 0.3 | 92.0 | 5.7 | 2.0 |
| Pt/Ga-SiO ₂ (80) | 0.43 | 0.5 | 37.1 | 6.0 | 56.4 |
| Pt/Sn-SiO ₂ (95) | 0.36 | 0.5 | 63.1 | 5.5 | 30.9 |
| Pt/TiO ₂ (100) | 0.29 | 0.9 | 46.1 | 6.7 | 46.3 |

353 K, conversion < 10%, 1 bar, tubular reactor, metal loading 5.0–7.2%

It was concluded that

- C=O hydrogenation is favored by Pt-TiO_x and Pt-GaO_x and bimetallic particles of Pt-Sn and Pt-Ni
- C=C hydrogenation takes place at the surface of the pure metals

Bimetallic Pt/Sn catalysts find broad application for dehydrogenation reactions. The best supports for this purpose are alumina, ZnAl₂O₄ or MgAl₂O₄. The influence of tin as well as of the support was determined. We will only briefly name the effects which have been described.

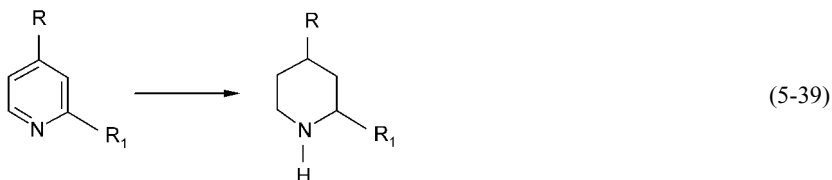
Influence of tin:

- Promoter: Sn = promoter for Pt, improves activity, selectivity and stability of the catalysts
- Electronic effects: Sn content up to 15% is sufficient to fill the 5d-band of Pt with electrons; less coke formation, less hydrogenolysis of C-C bonds
- Ensemble effect: dehydrogenation requires smaller Pt cluster or well dispersed Pt centers; alloying causes dilution of the Pt atoms, smaller ensembles

Influence of the support:

- Causes surface-acidity
- Improves stability during reaction and catalyst regeneration
- Stabilizes the Pt dispersion during all steps of the catalyst treatment, especially during coke removal by combustion
- May have chemical interactions with promoters
- Affects the pore size distribution

Another example for the kind of action of bimetallic catalysts is shown by the promoter effect of Rh improving the selectivity for the hydrogenation of a substituted pyridine [41]. From Table 5-19 can be seen that adjusting the ratio of the metals increases the selectivity of the reaction (Eq. 5-39).



Alloying with active or inactive metals can both accelerate desired reactions and suppress undesired reactions. For example, the addition of Sn to Pd gives selective catalysts for the removal of acetylene from ethylene streams. Similar effects are also observed for Zn, Pb, Ag, and Au [T41]. On alloying Pd with inactive Au, the rate of the reaction between H₂ and O₂ is increased by a factor of 50. As an additive to Pt, Au increases the rate of isomerization of *n*-hexane tenfold. These effects are explained in terms of a “widening” of the metal–metal bond by another metal.

Table 5-19 Hydrogenation of a pyridine derivative with alumina supported bimetallic catalysts [41]

| Catalyst | Selectivity (%) | Reaction time (hrs) |
|------------------|-----------------|---------------------|
| 5% Rh | 94 | 9 |
| 4% Rh, 2% Pt | 96–98 | 5 |
| 4% Pt, 1% Rh | 96–98 | 5 |
| 4.5% Pd, 0.5% Rh | 96–98 | 5 |

The range of variation of the catalytic properties of the noble metals is demonstrated by some industrial examples (Table 5-20) [T23].

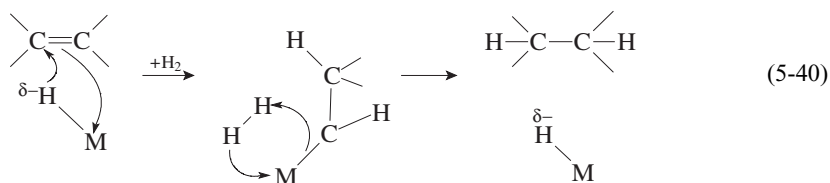
In more recent work, bimetallic Pd catalysts were investigated in the hydrogenation of saturated and unsaturated aldehydes, and fundamental mechanisms were determined [T32]. The following activity series was found for the hydrogenation of crotonaldehyde with metals of groups 8–10:

**Table 5-20** Modification of the catalytic properties of the platinum group metals by addition of other metals [T23]

| Base metal | Additive | Reaction | Effect of additive |
|------------|----------------|---|---|
| Pt | 5–20% Rh | ammonia oxidation | increased NO yield, lower Pt losses |
| Ag | Au | ethylene oxidation | higher selectivity of ethylene oxide formation |
| Ag | 10% Au | cumene oxidation | increased rate of formation of cumene hydroperoxide |
| Pt | Ge, Sn, In, Ga | dehydrogenation and hydrocracking of alkanes | increased lifetime due to lower carbon deposition |
| Pt | Sn + Re | dehydrocyclization and aromatization of alkanes | increased catalyst activity and stability |
| Pt | Pb, Cu | dehydrocyclization and aromatization of alkanes | effectivity of aromatization |
| Pt, Pd, Ir | Au | oxidative dehydrogenation of alkanes, <i>n</i> -butene to butadiene, methanol to formaldehyde | improved selectivity |
| Ir | Au (Ag, Cu) | hydroforming of alkanes and cycloalkanes | high aromatics yield above 500 °C |
| Pd | Sn, Zn, Pb | selective hydrogenation of alkynes to alkenes | |

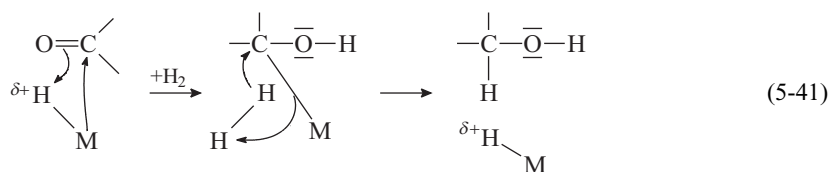
The opposite sequence applies in the hydrogenation of *n*-butyraldehyde to butanol. Both reactions are one-center processes in which the rate-determining step is the formation of a hemihydrogenated intermediate. The following mechanisms have been given for both reactions:

- 1) Hydrogenation of the alkene in a nucleophilic ligand addition reaction:



Electron-donor second metals should increase the nucleophilicity

- 2) Hydrogenation of the carbonyl group in an electrophilic ligand addition reaction:



Electron-acceptor second metals should increase the electrophilicity

The hydrogenation of the double bond in crotonaldehyde to form butyraldehyde proceeds smoothly with pure Pd/Al₂O₃ supported catalysts (Eq. 5-40). No significant influence of the alloying elements Fe, Sn, and Pb was found. However, these alloying elements accelerate the hydrogenation of butyraldehyde according to Equation (5-41). It was concluded that these elements act as electron acceptors and thus favor the electrophilic ligand addition reaction of hydrogen.

However, this is in disagreement with other results of test reactions reported in the literature, which found an electron-donor function for Fe, Sn, and Pb, partly by IR spectroscopy. This is a further example of the inconsistency of catalyst concepts, which are better regarded as working hypotheses.

5.3.3.3 Semiconductors [16, 35, T27]

Semiconductors are a group of nonmetallic solids whose electron structure is better understood than that of the metals. The band model, already discussed above, is useful for explaining the semiconductor character and catalytic properties of this class of substances.

Two energy bands are present in these crystalline solids: the lower-energy, electron-containing valence band and the considerably higher lying conduction band. The valence band contains all the electrons of the chemical bonds and the ionic

charges in the substance; it has no conductivity. The conduction band contains allowed electronic states, which, however, are all unoccupied.

The electronic properties of the solid depend on the size of the forbidden zone between the two bands. For semiconductors a distinction is made between *i*- (intrinsic), *n*-, and *p*-type semiconductors [T27]. In the *i*-type semiconductors electrons result from the splitting of homopolar bonds in the solid under the action of heat or light (photoconductivity) (Fig. 5-29).

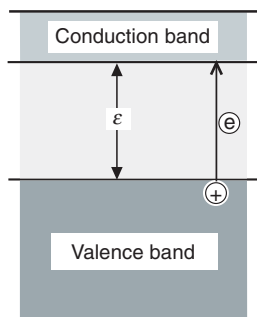


Fig. 5-29 Intrinsic semiconductor with excitation energy

These excited electrons can jump over the forbidden zone and occupy free states in the conduction band. At the same time a gap arises in the valence band, known as a positive hole. The size of the forbidden zone that must be overcome can be determined. One measure for this is the wavelength at which optical absorption begins. The corresponding energy ϵ is sufficient to raise an electron from the uppermost level of the valence band into the lowest level of the conduction band. Table 5-21 gives examples of crystals with the Si structure that are regarded as semiconductors.

Table 5-21 Excitation energies of semiconductors

| Substance | Excitation energy ϵ , eV (Fig. 5-29) |
|-------------|---|
| C (diamond) | 5.2 |
| Si | 1.09 |
| Ge | 0.6 |
| Sn (gray) | 0.08 |

The fraction of electrons of the valence band that are raised to the conduction band by thermal energy corresponds to the Boltzmann factor $\exp(-\epsilon/2kT)$. The *i*-type semiconductors play only a minor role in catalysis; the *n*- and *p*-type semiconductors are far more important. Nonstoichiometric oxides and sulfides are of industrial importance. The conductivity of these materials is low but can be considerably increased by doping with foreign atoms.

Assume that some of the building blocks of the crystal are replaced by foreign atoms that are electron donors, that is, atoms that readily release electrons on heating. These electrons are located in the forbidden zone, just below the conduction band, and therefore require only a small ionization energy E_i to reach the conduction band (Fig. 5-30a). The positive charge then remains localized on the donor atoms, and we have pure electron conductivity (n conductivity, $n = \text{negative}$).

It is also possible to incorporate electron acceptors in the crystal lattice. They readily take up an electron from the valence band (Fig. 5-30b). On heating, an electron from the valence band enters the acceptor level and remains there, so that a positive hole is generated in the valence band. Thus we now have pure p -type conductivity ($p = \text{positive}$), and the ionization energy E_i in this case is also low.

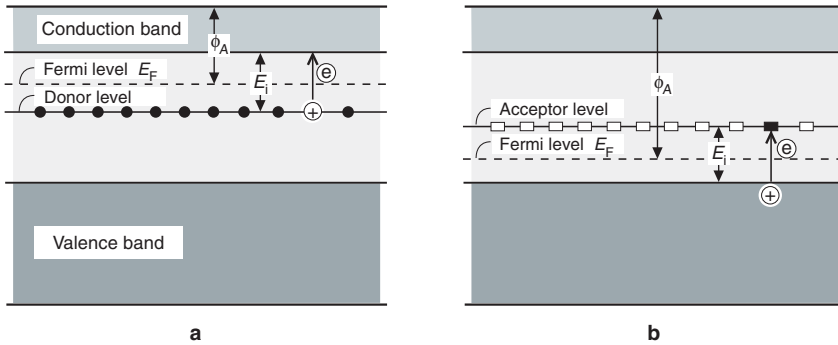
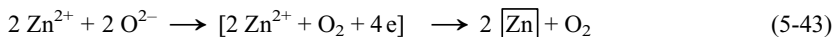
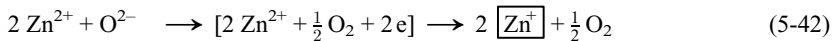


Fig. 5-30 Semiconductors and how they function: a) n -type semiconductor; b) p -type semiconductor

In semiconductors the Fermi level lies in the forbidden zone. It is the electrochemical potential intermediate between the highest filled and the lowest empty band. The Fermi level can easily be measured, and it is much higher in n -type semiconductors than in p -type semiconductors. Figure 5-30 also shows the corresponding work functions ϕ_A .

What connection is there between the structure of semiconductors and their properties? As already mentioned nonstoichiometric semiconductor oxides play an important role. On heating, their crystal lattices tend to release or take up oxygen. For an n -type semiconductor such as ZnO, the release of oxygen is described by Equations 5-42 and 5-43.



The semiconductor capability of ZnO in this case is due to the Zn^+ ions and Zn atoms formed by reaction with oxide ions. The above two reactions can be result from raising the temperature or by reaction with reducing gases such as H_2 , CO , and hydrocarbons

at room temperature. The Zn ions and atoms occupy interlattice sites and act as electron donors. An equivalent number of quasifree electrons gives electrical neutrality. The formula for the nonstoichiometric compound can be written Zn_{1+x}O .

If oxygen is chemisorbed on the ZnO, the conductivity is lowered because the oxygen acts as an electron acceptor (Eq. 5-44).



Chemisorbed hydrogen acts as an electron donor and increases the conductivity according to the reaction:



For a *p*-type semiconductor like NiO, the take up of oxygen by the lattice is described by Equation 5-46.



The incorporation of an O_2 molecule in the lattice in the form of O^{2-} ions leads to formation of four Ni^{3+} ions, each of which gives rise to a positive hole, whose mobility in the lattice is responsible for the observed conductivity.

The *p*-type or defect semiconductor has the formula Ni_{1-x}O . Metals that form such *p*-type oxides are those that exist in several oxidation states. The oxides contain the lower oxidation state form (e.g., Ni^{2+} , Co^{2+} , Cu^+), which can then enter the higher oxidation state (Ni^{3+} , Co^{3+} , Cu^{2+}). The *n*-type oxides, in contrast, are those that exist in only one oxidation state or in which the highest state is present (e.g., ZnO, TiO_2 , V_2O_5 , MoO_3 , Fe_2O_3).

The conductivity of both *n*- and *p*-type oxides is generally low. How can the increased conductivity due to doping be explained? In *p*-type semiconductors the number of positive holes must be increased, and this can be achieved by incorporating another oxide of lower oxidation state in the lattice. Thus replacing Ni^{2+} ions by Li^+ ions in the nickel oxide lattice leads to an excess of O^{2-} ions (to give electrical neutrality) and formation of Ni^{3+} ions. Doping with trivalent ions such as Cr^{3+} leads to the opposite effect.

In contrast, in an *n*-type semiconductor like ZnO, doping with Ga_2O_3 , Cr_2O_3 , or Al_2O_3 leads to increased conductivity, while addition of Li_2O lowers it. Only small amounts of foreign atoms are required for doping, normally less than 1%.

The general behavior of nonstoichiometric semiconductor oxides is summarized in Table 5-22. Table 5-23 classifies the most important oxides according to their electronic behavior.

There are several possibilities for measuring the semiconductor properties of a substance. One of these is to determine the conductivity of the solid at various temperatures; this describes the magnitude of the effect and its energy level. Other possibilities are to investigate the effect of photoelectric and photoelectromagnetic effects on the conductivity and the electron work function.

Table 5-22 Behavior of nonstoichiometric semiconductor oxides

| | <i>n</i> -Type | <i>p</i> -Type |
|--|--|-----------------------------|
| Oxides with ions in interlattice sites | ZnO, CdO | UO ₂ |
| Oxides with vacant lattice sites | TiO ₂ , ThO ₂ , CeO ₂ | Cu ₂ O, NiO, FeO |
| Type of conductivity | electrons | positive holes |
| Addition of M ₂ O | lowers conductivity | increases conductivity |
| Addition of M ₂ ^{III} O ₃ | increases conductivity | lowers conductivity |
| Adsorption of O ₂ , N ₂ O | lowers conductivity | increases conductivity |
| Adsorption of H ₂ , CO | increases conductivity | lowers conductivity |

Table 5-23 Classification of the metal oxides according to their electronic properties

| <i>n</i> -Type | <i>p</i> -Type | <i>i</i> -Type (intrinsic semiconductors) | Isolators |
|---|--|--|---|
| <i>Oxides of main group elements</i> | | | |
| ZnO, GeO ₂ , CdO, HgO, SnO ₂ , As ₂ O ₅ , Sb ₂ O ₅ , PbO ₂ , Bi ₂ O ₅ ; Al ₂ O ₃ (at high temperatures) | NiO, Cr ₂ O ₃ , MnO, FeO, CoO, Cu ₂ O, Ag ₂ O, PtO | Fe ₃ O ₄ , Co ₃ O ₄ , CuO | BeO, B ₂ O ₃ , MgO, Al ₂ O ₃ , SiO ₂ , P ₂ O ₅ , CaO, SrO, BaO |
| <i>Oxides of transition metals</i> | | | |
| Sc ₂ O ₃ , TiO ₂ , V ₂ O ₅ , Fe ₂ O ₃ , ZrO ₂ , Nb ₂ O ₅ , MoO ₃ , Ta ₂ O ₅ , HfO ₂ , WO ₃ , UO ₃ | | | |

In practice the results of these measurements are the subject of controversy. A solid can contain various impurities (e. g., Zn and Zn⁺ in ZnO) and can have both donor and acceptor levels. The measurements can be carried out on the isolated solid or in the presence of reactants. Interpretation of conductivity, ionization energy, and work function data is difficult. Once again, surface effects must be examined separately from effects inside the lattice.

Thus, similar to the case for metals, the applicability of electronic theory to catalysis is limited. The predictions often contradict experimental results; for example:

- 1) Oxides and sulfides of the transition metals are the most active, most selective, and industrially most important catalysts. According to electronic theory, numerous other semiconductors should have good catalytic properties, which could be

influenced by modification. However, apparently chemical factors are predominant in the catalytic activity.

- 2) Additives that lead to large changes in the conductivity ought to strongly influence the catalytic properties of the material. Semiconductor oxide and sulfide catalysts are, however, considerably less susceptible to poisoning than metal catalysts. Furthermore, the composition of semiconductor mixed crystals can be varied over a wide range without affecting their catalytic properties.

In the case of this concept, too, empirical findings are of greater interest than exact theoretical predictions of catalytic activity. It is particularly useful for explaining many chemisorption effects and for oxidation reactions.

It can be of practical importance to modify the electronic properties of cheap semiconductor catalysts by doping such that their activity corresponds to that of expensive noble metal catalysts. Two industrial examples of such substitutions are the SCR process (waste-gas purification) and the selective oxidation of methanol to formaldehyde.

Chemisorption on Semiconductors

The chemisorption of simple gases on semiconductors can be relatively simply understood in terms of the chemical reaction of the adsorbate with the catalyst. Reducing gases like hydrogen and CO are strongly and irreversibly adsorbed. On heating, only water and carbon dioxide are detectable. On adsorption, H₂ mainly undergoes heterolytic dissociation (Eq. 5-47):



On heating, the hydroxyl ion is decomposed to water and anionic defects, and a corresponding number of cations are reduced to atoms.

On *n*-type semiconductors, H₂ and CO almost totally cover the surface, whereas chemisorption on *p*-type semiconductors is less extensive. In this strong chemisorption a free electron or positive hole from the lattice is involved in the chemisorptive bonding. This changes the electrical charge of the adsorption center, which can then transfer its charge to the adsorbed molecule.

The change in the electrical charge density on the surface can hinder the further adsorption of molecules of the same gas. A decrease in the heat of adsorption with increasing degree of coverage is then observed, and hence a deviation from the Langmuir adsorption isotherm occurs.

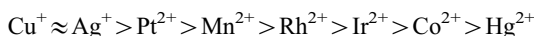
Chemisorption of CO usually occurs initially on metal cations, after which it reacts with an oxide ion according to Equation 5-47. This reaction can eventually lead to complete reduction of the oxide to the metal.



When oxygen is adsorbed on an *n*-type semiconductor, electrons flow from the donor level, and O⁻ and O²⁻ ions can be observed. The surface of the solid be-

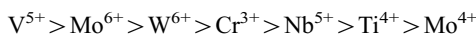
comes negatively polarized, and the adsorption of further oxygen requires more and more energy. Therefore the adsorption of oxygen on *n*-type semiconductors is subject to very rapid auto-inhibition. If *n*-type semiconductors like ZnO have their exact stoichiometric composition then they can not chemisorb oxygen. If they are oxygen deficient, they can chemisorb precisely the amount of oxygen required to fill the anionic defects and reoxidize the zinc atoms.

Metals that favor the adsorption of oxygen have five, seven, eight, or ten d electrons. The order of preference is:



Therefore the corresponding *p*-type semiconductors Cu₂O, Ag₂O, MnO, and PtO are highly effective catalysts for the activation of oxygen.

In *n*-type semiconductors, metal ions having one, two, or five d electrons are advantageous for the adsorption of oxygen. The following series was determined experimentally:

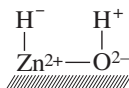


Accordingly, *n*-type semiconductors like V₂O₅, MoO₃, WO₃, Cr₂O₃, and TiO₂ are effective oxidation catalysts.

We have already encountered the chemisorption of oxygen on *p*-type oxides (Eq. 5-46). It results in high degrees of coverage and eventually in complete coverage of the surface by O⁻ or O²⁻ ions. At the same time Ni²⁺ ions are oxidized at the surface (Eq. 5-49). The heat of adsorption remains practically constant while the surface becomes saturated with oxygen.



The course of reaction on a semiconductor oxide may also depend on the sites to which the starting materials are bound and the manner in which they are bound. Consider the adsorption of hydrogen. It has been shown that hydrogen is heterolytically cleaved on a ZnO surface, so that simultaneous formation of a donor and an acceptor takes place. Active hydrides are bound to the ZnO surface:



Cr₂O₃ can heterolytically cleave H₂ in two ways:





The adsorption of various gases on special TiO₂ surfaces with surface defects (oxygen holes) has been studied in detail. The following results were obtained [17, 35];

- H₂ is dissociatively bound on Ti
- O₂ is dissociatively bound and fills O₂ holes
- CO is bound molecularly on Ti atoms with O₂ holes
- CO₂ reacts with O²⁻ ions to form surface carbonate; this is not influenced by the O₂ holes

All of these findings are important for understanding reaction mechanisms on semiconductor catalysts.

Reactions on Semiconductor Oxides [T20, T40]

The knowledge obtained about chemisorption on semiconductor oxides makes possible a better understanding of the behavior of these materials as oxidation catalysts. An oxidation reaction consists of several steps:

- 1) Formation of an electron bond between the starting material to be oxidized (e.g., a hydrocarbon) and the catalyst; chemisorption of the starting material.
- 2) Chemisorption of oxygen.
- 3) Transfer of electrons from the molecule to be oxidized (the donor) to the acceptor (O₂) by the catalyst.
- 4) Interaction between the resulting ion, radical, or radical ion of the starting material and the oxygen ion with formation of an intermediate (or the oxidation product).
- 5) Possible rearrangement of the intermediate.
- 6) Desorption of the oxidation product.

Hence the oxidation catalyst must be capable of forming bonds with the reactants and transferring electrons between them. Oxides of the *p*-type, with their tendency to adsorb oxygen up to complete saturation of the surface, are more active than *n*-type oxides. Unfortunately, activity and selectivity mostly do not run parallel, and the *p*-type semiconductors are less selective than the *n*-type semiconductors. The *p*-type semiconductors can often cause complete oxidation of hydrocarbons to CO₂ and H₂O, while the *n*-type semiconductor oxides often allow controlled oxidation of the same hydrocarbons to be performed.

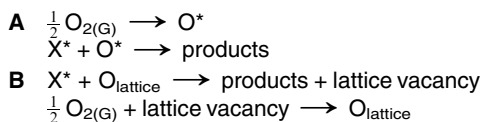
The ratio of adsorbed oxygen to hydrocarbon on *p*-type semiconductor oxides is generally high and is difficult to control even at low partial pressures of oxygen. The result is often complete combustion of the hydrocarbon. In contrast the amount of adsorbed oxygen on *n*-type semiconductors is generally small and can readily be controlled by means of the nature and amount of dopant, making selective hydrocarbon oxidation possible.

However, in practice neither *p*- nor *n*-type semiconductors are good catalysts for highly selective oxidations. Experience has also shown that a combination of the two semiconductor types also does not give any outstanding results with respect to activity and selectivity. Nevertheless, many simple oxidation reactions have been investigated with semiconductor catalysts, as we shall see in the following examples.

Variations in the selectivity of oxidations is explained in terms of:

- Electronegativity differences
- Ionization potentials of the metals
- Strength of oxygen bonding on the surface of the oxidation catalyst (“removability of lattice oxygen”)

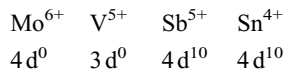
Simple two-step oxidation/reduction mechanisms are often used to explain industrial reactions. The oxidation of a molecule X can proceed by two mechanisms (Scheme 5-3).



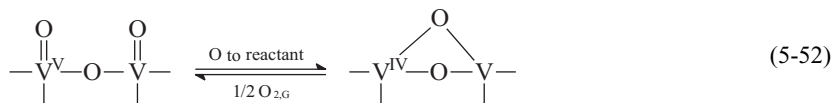
Scheme 5-3 Mechanisms of oxidation [T22]

In case **A**, O₂ is more rapidly adsorbed than the substrate X, and X* then reacts to remove this “excess” oxygen. Oxidation then proceeds through to the final products carbon dioxide and water.

In case **B**, adsorbed molecules of the starting material react with lattice oxygen. The result is selective oxidation, as is observed for partially oxidized molecules such as carbonyl compounds and unsaturated species in particular. Selective catalysts that react according to this Mars–van Krevelen mechanism formally contain a cation with an empty or filled d orbital, for example:



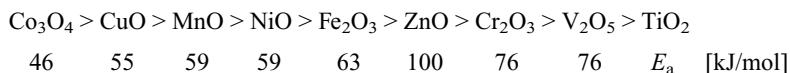
Metals in their highest oxidation states readily release lattice oxygen, formally as O²⁻. The well-known V₂O₅ catalysts have been intensively investigated. It was found that the rate of oxidation depends on the number of V=O bonds on the surface, and this was confirmed for the oxidation of H₂, CO, ethylene, butenes, butadiene, and xylene. The decisive step is the transition of V^V into the lower oxidation state V^{IV} (Eq. 5-52). A similar description can be applied to the oxidation of methanol to formaldehyde on Mo=O bonds.



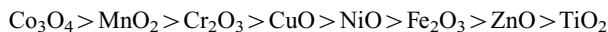
Metal oxides, especially those of the transition metals, can oxidize, dehydrogenate, decarboxylate, decarbonylate, and cleave C–C bonds. Numerous empirical activity and selectivity series can be found in the literature [32, T41].

Activity Series

For the oxidation of H₂ in excess oxygen:



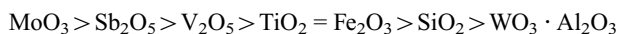
Oxidation of ammonia:



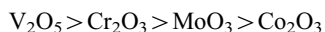
For both the above series the dissociative adsorption of oxygen is the rate-determining step.

Selectivity series are of greater practical importance.

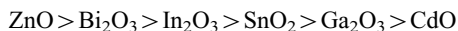
Oxidation of propene to acrolein:



Oxidation of benzene to maleic anhydride:



Oxidative dimerization and ring closing of propene to give 1,5-hexadiene and benzene:

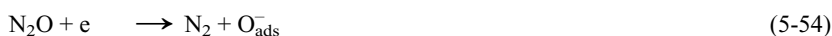


These few examples show that there can be no generally valid selectivity series for oxidation catalysts; each reaction must be investigated individually. In the following section we shall discuss some well-known reactions in more detail.

A well-investigated model reaction is the decomposition of N₂O (Eq. 5-53).



The mechanism is described as follows:





The release of electrons to the catalyst is the rate-determining step; in addition, a good catalyst should readily adsorb oxygen. The transfer of an electron from adsorbed O^- only takes place if the Fermi level of the surface is lower than the ionization potential of adsorbed O^- . This situation is more likely for *p*-type semiconductors. An activity series has been given for this reaction, the criterion being the temperature at which decomposition begins. The catalysts can be classified in three groups, as shown in Figure 5-31. As expected, the *p*-type semiconductor oxides are the most active catalysts, followed by the insulator oxides, and finally the *n*-type semiconductor oxides. This ranking has been verified by subsequent work, and relative activities have been determined. The overall trend does not follow any correlative relationship, and the results are presumably influenced by other effects such as dispersity, impurities, and number and symmetry of the active centers. The influence of donors on NiO catalysts can be clearly be seen, as the following series shows [T35]:



Thus *p*-type doping has a positive effect, and *n*-type doping, a negative one.

A donor reaction was also found to be rate-determining for the *n*-type semiconductor catalyst ZnO, which showed considerably higher activity after doping with Li_2O . The oxidation of CO (Eq. 5-56) has also been thoroughly investigated with the *p*-type semiconductor NiO and the *n*-type semiconductor ZnO as catalyst (Table 5-24).

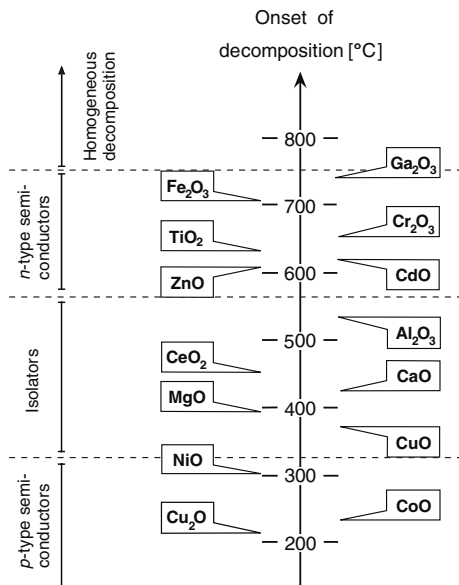


Fig. 5-31 Relative activities of metal oxides in the decomposition of N_2O [5]

Table 5-24 Oxidation of CO with metal oxide catalysts

| Catalyst | E_a [kJ/mol] |
|---|----------------|
| 1. NiO (<i>p</i>) | <u>63</u> |
| Doped with Cr ₂ O ₃ | 80 |
| Doped with Li ₂ O | <u>50</u> |
| ----- | |
| 2. ZnO (<i>n</i>) | <u>118</u> |
| Doped with Ga ₂ O ₃ | <u>84</u> |
| Doped with Li ₂ O | 134 |

As expected the *p*-type semiconductor NiO is the better catalyst. An increased *p*-type conduction due to Li₂O and a decrease due to Cr₂O₃ is understandable. It is assumed that a donor step is rate-determining, namely, the chemisorption of CO.



This assumption is supported by the observation that the reaction is first order in CO. The chemisorption of O₂ (Eq. 5-58), an acceptor step, is fast, and the reaction rate is not dependent on the oxygen partial pressure.



The final step is neutral and follows the Langmuir–Hinshelwood mechanism (Eq. 5-59).



The influence of donors on ZnO at first appears remarkable. Here one would expect that increasing the *n*-type conductivity by adding trivalent donors would lower the reaction rate. However, this does not happen. This leads to the conclusion that in this case an acceptor reaction is the rate-determining step. Presumably it is the chemisorption of oxygen, since considerable dependence of the reaction rate on the oxygen partial pressure was observed. The example shows how the reaction mechanism can change from catalyst to catalyst.

The next reaction that we will study is the decomposition of ethanol (Eq. 5-60). Depending on the catalyst, dehydrogenation (A) or dehydration (B) can occur. Table 5-25 summarizes the results [T35].

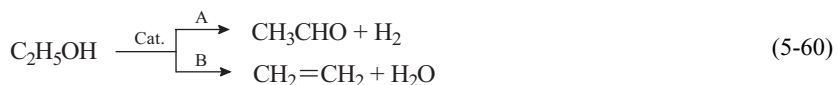


Table 5-25 Decomposition of ethanol on semiconductor oxides

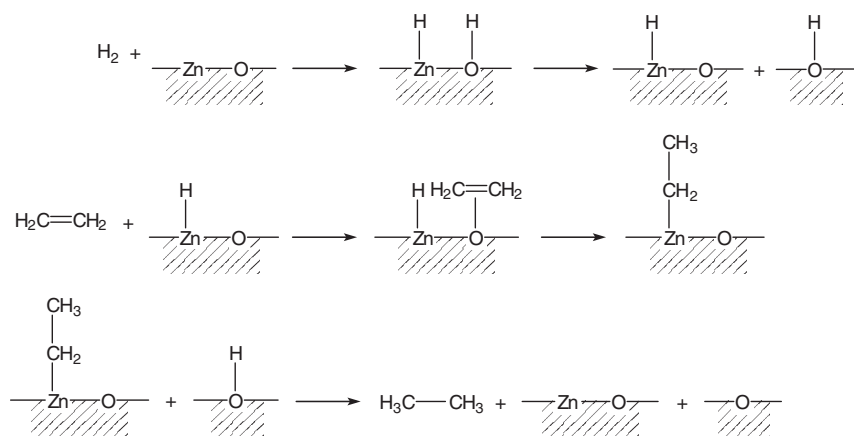
| Catalyst | | Decomposition of ethanol [%] | |
|----------------------------------|---|--------------------------------------|--|
| | | CH ₃ CHO + H ₂ | C ₂ H ₄ + H ₂ O |
| γ-Al ₂ O ₃ | ↓ | | |
| Cr ₂ O ₃ | | increasing | 98.5 |
| TiO ₂ | | <i>n</i> -type | 91 |
| ZrO ₂ | | character | 63 |
| Fe ₂ O ₃ | | | 45 |
| ZnO | | 86 | 14 |
| | | 95 | 5 |

The results can easily be explained. The extent of dehydrogenation increases with rising Fermi level and increasing *n*-type character, while dehydration follows the opposite trend.

The hydrogenation of ethylene on the catalyst ZnO at ca. 100°C has been thoroughly studied by IR spectroscopy. The catalytic centers on the surface are ZnO pairs. Adsorption measurements have shown that these pairs lie spatially far apart on the surface [T24]. We have already seen that ZnO can cleave hydrogen heterolytically. The hydrogen atom bound to oxygen can be transferred to other oxygen atoms in the lattice (Scheme 5-4).

The starting material ethylene is also initially bound to oxygen by physisorption and then chemisorbed. The reaction of neighboring hydrogen and ethylene ligands leads to formation of a σ -ethyl complex on Zn. This complex is then hydrogenated to ethane by chemisorbed H, which migrates from oxygen to Zn centers.

Binary oxide catalysts are of major industrial importance. Such compounds are combinations of the oxides of Fe, Co, Ni, Cu, and Zn with those of Cr, Mo, and W.



Scheme 5-4 Hydrogenation of ethylene on ZnO

They form mixed oxide phases such as chromites, molybdates, and tungstates. Important industrial processes involving mixed oxides are:

- Oxidation of methanol to formaldehyde: Fe/Mo, Fe/W
- Selective hydrogenation and dehydrogenation: Cu/Cr
- Desulfurization, denitrogenation, and deoxygenation: Co/Mo, Ni/Mo
- Methanol synthesis: Zn/Cr, Zn/Cu
- CO conversion: Fe/Cr

In methanol synthesis Cu^I ions are dispersed in a ZnO matrix. Copper chemisorbs CO, and ZnO sites adsorb hydrogen. The heterolytically cleaved hydrogen reacts with the chemisorbed CO to give CH–OH fragments, which are further hydrogenated to methanol.

The Cr₂O₃/Al₂O₃ catalysts are used for the dehydrogenation of butanes to butenes and butadiene. With the addition of alkali metal oxides, they are used for the aromatization of *n*-alkanes. In these catalysts Al₂O₃ does not act only as a support, it also forms mixed phases with the chromium oxide. The active centers in these catalysts are Cr²⁺ and Cr³⁺ ions [T41].

Semiconductor oxides are also important support materials. Even if a support is inactive in the reaction under consideration, it can considerably change the reactivity of the catalyst that it supports. As an example, metals such as Ni and Ag are often applied to doped Al₂O₃ by vapor-phase deposition. The resulting catalyst system behaves like a rectifier in that electrons flow from the support through the catalyst metal to the reactants (Eq. 5-61). Hence in this case acceptor reactions are favored.



Such systems are of course less well suited to donor reactions, for which a *p*-doped support with an electron-withdrawing effect would be more favorable. There are many examples of support effects, which are discussed in more detail in Section 5.4.

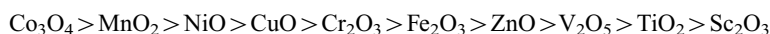
Major influences have been observed in the reactions listed in Table 5-26.

Table 5-26 Reactions with supported catalysts

| Reaction | Catalyst |
|------------------------|---|
| Formic acid cleavage | Ni/Al ₂ O ₃ Ag/SiC |
| Ethylene hydrogenation | Ni/ZnO |
| Aldehyde hydrogenation | Pd/C |

Finally let us summarize the knowledge gained in some general rules [T40]:

- 1) Transition metal oxides catalyze oxidation and dehydrogenation reactions.
- 2) Simple oxides with several stable oxidation states are generally the most active catalysts.
- 3) Alkalis generally stabilize high oxidation states, and acids, low oxidation states.
- 4) Activity and selectivity often follow opposite trends in catalytic oxidations.
- 5) Metal oxides with d^0 or d^{10} electronic structures are often selective oxidation catalysts.
- 6) Activity correlates with
 - the strength of bonding of oxygen to the surface
 - the heat of formation of the metal oxide
 - the number of O atoms in the oxide
 - the availability of lattice oxygen
- 7) The catalytic activity in the oxidation of H_2 , CO, or hydrocarbons correlates with the bonding energy of oxygen on the surface:



For a fundamental understanding of catalytic reactions, it is not sufficient to simply consider the global electronic properties of the catalyst. The surface geometry, the orbital structures of catalyst and starting materials, and other effects must also be considered. Refinement of the electronic concept of semiconductor catalysis is therefore essential.

5.3.3.4 Isolators: Acidic and Basic Catalysts [T24, T39, T41]

Catalysts belonging to this group are less common, and their activity for redox reactions is relatively low, at least at low temperatures. The solid oxides of the third period Na_2O , MgO , Al_2O_3 , SiO_2 , and P_2O_5 are insulators, and they exemplify the transition from basic through amphoteric to acidic character. The oxides of the elements of other periods behave similarly.

Since the catalytic properties can not be explained directly by means of electronic properties, it is appropriate to introduce another catalyst concept. In this case, the acid/base concept is suitable. Well-known catalysts with insulator properties are Al_2O_3 , aluminosilicates, SiO_2/MgO , silica gels, phosphates such as $AlPO_4$, and special clays activated by chemical treatment. All these catalysts have acid centers on their surface.

A special class of crystalline aluminosilicates are the highly active and selective zeolites, which are discussed separately in Chapter 7.

In comparison, the basic catalysts play only a minor role. Well-known acidic/basic catalysts are listed in Table 5-27.

Table 5-27 Classification of acid/base catalysts [T41]

| Solid acid catalysts | Solid basic catalysts |
|--|--|
| 1. Oxides such as Al_2O_3 , SiO_2 , TeO_2 | 1. Oxides, hydroxides, and amides of alkali and alkaline earth metals (also on supports) |
| 2. Mixed oxides such as $\text{Al}_2\text{O}_3/\text{SiO}_2$, MgO/SiO_2 , $\text{ZrO}_2/\text{SiO}_2$, heteropolyacids | 2. Anion exchangers |
| 3. Mineral acids (H_3PO_4 , H_2SO_4) on solid porous supports | 3. Alkali and alkaline earth metal salts of weak acids (carbonates, carbides, nitrides, silicates, etc.) |
| 4. Cation exchangers | 4. Superbases: MgO doped with Na |
| 5. Salts of O-containing mineral acids; heavy metal phosphates, sulfates, tungstates | |
| 6. Halides of trivalent metals (e. g., AlCl_3) on porous supports | |
| 7. Zeolites (H form) | |
| 8. Superacids: ZrO_2 or TiO_2 , treated with H_2SO_4 | |

Surface Acidity

Oxidic catalysts with acidic properties catalyze many industrial reactions, including the dehydration of alcohols, the hydration of olefins, cracking processes, and olefin polymerization. How does the acidity of such solids arise?

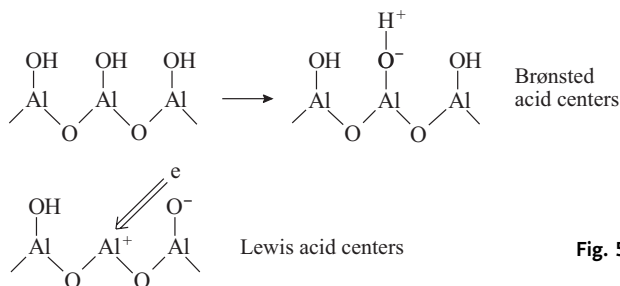
For surface acids a distinction is made between protic (Brønsted centers) and non-protic (Lewis centers). Brønsted centers can release surface protons, while Lewis centers represent surface acceptor sites for electron pairs and thus bind nucleophiles.

Let us consider the role of Brønsted and Lewis centers in catalysis, using the example of aluminum oxide. Aluminum oxide contains bound water, the amount depending on the temperature. Freshly precipitated, water-containing Al_2O_3 is completely hydroxylated on the surface up to a temperature of 100°C . The OH groups act as weak Brønsted acids. Above 150°C the OH groups are gradually lost as water. This dehydroxylation liberates some of the Al atoms in the second layer, and these act as Lewis acid centers. At 400°C the surface of partially dehydroxylated Al_2O_3 exhibits Lewis acid sites with coordination holes (Al^{3+} ions), Lewis base sites (O^{2-} ions), and Brønsted acid sites (Fig. 5-32).

At 900°C the fully dehydroxylated Al_2O_3 exhibits only Lewis acid and Lewis base sites.

It has been shown that the Brønsted acid sites are largely responsible for the polymerization of olefins, the cracking of cumene, and the disproportionation of toluene to benzene and xylene. In contrast, a strong influence of the Lewis acid centers was found in the decomposition of isobutane [32].

The catalytic function of solid acids and bases is fundamentally similar to that of their counterparts in liquid systems. Thus the Brønsted equation is also applicable

Fig. 5-32 Acid centers in Al_2O_3

to heterogeneous catalysis. Since surface-acidic compounds do not dissociate, in contrast to liquid systems, the Brønsted equation in its special form for concentrated acids applies (Eq. 5-62).

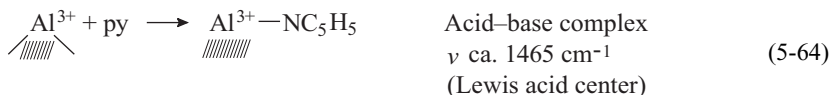
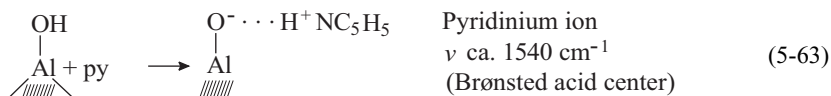
$$\lg k = \lg a + \alpha H_0 \quad (5-62)$$

where k is the rate constant of the catalytic reaction, α is a measure of the proton transfer ($\alpha < 1$), a is a constant for a particular class of reaction, and H_0 is the Hammett logarithmic acidity function, a measure of the protonation of the acid.

The acidity function H_0 gives information on the acid centers of a catalyst. It can be determined by means of a series of calibrated bases in the presence of special indicators, and in this way, comparison to sulfuric acid of known strength can be made.

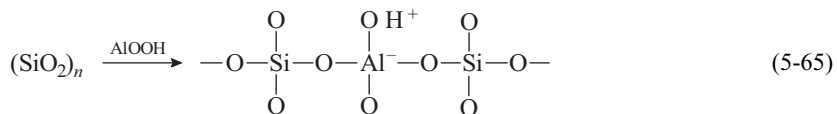
Other methods for determining the surface acidity of a catalyst are also available. For example the sum of Brønsted and Lewis centers can be determined by chemisorption of basic substances such as ammonia, quinoline, and pyridine.

Infrared spectroscopy is a powerful method that allows the direct determination of the Brønsted centers. When pyridine (py) is adsorbed on the catalyst simultaneous determination of both types of center is possible, since it is bound to Brønsted centers in the form of a pyridinium ion through a hydrogen bond (Eq. 5-63), whereas on Lewis acid centers, adsorption occurs by a coordinative acid–base interaction (Eq. 5-64).



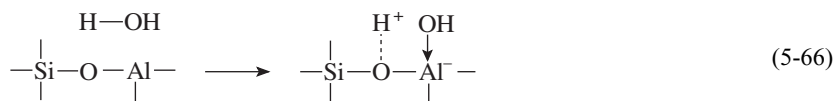
In comparison with Al_2O_3 , Lewis centers are not so readily formed on the surface of SiO_2 since the OH groups are very strongly bound, so that Brønsted acidity predominates, albeit in a weak form, comparable to acetic acid.

The aluminosilicates have major industrial importance as cracking catalysts. These are derived formally from silicates by partially replacing the Si atoms in the silicate framework by Al atoms [32]. Since each Al center has one nuclear charge less than Si, each Al center has a formal negative charge, which requires additional cations for neutralization. If these are protons, then a very strong, high-polymer acid is formally obtained (Eq. 5-65).

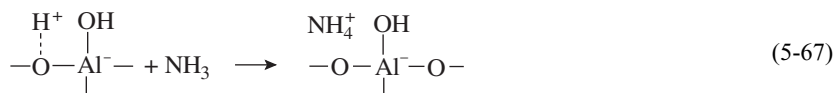


The acidity of these catalysts can be determined by titration with alkalis or by poisoning with nitrogen bases such as ammonia and quinoline. Good information about the active centers and the species adsorbed on them can be obtained by ESR spectroscopy.

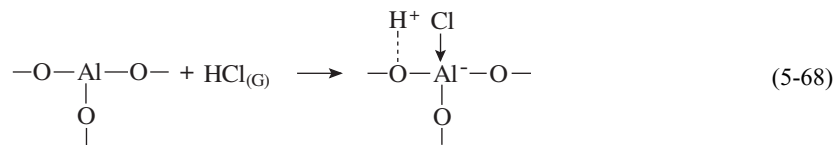
In contrast to Al_2O_3 , aluminosilicates exhibit pronounced Brønsted acidity. This can be explained in terms of dissociatively adsorbed water on the surface (Eq. 5-66).



According to Equation 5-66, the Al center can form its fourth bond with a free electron pair of a hydroxide anion. At the same time, the proton can react with a free electron pair of a neighboring O atom, and the formation of a partial bond results in a Brønsted acid center. The Si^{4+} center, which is more electropositive than Al^{3+} , weakens the O–H bond and increases the acidity. Experimentally it was found that maximum acidity occurs at ca. 30 % Al_2O_3 . This model also allows the chemisorption of ammonia on Brønsted centers to be explained (Eq. 5-67).



It also allows the pronounced increase in the Brønsted acidity resulting from the adsorption of HCl on aluminosilicates to be understood (Eq. 5-68).



Dehydration of organic molecules can occur on surface acids, for example, the conversion of alcohols to ethers and ketones. A good example is the reaction of ethanol on modified Al_2O_3 catalysts of various acidities (Table 5-28).

Table 5-28 Performance of aluminum oxides in the dehydration of ethanol [7]

| Relative acidity ^{a)} at 175 °C | SiO ₂ [%] | Na ₂ O [%] | Conversion [%] | Selectivities | | C(coke) [%] |
|--|----------------------|-----------------------|----------------|---------------|-----------|-------------|
| | | | | Ethene [%] | Ether [%] | |
| 0.021 | 0.02 | 0.25 | 66.1 | 25.3 | 70.1 | 0.1 |
| 0.046 | 0.01 | 0.06 | 98.8 | 99.2 | 0.2 | 0.2 |
| 0.060 | 0.13 | 0.03 | 85.7 | 89.2 | 0.1 | 0.5 |

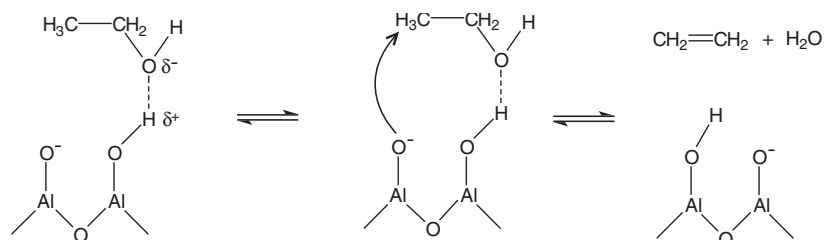
a) mmol NH₃/g Al₂O₃

The commercially available aluminas used here contain SiO₂ and Na₂O as the main impurities. Apparently both components influence the conversion and the selectivity with respect to ethylene. The dehydration proceeds by a cyclic mechanism involving the action of an acid and a basic center (Fig. 5-33).

Silica increases the acid content of the surface, and Na₂O influences the basicity. The parameter measured was the relative acidity by ammonia adsorption. The presence of SiO₂ or Na₂O results in an equilibrium between Brønsted acid centers, Lewis acid centers, and Lewis base centers. The catalyst with medium acidity has both the highest activity and the highest selectivity for ethylene. The weakly acidic catalyst with the highest Na₂O content allows greater formation of ether.

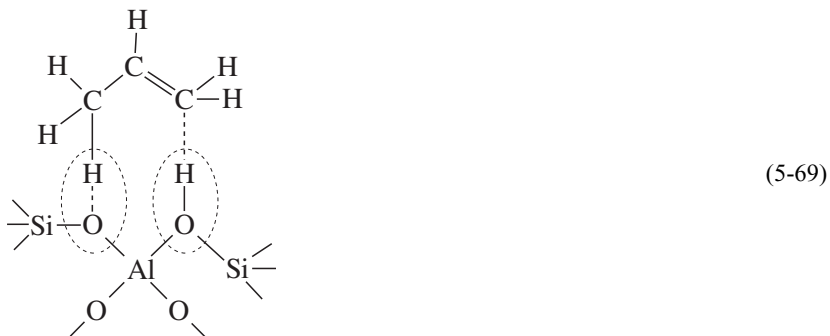
Another important factor in industrial reactions is coke formation. As expected, the catalyst with the highest content of SiO₂ (highest acid content) has the most pronounced tendency for coke formation. This is explained by increased formation of carbenium ions, which undergo fast coupling and polymerization reactions that eventually lead to involatile deposits on the surface. This also leads to lower activity and selectivity of the catalyst.

A further finding was that only the moderately active Brønsted acid centers are responsible for dehydration, and that Lewis acid centers such as Al³⁺ are not involved. Evidence for this is that the addition of small amounts of bases such as NH₃ or pyridine does not inhibit the reaction. The formation of ether on Al₂O₃ is explained by a Langmuir–Hinshelwood mechanism, in which two adjacently adsorbed

**Fig. 5-33** Mechanism of gas-phase dehydration of ethanol on aluminum oxide

intermediate alcohol fragments—for example, one bound as an alkoxide $-\text{OC}_2\text{H}_5$ and the other by hydrogen bonding—react with one another.

The chemisorption of olefins on an aluminosilicate catalyst is also believed to proceed by a mechanism similar to that shown in Figure 5-33. As shown in Equation 5-69, the olefin couples with an acid/base pair, that is, a bridging hydroxyl group and a lattice oxygen center on the surface, probably as the result of a direct geometrical correspondence.

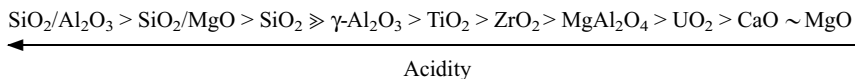


Acidic aluminosilicate-based catalysts are of major industrial importance. In terms of product quantity, the most important catalytic process is the cracking of crude oil. The reaction is initiated by the reaction of a Brønsted acidic surface with alkenes in which addition of a proton to the double bond gives chemisorbed carbenium ions (Eq. 5-70).



Cleavage of long-chain hydrocarbons is accompanied by extensive isomerization, polymerization, and alkylation of the initial products and formation of aromatic hydrocarbons. The same reactions occur in the the homogeneously catalyzed reaction initiated by protons or Lewis acids (BF_3 , AlCl_3).

It has been shown in many cases that the acid strength of a catalyst of given composition is often comparable to its activity. Thus the polymerization of olefins and the formation of coke depend on the catalyst acidity, for which the following series is given [T40]:



Experience has shown that much stronger acids are formed when two oxides whose cations have different coordination numbers or oxidation states are combined. Such catalysts with a broad activity spectrum are listed in Table 5-29. The acid

Table 5-29 Acid strength of binary mixed oxides [T41]

| Components A–B | A [%] | Specific surface area [m ² /g] | Acid strength (Hammett function H_0) |
|--|-------|--|---|
| Al ₂ O ₃ –SiO ₂ | 94 | 270 | –8.2 (\approx 90% H ₂ SO ₄) |
| ZrO ₂ –SiO ₂ | 88 | 448 | –8.2 to –7.2 |
| Ga ₂ O ₃ –SiO ₂ | 92.5 | 90 | –8.2 to –7.2 |
| BeO–SiO ₂ | 85 | 110 | –6.4 |
| MgO–SiO ₂ | 70 | 450 | –6.4 |
| Y ₂ O ₃ –SiO ₂ | 92.5 | 118 | –5.6 (\approx 71% H ₂ SO ₄) |
| La ₂ O ₃ –SiO ₂ | 92.5 | 80 | –5.6 to –3.2 |

strength and catalytic activity of such solid acids correspond to those of mineral acids. The major advantage of solid acids is their thermal stability, which allows them to be used at much higher temperatures.

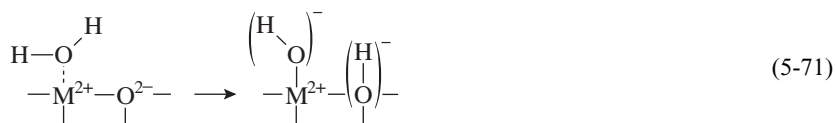
Some interesting results with acid catalysts in selected reactions such as isomerization, polymerization, and cracking reactions confirm the influence of the catalyst acidity (Table 5-30).

Table 5-30 Acidic catalysts for various reactions arranged in order of increasing acidity [T33]

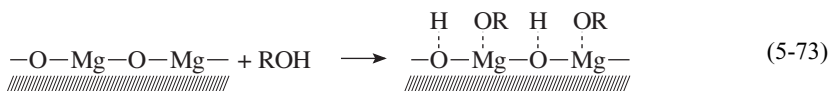
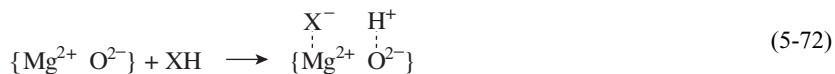
| Acid catalyst | Isomerization of <i>n</i> -pentane (Pt + support); Reaction temperature [°C] | Polymerization of propene at 200 °C; Conversion [%] | Cracking of <i>n</i> -heptane (temperature [°C] for 10% conversion) |
|--|--|---|---|
| α -Al ₂ O ₃ | inactive | 0 | inactive |
| SiO ₂ | inactive | 0 | inactive |
| ZrO ₂ | inactive | 0 | inactive |
| TiO ₂ | inactive | 0 | inactive |
| Al ₂ O ₃ , small surface area | 500 | <1 | inactive |
| Al ₂ O ₃ , large surface area | 450 | 0–5 | 490 |
| Al ₂ O ₃ , chlorinated | 430 | 10–20 | 475 |
| SiO ₂ –MgO | 400 | 20–30 | 460 |
| Heteropoly acids | unstable | 70–80 | unstable |
| Al ₂ O ₃ , fluorinated | 380 | >80 | 420 |
| Aluminosilicate | 360 | >90 | 410 |
| Zeolites, exchanged | 260 | >95 | 350 |
| Solid phosphoric acid | – | 90–95 | unstable |
| AlCl ₃ , HCl/Al ₂ O ₃ | 120 | 100 | 100 |

Basic Catalysts [16]

Solid basic catalysts are used in only a few industrial processes. The most important group is made up of the compounds of the alkali and alkaline earth metals. Magnesium oxide has been thoroughly investigated [35]. On the surface of alkaline earth metal oxides, water undergoes rapid heterolytic cleavage, covering the surface with hydroxyl groups (Eq. 5-71; cf. Al_2O_3).



Ion pairs on the surface of MgO can also heterolytically cleave the Brønsted acids HX (Eq. 5-72), acetylene, acetic acid, and alcohols (Eq. 5-73).



The heterolytic cleavage of the alcohol to give RO^- and H^+ explains why alkaline earth metal oxides, especially magnesium oxide, are good catalysts for the dehydrogenation of alcohols.

Increasing dehydroxylation resulting from activation at higher temperatures increases the base strength of MgO. Highly dehydroxylated MgO is such a strong base that it deprotonates the weak Brønsted acids NH_3 ($\text{p}K_{\text{a}} = 36$) and propene ($\text{p}K_{\text{a}} = 35$). Heterolytic cleavage of H_2 on MgO has even been demonstrated.

On alkaline earth metal oxides butene is adsorbed as methylallyl anions $(\text{CH}_3-\text{CH}=\text{CH}=\text{CH}_2)^-$. This carbanion is an intermediate in the double bond isomerization of butene. Adsorption was shown to be stronger on CaO (higher basicity) than on MgO. Activation of CaO at 700–900 °C results in maximum Lewis basicity and optimum activity for the isomerization to 2-butene.

Magnesium oxide is a good “solvent” for 3d transition metal ions. For example, Co^{2+} and Ni^{2+} ions are very well dispersed on MgO. The covalent component of the cation–anion bonding lowers the basicity of the oxide, making it “softer”. In the hydrogenation of CO, Co/MgO, and Ni/MgO supported catalysts give higher yields of C_2 and C_3 products than those with Al_2O_3 as support.

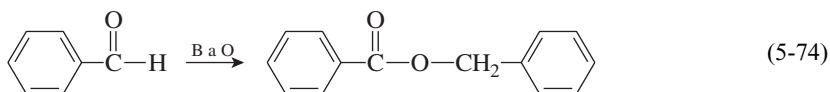
In the dehydrogenation of alcohols, Co^{2+} ions also increase the selectivity of the reaction. Alkaline earth metal oxides are good catalysts for the dehydrohalogenation of alkyl halides at 100–250 °C. The elimination of hydrogen halide proceeds by a highly selective E2 reaction. The following selectivity series was found for the *trans* elimination:



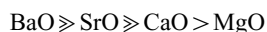
It reflects well the decreasing basicity of the oxides.

Thermally activated MgO, CaO, and BaO can even be used as catalysts for the hydrogenation of alkenes and dienes.

The reaction of benzaldehyde with activated oxides gives the Tischchenko product benzyl benzoate (Eq. 5-74).



The following reactivity series was found for this reaction:



The most active basic catalysts are alkali metals supported on alumina. Thus the catalyst 5% Na/Al₂O₃ results in complete conversion of 1-butene to 2-butene at 20 °C. Longer chain α -olefins are also readily isomerized by this highly active catalyst.

Reactions for the oxidative coupling of methane are also of much interest. This can be carried out with Li₂CO₃-doped MgO. Good selectivities for ethylene and ethane have been achieved.

In spite of these many examples, only a few base-catalyzed reactions are carried out industrially. Examples are:

- Condensation of acetone to diacetone alcohol with Ba(OH)₂ or Ca(OH)₂ supported catalysts
- Disproportionation of methylcyclopentene to methylcyclopentadiene and methylcyclopentane with sodium
- Dimerization of propene to 2-methylpentene with supported alkali metal catalysts
- Side-chain alkylation of toluene with Na/Al₂O₃
- Polymerization of butadiene with sodium

► Exercises for Section 5.3.3

Exercise 5.23

Classify the following as semiconductor catalysts (S), acid catalysts (A), or insulators (I):

Pd Al₂O₃ ZnO aluminosilicates MgO CoO zeolites

Exercise 5.24

Oxides such as Cu₂O, NiO, and CoO have a high adsorption capacity for CO.

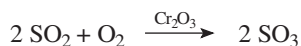
- a) Which type of semiconductor are the above-mentioned oxides?
- b) How is the reaction with the starting material CO designated?
- c) What is the effect of doping the oxides with Li₂O?

Exercise 5.25

Which types of semiconductor are represented by the following oxides:

**Exercise 5.26**

The oxidation of SO_2 can be carried out on chromium(III) oxide catalysts.



This oxidation catalyst can be both *n* and *p* doped by various additives. The activation energy of the reaction increases with *n*-type doping and decreases on *p*-type doping.

Discuss these findings.

Exercise 5.27

A donor step is the rate-determining step in a hydrogenation reaction. The following catalysts are available:

- Ni
- Ni on Al_2O_3 (*n* donor)
- Ni on CoO (*p* donor)

Which order of catalytic activity can be expected. Give a reason for this.

Exercise 5.28

In the conversion of methane to ethane and ethene, MnO is used as catalyst. Hydrogen abstraction from methane is observed as an intermediate step. On doping the catalyst with Li_2O , the selectivity of the reaction increases considerably. Explain the course of the reaction.

Exercise 5.29

The selective oxidation of *n*-butane to maleic anhydride is an industrial process. Butane behaves as a weak base towards metal oxides.

Which properties should a metal oxide catalyst for this reaction have?

Exercise 5.30

- Explain how a solid can react as an acid, using Al_2O_3 as an example.
- Arrange the following oxides in order of relative acidity:



Exercise 5.31

Aluminosilicate surfaces are classified as strong Brønsted acids, whereas silica gel is a weak acid.

Give an explanation for the increased acidity when Al^{3+} is present in the silicon dioxide lattice.

Exercise 5.32

How can the acidity of aluminosilicates be measured?

Exercise 5.33

Explain the cationic polymerization of alkenes on aluminosilicate surfaces with the aid of a reaction equation.

5.4**Catalyst Performance**

5.4.1

Factors which Affect the Catalyst Performance

Catalysis is a multidisciplinary subject that has a lot of aspects. It is obvious that a good catalyst should possess high activity. A high activity allows relatively small reactor volumes, short reaction times, and operation under mild conditions. High selectivity is often more important than high activity. Furthermore, a catalyst should maintain its activity and selectivity over a period of time, i. e. it should have sufficient stability. In summary, important properties of an industrial catalyst are shown in Fig. 5-34.

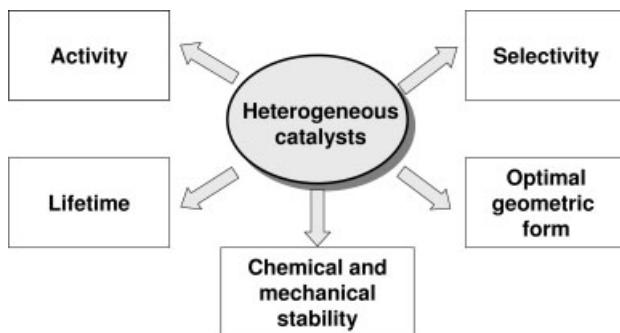


Fig. 5-34 Important properties of an industrial catalyst

Catalysts are developed for specific processes, e.g. for a specific reaction in a specific reactor under specific reaction conditions. Therefore, there are many requirements for an industrial catalyst:

- High activity/unit of reaction volume
- High selectivity with reference to the desired product at the required conversion in the reactor
- Sufficient stability with regard to deactivation
- Possibilities for regeneration, especially for fast deactivation processes
- Reproducible production method
- Sufficient thermal stability against sintering, structural change or loss via gas phase (e.g. if H₂O-vapor is produced as side product)
- High compressive strength (with reference to the catalyst bed and shape of the catalyst!)
- High resistance against mechanical stress

The catalytic performance can be affected by many influences such as

- Active phase (metal, metal oxide; type, morphology ...)
- Support (type, texture, chirality ...)
- Environment of the reaction (solvent etc)
- Promoters (inorganic, organic, chiral)
- Inhibitors

For a good understanding of catalysis it is crucial to have a good idea of the structure (both chemical and physical) of a catalyst. The properties of a catalyst can be manipulated by any process that alters the properties of its surface, because the nature of the individual sites at the surface is responsible for the activity, selectivity and stability of the catalyst.

5.4.2

Supported Catalysts [T32, T35]

Supported catalysts represent the largest group of heterogeneous catalysts and are of major economic importance, especially in refinery technology and the chemical industry. Supported catalysts are heterogeneous catalysts in which small amounts of catalytically active materials, especially metals, are applied to the surface of porous, mostly inert solids – the so-called supports. The supports can have special forms such as pellets, rings, extrudates, and granules.

Typical catalyst supports are porous solids such as aluminum oxides, silica gel, MgO, TiO₂, ZrO₂, aluminosilicates, zeolites, activated carbon, and ceramics. Table 5-31 lists widely used catalyst supports.

What are the reasons for the predominant use of supported catalysts in industry?

- **Costs.** The catalytically active components of supported catalysts are often expensive metals. Since this active component is applied in a highly dispersed form, the metal represents only a small fraction of the total catalyst mass. For example, the metals Rh, Re, and Ru are highly effective hydrogenation catalysts for aromatic hydrocarbons. They are sometimes used in mass fractions as low as 0.5 % on Al₂O₃ or activated carbon.

Table 5-31 Important catalyst supports and their applications

| Support | Specific surface area, m ² /g | Applications |
|----------------------------------|--|---|
| Alumina | | |
| γ-Al ₂ O ₃ | 160–300 | cracking, hydrogenation, dehydrogenation, metathesis |
| α-Al ₂ O ₃ | 5–10 | selective hydrogenation of acetylene; selective oxidation (ethylene oxide) |
| Aluminosilicates | up to 180 | cracking reactions, dehydrations, isomerizations, ammoxidation |
| Silica SiO ₂ | 200–1000 | polymerization, hydrogenation, oxidation, NO _x reduction (SCR process) |
| Titania TiO ₂ | 40–200 | TiO ₂ on SiO ₂ : oxidation of <i>o</i> -xylene to phthalic anhydride; V ₂ O ₅ /TiO ₂ selective oxidation |
| Activated carbon | 600–1200 | vinylation with acetylene, selective hydrogenation with noble metal catalysts (fine chemicals) |
| Corundum ceramic | 0.5–1 | selective oxidation (ethylene oxide, benzene to maleic anhydride, <i>o</i> -xylene to phthalic anhydride) |
| Diatomaceous earth | up to 200 | hydrogenation |
| Clays | 50–300 | hydrogenation, condensation |
| Zeolites | 300–600 | refinery processing, bifunctional catalysis, organic syntheses |
| Cordierite monoliths | | mechanical supports: automotive exhaust gascleaning |

- **Activity.** The high activity leads to fast reaction rates, short reaction times, and maximum throughput.
- **Selectivity** facilitates the following: maximum yield, elimination of side products, and lowering of purification costs; it is the most important target parameter in catalyst development.
- **Regenerability** helps keep process costs low.

Which factors influence these properties? The main factors are the choice of the most suitable support material and the arrangement of the metal atoms in the pore structure of the support. In choosing catalyst supports, numerous physical and chemical aspects and their effects must be taken into account (Table 5-32).

The tasks of catalyst supports are as follows:

- Fixation of the active components
- Formation of high dispersed particles of the active component
- Stabilization of the active component
- Enlargement of the specific surface area

Table 5-32 Selection of catalyst supports [T40]

| Physical aspects | Chemical aspects |
|--|--|
| Specific surface area (→ activity, distribution of active components) | specific activity (→ adaption to heat evolution) |
| Porosity (→ mass and heat transport) | |
| Particle size and shape (→ pore diffusion, pressure drop) | |
| Mechanical stability (→ abrasion, durability) | interaction with active components (→ selectivity, bifunctional catalysts) |
| Thermal stability (→ catalyst lifetime, regenerability) | |
| Bulk density (active component content per unit reactor volume) | catalyst deactivation (→ stabilization against sintering, poisoning) |
| Dilution of overactive phases (→ heat evolution, avoidance of hot spots) | |
| Separability (filterability of powder catalysts) | No interaction with reactants or solvents |

The main function of the catalyst support is to increase the surface area of the active component. Catalytic activity generally increases with increasing catalyst surface area, but a linear relationship can not be expected since the reaction rate is often strongly dependent on the structure of the catalyst surface. However, in many reactions, the selectivity decreases when the catalytic surface is enlarged. As a general rule, catalysts for the activation of hydrogen (hydrogenation, hydrodesulfurization, hydrodenitrogenation) require high support surface areas, while selective oxidations (e. g., olefin epoxidation) need small support surface areas to suppress problematic side reactions.

The choice of the appropriate catalyst support for a particular active component is important because in many reactions the support can significantly influence the reaction rate and the course of the reaction. The nature of the reaction system largely determines the type of catalyst support.

If a support material with a large surface area such as activated carbon is used as support, then the metal is present as discrete crystallites, only a few atomic layers thick, with a very high surface area.

In batch liquid-phase reactions, powder supports are used exclusively, whereas in gas-phase and continuous liquid-phase reactions (trickle columns), supports in pellet or granule form can be employed (see Chapter 14).

The pore structure of the support can also have an influence on the role of the active component, since the course of the reaction is often strongly dependent on the rate of diffusion of the reactants. Furthermore, the size of the support surface can limit the exploitable metal concentration.

Many commercially available catalyst supports, for example, activated carbon and alumina, are offered in various particle sizes, each having a series of different specific surface areas and pore size distributions.

The choice of catalyst support may be restricted by the reaction conditions. Thus the support must be stable under the process conditions and must not interact with the solvent and the starting materials. Depending on the process, supported catalysts can have a low (e.g., 0.3 % Pt/Al₂O₃, 15 % Ni/Al₂O₃) or a high loading (e.g., 70 % Ni/Al₂O₃, Fe/Al₂O₃).

In supported metal catalysts, the support does not only ensure high dispersion of the metal; there are also interactions between metal and support due to various physical and chemical effects:

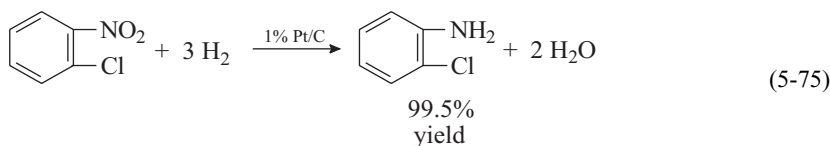
- Electronic effects: electron transfer up to formation of chemical bonds
- Adhesive forces (van der Waals forces)
- Formation of reduced support species on the metal surface
- Formation of new phases at the boundary surface

Electronic effects and their causes have already been treated in Section 5.3.3; they result from the *n*- or *p*-type semiconductor properties of the support material. The interactions can impair the chemisorption capability and effectiveness of a catalyst, as well as restricting the mobility of the disperse phase and delaying its sintering.

In the last few years, the concept of strong metal–support interaction (SMSI) has gained considerable importance [18]. It was introduced in 1978 to explain certain peculiarities in the chemisorption of H₂ and CO on TiO₂-supported platinum group metals. The catalysts were subjected to high-temperature reduction with H₂ (400 °C), after which a strong decrease in the adsorption capacity for H₂, CO, and NO was found. The effect is also exploited in chemical syntheses: platinum group metals on TiO₂ can considerably influence the catalytic activity and product selectivity in the hydrogenation of CO.

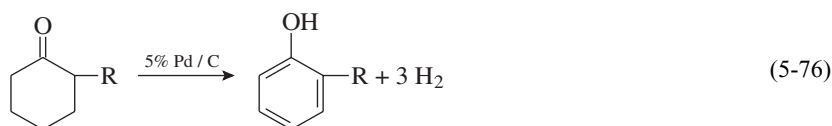
In the following we shall discuss some examples of the industrial use of supported catalysts and the above-mentioned metal–support interactions.

Hydrogenation is one the oldest and most widely used applications for supported catalysts. The usual metals are Co, Cu, Ni, Pd, Pt, Re, Rh, Ru, and Ag. There are numerous catalysts for special applications. Most hydrogenation catalysts consist of an extremely fine dispersion of the active metal on activated carbon, Al₂O₃, aluminosilicates, zeolites, kieselguhr, or inert salts such as BaSO₄ [22]. An example is the selective hydrogenation of chloronitrobenzene (Eq. 4-75).



Usually, palladium catalysts are used for the industrial hydrogenation of nitro compounds, but Pd is also an excellent catalyst for the dehydrochlorination reaction, so that aniline is predominantly formed. Therefore, a new, high-selectivity Pt/C catalyst was developed, which gives the desired product *o*-chloroaniline without affecting the rate of hydrogenation.

In the dehydrogenation of cyclohexanone derivatives (Eq. 5-76), an activated carbon support in which the palladium is uniformly distributed in the support structure is recommended. With increasing ordering of the metal, the catalyst exhibits an increasing metal dispersion and therefore a higher resistance to thermal sintering. Sintering would lead to crystal growth and deactivation of the catalyst.



The hydrogenolysis of ethane on supported nickel catalysts is a good example for the influence of the degree of dispersion of the metal (Table 5-33). It is known that nickel is more highly dispersed on SiO_2 than on Al_2O_3 , and at the same time there is an influence on the crystallite form. A further influence is due to the acid centers of aluminum oxide, which lead to more extensive coke formation, deactivating the nickel catalyst.

Table 5-33 Hydrogenolysis of ethane on supported nickel catalysts (10 % Ni) [T35]

| Support | Reaction rate [mol m ⁻² metal h ⁻¹ · 10 ⁶] |
|--|---|
| SiO ₂ | 151 |
| Al ₂ O ₃ | 57 |
| SiO ₂ /Al ₂ O ₃ | 7 |

The dehydrogenation of cyclohexane to benzene can be explained well in terms of electronic effects (Table 5-34). The benzene selectivity decreases on going from TiO₂ to SiO₂, and this corresponds to the decreasing *n* character of the support material. Apparently, weak *n*-type semiconductor oxides are the most effective supports for this reaction. In contrast, the strong *n*-type semiconductor ZnO, which has a higher electron concentration than TiO₂, gives no reaction.

Table 5-34 Dehydrogenation of cyclohexane to benzene on supported platinum catalysts at 773 K [T28]

| Catalyst | Benzene (%) |
|-----------------------------------|-------------|
| Pt/ZnO | — |
| Pt/TiO ₂ | 76.1 |
| Pt/Al ₂ O ₃ | 59.8 |
| Pt/MgO | 32.3 |
| Pt/SiO ₂ | 23.1 |

Extensive investigations have been carried out on the industrially important hydrogenation of CO. Here we shall discuss just a few of the results, some of which are contradictory [T28]. High activities and selectivities for the formation of methanol were found for the catalysts Pd on La_2O_3 , MgO, or ZnO, but high activities and selectivities for the formation of methane with Pd on TiO_2 or ZrO_2 (Table 5-35). It is no surprise that a high proportion of dimethyl ether is formed with the acidic support Al_2O_3 . However, these investigations did not take degree of dispersion of the metal into consideration.

Table 5-35 Hydrogenation of CO on supported Pd catalysts [T28]

| Catalyst | Selectivities (%) | | | |
|-----------------------------|------------------------|-----------------------------|---------------|-----------------|
| | CH_3OH | $\text{CH}_3\text{-O-CH}_3$ | CH_4 | C_{2+} |
| Pd powder | 75.0 | 0 | 8.8 | 16.2 |
| Pd/MgO | 98.4 | 1.2 | 0.3 | 0.2 |
| Pd/ZnO | 99.8 | 0 | 0.1 | 0.2 |
| Pd/ Al_2O_3 | 33.2 | 62.7 | 3.3 | 0.8 |
| Pd/ La_2O_3 | 99.0 | 0 | 0.5 | 0.5 |
| Pd/ SiO_2 | 91.6 | 0 | 1.5 | 0.2 |
| Pd/ TiO_2 | 44.1 | 8.6 | 42.1 | 5.2 |
| Pd/ ZrO_2 | 74.7 | 0.5 | 22.3 | 2.5 |

The hydrogenation of CO can be influenced by means of the support composition and by varying the degree of dispersion of the metal. Thus it is assumed that for metals of Groups 8–10, a low degree of dispersion favors formation of hydrocarbons, and a high degree of dispersion, the formation of oxygen-containing compounds.

Relative activities in CO hydrogenation measured for supported rhodium catalysts are listed in Table 5-36. These experimental findings are supported by H_2 chemisorption measurements and active rhodium centers.

Table 5-36 Relative activities of supported Rh catalysts in the hydrogenation of CO [T28]

| Support | Relative activity |
|-------------------------|-------------------|
| TiO_2 | 100 |
| MgO | 10 |
| Al_2O_3 | 5 |
| CeO_2 | 3 |
| SiO_2 | 1 |

In another investigation with supported rhodium catalysts, it was found that the oxidation state of the rhodium influences the type of chemisorption of CO and hence the product distribution according to Equation 5-77.



Thus dissociative chemisorption of CO leads to hydrocarbons, and associative chemisorption to alcohols as final product (Table 5-37).

Table 5-37 Influence of support materials on the hydrogenation of CO with rhodium catalysts [T22]

| Catalyst | Active catalyst | Chemisorption of CO | Products |
|---|-----------------|------------------------------|---|
| Rh/SiO ₂ | Rh(0) | dissociative | CH _x |
| Rh/ZrO ₂ | Rh(0), Rh(I) | dissociative/ associative | 42 % ethanol 12 % methanol 32 % CH ₄ |
| Rh/ZnO Rh/La ₂ O ₃ | Rh(I) | associative | 94 % methanol |

In CO hydrogenation with supported copper catalysts (Table 5-38), the results were explained in terms of electronic effects of the support material [13]. The differing CO hydrogenation activity of the catalysts reflects the electronic interaction between the Cu particles on the surface and the support. With *p*-type semiconductors such as Cr₂O₃ and ZrO₂, which have higher work functions than copper metal, higher activity than with pure copper is observed. This is explained by the fact that in this case, electron density can flow from copper to the support. With the insulators SiO₂ and Al₂O₃, the activity corresponds roughly to that of copper; no electrons

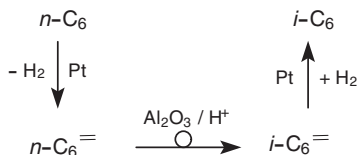
Table 5-38 Supported copper catalysts for the hydrogenation of CO [13]

| Catalyst | Work function of the support [eV] | TON · 10 ³ of CO ^{a)} | Semiconductor type of support |
|--|-----------------------------------|---|-------------------------------|
| 5 % Cu/ZrO ₂ | 5.0 | 0.41 | <i>p</i> |
| 5 % Cu/Cr ₂ O ₃ | 5.8 | 0.24 | <i>p</i> |
| 5 % Cu/graphite | 4.8 | ≤ 0.04 | <i>n</i> (metalloid) |
| 5 % Cu/ZnO | 4.6 | ≤ 0.03 | <i>n</i> |
| 20 % Cu/Al ₂ O ₃ | — | ≤ 0.01 | isolator |
| 20 % Cu/SiO ₂ | — | ≤ 0.02 | isolator |
| 5 % Cu/TiO ₂ | 3.0 | ≤ 0.01 | <i>n</i> |
| 5 % Cu/MgO | 3.5 | ≤ 0.01 | <i>n</i> |
| Cu metal | 4.55 | ≤ 0.02 | (metal) |

a) TON = mol CO/atom surface metal × s; H₂/CO = 3; flow rate 60 mL/min, normal pressure, 275 °C; all catalysts have approximately the same particle size.

can be taken up by the support. In the case of *n*-type semiconductors such as TiO₂ and MgO, charge transfer from copper to support can not take place, and the catalytic activities are lower than with pure copper.

The next example shows how catalyst bifunctionality can arise from the support material. Platinum metal dehydrogenates naphthenes to give aromatic compounds, but it is not able to isomerize or cyclize *n*-alkanes. This function is adopted by the Al₂O₃ support with its acidic properties. The cooperation of the two catalyst components is shown schematically for the reforming of *n*-hexane in Scheme 5-5 [T20].

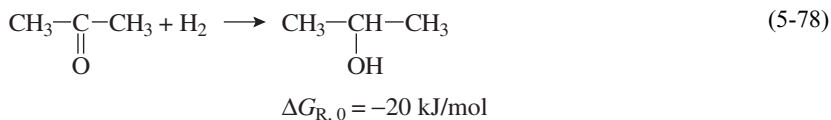


Scheme 5-5 Reforming of *n*-hexane on a Pt/Al₂O₃ supported catalyst

It was shown that neither Pt nor the support material Al₂O₃ can isomerize the alkane starting material. However, acidic Al₂O₃ centers can isomerize *n*-alkenes, which are then hydrogenated to isoalkanes on Pt. During the activation phase of the catalyst, chlorine is added to achieve the necessary acidity.

The final examples deal with SMSI effects [18]. In the hydrogenation of CO on Pt/TiO₂ catalysts, a 100-fold increase in catalyst turnover number was observed after high-temperature reduction. In the high-temperature reduction, the chemisorption capacity for both starting materials, CO and H₂, was drastically lowered, but no sintering of the metal occurred. It has been shown that partially reduced TiO_x species are distributed over the Pt surface. Interestingly, in spite of the higher catalyst activity, a higher activation energy was measured rather than a lower one [37].

A further example is the model reaction of hydrogenation of acetone to isopropanol (Eq. 5-78).



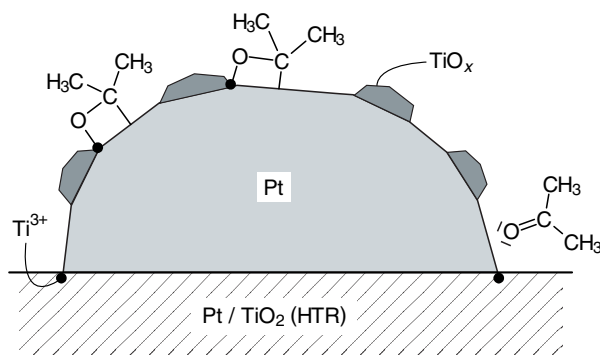
Kinetic measurements on a Pt catalyst showed no dependence on the size of the crystallites. On an inert SiO₂ support the catalyst turnover number remained virtually constant over the particle size range 2–1000 nm; that is, the reaction is structure-insensitive. With a TiO₂ support, the TON was increased by a factor of 500 following high-temperature reduction (Table 5-39).

Langmuir–Hinshelwood kinetics involving competitive adsorption of acetone molecules and hydrogen atoms were postulated, and it was assumed that adsorbed acetone dominates. The SMSI effect is explained by the fact that the oxygen atom of the carbonyl group is more effectively activated than in conventional platinum catalysis. It is assumed that the oxygen atom is adsorbed on particularly active Ti³⁺ cen-

Table 5-39 SMSI effect in the hydrogenation of acetone to isopropanol on supported platinum catalysts [37]

| Catalyst | TON · 10 ² [s ⁻¹] | E _a [kJ/mol] |
|-------------------------------------|--|-------------------------|
| Pt/SiO ₂ | ca. 1.1 | 67 ± 2,5 |
| Pt/η-Al ₂ O ₃ | 2.4 | 78 |
| Pt/TiO ₂ (LTR) | ca. 2.8 | 59 ± 2,9 |
| Pt/TiO ₂ (HTR) | ca. 565 | 68 ± 8,3 |

Reaction conditions: 303 K, 0.1 MPa, H₂/acetone = 3.06; LTR = low-temperature reduction, HTR = high-temperature reduction.

**Fig. 5-35** Model for the hydrogenation of acetone (SMSI effect) [37]

ters of the partially reduced TiO_x islands on the platinum at the metal/support boundary (Fig. 5-35).

An SMSI effect was also demonstrated in the hydrogenation of crotonaldehyde, and a surprising change in the selectivity of the reaction was observed. With Pt/SiO₂ and Pt/Al₂O₃ catalysts, only butyraldehyde or butanol, respectively, is obtained as hydrogenation product; with Pt/TiO₂ a considerable selectivity of 37% for the unsaturated crotyl alcohol is reported.

Another interesting reaction is the reforming of methane with CO₂ to produce synthesis gas (Eq. 5-79). This endothermic reaction is said to be suitable for storing solar energy in chemical substances [14].

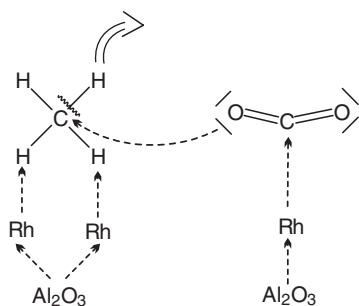


The support is a ceramic honeycomb with a washcoat of Al₂O₃ that contains the rhodium metal catalyst (0.2%). Indications of the mechanism of the reaction are provided by literature data on analogous reactions:

- Al₂O₃ has acidic properties and can catalyze the formation of CH₃⁺. At higher temperatures it behaves as an *n*-type semiconductor.

- When CO_2 is adsorbed, it accepts electrons from catalysts with n -type semiconductor properties, but releases electrons to catalysts with p -type semiconductor properties (Lewis amphoteric behavior).
- When a metal is applied to an n -type semiconductor, its electron density increases.
- The SMSI effect influences the binding between support and metal. The bonds can take on ionic character or undergo geometric changes.

Combining these facts leads to the mechanism shown in Scheme 5-6. Methane is the first species to be adsorbed and is partially dehydrogenated. The CO_2 reacts with the methane fragment either from the gas phase or from the adsorbed phase. In the adsorption process, electron flow from the support, through the metal, and to the reactant is assumed for both starting materials. The electrons of CO_2 attack the partially dehydrogenated methane, whereby CO is formed. In the final step hydrogen is split off and desorbed.



Scheme 5-6 Reforming of methane with CO_2 on supported $\text{Rh}/\text{Al}_2\text{O}_3$ catalysts [14]

Chemical interactions between metal and support are also observed on main group metal oxides such as SiO_2 , Al_2O_3 , and MgO , which can normally be regarded as chemically highly inert. Strong interactions have also been found between various metals of Groups 8–10 and carbon supports. Palladium and nickel form carbide supports, and the transformation of carbon and the encapsulation of metal crystallites have been proven [18].

5.4.3

Promoters [39]

Promoters are substances that are themselves not catalytically active but increase the activity of catalysts. The function of these substances, which are added to catalysts in amounts of a few per cent, has not been fully elucidated. There are four types of promoters:

- **Structure promoters** increase the selectivity by influencing the catalyst surface such that the number of possible reactions for the adsorbed molecules decreases and a favored reaction path dominates. They are of major importance since they

are directly involved in the solid-state reaction of the catalytically active metal surface.

- **Electronic promoters** become dispersed in the active phase and influence its electronic character and therefore the chemical binding of the adsorbate.
- **Textural promoters** inhibit the growth of catalyst particles to form larger, less active structures during the reaction. Thus they prevent loss of active surface by sintering and increase the thermal stability of the catalyst.
- **Catalyst-poison-resistant promoters** protect the active phase against poisoning by impurities, either present in the starting materials or formed in side reactions.

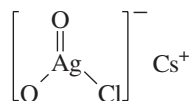
A catalyst may contain one active component and one or more promoters. The fraction of active components usually exceeds 75 %. Since the above four effects tend to overlap in practice, it is sometimes difficult to precisely define the function of a promoter.

Promoters are the subject of great interest in catalyst research due to their remarkable influence on the activity, selectivity, and stability of industrial catalysts. Many promoters are discovered serendipitously; few are the result of systematic research. This sector of catalyst research is often the scene of surprising discoveries.

Before we discuss some examples of function of promoters, let us examine an overview of promoters for industrial catalysts (Table 5-40).

Structure promoters can act in various ways. In the aromatization of alkanes on Pt catalysts, nonselective dissociative reaction paths that lead to gas and coke formation can be suppressed by alloying with tin. This is attributed to the ensemble effect, which is also responsible for the action of alkali and alkaline earth metal hydroxides on Rh catalysts in the synthesis of methanol from CO/H₂ and the hydroformylation of ethylene. It was found that by means of the ensemble effect the promoters block active sites and thus suppress the dissociation of CO. Both reactions require small surface ensembles. As a result, methanol production and insertion of CO into the alkene are both positively influenced.

Promoters can also influence catalytically active phases by stabilizing surface atoms in certain valence states. An example is the effect of chlorine on silver catalysts in the oxidation of ethylene to ethylene oxide. Silver oxide chloride phases were detected on the surface. The selective epoxidation between the electrophilic oxygen and the electron-rich double bond of ethylene is optimized. Cesium promoters stabilize these silver oxide chloride phases of the type



under reaction conditions.

Another example of a structure promoter is Al₂O₃ in ammonia synthesis. It was long assumed that Al₂O₃ hinders the sintering of the iron following reduction of the catalyst, but it is now believed that Al₂O₃ favors the formation of highly catalytically active (111) surfaces of the iron catalyst.

Table 5-40 Examples of promoters in the chemical industry [T41]

| Catalyst (use) | Promoters | Function |
|--|--------------------------------|---|
| Al ₂ O ₃ (support and cat.) | SiO ₂ , | increase thermal stability |
| | ZrO ₂ , P | |
| | K ₂ O | poisons coke formation on active centers |
| | HCl | increases acidity |
| | MgO | slows sintering of active components |
| SiO ₂ /Al ₂ O ₃ (cracking catalyst and matrix) | Pt | increased CO oxidation |
| Pt/Al ₂ O ₃ (cat. reforming) | Re | lowers hydrogenolysis activity and sintering |
| MoO ₃ /Al ₂ O ₃ (hydrotreating, HDS, HDN) | Ni, Co | increased hydrogenolysis of C–S and C–N bonds |
| | P, B | increased MoO ₃ dispersion |
| Ni/ceramic support (steam reforming) | K | improved coke removal |
| Cu/ZnO/Al ₂ O ₃ (low-temperature conversion) | ZnO | decreased Cu sintering |
| Fe ₃ O ₄ (NH ₃ synthesis) | K ₂ O | electron donor, favors N ₂ dissociation |
| | Al ₂ O ₃ | structure promoter |
| Ag (EO synthesis) | Alkali metals | increase selectivity, hinder crystal growth, stabilize certain oxidation states |

Next, let us take a closer look at electronic effects. Potassium is used as a promoter in many catalytic reactions. The hydrogenation of CO and ammonia synthesis are two well-known examples. The strongly electropositive potassium (or, more often, the oxide K₂O) provides electrons that flow to the metal and then into the chemisorbed molecule. In this way, π backbonding into the π^* orbitals of the adsorbate is considerably strengthened. Figure 5-36 explains this for the example of nitrogen.

The promoter potassium facilitates the dissociation of N₂ and thus increases the rate of formation of NH₃. In investigations of the chemisorption of N₂ on the less active (100) and (110) iron surfaces, it was shown that low concentrations of potassium increase the heat of chemisorption of molecular nitrogen by 16 kJ/mol and increase the rate of N₂ dissociation 300-fold.

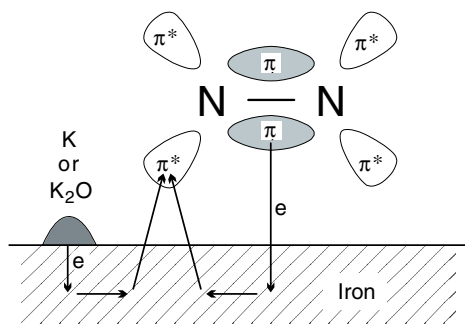


Fig. 5-36 The action of potassium promoters in the dissociative chemisorption of N_2 on iron catalysts

This is direct evidence that the rate-determining step in ammonia synthesis is the chemisorption of nitrogen. Commercial iron catalysts contain ca. 1.8 mol% K. The electron-donor capability of potassium depends strongly on the degree of coverage θ and therefore on the promoter concentration in the catalyst, as has been shown by measurements of the heat of adsorption of potassium on transition metal surfaces. At low degrees of coverage, values of around 250 kJ/mol were measured, which corresponds to complete ionization of the atom. At high degrees of coverage, partial depolarization of the charged potassium species leads to neutralization. At $\theta = 50\%$, the heat of adsorption drops to about 97 kJ/mol, which corresponds to the heat of sublimation of potassium metal. The adsorbed atoms are then clearly no longer ionized. Similar effects were found in the hydrogenation of CO with the transition metals Pt, Ni, and Ru.

Potassium increases the reaction rate and the selectivity for C_{2+} hydrocarbons, as would be expected if dissociation of CO is more facile. Evidence for this is that in the presence of potassium, the CO desorption temperature is 100–200 K higher and the heat of chemisorption increases by 20–50 kJ/mol. Vibrational spectroscopy showed that with increasing degree of coverage by potassium, the CO stretching frequency of 1875 and 2120 cm^{-1} ($\theta = 0$) decreases to 1565 cm^{-1} ($\theta = 0.6$). Thus the influence of potassium lowers the CO bond order from 2 to 1.5, so that CO dissociation can more readily occur.

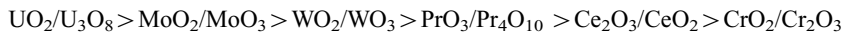
It was also shown for rhodium catalysts that at low pressures CO is molecularly adsorbed but dissociates in the presence of potassium promoters.

Besides the purely electronic effects that we have discussed up to now, the promoter can also form direct chemical bonds with the adsorbate. An example is the influence of alkali metal cations on the synthesis of methanol with copper catalysts. Sodium and potassium hydroxide can react with CO under relatively mild conditions to form alkali metal formates, which are hydrogenated to methanol by hydrogen dissociatively adsorbed on copper.

Purely chemical promoter effects are also observed with methanation catalysts. The water formed in the reaction is adsorbed on the active centers of the catalyst and thus blocks them. The water can be removed by electron-deficient compounds (Eq. 5-80).



The resulting hydrogen is then desorbed. Various reducible transition metal oxides have been tested as promoters, and the following activity series was found:



Hence the promoter of choice is UO_2 , which is added to the catalyst in small amounts.

An interesting promoter effect is exhibited by K_2SO_4 in the oxidation of methanol to formaldehyde on V_2O_5 catalysts. The addition of 10–20 % K_2SO_4 drastically increases the reaction rate and raises the selectivity from 85 to 97 %. In this case, too, the potassium releases electrons to the oxide, weakening the coordinative $\text{V}=\text{O}$ bond and accelerating the reaction. Promoters are also developed to strengthen the support or the active component. An important function is influencing the stability of support materials. Oxidic supports can exist in numerous different phases. For Al_2O_3 the preferred phase is $\gamma\text{-Al}_2\text{O}_3$. This oxide has a defect spinel structure, high surface area, a certain degree of acidity, and forms solid solutions with transition metal oxides such as NiO and CoO . Above 900°C $\gamma\text{-Al}_2\text{O}_3$ is transformed into $\alpha\text{-Al}_2\text{O}_3$, which has a hexagonal structure and a smaller surface area. Such high temperatures can occur during catalyst regeneration. Even at lower temperatures a slow phase transition occurs, which shortens the catalyst lifetime. The incorporation of small amounts (1–2 %) of SiO_2 or ZrO_2 in $\gamma\text{-Al}_2\text{O}_3$ shifts the $\gamma\text{-}\alpha$ transition to higher temperature and increases the stability of the catalyst.

Promoters are often used to suppress undesired activity of support materials, such as coke formation. Coking is due to cracking reactions on Brønsted acid centers, followed by an acid-catalyzed polymerization to give $(\text{CH}_x)_n$ chains, which cover the active centers on the surface and block the pores. Removal of the coke by incineration can lead to loss of activity due to sintering. Acidic centers are best neutralized by bases, preferably alkali metal compounds. Potassium, added as K_2CO_3 during catalyst production is the most effective at minimizing the coking tendency of Al_2O_3 supports.

In the steam reforming of naphtha, potassium promoters accelerate the reaction of carbon with steam. However, this leads to formation of KOH , which sublimates. In this case, potassium aluminosilicate was successfully used as promoter. In the presence of steam and CO_2 it decomposes into K_2CO_3 and KOH to an extent that is just sufficient to remove the coke that is formed. This prolonged catalyst lifetimes to 4–5 years [T35].

Finally, let us take a closer look at the influence of promoters on hydrodesulfurization catalysts. In this important refinery technology reaction, $\text{CoMo}/\text{Al}_2\text{O}_3$ supported catalysts are used. The schematic reaction sequence is shown in Equation 5-81.



Hydrogenolysis of the C–S bond is followed by hydrogenation of the resulting alkene. Since the starting materials range from low-boiling compounds to heavy resi-

dues, a wide range of technologies is used. However, the fundamental chemistry of the processes is in all cases the same.

Precipitated γ - Al_2O_3 -based catalysts with a large surface area (ca. $250 \text{ m}^2/\text{g}$) are used. Amounts of about 1% SiO_2 act as texture stabilizer. Cobalt and molybdenum salts are calcined on the support and form oxides such as MoO_3 , CoO , Co_3O_4 , and CoAl_2O_4 in a solid-state reaction. The key precursor of the active component is MoO_3 , which is activated by sulfiding to give microcrystalline MoS_2 in which small amounts of Co^{2+} ions are incorporated. Active “CoMoS” centers increase the activation of hydrogen and thus facilitate the cleavage of sulfur. It is assumed that Co acts as a structure promoter and leads to increased dispersion of the sulfided species.

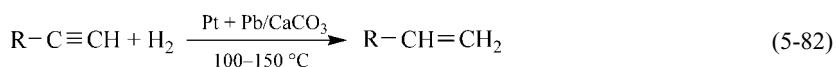
For high-boiling starting materials the catalysts also contain K and P promoters to neutralize acid centers, suppress coking, and to increase the dispersion of the molybdenum component. The last example – even in this strongly simplified form – gives an impression of just how complex the interaction between catalyst components, support materials, and promoters can be, and shows that adapting a catalyst to the requirements of an industrial process is a time-consuming, creative task.

5.4.4

Inhibitors

An inhibitor is a substance that reduces the rate of a catalytic reaction, often as a result of bonding chemically to the catalyst. Examples are

- Pt or Pd catalysts on CaCO_3 , poisoned by Pb (Lindlar’s catalyst). They enable selective reduction of triple bonds to double bonds (Eq. 5–82).



- Aprotic solutions (which act by forming H bonds with catalyst molecules in competition with other reactant molecules)
- Structural effectors in enzyme catalysis which bond to the active sites

A strong inhibitor is a catalyst poison, e. g. sulfur for Ni hydrogenation catalysts. For example, partially sulfided Ni catalysts are applied for the selective hydrogenation of alkynes (lower activity than Lindlar’s catalyst, reaction temperature $200\text{--}250\text{ }^\circ\text{C}$, continuous feed of 1 ppm H_2S to the reactant).

► Exercises for Section 5.4

Exercise 5.34

What are the main interactions that can occur between metals and support materials?

Exercise 5.35

What is meant by the term “texture” of a catalyst support?

Exercise 5.36

The chemisorption properties of platinum group metals for CO and H₂ are less pronounced on TiO₂ supports.

The chemisorption of H₂ is reduced on Ni/SiC and SiO₂; formation of Ni–Si alloys is assumed.

Which effect could be responsible for this?

Exercise 5.37

Which catalyst properties can be influenced by promoters?

Exercise 5.38

What influence do potassium promoters have on acidic cracking catalysts?

5.5

Catalyst Deactivation and Regeneration [6]

Catalysts have only a limited lifetime. Some lose their activity after a few minutes, others last for more than ten years. The maintenance of catalyst activity for as long as possible is of major economic importance in industry. A decline in activity during the process can be the result of various physical and chemical factors, for example:

- Blocking of the catalytically active sites
- Loss of catalytically active sites due to chemical, thermal, or mechanical processes

An overview of catalyst deactivation in large-scale industrial processes is given in Table 5-41.

Catalyst deactivation, also known as ageing, is expressed by the decrease in catalyst activity with time. Catalyst activity a is the ratio of the reaction rate at a given time t to the reaction rate at the time that use of the catalyst began ($t = 0$; Eq. 5-83).

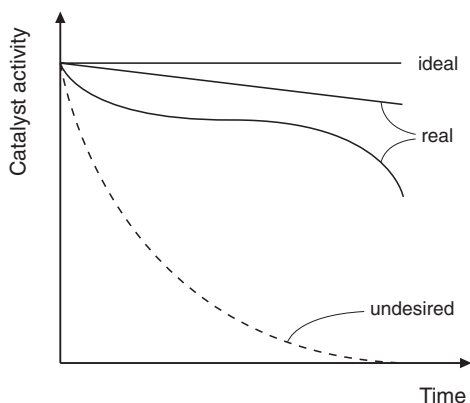
$$a(t) = \frac{r(t)}{r(t=0)} \quad (5-83)$$

Table 5-41 Causes of deactivation in large-scale industrial processes

| Reaction | Reaction conditions | Catalyst | Catalyst lifetime [years] | Deactivation process |
|---|---------------------------|---|---------------------------|---|
| Ammonia synthesis $N_2 + 3 H_2 \rightarrow 2 NH_3$ | 450–550 °C 200–500 bar | Fe/K ₂ O/Al ₂ O ₃ | 5–10 | slow sintering |
| Methanization $CO + 3 H_2 \rightarrow CH_4 + H_2O$ | 250–350 °C 30 bar | Ni/Al ₂ O ₃ | 5–10 | slow poisoning by S and As compounds |
| Methanol synthesis $CO + 2 H_2 \rightarrow CH_3OH$ | 200–300 °C 50–100 bar | Cu/Zn/Al ₂ O ₃ | 2–8 | slow sintering |
| Hydrosulfurization of light petroleum | 300–400 °C 35–70 bar | CoS/MoS ₂ /Al ₂ O ₃ | 0.5–1 | deposits (decomp. of sulfides) |
| NH ₃ Oxidation $2 NH_3 + 2,5 O_2 \rightarrow 2 NO + 3 H_2O$ | 800–900 °C 1–10 bar | Pt net | 0.1–0.5 | loss of platinum, poisoning |
| Catalytic cracking | 500–560 °C 2–3 bar | zeolites | 0.000002 | rapid coking (continuous regeneration) |
| Benzene oxidation to maleic anhydride $C_6H_6 + O_2 \rightarrow C_4H_2O_3$ | 350 °C 1 bar | V ₂ O ₅ /MoO ₂ /Al ₂ O ₃ | 1–2 | formation of an inactive vanadium phase |

The course of the activity of an industrial catalyst with time can be described by means of several basic types (Fig. 5-37).

Not only does the decreasing catalyst activity lead to a loss of productivity, it is also often accompanied by a lowering of the selectivity. Therefore, in industrial processes great efforts are made to avoid catalyst deactivation or to regenerate deactivated catalyst. Catalyst regeneration can be carried out batchwise or preferably continuously while the process is running.

**Fig. 5-37** Deactivation behavior of catalysts [8]

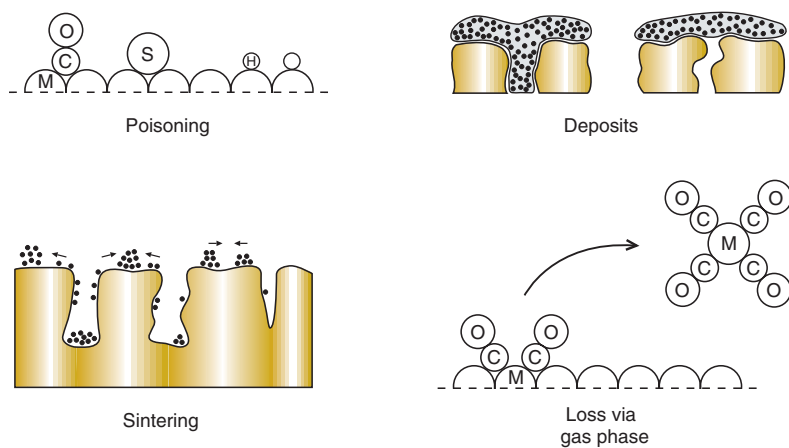


Fig. 5-38 Mechanisms of catalyst deactivation (M = metal) [8]

In this chapter we will encounter the most important mechanisms of catalyst deactivation and discuss possible methods of catalyst regeneration [T35].

The four most common causes of catalyst deactivation are:

- Poisoning of the catalyst. Typical catalyst poisons are H_2S , Pb, Hg, S, P
- Deposits on the catalyst surface block the active centers and change the pore structure (e. g., coking)
- Thermal processes and sintering of the catalyst lead to a loss of active surface area
- Catalyst losses by evaporation of components (e. g., formation of volatile metal carbonyls with CO)

These processes are shown schematically in Figure 5-38. We will now discuss these effects in more detail and examine some examples from the chemical industry.

5.5.1

Catalyst Poisoning

Catalyst poisoning is a chemical effect. Catalyst poisons form strong adsorptive bonds with the catalyst surface, blocking active centers. Therefore, even very small quantities of catalyst poisons can influence the adsorption of reactants on the catalyst. The term catalyst poison is usually applied to foreign materials in the reaction system. Reaction products that diffuse only slowly away from the catalyst surface and thus disturb the course of the reaction are referred as inhibitors. Table 5-42 lists some catalyst poisons and inhibitors and the way in which they act.

In the investigation of catalyst deactivation by poisoning, the distribution of the active centers, the stoichiometry, and diffusion are of decisive importance. In the following, poisoning of the most important classes of catalysts, i. e., metals, semi-conductors, and acidic insulators, is discussed.

Table 5-42 Catalyst poisons and inhibitors in chemical processes [T41]

| Process | Catalyst | Catalyst poison, inhibitor | Mode of action |
|---------------------------|---|---|---|
| NH ₃ synthesis | Fe | S, Se, Te, P, As compounds, halogens | poison: strong chemisorption or formation of compounds |
| | | O ₂ , H ₂ O, NO | weak poison: oxidation of Fe surface; reduction possible but causes sintering |
| | | CO ₂ | inhibitor: reaction with alkaline promoters |
| | | CO | poison and inhibitor: strong chemisorption, reduction to methane; accelerates sintering |
| | | unsaturated hydrocarbons | inhibitor: strong chemisorption, slow reduction |
| Hydrogenation | Ni, Pt, Pd, Cu | S, Se, Te, P, As compounds, halogens | poison: strong chemisorption |
| | | Hg and Pb compounds | poison: alloy formation |
| | | O ₂ | poison: surface oxide film |
| | | CO | Ni forms volatile carbonyls |
| Catalytic cracking | alumino-silicates | amines, H ₂ O, Ni, Fe, V, (porphyrins) | inhibitor: blocking of active sites |
| | | coke | poison: blocking of active sites |
| NH ₃ oxidation | Pt/Rh | P, As, Sb compounds; Pb, Zn, Cd, Bi | poison: alloy formation, catalyst net becomes brittle |
| | | rust | decomposes NH ₃ |
| | | alkali metal oxides | poisons: react with Rh ₂ O ₃ |
| SO ₂ oxidation | V ₂ O ₅ / K ₂ S ₂ O ₇ | As compounds | inhibitor → poison; compound formation |
| Ethylene oxide synthesis | Ag | halogenated hydrocarbons | inhibitor: increase selectivity |

5.5.2

Poisoning of Metals

Metal catalysts are highly sensitive to small amounts of certain impurities in the reaction medium. Catalytically active metals make their d orbitals available for adsorption, and this is the key to understanding both their catalytic activity and their sensitivity to poisons.

Poisons for metals can be classified in three groups:

- Nonmetallic ions
- Metal ions
- Unsaturated molecules

Particularly strong catalyst poisons are the ions of elements of groups 15 (N, P, As, Sb, Bi) and 16 (O, S, Se, Te). The poisoning activity depends on the presence of electron lone pairs, which have been shown to form dative bonds with transition metals on chemisorption. If these are involved in bonding to other elements, then the ions are nonpoisons:

Poisons: H₂S, thiophene, NH₃, PH₃, AsH₃

Nonpoisons: SO₄²⁻, NH₄⁺, PO₄³⁻, AsO₄³⁻, sulfones

The poisoning effect of metal ions depends on the number of d electrons. Metals with an empty d shell, such as alkali and alkaline earth metals, and those with less than three d electrons are nonpoisons, as shown in the following for the example of platinum:

Poisons: Zn²⁺, Cd²⁺, Hg²⁺, In³⁺, Tl⁺, Sn²⁺, Pb²⁺, Cu⁺, Cu²⁺, Fe²⁺, Mn²⁺, Ni²⁺, etc.

Nonpoisons: Na⁺, Be²⁺, Mg²⁺, Al³⁺, La³⁺, Ce³⁺, Zr⁴⁺, Cr²⁺, Cr³⁺

Metals readily adsorb unsaturated molecules such as CO and olefins. If they are adsorbed irreversibly in molecular form, then they act as poisons. If dissociation or decomposition occurs, then this can lead to deactivation by coking.

Because of the wide range of chemisorption bond strengths, various effects can occur in the hydrogenation of two unsaturated molecules. Inhibition can range from favored hydrogenation of one component to complete suppression of a reaction in the presence of extremely small quantities of a second unsaturated component. Examples are the poisoning of Pt and Ni hydrogenation catalysts by CO or CN⁻ and the slower hydrogenation of cyclohexene in the presence of small amounts of benzene.

Halogens and volatile nitrogen compounds generally act as weak catalyst poisons or inhibitors and lead to a reversible or temporary lowering of the catalyst activity.

Catalyst poisoning can be reversible or irreversible, depending on the reaction conditions. For example, sulfur poisoning of nickel catalysts is irreversible at low temperatures, and methanation catalysts can not be regenerated, even by treatment with hydrogen. At higher temperatures sulfur can be removed by hydrogenation and steam, so that nickel catalysts for steam reforming are considerably more resistant to sulfur-containing poisons.

Poisoning of metal catalysts can best be avoided by pretreatment of the reactants by:

- Chemical treatment (expensive; can lead to other impurities)
- Catalytic treatment (very effective for organic poisons)
- Use of adsorbers (e.g., ZnO to remove sulfur-containing compounds in natural gas reforming)

The incorporation of promoters can also neutralize catalyst poisons. Thus the sulfur poisoning of nickel catalysts is reduced by the presence of copper chromite since copper ions readily form sulfides.

The appropriate treatment method and the decision whether the catalyst or the process should be modified requires detailed knowledge of the cause of deactivation.

5.5.3

Poisoning of Semiconductor Oxides

Because of the presence of electron-donor or electron-acceptor centers with special surface geometries and the fact that redox reactions are favored, general statements about the poisoning of semiconductor catalysts can hardly be made. Any molecule that is strongly adsorbed on the surface is a potential poison.

Up to now there have been no theoretical models of the poisoning of semiconductor catalysts. They are quite resistant to poisoning, the addition of several per cent of foreign materials being required to give a noticeably lower activity.

5.5.4

Poisoning of Solid Acids

The poisoning of acid centers can easily be explained. Acid centers can be neutralized and thus poisoned by basic compounds such as alkali and alkaline earth compounds and especially organic bases. Alkali and alkaline earth compounds are normally used as promoters and are generally not present in process streams.

In contrast, nitrogen-containing bases are contained in many crude-oil fractions. In a typical starting material, 25–35 % of the nitrogen compounds have basic character. The sensitivity of solid acids towards these poisons correlates directly with their basicity. For example, pyridine, quinoline, amines, and indoles are basic, while pyrrole and carbazole are nonbasic. These poisons are best removed by hydrogenation, together with sulfur and most of the heavy metal poisons.

However, in some cases partial catalyst poisoning is desired, for example to lower the catalyst activity or to influence the selectivity. A well-known example is the addition of ppm quantities of H₂S in catalytic reforming with nickel catalysts. Compared to platinum, nickel has a higher hydrogenolysis activity, which leads to formation of gases and coke. Sulfur selectively poisons the most active hydrogenolysis centers and thus drastically influences the selectivity towards the desired isomerization reactions.

Other partially poisoned catalysts have long been used in the laboratory. Supported palladium catalysts, poisoned with lead (Lindlar catalysts), sulfur, or quinoline, are used for the hydrogenation of acetylenic compounds to *cis*-olefins. Another

application of this type of catalyst is the removal of traces of phenylacetylene (200–300 ppm) from styrene by selective hydrogenation.

In the Rosenmund reaction (Eq. 5-84), acid chlorides are hydrogenated to aldehydes. The catalyst is a supported palladium catalyst (5% Pd/BaSO₄) poisoned by sulfur compounds such as quinoline, tiourea, or thiophene to prevent further reduction of the aldehyde.



5.5.5

Deposits on the Catalyst Surface

The blocking of catalyst pores by polymeric components, especially coke, is another widely encountered cause of catalyst deactivation. In many reactions of hydrocarbons, side reactions lead to formation of polymers. If these are deposited near the pore openings, catalyst activity and selectivity can be influenced due to impaired mass transport into and out of the pores.

At high temperatures (above 200 °C) these polymers are dehydrogenated to carbon, a process known as coking. Especially catalysts with acidic or hydrogenating/dehydrogenating properties cause coking. Coking on acid centers is observed with zeolite and aluminosilicate catalysts and with acidic supports. The extent of coke formation depends directly on the acidity.

The precursors for coke formation are mainly aromatic and olefinic hydrocarbons, which are either contained in the starting materials or are formed as intermediate products in the process.

In some processes, 5–10% zeolite is added to amorphous cracking catalysts. This increases the activity by several orders of magnitude and drastically reduces coke formation. This is another example of shape-selective catalysis by zeolites, in which the coke-forming intermediates are restricted by the zeolite pores (see Section 7.3.1).

With dehydrogenation catalysts (metals, oxides, sulfides), coke is formed in a different manner than acid cleavage of hydrocarbons. Dehydrogenation steps, followed by hydrogenolysis, lead to formation of carbon fragments C_x. These are highly reactive and are bound in a carbide-like fashion or are present as pseudo-graphite. In the presence of acid support materials, the C fragments migrate from the dehydrogenation centers of the metal to the support, where they are cleaved analogously to acid catalysts (Fig. 5-39).

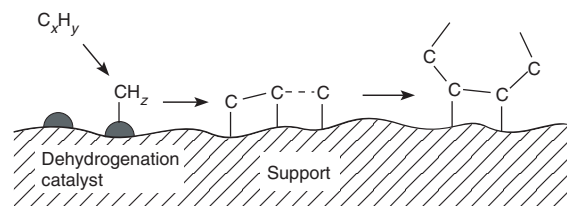


Fig. 5-39 Dehydrogenative coking

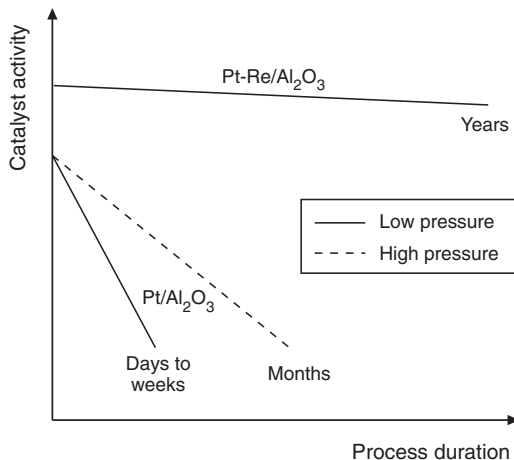


Fig. 5-40 Catalyst deactivation in reforming processes [T35]

Dehydrogenative coking mainly occurs in catalytic reforming, hydrodesulfurization, and in cases of metal contamination of the starting materials. In catalytic reforming processes, bimetallic catalysts are successfully used. Addition of Re to Pt greatly increases the stability of the catalyst, as depicted schematically in Figure 5-40. Rhenium inhibits both coking and sintering of the catalyst and thus has a favorable effect on deactivation during the process and on the frequency of regeneration. By using supported Re/Pt catalysts, the catalyst lifetime can be extended from a few weeks to several years, whereby, however, the H₂ pressure also plays a role. Metal impurities in the starting materials play a role in hydrodesulfurization and hydrodenitrogenation processes. Crude oil fractions contain heavy metal impurities in the form of porphyrins of Fe (up to 150 ppm), Ni (up to 50 ppm) and V (up to 100 ppm). These porphyrins are preferentially adsorbed on Al₂O₃ and aluminosilicates and then decompose to finely divided metals. Nickel is the most active. When the catalyst is regenerated, these metals are oxidized, and the resulting oxides can act as strong oxidizing agents (e.g., V₂O₅). These metals and their oxides have several negative effects: they block active centers, have high catalytic activity, and have a strong coking effect.

Therefore, heavy metals must be removed from crude oil fractions. Various processes are used: chemical or adsorptive removal of the porphyrins, or demetallation by hydrogenation and binding the metals on Al₂O₃. Another effective method is the use of additives. For example, the heavy metals can be alloyed by adding antimony, after which they are deposited on the catalyst in a different form.

Coking of catalysts can be reduced by increasing the hydrogen partial pressure or by partial neutralization of the acid sites with promoters, as we have already seen. Coke that has already formed is removed by periodic regeneration of the catalyst. The deactivated catalyst is purified by controlled combustion of the carbon layer. In fluidized-bed crackers the catalyst circulates continuously between the reactor and the regenerator, in which combustion takes place. The heat of combustion is used to maintain the catalyst at the temperature of the slightly endothermic cracking reaction.

5.5.6

Thermal Processes and Sintering

Thermal influences can often affect the catalyst composition. In many cases one or more metastable phases are formed from the active components or the support materials. Phase changes can limit the catalyst activity or lead to catalyst–substrate interactions. We have already dealt with the transformation of γ - Al_2O_3 into α - Al_2O_3 with its lower surface area. Another example is the phase transformation of TiO_2 from anatase to rutile in $\text{V}_2\text{O}_5/\text{TiO}_2$ /corundum catalysts for the oxidation of *o*-xylene to phthalic anhydride.

Sintering is a well-known phenomenon in metallurgy and ceramics technology. Sintering processes are also of importance in catalysis, even at low temperatures. Reasons for this are the extremely small crystallites, porous supports, and reactive gases. Catalyst atoms already become mobile at temperatures between one-third and one-half of the melting point.

The rate of sintering increases with increasing temperature, decreasing crystallite size, and increasing contact between the crystallite particles. Other factors are the amount and type of impurities on the crystallite surface and the support composition in supported catalysts.

Increased sintering can also occur if the active catalyst components form volatile compounds with the reactants. An example is the sintering of copper catalysts in the presence of chlorine compounds.

The main effect of sintering is loss of active surface area and the resulting decrease in catalyst activity. However, a change in selectivity can also occur, especially in the case of structure-sensitive reactions. Extensive investigations of sintering have been carried out on highly dispersed metals such as $\text{Pt}/\text{Al}_2\text{O}_3$.

An informative example is naphtha reforming, in which the influence of regeneration also becomes apparent. The data in Table 5-43 suggest that regeneration of the catalyst by combustion of the coke leads to an increase in crystallite size, since the catalyst activity, measured by H_2 adsorption, decreases steadily with time, in spite of regeneration. Studies of the reforming process with model substances found major changes in

Table 5-43 Naphtha reforming with 0.6% $\text{Pt}/\text{Al}_2\text{O}_3$: catalyst deactivation and regeneration [T35]

| Catalyst state | Adsorbed hydrogen [$\text{cm}^3/\text{g cat.}$] |
|---------------------|--|
| Fresh | 0.242 |
| Coked, 1 d (1% C) | 0.054 |
| Regenerated | 0.191 |
| Coked, 1 d (1% C) | 0.057 |
| Regenerated | 0.134 |
| Coked, 5 d (2.5% C) | 0.033 |
| Regenerated | 0.097 |

selectivity. For example, it was found that with increasing crystallite diameter aromatics formation due to dehydrocyclization decreases, isomerization reactions increase, and the hydrocracking activity remains roughly the same.

Another example is industrial ethylene oxide synthesis. Here, too, it was shown that a decrease in the Ag surface area due to sintering is responsible for the deactivation of the catalyst.

A final example is the selective catalytic reduction of nitrogen oxides on vanadium titanium oxides (SCR process) [20]. The catalyst consists of V_2O_5 on a TiO_2 (anatase) support. Above about $350^\circ C$ the less thermally stable TiO_2 sinters, and the anatase surface becomes much smaller. This results in recrystallization of the vanadium pentoxide, which is now present in excess, and growth of threadlike and platelet V_2O_5 crystallites is observed. This results in undesired side reactions such as increased N_2O formation. The thermal stability of the catalyst can be improved by stabilizing the support (addition of sulfate) or by modifying the active components (addition of tungsten oxide).

In general, the effects of sintering can be counteracted by the following measures:

- Addition of stabilizing additives (promoters) to the active components or their dispersion on the surface of the support (e. g., nickel can be stabilized by Cr_2O_3)
- Redispersion of the metals (e. g., chlorine treatment of Pt/ Al_2O_3 reforming catalysts: volatile $PtCl_2$ is re-adsorbed on Al_2O_3 and finely distributed)

5.5.7

Catalyst Losses via the Gas Phase

High reaction temperatures in catalytic processes can lead to loss of active components by evaporation. This does not only occur with compounds that are known to be volatile (e. g., P_2O_5 in H_3PO_4 , silica gel, $HgCl_2$ /activated carbon), but also by reaction of metals to give volatile oxides, chlorides, or carbonyls. In the oxidation of ammonia on Pt/Rh net catalysts (Ostwald nitric acid process), the catalyst reacts with the gas phase to form volatile PtO_2 . Furthermore, porous platinum growths are observed on the surface. This can be prevented by addition of rare earth oxides.

In hydrogenation processes with molybdenum-containing catalysts, too high a temperature during regeneration due to the occurrence of hot spots can lead to the formation of MoO_3 , which evaporates at temperatures above $800^\circ C$ with irreversible loss of activity.

Another example is the use of nickel catalysts in the methanation of synthesis gas. If the temperature of the catalyst bed drops below $150^\circ C$, catalyst is lost by formation of highly toxic nickel tetracarbonyl.

We will now examine some models of catalyst deactivation processes. Given the various causes of catalyst deactivation, it is not surprising that numerous mechanisms and models can be found in the literature.

A relatively simple model of deactivation kinetics is based on Langmuir adsorption. It is assumed that the total number of active surface sites of the catalyst Z_{tot} decreases with increasing lifetime or operating time t' , for example, due to poisoning

by a component of the starting material. For a monomolecular reaction, the kinetics are then described by Equation 5-85.

$$r = \frac{k'_s Z_{\text{tot}} K_1 p_1}{1 + K_1 p_1} = \frac{k_1 p_1}{1 + K_1 p_1} \quad (5-85)$$

The rate of deactivation r_d is defined as the rate of decrease of the activity a with time and can be determined separately (Eq. 5-86).

$$r_d = \frac{da}{dt'} \quad (5-86)$$

In our model r_d can be attributed to the change in the active surface sites. The rate of deactivation depends on the temperature, the activity of the catalyst a , the concentration of the deactivating component c_d , and the activation energy of the process E_d (Eq. 5-87).

$$-r_d = k_{d,0} e^{-(E_d/RT)} \cdot f(a, c_d) \quad (5-87)$$

A very high activation energy of 290 kJ/mol is found for the reforming of heptane on Pt/Al₂O₃ catalysts, for example.

Quantitatively, the rate of loss of activity can often be expressed as a power law of the type given in Equation 5-88.

$$-r_d = -\frac{da}{dt'} = k_d a^n c_d^m \quad (5-88)$$

If there is no deactivation by poisoning, then $m = 0$. This could then be a process of deactivation by sintering. With the simplifying assumption $n = 1$, Equation 5-88 becomes:

$$-r_d = -\frac{da}{dt'} = k_d a \quad (5-89)$$

Integration of Equation 5-89 between $t' = 0$ and t' gives:

$$a(t') = a(t' = 0) \cdot e^{-k_d t'} \quad (5-90)$$

Since by definition $a(t' = 0) = 1$, we obtain the simple exponential equation:

$$a(t') = e^{-k_d t'} \quad (5-91)$$

Such exponential equations can sometimes also describe deactivation by poisoning, provided the concentration of the catalyst poison is constant. Examples are the hydrogenation of ethylene on copper catalysts (poisoning by CO) and the dehydrogenation of alkanes on Cr/Al₂O₃ catalysts.

For sintering processes, the decrease in activity can often be described by a second-order equation. We then obtain:

$$-r_d = k_d a^2 \quad (5-92)$$

and after integration

$$a(t') = \frac{1}{1 + k_d t'} \quad (5-93)$$

Examples for the application of this hyperbolic law are the dehydrogenation of cyclohexane on Pt/Al₂O₃ catalysts and the hydrogenation of isobutene on Ni catalysts.

After many examples of catalyst deactivation, let us look at the process of catalyst regeneration. The catalyst activity varies with time as shown in Figure 5-41. The activity decreases with increasing operating time in a manner that depends on the reaction conditions and the deactivation kinetics. First, attempts are made to make the deactivation slower by adjusting the operating parameters (e.g., raising the temperature, increasing the pressure in hydrogenation reactions).

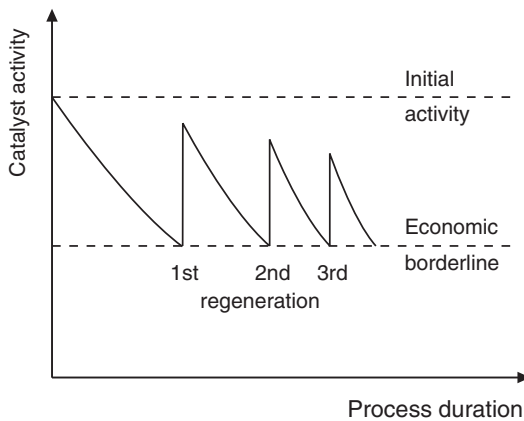


Fig. 5-41 Catalyst regeneration and loss of activity during a process

The loss of activity can be gradual or very rapid. Examples are the hydrogenative treatment of naphtha, with catalyst lifetimes of several years, and catalytic cracking, in which strong catalyst deactivation occurs after a few minutes. In all cases the deactivation reaches an extent at which the conversion or other process parameters are below specification, and the catalyst must be replaced or regenerated. In practice, the original activity is not attained due to a permanent secondary deactivation. When regeneration steps are no longer economically viable, the catalyst must be completely replaced.

In this chapter we have described the importance of catalyst deactivation in industrial processes. Detailed knowledge of the cause of deactivation is a prerequisite for catalyst modification and process control.

► Exercises for Section 5.5**Exercise 5.39**

What are the effects of catalyst deactivation?

Exercise 5.40

How can catalyst deactivation be measured experimentally?

Exercise 5.41

Catalysts based on Al_2O_3 are often regenerated by combustion of coke deposits. Which negative effects can occur here?

Exercise 5.42

Why must particular care be taken when nickel catalysts are used in industrial carbonylation reactions?

Exercise 5.43

Platinum metal catalysts are strongly inhibited by halides. Which order of inhibition activity can be expected for the halides?

Exercise 5.44

Zeolites are the preferred catalysts for cracking reactions.

- a) How does their deactivation occur?
- b) How are cracking catalysts regenerated?

5.6**Characterization of Heterogeneous Catalysts [3, 28]**

Both the physical and the chemical structure of a catalyst must be known if relationships between the the material structure of the catalyst and activity, selectivity, and lifetime are to be revealed. The available methods include classical procedures and state-of-the-art techniques for studying the physics and chemistry of surfaces [33].

The physical properties of pore volume, pore distribution, and BET surface area are nowadays routinely monitored in the production and use of industrial catalysts. In contrast, the chemical characterization of catalysts and microstructural investigations, especially of the catalyst surface, are far more laborious and are rarely carried out in industry.

As we have already seen in many examples, the upper atomic layers often have a different composition to that in the catalyst pellet. Promoters, inhibitors, and catalyst poisons can also be deposited. Therefore, in order to understand heterogeneous cata-

lysis, information about the nature and structure of the upper atomic layers is required. Up to about 35 years ago, chemisorption processes were the only methods available for the indirect characterization of the catalyst surface. Only in the 1970s did instruments for the analysis of surfaces become commercially available, opening up new possibilities for fundamental catalyst research [21].

In this section we will encounter some methods for characterizing catalysts and discuss their capabilities and limitations. Most chemical engineers working in catalyst development are not experts in complex industrial analytical chemistry, and only a few major companies and research institutes can afford surface analysis equipment. For these reasons we shall dispense with the details of methods and apparatus and concentrate on practical applications.

Figure 5-42 gives an overview of the common methods of catalyst investigation.

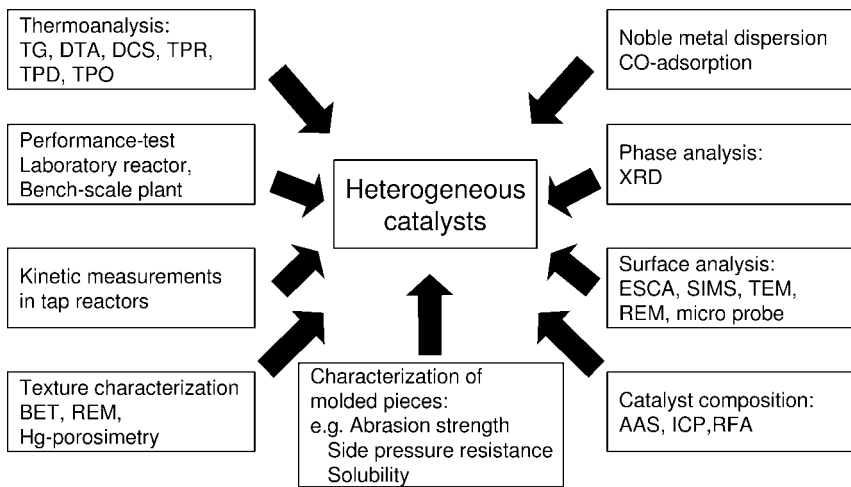


Fig. 5-42 Instruments of catalyst investigation

5.6.1

Physical Characterization [T41]

The main terms for describing physical catalyst properties are as follows:

- Morphology: steric conditions and topology of the surface
- Porosity: share of the hollow space (pore volume) of a catalyst pellet
- Texture: generally refers to the pore structure of the particles (pore size, pore size distribution, pore shape)

An important property of catalysts is the distribution of pores across the inner and outer surfaces. The most widely used method for determining the pore distribution in solids is mercury porosimetry, which allows both mesopores (pore radius 1–25 nm) and macropores (pore radius >25 nm) to be determined. The pore size

distribution is determined by measuring the volume of mercury that enters the pores under pressure. The measurement is based on Equation 5-94.

$$p = \frac{2\pi\sigma\cos\alpha}{r_p} \quad (5-94)$$

p = pressure
 σ = surface tension of Hg
 α = contact angle Hg/solid
 r_p = radius of the cylindrical pores

Pressures of 0.1 to 200 MPa allow pore sizes in the range 3.75–7500 nm to be determined. Since the pores are not exactly cylindrical, as assumed in Equation 5-94, the calculated pore sizes and pore size distributions can differ considerably from the true values, which can be determined by electron microscopy.

Mercury porosimetry is advantageously used for characterizing various shaped industrial catalysts in which diffusion processes play a role. The macropore distribution is of major importance for the turnover and lifetime of industrial catalysts and is decisively influenced by the production conditions.

For the actual catalytic reaction, the distribution of meso- and micropores is of greater importance. The specific pore volume, pore size, and pore size distribution of microporous materials are determined by gas adsorption measurements at relatively low pressures (low values of p/p_0 = pressure/saturation pressure). The method is based on the pressure dependence of capillary condensation on the diameter of the pores in which this condensation takes place. To calculate the pore size distribution, the desorption isotherm is also determined. Thus a distinction can be made between true adsorption and capillary condensation. The latter is described by the Kelvin equation (Eq. 5-95).

$$\ln \frac{p}{p_0} = \frac{V}{RT} \frac{2\sigma\cos\theta}{r_p} \quad (5-95)$$

V = molar volume
 σ = surface tension of adsorbate
 θ = contact angle adsorbate/solid
 r_p = radius of the cylindrical pores

Micropores occur in particular in zeolites and activated carbons. They can lead to false values of BET surface areas due to capillary condensation.

The specific surface area (in m^2/g) of a catalyst or a support material can be determined by the proven BET method. The volume of a gas (usually N_2) that gives monomolecular coverage is measured, allowing the total surface area to be calculated. The equilibrium isotherms are of the form shown in Figure 5-43.

In Figure 5-43 the adsorbed volume is plotted against p/p_0 (p = pressure, p_0 = saturation pressure). At low pressures monolayer adsorption obeys the Langmuir equation (Eq. 5-96).

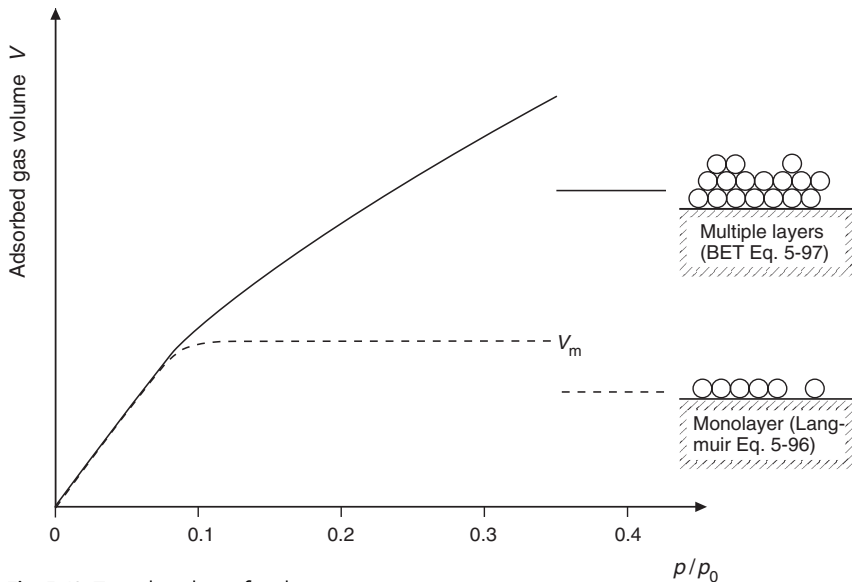


Fig. 5-43 Typical isotherm for physisorption

$$\frac{V}{V_M} = \frac{K(p/p_0)}{[1 + K(p/p_0)]} \quad (5-96)$$

V_M = volume of the monolayer

K = constant

However, above about $p/p_0 = 0.1$, multilayer adsorption becomes important. A theoretical model for describing such adsorption processes was developed by Brunauer, Emmett, and Teller, who formulated the familiar BET equation (Eq. 5-97) [T35].

$$\frac{V}{V_M} = \frac{c p}{[p_0 - p][1 + (c - 1) p/p_0]} \quad (5-97)$$

c includes the heat of adsorption and condensation and is constant for a particular class of compounds (i. e., oxides, metals) with values of over 100.

Equation 5-97 applies up to $p/p_0 = 0.3$, above which capillary condensation begins, initially in the smallest micropores and finally in the mesopores when p/p_0 approaches unity. The determination of V_M by means of Equation 5-97 is impractical, and a much better method was developed by transforming Equation 5-97 into a linear equation (Eq. 5-98).

$$\frac{p}{V(p_0 - p)} = \frac{1}{V_M c} + \frac{(c - 1)}{V_M c} (p/p_0) \quad (5-98)$$

Then V_M can easily be determined from the slope m and the ordinate intersection y .

From the difference between the BET surface area and the surface area measured by mercury porosimetry, the micropore fraction of materials such as zeolites and activated carbons can be determined.

Table 5-44 lists typical surface areas of catalysts and supports.

Table 5-44 Specific surface areas of catalysts and support materials

| Catalyst/support | Specific surface area [m ² /g] |
|--|---|
| H-zeolite for cracking processes | 1000 |
| Activated carbon | 200–2000 |
| Silica gel | 200–700 |
| Aluminosilicates | 200–500 |
| Al ₂ O ₃ | 50–350 |
| Ni/Al ₂ O ₃ (hydrogenation cat.) | 250 |
| CoMo/Al ₂ O ₃ (HDS) | 200–300 |
| Fe–Al ₂ O ₃ –K ₂ O (NH ₃) | 10 |
| Bulk catalyst | 5–80 |
| V ₂ O ₅ (partial oxidation) | 1 |
| Noble metal/support | 0–10 |
| Pt wire (NH ₃ oxidation) | 0.01 |

Although the specific surface area is one of the most important parameters in heterogeneous catalysis, it must be taken into account that especially in the case of supported catalysts, there is no direct relationship between catalyst activity and the physical surface of the catalyst. Such predictions can only be made with the aid of chemisorption measurements. Here the number of catalytically active surface atoms is determined by chemisorption of appropriate gases such as H₂, O₂, CO, NO, and N₂O at room temperature or above (Fig. 5-44). The choice of gas depends on the metal (Table 5-45).



Fig. 5-44 Sorptometer (catalysis laboratory, FH Mannheim, Germany)

Table 5-45 Specific chemisorption for the characterization of metal surfaces

| Adsorbate | Metal | T [°C] | Advantages | Disadvantages |
|------------------|-----------------------------|-------------------------|--|---|
| H ₂ | Pt, Pd, Ni | 0–20 –78 –195 | dissociative chemisorption, low adsorption on support, negligible physisorption, simple stoichiometry | possible hydride formation, sensitive to impurities |
| CO | Pt, Pd Ni, Fe, Co | 0–25 –78 –195 | no solution in volume | physisorption at low tem- peratures bridging and linear binding, risk of carbonyl formation or dissociation |
| O ₂ | Pt, Ni Ag Cu | 25 200 –195 | low adsorption on oxide supports | physisorption at low tem- peratures, oxidation possible |
| N ₂ O | Cu, Ag | 25 | low adsorption on oxide supports, very little oxidation | complicated measurement (volumetric not possible) |

Table 5-45 lists the advantages and disadvantages of the adsorbates. It can be seen that the adsorbates are not specifically suited to just one type of metal, so that chemisorption on multimetal catalysts has only limited applicability.

Apart from the adsorbates listed in Table 5-45, the so-called surface titration method is used to determine Pt and Pd on supports. The method is based on the dissociative chemisorption of H₂ or O₂, followed by reaction with chemisorbed O₂ or H₂, respectively. A problem is the reaction mechanism, which is still the subject of debate in the literature.

Given knowledge of the adsorption stoichiometry, the amount of material adsorbed on a supported catalyst can be used to determine the dispersion of the active component.

The volume of adsorbed gas gives the active surface. The number of active metal atoms is given per gram of catalyst, that is, the degree of dispersion. Normally, a direct proportionality between the measured number of surface atoms and the number of active centers can be assumed. Knowledge of the dispersion allows comparison of the catalyst activity on the basis of reaction rate per unit metal surface.

To a certain extent, chemisorption techniques are also applicable to oxides [33].

Temperature-Programmed Desorption [43, 44]

Temperature-programmed desorption (TPD) is extensively applied for catalyst characterization. Commonly used molecules are NH₃, H₂, CO and CO₂. From the desorption pattern much useful information can be obtained. TPD allows kinetic experiments in which the desorption rate from the surface is followed while the temperature of the substrate is increased continuously in a controlled way, usually in a linear

ramp. TPD is used to characterize adsorption states and to determine the kinetics of desorption. Qualitatively TPD can be interpreted simply because the higher the desorption temperature the more strongly is the adsorbate bonded to the surface. Since the area under a TPD curve is proportional to the coverage, TPD spectra allow determination of relative coverages.

TPD is used to determine

- The adsorbate layer
- The amount of desorbed molecules as a function of the temperature
- The behavior of the catalyst during calcination with an inert carrier gas
- The interaction of probe molecules such as ammonia with zeolites for acidity measurements

Chemisorbed molecules are bonded to the surface by forces dependent on the nature of the active site. For instance, ammonia will be strongly adsorbed on acid sites, whereas it is only weakly adsorbed on basic sites. Figure 5-45 shows schematically a TPD pattern of ammonia desorption from H-ZSM-5.

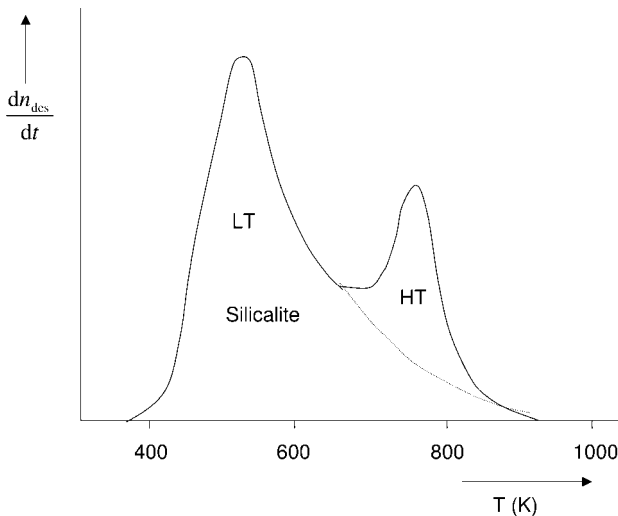


Fig. 5-45 Scheme of a TPD spectrum of ammonia desorbing from zeolite [43]

The desorption spectrum consists of two broad overlapping peaks. The first (low-temperature LT) peak is assigned to NH_3 desorbing from weak acid or non-acidic sites such as be built from silicalite. The high-temperature peak (HT) is due to ammonia desorbed from strong acid sites. Thus, the peak temperatures can be correlated to the acid strength of the adsorption sites. But it should be mentioned that the technique does not clearly discriminate between Lewis and Brönsted sites.

5.6.2

Chemical Characterization and Surface Analysis

Of particular importance are the composition, i.e., the distribution of elements in the catalyst, and the detection of phases and surface compounds. Also of interest are differences in composition between catalyst volume and catalyst surface, as well as interactions between active components and support materials and between the active components themselves.

These phenomena are best studied by advanced spectroscopic methods. Since the solid surface plays the decisive role in heterogeneous catalysis, methods for the characterization of surfaces are of major importance in modern catalyst research [28].

Catalyst surfaces, surface compounds, metals dispersed on supports, and adsorbed molecules are investigated by electron spectroscopy, ion spectroscopy, analytical microscopy, and other methods [12, 33].

We will first discuss methods with which the structure of the surface is determined, and then those that determine the chemical composition of the surface (catalyst and substrate). Finding relationships between the structures of material and the catalyst activity requires high-resolution investigation of the microstructure of the catalyst. Since heterogeneous catalysts are often highly nonuniform solids, correct sampling, sample preparation, and choice of the appropriate method are important if meaningful results are to be obtained.

Temperature-Programmed Reaction Methods [44, 45]

Temperature-programmed methods are techniques in which a chemical reaction is monitored while the temperature is increased linearly in time. There are used several methods: temperature-programmed reduction (TPR), oxidation (TPO), and sulfidation (TPS). The equipment for these investigations is relatively simple. The catalyst is placed in a tubular reactor and with TPR the O-releasing catalyst is reduced in a flow of inert gas, usually Ar or N₂ containing a few % of H₂. The off-gases are continuously monitored by a mass spectrometer and the consumption of hydrogen is recorded as a function of the reaction temperature. The reactor is controlled by a processor, which heats the reactor at a linear rate of 0.1 to 20 °C/min. The process is shown schematically in Figure 5-46.

The complete reduction of a catalyst can be determined by TPR method. Integration of the H₂ consumption signal allows the determination of the total amount of hydrogen used to titrate the reactive oxygen in the catalyst and is expressed in moles of H₂ per mol of metal atoms.

Catalysts for hydrotreatment reactions such as hydrodesulfurization (HDS), based on alumina-supported Mo or W (promoters Co or Ni) are active in the sulfided state. Thus, the oxidic catalyst precursors have to be activated by treating with a mixture of H₂S and H₂. This sulfidation process can be studied by TPS.

Temperature-programmed oxidation is an equally valid technique to determine the amount of reduced species in a catalyst material. The experimental setup of TPO equipment is identical to that of a TPR. Therefore, both techniques can easily be

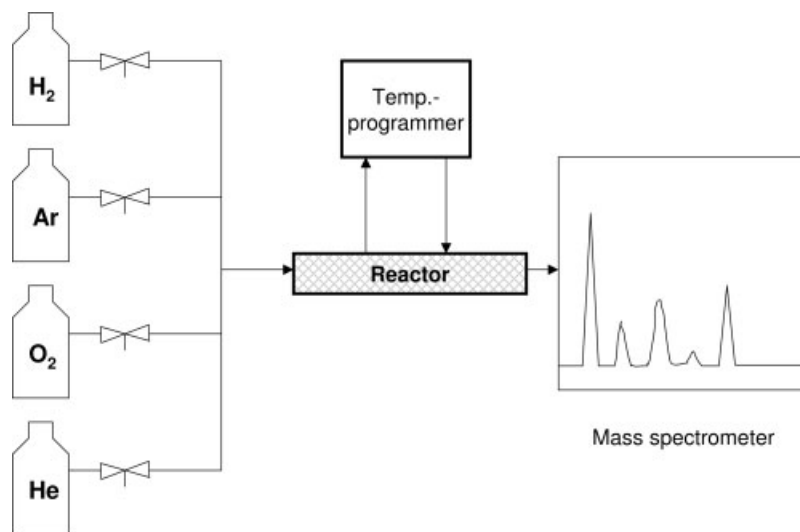


Fig. 5-46 Principle of a device for temperature programmed reduction TPR [45]

combined. The combination of such a TPR/TPD setup with CO temperature-programmed desorption (TPD), moreover, allows the titration of coordinatively unsaturated metal centers on the catalyst surface as a function of the TPR/TPO pretreatment.

Transmission Electron Microscopy

This method allows the size distribution and shape of metal particles in supported and unsupported catalysts to be characterized down to the level of atomic resolution [27].

Scanning transmission electron microscopy (STEM) uses X-ray backscattering analysis to obtain information on the size, morphology, and chemical composition of the active components on support materials (Fig. 5-47).

Examples of Applications:

- Dispersion measurements on Pd/SiO₂ catalysts: good agreement with chemisorption measurements
- Sintering, segregation, and redispersion of metal particles as a result of oxidative treatment
- Study of coking processes
- Detection of surface impurities and surface poisoning

Low-Energy Electron Diffraction (LEED) [9, 25]

Electrons with kinetic energies in the range 2–200 eV are important tools for the investigation of surface properties. Since such electrons interact with the electrons of the solids, they penetrate to a depth of only a few atomic layers, or are emitted from

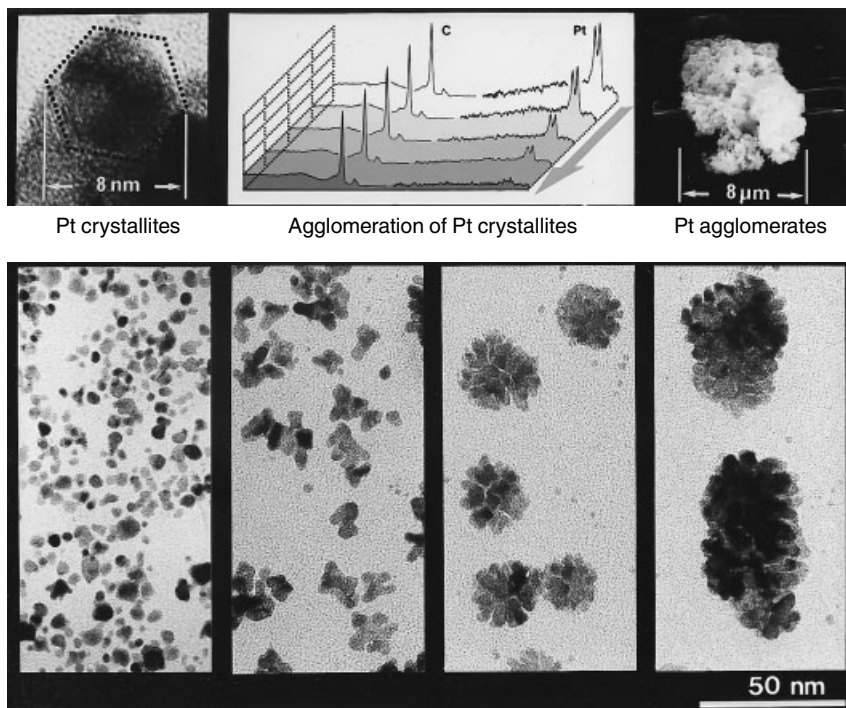


Fig. 5-47 Agglomeration of platinum crystallites in a platinum/graphite catalyst: quantification of the process by XPS (top middle) and visualization by TEM (bottom) (BASF, Ludwigshafen, Germany)

a depth of a few atomic layers in emission processes. Their energy and angular distribution provide information on the properties of the surface region.

In the LEED method, low-energy electrons with high cross sections undergo elastic scattering from atomic cores. Since their wavelengths are comparable to interatomic distances, diffraction effects are observed with single-crystal surfaces. This allows the spatial arrangement of the atoms in the surface region, and hence the periodic structure of the catalyst surface to be determined.

In principle, the LEED method provides the same information about surfaces as is obtained for the interior of solids by X-ray structure analysis.

Examples of Applications:

- Changes in the structure of nickel surfaces on chemisorption of oxygen
- Ordered surface structures in the adsorption of CO on Pd surfaces
- Detection of competitive adsorption of CO and O₂ on Pd surfaces
- Surfaces of Au, Ir, Pt, and semiconductors: structures other than those expected from the lattice geometry

IR Spectroscopy [12]

Infrared spectroscopic investigations in special cuvettes can be used to characterize active centers on catalyst surfaces and chemisorbed molecules. Catalysts on strongly absorbing supports, such as activated carbons, can be studied by reflection IR spectroscopy.

Examples of Applications:

- Detection of Brønsted acid and Lewis acid surface groups with chemisorbed pyridine
- Ethylene chemisorption on isolated Pd atoms by means of matrix-isolation techniques (metal vapor, 10–30 K, xenon matrix, high vacuum): detection of chemisorption complexes
- Proof of metal oxo compounds (Mo, V) as oxidation catalysts
- IR bands of chemisorbed NO for the characterization of supported metal catalysts, e. g., Mo/Al₂O₃, Pt–Re/Al₂O₃, cracking catalysts

Electron Spectroscopy for Chemical Analysis (ESCA)

This widely used method is particularly suitable for the analysis of surface composition [19]. In an ESCA spectrometer, a sample is exposed to X-ray radiation (Fig. 5-48).



Fig. 5-48 Investigation of a catalyst surface in an ESCA apparatus (BASF, Ludwigshafen, Germany)

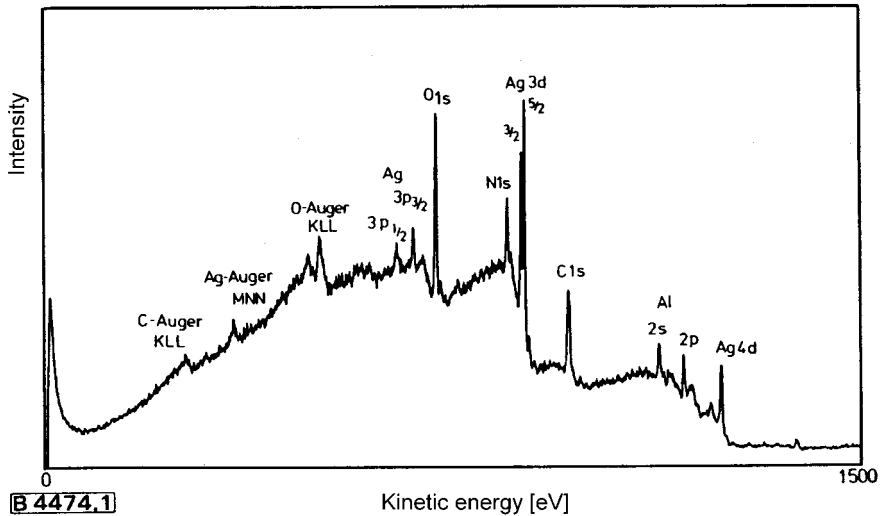


Fig. 5-49. ESCA spectrum of an Ag/Al₂O₃ supported catalyst [25]

The photoelectrons formed in the probe by ionization are analyzed according to their kinetic energy. From this, the binding energy can be determined and therefore the element identified. The chemical shift of these energy values gives information about the bonding and oxidation state of the elements. ESCA can be used to detect all elements other than hydrogen in the upper 5–10 nm of the catalyst surface.

Figure 5-49 shows the ESCA spectrum of a silver catalyst supported on Al₂O₃. Both the sharp photoelectron lines and the broader Auger electron lines can be seen on a background of scattered electrons. The lines can be assigned by means of tabulated values of the bond energies of the main components of the catalyst [25].

Examples of Applications:

- Distinction between Al metal and Al₂O₃
- Distinction between aliphatic carbon and acid carbon
- Changes in the oxidation state of tin on pretreatment of a Pd/Sn catalyst
- Effect of pretreatment on the structure and composition of Mo/Al₂O₃ desulfurization catalysts
- Distinction between Fe⁰ and Fe^{III} in ammonia synthesis catalysts

Auger Electron Spectroscopy (AES)

In this method the surface of the sample is bombarded with high-energy (1–5 keV) electrons [32]. Similarly to ESCA, photoelectrons are generated. The remaining atom, which now has an electron missing from the K shell, has two possibilities for filling this hole. One possibility is X-ray fluorescence, in which an electron from a higher shell fills the hole, and the energy that is released is emitted as an X-ray

quantum. The competing process is Auger emission, in which an electron fills the hole, and the energy released is transferred to a valence electron, which exits the probe as a so-called Auger electron. Similar relationships apply as in ESCA.

The kinetic energy of the Auger electron allows the element to be inferred, and the intensity is a measure of the concentration. Information is obtained for the upper 5 nm. The advantage of AES is that the electron beam can be very tightly focussed. Since the electron beam can be moved across the surface, it is possible to measure a concentration profile along a line or to generate figures. A disadvantage is the relatively low sensitivity and damage to the sample. AES is mainly suited to the determination of surface composition and changes therein.

Examples of Applications:

- Alkyne hydrogenation on NiS catalysts: Ni_3S_2 on the nickel surface is active in selective hydrogenation, but NiS is not
- Determination of the Si/Al ratio in zeolite crystals and on their surfaces

Ion Scattering Spectroscopy (ISS)

In this method a surface is bombarded with noble gas ions, and the kinetic energy of the ions is measured after impact with the surface [21, 31]. In simple terms, this can be regarded as playing billiards with the uppermost atoms of the surface. Since the mass and energy of the noble gas ions prior to impact are known, mechanical energy and impulse equations can be used to calculate the mass of the impacted surface atom. In this way a sort of elemental analysis of the uppermost atomic layer is obtained. A disadvantage is that the lines in ISS spectra are relatively broad, and information about bonding is not obtained.

Comparing the ISS spectra of an unused and a used silver catalyst for ethylene oxide synthesis shows how the alkali metal promoter on the catalyst behaves during the process (Fig. 5-50). In time, the alkali metal promoter spreads across the surface of the catalyst [25].

Secondary Ion Mass Spectrometry (SIMS)

In this method the surface is also bombarded with noble gas ions (primary ions; 1–10 keV) [9, 31]. In each impact, atoms, groups of atoms, or secondary ions are knocked out of the surface. The charged fragments—both positive and negative ions—are analyzed in a mass spectrometer. SIMS can be used to detect all the elements of the periodic table and their isotopes. By using low-energy ion beams, the depth of penetration can be kept so low that exclusively information about the uppermost atomic layers is obtained (static SIMS). More energetic ion beams can be used to remove the surface layer by layer to obtain a depth-profiled analysis over a range of a few nanometers to several micrometers (dynamic SIMS). This is the most sensitive method of depth-profiled trace analysis of solids. The detection limit is 5×10^{14} atoms/cm³ or one particle in 10^8 , i. e., near the ppb range.

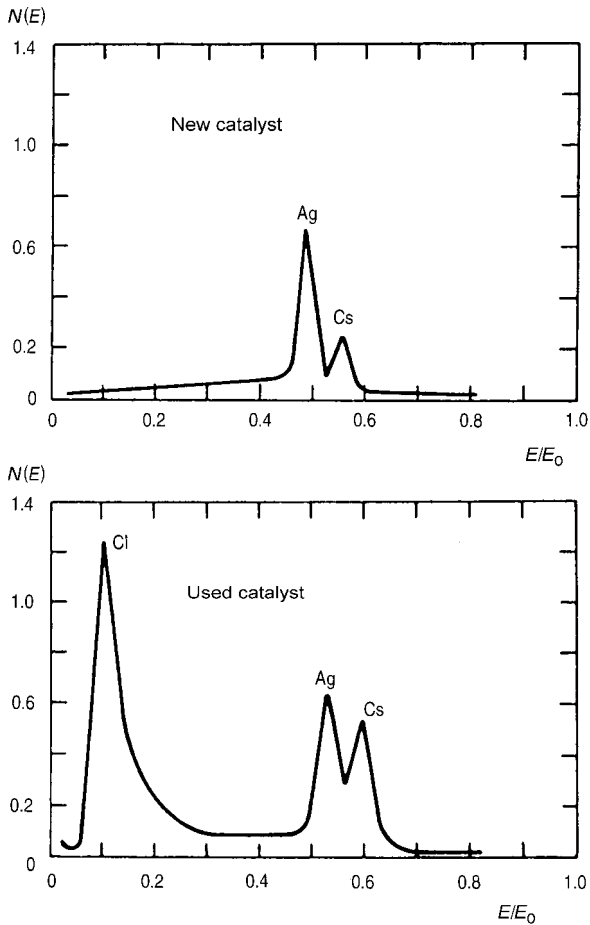


Fig. 5-50 ISS spectra of a new and used ethylene oxide catalyst [26]

Examples of Applications:

- Changes in the Si/Al ratio in the interior of cracking catalysts relative to the particle surface
- Effects of metals in exchanged zeolites
- Proof of the segregation of Pt on the surface of Pt/Re catalysts
- Determination of the surface composition of Cu, Co, and Ni spinels MA_2O_4
- The action of CO on Ni surfaces: detection of $NiCO^+$ and Ni_2CO^+ , i. e., associative chemisorption

Of course, the above-mentioned methods all have advantages and disadvantages. Therefore, it is best to use a combination of methods, e. g., surface analysis, microscopy, and chemisorption measurements.

The main problem of surface analysis methods is that many of them are restricted to special measurement conditions (defined single-crystal surfaces, low temperatures, ultrahigh vacuum). It is questionable whether these results are extrapolable to the behavior of industrial catalysts under process conditions (pressure, high temperatures, impurities). Table 5-46 gives a comparison.

Table 5-46 Comparison of surface physics and industrial heterogeneous catalysis

| Surface physics | Industrial heterogeneous catalysis |
|---|------------------------------------|
| Ideal, well-defined surface (single crystals) | complex, poorly defined surface |
| Very pure surface | highly contaminated surface |
| Pressure ca. 10^{-8} mbar | pressure up to 300 bar |
| Equilibrium | kinetically controlled |

Nevertheless, in the last few years many successes have been achieved that bridge the gap between pure research and applied catalysis. In any case, electron microscopy and surface analysis have made a decisive contribution to the development, optimization and monitoring of catalysts.

► Exercises for Section 5.6

Exercise 5.45

The following physicochemical catalyst properties are to be determined:

- A) Surface complexes
- B) Number and type of active centers
- C) Specific surface area and pore radius distribution
- D) Element distribution on the pore surface
- E) Bonding state of the elements
- F) Crystal structure
- G) Crystallite size

Which of the following methods are suitable for determining the above properties: ESCA, BET method, reflection IR spectroscopy, SIMS, X-ray structure analysis, scanning electron microscopy, temperature-programmed desorption, ESR.

Exercise 5.46

In a sorptometer, chemisorption measurements are carried out with various gases such as H₂, CO, NO and N₂O at room temperature or at higher temperatures. Which catalyst properties are measured?

- Specific pore volume and pore size
- Number of active surface atoms per gram of catalyst
- True catalyst density
- Selectivity of catalysts
- Degree of dispersion
- Pore size distribution

Exercise 5.47

A sample of γ -Al₂O₃ that was heated to 200 °C, cooled, and then pretreated with pyridine exhibits IR bands at 1540 and 1465 cm⁻¹. Explain this finding.

Exercise 5.48

On a supported nickel catalyst, two strong C–O stretching bands are observed in the IR for chemisorbed CO at 1915 and 2035 cm⁻¹. Interpret the position of the bands. How is the CO bound to the metal?

Exercise 5.49

Carbon dioxide adsorbed on a Rh(111) surface gives the same IR spectrum as adsorbed CO. What can be said about the manner in which the gas is adsorbed?

Exercise 5.50

Ethylene undergoes a reaction on a supported Pd/SiO₂ catalyst. The IR band of the adsorbed molecule is observed at 1510 cm⁻¹. Olefins usually have a band at ca. 1640 cm⁻¹. Give an explanation.

Exercise 5.51

What is the LEED method, and what can be measured with it?

Exercise 5.52

What instrument would you need to determine the state of reduction for an alumina-supported nickel catalyst?

Exercise 5.53

Recommend a method for doing routine measurements for comparison of acidic zeolites.

6 Catalyst Shapes and Production of Heterogeneous Catalysts

6.1 Catalyst Production [1, T41]

Industrial catalysts are generally shaped bodies of various forms, e. g., rings, spheres, tablets, pellets (Fig. 6-1). Honeycomb catalysts, similar to those in automobile catalytic converters, are also used. The production of heterogeneous catalysts consists of numerous physical and chemical steps. The conditions in each step have a decisive influence on the catalyst properties. Catalysts must therefore be manufactured under precisely defined and carefully controlled conditions [14].

Since even trace impurities can affect catalyst performance, strict quality specifications apply for the starting materials. Successful catalyst production is still more



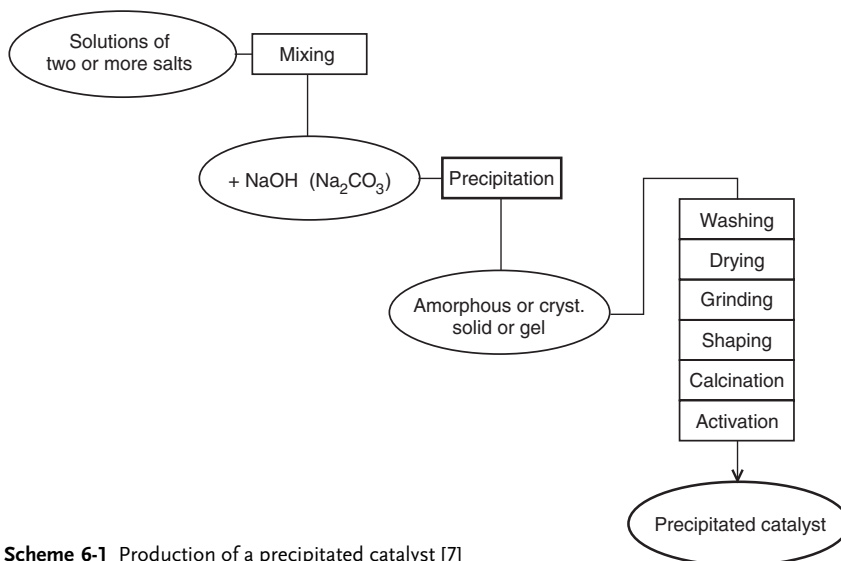
Fig. 6-1 Various shaped catalyst bodies (BASF, Ludwigshafen, Germany)

of an art than a precise science, and much company know-how is required to obtain catalysts with the desired activity, selectivity, and lifetime.

Depending on their structure and method of production, catalysts can be divided into three main groups [8]:

- Bulk catalysts
- Impregnated catalysts
- Shell catalysts

Bulk catalysts are mainly produced when the active components are cheap. Since the preferred method of production is precipitation, they are also known as precipitated catalysts. Precipitation is mainly used for the production of oxidic catalysts and also for the manufacture of pure support materials. One or more components in the form of aqueous solutions are mixed and then coprecipitated as hydroxides or carbonates. An amorphous or crystalline precipitate or a gel is obtained, which is washed thoroughly until salt free. This is then followed by further steps: drying, shaping, calcination, and activation (Scheme 6-1)



Scheme 6-1 Production of a precipitated catalyst [7]

The production conditions can influence catalyst properties such as crystallinity, particle size, porosity, and composition.

In the shaping step, the catalyst powder is plastified by kneading and pelletized by extrusion or pressed into tablets after addition of auxiliary materials (Fig. 6-2). The influence of the shaping process on the mechanical strength and durability of the catalyst should not be underestimated. When reactors are filled with catalyst, a dropping height of 6–8 m is usual, and bed heights of up to 10 m are possible. Furthermore, industrial catalysts are subject to high temperatures and also often to changing temperatures.



Fig. 6-2 Production of noble metal catalysts at the company Degussa, Hanau–Wolfgang, Germany

Typical examples of precipitated catalysts are:

- Iron oxide catalysts for high-temperature CO conversion (Fe_2O_3 with addition of Cr_2O_3)
- Catalysts for the dehydrogenation of ethylbenzene to styrene (Fe_3O_4)

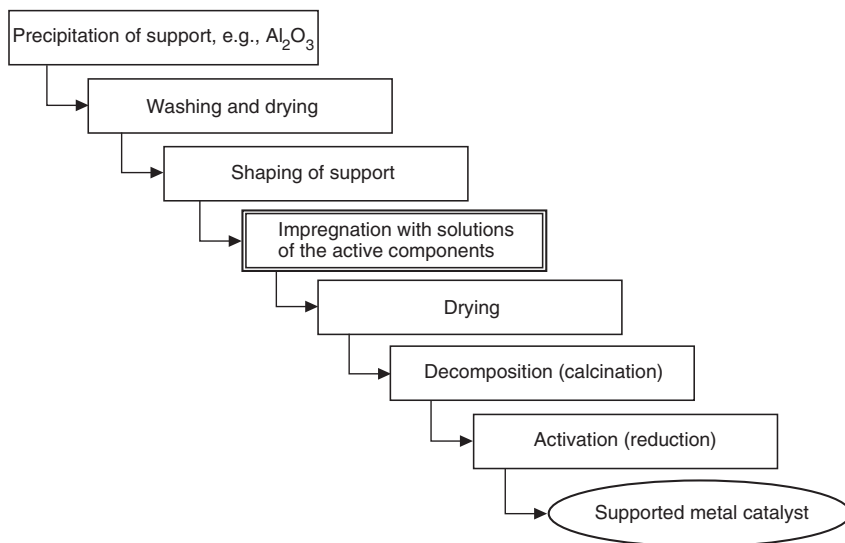
Highly homogeneous catalysts can be obtained by using mixed salts or mixed crystals as starting materials, since in this case the ions are already present in atomically distributed form. Readily decomposable anions such as formate, oxalate, or carbonate are advantageous here.

Examples:

- $\text{Cu}(\text{OH})\text{NH}_4\text{CrO}_4$ as a precursor for copper chromite (Adkins catalyst)
- $\text{Ni}_6\text{Al}_2(\text{OH})_{16}\text{CO}_3 \cdot 4\text{H}_2\text{O}$ decomposes to give a supported $\text{Ni}/\text{Al}_2\text{O}_3$ catalyst

One of the best known methods for producing catalysts is the impregnation of porous support materials with solutions of active components [9,10]. Especially catalysts with expensive active components such as noble metals are employed as supported catalysts. A widely used support is Al_2O_3 . After impregnation the catalyst particles are dried, and the metal salts are decomposed to the corresponding oxides by heating. The process is shown schematically in Scheme 6-2.

In the impregnation process, active components with thermally unstable anions (e.g., nitrates, acetates, carbonates, hydroxides) are used. The support is immersed



Scheme 6-2 Production of supported metal catalysts by impregnation

in a solution of the active component under precisely defined conditions (concentration, mixing, temperature, time). Depending on the production conditions, selective adsorption of the active component occurs on the surface or in the interior of the support. The result is nonuniform distribution.

To achieve the best possible impregnation, the air in the pores of the support is removed by evacuation, or the support is treated with gases such as CO_2 or NH_3 prior to impregnation. After impregnation, the catalyst is dried and calcined.

For large-scale manufacture the so-called incipient wetness impregnation (also called pore volume, or dry or capillary impregnation) is the most advantageous method. In this approach the support is brought into contact with a solution the volume of which corresponds to the total pore volume of the solid and which contains the appropriate amount of precursor compound. The principle of this method is shown in Figure 6-3.

If catalysts with high loadings of the active compounds are to be made, limited solubility of the precursor compound may cause problems, and multiple impregnations may have to be applied. With incipient wetness impregnation, even precursor compounds which do not interact with the support can be deposited when the solvent is removed during a subsequent drying procedure. This can be illustrated with Figure 6-4.

The rate of drying depends on the temperature and the gas throughput. From Figure 6-4 it can be seen that the rate of drying strongly affects the metal distribution of the catalyst particles.

There can be obtained catalysts with egg-yolk, egg-shell, and homogeneous metal distributions.

Calcination is heat treatment in an oxidizing atmosphere at a temperature slightly higher than the intended operating temperature of the catalyst. In calcina-

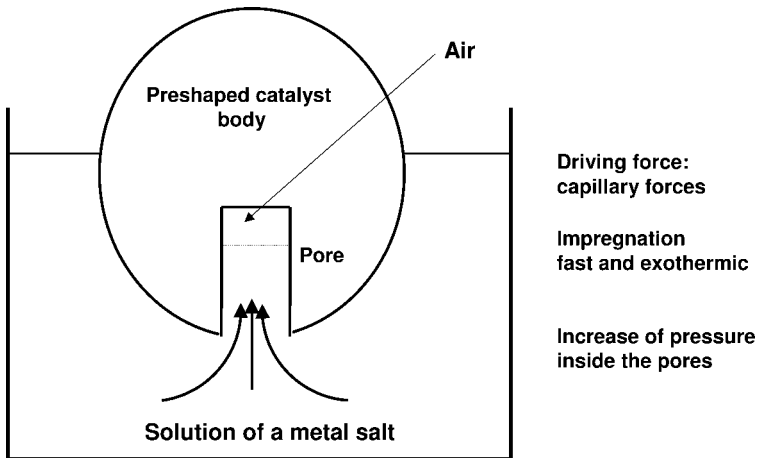


Fig. 6-3 Principle of catalyst preparation by incipient wetness impregnation

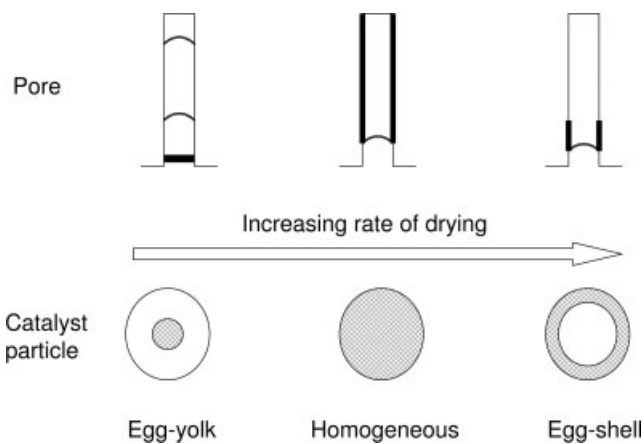


Fig. 6-4 Influence of the rate of drying on the profile of pores and particles

tion numerous processes can occur that alter the catalyst, such as formation of new components by solid-state reactions, transformation of amorphous regions into crystalline regions, and modification of the pore structure and the mechanical properties.

In the case of supported metal catalysts, calcination leads to metal oxides as catalyst precursors, and these must subsequently be reduced to the metals. This reduction can be performed with hydrogen (diluted with nitrogen), CO, or milder reducing agents such as alcohol vapor. In some cases reduction can be carried out in the production reactor prior to process start-up. Here temperature control is a problem.

Impregnated catalysts have many advantages compared to precipitated catalysts. Their pore structure and specific surface area are largely determined by the support. Since support materials are available in all desired ranges of surface area, porosity, shape, size, and mechanical stability, impregnated catalysts can be tailor-made with respect to mass transport properties [9].

In individual cases it is possible to achieve almost molecular distribution of the active components in the pores. As a rule, however, the active substance is distributed in the form of crystallites with a diameter of 2–200 nm. This fine distribution on the support not only ensures a particularly favorable surface to volume ratio and hence makes good use of the active components, some of which are expensive, it also reduces the risk of sintering.

In general, with increasing loading, catalyst activity eventually reaches a limiting value. Therefore, for economic reasons the catalyst loading is 0.05–0.5 % for noble metals, and 5–15 % for other metals. Examples of industrial impregnated catalysts are:

- Ethylene oxide catalysts in which a solution of a silver salt is applied to Al_2O_3
- Catalysts in the primary reformer of ammonia synthesis, with 10–20 % Ni on $\alpha\text{-Al}_2\text{O}_3$
- Catalysts for the synthesis of vinyl chloride from acetylene and HCl: HgCl_2 /activated carbon; HgCl_2 is applied from aqueous solution

Catalysts in which the active component is a finely divided metal are often pyrophoric. The catalyst can be better handled after surface oxidation of the active component (passivation). Reactivation is then carried out in the start-up phase under process conditions.

Shell catalysts consist of a compact inert support, usually in sphere or ring form, and a thin active shell that encloses it [4]. Since the active shell has a thickness of only 0.1–0.3 mm, the diffusion paths for the reactants are short. There are many heterogeneously catalyzed reactions in which it would be advantageous to eliminate the role of pore diffusion. This is particularly important in selective oxidation reactions, in which further reactions of intermediate products can drastically lower the selectivity. An example is acrolein synthesis: two catalysts with the same active mass but different shell thicknesses differed greatly in selectivity at the high conversions desired in industry (Fig. 6-5). Therefore, if acrolein synthesis is to be operated economically, the shell thickness must be optimized.

The best known method for producing shell catalysts is the controlled short-term immersion of strongly adsorbing support materials. A well-known example is the platinum shell catalyst, which can easily be prepared with low loading and a high degree of dispersion. The support is immersed in solution of hexachloroplatinic acid (H_2PtCl_6), and an outer layer of adsorbed PtCl_4^{2-} ions is formed. The adsorption of the hexachloroplatinic acid is so fast that diffusion of the solution into the pores is rate-determining. The treated catalyst particles are then dried without washing and calcined to generate the metal [T35]. Figure 6-6 shows how different impregnation techniques can be used to obtain supported catalysts with special distributions of the metal.

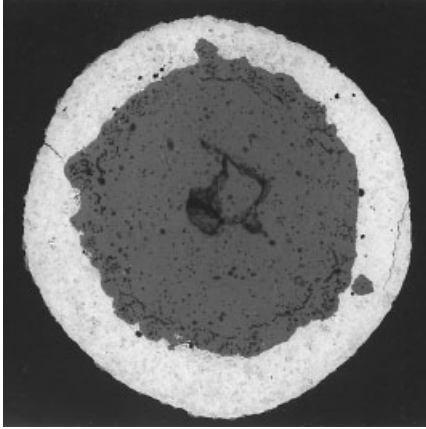


Fig. 6-5 Cross section of a shell catalyst (magnification $18\times$). Influence of the shell thickness on the selectivity of acrolein synthesis (BASF, Ludwigshafen, Germany):

| Shell thickness [μm] | 150 | 400 |
|-----------------------------------|-----|-----|
| Selectivity [%] at 99% conversion | 89 | 82 |

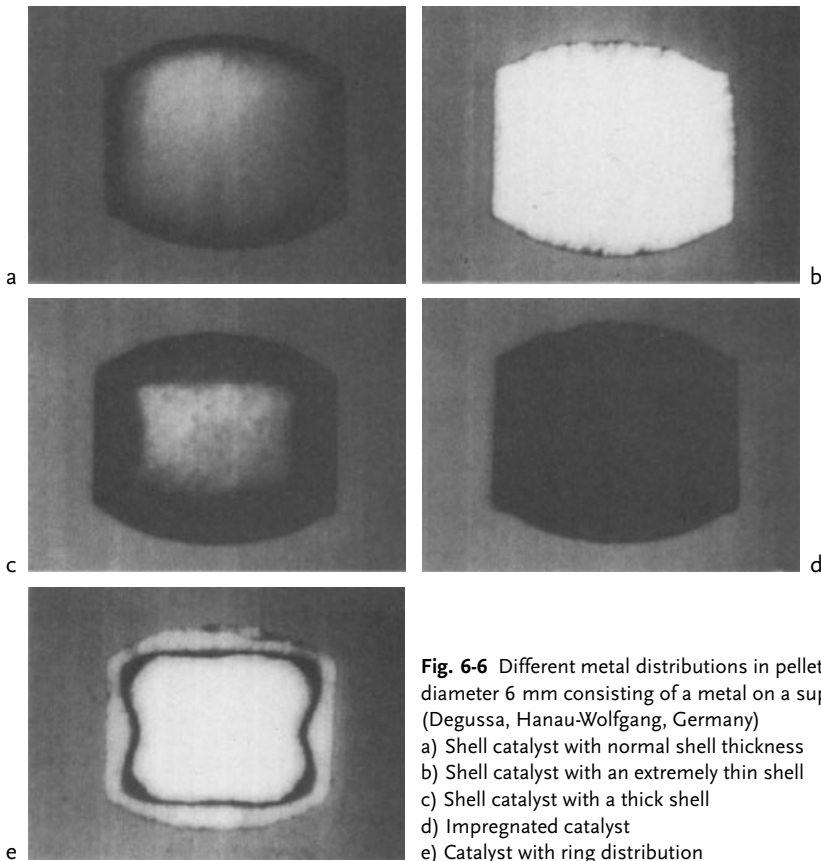


Fig. 6-6 Different metal distributions in pellets of diameter 6 mm consisting of a metal on a support (Degussa, Hanau-Wolfgang, Germany)

- a) Shell catalyst with normal shell thickness
- b) Shell catalyst with an extremely thin shell
- c) Shell catalyst with a thick shell
- d) Impregnated catalyst
- e) Catalyst with ring distribution

The advantages of shell catalysts are short transport or diffusion paths, a pore structure independent of the support, and better heat transport in the catalyst layer. Examples of industrial applications of shell catalysts are:

- Selective oxidation reactions, e.g., production of acrolein from propene and of phthalic anhydride from *o*-xylene
- Purification of automobile exhaust gases
- Selective oxidation of benzene to maleic anhydride: vanadium molybdenum oxide on fused corundum (catalytically inactive support without pores)
- Autothermal decomposition of liquid hydrocarbons on NiO/ α -Al₂O₃ shell catalysts (high selectivity for lower alkenes [4])

In this chapter we have seen how the different steps of catalyst production can affect the functional properties of catalysts, such as activity and selectivity, and their morphology (Fig. 6-7).

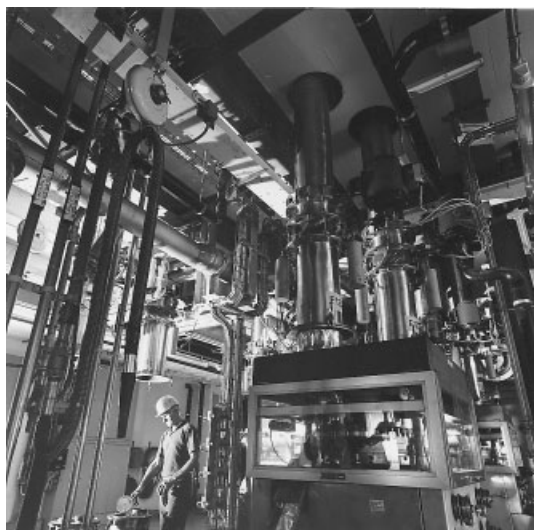


Fig. 6-7 Modern catalyst production plant (BASF, Ludwigshafen, Germany)

Because of the numerous influencing parameters, prediction of the catalytic properties is not possible. They can only be determined by measurement of the reaction kinetics. This makes it clear why catalyst production is based on special company know-how and that not all details are publicized.

6.2 Immobilization of Homogeneous Catalysts

As we have seen in Chapter 3, the industrial use of homogeneous catalysts often leads to problems with catalyst separation and recycling, recovery of the often valuable metal, and short catalyst lifetimes. Therefore, in the last twenty years or so, extensive studies have been carried out on the development of heterogenized homogeneous catalysts, which are intended to combine the advantages of homogeneous catalysts, in particular high selectivity and activity, with those of heterogeneous catalysts (ease of separation and metal recovery). Hence attempts are made to convert organometallic complex catalysts to a form that is insoluble in the reaction medium. This is generally achieved by anchoring a suitable molecule on an organic or inorganic polymer support.

In the following, we will discuss such methods for obtaining immobilized homogeneous catalysts, which are also known as fixed catalysts or hybrid catalysts, and the potential applications of this interesting class of catalysts [3]. To come to the most important point first: the ideal immobilized metal complex for industrial applications has not yet been found, as is shown by weighing up the advantages and disadvantages of this type of catalyst.

Advantages:

- 1) Separation and recovery of the catalyst from the product stream is straightforward. This is the main advantage of heterogenization.
- 2) Multifunctional catalysts can be obtained in which more than one active component is bound to a carrier.
- 3) Highly reactive, coordinatively unsaturated species that can not exist in solution can be stabilized by heterogenization.

Disadvantages:

- 1) The immobilized homogeneous catalysts are not sufficiently stable. The valuable metal is continuously leached and carried away with the product stream.
- 2) The problems of homogeneous catalysts, such as corrosion, catalyst recovery, and catalyst recycling, have so far not been satisfactorily solved.
- 3) Lower catalytic activity than homogeneous catalysts because of: poor accessibility of the active sites for the substrate, steric effects of the matrix, incompatibility of solvent and polymer, deactivation of active centers.
- 4) Inhomogeneity due to different linkages between support matrix and complex.

Particularly intensive investigations have been carried out on catalysts for reactions with CO or alkenes. These reactions, which are typical transition metal catalyzed conversions, provide the best possibility for assessing the properties of heterogenized catalysts. Examples are given in the following overview (Table 6-1). All the examples show that the reaction mechanisms with homogeneous and heterogeneous catalysis are in many respects similar. However, care must be taken in

comparing soluble and matrix-bound catalysts, since the matrix can be regarded as a ligand. Thus at least one coordination site of the complex catalyst is no longer available for the catalytic cycle. It is difficult to find the corresponding ligands required for a comparison. For example, a monodentate phosphine ligand like PPh_3 is not directly comparable to a polystyrene matrix with phosphine groups. For meaningful comparisons, the less common multidentate ligands must be used in solution.

Table 6-1. Comparison of homogeneous and heterogenized catalysts in industrial reactions

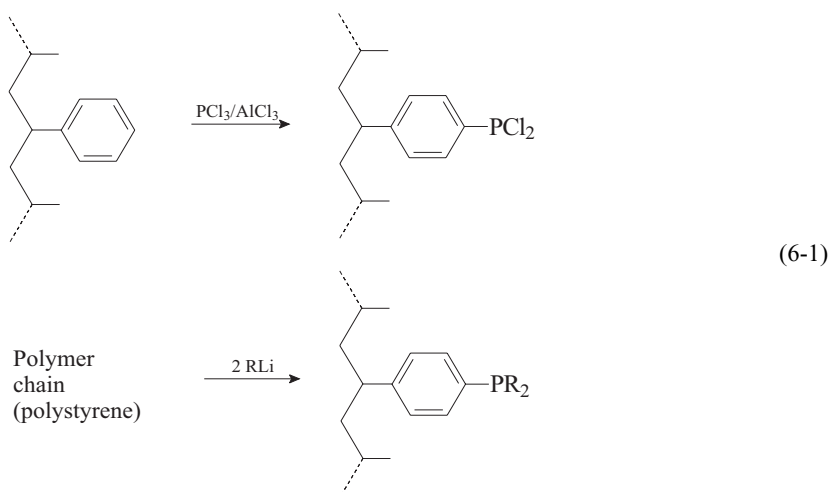
| Reaction | Homogeneous catalyst | Heterogenized catalyst |
|---|--|--|
| Hydroformylation of olefins (oxo synthesis) | Co or Rh complex | Co or Rh complex on polymer or SiO_2 support matrix |
| Oxidation of olefins (Wacker process) | $[\text{PdCl}_4]^{2-}$ | PdCl_2 on support matrix |
| Carbonylation of methanol to acetic acid | $[\text{Rh}(\text{CO})_2\text{I}_2]^- + \text{HI}$ | " RhCl_3 " on activated carbon or $[\text{RhCl}(\text{CO})\text{PR}_n]$ on modified polystyrene |
| Hydrogenation of olefins | $[\text{Rh}(\text{PPh}_3)_3\text{Cl}]$ | $[\text{Rh}(\text{PPh}_3)_n\text{Cl}]$ on polymer support |

There are four basic ways of fixing transition metal complexes on a matrix:

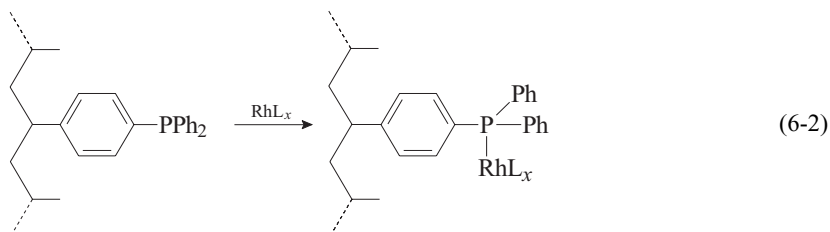
- 1) Chemical bonding on inorganic or organic supports
- 2) Production of highly dispersed supported metal catalysts
- 3) Physisorption on the surface of oxidic supports (supported solid phase catalysts, SSPC)
- 4) Dissolution in a high-boiling liquid that is adsorbed on a porous support (supported liquid phase catalysts, SLPC)

The immobilization of organometallic complexes on inorganic or organic supports is the most widely used method. Basically the supports act as high molecular mass ligands and are obtained by controlled synthesis. The bonding can be ionic or coordinative. The main aim of the process is to bind the complexes on the solid surface in such a manner that its chemical structure is retained as far as possible. A common method is the replacement of a ligand by a bond to the surface of the solid matrix. This means that a reactive group must be incorporated in the surface during production of the support.

Numerous polymer syntheses and organometallic syntheses are available for the construction of functionalized supports; Equation 6-1 gives just one example.

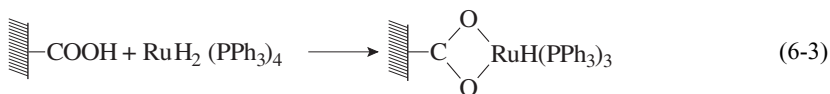


Here triphenylphosphine, the most important ligand in organometallic catalysis, is coupled to the benzene rings of cross-linked polystyrene. An anchored catalyst is then formed by coordination of the phosphine group to the metal center of a rhodium complex (Eq. 6-2).



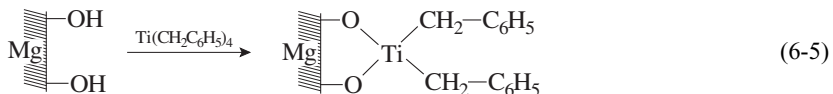
The degree of swelling of this copolymer in organic solvents is controlled by means of the amount of divinylbenzene. Hard copolymers of this type take up metal complexes only on the surface. The physical properties of the support can be varied by means of the polymerization method; the metal loading can also be controlled well.

There are many reactions available for applying the organometallic complexes to the surface. Two examples are shown in Equations 6-3 and 6-4.

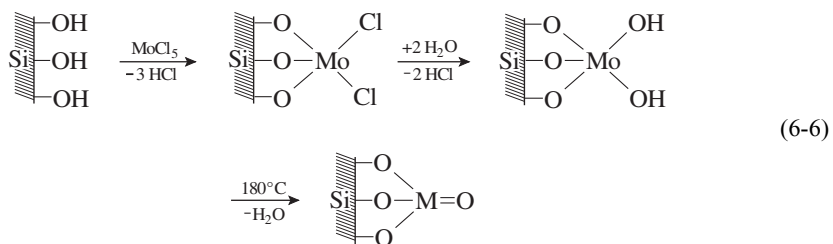


Disadvantages of the organic polymer supports are low mechanical durability (e. g., in stirred tank reactors), poor heat-transfer properties, and limited thermal stability (up to max. 150 °C).

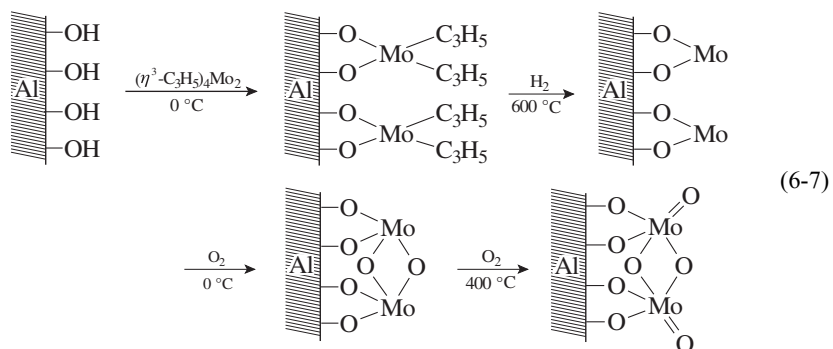
There are also several methods available for producing inorganic supports. Here we will discuss a few basic methods. The most important method is the reaction of inorganic supports having surface hydroxyl groups with metal alkyls (Eq. 6-5).



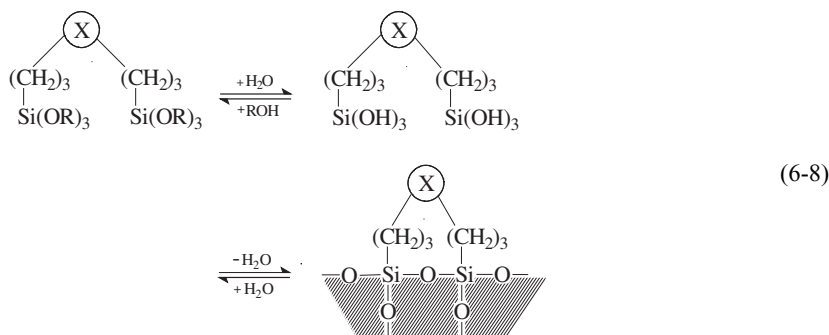
Alkoxides and halides can also be attached to surfaces. Subsequent hydrolysis and dehydration lead to terminal metal oxo structures (Eq. 6-6).



Such immobilized molybdenum oxide catalysts are active in selective oxidation reactions. For example, methanol can be oxidized with air to methyl formate at ca. 500 K with 90–95 % selectivity [T22]. The catalyst obtained from γ - Al_2O_3 and tetrakis(η^3 -allyl)dimolybdenum (Eq. 6-7) is considerably more active in ethylene hydrogenation and olefin metathesis than the catalysts prepared by conventional fixation of $[\text{Mo}(\text{CO})_6]$ followed by calcination.



Organofunctional polysiloxanes are a versatile group of catalysts developed by the company Degussa [13]. These are solids with a silicate framework obtained by hydrolysis and polycondensation of organosilicon compounds (Eq. 6-8).



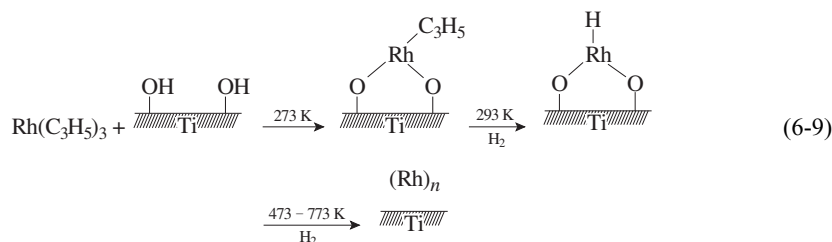
X = functional group: sulfane, phosphine, amine

This class of substances is characterized by broad chemical modifiability, a high capacity for functional groups, high temperature and ageing resistance, and insolubility in water and organic solvents. The heterogenized organopolysiloxane catalysts are marketed as abrasion-resistant spheres of various particle sizes. In particular the phosphine complexes of Ru, Pd, Ir, and Pt are interesting catalysts for hydrogenation, hydroformylation, carbonylation, and hydrosilylation

6.2.1

Highly Dispersed Supported Metal Catalysts [T22]

This method is used to obtain a very fine distribution of metal on a support by decomposition of organometallic compounds (so-called grafted catalysts). For example, by treating TiO_2 with η^3 -allyl complexes of rhodium followed by decomposition, highly active hydrogenation and hydrogenolysis catalysts are obtained (Eq. 6-9). Similar catalysts based on polysiloxanes are produced by Degussa; Pd, Rh, and Pt systems are available.



$(\text{Rh})_n$ = small aggregates of 25 or more Rh atoms with particle diameters of ca. 1.4 nm

6.2.2

SSP Catalysts [6, 11]

In this group of catalysts, organometallic complexes are anchored on the inner surface of porous supports, mainly by physisorption. These catalysts can be used as catalyst beds through which the reaction medium flows. For example, the complex

$[\text{Rh}(\eta^3\text{-C}_3\text{H}_5)(\text{CO})(\text{PPh}_3)_2]$ is adsorbed on $\gamma\text{-Al}_2\text{O}_3$ and used as a hydrogenation catalyst. The fixed complexes often exhibit considerably lower activity and selectivity than in the homogeneous phase, and this limits their range of applications. The SLP catalysts are a better alternative.

6.2.3

SLP Catalysts [11, 15]

In this process a solution of the complex in a high-boiling solvent spreads out on the inner surface of a porous support, which generally consists of an inorganic material such as silica gel or chromosorb. The reaction takes place in the liquid film, which the starting materials reach by diffusion. The products are also transported away by diffusion out of the film, which is retained on the support.

The use of SLP catalysts is generally restricted to the synthesis of low-boiling compounds. Oxo synthesis with SLP catalysts has been the subject of much interest. An example is the hydroformylation of propene with $[\text{RhH}(\text{CO})(\text{PPh}_3)_3]$ in liquid triphenylphosphine on $\gamma\text{-Al}_2\text{O}_3$. The starting material and the C_4 aldehyde are present in the gas phase. In a pilot plant at DSM, low selectivity was found and diffusion problems were encountered. Further examples are the oxidation of ethylene to acetaldehyde with aqueous solutions of PdCl_2 and CuCl_2 on kieselguhr, and the oxychlorination of alkenes with a $\text{CuCl}_2/\text{CuCl}/\text{KCl}/\text{rare earth halide}$ melt on silica gel [T22].

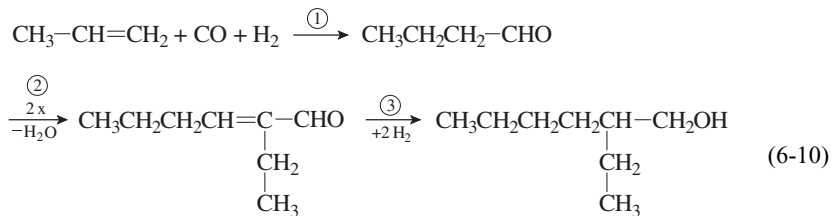
From these examples, most of which are based on laboratory investigations, it becomes clear that heterogenization is not a general method for solving problems in catalysis. It is, however, an interesting addition to the spectrum of catalytic methods.

Finally we shall discuss some examples in which heterogenized catalysts have been successfully used in industrial processes.

Chromium complexes on the basis of chromocene or chromium salts on SiO_2 are used for the polymerization of α -olefins and for the production of linear polyethylene in the Phillips process. The structure of the active surface species is unknown.

Heterogenized titanium complexes are used for the polymerization of propylene and give high yields of isotactic polypropylene [T31].

Another example for the use of a multifunctional solid catalyst is the Aldox process for the production of 2-ethylhexanol (Eq. 6-10).



In industry the hydroformylation (reaction 1) is catalyzed by Rh or Co complexes in solution. The aldol condensation (reaction 2) is acid or base catalyzed, and the hydrogenation of the unsaturated aldehyde (reaction 3) is catalyzed by metals such

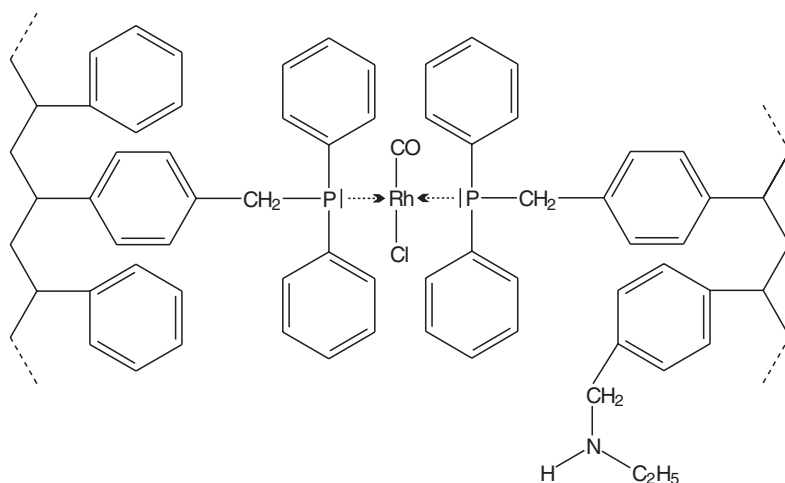


Fig. 6-8 Multifunctional, polymer-fixed solid catalyst for the Aldox process [16]

as nickel. On this basis a catalyst with a metal function (Rh) and a base function (amine) was developed (Fig. 6-8), and is active for the formation of 2-ethylhexanol. The rhodium center catalyzes the hydroformylation and the partial hydrogenation of the aldol product, in which the aldehyde group is retained, while the amino group catalyzes the aldol condensation [16].

These examples show that the area of heterogenization of catalysts represents an enormous potential for research. Some of these catalysts show high activities under mild conditions with interesting and sometimes unexpected selectivities. The processes for the production of these catalysts, the investigation of their precise structures, and the elucidation of their reaction mechanisms are still at an early stage.

It would seem that the use of heterogenized catalysts is best suited to small molecules (oxidation, hydrogenation), and that inorganic supports are more promising than organic supports. The field of heterogenization has led to a closer approach between heterogeneous and homogeneous catalysis.

► Exercises for Chapter 6

Exercise 6.1

Which are the main physical properties of a catalyst that are influenced by the production conditions?

Exercise 6.2

What are the advantages of impregnated catalysts compared with precipitated catalysts?

Exercise 6.3

Name porous supports with which impregnated catalysts can be manufactured.

Exercise 6.4

Which two types of support are preferentially used for oxidation catalysts?

Exercise 6.5

For which reactions are supported catalysts impregnated near the surface particularly suitable?

Exercise 6.6

- Why do monolith and honeycomb catalysts have to be coated before they are loaded with catalyst?
- What is this initial coating called?

Exercise 6.7

- What are the advantages of shell catalysts compared to bulk catalysts?
- What is the preferred support material for shell catalysts?

Exercise 6.8

Why have numerous dinuclear and multinuclear metal complexes (clusters) been tested in the synthesis of glycol from CO/H₂?

Exercise 6.9

What are the advantages of heterogenized metal catalysts compared to conventional heterogeneous catalysts?

Exercise 6.10

A phosphine-modified plastic matrix is treated with iron pentacarbonyl. What reaction can be expected?

**Exercise 6.11**

What are the disadvantages of organic polymer supports for the production of immobilized homogeneous catalysts?

Exercise 6.12

How are SLP catalysts produced?

7

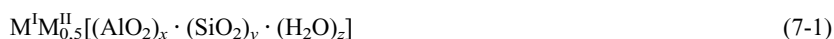
Shape-Selective Catalysis: Zeolites

7.1

Composition and Structure of Zeolites [5, 6]

Zeolites are water-containing crystalline aluminosilicates of natural or synthetic origin with highly ordered structures. They consist of SiO_4 and AlO_4^- tetrahedra, which are interlinked through common oxygen atoms to give a three-dimensional network through which long channels run.

In the interior of these channels, which are characteristic of zeolites, are water molecules and mobile alkali metal ions, which can be exchanged with other cations. These compensate for the excess negative charge in the anionic framework resulting from the aluminum content. The interior of the pore system, with its atomic-scale dimensions, is the catalytically active surface of the zeolites. The inner pore structure depends on the composition, the zeolite type, and the cations. The general formula of zeolites is



where M^{I} and M^{II} are preferentially alkali and alkaline earth metals. The indices x and y denote the oxide variables, and z is the number of molecules of water of hydration. The composition is characterized by the Si/Al atomic ratio or by the molar ratio M

$$M = \frac{\text{SiO}_2}{\text{Al}_2\text{O}_3} \quad (7-2)$$

and the pore size of zeolites by the type (A, X, Y).

Zeolites are mainly distinguished according to the geometry of the cavities and channels formed by the rigid framework of SiO_4 and AlO_4^- tetrahedra. The tetrahedra are the smallest structural units into which zeolites can be divided. Linking these primary building units together leads to 16 possible secondary building blocks (polygons), the interconnection of which produces hollow three-dimensional structures.

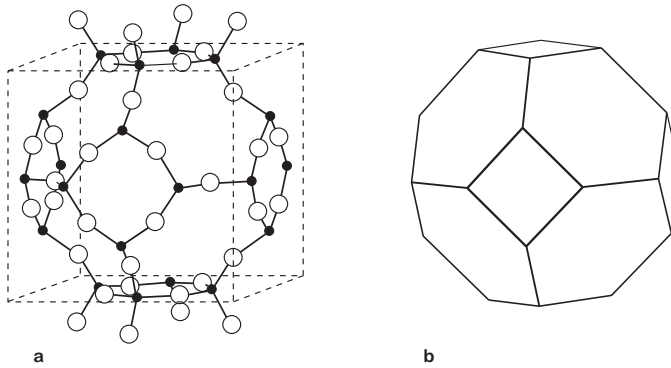


Fig. 7-1 Truncated octahedra as structural units of zeolites
 a) Sodalite cage (β -cage)
 b) Sodalite cage (schematic)

The entrances to the cavities of the zeolites are formed by 6-, 8-, 10-, and 12-ring apertures (small-, medium-, and widepore zeolites). A series of zeolites is composed of polyhedra as tertiary building units. These include truncated octahedra (sodalite or β -cage, Fig. 7-1), composed of 4- and 6-rings, which can be connected in various manners to give the fundamental zeolite structures. The sodalite cage, which consists of 24 tetrahedra, is generally depicted schematically as a polygon, generated by connecting the centers of neighboring tetrahedra with a line. Each vertex of this polyhedron then represents a silicon or aluminum atom, and the midpoint of each edge, an oxygen atom.

The structure of zeolite A, a narrow-pore zeolite, is formed by linking the square faces of the polyhedra via intermediate cubic units (Fig. 7-2). The cavity formed by linking eight truncated octahedra is known as the α -cage (Fig. 7-2). It is larger than the β -cage. The wide-pored zeolite Y (faujasite) is formed when the truncated octahedra are linked together by hexagonal prisms. The resulting cavity is larger than the α -cage of zeolite A (Fig. 7-3).

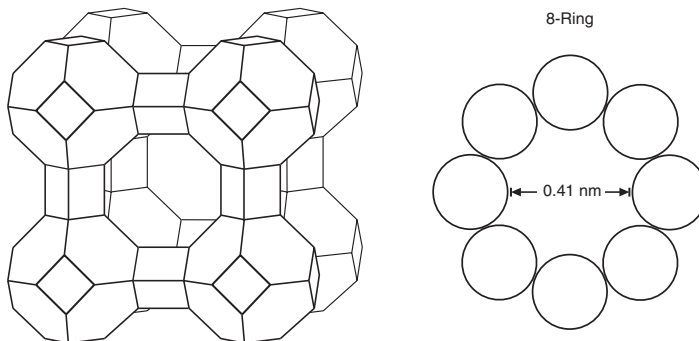


Fig. 7-2 Framework structure of zeolite A with α -cage

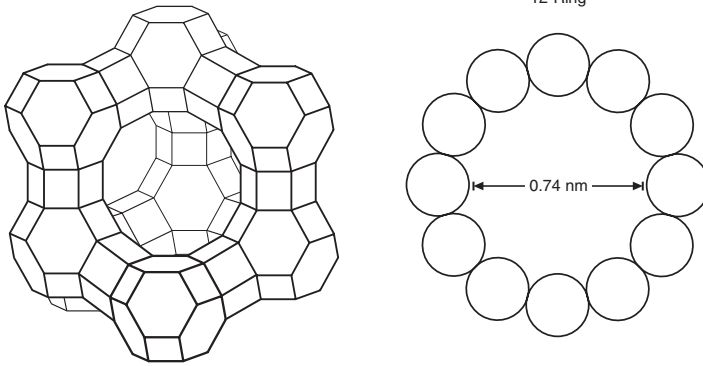


Fig. 7-3 Y zeolite (faujasite)

Representatives of the medium-pore zeolites are the so-called pentasils, which belong to the silicon-rich zeolites. In contrast to the structures described above, their polyhedra are composed of 5-rings as secondary building units. These so-called 5-1 units are structurally analogous to methycyclopentane. Linking of the resulting chains gives a two-dimensional pore system in which linear or zig-zag channels are intersected by perpendicular linear channels (Fig. 7-4). An advantage of these zeo-

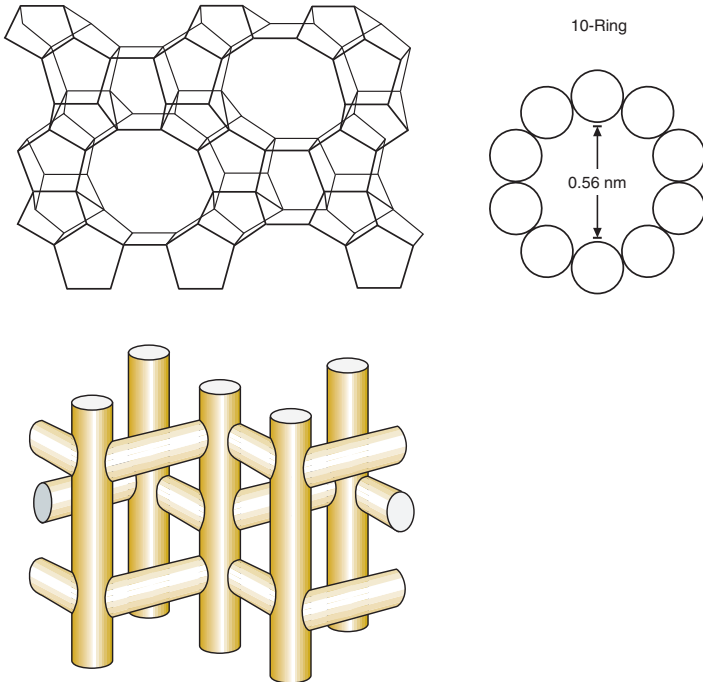


Fig. 7-4 Pentasil zeolite with channel structure

Table 7-1. Characteristics of important zeolites

| Type | Pore diameter [nm] | Pore aperture |
|-----------------------|--------------------|---------------------|
| Zeolite Y (faujasite) | 0.74 | 12-ring |
| Pentasil zeolite | 0.55 × 0.56 | 10-ring (ellipsoid) |
| Zeolite A | 0.41 | 8-ring |
| Sodalite | 0.26 | 4-ring |

lites is the uniform channel structure, in contrast to the zeolites A and Y, in which the pore windows provide access to larger cavities. A well-known representative of this class of zeolites is ZSM-5 (from zeolite Socony Mobil no. 5).

Table 7-1 lists the most important synthetic zeolites.

7.2

Production of Zeolites [T32]

Zeolite syntheses start from alkaline aqueous mixtures of aluminum and silicon compounds. The reactions are sometimes carried out at atmospheric pressure but more often in a high-pressure autoclave. The controlled crystallization of a particular zeolite requires careful control of the concentration and stoichiometry of the reaction partners, the temperature, and the shearing energy of the stirrer. After mixing of the liquid phase and formation of a gel, a transition of the gel phase in to the liquid aqueous phase occurs, whereby crystalline zeolites are formed from the amorphous particles.

The silicon-rich pentasils are mainly synthesized in the presence of organic cations. Their open structures seem to be formed around hydrated cations or other cations such as NR_4^+ . In particular, templates such as tetrapropylammonium hydroxide are used, and are of decisive importance for the crystallization of the zeolite structures. The C, H, and N of the tertiary ammonium cation is removed in the subsequent calcination of the microcrystalline product.

Zeolite structures can also be modified after synthesis, the simplest being the exchange of extra-framework species. The Si/Al ratio can also be changed by dealumination procedures which involve steaming, acid treatment, and ammonium exchange. Other atoms, such as B, Ga, Fe and Ti can also be introduced into the zeolite framework. For example, the well-known oxidation catalyst TS1 is synthesized hydrothermally from, e.g., tetraethyl orthotitanate, tetraethyl orthosilicate (Si:Ti ratio is typically 30–50), tetrapropylammonium hydroxide, and water. The reaction is carried out at 160–180 °C, followed by calcination at 550 °C. Keeping the Si:Ti ratio high ensures that the Ti atoms occupy lattice sites with no near neighbour Ti atoms. This is a prerequisite for an active catalyst. The typical pore size is of the order of 0.55 nm, thus endowing the catalyst with shape selectivity, but thereby restricting its use to small substrates.

7.3 Catalytic Properties of the Zeolites [2–4]

In 1962 the zeolites were introduced by Mobil Oil Corporation as new cracking catalysts in refinery technology. They were characterized by higher activity and selectivity in cracking and hydrocracking. At the end of the 1960s, the concept of shape-selective catalysis with zeolites was introduced to petrochemistry (Selectoforming process), and the zeolites became of increasing importance in catalysis research and applied catalysis [6].

Since then chemists worldwide have prepared numerous “tailor-made” modified zeolites, and the synthetic potential for the production of organic intermediates and high-value fine chemicals is enormous. How can the success of this new class of catalysts in industry and academe be explained? It is due to the outstanding catalytic properties of the zeolites. No other class of catalysts offers so much potential for variation and so many advantages in application. Their advantages over conventional catalysts can be summarized as follows:

- Crystalline and therefore precisely defined arrangement of SiO_4 and AlO_4^- tetrahedra. This results in good reproducibility in production.
- Shape selectivity: only molecules that are smaller than the pore diameter of the zeolite undergo reaction.
- Controlled incorporation of acid centers in the intracrystalline surface is possible during synthesis and/or by subsequent ion exchange.
- Above 300°C pentasils and zeolite Y have acidities comparable to those of mineral acids.
- Catalytically active metal ions can be uniformly applied to the catalyst by ion exchange or impregnation. Subsequent reduction to the metal is also possible.
- Zeolite catalysts are thermally stable up to 600°C and can be regenerated by combustion of carbon deposits.
- They are well suited for carrying out reactions above 150°C , which is of particular interest for reactions whose thermodynamic equilibrium lies on the product side at high temperatures.

Let us first take a closer look at the most important properties of the zeolites:

- Shape selectivity
- Acidity

7.3.1 Shape Selectivity [1]

We have seen that the inner pore system of the zeolites represents a well-defined crystalline surface. The structure of the crystalline surface is predetermined by the composition and type of the zeolite and is clearly defined. Such conditions are otherwise found only with single-crystal surfaces.

The accessibility of the pores for molecules is subject to definite geometric or steric restrictions. The shape selectivity of zeolites is based on the interaction of re-

actants with the well-defined pore system. A distinction is made between three variants, which can, however, overlap:

- Reactant selectivity
- Product selectivity
- Restricted transition state selectivity

Figure 7-5 shows these schematically with examples of reactions.

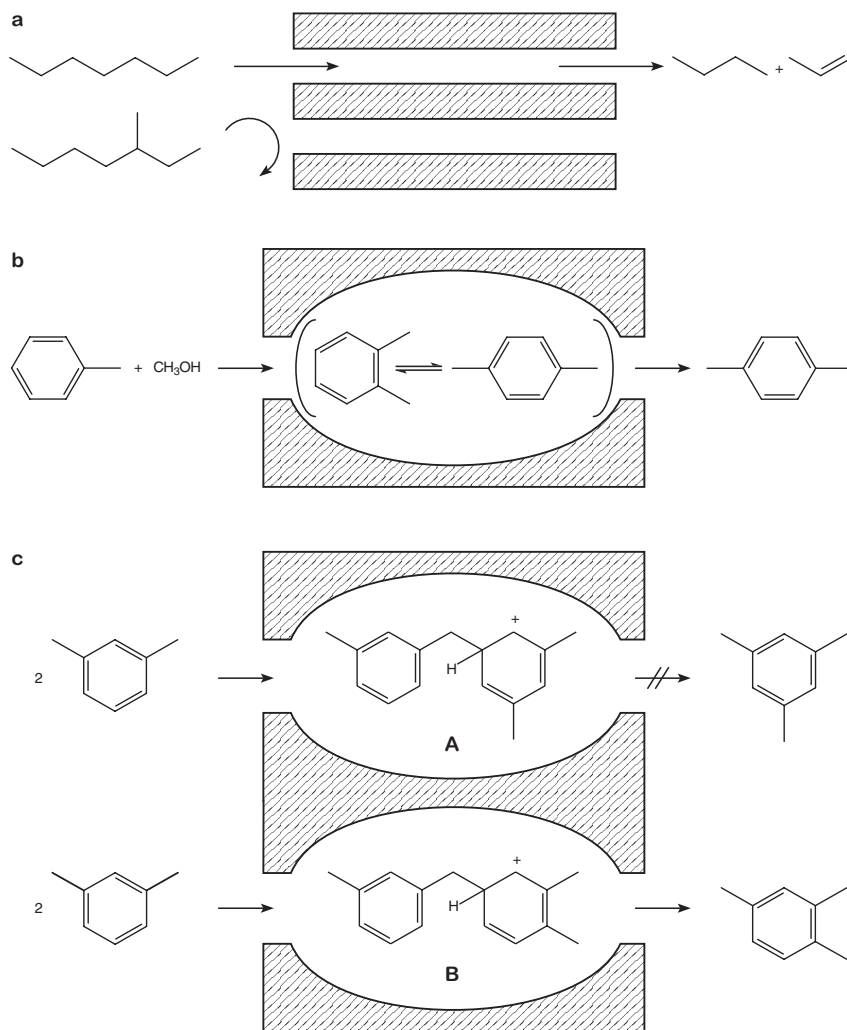


Fig. 7-5 Shape selectivity of zeolites with examples of reactions

- a) Reactant selectivity: cleavage of hydrocarbons
- b) Product selectivity: methylation of toluene
- c) Restricted transition state selectivity: disproportionation of *m*-xylene

7.3.1.1 Reactant Selectivity

Reactant selectivity means that only starting materials of a certain size and shape can penetrate into the interior of the zeolite pores and undergo reaction at the catalytically active sites. Starting material molecules that are larger than the pore apertures can not react (Fig. 7-5 a). Hence the term “molecular sieve” is justified.

Table 7-2 compares the pore apertures of some zeolites with the kinetic molecular diameters of some starting materials. On the basis of these data, a preliminary choice of a suitable zeolite for a particular starting material can be made. However, it should not be forgotten that molecules are not rigid objects and that the kinetic diameter gives only a rough estimate of the molecular size.

Table 7-2 Molecular diameters and pore sizes of zeolites [7, T32]

| Molecule | Kinetic diameter [nm] | Zeolite, pore size [nm] | |
|---|-----------------------|-------------------------|-------------------------|
| He | 0.25 | KA | 0.3 |
| NH ₃ | 0.26 | LiA | 0.40 |
| H ₂ O | 0.28 | NaA | 0.41 |
| N ₂ , SO ₂ | 0.36 | CaA | 0.50 |
| Propane | 0.43 | Erionite | 0.38 × 0.52 |
| <i>n</i> -Hexane | 0.49 | ZSM-5 | 0.54 × 0.56/0.51 × 0.55 |
| Isobutane | 0.50 | ZSM-12 | 0.57 × 0.69 |
| Benzene | 0.53 | CaX | 0.69 |
| <i>p</i> -Xylene | 0.57 | Mordenite | 0.67–0.70 |
| CCl ₄ | 0.59 | NaX | 0.74 |
| Cyclohexane | 0.62 | AlPO-5 | 0.80 |
| <i>o</i> -, <i>m</i> -Xylene | 0.63 | VPI-5 | 1.20 |
| Mesitylene | 0.77 | | |
| (C ₄ H ₉) ₃ N | 0.81 | | |

The catalytic characterization of zeolites is generally carried out with the aid of test reactions [8]. For example, the constraint index CI (Table 7-3) compares the relative rate of cracking of a 1 : 1 mixture of *n*-hexane (molecular diameter 0.49 nm) and 3-methylpentane (molecular diameter 0.56 nm).




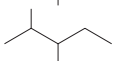
The CI is strongly dependent on the pore size of the zeolite. Small values between zero and two mean little or no shape selectivity (large-pore zeolites), values between two and 12 a medium selectivity (medium-pore zeolites), and values higher than 12 a high shape selectivity (small-pore zeolites).

Thus erionite, with the smallest pore opening of 0.38–0.52 nm, has the highest shape selectivity. It was found that with certain zeolites, the linear alkane *n*-hexane is cracked 40–100 times faster than the branched isomer 3-methylpentane. This is exploited industrially in the Selectoforming process, in which erionite is added to the reforming catalyst.

Table 7-3 Constraint index (CI) for some typical catalysts at 316 °C [T28]

| Zeolite | CI |
|--|-----|
| Aluminosilicate, amorphous (at 510 °C) | 0.6 |
| HY | 0.4 |
| H-Mordenite | 0.4 |
| ZSM-4 | 0.5 |
| ZSM-12 | 2.3 |
| Offretite | 3.7 |
| ZSM-5 | 8.3 |
| ZSM-11 | 8.7 |
| Erionite | 40 |

Table 7-4 Relative rate of cleavage of heptanes on H-ZSM-5 at 325 °C [T35]

| C ₇ Alkane | r _{rel} |
|---|------------------|
|  | 1.00 |
|  | 0.52 |
|  | 0.38 |
|  | 0.09 |

Especially ZSM-5 is used for shape-selective reactions. Numerous alkanes with various chain lengths and degrees of branching have been investigated.

The next example shows results for the cracking of heptane isomers over H-ZSM-5 (Table 7-4).

In this case, the critical diameters of the starting material molecules are equal to or slightly larger than the pore openings of the zeolite, but as a result of molecular vibrations under the reaction conditions, are able to enter the zeolite pores, where they react. Here the reactions are largely diffusion controlled.

In particular, the ability of ZSM-5 to cleave unbranched and monomethyl-branched alkanes with retention of more highly branched and cyclic isomers is exploited industrially in the dewaxing process to lower the solidification point of lubricants and in reforming processes to obtain high-octane gasolines (M Forming process) [3].

Another example of reactant selectivity is the dehydration of butanols. On CaA zeolites, the straight-chain alcohol, which fits in the zeolite pores, is much more rapidly dehydrated than isobutanol, which has a larger molecular diameter [T24]. In spite of the considerable molecular sieve effect, 100 % selectivity is often not at-

tained because the starting materials can also react to a small extent on the outer surface of the zeolite crystals.

7.3.1.2 Product Selectivity

Product selectivity arises when, corresponding to the cavity size of a zeolite, only products of a certain size and shape that can exit from the pore system are formed. Well-known examples of product selectivity are the methylation of toluene (Fig. 7-5b) and the disproportionation of toluene on ZSM-5.

In both reactions all three isomers *o*-, *m*-, and *p*-xylene are formed. The desired product *p*-xylene can be obtained with selectivities of over 90 %, although the thermodynamic equilibrium corresponds to a *p*-xylene fraction of only 24 %. This is explained by the fact that for the slimmer molecule *p*-xylene has a rate of diffusion that is faster by a factor of 10^4 than those of the other two isomers. These isomerize relatively rapidly in the zeolite cavity, and the *p*-xylene diffuses out of the cavity. The selectivity can be further influenced by, for example:

- Increasing the size of the zeolite crystals
- Incorporation of cations or other organic materials in the pore structure
- Closing some of the pore apertures

An industrial application is the Mobil Oil selective toluene disproportionation process (STDP) [T32].

Another example of product selectivity is the alkylation of toluene with ethylene to give ethyltoluene (Table 7-5). The comparison with the conventional Friedel–Crafts catalyst shows the clear advantages of the highly selective zeolite catalyst.

Table 7-5 Product distribution in the ethylation of toluene [T32]

| Ethyltoluene | Selectivity (%) Catalyst | |
|--------------|-----------------------------|-------|
| | AlCl ₃ /HCl | ZSM-5 |
| <i>p</i> - | 34.0 | 96.7 |
| <i>m</i> - | 55.1 | 3.3 |
| <i>o</i> - | 10.9 | 0 |

This form of shape selectivity can also have disadvantages. Large molecules that are unable to leave the pores can be converted to undesired side products or undergo coking, deactivating the catalyst.

7.3.1.3 Restricted Transition State Selectivity

This third form of shape selectivity depends on the fact that chemical reactions often proceed via intermediates. Owing to the pore system, only those intermediates that have a geometrical fit to the zeolite cavities can be formed during catalysis.

This selectivity occurs preferentially when both monomolecular and bimolecular rearrangements are possible. In practice, it is often difficult to distinguish restricted transition state selectivity from product selectivity.

An example is the disproportionation of *m*-xylene to toluene and trimethylbenzenes in the wide-pored zeolite Y (Fig. 7-5c). In the large zeolite cavity, bulky diphenylmethane carbenium ion transition states can be formed as precursors for methyl group rearrangement, whereby the less bulky carbenium ion **B** is favored. Thus the reaction product consists mainly of the unsymmetrical 1,2,4-trimethylbenzene rather than mesitylene (case **A**). In contrast, in ZSM-5, with its medium sized pores, monomolecular xylene isomerization dominates, and the above-mentioned disproportionation is not observed as a side reaction.

Restricted transition state selectivity is also of importance in the alkylation of benzene with ethylene to give ethylbenzene. High selectivities for ethylbenzene are achieved on H-ZSM-5 owing to suppression of side reactions. These high selectivities were also explained by the fact that the possible bimolecular disproportionation of ethylbenzene is suppressed.

H-ZSM-5 is also used as catalyst in the large-scale MTG (methanol to gasoline) process. The products are hydrocarbons, aromatics in the benzene range, and water. The reaction is based on the dehydration of methanol to dimethyl ether, followed by numerous reactions that proceed via carbenium ion intermediates. The largest molecules observed, e.g., durene (1,2,4,5-tetramethylbenzene), correspond to the high-boiling components of gasoline. The favorable product distribution in this process can be attributed to restricted transition state selectivity.

Restricted transition state selectivity also influences the cracking of alkenes. In the cracking of hexenes with H-ZSM-5, the following order of reactivity is observed:

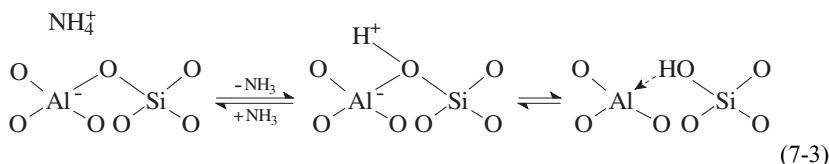


The sequence is exactly opposite to that of conventional acid catalysis: The reactants that are best able to form carbenium ions in solution are the least reactive with zeolite catalysis. The restricted transition state selectivity suppresses cracking of the more highly branched hydrocarbons in the cavities [T25].

7.3.2

Acidity of Zeolites [T24, T32]

In the last chapter we have already learnt of the importance of the hydrogen form of the zeolites (H-zeolites). Zeolites in the H form are solid acids whose acid strength can be varied over a wide range by modification of the zeolites (ion exchange, partial dealumination, and isomorphic substitution of the framework Al and Si atoms). Direct replacement of the alkali metal ions by protons by treatment with mineral acids is only possible in exceptional cases (e.g., mordenite and the high-silicon zeolite ZSM-5). The best method is exchange of the alkali metal ions by NH_4^+ ions, followed by heating the resulting ammonium salts to 500–600 °C (deammonization; Eq. 7-3).



Infrared investigations have shown that the protons are mainly bound as silanol groups but have a strongly acidic character due to the strongly polarizing influence of the coordinatively unsaturated aluminum center. Brønsted acid centers are generally the catalytically active sites of H-zeolites.

Weak to moderately strong acid sites can be generated in zeolites by ion exchange with multivalent cations. Owing to the polarizing effect of the metal cations, water is dissociatively adsorbed, and the equilibrium of Equation 7-4 is established.



The following order of Brønsted acidity is given for cation-exchanged zeolites:

H form \gg La form $>$ Mg form $>$ Ca form $>$ Sr form $>$ Ba form

The influence of the exchanged ions is considerable, as shown by the example of cumene dealkylation on faujasite (Table 7-6). Reasons for the large differences in reactivity are the different charges on the ions, and the decreasing ionic radii from Na^+ to H^+ and the associated polarizing power of the ions.

Table 7-6 Effect of the metal ion in faujasite on the dealkylation of cumene [T35]

| Cation | Relative activity |
|--------------------------------------|-------------------|
| Na^+ | 1.0 |
| Ba^{2+} | 2.5 |
| Sr^{2+} | 20 |
| Ca^{2+} | 50 |
| Mg^{2+} | 1.0×10^2 |
| Ni^{2+} | 1.1×10^3 |
| La^{3+} | 9.0×10^3 |
| H^+ | 8.5×10^3 |
| ----- | |
| $\text{SiO}_2/\text{Al}_2\text{O}_3$ | 1.0 |

The incorporation of transition metal ions into zeolites leads to interesting bifunctional catalysts in which metal and acid centers can act simultaneously.

Another major influence on the acidity of zeolites is the Si/Al ratio. The zeolites can be classified according to increasing Si/Al ratio and the associated acid/base properties (Table 7-7).

Table 7-7 Classification of acidic zeolites according to increasing Si/Al ratio [T24]

| Si/Al ratio | Zeolite | Acid/base properties |
|----------------------------|---|--|
| Low (1–1.5) | A, X | relatively low stability of lattice; low stability in acids; high stability in bases; high concentration of acid groups of medium strength |
| Medium (2–5) | erionite chabazite chinoptilolite mordenite Y | |
| High (ca. 10 to ∞) | ZSM-5; dealuminated erionite, mordenite Y | relatively high stability of the lattice; high stability in acids; low stability in bases; low concentration of acid groups of high strength |

Since the ion-exchange capacity corresponds to the Al^{3+} content of the zeolites, those with lower Si/Al ratios have higher concentrations of active centers.

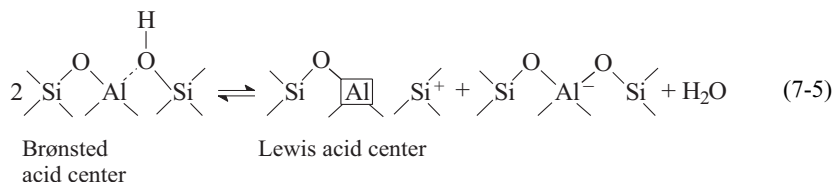
Zeolites with high concentrations of protons are hydrophilic and have high affinities for small molecules that can enter the pores. Zeolites with low H^+ concentrations, such as silicalite, are hydrophobic and can take up organic components (e.g., ethanol) from aqueous solution. The boundary lies at a Si/Al ratio of around 10.

The stability of the crystal lattice also increases with increasing Si/Al ratio. The decomposition temperatures of zeolites are in the range 700–1300 °C. Zeolites of low aluminum content are produced by dealumination with a reagent such as SiCl_4 , which removes aluminum from the framework with formation of AlCl_3 . Zeolite Y, which is produced by this method or by hydrothermal treatment with steam at 600–900 °C, is regarded as ultrastable and is employed in cracking catalysts.

The highest proton-donor strengths are exhibited by zeolites with the lowest concentrations of AlO_4^- tetrahedra such as H-ZSM-5 and the ultrastable zeolite HY. These are superacids, which at high temperatures (ca. 500 °C) can even protonate alkanes. It was found that the acid strength depends on the number of Al atoms that are adjacent to a silanol group. Since the Al distribution is nonuniform, a wide range of acid strengths results.

The nonuniform distribution of the proton-active centers in zeolites can be measured by temperature-controlled desorption of adsorbed organic bases. The bases that are adsorbed on the centers of highest activity require the highest temperature for desorption. The IR spectra of adsorbed bases such as ammonia and pyridine give information about the nature of the adsorption centers. For example, the pyridinium ion is indicative of proton-donor sites. NMR and ESR spectroscopy are also useful for elucidating the nature of acid centers.

When an H-zeolite is heated to high temperature, water is driven off and coordinatively unsaturated Al^{3+} ions are formed. These are Lewis acids (Eq. 7-5).



Bases like pyridine are more strongly bound to such Lewis acid centers than to Brønsted acid centers, as can be shown by IR spectroscopy and temperature-controlled desorption. Figure 7-6 shows the transformation of Brønsted into Lewis acid centers on calcination of an HY zeolite, monitored by IR spectroscopic measurements on the adsorption of pyridine.

As catalysts, zeolites combine the advantages of high density of catalytically active centers with high thermal stability. Practically all reactions that are catalyzed by acids in solution or by acidic ion exchangers are also catalyzed by acid zeolites. Hundreds of examples are known. However, there are differences to conventional acid–base reactions, as we shall see below.

A simple example is the cracking of alkanes by zeolites with a low density of acid groups. H-ZSM-5 can be regarded as an “ideal solution” of acidic groups, since they are too far apart to influence one another. At low Al contents (up to 4% Al_2O_3) there is a direct relationship between the catalytic activity in the cracking of *n*-hexane and

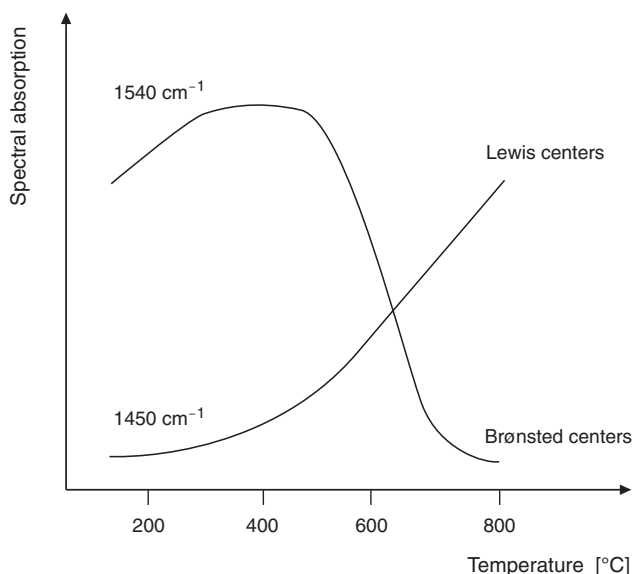


Fig. 7-6 Calcination of an HY zeolite: equilibrium between Brønsted and Lewis acid centers [9]

the concentration of Al^{3+} ions in the zeolite, which can be measured by Al NMR spectroscopy. Since each acidic group has a neighboring AlO_4^- tetrahedron, the activity is proportional to the aluminum concentration [T24].

In contrast, in the cracking of *n*-octane on H-mordenite, maximum catalytic activity occurs at a $\text{SiO}_2/\text{Al}_2\text{O}_3$ ratio of about 20. How can this finding be explained? On dealumination, the number of acidic centers decreases, but the acidity of the remaining centers increases up to a degree of dealumination of ca. 50 %. The opposite effects of the concentration of acid centers and their acid strength are superimposed, so that maximum reactivity is reached at a certain $\text{SiO}_2/\text{Al}_2\text{O}_3$ ratio.

The next example is the ethylation of the aromatic compounds benzene and phenol. With normal acid catalysis in solution, ethylene reacts with phenol more rapidly than with benzene, since the more electron-rich ring in phenol more readily undergoes electrophilic attack by the ethyl cation. In zeolites, however, the situation is reversed, and benzene reacts faster than phenol. This has been explained in terms of competitive adsorption. First, the ethylene must be protonated (Eq. 7-6).



The carbenium ion is “solvated” by the polar, anionic environment of the zeolite pore. The highly reactive carbenium ion can alkylate an aromatic molecule from the surrounding medium. However, if phenol is present in the zeolite pore, then a competing reaction occurs with the less polar olefin at the acid sites. Adsorption of phenol (Eq. 7-7) is favored.



This leads to blocking of the catalytically active centers. However, above 200 °C the influence of phenol adsorption is weaker, some ethylene can be adsorbed, and partial alkylation of phenol is observed [T24].

The composition and therefore the catalytic properties of zeolites can also be influenced by modification of the zeolites. In the following we shall discuss two modification processes in more detail: isomorphic substitution and doping with metals.

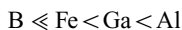
7.4

Isomorphic Substitution of Zeolites [T24, T32]

The isomorphic substitution of the tetrahedral centers of the zeolite framework is another possibility for producing new catalysts. A prerequisite is that the ions have a coordination number of four with respect to oxygen and an ionic radius corresponding to the zeolite framework.

The Al centers can be replaced by trivalent atoms such as B, Fe, Cr, Sb, As, and Ga, and the Si centers by tetravalent atoms such as Ge, Ti, Zr and Hf. Silicon enrichment up to a pure SiO_2 pentasil zeolite (silicalite) is also possible [4].

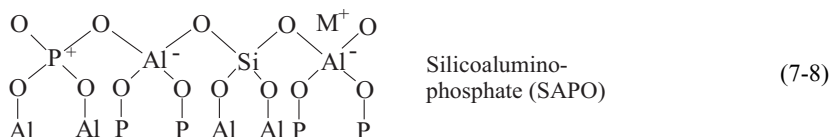
Isomorphous substitution affects zeolite properties such as shape selectivity (influences on the framework parameters), acidity, and the dispersion of introduced components. The following sequence was found for the acidity of ZSM-5 zeolites:



Thus the weakly Brønsted acidic boron zeolites allow acid-catalyzed reactions to be carried out with high selectivity. Gallium substitution gives effective, sulfur-resistant catalysts for the synthesis of aromatics from lower alkanes, without the need for noble metal doping [8]. The nonacidic titanium silicalite exhibits very interesting properties in selective oxidation reactions with H_2O_2 [T32].

In addition, a completely new class of zeolite-like materials has been synthesized from Al and P compounds, namely the aluminophosphate (AlPO_4) molecular sieves. In contrast to the zeolites, the frameworks of the aluminophosphates are electrically neutral, contain no exchangeable ions and are largely catalytically inactive.

In 1988 Davis succeeded in preparing an aluminophosphate with a pore aperture of 1.2 nm: VPI-5 (Virginia Polytechnical Institute no. 5) is the molecular sieve with the largest pore width known up to now [6]. Many possibilities exist for modifying aluminophosphates. Replacing part of the framework P atoms by Si gives the silicoaluminophosphates, which have catalytic properties. Various metals have been introduced into both classes of materials, as shown in the following formula (Eq. 7-8). The catalytic properties of these compounds have barely been explored [7].

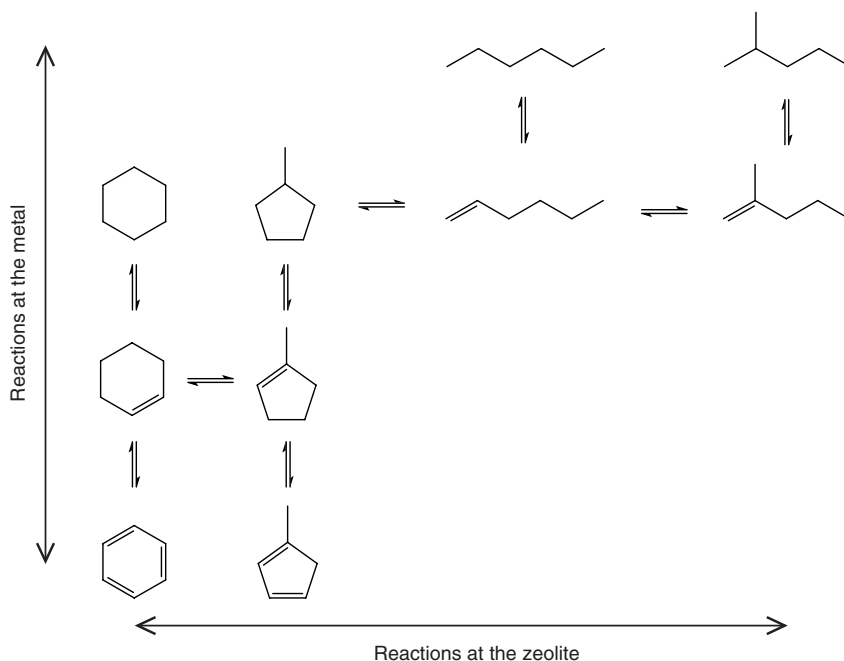


7.5

Metal-Doped Zeolites [T32]

Zeolites are especially suitable as support materials for active components such as metals and rare earths. With rare earths, the activity of the catalyst and its stability towards steam and heat can be increased. Suitable metals are effective catalysts for hydrogenations and oxidations, whereby the shape selectivity of the carrier is retained. Important factors influencing the reactions of such bifunctional catalysts are the location of the metal, the particle size, and the metal-support interaction.

The bifunctionality of metal-doped zeolite catalysts is explained here for the important example of isomerization and hydrogenation. The metal content facilitates the hydrogenation and dehydrogenation steps, while the acid-catalyzed isomerization step takes place under the restricted conditions of the zeolite cavities (Scheme 7-1).



Scheme 7-1 Bifunctionality of metal-doped zeolites: isomerization and hydrogenation

Bifunctional catalysts are used in many reactions, including hydrocracking, reforming, and dewaxing processes. They usually contain ca. 0.5 % Pt, Pd, or Ni. An advantage of nickel-containing hydrocracking catalysts is their lower hydrogenolysis activity compared to conventional catalysts.

A further example is acid-catalyzed disproportionation with [Pt]H-ZSM-5 as catalyst. The metal performs the hydrogenative cleavage of more highly aggregated molecules that would otherwise cause coking of the catalyst.

It is understandable that transition metals and transition metal complexes that are used in large-scale industrial processes are also incorporated into zeolites so as to exploit their shape selectivity. Examples are:

- Zeolite X with Rh^{3+} or Ni^{2+} : oligomerization of alkenes
- [Rh]-zeolites: carbonylation reactions (oxo synthesis, methanol carbonylation)
- [Pd^{II}][Cu^{II}]-zeolites: oxidation of ethylene to acetaldehyde in the Wacker process
- [Ru]-zeolites: photosensitization of oxygen

Finally, we shall discuss two examples that demonstrate the shape selectivity of bifunctional zeolite catalysts. Thus the diffusivity of *trans*-2-butene in zeolite CaA is 200 times higher than that of *cis*-2-butene. Doping with Pt allows selective hydrogenation of *trans*-2-butene to be carried out [T35]. Also of interest is shape selective hydrogenation on [Pt]ZSM-5, which is compared to hydrogenation on a conventional supported Pt catalyst in Table 7-8. With the zeolite catalyst, hydrogenation of the unbranched alkene is favored.

Table 7-8 Shape-selective hydrogenation [T32]

| Alkene | Reaction temperature [°C] | Conversion [%] | |
|-----------------------|---------------------------|----------------|-----------------------------------|
| | | [Pt]ZSM-5 | Pt/Al ₂ O ₃ |
| Hexene | 275 | 90 | 27 |
| 4,4-Dimethyl-1-hexene | 275 | <1 | 35 |
| Styrene | 400 | 50 | 57 |
| 2-Methylstyrene | 400 | <2 | 58 |

7.6

Applications of Zeolites [5, 8]

Zeolites have a wide range of applications. They are used as replacements for phosphates in laundry detergents, as adsorbents for purification and separation of materials, and as catalysts. The detergents industry has the largest demand for zeolites (ca. 1.2×10^6 t/a in 1994) and the highest growth rate. Demand for zeolite catalysts is also growing, and in 1994 amounted to ca. 115 000 t/a.

Table 7-9 lists important catalytic processes involving zeolites.

Table 7-9 Important catalytic processes involving zeolites

| Process | Starting material | Zeolite | Products |
|----------------------------|----------------------------|----------------------------------|-------------------------------|
| Catalytic cracking | crude oil | faujasite | gasoline, heating oil |
| Hydrocracking | crude oil + H ₂ | faujasite | kerosene |
| Dewaxing | middle distillate | ZSM-5, mordenite | lubricants |
| Benzene alkylation | benzene, ethene | ZSM-5 | styrene |
| Toluene disproportionation | toluene | ZSM-5 | xylene, benzene |
| Xylene isomerization | isomer mixture | ZSM-5 | <i>p</i> -xylene |
| MTG | methanol | ZSM-5 | gasoline |
| MTO | methanol | ZSM-5 | olefins |
| Intermediate products | diverse | acidic and bifunctional zeolites | chemical raw materials |
| SCR process | power station flue gases | mordenite | NO _x -free off-gas |

Zeolite catalysts are mainly used in refinery technology and petrochemistry [3]:

- Catalytic Cracking (FCC). Here heavy heating oil is converted to middle distillate and high-octane gasoline with cerium- and lanthanum-doped Y zeolites. Advantages compared to conventional thermal cracking processes are the better conversion yields and product quality, albeit at the expense of slightly less flexibility with regard to starting materials.
- Hydrocracking. In this environmentally friendly process, which operates in a closed system with 100 % conversion of heavy crude oil fractions, zeolite is used as a support for a hydrogenating component such as Pd. Bifunctional catalysis is achieved in which the cracking activity of the acidic zeolite is combined with the hydrogenation activity of the palladium.
- Dewaxing Process. In this industrial catalytic hydrocracking process, waxy C₁₆₊ paraffins are cracked and partly converted to aromatics.
- Methanol to Gasoline Process (MTG) Process. Methanol, produced from natural gas or coal, can be converted to high-quality, aromatics-rich gasoline in a two-stage fixed- or trickle-bed process with pentasil catalysts. Natural gas based production and cleavage of methanol has been operated since 1985 in New Zealand, where it covers one-third of gasoline demand.
- Methanol to Olefins Process (MTO) Process. Methanol can be converted to olefins by using modified pentasil catalysts. This interesting process, which is not yet used on an industrial scale, will presumably be of practical importance some time in the future.

Besides these processes, which lead to a wide product spectrum, controlled large-scale acid-catalyzed organic syntheses can also be carried out:

- Mobil–Badger Process. This process is a selective gas-phase alkylation of aromatics on pentasil zeolites. Ethylbenzene is produced from ethylene and benzene in a multistage adiabatic reactor. Compared to the conventional process of homogeneous catalysis with AlCl₃ as Friedel–Crafts catalyst, this heterogeneously catalyzed process has several advantages. These include economic and environmental advantages (e. g., up to 95 % heat recovery at a reaction temperature of 400 °C), straightforward regenerability, no problems in separating and recovering the catalyst, and freedom from the corrosion and waste-disposal problems encountered with AlCl₃ as catalyst.
- Xylene Isomerization. This industrial process for obtaining higher contents of *p*-xylene in C₈ aromatics cuts is carried out on pentasil zeolites at 400 °C, generally in the presence of hydrogen. The *para*-selective xylene isomerization and the disproportionation of toluene are among the industrially established processes.

In environmental protection, the use of zeolite catalysts in SCR technology for the denitrogenation of flue gases (e. g., from coal-fired power stations) is the subject of many publications and patent applications (companies: Norton and Degussa).

However, up to now the high prices and steam sensitivity of zeolites have prevented industrial realization.

In the last 20 years, the use of zeolites in the organic synthesis of intermediate products and fine chemicals has made rapid developments [4]. Especially pentasil zeolites have been used with great success. The syntheses can involve a whole series of steps, some of which are quite complicated. An overview is given in Table 7-10.

Table 7-10. Organic syntheses with zeolite catalysts [8]

Alkylations

Alkylation of arenes, side-chain alkylation, alkylation of heteroaromatics

Halogenation and nitration of arenes, substitution reactions of aliphatics

Ether and ester formation, thiols from alcohols and H₂S, amines from alcohols and NH₃ (mordenite, erionite)

Isomerizations

Isomerization of arenes and aliphatics, double bond isomerizations

Rearrangements

Skeletal rearrangement of alkanes, olefins, and functionalized compounds; pinacolone rearrangement; Wagner-Meerwein rearrangement; epoxide rearrangement; rearrangement of cyclic acetals

Additions and eliminations

Hydration and dehydration, additions to and eliminations from alcohols and acids, additions to N- and S-containing compounds, addition to epoxides

Hydrogenation and dehydrogenation

Dehydrocyclization

Hydroformylation

Oxidations

Oxidation with oxygen and peroxides

Condensations

Aldol condensations; synthesis of N heterocycles, isocyanates, nitriles; O/N exchange in cyclic compounds

Apart from simple mechanisms (condensation, hydrogenation, substitutions, alkylations), more complicated reactions can also be performed (Wagner-Meerwein and pinacolone rearrangements, syntheses of heterocycles) [8].

The application potential of zeolite catalysts in organic synthesis is by no means exhausted, and base catalysis remains practically unexplored. Thus the zeolites still have huge potential for future research and development.

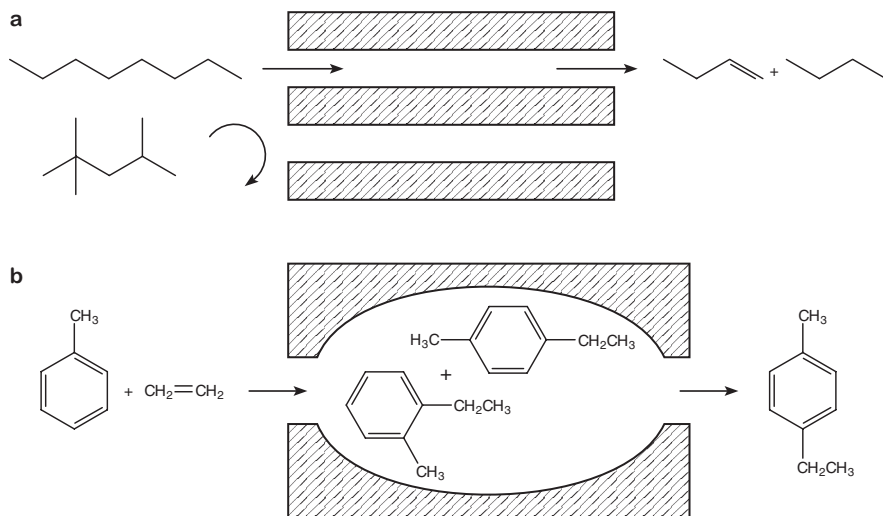
► Exercises for Chapter 7

Exercise 7.1

- What are zeolites?
- What are the three main possibilities for modifying zeolites?

Exercise 7.2

The following figure was found in a textbook:



Explain these reactions. Which catalyst properties make reactions a and b possible?

Exercise 7.3

Name several advantages that zeolite catalysts have compared to conventional catalysts.

Exercise 7.4

A mixture of olefins is hydrogenated with different catalysts at 275 °C. The following results were obtained:

| Catalyst | % Hydrogenation | |
|--|-----------------|-----------------------|
| | 1-Hexene | 4,4-Dimethyl-1-hexene |
| 1% Pt/Cs-ZSM-5 | 90 | 1 |
| 0.5% Pt/Al ₂ O ₃ | 27 | 35 |

Explain the differing selectivities.

Exercise 7.5

What is shape-selective catalysis?

Exercise 7.6

In the industrial synthesis of gasoline hydrocarbons, two processes compete with one another: Fischer–Tropsch synthesis and methanol cleavage (MTG process). Starting from synthesis gas, the methanol cleavage is two-stage process but still has advantages over the one-step Fischer–Tropsch synthesis. Why is this so?

Exercise 7.7

What are H-zeolites and how are they prepared?

Exercise 7.8

In the large-scale industrial production of methylamines, methanol and NH_3 are reacted at 350–500 °C and ca. 20 bar in the presence of Al_2O_3 . A mixture of mono-, di-, and trimethylamine is obtained with an equilibrium content of ca. 62 % trimethylamine. However, trimethylamine is of only minor economic importance.

Suggest how the product spectrum could be modified to favor mono- and dimethylamine.

Exercise 7.9

- In its protonated form ZSM-5 catalyzes the reaction of ethylene with benzene to give ethylbenzene. Suggest a plausible mechanism for this alkylation reaction.
- It is possible to produce the pure SiO_2 analogue of ZSM-5. Can it be expected that it will be an active catalyst for the alkylation of benzene?

Exercise 7.10

The kinetics of the alkylation of benzene with a rare earth zeolite Y is described by the equation:

$$r = \frac{k c_{\text{O}} c_{\text{T}}}{1 + K_{\text{O}} c_{\text{O}}} \quad \text{O} = \text{olefin}, \text{T} = \text{toluene}$$

What can be said about the mechanism of zeolite-catalyzed alkylation?

Exercise 7.11

The hydrothermal treatment (100–300 °C) of aluminophosphate gels in the presence of organic amines and quaternary ammonium bases leads to AlPO_4 molecular sieves with open pores and channels.

How do they differ from conventional zeolites?

Exercise 7.12

How can zeolites of low aluminum content be manufactured?

8 Heterogeneously Catalyzed Processes in Industry

8.1

Overview [T23, T31, T41]

Modern industrial chemistry is based on catalytic processes. Heterogeneous catalysts are used on a large scale in the following areas:

- Production of organic and inorganic chemicals
- Crude oil refining and petrochemistry
- Environmental protection
- Energy conversion processes

We will now give an overview of the most important catalytic processes and the process conditions.

8.1.1

Production of Inorganic Chemicals [21]

The production of hydrogen and synthesis gas mixtures (CO/H_2) from methane and higher hydrocarbons by steam reforming involves numerous reaction steps with different catalysts. The synthesis of ammonia and the oxidation of SO_2 to SO_3 are long-known equilibrium reactions in which the target product is removed from the product stream and the unchanged starting material is recycled.

The oxidation of ammonia to nitrous gases is a fast high-temperature reaction for the production of nitric acid (Ostwald process). The Claus process is an important petrochemical process for obtaining sulfur from H_2S , which results from the desulfurization of petroleum and natural gas (hydrodesulfurization). One-third of the H_2S is combusted to SO_2 , which reacts with the remaining H_2S (see Table 8-1).

8.1.2

Production of Organic Chemicals [9, 15]

Heterogeneous catalysts are used on a large scale in the production of organic chemicals. The processes can be classified according to reaction type (Table 8-2).

Catalytic hydrogenations are preferably carried out with metal catalysts based on Ni, Co, Pd, or Pt. In selective hydrogenations, undesired side reactions such as dou-

Table 8-1 Heterogeneous catalysis for the production of industrial gases and inorganic chemicals [T41]

| Process or product | Catalyst (main components) | Conditions |
|---|--|--------------------------|
| Steam reforming of methane $\text{H}_2\text{O} + \text{CH}_4 \rightarrow 3\text{H}_2 + \text{CO}$ | Ni/Al ₂ O ₃ | 750–950 °C, 30–35 bar |
| CO conversion $\text{CO} + \text{H}_2\text{O} \rightleftharpoons \text{H}_2 + \text{CO}_2$ | Fe/Cr oxides Cu/Zn oxides | 350–450 °C 140–260 °C |
| Methanization (SNG) $\text{CO} + 3\text{H}_2 \rightarrow \text{CH}_4 + \text{H}_2\text{O}$ | Ni/Al ₂ O ₃ | 500–700 °C, 20–40 bar |
| Ammonia synthesis | Fe ₃ O ₄ (K ₂ O, Al ₂ O ₃) | 450–500 °C, 250–400 bar |
| Oxidation of SO ₂ to SO ₃ | V ₂ O ₅ /support | 400–500 °C |
| Oxidation of NH ₃ to NO (nitric acid) | Pt/Rh nets | ca. 900 °C |
| Claus process (sulfur) $2\text{H}_2\text{S} + \text{SO}_2 \rightarrow 3\text{S} + 2\text{H}_2\text{O}$ | bauxite, Al ₂ O ₃ | 300–350 °C |

ble bond isomerization or *cis/trans* isomerization in fat-hardening processes must be avoided. The hydrogenation of CO to methanol is of major industrial importance.

Dehydrogenation is the reverse reaction of hydrogenation. It is preferably carried out with metal oxide catalysts, but metal catalysts are also used at low temperatures since they favor the hydrogenolysis of C–C bonds.

In *oxidation* processes heterogeneous catalysts are mainly used in gas-phase processes. In the oxidation of ethylene to ethylene oxide, supported silver catalysts are used; in the other examples, reducible metal oxide catalysts are used. In *ammoxidation* nitriles and HCN are obtained by using NH₃/O₂ mixtures. The *oxychlorination* of ethylene with HCl/O₂ is used for the production of vinyl chloride.

Acid catalysts are mainly used in alkylation processes, but also for hydration, dehydration, and condensation reactions. In olefin reactions, heterogeneous catalysts are mainly employed for metathesis reactions and the production of polymers.

8.1.3

Refinery Processes

In crude oil processing, catalytic processes are used to produce products such as gasoline, diesel, kerosene, heating oil, aromatic compounds, and liquefied petroleum gas (LPG) in high yield and good quality.

Bifunctional catalysts with acid and metallic components are used in reforming, hydrocracking, and isomerization; acid catalysts in cracking; and supported metal oxide/sulfide catalysts in hydrotreating for the removal of S, N, and O (hydrofining, hydrotreating). The most important processes in refinery technology are listed in Table 8-3.

Table 8-2 Heterogeneously catalyzed processes for the production of organic chemicals [T41]

| Process or product | Catalyst | Conditions |
|--|--|------------------------------------|
| <i>Hydrogenation</i> | | |
| Methanol synthesis | ZnO–Cr ₂ O ₃ | 250–400 °C, 200–300 bar |
| CO + 2 H ₂ → CH ₃ OH | CuO–ZnO–Cr ₂ O ₃ | 230–280 °C, 60 bar |
| Fat hardening | Ni/Cu | 150–200 °C, 5–15 bar |
| Benzene to cyclohexane | Raney Ni | liquid phase 200–225 °C, 50 bar |
| | noble metals | gas phase 400 °C, 25–30 bar |
| Aldehydes and ketones to alcohols | Ni, Cu, Pt | 100–150 °C, bis 30 bar |
| Esters to alcohols | CuCr ₂ O ₄ | 250–300 °C, 250–500 bar |
| Nitriles to amines | Co or Ni on Al ₂ O ₃ | 100–200 °C, 200–400 bar |
| <i>Dehydrogenation</i> | | |
| Ethylbenzene to styrene | Fe ₃ O ₄ (Cr, K oxide) | 500–600 °C, 1.4 bar |
| Butane to butadiene | Cr ₂ O ₃ /Al ₂ O ₃ | 500–600 °C, 1 bar |
| <i>Oxidation</i> | | |
| Ethylene to ethylene oxide | Ag/support | 200–250 °C, 10–22 bar |
| Methanol to formaldehyde | Ag cryst. | ca. 600 °C |
| Benzene or butene to maleic anhydride | V ₂ O ₅ /support | 400–450 °C, 1–2 bar |
| <i>o</i> -Xylene or naphthalene to phthalic anhydride | V ₂ O ₅ /TiO ₂ V ₂ O ₅ -K ₂ S ₂ O ₇ /SiO ₂ | 400–450 °C, 1.2 bar |
| Propene to acrolein | Bi/Mo oxides | 350–450 °C, 1.5 bar |
| <i>Ammoxidation</i> | | |
| Propene to acrylonitrile | Bi molybdate (U, Sb oxides) | 400–450 °C, 10–30 bar |
| Methane to HCN | Pt/Rh nets | 800–1400 °C, 1 bar |
| <i>Oxychlorination</i> | | |
| Vinyl chloride from ethylene + HCl/O ₂ | CuCl ₂ /Al ₂ O ₃ | 200–240 °C, 2–5 bar |
| <i>Alkylation</i> | | |
| Cumene from benzene and propene | H ₃ PO ₄ /SiO ₂ | 300 °C, 40–60 bar |
| Ethylbenzene from benzene and ethylene | Al ₂ O ₃ /SiO ₂ or H ₃ PO ₄ /SiO ₂ | 300 °C, 40–60 bar |
| <i>Olefin reactions</i> | | |
| Polymerization of ethene (polyethylene) | Cr ₂ O ₃ /MoO ₃ Cr ₂ O ₃ /SiO ₂ | 50–150 °C, 20–80 bar |

Table 8-3 Heterogeneously catalyzed processes in refinery technology [T41]

| Process or product | Catalyst | Conditions |
|---|--|--------------------------------------|
| Cracking of kerosene and residues of atmospheric crude oil distillation to produce gasoline | Al ₂ O ₃ /SiO ₂ zeolites | 500–550 °C, 1–20 bar |
| Hydrocracking of vacuum distillates to produce gasoline and other fuels | MoO ₃ /CoO/Al ₂ O ₃ Ni/SiO ₂ -Al ₂ O ₃ Pd zeolites | 320–420 °C, 100–200 bar |
| Hydrodesulfurization of crude oil fractions | NiS/WS ₂ /Al ₂ O ₃ CoS/MoS ₂ /Al ₂ O ₃ | 300–450 °C, 100 bar H ₂ |
| Catalytic reforming of naphtha (high-octane gasoline, aromatics, LPG) | Pt/Al ₂ O ₃ bimetal/Al ₂ O ₃ | 470–530 °C, 13–40 bar H ₂ |
| Isomerization of light gasoline (alkanes) and of <i>m</i> -xylene to <i>o/p</i> -xylene | Pt/Al ₂ O ₃ Pt/Al ₂ O ₃ /SiO ₂ | 400–500 °C, 20–40 bar |
| Demethylation of toluene to benzene | MoO ₃ /Al ₂ O ₃ | 500–600 °C, 20–40 bar |
| Disproportionation of toluene to benzene and xylenes | Pt/Al ₂ O ₃ /SiO ₂ | 420–550 °C, 5–30 bar |
| Oligomerization of olefins to produce gasoline | H ₃ PO ₄ /kieselguhr H ₃ PO ₄ /activated carbon | 200–240 °C, 20–60 bar |

8.1.4

Catalysts in Environmental Protection [10, 12]

As early as the 1940s, supported Pt/Al₂O₃ catalysts were used in the USA for the catalytic purification of off-gases by oxidation. In 1975 the purification of automobile exhaust emissions became required by law, and similar laws were later introduced in western Europe and Japan. The catalytic converters are monolithic supports coated with platinum and other noble metals (Fig. 8-1). Of major importance is the catalytic purification of the flue gases from power stations, in which the nitrous gases are converted to nitrogen and water by treatment with ammonia. Heterogeneous catalysts also have numerous applications in the catalytic afterburning of impurities or odoriferous components in industrial off-gases. Table 8-4 lists some examples.

Catalytic afterburning can solve various emission problems without generating secondary pollutants. There are numerous examples of off-gas purification in the chemical industry, the textile and furniture industry, and in printing works (see Section 10.3). Catalytic afterburning units (Fig. 8-2) are also successfully used for removing odors, e. g., in the foodstuffs industry.



Fig. 8-1 Supported metal catalyst with large reaction surface (Doduco)

Table 8-4 Heterogeneous catalysts in environmental protection [T32]

| Process | Catalyst | Conditions |
|--|---|---|
| Automobile exhaust control (C_nH_m , CO, NO_x) | Pt, Pd, Rh, washcoat Al_2O_3 , ceramic monolithes, rare earth oxide promoters | 400–500 °C, 1000 °C short-term |
| Flue gas purification (SCR): removal of NO_x with NH_3 | Ti, W, V mixed oxides as honeycomb bulk catalysts Ti, W, V oxides on inert honeycomb supports | hot denitrification (400 °C) cold denitrification (300 °C) |
| Combined denitrification and desulfurization (DESONOX process) | SCR catalyst + V_2O_5 honeycomb catalyst, catalyst bed | up to 450 °C |
| Catalytic afterburning (off-gas purification) | Pt/Pd; $LaCeCoO_3$ (perovskite); oxides of V, W, Cu, Mn, Fe; supported catalyst (honeycomb monolith or catalyst bed) or bulk catalyst | 150–400 °C 200–700 °C |



Fig. 8-2 Catalytic afterburning of the off-gases from a cyclohexanone plant (BASF, Antwerp)

8.2

Examples of Industrial Processes – Bulk Chemicals

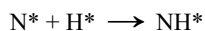
8.2.1

Ammonia Synthesis [11, 16]

The synthesis of ammonia from nitrogen and hydrogen is one of the most important processes in the chemical industry; over 100×10^6 t/a of ammonia is produced worldwide. The Haber–Bosch process, introduced in 1913, was the first high-pressure industrial process. Ammonia synthesis is carried out at ca. 300 bar and 500°C on iron catalysts with small amounts of the promoters Al_2O_3 , K_2O , and CaO .

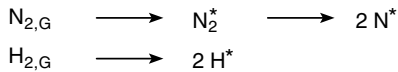
Extensive investigations of the mechanism of ammonia synthesis have shown that the rate-determining step is the dissociation of coordinatively bound nitrogen molecules on the catalyst surface. Hydrogen is much more readily dissociated on the catalyst surface. The adsorbed species then undergo a series of insertion steps, in which ammonia is formed stepwise and is finally desorbed (Scheme 8-1).

At moderately high pressures the reaction rate is independent of the hydrogen pressure and first order with respect to nitrogen. The stationary occupation by N^* atoms is low, and this indicates that the dissociative adsorption of N_2 is rate-determining. At higher hydrogen pressures, there is a fractional reaction order in H_2 corresponding to displacement of the rate-determining step towards

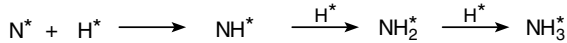


The elucidation of the reaction mechanism has occupied catalysis researchers up to the present day [11]. Over 20 000 catalysts have been tested, but none has been

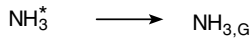
1) Dissociative chemisorption of starting materials



2) Reaction of adsorbed atoms



3) Desorption of product



Scheme 8-1 Simplified mechanism of ammonia synthesis

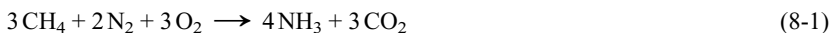
found that operates at room temperature. Catalytic activity is exhibited by metals that chemisorb N_2 dissociatively with relatively strong binding, especially the metals of Groups 6–8 with d gaps, on which large amounts of H_2 are also rapidly chemisorbed. The activity increases with increasing heat of adsorption of N_2 in the order:



Other metals are more active in cleaving the $\text{N} \equiv \text{N}$ bond (e.g., Li) but the resulting metal nitrides are too stable to take part in a catalytic cycle.

For economic reasons, industrial catalysts consist of smelted iron oxides (60–70 % Fe) mixed with oxides of Al, Ca, Mg, and K, ground to 6–20 mm. During the activation of the catalyst by reduction, iron crystallites are formed with an interconnected pore system and an inner surface area of 10–20 m^2/g . The surface is partially covered by promoter oxides.

The industrial production of ammonia from natural gas involves eight different catalytic steps (Scheme 8-2). The overall reaction equation is given in Equation (8-1).

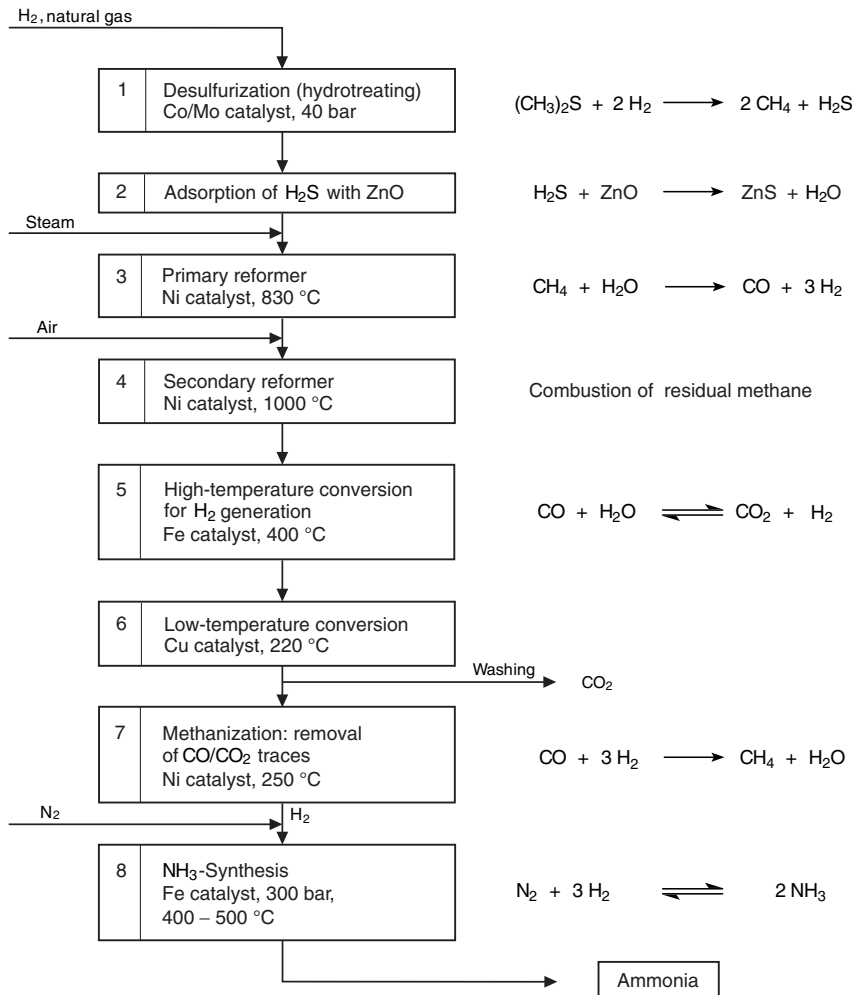


The thermodynamic energy requirement is 2×10^7 kJ/t NH_3 , which represents the theoretical minimum for all conceivable processes. Modern processes for the production of ammonia from natural gas have energy consumptions of around 3×10^7 kJ/t NH_3 , i.e., only 1.5 times the theoretical minimum energy consumption. Today much of the energy requirement can be covered by means of heat recovery. Modern ammonia plants produce up to 2000 t/d.

8.2.2

Hydrogenation [2, 6]

With increasing crude oil prices, there is a growing trend towards renewable raw materials. Fats (triglycerides) are being used in increasing quantities as raw materials in the chemical industry. The glycerides are oxidized, hydrogenated, and ami-

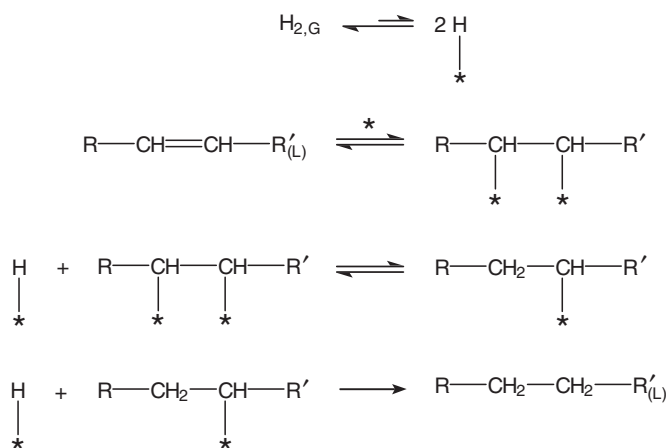


Scheme 8-2 Synthesis of ammonia from natural gas

nated to remove undesired functional groups, to shorten the chain length, or to introduce other functional groups. Many of these steps are carried out catalytically, and for economic reasons should take place at low temperatures and pressures in order to attain high selectivities [5, 13].

An important process in the foods industry is the hardening of vegetable oils, for example, the production of margarine by hydrogenation of double bonds. In this process an oil is converted to a solid that should have high stability towards oxidation, which leads to rancidity. The main aim in an industrial process is to remove linoleic acid (three C–C double bonds) as completely as possible while minimizing conversion of the desired oleic acid (one C–C double bond) to the saturated stearic acid.

The hydrogenation is carried out at ca. 3 bar hydrogen pressure with a suspension of supported Ni/SiO₂ catalyst in the liquid phase at 200–210 °C, usually in a batch process. The reaction is terminated by stopping the supply of hydrogen and lowering the temperature to ca. 100 °C. The strength of adsorption on the catalyst decreases with increasing degree of saturation of the fats. Therefore, the more highly unsaturated side chains are preferentially hydrogenated. The rate of hydrogenation is generally zero order with respect to the concentration of the oil and first order with respect to the hydrogen pressure. This indicates that the nickel surface is largely covered with unsaturated molecules, whereas hydrogen is only weakly adsorbed. A highly simplified reaction mechanism is shown in Scheme 8-3; the last step is rate-determining.



Scheme 8-3 Reaction steps in the hydrogenation of fats [T22]

The highly unsaturated triglycerides can be hydrogenated to oleic acid with high selectivity by using copper catalysts, but traces of copper remain in the margarine, which excludes the industrial use of copper catalysts. A typical hydrogenation plant hydrogenates oil in a stirred tank in batches of up to 15 t and produces about 90 t/d of hardened fat.

Noble metal catalysts such as Pd and Pt are being increasingly used in oil and fat treatment processes since they have a less pronounced tendency to remove functional groups. The choice of catalyst and its optimization are of growing importance in this area. For example, a Pd shell catalyst is used advantageously for the hydrogenation of soya oil to edible oil. In this process the content of linolenic acid must be reduced to less than 2 % without hydrogenating the other unsaturated fatty acids. In spite of the small metal surface area, the shell catalyst is the most suitable, since the metal is most readily accessible for the bulky triglyceride molecules. The Pd catalysts have higher activity and can be more easily recovered. The high cost of the noble metal is made up for by the low metal concentration. While nickel

catalysts are used in concentrations of 0.04 % relative to the oil to be hydrogenated, concentrations of platinum of less than 0.005 % are sufficient [13].

Another area of major industrial importance is the production of oleochemical raw materials such as fatty acids, fatty acid methyl esters, fatty alcohols, and glycerol. The company Henkel is the world's largest processor of renewable fats and oils, with a capacity of 10^6 t. Tailor-made catalysts are used in most oleochemical reactions.

A successful catalyst development in the last few years has made possible the direct hydrogenation of fats to fatty alcohols in a one-stage process. The laborious transesterification of the the fats can be dispensed with. Beside the high-quality coconut and palm oils, lower quality, acid-containing fats and oils can now be hydrogenated by using new acid-stable copper chromite spinel catalysts.

8.2.3

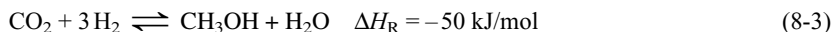
Methanol Synthesis [T22, T41]

The synthesis of methanol from CO and H₂ (Eq. 8-2) has been known since the early 1920s. Mittasch found oxygen-containing compounds during investigations of ammonia synthesis at BASF. In 1923 the first large-scale methanol plant operating with synthesis gas was erected in Germany.

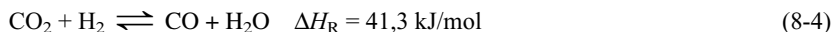


The high-pressure process, which used to be exclusively operated, is carried out with ZnO/Cr₂O₃ catalyst at 250–350 bar and 350–400 °C. The development of more active, copper-based catalysts allowed the process to be carried out in the pressure range 50–100 bar and at lower temperatures. This improved the economics of the process. The low-pressure processes were developed by ICI and Lurgi and introduced in the mid-1960s.

Let us examine the mechanism of methanol synthesis [18]. In 1962 the activating effect of CO₂ in the synthesis gas was discovered. When cracked gas (CO + 3H₂) from methane-rich natural gas is used, CO₂ is added to the synthesis gas and it consumes more H₂ than the CO (Eq. 8-3).



Another side reaction is the water-gas shift equilibrium (Eq. 8-4).

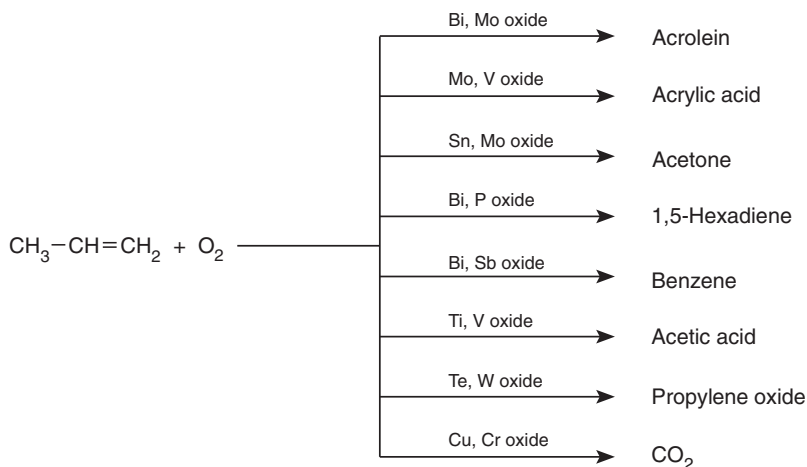


Thus the question of what is the actual carbon source in methanol synthesis can not be unambiguously answered. Two mechanisms have been suggested to explain the formation of methanol on the heterogeneous catalyst. In the first mechanism (Eq. 8-5), adsorbed CO reacts on active copper centers of the surface with dissociatively adsorbed hydrogen in a series of hydrogenation steps to give methanol.

that selectivities of over 90 % are achieved in some cases. Thus the space–time yields of the processes could be improved and better use made of the raw materials.

Selective oxidation still offers interesting development possibilities for the chemical engineer [8]. Here we shall consider the oxidation and ammoxidation of propene, which both proceed by a similar mechanism, in more detail.

In the selective oxidation of propene, metal oxides are mainly used as catalysts, and many different products are obtained (Scheme 8-5), depending on the catalyst used [19].



Scheme 8-5 Oxidation of propene on various metal oxide catalysts

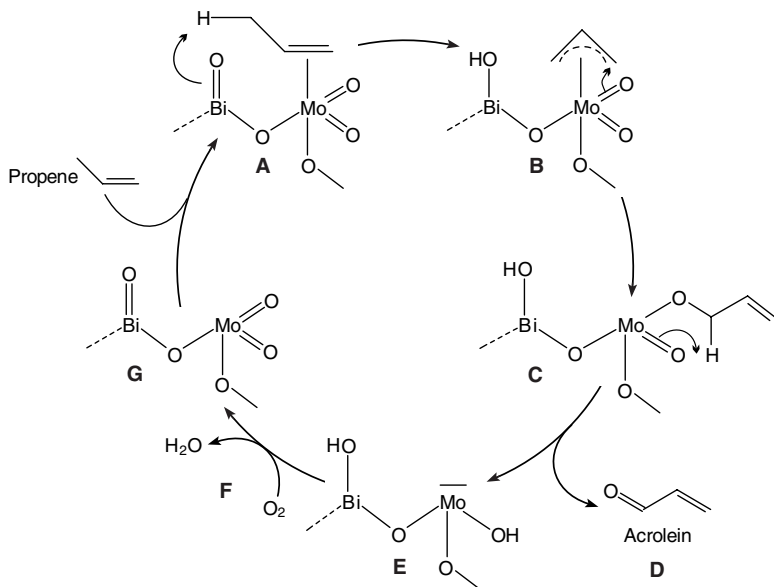
The catalytic oxidation of propene leads preferentially to formation of acrolein (Eq. 8-7).



$$\Delta H_{\text{R}} = -368 \text{ kJ/mol}$$

Carbon dioxide, acetaldehyde, and acrylic acid are formed as side products. A technical breakthrough was achieved by Standard Oil of Ohio (SOHIO) with the discovery of the bimetallic bismuth molybdate and bismuth phosphomolybdate catalysts. Propene is oxidized with air on a $\text{Bi}_2\text{O}_3/\text{MoO}_3$ catalyst at 300–400 °C and 1–2 bar in a fixed-bed tubular reactor, which allows effective removal of heat from the exothermic reaction [15].

The mechanism of the allyl oxidation of propene is explained in terms of a reaction cycle [19]. As shown in Scheme 8-6, propene and air do not react directly with one another. Instead, the propene initially forms a π complex **A** with an Mo center of the bismuth molybdate catalyst. Hydrogen abstraction by an oxo oxygen atom on bismuth leads to formation of a hydroxyl group and a π -allyl complex at Mo **B**, whereby one

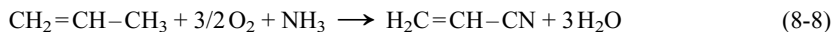


Scheme 8-6 Oxidation of propene to acrolein on Bi/Mo catalysts [19]

electron flows into the lattice. Transfer of oxygen to the allyl group forms an Mo–allylate bond, and a further hydrogen abstraction (C) on the same Mo center leads to formation of acrolein, which is desorbed from the catalyst surface (D). In these steps, three electrons flow into the lattice, and what remains is an oxygen-deficient bismuth molybdate with OH groups (E). This reacts with atmospheric oxygen with cleavage of water (F) and re-formation of the original catalyst (G). In the reoxidation of the catalyst, an O_2 molecule is reduced to O^{2-} ions by four electrons, available in the lattice. The oxide ions then diffuse to the lattice vacancies.

How can the side products of the oxidation reaction be explained? It can be assumed that the allylmolybdenum complex (B) is cleaved into C_1 and C_2 fragments, which result in acetaldehyde and CO_2 , the latter presumably via formaldehyde as intermediate. Carbon dioxide can, however, also be formed by total oxidation of propene.

The true SOHIO process is in fact the ammoxidation of propene with NH_3 and atmospheric oxygen in a highly exothermic reaction to give acrylonitrile (Eq. 8-8).

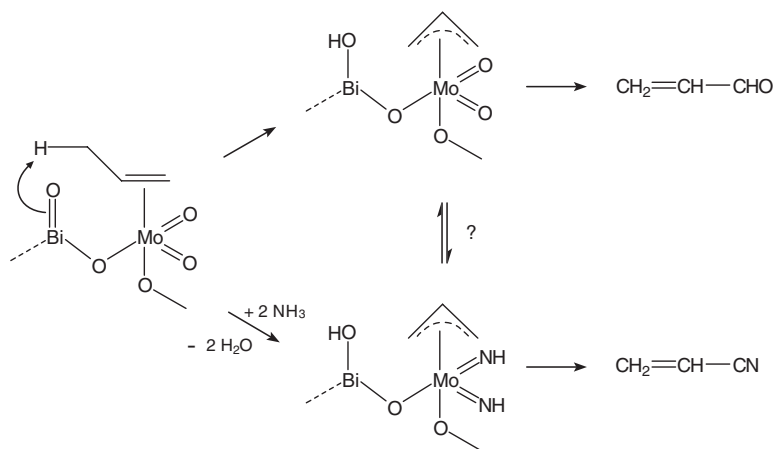


$$\Delta H_R = -502 \text{ kJ/mol}$$

In this process the activated methyl group in the allylic position is converted to a nitrile. In the SOHIO process, stoichiometric quantities of propene and ammonia are treated with an excess of oxygen in a fluidized-bed reactor at ca. $450^\circ C$ and 1–2 bar. The catalysts used today contain several multivalent main group metals (Bi^{3+} , Sb^{3+} ,

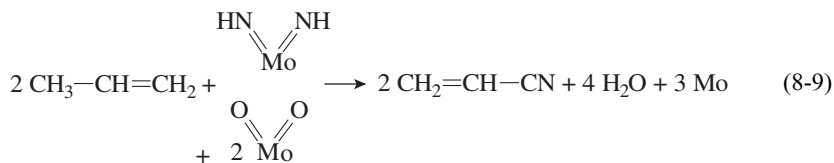
Te⁴⁺), molybdenum, and a redox component (Fe^{2+/3+}, Ce^{3+/4+}, U^{5+/6+}) in a solid oxide matrix. However, most research investigations deal with the standard bismuth molybdate catalyst, which can be simply formulated as Bi₂O₃ · n MoO₃ [23].

Besides oxidizing propene and being regenerable by atmospheric oxygen, the catalyst must also activate ammonia. In spite of numerous experimental findings, the mechanism of ammoxidation is still largely speculative. According to Scheme 8-7 the BiO group abstracts hydrogen from the alkane, and this leads to formation of a π-allyl complex at the Mo center. The actual allyl oxidation and the NH₃ activation then take place on the molybdenum side. It is assumed that by reaction with ammonia the oxomolybdenum groups are partly converted to iminomolybdenum groups, which are responsible for the C–N bond-forming reaction to give acrylonitrile.



Scheme 8-7 Postulated reaction mechanism for the ammoxidation of propene [13]

The oxidation is a six-electron process, and it is regarded as certain that the α -H abstraction with formation of the π -allyl complex is the rate-determining step. Both the dioxomolybdenum cations and the diimino species are believed to be involved in the formation of acrylonitrile. On the basis of selectivity measurements, the stoichiometry shown in Equation 8-9 was assumed [L32].



In the industrial process the acrylonitrile selectivity is greater than 70 %, and the side products are acetonitrile (3–4 %), HCN (ca. 15 %), CO₂, acrolein, and acetaldehyde. After washing with water, the acrylonitrile is purified by multistage distillation to give a purity of >99 %, as is required for the production of fibers. The acet-

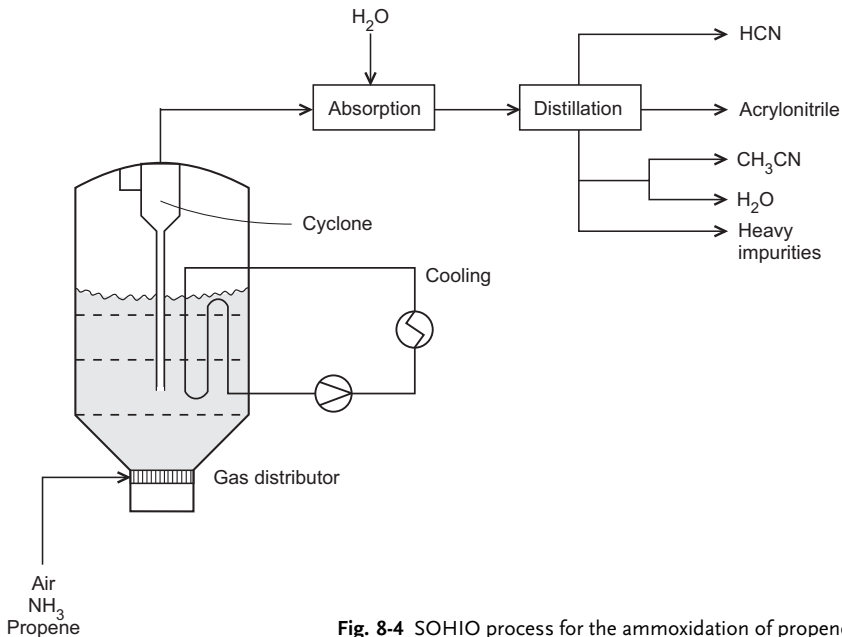


Fig. 8-4 SOHIO process for the ammoxidation of propene

onitrile byproduct is isolable but is usually incinerated. Figure 8-4 shows a scheme of the SOHIO process.

The SOHIO ammoxidation process was developed since 1957. Production capacity for acrylonitrile, the most important product derived from propene, is greater than 4×10^6 t/a, of which over 70 % is produced by the SOHIO process. Plants are constructed with capacities of up to 180000 t/a. There are numerous variants of ammoxidation, the following products also being produced by this process:

- Methacrylonitrile from isobutene
- Hydrogen cyanide from methane
- Phthalodinitrile from *o*-xylene
- Nicotine nitrile from β -picoline

8.2.5

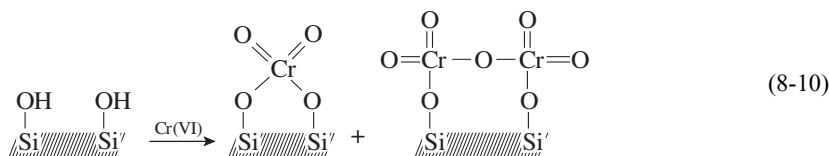
Olefin Polymerization [15]

The polymerization of olefins has been carried out industrially for decades and can be performed by various mechanisms. The high-pressure radical polymerization of ethylene leads to low-density polyethylene (LDPE, $\rho = 0.92\text{--}0.93$ g/cm³). In the mid-1950s Ziegler achieved the low-pressure polymerization of ethylene and propylene (up to 10 bar, 50–150 °C) by using organometallic catalysts based on TiCl₄/Al(C₂H₅)₃. The Ziegler catalysts give less branched, linear high-molecular polyethylene (high-density polyethylene, HDPE; $\rho = 0.94\text{--}0.97$ g/cm³). Using this catalyst

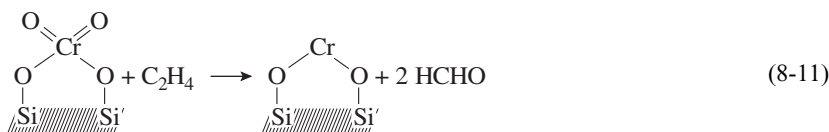
system, Natta succeeded in manufacturing crystalline, isotactic polypropylene, and around the same time, the company Phillips in the USA developed silica-supported chromium catalysts.

In the following we shall take a closer look at supported catalysts for the polymerization of olefins [T22]. Oxides of Cr and Ti on various support materials have high activities for the polymerization of ethylene to linear chains (HDPE). The processes operate at relatively low ethylene pressure (20–30 bar) in the temperature range 130–150 °C (solution polymerization) or 80–100 °C (suspension and gas-phase polymerization).

The Phillips catalysts are manufactured by impregnating amorphous silica gel with chromates up to a metal loading of ca. 1%. The material is then dried and calcinated at 500–1000 °C. The surface silanol groups react with the chromate groups to give a disperse monolayer of chromate and dichromate esters (Eq. 8-10).



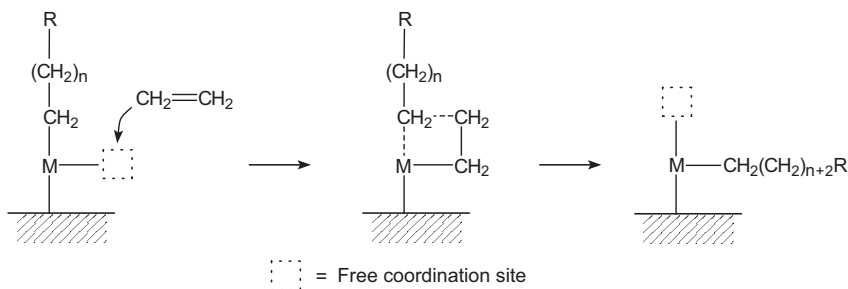
However, it is assumed that the active centers are coordinatively unsaturated Cr^{II} or Cr^{III} centers that are generated by reaction with ethylene (Eq. 8-11). It is also possible to convert the chromate deposited on the silica surface to an active form by high-temperature reduction with CO. In an alternative method of catalyst production, low-valent organochromium compounds such as chromocene and tris(η^3 -allyl)-chromium are used as catalyst precursors.



Similar to the polymerization of ethylene on Ziegler catalysts, the first reaction step is the coordination of an ethylene molecule at a Cr^{II} center. The initiator of the polymerization reaction is thought to be a Cr–H group, into which ethylene inserts to form an ethyl ligand (Eq. 8-12). It was shown that only isolated Cr centers on the surface are catalytically active.



Coordinatively unsaturated transition metal centers are the prerequisite for olefin polymerization in both Phillips and Ziegler–Natta catalysts, and this makes it possible to simultaneously bind the monomer and the growing chain. This does not occur



Scheme 8-8. Polymerization of ethylene at a metal center (M)

by a redox reaction, since the transition metal does not change its oxidation state during the polymerization process. The chain-growth process can be described as shown in Scheme 8-8.

The chain-growth mechanism involves the insertion of two CH_2 units between the metal center M and the original alkyl chain, so that chain branching can not occur in the growing polymer. Thus the vacant site on the transition metal atom simply changes its position. Chain branching can be introduced in a controlled fashion by copolymerizing ethylene with short-chain terminal alkenes, which leads to modified polymer properties.

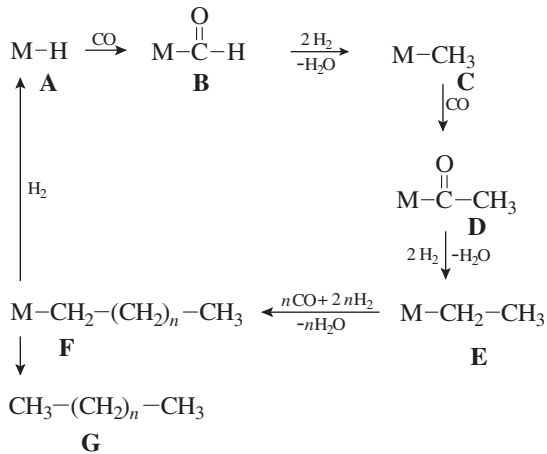
► Exercises for Sections 8.1 and 8.2

Exercise 8.1

The following industrial processes are to be carried out. Which of the catalysts A–L is potentially suitable for which reaction?

- 1) Alkylation of benzene to ethylbenzene
- 2) Cracking of higher hydrocarbons
- 3) Dehydration of amides to amines
- 4) Dehydration of ethylbenzene to styrene
- 5) Esterification
- 6) Hydrogenation of CO to methanol
- 7) Hydrogenation of vegetable oils
- 8) Isomerization of pentane to isopentane
- 9) Oxidation of ammonia to nitrogen oxides
- 10) Oxidation of SO_2 to SO_3
- 11) Reforming processes for the production of aromatics
- 12) Oxidation of methanol to formaldehyde

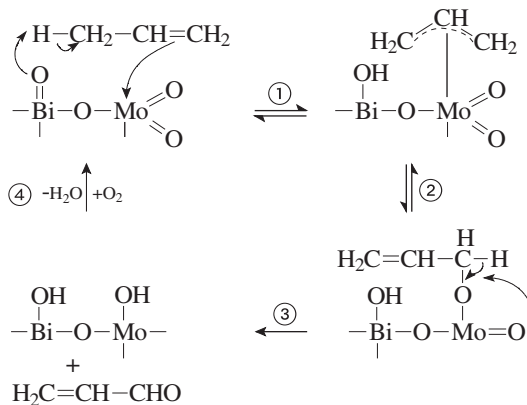
Pt/support (A), zinc chromite (B), V_2O_5 (C), Pt (D), Al_2O_3 (E), Ag (F), aluminosilicates (G), zeolites (H), Ni (I), iron oxides/promoter (J), ion-exchange resins (K), CuO (L).



Explain the individual reactions to give the products A–G.

Exercise 8.7

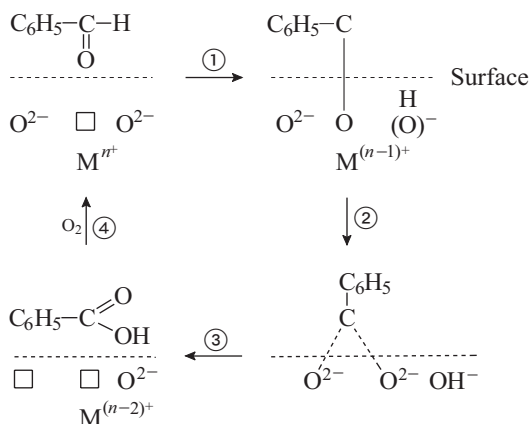
The following mechanism is given for the oxidation of propene to acrolein on bis-muth molybdate catalysts:



Explain the course of the reaction with the steps 1–4.

Exercise 8.8

The oxidation of benzaldehyde on an $\text{SnO}_2/\text{V}_2\text{O}_5$ catalyst is described as follows (\square represents an anion vacancy in the catalyst surface):



Explain the course of the reaction with the steps 1–4.

8.3

Fine Chemicals Manufacture

8.3.1

Fine Chemicals and their Synthesis [7]

Driven by demands for increased and sustained profitability since more than 20 years there has been a worldwide shift away from traditional commodity chemicals towards high added value fine chemicals production. This can be easily accounted for an increased competition in commodity chemicals.

As with bulk chemicals, fine chemicals are identified according to specifications (what they are). In contrast, specialties are identified according to performance (what they can do).

Fine chemicals include:

- Advanced intermediates
- Bulk drugs
- Bulk pesticides
- Active ingredients
- Bulk vitamins
- Flavor and fragrance chemicals
- Pharmaceuticals
- Dyes
- Food additives
- Cosmetics
- Vitamines
- Photochemicals etc.

Especially biologically active compounds, which include pharmaceuticals, crop protection chemicals, flavors, fragrances, and food additives, have provided a strong driving force for the use of homogeneous catalysts and special heterogeneous catalysts.

Fine or speciality chemicals, unlike the traditional commodity products, have complex chemical structures and properties that justify a high selling price. In high added value products, where relatively small quantities of products are manufactured, factors such as catalyst costs, separation of product from catalyst and reactants, recycling and regeneration of catalysts, etc., assume reduced significance relative to that in the manufacture of commodity chemicals. This is understandable because these costs can be more readily absorbed in the relatively high value of the products. In fine chemistry there are generally small-scale processes and usually reactions are carried out batch-wise rather than continuously. Typical plant types are the so-called Multi-Product Plant and Multi-Purpose Plant.

Fine chemicals differ from bulk chemicals in many aspects, as can be seen in Table 8-5.

Table 8-5 Fine versus bulk chemicals [7]

| | Bulk chemicals | Fine chemicals |
|----------------------|--|--|
| Volume (t/a) | >10,000 | < 10,000 |
| Price (\$/kg) | <10 | >10 |
| Lifecycle | long | relatively short |
| Molecules | simple | complex, several functionalities |
| Applications | many | limited number (often one) |
| Synthesis | few steps one or few routes | multi steps various routes |
| Catalysis | often | exception |
| Processing | continuous, mostly gas phase, fixed bed | batch, multi-step mostly liquid phase |
| By-products (kg/kg) | low | high |
| Waste per kg product | relatively low | high |

Specific for fine chemistry is the formation of relatively large amounts of by-products. In fine chemistry, catalysis does not play the important role as it does in the production of bulk chemicals. Multistep synthesis reactors are common and they usually consist of a number of stoichiometric reactions rather than catalytic reactions. These reactions often result in the formation of large amounts of by-products, predominantly inorganic salts.

In recent years two trends have become visible in the manufacture of fine chemicals:

- 1) Custom synthesis.
- 2) Specialization in groups of processes or products that are derived from specific raw materials (chemical trees).

Many companies specialize in the production of chemicals grouped in “chemical trees” characterized by the same chemical roots (compounds) or the same/similar method of manufacturing. Examples for different special technologies in fine chemistry are as follows:

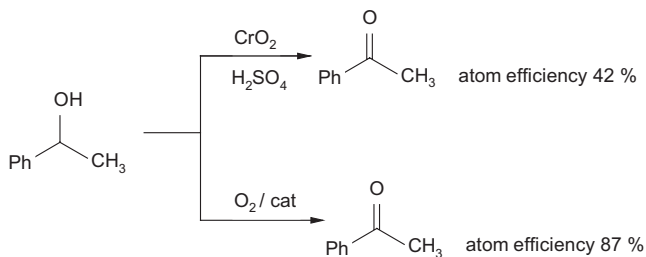
- Hydrogenation
- Oxidation
- C-C-coupling
- Reduction of NO₂-groups
- Cyanid-chemistry
- Amino acid synthesis
- Oligomerization
- Hydrocyanation
- Electrochemistry
- Metathesis
- Carbonylation
- Asymmetric synthesis
- Multiple phase catalysis

Zero emission plants, environmentally benign or green chemistry, and sustainable development have become more and more important since the 1990s. Thus, environment-economics have become a major driving force in technological innovation. The major aim of successful developing fine chemicals is, to design more precision into organic synthesis. Chemists use the concept of selectivity as a measure of how efficiently a synthesis is performed. However, one category of selectivity is largely ignored by organic chemists, the “atom selectivity” or what is variously called “atom economy” or “atom efficiency”. The complete disregard of this parameter is the root cause of the waste problem in fine chemicals manufacture.

The *atom efficiency* concept is a useful tool for rapid evaluation of the amount of waste that will be generated by alternative routes to a particular product. It is calculated by dividing the molecular weight of the desired product by the sum total of the molecular weights of all the substances produced in the stoichiometric equation of the reactions in question. The comparison is made on a theoretical (i. e. 100%) chemical yield basis.

Scheme 8-9 shows a simple illustration of the concept for acetophenone production by oxidation of the corresponding alcohol α -phenylethanol [7]. The older oxidation with chromium oxide leads to some side products and the atom efficiency is only 42%. Modern homogeneous or heterogeneous catalyzed oxidation results in an atom efficiency of 87% (MW 120 + 18 (water) = 138; 120/138 = 0.87).

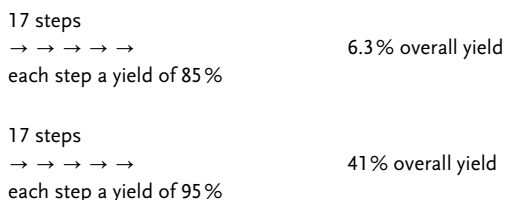
As noted above, a prime cause of waste generation is the use of stoichiometric inorganic reagents. Hence, the solution is simple: replacement of antiquated stoichiometric methodologies with cleaner catalytic alternatives, e.g. catalytic hydrogenations, catalytic oxidations with O₂ or H₂O₂ and catalytic carbonylations.



Scheme 8-9 Atom efficiency in acetophenone production [7]

Catalysis is the key to increasing the selectivity. With complex reaction pathways, selectivity is the key problem to make the process profitable. Selectivity can be controlled by chemical factors such as chemical route, solvent, catalyst and operation conditions, but it is also strongly dependent on engineering solutions.

Fine chemicals manufacture often requires numerous reactions with different yield in each step. The impact of catalysis will be illustrated in the next example (Scheme 8-10):



Scheme 8-10 Influence of yield improvement in a multi-step process

What we can see is, that a moderate enlargement of the yield of each reaction step leads to a significant increase of the overall yield of the process. Catalysis can improve yield and can cut down reaction steps, too. Not surprisingly, catalysis is and will be more and more applied in fine chemistry. In that respect, fine chemistry can benefit from the experience in bulk chemistry. The use of catalysis, including biocatalysis, in the fine chemicals industry has already resulted in much improved efficiency, but further progress is possible and needed.

Some general comments on catalysis in fine chemical synthesis are summarized as follows:

- Historically non-catalytic routes were used
- Pressure on production cost
- Need of waste minimization
- Catalysts can cut out processing steps in multistep processes
- Atom efficiency should be maximized
- Catalysts can offer new routes
- Safety aspects (toxicity) are important
- Catalysts can make new products
- Catalysts allow easier continuous operation change in raw materials

8.3.2

Selected Examples of Industrial Processes

Figure 8-5 gives an overview of the most important reaction types in fine chemical synthesis.

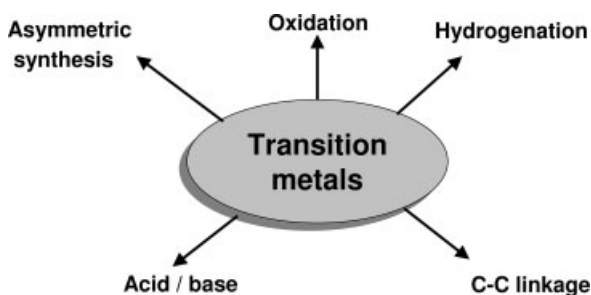


Fig. 8-5 Use of metal catalysis in fine chemical synthesis

Examples of these technologies with the exception of asymmetric catalysis (cf. Section 3.3) will be delineated in the following sections.

8.3.2.1 **Hydrogenation**

Hydrogenation reactions are widely used in fine chemicals manufacture, for example 10–20% of all the reaction steps in the synthesis of vitamins are catalytic hydrogenations.

Characteristics

Catalysts most frequently used are noble metals, on various supports, generally performed in liquid phase

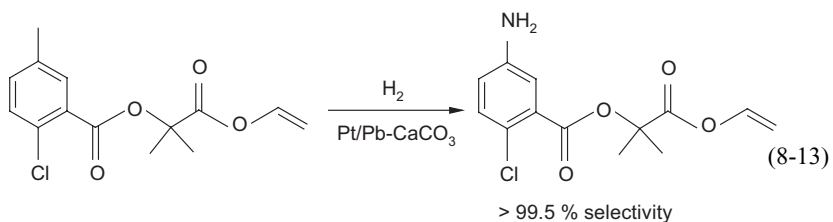
- Relatively mild conditions of temperature and pressure (1–40 bar)
- Reduction of one organic function in the presence of other reducible functions, e. g. selective reduction of a carbon-carbon double bond in the presence of –CHO, –NO₂ or –CN
- A high degree of chemo-, regio-, stereoselectivity is very important
- Most processes are performed batch-wise using powder catalysts in stirred tank or loop-type reactors with sizes up to 10 m³

Molecular hydrogen is by far the cheapest reductive agent. In addition, it is either completely added to the starting molecule or it yields hydrogenolysis by-products which normally can be easily disposed. Consequently, these reductions are particularly popular in the fine chemicals industry. Careful adjustment of all experimental parameters, including type and amount of catalyst, solvent, temperature, pressure, and degree of mixing (e. g. stirring speed), is necessary to maximize the yield of the desired product (Fig. 8-6). Here we can only discuss a few basic principles.

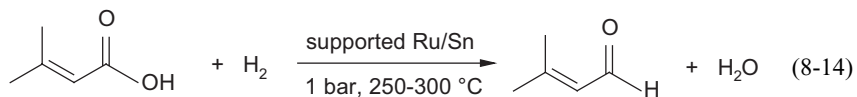


Fig. 8-6 Operation of a continuous high-pressure hydrogenation plant (CATATEST plant, VINCI technologies, France; high-pressure laboratory, FH Mannheim, Germany)

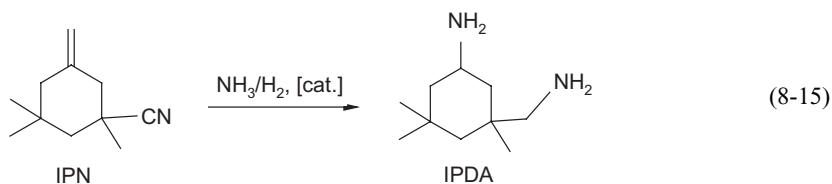
Equation 8-13 shows an example for a chemoselective hydrogenation of a nitro-group in the presence of C=C, C=O, C≡N, as well as Cl- or Br-substituents (Novartis) [7]:



Another example (Eq. 8-14) deals with the direct hydrogenation of carboxylic acids to the corresponding aldehydes using a bimetallic Ru/Sn-catalyst (Rhône-Poulenc, 1998) [7]:



A key step in the large-scale production of isophorone diamine (IPDA, Degussa) is simultaneous hydrogenation of a nitrile group and reductive amination of a keto function from isophoronenitrile (IPN) to give the corresponding diamine using a catalyst based on cobalt, nickel or ruthenium or mixtures thereof (Eq. 8-15) [4]:



The best catalyst can only be found by experiment (Fig. 8-7).

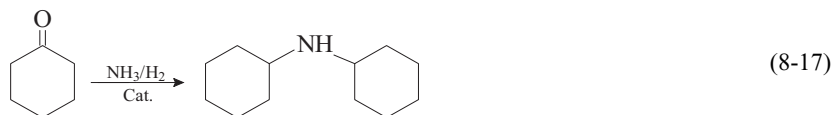


Fig. 8-7 A hydrogenation catalyst is introduced into a pilot plant in order to test it under process-relevant conditions (BASF, Ludwigshafen, Germany)

Catalytic reactions often give surprising results. An interesting result is the reductive amination of aldehydes and ketones. The keto compounds react with primary or secondary amines or ammonia in the presence of H_2 and a suitable catalyst (e.g., Pd) to give a new amine. Thus, as expected, 2-methylcyclohexanone is converted to 2-methylcyclohexylamine (Eq. 8-16).



Under the same reaction conditions, the unsubstituted cyclohexanone forms dicyclohexylamine (Eq. 8-17). The reasons for this behavior have not yet been completely elucidated [T20].



8.3.2.2 Oxidation [22]

Whereas in bulk chemicals manufacture the choice of oxidant is largely restricted to molecular oxygen, the economics of fine chemicals production allow a broader choice of oxidants such as H_2O_2 or other peroxides. Increasingly stringent environmental constraints are making the industrial use of classical stoichiometric oxidants such as dichromate, permanganate, and manganese dioxide prohibitive. There is a general trend toward substitution of such antiquated technologies by catalytic methods that do not generate aqueous effluents containing large quantities of inorganic salts (Fig. 8-8).

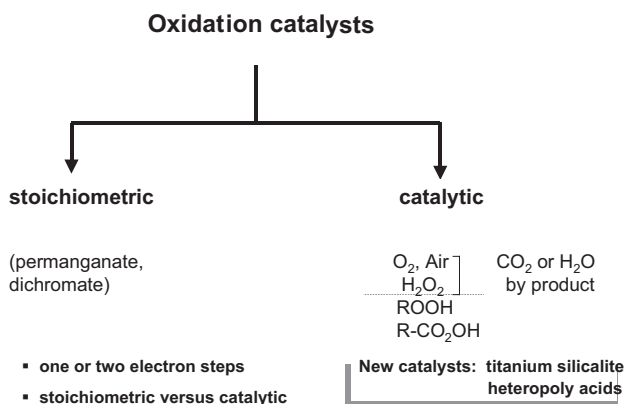
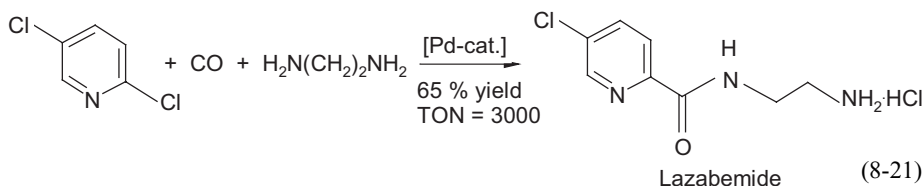


Fig. 8-8 Comparison of stoichiometric and catalytic routes in oxidation processes

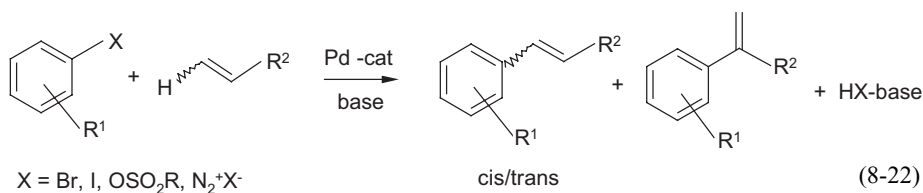
Even though hydrogen peroxide is more expensive than oxygen, it is often the oxidant of choice for fine chemicals because of its simplicity of operation. An extremely versatile catalyst for a variety of synthetically useful oxidations with aqueous hydrogen peroxide is the zeolite catalyst titanium(IV) silicalite (TS-1), developed by Enichem. This catalyst is obtained by isomorphic substitution of Si by Ti in molecular sieve materials such as silicalite (the all-silica analogue of ZSM-5) and zeolite beta. These catalysts have become known as “redox molecular sieves”, they can be used several times for liquid phase processes.

Thus, the TS-1 catalyzed hydroxylation of phenol to a 1:1 mixture of catechol and hydroquinone was commercialized by Enichem [22]. This process offers higher selectivities at higher phenol conversions, compared to other catalytic systems (Eq. 8-18).

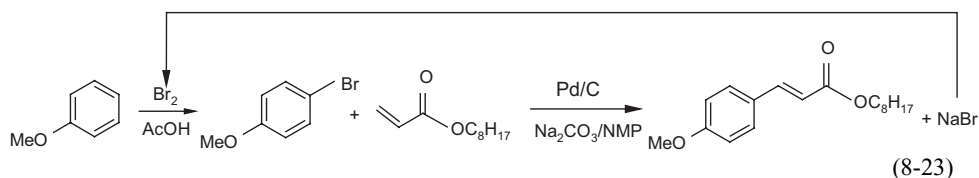
Hoffmann La Roche has developed a process for the anti-Parkinsonian drug, lazabemide, by amidocarbonylation of 2,5-dichloropyridine [7]. This one-step route affords lazabemide hydrochloride in 65% yield with 100% atom efficiency and replaced an original synthesis that involved eight steps with an overall yield of 8% (Eq. 8-21).



Another method that is widely used for C-C bond formation is the *Heck coupling* [3]. The arylation of olefinic double bonds is mostly catalyzed by palladium complexes in homogeneous solution. Important advantages of this reaction are the broad availability of aryl bromides and chlorides and the tolerance of the reaction for a wide variety of functional groups. There were also developed heterogeneous Pd/C catalysts which exhibit high activity for the Heck reaction of aryl halides with olefins. The reaction conditions are 80–200 °C, solvents (NMP, DMF, toluene/water), base addition is necessary (NaOAc, amines, alkali carbonates). The reaction scheme can be described as follows (Eq. 8-22).



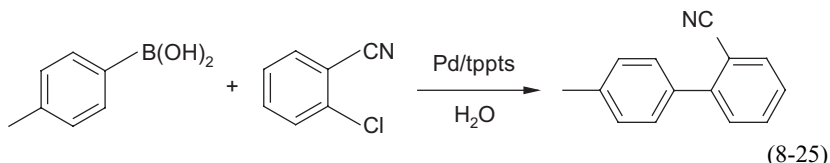
Formally a vinylic hydrogen is replaced by an aryl group during this reaction. The preferred substrates are aryl bromides and aryl iodides, especially bearing electron-withdrawing substituents. Aryl chlorides, which have a much lower reactivity, require higher Pd loadings as heterogeneous catalysts are used. Until now, several industrial production processes have been described using Heck coupling. As example may serve octyl-4-methoxycinnamate, the most common UV-B sunscreen. In the first step, anisole is brominated in the *p*-position. The following Heck coupling with octyl acrylate at 180 °C using a Pd/C catalyst leads to the final product (Eq. 8.23). The advantages of this commercial process are that the resulting salt NaBr is recycled to bromine and that the Pd catalyst can easily be separated from the product [3].



A closely related cross coupling reaction, the so-called *Suzuki coupling* of aryl-boronic acids with aryl halides leads to biphenyl groups under very mild conditions in the presence of a Pd catalyst. Due to the stability, ease of preparation and low toxicity of the boronic acid compounds, the reaction has attracted much attention. The general reaction scheme can be depicted as follows (Eq. 8-24).



For example, *o*-tolyl-benzonitrile, is produced by Clariant using the Suzuki coupling (Eq. 8-25). The compound is a key intermediate for the production of a series of so-called angiotensin-II receptor antagonists against high blood pressure [3].

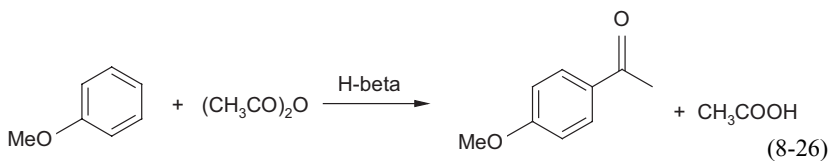


In general, aryl chlorides are not reactive enough for Pd catalysts. However, in this special case, the aryl-chlorine bond is highly activated by the strongly electron-withdrawing nitrile group in *o*-position. The coupling reaction is carried out in a two-phase process using a water-soluble sulfonated Pd-phosphine complex.

8.3.2.4 Acid/Base Catalysis [7]

Catalysis by solid acids and bases is another area of current interest for the industrial manufacture of fine chemicals. In many cases strong mineral or Lewis acids (i.e. H_2SO_4 or AlCl_3) which are often used in stoichiometric quantities, can be replaced by recyclable solid acids such as zeolites and clays.

For example, the Friedel-Crafts-acylation of anisole with acetic anhydride with the acidic zeolite H-beta leads to *p*-methoxyacetophenone in fixed-bed operation (Eq. 8-26). Compared with the traditional process, using more than one equivalent of AlCl_3 (Eq. 8-27), the number of unit operations could be reduced from 12 to 2 by Rhône-Poulenc.



Important aspects of both processes are compared in Table 8-6. It is clear that the use of solid acid catalysts is proving advantageous.

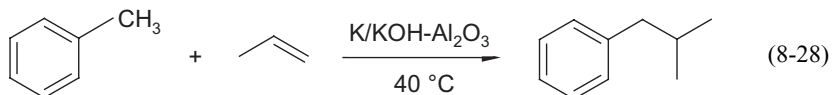
Table 8-6 *p*-Methoxyacetophenone via zeolite-catalyzed versus classical Friedel–Crafts acylation [7]

| Homogeneous process | Heterogeneous process |
|--|---|
| $\text{AlCl}_3 > 1$ equiv., stoichiometric | zeolite H-beta, catalytic and regenerable |
| Solvent | – |
| Hydrolysis of products | no water necessary |
| Phase separation | – |
| 85–95% yield | > 95% yield, higher purity |
| 4.5 kg aqueous effluent per kg | 0.035 kg aqueous effluent per kg |

There are also some examples of commercially applied solid base catalysts in fine chemistry:

- Hydrotalcite clays as solid bases can catalyze aldol-condensations or Knoevenagel-condensations
- Bulky guanidine derivatives/zeolite Y can act as “ship in a bottle” catalysts
- Solid super bases can be prepared by successive treatment of γ -alumina with alkali metal hydroxide and alkali metal

For example, isobutylbenzene as starting material for ibuprofen synthesis is produced by side-chain alkylation of toluene with solid super-base by Sumitomo (Eq. 8-28).



These few illustrative examples can only briefly describe the application of catalysis in fine chemicals production. In future, companies will choose more catalytic routes since these are mostly shorter and lead to cheaper processes than noncatalytic processes.

► Exercises for Section 8.3

Exercise 8.9

Characterize fine chemicals and their behavior in processing.

Exercise 8.10

Distinguish among the following forms of selectivity: chemoselectivity, regioselectivity, stereoselectivity.

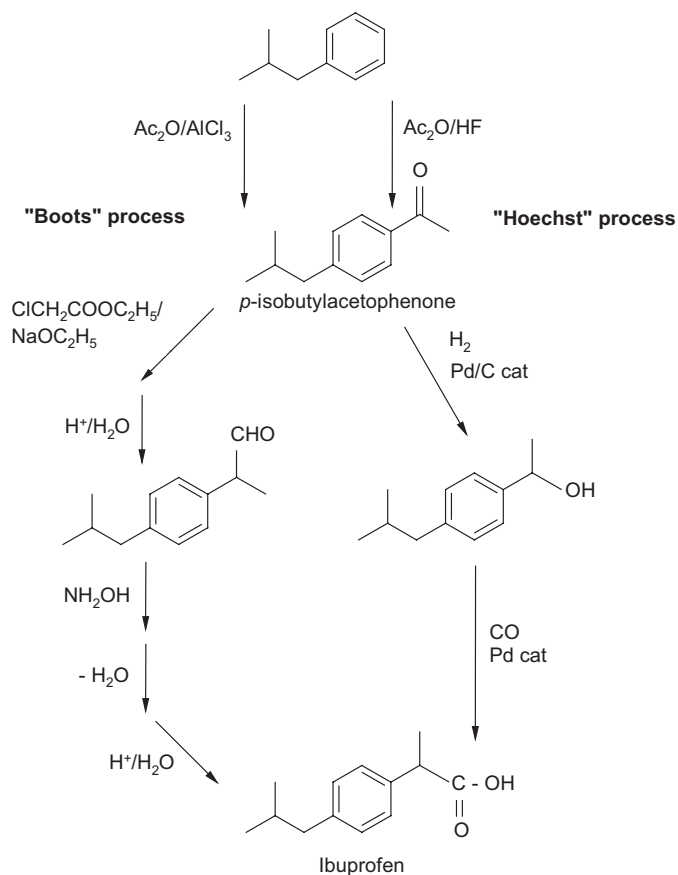
Exercise 8.11

A trend in fine chemistry is the use of reactants that do not produce by-products with unfavorable properties. Give examples for

- Oxidation
- Hydrogenation and
- Acid-base catalysis

Exercise 8.12

Ibuprofen can be manufactured via two routes, the classical Boots process (the inventor of the drug) and a new route developed by Hoechst Celanese. Both routes share the intermediate, *p*-isobutylacetophenone. Compare both processes:



9

Electrocatalysis

9.1

Comparison Between Electrocatalysis and Heterogeneous Catalysis [5, 9]

Electrochemistry is the surface science studying the physicochemical phenomena at the interface between an electrode and the electrolyte. The aim of electrocatalysis is to accelerate electrochemical reactions taking place at the electrode surface.

The most important parameters in electrocatalysis are the overpotentials, which arise from the losses due to the kinetics at the electrodes and transport losses in the electrolyte. The goal is to have low overpotentials η_i at high currents. In electrocatalysis the current is referred to the electrode surface thus obtaining the current density j . The dependence between overpotentials η and current density j is described by the Tafel equation (Eq. 9-1)

$$\eta = A + S \log \frac{j}{j_0} \quad (9-1)$$

in which S is called the Tafel slope and j_0 is the exchange current density, that is correlated with the heterogeneous rate constant k_0 (Eq. 9-2).

$$j_0 = z F k_0 c \quad (9-2)$$

where z is the number of exchanged electrons and c the concentration of electrochemical active species. The electrocatalyst for an desired electrochemical reaction is optimal, when η is low with high exchange current density and low Tafel slope.

If we restrict our discussion to the catalytic effect of the nature and structure of the electrode material and we consider systems with polar liquid components (for instance, water or aqueous solutions) it is relatively easy to find a link between electrocatalysis and liquid phase heterogeneous catalysis. It is a well known fact that electrochemists learned a lot from catalytic people and many important ideas were taken from catalysis. The classical work of hydrogen overpotential were based on the recognition of the importance of catalytic effects. During the last decades, the effort to develop efficient fuel cells, oriented again the attention of electrochemist towards catalysis.

Electrocatalysis is the phenomenon that electrode reactions can be accelerated by structural or chemical modification of the electrode surface and by additives to the electrolyte. Structural modifications include changes in surface geometry (crystal planes, clusters, adatoms), and variations in the electronic state of the catalyst material. Electrode reactions are connected with a transfer of electric charge carriers through the interface between the electrode and the electrolyte. These charge carriers can be ions or electrons.

Very close to heterogeneous catalysis are redox reactions at electrodes where only electrons pass the interface and the electrode surface remains unaffected after the reaction has reached a steady state. But there is still a basic difference to heterogeneous chemical reactions being catalyzed by a solid. In the case of an electrode reaction, the catalyst contributes one of the reactants to the process, the electrons, which are either consumed or generated in the net reaction. Charge transfer rates and electrosorption equilibria depend exponentially on electrode potential. Therefore, the driving force of an electrode reaction is not only controlled by the chemical forces, which depend on temperature, pressure, reactant concentrations etc., but also by electrical forces which affect the rate of electron transfer through the interface.

These electric forces can be characterized by the so-called electrode potential relative to a suitable reference electrode which can be altered in an electrolysis cell by an external voltage applied to this cell. A great advantage is that the rate of the reaction can be followed with high sensitivity in the form of the electric current passing the electrode interface.

The closest resemblance between electrocatalysis and heterogeneous catalysis exists in the role of adsorption and chemisorption of the reactants or of intermediates of a reaction on the rate of the process. The main field of electrocatalysis are redox reactions which occur in several steps. Slow intermediate chemical reactions in multielectron electrode reactions that are usually hindered due to chemical kinetics, can often be accelerated very strongly by means of heterogeneous catalysis at the electrode surface.

9.2

Electrochemical Reactions and Electrode Kinetics

9.2.1

Hydrogen Electrode Reaction [5]

The classical example of electrocatalysis is the electrochemical evolution of molecular hydrogen from aqueous electrolytes and the reverse process, the electrolytic oxidation of molecular hydrogen on metal electrodes. In these reactions, hydrogen atoms are formed as intermediates and remain adsorbed on the electrode. The strength of the adsorption becomes decisive for the rate of the reaction.

Electrocatalysts for cathodic hydrogen evolution or its oxidation and catalysts for chemical hydrogenation are essentially the same: platinum and the transition metals of group 10 of the periodic table. Hence, for catalysis and electrocatalysis the same correlation of catalytic activity in terms of exchange current density (mA/cm^2) and

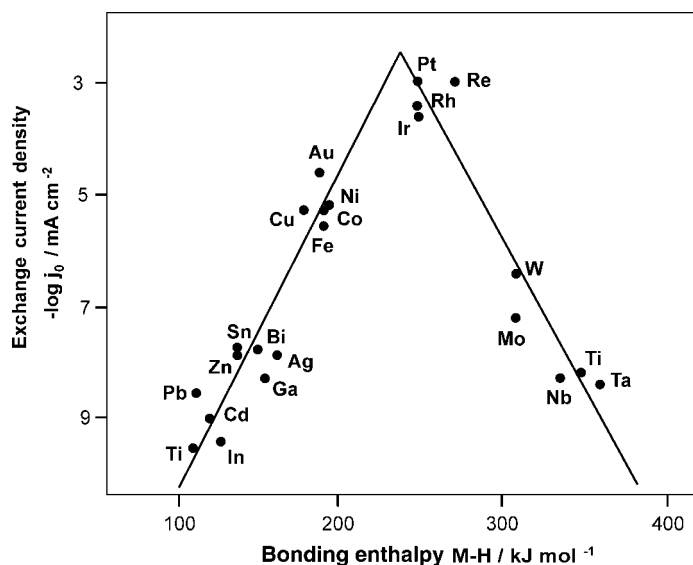
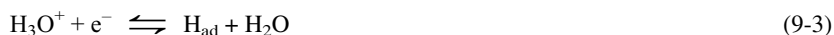


Fig. 9-1 Hydrogen volcano curve: logarithm of exchange current density of H₂ reaction vs. enthalpy of hydrogen adsorption at different metals. (Courtesy V. M. Schmidt, Mannheim, Germany)

hydrogen adsorption enthalpy at the respective metal catalyst prevails, the volcano curve (Fig. 9-1).

Figure 9-1 illustrates, that the catalytic activity of those metals is optimum which adsorb hydrogen only to a moderate extent and can thus assist H₂ splitting without hindering its desorption. The process in acidic solution can be described by the following steps (Eqs. 9-3 and 9-4):



Reaction (9-3) is called the Volmer reaction or proton discharge and reaction (9-4) the Heyrovsky reaction or electrochemical desorption. Both reactions are not the only ones possible. Desorption of the adsorbed hydrogen may also proceed according to the Tafel reaction (Eq. 9-5):



Eq. (9-5) describes the pure chemical dimerization of two adsorbed hydrogen atoms, the chemical recombination, which should not be directly affected by the electrode potential.

Reactions 9-3 and 9-4 are connected by a charge transfer through the electrode/electrolyte interface, their rates therefore depend on the electrode potential relative to the electrolyte.

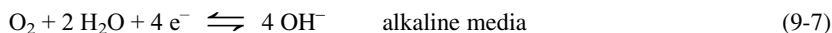
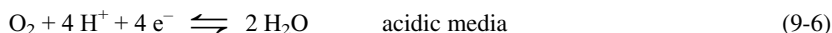
The thermodynamic activity of adsorbed H atoms depends not only on their total concentration but also on the individual properties of the electrode surface, its local crystallographic orientation, its morphology and the presence and concentration of defects in the lattice structure. All these effects influence the activation energies of the reactions, too.

We are able to give a thermodynamic basis for the distinction between catalytic and electrocatalytic approach to a given system. In the case of catalytic hydrogenation H_2 and H^+ should be considered as components of the system. In contrast to this, treating the system in terms of electrocatalysis H^+ and electrons have to be considered as components.

9.2.2

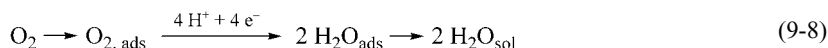
Oxygen Electrode Reaction [6, 9]

The electrocatalytic reduction of oxygen according to the overall equations following a direct four-electron pathway (Eqs. 9-6 and 9-7):

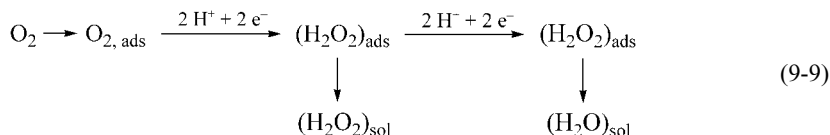


can occur via various mechanisms. However, two main types of mechanisms should be distinguished.

- a) The complete reduction occurs on the surface without formation of intermediates desorbing from the surface (Eq. 9-8):



- b) The reduction occurs in two distinct steps, hydrogen peroxide is formed as an identifiable intermediate (peroxide pathway) (Eq. 9-9):



An optimum catalysis of the oxygen electrode reaction depends on a critical compromise of adsorption energies of the intermediates. It is, therefore, not surprising that no electrocatalyst has been found where this reaction occurs reversibly at ambient temperatures. In both directions rather large overvoltages are required to reduce O_2 to H_2O or to oxidize H_2O to O_2 .

Electrochemistry offers a wide variety of possibilities of studying surfaces of solid conductive systems such as metal catalysts. It has been proved that voltammetric methods constitute a very sensitive tool for the characterization of the state of a sur-

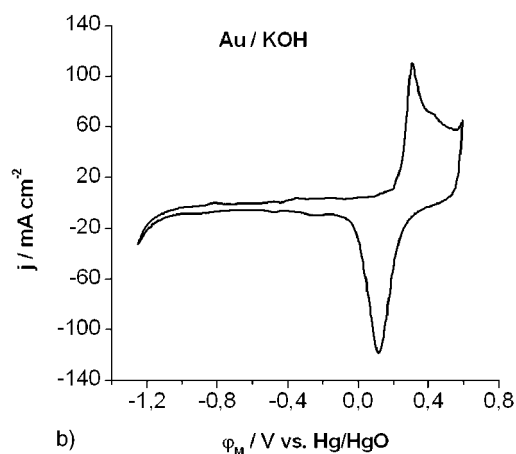
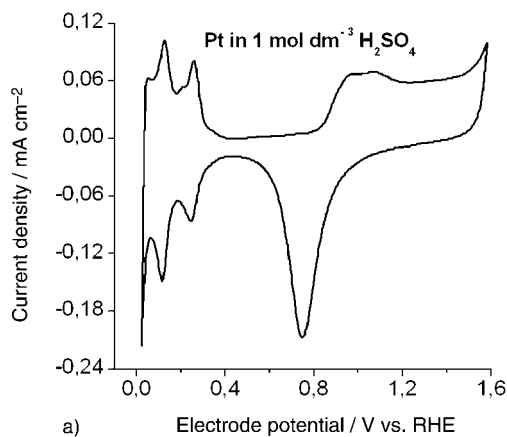
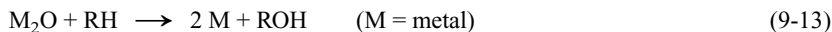


Fig. 9-2 Cyclic voltammetry of two electrocatalysts: a) Pt in acidic electrolyte solution, b) Au in alkaline electrolyte solution. The potential scan rate: $\nu = 50$ mV/s; two different reference electrodes were used, RHE: reversible hydrogen electrode, Hg/HgO: mercury/mercury oxide electrode. (Courtesy V. M. Schmidt, Mannheim, Germany)

face. A significant effort has been made to explain the behavior of polycrystalline surfaces by the combination of effects originating from well-defined crystal faces.

The hydrogen and oxygen adsorption is reflected by more or less defined peaks on the cyclic voltammetric curves. Evidently, the shape of these curves depends on the nature of the catalyst and the state of its surface. For example, a characteristic cyclic voltammetric curve is shown in Figure 9-2.

Anodic oxygen evolution and cathodic reduction of O₂ as well as anodic oxidation of organics are catalyzed by the same metals or metal oxides. The latter are also used in chemical catalysis for catalytic oxidation of organic compounds. These catalysts undergo relatively easy redox conversion with oxygen or are oxidized anodically to a higher valency state at potentials which are close to the oxygen equilibrium potential, thus facilitating the transfer of oxygen from oxidized surface groups of the catalyst to organic substrates (Eqs. 9-10 to 9-13).



The reaction overpotential versus enthalpy of formation for different transition metal oxides is shown in Figure 9-3.

Going from lower to higher oxides a type of volcano curve of anodic O_2 -evolution, is obtained.

In practice, there are two different kinds of electrochemical reactions of technical importance.

In *direct electrochemical reactions* the substrate undergoes a heterogeneous redox reaction at the electrode surface within the Helmholtz layer. The thus formed reactive intermediate, i.e. a radical ion, undergoes the chemical follow-up reaction to the product in the reaction layer. There are steep concentration gradients near the electrode. Second-order reactions of the intermediates can thus be obtained at high current densities.

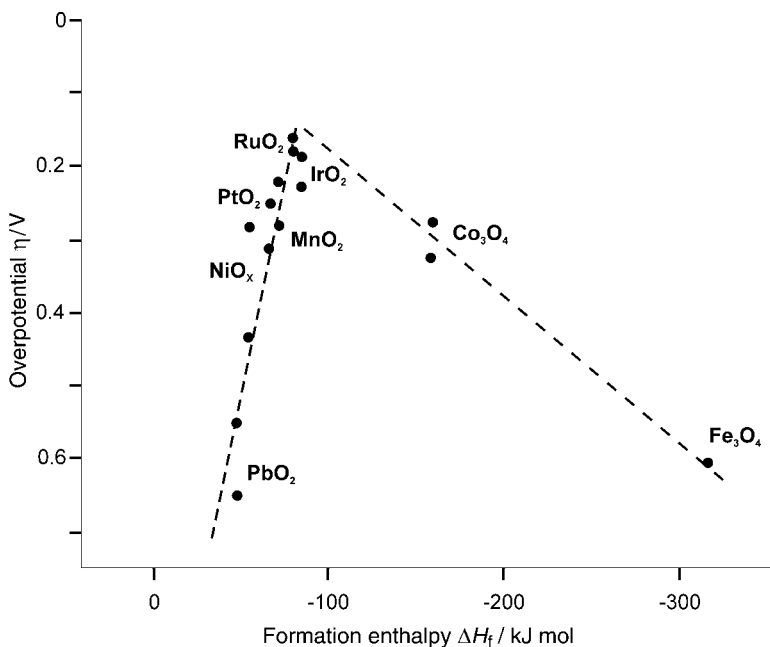


Fig. 9-3 Oxygen volcano curve: overpotential at 0.1 mA/cm^2 vs. formation-enthalpy of different metal oxides. (Courtesy V. M. Schmidt, Mannheim, Germany)

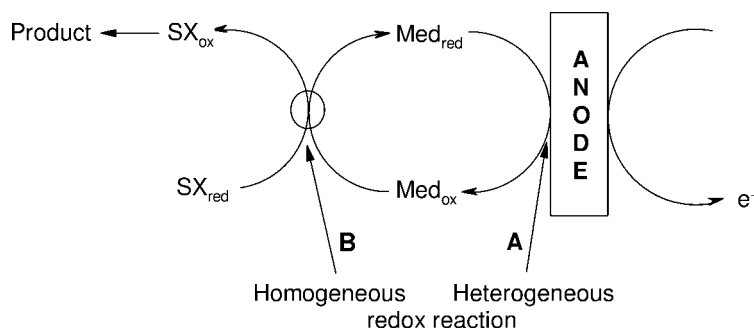


Fig. 9-4 Scheme of an indirect electrochemical process
(Med = mediator, redox catalyst; S = substrate)

In *indirect electrochemical reactions*, the heterogeneous reaction between the substrate and the electrode is replaced by a homogeneous redox reaction in solution between the substrate and an electrochemically activated and regenerated redox catalyst (Fig. 9-4).

First-order reactions may be favored under these conditions. In addition, overpotentials for the reaction of the substrate at the electrode may be avoided and reactions may be accelerated. Furthermore, if electrode passivation causes problems for direct electrolyses, an indirect pathway could be an advantage. In indirect processes often there are obtained better selectivities with redox catalysts.

Two types of redox catalysts are used in indirect electrolyses (Fig. 9-4):

- A) pure, outer-sphere or nonbonded electron transfer agents and
- B) redox reagents which undergo a homogeneous chemical reaction which is intimately combined with a redox-step.

In case A the mediator catalyzes the electron exchange between the electrode and the substrate. Advantages of this processing are as follows: reduced overvoltages, passivation of electrodes may be avoided, increase of the reaction rate.

In case B, the homogeneous redox reaction of the electrogenerated and regenerated redox catalyst consists of a chemical reaction. For oxidations, these reactions may be hydride ion or hydrogen atom abstraction, oxygen transfer or an intermediate complex or bond formation. For reductions, hydride or carbanion transfer from a metal complex is often observed. In all these cases, very large potential differences between the standard potential of the substrate and the redox catalyst may be overcome. All chemical steps involved must be very fast for an efficient redox system. If metal complexes are used as redox catalysts, a good selection of the metal ions and the ligands is necessary. For oxidations, also halide ions are applied. Typical examples of inorganic redox couples which are used for indirect electrolyses are:

- For oxidations:

Ce(III)/Ce(IV); Cr(III)/Cr(VI); Mn(II)/Mn(III); Mn(II)/Mn(IV);
Ni(OH)₂/NiOOH; I⁻/I₂; Br⁻/Br₂; Cl⁻/ClO⁻.

- For reductions:

Sn(IV)/Sn(II); Cr(III)/Cr(II); Ti(IV)/Ti(III); Zn(II)/Zn; Na(I)/NaHg.

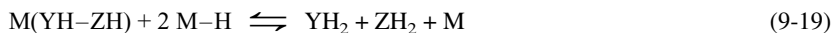
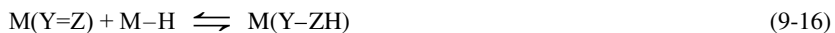
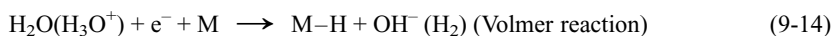
9.3

Electrocatalytic Processes

9.3.1

Electrocatalytic Hydrogenation [4, 8]

Hydrogenation of organic compounds is a very important reaction from the synthetic point of view. The electrocatalytic hydrogenation proceeds by the following steps (Eqs. 9-14 to 9-19):



In the first step of the reaction sequence (Eq. 9-14), the chemisorbed hydrogen M-H is generated by the electroreduction of water (or hydronium ions) at a cathode characterized by a low hydrogen overvoltage. The chemisorbed hydrogen that is formed is very reactive, it reacts with an organic unsaturated molecule Y=Z exactly as in catalytic hydrogenation (Eqs. 9-15 to 9-18). If the Y-Z bond is sufficiently weak, hydrogenolysis of the adsorbed hydrogenated molecule, shown in Eq. (9-19) can occur.

Electrochemical hydrogenation has several advantages over catalytic hydrogenation. Firstly, the kinetic barrier due to the splitting of the hydrogen molecules is bypassed, as is the mass transport of the poorly soluble hydrogen molecules. Elevated temperatures and high pressures can be avoided; hence, the reaction conditions are milder. In addition, the amount of chemisorbed hydrogen may be controlled by the current density or the potential. Secondly, the fact that a cathodic potential is applied to the catalyst in electrochemical hydrogenation can, in some cases, diminish or even prevent the adsorption of poisons. The main disadvantage of electrochemical hydrogenation, compared with catalytic hydrogenation, is the necessity of separation of reduction products from the supporting electrolyte. We will present some practical examples of the electrochemical hydrogenation as follows.

Catalytic hydrogenations are favored at low overpotential electrodes (Pt, Ni, C, Fe) whereas direct electroreductions and dimerizations would be most efficient at high-overpotential electrodes (Hg, Pb, Cd). Hydrogen overpotential values vary from 0.0 V for platinized platinum to 1.2 V for Cd relative to the normal hydrogen electrode. High- and low-hydrogen overvoltage electrodes are used on an industrial scale.

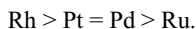
Noble metals are catalytically very active, and many studies have been carried out on their surfaces, especially platinum, palladium, and rhodium. Noble metals have been used as polycrystalline metals or monocrystals, metal blacks, metals supported on graphite, microparticles incorporated into redox active polymers, etc. The activity of these materials towards the electrocatalytical hydrogenation depends mainly on the nature of the metal, pH, and supporting electrolyte, and the state of the surface.

Platinum is among the most active catalysts. Ethylene is reduced to ethane on Pt, Pd, and Ru electrodes. Electrocatalytic hydrogenation of acetone, acetaldehyde, and acetophenone on platinized Pt in acidic solution produces the corresponding hydrocarbons, whereas in alkaline media, alcohols or dimers are obtained. Phenol may be reduced to cyclohexanol on Pt in acidic solutions. Pt deposited or supported on carbon is more active than platinized Pt. However, the highest yield was observed on Rh/C. Substituted phenols are more difficult to reduce than the unsubstituted phenol.

With Pd black electrodes, many organic compounds such as nitriles, alkynes, alkenes, aldehydes, carbonic acids, anthracene, etc. can be reduced. The electrocatalytic hydrogenation of benzaldehyde on a Pd electrode, deposited on carbon felt at potentials below the limiting current, gave a uniform deposit and produced principally benzyl alcohol with small amount of toluene, whereas Pd deposited at potentials corresponding to the limiting current formed irregularly distributed clusters, and the main product was toluene [8].

Another method of carrying out the electrocatalytic hydrogenation of organic compounds consists of deposition of metallic particles (Au, Pt) on both sides of a polymer electrolyte (Nafion). During electrolysis, oxygen and protons are produced on the anode, which is in contact with water. Protons migrate through the membrane, to be reduced on the cathode, thereby forming adsorbed hydrogen active in hydrogenation of olefinic compounds like dimethyl maleate, cyclooctene, and α -methylstyrene. An advantage of this method is that it is working without any supporting electrolyte, facilitating the separation of the products.

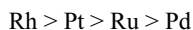
The electrocatalytic hydrogenation of cyclohexanone to cyclohexanol was carried out using various supported catalysts [4]. The hydrogen generation takes place on the metallic sites, whereas the organic substrate is adsorbed on alumina or activated carbon acting as support. The electrocatalytic activity of metals dispersed on alumina particles decreased in the order



The ability of a metal to promote electrohydrogenation catalysis of a specific type of bond is not well understood. In the electrocatalytic hydrogenation process, where

atomic hydrogen is produced on metal by water electrolysis, the two key parameters are the kinetics of water electroreduction to hydrogen gas on a selected metal (characterized by the overpotential η) and the strength of the hydrogen-metal bond, described by ΔH_{ads} , the adsorption enthalpy of hydrogen on the metal.

On an activated carbon matrix, the electrocatalytic activity for the cyclohexanone hydrogenation decreases in the following order:

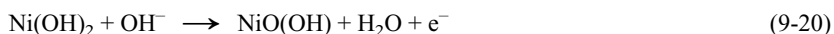


Rhodium is a very good metal catalyst for the hydrogenation of ketones because it shows the same activity in the presence of both adsorbents. It was stated that the electrocatalytic hydrogenation of cyclohexanone is largely dependent on the nature of both the metal nanoaggregates dispersed on a nonconductive matrix particle and the support particle. This reaction is improved by the use of activated carbon as the matrix material compared to alumina. It is deduced that the use of a very strong adsorbent matrix material for organic molecules, that is, activated carbon, is better than the use of a moderate adsorbent such as alumina.

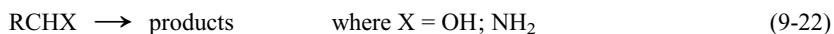
9.3.2

Electrocatalytic Oxidation [6, 7]

An advantage in electrocatalysis is realized with redox catalysts anchored to the surface of the solid face. The most important examples of these anchored systems are those where an oxide layer covers the surface. In this respect the nickel oxide/hydroxide electrode should be mentioned [6]. A $\text{Ni}(\text{OH})_2$ layer can be easily formed at any inert electrode surface and its oxidation can be achieved by shifting the potential of the electrode to an appropriate value (Eq. 9-20):



The nickel(III)-oxide-hydroxide thus prepared can be regarded as an active oxidation agent. Holding the potential of the electrode at this value and adding a reacting organic substrate to the solution phase the oxidation of the organic species takes place. The first steps of this oxidation can be formulated as follows (Eqs. 9-21 and 9-22):

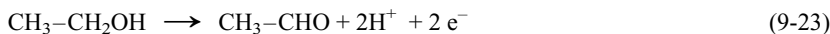


With regard to Eq. (9-20) a steady state coverage with $\text{NiO}(\text{OH})$ will be attained, i.e. continuous oxidation reaction with a continuous current flow will be observed under potentiostatic conditions. All this means that the nickel oxide catalyst is turned into a nickel oxide electrocatalyst, that can be used in electrosynthesis. The most important synthetic reactions employing such electrodes are as follows:

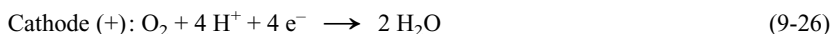
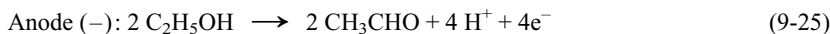
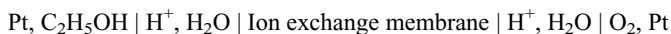
- Primary alcohols → carboxylic acids
- Secondary alcohols → ketones
- Primary amines → nitriles

A technologically important version of the first reaction is the oxidation of diacetone-L-sorbose to diaceto-2-keto-L-gulonic acid.

The oxidation of alcohols to aldehydes or ketones assumes new importance with long term attention to biomass based economics. Acetaldehyde, the product of ethanol oxidation, is of special interest since it can be utilized in the synthesis of other basic chemicals such as acetic acid, butanol, etc. [6]. The following Equations 9-23 and 9-24 can be formulated:



In this case the electrocatalytic oxidation of ethanol is coupled with the electrocatalytic reduction of oxygen. This reaction can be carried out with modern oxidation cells containing ion exchange membranes instead of liquid electrolytes, represented by the following arrangement including Equations 9-25 and 9-26.

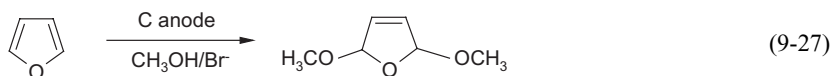


9.3.3

Electrochemical Addition [9]

As industrial important anodic addition reaction can be mentioned the synthesis of chiral 1,2-diols by indirect electrolysis. This reaction can be carried out, using a double mediator system consisting of ferricyanide and osmium tetroxide in the presence of chiral ligands. As an alternative to ferricyanide, electrogenerated iodine may be used. This reaction can be seen as an electrochemical variant of the asymmetric bishydroxylation introduced by Sharpless (Fig. 9-5).

The dimethoxylation of furan and furan derivatives using bromide redox catalyst gives 2,5-dimethoxy-2,5-dihydrofurans which can serve as interesting synthetic intermediates (Eq. 9-27):



This process is commercialized by BASF for the formation of succinic dialdehyde and by Otsuka, Japan, for the synthesis of maltol and ethyl maltol.

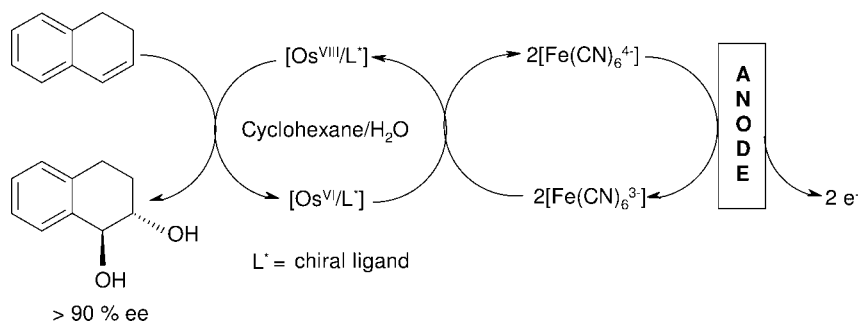


Fig. 9-5 Electrocatalytic asymmetric bishydroxylation using a double mediator system in the presence of chiral ligands

9.3.4

Electrocatalytic Oxidation of Methanol [8]

In this section we will discuss the role of surface modification to enhance electrocatalytic oxidation of methanol, one of the interesting components for fuel cell technology. Perhaps the most successful promoter of methanol electrooxidation is ruthenium. Pt/Ru catalysts appear to exhibit classical bifunctional behavior, whereas the Pt atoms dissociate methanol and the ruthenium atoms adsorb oxygen-containing species. Both platinum and ruthenium atoms are necessary for complete oxidation to occur at a significant rate. The bifunctional mechanism can account for a decrease in poisoning from methanol, as observed for Pt/Ru alloys. Indeed, CO oxidation has been attributed to a bifunctional mechanism that reduces the overpotential of this reaction by 0.1 V on the Pt/Ru surface.

Furthermore, a modifier may alter the electronic nature of the electrode. By changing the electric field at the surface, a modifier may affect the reactant-substrate interactions. A change in reactant-substrate interactions may be manifested, for instance, in a change in molecular orientation of the reactant molecule adsorbed on the surface. Clear evidence does exist for the influence of surface electronic properties on catalytic reactions. It is apparent that a modifier which acts through an electronic effect could influence both reaction kinetics and the tendency to poison.

Pt/Ru alloys exhibit lower susceptibility to poisoning than does pure platinum, as can be shown by a slower decay in current-time curves following a potential step. The reaction of methanol on Pt/Ru alloys results in CO₂ production at lower potential than does reaction on pure Pt, indicating enhanced complete oxidation by the ruthenium. When a high coverage of adsorbed CO develops on the Pt sites, the Ru sites facilitate its oxidation.

The promotion of methanol electrooxidation by tin modifier has been studied, too. The presence of tin appears to enhance the reaction at low potential, increasing the production of CO₂. The kinetic enhancement observed most likely result from an increase in the number of active catalyst sites for reaction due to decreased poisoning.

9.4 Electrocatalysis in Fuel Cells

9.4.1

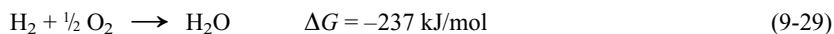
Basic Principles [2, 10]

Fuel cells are galvanic cells, in which the free energy of a chemical reaction is converted into electrical energy via an electrical current. The Gibbs free energy change of a chemical reaction is related to the cell voltage via Equation 9-28:

$$\Delta G = -nF\Delta U_0 \quad (9-28)$$

where n is the number of electrons involved in the reaction, F is the Faraday constant, and ΔG_0 is the voltage of the cell for thermodynamic equilibrium in the absence of a current flow.

The anode reaction in fuel cells is either the direct oxidation of hydrogen or the oxidation of methanol. An indirect oxidation via a reforming step can also occur. The cathode reaction in fuel cells is oxygen reduction, in most cases from air. For the case of a hydrogen/oxygen fuel cell the overall reaction according to Equation 9-29 is:



with an equilibrium cell voltage for standard conditions at 25 °C (Eq. 9-30) of:

$$\Delta U_0 = \frac{-\Delta G}{nF} = 1.23 \text{ V} \quad (9-30)$$

Fuel cell catalysis occurs in two parts of the fuel cell system: in the processing of the fuel before feeding it into the fuel cell stack and in the catalysts at the electrodes of the fuel cell.

Figure 9-6 describes a fuel cell system including all parts of a process: the fuel cell catalysis itself, gas processing (e. g., reforming of hydrocarbons like methane or methanol) and the catalytic burner for the off-gases [3].

As mentioned before, reactions at the surface of catalysts in electrochemical cells have much in common with heterogeneous chemical reactions. In both cases a mass transfer of species to and from the surface of the catalyst occurs. If more than just one reaction step has to be catalyzed, two or more different catalytic materials are required in the form of a bi- or multifunctional electrocatalyst.

Using only small amounts of catalytic material, the current density, which represents the rate of reaction per square centimeter of electrode surface, has to be as high as possible. Hence, the catalyst has to be finely distributed, in most cases on a suitable support such as high surface area carbon or graphite. The role of adsorption and chemisorption of reactants and/or intermediates on the rate of the processes is very similar to that in heterogeneous catalysis.

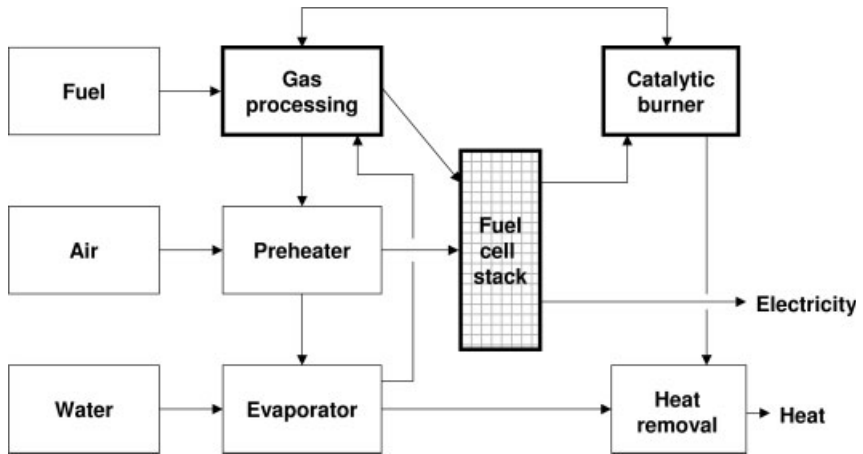


Fig. 9-6 Complete fuel cell system including gas processing

9.4.2

Types of Fuel Cell and Catalyst [1, 3]

Depending of the fuel applied and the nature of electrolyte, six fuel cells can be distinguished. These fuel cell systems are listed in Table 9-1.

With the exception of the direct methanol fuel cell (DMFC), characterization and nomenclature of the different systems is by the electrolyte and associated operating temperature. These features also govern the requirements of the electrocatalysts which control the reactions. The DMFC stands alone in involving a carbonaceous fuel (methanol) fed directly to the anode; all others use hydrogen as the anode fuel, either as a pure gas, or as a hydrogen-rich gas mixture. A catalytic steam reformer, or partial oxidation reactor, fed with methanol (or methane) is used to generate the hydrogen-rich gas mixture suitable for the fuel cell anode. This reformer/fuel cell system, fed with methanol, is sometimes referred to as the indirect methanol fuel

Table 9-1 Types of fuel cell

| | AFC | PEMFC | PAFC | MCFC | SOFC | DMFC |
|-------------|----------------|------------------------------------|---|--------------------------------------|--------------------------------------|----------|
| Electrolyte | KOH | Polymer | H ₃ PO ₄ | Molten carbonate | Ceramic | Polymer |
| Temp. (°C) | <100 | 60–120 | 160–220 | 600–800 | <1000 | 60–120 |
| Fuel | H ₂ | H ₂ , reformed methanol | H ₂ , reformed CH ₄ | H ₂ , CO, CH ₄ | H ₂ , CO, CH ₄ | methanol |

AFC = alkaline fuel cell; PEMFC = proton exchange membrane fuel cell; PAFC = phosphoric acid fuel cell; MCFC = molten carbonate fuel cell; SOFC = solid oxide fuel cell; DMFC = direct methanol fuel cell.

cell, since in contrast to the DMFC, it is still hydrogen that is ultimately oxidised on the fuel cell anode.

The *proton exchange membrane fuel cell* is unusual in that its electrolyte consists of a layer of solid polymer (mostly Nafion-membranes by DuPont) which allows protons to be transmitted from one face to the other [11]. It basically requires hydrogen and oxygen as its inputs, though the oxidant may also be ambient air, and these gases must be humidified. It operates at a low temperature because of the limitations imposed by the thermal properties of the membrane itself. The operating temperatures are around 90 °C. The PEMFC can be contaminated by carbon monoxide, reducing the performance by several percent for contaminant in the fuel in ranges of tens of percent. It requires cooling and management of the exhaust water in order to function properly. Figure 9-7 describes the principle of a PEM fuel cell with well-known nafion membrane.

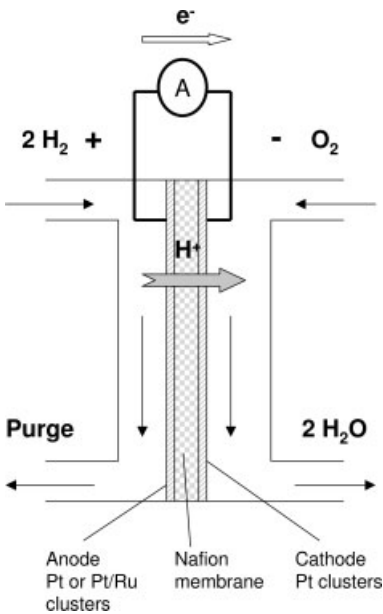


Fig. 9-7 Scheme of a PEM fuel cell

The main focus of current PEMFC designs is transport applications, as there are advantages to having a solid electrolyte for safety, and the heat produced by the fuel cell is not adequate for any form of cogeneration. It now appears, however, that there is a strong possibility of using the PEMFC in very small scale localised power generation, where the heat could be used for hot water or space heating. If it does prove possible to use this particular type of fuel cell for both transport and power generation, then the advantages generated by economies of scale and synergy between the two markets could make the introduction of the technology easier than in other cases.

Figure 9-8 shows a laboratory fuel cell device for education, consisting of fuel cell stack with four PEM fuel cells, different hydrogen gas supply devices (hydrogen

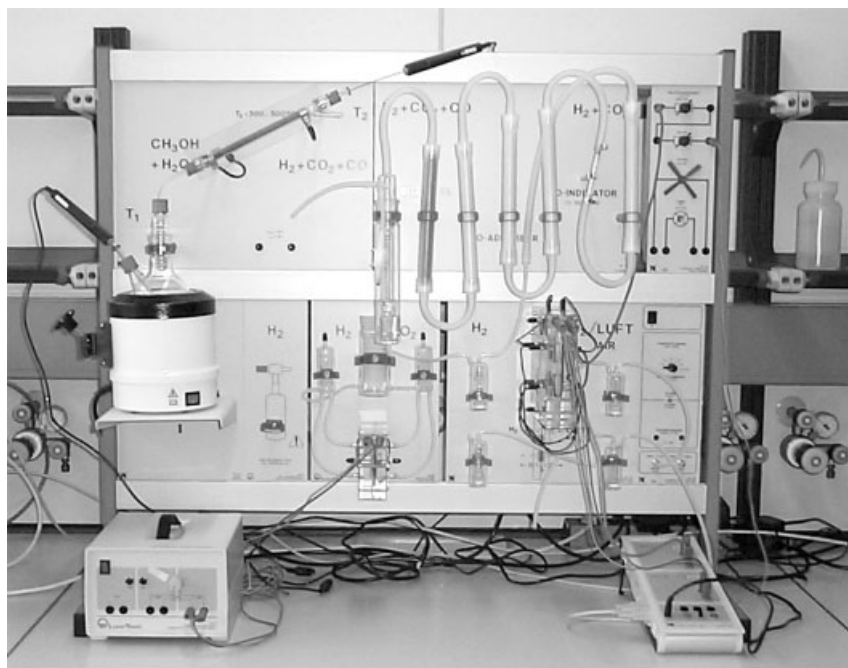


Fig. 9-8 Fuel cell device for education (Leybold Didactic; University of Applied Sciences Mannheim, Germany, Institute of Chemical Process Engineering)

tank, water electrolysis cell, methanol converter), air pump for oxygen supply, and automatic data acquisition by PC.

Apart from exhibiting electrocatalytic activity towards the electrode reactions, the electrocatalysts must be stable within the working cell. For the *alkaline fuel cell* (AFC) this is relatively easy since many electrocatalytic materials are adequately stable in alkaline solutions. The fact that the AFC is very sensitive to the presence of CO_2 , either in the fuel stream or in the air stream, has limited its application substantially to those situations where very pure hydrogen and very pure oxygen can be supplied.

For the fuel cells employing acidic electrolytes, stability of the electrocatalysts is much more difficult to realize. Many electrocatalysts have been examined over many years for their application to fuel cells. The nature of preferred electrocatalysts is critically dependent on the kind of fuel cell.

The high temperature *molten carbonate* and *solid oxide fuel cells* (MCFC and SOFC) present difficulties of thermal stability as well as compatibility with the electrolyte. Currently preferred electrocatalysts for the various cells are listed in Table 9-2.

Since most electrocatalysts for fuel cells are made from noble metals, particularly platinum, it is of practical importance, to minimise the loadings of the electrocatalysts over the electrodes and to maximise their effective utilization in the electrode structure.

Table 9-2 Electrocatalysts for the main fuel cell systems [1, 3]

| Fuel cell | Anode catalyst | Cathode catalyst |
|-----------|--|---|
| AFC | Pt/Au, Pt, Ag, Ni, Ni/Ti, Pt/Pd | Pt/Au, Pt, Ag, Pt on carbon, Ag or different perovskites or spinels |
| PEMFC | Pt, Pt/Ru | Pt, Pt/C, Pt alloys |
| PAFC | Pt | Pt/Cr/Co, Pt/Ni |
| MCFC | Ni, Ni/Cr | Li/NiO |
| SOFC | Ni/ZrO ₂ (Y)-cermet layers | perovskites, e. g. LaMnO ₃ , LaSrMnO ₃ |
| DMFC | Pt/Ru, Pt/Sn, Pt/WO ₃ | Pt, metal chelates, thiospinels |

9.4.3

Important Reactions in Fuel Cell Technology

9.4.3.1 The Anodic Reaction [1,2]

The oxidation of hydrogen occurs readily on Pt-based catalysts. The kinetics of this reaction is very fast on Pt catalysts and in a fuel cell the oxidation of hydrogen at higher current densities is usually controlled by mass-transfer limitations. The oxidation of hydrogen also involves the adsorption of the gas onto the catalyst surface followed by a dissociation of the molecule and electrochemical reaction to two hydrogen ions as follows (Eqs. 9-31 and 9-32):



Where $\text{Pt}_{(s)}$ is a free surface site and Pt-H_{ads} is an adsorbed H-atom on the Pt active site. The overall reaction of hydrogen oxidation is according Eq. (9-33):



Pure hydrogen provides the best fuel for the fuel cell anode. The manufacture of hydrogen from reformed natural gas, propane or alcohols (mainly methanol) provides a variable source. The reforming reaction does not, however, provide pure hydrogen; rather it produces a mixture of gases as output: H₂, CO₂, N₂ and CO. This mixture is hydrogen-rich, but the other components can restrict the performance of the anodes severely. Of most significance here is the production of carbon monoxide. CO is a severe anode catalyst poison. Amounts of less than 100 ppm CO in the gas feed can heavily poison the Pt catalyst. CO is itself very difficult to oxidize electrocatalytically at low overpotentials. Primarily, the effect appears to involve the adsorption of the CO to the electrocatalyst; once adsorbed, it is difficult to remove.

One method of combating poisoning of hydrogen electrodes by CO is to modify the catalyst using an approach in which the relative strength of the chemisorbed CO bond is reduced. It is more than 30 years since the discovery of Pt/Ru as an electrocatalyst which is relatively tolerant of CO (relative to pure Pt), and no significantly better electrocatalytic system has yet been found.

An alternative method of approaching the poisoning effect of carbon monoxide is to clean up the reformed fuel stream prior to admission to the fuel cell. For instance, methanol is fed to a reforming processor which produces a gas stream containing approximately 55% H₂, the required fuel mixed with 22% CO₂, 21% N₂ and 2% CO. The overall process is achieved by combining the exothermic partial oxidation reaction with an endothermic steam reforming reaction over the same catalyst particles. This achieves a very high rate of internal heat transfer and a very easily controlled reactor. In the last step the reformer output can then be fed to a „clean-up“ reactor where the fuel is reacted further with air to reduce the CO content from 2% to 10 ppm, a far more viable concentration for the electrocatalysts used in the low temperature fuel cell.

9.4.3.2 The Cathodic Reaction [10, 11]

The reduction of oxygen is itself a complex electrochemical process. As described in Section 9.2, O₂ reduction is considered to proceed along two parallel pathways, the direct four-electron pathway and the peroxide pathway (Eq. 9-9). Both pathways are compared in Figure 9-9.

If the O₂ molecule is adsorbed so that its axis is parallel to the catalyst surface, it divides into adsorbed oxygen atoms; these can be reduced and protonated to give water (Fig. 9-9, left side). The right-hand side shows the oxygen molecule adsorbed

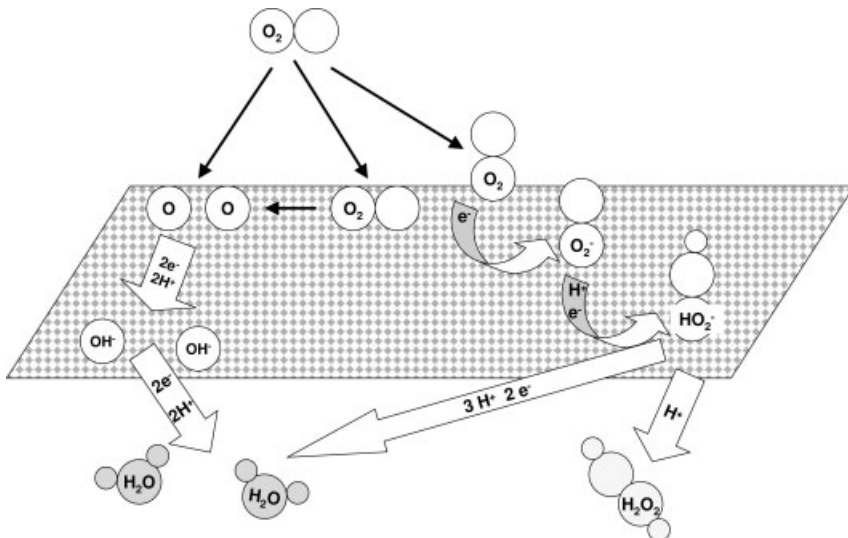


Fig. 9-9 Different reaction pathways for electrochemical oxygen reduction in acidic electrolytes [1]

with its axis vertical to the catalyst surface. In this case the O_2 molecule does not cleave; instead the peroxide anion HO_2^- is formed by partial reduction as an adsorbed intermediate. This intermediate can then be further reduced to water, or it can be protonated and leave the surface as hydrogen peroxide. Due to the complexity of this process, the cathode reaction requires a significant overpotential. Despite enormous research effort to find effective catalysts for oxygen reduction, the activation overpotential is at least 300–400 mV at current densities appropriate for fuel cell applications. Similar large polarization is observed for O_2 evolution. No material has yet been found, which optimally catalyses both processes.

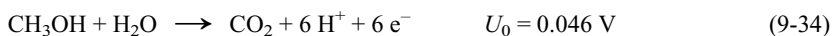
In alkaline solution the peroxide pathway is dominant and relatively fast. Organic or inorganic impurities at the surface favor this pathway. Generally, Pt is the most active catalyst. The reduction kinetics are faster in concentrated KOH or NaOH than in concentrated H_3PO_4 or H_2SO_4 . At highly dispersed Pt on carbon support, the reduction occurs predominantly via the four-electron pathway.

In alkaline and neutral solutions silver and carbon are also used as catalysts. In acid electrolytes carbon is not effective for O_2 reduction. New ways for oxygen reduction catalysis have been offered via the interaction of O_2 with transition metal complexes, as demonstrated for the face-to-face Co-Co-4 porphyrin and a number of transition metal macrocycles on carbon, graphite, or metal substrates. Heat treatment at 700–1200 K of macrocycles such as cobalt tetramethoxyphenyl porphyrin (Co-TMPP) and Fe-(TMPP) improve the activity in alkaline and acid media, respectively.

9.4.3.3 Methanol Oxidation [2, 10]

The direct methanol fuel cell is a special form of low-temperature fuel cells based on PEM technology. In the DMFC, methanol is directly fed into the fuel cell without the intermediate step of reforming the alcohol into hydrogen. Methanol is an attractive fuel option because it can be produced from natural gas or renewable biomass resources. It has the advantage of a high specific energy density, since it is liquid at operation conditions. The DMFC can be operated with liquid or gaseous methanol/water mixtures.

Very few electrode materials have been shown to be capable of adsorbing methanol in acidic media, and of these only Pt-based materials display a high enough stability and activity to be attractive as catalysts. The overall reaction mechanism for methanol oxidation is (Eq. 9-34):



It is assumed that the oxidation of methanol on Pt based catalysts proceeds by the adsorption of the molecule followed by several steps of deprotonation. A scheme for this adsorption is given in Figure 9-10.

The scheme shows that CO is formed during the oxidation of methanol. This CO species can block the surface of the catalyst and hinder any further reaction. For this reason a number of co-metals are usually added to the Pt catalyst to facilitate CO re-

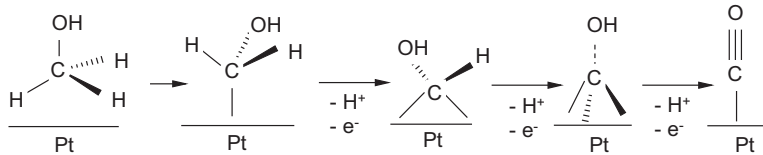
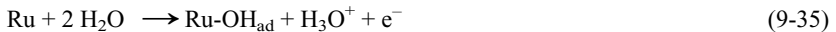


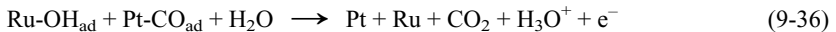
Fig. 9-10 Scheme of methanol oxidation on Pt catalysts [2]

removal by oxidation to CO_2 . This can be achieved by oxidising the CO species using oxygen containing species adsorbed at the surface either from the water in solution or hydroxide ions.

Much research has been carried out on catalysts for methanol oxidation (see also Section 9.3.4) to find a catalyst which can avoid the poisoning effect of the CO species. Several promoters have been found to increase the activity of the Pt catalyst. One of the most important and most investigated promoter is Ru. A bimetallic alloy consisting of Pt and Ru supported on carbon has thus far been one of the major research interests in DMFC technology. The action of Ru can be explained as follows. The adsorption of H_2O molecules at Ru surfaces takes place with lower overvoltages (Eq. 9-35).



The subsequent oxidation of CO_{ad} occurs by the adsorbed OH species (Eq. 9-36).



Other promoters such as Sn, Os, W, Mo and other metals have also been investigated for methanol oxidation and CO poisoning.

What we have seen is, that electrocatalysts are vital components of fuel cell systems. Much progress has been made over the years in improving their effectiveness both for anode and cathode reactions. There is nevertheless scope for considerable improvement in the performance of the electrocatalysts, particularly at the air cathode, where large activation overpotentials should be overcome. With the anode reaction also, electrocatalysts more tolerant to carbon monoxide should allow the use of less pure hydrogen and stimulate performance. There is much room for further improvement in the design of catalysts for use in fuel cells, by increasing both activity and durability.

► Exercises for Chapter 9

Exercise 9.1

Electrode reactions can be accelerated by means of electrocatalysis. Give reasons.

Exercise 9.2

In which way can the thermodynamic activity of adsorbed H atoms be affected at electrode surfaces?

Exercise 9.3

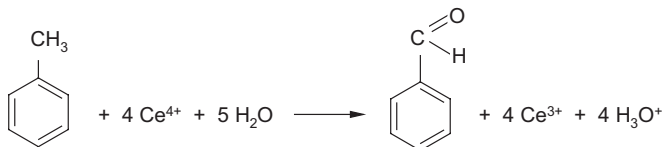
Provide the main advantages of electrochemical hydrogenation.

Exercise 9.4

What kinds of electrodes are favored for electrocatalytic hydrogenations?

Exercise 9.5

Explain the following electroorganic synthesis of benzaldehyde from toluene:



The redox system $\text{Ce}^{4+}/\text{Ce}^{3+}$ is diluted in perchloric acid.

Exercise 9.6

Which fuel cell reaction requires a higher overpotential?

- the anodic reaction
- the cathodic reaction

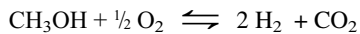
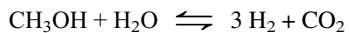
Explain the difference.

Exercise 9.7

Despite methanol is an attractive fuel, the direct methanol fuel cell DMFC has some disadvantages in comparison with the PEMFC using H_2 as fuel. List some reasons.

Exercise 9.8

Hydrogen as a feed for fuel cells can be produced from methanol by steam reforming with CuO/ZnO/Al₂O₃ catalysts at 200–300 °C. The following reactions occur:



In addition to CO₂ and H₂ the produced gas stream contains ~2% CO. Give the reason.

Exercise 9.9

Why is the PEM fuel cell so sensitive to CO, while the SOFC or the MCFC cell are not?

10

Environmental Catalysis and Green Chemistry

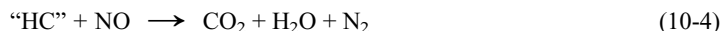
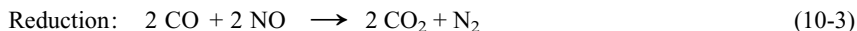
Traffic and industry are the most important sources of air pollution. They are responsible for the emission of CO, nitrogen oxides (NO_x), sulfur oxides (SO_x), and all sorts of volatile organic compounds (VOCs). Therefore, environmental catalysts are necessary for cleaning flue gases. Here we concentrate only on some topics, namely

- Automotive exhaust catalysis
- NO_x removal systems
- Catalytic afterburning of VOCs

10.1

Automotive Exhaust Catalysis [2, 3]

For the conversion of automotive exhaust gases the three-way catalyst (TWC) enables the removal of the three pollutants CO, NO and hydrocarbons („HC“) in the following manner (Eqs. 10-1 to 10-4):



The three-way catalyst allows the treatment of the two reducing pollutants, CO and “HC” (C_xH_y), and the oxidizing pollutant, NO_x, it has been in use since 1979. All reactions are running simultaneously, therefore, the composition of the exhaust gas must be carefully adjusted to an air-to-fuel ratio of 14.7 using an oxygen sensor (the so-called lambda-probe). At higher oxygen content, that means under lean-burning conditions with air-to-fuel ratios of about 20 : 1, the NO_x reduction is extremely difficult. This negative effect is reasonable, because the CO oxidation reaction consumes too much CO and hence the NO conversion fails. On the other hand, if the oxygen content is too low all of the NO_x is converted, but hydrocarbons and CO

are not completely oxidized. The actual support of a monolith is called „washcoat“, which provides a high surface area for the active catalyst.

The three-way catalyst compositions is 70% cordierite substrate ($MgAl_2O_4$) and the washcoat:

- 20–25% γ - Al_2O_3 (or α - Al_2O_3 , ZrO_2)
- < 10% CeO_2 , BaO , etc. (oxygen storage, stabilizer)
- 0.2–0.6% Pt, Pd (CO, HC conversion)
- 0.04–0.06% Rh (NO_x activity)

The three-way catalyst represents a remarkably successful area of catalytic technology. The main shortcoming of the three-way catalyst is only, that it is not good enough under lean (oxygen-rich) conditions.

10.2

NO_x Removal Systems

The main technologies to remove NO_x are as follows:

- The selective catalytic reduction (SCR) (Eq. 10-5):



- The catalytic decomposition to elements (Eq. 10-6):



10.2.1

Selective Catalytic Reduction of Nitrogen Oxides [8]

Selective catalytic reduction (SCR; DENOX process) is the reduction of NO and NO_2 (NO_x) by ammonia in the presence of oxygen to give molecular nitrogen. Since the 1970s SCR processes have been used to an increasing extent for the catalytic after-treatment of flue gases from power stations and furnaces. In Germany the limiting NO_x value for new coal-fired plants with a power output of 300 MW is 200 mg/m^3 . Such low NO_x levels can only be achieved by applying secondary measures. The 3–12% oxygen in the flue gas also takes part in the reaction, as shown for NO in Equation 10-7.



It can be assumed that in the presence of an excess of oxygen, NO reacts with an equimolar quantity of NH_3 to give N_2 and H_2O .

The catalysts must be designed so that side reactions such as the oxidation of ammonia by oxygen (Eq. 10-8) and the formation of N_2O (Eq. 10-9) are suppressed. The oxidation of SO_2 to SO_3 must also be avoided.



Transition metal oxides on ceramic supports have proved to be particularly suitable as catalysts; for example: support: TiO₂ (ca. 90 %), active components: V₂O₅ (1.5–5 %), WO₂ (5–10 %), MoO₃, GeO₂. Sheet or honeycomb catalysts are used industrially, and the usual operating temperature is 350–400 °C. Figure 10.1 shows honeycomb catalysts for air purification.

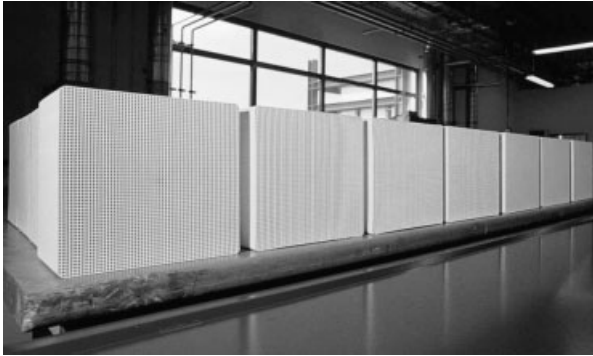


Fig. 10-1 Honeycomb catalysts for air purification (Süd-Chemie AG, Heufeld, Germany)

A mechanistic proposal (Fig. 10-2) explains the formation of N₂ besides N₂O and H₂O [12]. On the hydroxyl-group-containing surface of the oxide, ammonia is adsorbed on Brønsted acid centers with formation of an ammonium structure (step 1). In step 2, NO undergoes addition to the ammonium complex according to the Eley–Rideal mechanism. The resulting complex has two possible decomposition routes. In the major route (step 3 a), an N≡N bond is formed and N₂ and H₂O are cleaved off. In the following reaction (step 4 a), oxygen is filled up and water is released by the catalyst surface. In the minor route (step 3 b), lattice oxygen is abstracted from the catalyst, and N₂O and H₂O are formed. In step 4 b the oxygen vacancy is filled and water is cleaved off to regenerate the original catalyst.

In industry, two variants of the process compete with one another [7]. In the first variant, the SCR reactor is located in the high-dust high-temperature region directly after the boiler on the raw-gas side. The flue gas enters with a temperature of 300–450 °C and a dust content of 10–30 mg/m³ (high-dust configuration). Since this variant involves strong abrasion and more rapid poisoning of the catalyst, bulk catalysts on the basis of V, W, or Ti oxides are used. In the second variant, the SCR reactor is located after the flue gas purification and desulfurization stages (low-dust configuration). Since abrasion and poisoning are much lower in this case, honeycomb and sheet catalysts can also be used. A disadvantage is that the flue gas leaving the desulfurization stage at 50–70 °C must be heated to the reaction temperature of 300–350 °C.

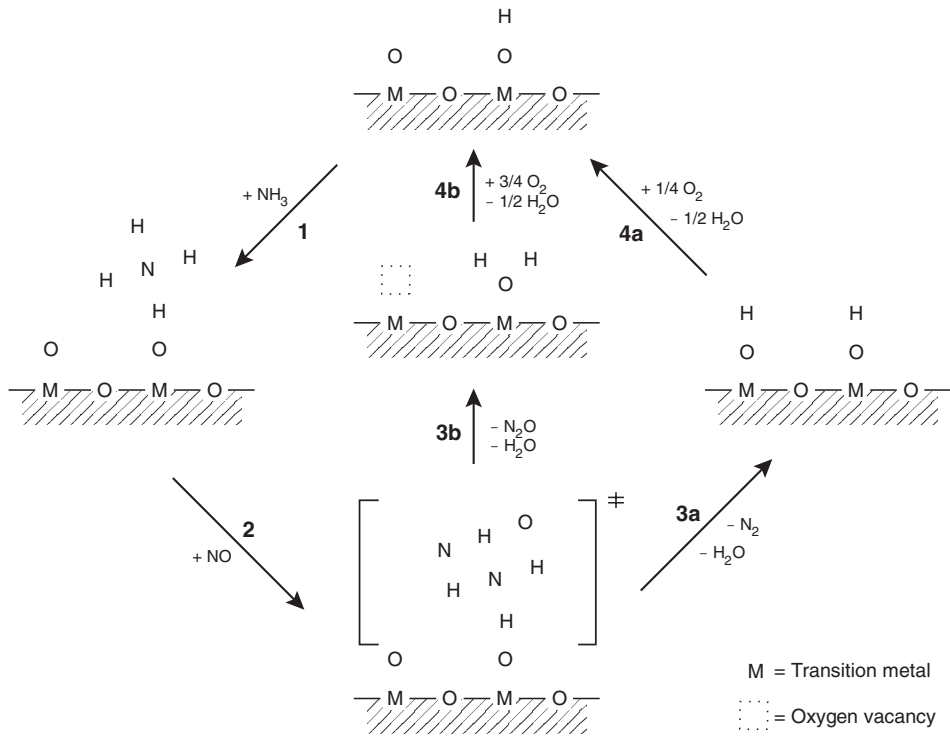


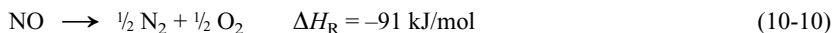
Fig. 10-2 Mechanism of the selective catalytic reduction of NO by NH₃ [12]

The SCR processes have become established in Western Europe, and the required TiO₂/V₂O₅ based honeycomb catalysts are produced by various European catalyst producers under a Japanese license.

10.2.2

NO_x Storage-Reduction Catalyst for Lean-Burning Engines

The NO_x abatement in Diesel and lean-burn Otto engine exhaust gases is of special interest. The direct decomposition of NO into N₂ and O₂ (Eq. 10-10) is a dream reaction for catalyst researchers:



The reaction is strongly exothermic, hence the equilibrium constant favors the reaction at low temperatures. It is well-known that Cu-zeolites can decompose NO directly to molecular oxygen and nitrogen, but unfortunately the zeolite is not stable under humid conditions. The main features of the Cu-ZSM-5 catalyst are:

- The reaction is a true decomposition and under controlled conditions a good material balance is achieved
- The decomposition passes through a reversible maximum with rising temperature at 500–600 °C
- The reaction order in NO is 1.0–1.2 and it may change with NO concentration
- Oxygen inhibits the reaction but the inhibition decreases with rising temperature
- Excess Cu loading in zeolite enhances the activity
- Sulfur compounds in the gas phase suppress the decomposition activity

Toyota has developed 1994a NO_x-storage-reduction (NSR) catalyst based on a two step process. The engine switches periodically between a long lean-burn stage and a very short fuel-rich stage. The NSR catalyst used in this process consists of two compounds: the active oxidation catalyst Pt and the NO_x storage compound based on BaO.

In the lean-burn stage all exhaust components are oxidized by the Pt catalyst and NO is oxidized to NO₂. The latter reacts with the basic storage compound BaO to yield Ba(NO₃)₂. In the fuel-rich stage which only lasts for seconds, the reducing agents CO, H₂, and hydrocarbons in the exhaust stream are able to reduce the Ba(NO₃)₂ to give N₂, CO₂ and H₂O. Figure 10-3 illustrates the overall process.

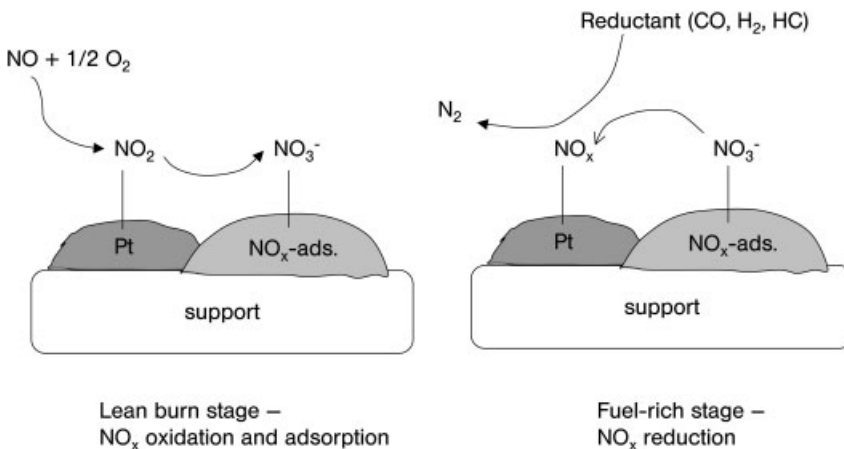


Fig. 10-3 Action of a NO_x-storage-reduction catalyst

Note that BaO is not a catalyst but reacts only in a stoichiometric manner with NO₂. A major difficulty limiting the general applications of the NSR catalyst is the sulfur sensitivity. Therefore, up to now this concept is only applicable in markets where low-sulfur fuels (< 30 ppm S) are available, such as in Japan and Sweden. The NSR technology claims to meet future standards and will find wider application all over the world.

10.3

Catalytic Afterburning [5, 11]

Afterburning processes enable the removal of pollutants such as hydrocarbons and volatile organic compounds (VOCs) by treatment under thermal or catalytical conditions. Combinations of both techniques are also known. VOCs are emissions from various sources (e.g. solvents, reaction products etc. from the paint industry, enamling operations, plywood manufacture, printing industry). They are mostly oxidized catalytically in the presence of Pt, Pd, Fe, Mn, Cu or Cr catalysts. The temperatures in catalytic afterburning processes are much lower than for thermal processes, so avoiding higher NO_x levels. The catalysts involved are ceramic or metal honeycombs with washcoats based on cordierite, mullite or perovskites such as LaCoO₃ or Sr-doped LaCoO₃. Conventional catalysts contain Ba-stabilized alumina plus Pt or Pd.

Both thermal and catalytical exhaust gas purification systems operate at pollutant concentrations >1.5–3 g/Nm³ autothermally. Since the efficiency of internal heat recovery is 80–90%, no additional energy is required for heating the exhaust gas. Thus both processes are environmentally sound and economical in operation. In Table 10-1 are some working temperatures compared for both processes. Limitations for catalytical processing are the catalyst sensitivity towards poison and overheating.

Table 10-1 Comparison of process temperatures for the oxidation of VOCs in afterburning processes

| Pollutant | Temperature Catalytical processing (°C) | Temperature Thermal processing (°C) |
|---------------------|---|---|
| Formaldehyde | 300 | 800 |
| CO | 250 | 760 |
| Styrene | 250 | 760 |
| Solvents | 350 | 760 |
| Phenol/formaldehyde | 350 | 800 |
| Phenol/creosol | 400 | 800 |
| Ethylacetate | 350–400 | 760 |

Figure 10-4 illustrates schematically a typical course of an afterburning process.

The curve shows the dependence of conversion on process temperature. There can be defined typical conversion values and areas:

T 50: 50% of the initial concentration is to be oxidized (ignition temperature)

T 90: 90% of the initial concentration is to be oxidized

Conversion at maximum process temperature (which may be fixed before)

Area I: kinetic region

Area II: diffusion region

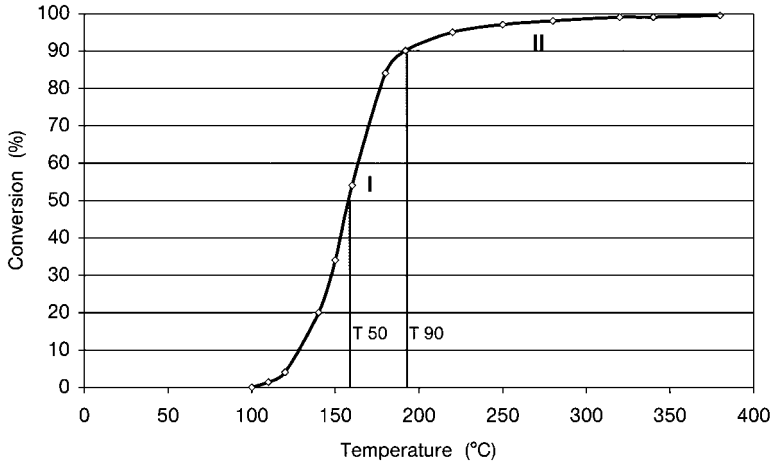


Fig. 10-4 Typical afterburning process of a hydrocarbon

Example [11]:

In formaldehyde processes the exhaust gas consists of 1.2–1.6 vol.% pollutants:

| | |
|---------------|------------|
| CO | 0.7–1.2% |
| Dimethylether | 0.1–0.4% |
| Methanol | 0.1–0.2% |
| Formaldehyde | 0.005–0.1% |

The feed gas is heated up to ca. 200 °C and can completely be oxidized by the catalyst. During this process the temperature rises up to 300–450 °C, dependent to the heat recovery system applied in the plant. The degree of conversion depends to the process temperature and the catalyst age. The following approximate results can be obtained:

| Catalyst temperature (°C) | Conversion of the pollutants [%] |
|---------------------------|----------------------------------|
| 300 | 90% |
| 350 | 99.0% |
| 450 | 99.9% |

With process temperatures of about 400 °C the following purification levels of the clean gas can be achieved over some years:

| | |
|----------------|----------------------|
| Formaldehyde | 10 mg/m ³ |
| Organic carbon | 20 mg/m ³ |

Figure 10-5 shows schematically a catalytic afterburning plant.

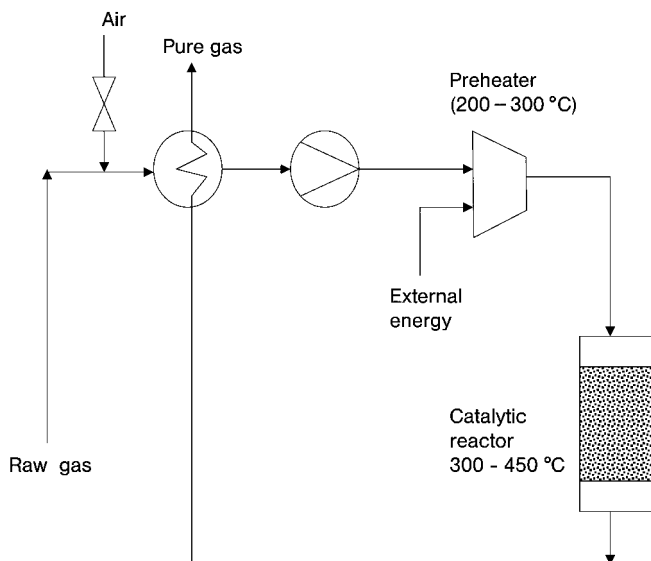


Fig. 10-5 Scheme of a catalytic afterburning plant

Finally, the catalyst design procedure for an afterburning process can be described as follows:

- Determination of pollutants, concentrations, limiting values (clean gas composition), poisons etc.
- Rough estimation: possible – yes or no
- Determination GHSV (gas hourly space velocity)
- Selection: pellets or monolith
- Estimation of the pressure drop
- Estimation of feed temperature, ΔT in the catalyst bed
- Catalyst weight (pellet height)
- Recommendation for a suitable catalyst
- Eventual test or new calculation

Advanced catalyst systems together with optimized engine management and process control can aid the achievement of the future low emission standards.

10.4

Green Chemistry and Catalysis [9]

Green chemistry, also called sustainable chemistry, was formally delineated in 1990 in the United States with the aim of preventing pollution through better process design rather than by managing emissions and waste – the “end of the pipe” solution. Catalysis is one of the fundamental pillars of green chemistry, the design of

chemical products and processes that reduce or eliminate the use and generation of hazardous substances. The design and application of new catalysts and catalytic systems are simultaneously achieving the dual goals of environmental protection and economic benefit [10].

Catalysis offers numerous green chemistry benefits including:

- Lower energy requirements
- Catalytic versus stoichiometric amounts of materials
- Increased selectivity
- Decreased use of processing and separation agents and
- Allows for the use of less toxic materials

Heterogeneous catalysis, in particular, addresses the goals of green chemistry by providing the ease of separation of product and catalyst, thereby eliminating the need for separation through distillation or extraction. In addition, environmentally benign catalysts such as clays and zeolites, may replace more hazardous catalysts currently in use.

Mass balances of alternative routes in chemical processing can be compared using measures such as the E factor and mass index S^{-1} . The E factor (ratio of waste [kg] to product unit [kg]) is an output orientated indicator, whereas the mass index S^{-1} (ratio of all raw materials [kg] to the product [kg]) is an input oriented indicator. These measures and the cost index CI (currency unit per kg product) clarify the benefits and drawbacks of changes in synthesis design, i.e. the strong and weak points, which must be addressed [6].

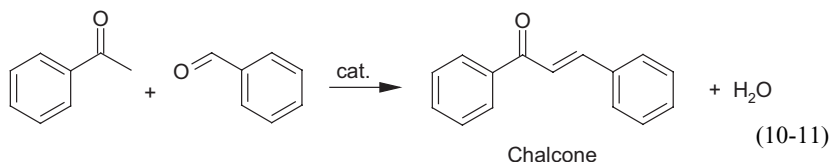
Waste is defined as everything that is produced during operation of the process, except the desired product. There is a substantial increase in E factors on going downstream from bulk chemicals ($<1-5$) to fine chemicals ($5 - >50$) and specialties ($25 - >100$). This reflects the more widespread use of stoichiometric reagents and multi-step syntheses in the latter sectors. Therefore, the longer term trend in fine chemicals manufacture is towards the use of the simplest raw materials – H_2 , O_2 , H_2O , H_2O_2 , NH_3 , CO , CO_2 – in low-salt, atom efficient processes employing homogeneous, heterogeneous, or biocatalysts.

10.4.1

Examples of Catalytical Processes

10.4.1.1 Aldol Condensation

The aldol condensation of benzaldehyde and acetophenone yields chalcone (Eq. 10-11) [6].



The aldol reaction is usually base-catalyzed, the results of the synthesis using different catalysts are demonstrated in Table 10-2.

Table 10-2 Results of the aldol condensation with various catalysts [6]

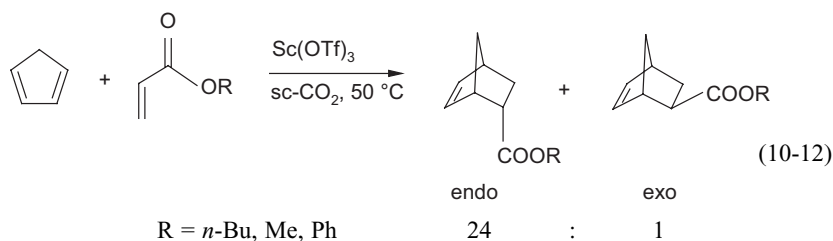
| Catalyst | Yield (%) | Mass index S^{-1} (kg/kg) | E factor (kg/kg) |
|--------------|-----------|-----------------------------|-------------------------|
| (a) KOMe | 75 | 5,6 | 4,6 |
| (b) NaOMe | 71 | 7,8 | 7,0 |
| (c) NaOH | 85 | 6,8 | 5,8 |
| (d) Nafion H | 78 | 2,7 | 1,7 (1,5) ^{a)} |

a) cat. d is reused (at least ten times)

The base catalysts must be neutralized and/or washed out during the work-up procedure. The solid-acid Nafion H, on the other hand, can be reused. Table 10-2 shows that the most effective procedure with regard to mass efficiency and E factor can be carried out with catalyst d. Not only solvents and auxiliary materials can be saved, but the catalyst too, is reusable without having a negative effect on the yield. This leads to a further decrease in the *E* factor. In conclusion, Nafion H seems to be an efficient catalyst for performing aldol condensation to yield chalcone in an environmentally friendly manner, i. e. avoiding the use of water and reducing the amount of solvent.

10.4.1.2 Diels-Alder Reaction [1]

Supercritical carbon dioxide (sc-CO₂) is an environmentally benign solvent that is providing a viable alternative to the traditional organic solvents. A Diels-Alder reaction between *n*-butyl acrylate and cyclopentadiene was investigated with the Lewis acid catalyst scandium tris (trifluoromethanesulfonate), primarily due to its solubility in sc-CO₂ (Eq. 10-12):

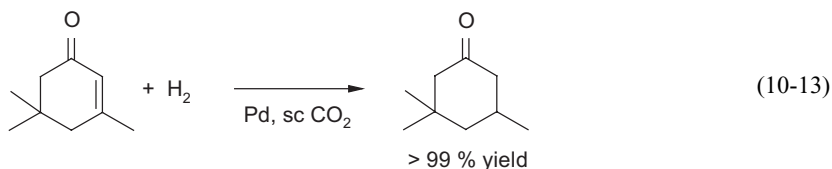


By varying the pressure of the solvent, endo:exo selectivity was maximized at 24:1, a significant improvement over selectivity achieved in conventional solvents (11:1). Green chemistry benefits of a less hazardous solvent, reduced energy usage,

ease of separation, and selectivity for waste minimization, as can be seen in this example [1].

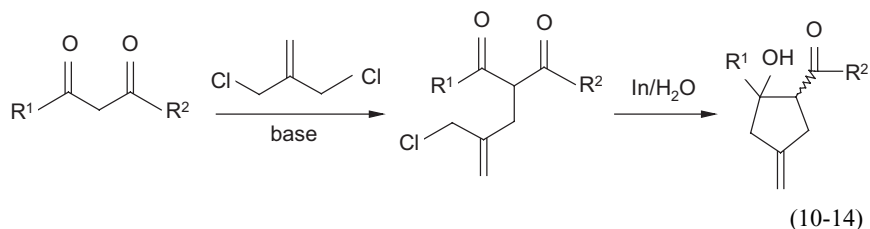
10.4.1.3 Hydrogenation [10]

The selective hydrogenation of an unsaturated cyclic ketone can be carried out successfully with Pd catalyst in supercritical CO₂ (Eq. 10-13):



10.4.1.4 Cyclization in Water [1]

A variety of reactions can be carried out in an aqueous environment given the right choice of catalyst. Water is an extremely attractive solvent choice. Allylation of 1,3-dicarbonyl compounds, for example, is efficiently promoted in water using an indium catalyst (Eq. 10-14).



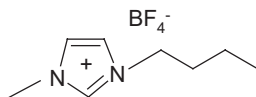
Metal mediated reactions in water have found applications in cyclization, ring expansion, and isomerization reactions.

10.4.1.5 Use of Ionic Liquids [1]

Ionic liquids (IL) are also gaining acceptance as alternatives to traditional organic solvents.

Ionic liquids are salts that are liquid at low temperatures. Unlike traditional solvents that can be described as molecular liquids, ionic liquids are composed of ions. This creates the potential to behave quite differently from conventional solvents. Due to the unique chemical physical properties of ionic liquids, they have been called „green solvents“.

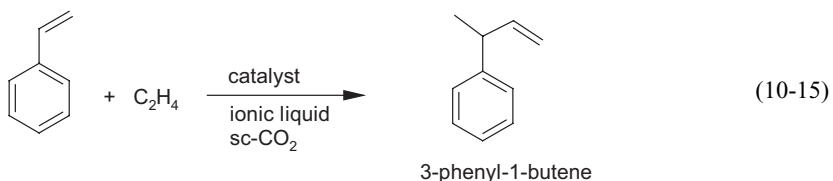
Especially room temperature ionic liquids (RTILs), such as those based on *N,N*-dialkylimidazolium ions, are interesting solvents for catalytic reactions, for example:



1-butyl-3-methylimidazolium-tetrafluoroborate

Ionic liquids are non-volatile and non-flammable, eliminating the hazards associated with volatile organic compounds (VOCs). In addition, the properties of ionic liquids may be tuned by varying the identities of the cations and anions, thereby tailoring the solvent to a specific application.

The ionic liquids show excellent extraction capabilities and allow catalysts to be used in a biphasic system for convenient recycling. For example, the hydrovinylation of styrene with ethene can be carried out successfully using an ionic liquid and supercritical CO_2 as solvent (Eq. 10-15). The ionic liquid dissolves the metal organic complex catalyst and sc-CO_2 facilitates mass transfer and continuous processing.



IFP France has developed dimerization, hydrogenation, isomerization, and hydroformylation reactions without conventional solvents. For butene dimerization a commercial process exists. There is formed a biphasic system with the catalyst in the IL phase, which is immiscible with the reactants and products. This system can be extended to a number of organometallic catalysts.

A variety of other reactions such as acylation of toluene, anisole, and chlorobenzene to give selectively *p*-isomer, alkylations, etc. have been conducted with ionic liquids.

► Exercises for Chapter 10

Exercise 10.1

Why is the automotive exhaust catalyst called a three-way catalyst?

Exercise 10.2

Which metals are used in the automotive catalyst and what reactions do they catalyze?

Exercise 10.3

What are the major compounds of exhaust gases?

Exercise 10.4

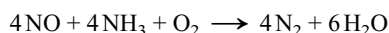
Describe how NO_x can be removed from the exhaust when a car operates under lean-burn conditions (i.e. oxygen rich). Why is it attractive to drive cars under lean-burn conditions?

Exercise 10.5

Explain the common characteristics of the NSR catalytic system for NO_x abatement based on the principle „oxidation before reduction“ employing the oxidation states of all stages.

Exercise 10.6

A BASF process proceeds according to the following equation:



- What is the significance of the process and what is it called?
- Catalysts and temperature range?

Exercise 10.7

You can select a suitable catalyst for a catalytic afterburning process from monoliths or pellets. Which process parameters are mainly influenced by your choice?

Exercise 10.8

Explain the atom efficiency concept by comparing the classical chlorohydrin route and the newer petrochemical ethylene oxide manufacture.

Exercise 10.9

What is an *E*-factor? Which processes usually have the highest *E*-factors?

Exercise 10.10

In the nitration of aromatic compounds, solid acid catalysts such as clays and zeolites are an alternative to the conventional process employing a mixture of $\text{HNO}_3/\text{H}_2\text{SO}_4$. List some reasons in view of green chemistry.

Exercise 10.11

Which advantages for process development can be offered by ionic liquids?

11

Photocatalysis

11.1

Basic Principles [3, 7]

Recently, the community is considering to turn over from an oil-based economy to a hydrogen-based economy due to the limitation of the earth's reserve of fossil fuels. The current way to produce hydrogen is still via fossil fuels. The main production route treats carbon (charcoal) with steam to produce synthesis gas, from which hydrogen can be obtained. CO₂ is produced as a by-product through this route. To overcome this problem water can be cleaved into hydrogen and oxygen. The production of one hydrogen molecule costs 2.42 eV, which is too high to be generated by heating water. Another energy source that can be used is electricity, but a disadvantage is that the energy costs are very high. A cheap alternative on the other hand is sunlight. At this point photocatalysis can play an important role.

Photocatalysis can be defined as follows: "A change in the rate of chemical reactions or their generation under the action of light in the presence of substances – called photocatalysts – that absorb light quanta and are involved in the chemical transformations of the reactants" [4]. Typical "photocatalysts" or "photosensitisers" are semiconductor materials. There are many chemical compounds which can act as photocatalysts, but only a very few of these materials are photochemically and chemically stable semiconductor photocatalysts, one compound dominates: titania (titanium dioxide) TiO₂.

A semiconductor has a manifold of electron energy levels filled with electrons – the valence band (VB) and also many higher energy levels that are largely vacant – the conduction band (CB). The energy difference between these two bands is called the bandgap energy (E_{bg}). A general photocatalytical reaction can be summarized by Eq. (11-1):



where the change in the Gibbs free energy for this reaction may be negative (the usual reported case) when photocatalysis occurs, or positive when photosynthesis occurs. The usual form of a semiconductor photocatalyst in reaction (11-1) is as par-

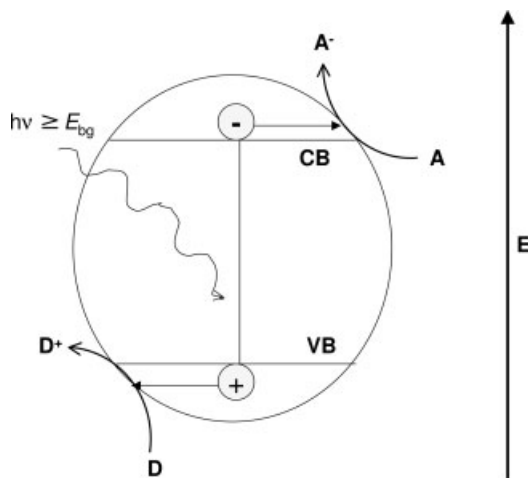


Fig. 11-1 Electron energetics for a photocatalytical reaction [3]

ticles of micrometre to nanometre diameter, which are aggregates of nanocrystals. These particles are used either as a powder dispersion or layered to form thin films (typically, 100–10 000 nm thick). The basic features of such materials for promoting a general chemical reaction, are shown in Figure 11-1.

Figure 11-1 shows the electron energetics associated with reaction (11-1), sensitized by a semiconductor particle. After excitation with light of ultra-bandgap energy has created an electron-hole pair, the following reactions can occur:

- Reduction of an electron acceptor A at the surface by a photogenerated electron
- Oxidation of an electron donor D at the surface by a photogenerated hole,
- Electron-hole recombination in the bulk or at the surface, which generates heat.

Electron-hole recombination usually dominates semiconductor photosensitization so the overall process is often not very efficient (typically <1%) with respect to photons.

Titania exists mainly as two crystalline forms, anatase and rutile. Anatase is generated by the usual low temperature production methods, such as alkaline hydrolysis of titanium(IV) compounds followed by calcination at moderate temperatures (400–500 °C). Anatase readily converts to rutile at elevated temperatures (>700 °C) although this phase change is often accompanied by extensive sintering. As a consequence, rutile usually has a much lower specific surface area (by a factor of 10 or more) than the anatase from which it was derived.

Titania is chemically and biologically inert, photostable, photoactive and cheap. The redox potentials of titania vary with pH, for anatase values as follows are given: $E_{CB} = -0.32$ V, $E_{VS} = 2.91$ V (vs. NHE and at pH 0). The high bandgap energies (E_{bg} anatase 3.23 eV, rutile 3.02 eV) show the major drawback in using them as photocatalysts is that they only strongly absorb UV light (rather than visible light).

Titania only absorbs 2–3% of the solar spectrum so is of limited use as a photosensitizer for any solar-driven system. Despite this, much research has been carried out

on titania-based systems for water reduction, oxidation and splitting, as the photo-generated electrons and holes on titania have favorable redox potentials ($E_{CB} < E^\circ(\text{H}^+/\text{H}_2)$ and $E_{VB} \gg E^\circ(\text{O}_2/\text{H}_2\text{O})$).

Thus, the photogenerated electrons on both rutile and anatase are sufficiently reducing to be able to reduce water to H_2 ($E^\circ(\text{H}^+/\text{H}_2) = 0 \text{ V}$). The photogenerated holes are more oxidising than fluorine ($E^\circ(\text{F}_2/\text{F}^-) = 2.85 \text{ V}$) and can oxidise water to form hydroxyl radicals ($E^\circ(\cdot\text{OH}/\text{H}_2\text{O}) = 2.31 \text{ V}$) or oxygen ($E^\circ(\text{O}_2/\text{H}_2\text{O}) = 1.23 \text{ V}$). Therefore, titania is the most used semiconductor in photosystems for water reduction, oxidation or cleavage.

11.2

Photoreduction and Oxidation of Water [6,7]

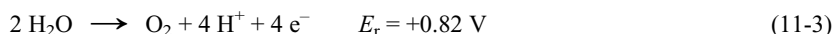
Present-day effort to convert solar energy into fuel or chemical feedstocks devolve upon discovering appropriate catalysts for the following reactions:

- Reduction of water to hydrogen (Eq. 11-2):



where E_r is the redox potential (with respect to the normal hydrogen electrode NHE in aqueous solution) at neutral pH.

- Generation of oxygen from water (Eq. 11-3):



- Simultaneous generation of H_2 and O_2 from water (Eq. 11-4):



If water is cleaved using a combination of the dielectronic reaction (11-2) and the tetraelectronic oxidation (Eq. 11-3), the free energy required per electron is only 1.23 V, i.e. the sum of the redox potentials, taking regard of signs, for both reactions.

In semiconductor photochemistry there are often used co-catalysts such as Pt or other transition metals. These co-catalysts are deposited on the surface of semiconductor particles. They act as traps or wells for any photogenerated electrons that may accumulate. The co-catalysts are assumed to reduce the overall probability of electron-hole recombination and so increase the overall efficiency of the photosystem. In the absence of oxygen but in the presence of water most platinum group metals will readily reduce water to H_2 . In this process, most metals stabilise the intermediate hydrogen atoms and catalyse their combination to form H_2 . For increased efficiency a sacrificial electron donor (D), such as EDTA or methanol, must be added to remove irreversibly any photogenerated holes or oxidising species, such as hydroxyl radicals, from the semiconductor surface. Therefore, most systems that

overall photoreduce water to H_2 utilise an sacrificial electron donor and a UV-absorbing semiconductor photocatalyst.

In water photooxidation by semiconductor photocatalysis, a sacrificial electron acceptor A, such as Fe^{3+} or Ag^+ ions, is usually added to the system to prevent accumulation of any photogenerated electrons. Transition metal oxides, such as RuO_2 or IrO_2 , which are recognised O_2 evolution catalysts, are often deposited on the surface of the semiconductor catalyst to improve the efficiency of water oxidation.

In the 1980s research into artificial photocatalytic systems for water splitting, reached a peak.

11.2.1

Water Reduction [3, 5]

Most photocatalysts are able to mediate water reduction to H_2 by electron donors only if a suitable H_2 catalyst is present. The system also works well if the catalyst is simply mixed in with the semiconductor in a finely divided form, for example Pt black. The basic overall process can be summarised as follows (Eq. 11-5):

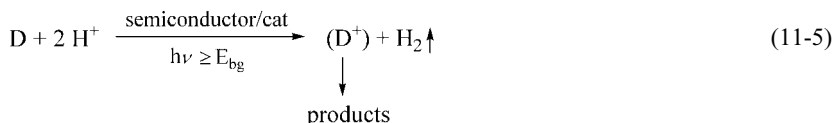


Figure 11-2 shows the electron transfer processes associated with reaction (11-5). The semiconductor is invariably TiO_2 (anatase).

There are now hundreds of photocatalyst systems for water reduction, some well known electron donors and hydrogen catalysts are as follows:

- Hydrogen catalysts: Pt, Pd, Rh, $Rh(bipy)_3^{3+}$, $Ru(bipy)_3^{2+}$
- Electron donors: glucose, EDTA, MeOH, i-PrOH, triethanolamine

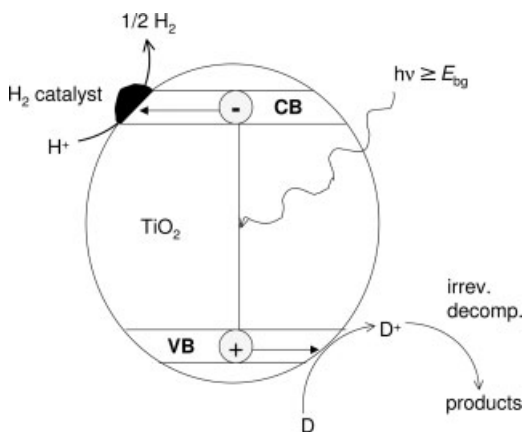


Fig. 11-2 Photoreduction of water by a sacrificial electron donor (D), sensitised by semiconductor particles with hydrogen catalyst [3]

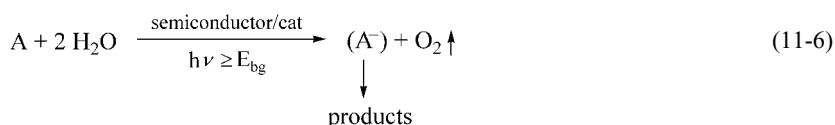
A $\text{Ru}(\text{bipy})_3^{2+}$ complex that acts as a photosensitizer is especially interesting, not only because it strongly absorbs visible light, but also because it possesses the appropriate redox properties and, in addition, it is known to undergo facile light-induced electron-transfer reactions.

The electron donor D is consumed in the process by a fast, irreversible decomposition of the oxidized D^+ species formed in the process. Certainly the quantum yields for hydrogen evolution are very low (typically 2–4%), because sunlight contains little UV, as mentioned earlier.

11.2.2

Water Oxidation [3]

The semiconductor sensitised photocatalytic oxidation of water by a sacrificial electron acceptor can be expressed by Eq. (11-6):



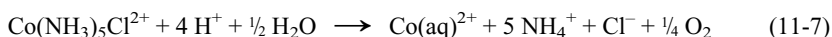
Oxygen photogeneration from water appears to be a less important process to study, because the H_2 -evolution system nominally provides a route to generate a useful fuel via alternative energy sources. Titania and WO_3 are the two most commonly used semiconductor sensitizers for water oxidation. In some cases an oxygen catalyst seems not to be needed, especially, if WO_3 is used as photosensitizer.

Some systems used in practice are as follows:

- Oxygen catalysts: Rh, Ru, Ir, Au, Pt, RuO_2 , none
- Electron acceptors: Fe^{3+} , $[\text{PtCl}_6]^{2-}$, Ag^+

An interesting photocatalytic system seems to be a ruthenium-trisbipyridine complex acting as sensitizer which absorbs visible light and is promoted to an excited state. Irradiation of the starting material, the photosensitizer $\text{Ru}(\text{bipy})_3^{2+}$, leads to the excited complex $^*\text{Ru}(\text{bipy})_3^{2+}$, the latter may be generated by oxidative quenching with the complex $\text{Co}(\text{NH}_3)_5\text{Cl}^{2+}$, which acts as an electron acceptor. Non-stoichiometric RuO_2 (best symbolized RuO_x), in the form of a powder, is a good catalyst for the thermal reduction of $\text{Ru}(\text{bipy})_3^{3+}$ by water with consequent evolution of oxygen.

Effectively, the ruthenium complex undergoes a catalytic cycle, while the $\text{Co}(\text{III})$ complex and water are consumed. The overall process of O_2 generation therefore involves the sacrificial consumption of the cobalt complex (Eq. 11-7):

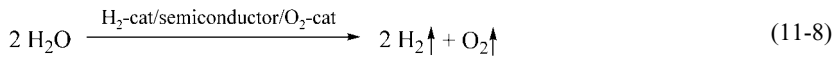


The successful choice of RuO_x as a redox catalyst was prompted by the fact that RuO_x anodes show high electrocatalytic activity (i. e. low overvoltage) for O_2 evolution in the electrolysis of water.

11.3

Photocleavage of Water [3, 6]

The semiconductor-sensitised photocleavage of water into hydrogen and oxygen can be summarised as follows (Eq. 11-8):



where the H_2 catalyst is usually Pt, and the O_2 catalyst is RuO_2 or nothing. The semiconductor photosensitiser is invariably titania or SrTiO_3 .

The use of photocatalysis for water cleavage is shown in Figure 11-3.

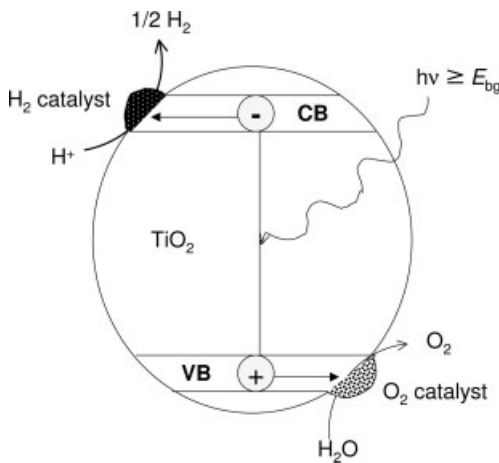


Fig. 11-3 Photocleavage of water, sensitised by semiconductor particles with both hydrogen and oxygen catalyst [3]

The photocatalyst uses a photon to excite an electron from the valence band to the conduction band: resulting is an excited state. The two protons, which are needed to generate hydrogen gas, can use the electrons that are excited in the photocatalyst. The hole in the valence band can be filled with an electron produced by the oxygen generation. A requirement for the photocatalyst is to have a bandgap higher than 2.43 eV, which is the energy needed for the splitting of water. The goal is to split water into hydrogen and oxygen by the use of redox-reaction. Catalyst 1 facilitates the hydrogen generation and catalyst 2 the oxygen generation. To enhance the speed of the reaction two things must happen. First, the association of protons needs to be quick and second, the electron generation needs to be high. The latter could be achieved by reducing the bandgap to a wavelength where the intensity in sunlight is very high.

The early claims of “bifunctional” photosynthetic systems with high quantum efficiencies (up to 30%) appear irreproducible and therefore unjustified. More recently, layered perovskite structures, such as $\text{K}_2\text{La}_2\text{Ti}_3\text{O}_{10}$ with Ni were described. The Ni acts as H_2 catalyst, there is no need of an O_2 catalyts.

The latest systems appear to work under visible light illumination without a noble metal-based H₂ and/or O₂ catalyst. There have been reported photocatalysts such as delafossite CuFeO₂, without a separate H₂ or O₂ catalyst, or In/Ni/Ta-oxides coated with NiO, or RuO₂ for visible-light activated water-splitting processes. However, all reported water-splitting systems are controversial and require confirmation [3].

There can be stated several requirements for developing a good photocatalyst for water cleavage [7]:

- The bandgap should be between 2.43 and 3.2 eV
- The valence band should be lower than the oxygen oxidation potential
- The conduction band should be higher than the hydrogen reduction potential
- The aid of a co-catalyst for hydrogen generation is necessary
- The photocatalyst must be able to split water in protons and hydroxyl anions
- The generation of water from molecular oxygen and hydrogen must be reduced
- Electron transport to the surface is necessary

Further work is certainly required to create a reproducible, stable, efficient photo-system for water splitting. For all systems this is still a long way from commercialization but it is an attractive goal for research in catalysis.

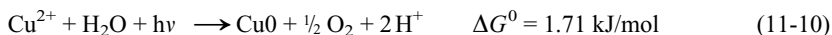
11.4

Other Reactions [2, 5]

Photoelectrosynthesis provided by the right catalysts offer some possibilities for converting inexpensive, readily available materials (H₂O, CO₂, N₂ or CO) into useful fuels. Other chemically useful products, such as chlorine (now prepared by electrolysis of NaCl demanding electrical energy) have been generated by photooxidation of chloride using TiO₂ electrode (Eq. 11-9):



Another elegant photoelectrosynthetic means now exists for executing the reduction of aqueous cupric solutions so as to generate O₂ and metallic copper (Eq. 11-10):

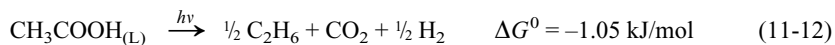


Preferential deposition of the Cu(0) occurs on the unilluminated side of a photo-active TiO₂.

A very interesting route to various amino acids (glycine, alanine, serine, aspartic acid, glutamic acid) from a mixture of CH₄, NH₃ and H₂O seems to be the reaction with irradiated suspensions of platinized TiO₂ (Eq. 11-11):



Another photocatalytic process that recently has been discussed, is the photo-Kolbe reaction (Eq. 11-12):



This reaction is induced by long-wavelength UV irradiation of an *n*-type TiO₂ photoanode in organic solvents. With platinized TiO₂ (anatase) powder under same conditions in aqueous acetic acid, methane becomes the major product.

Suspensions of semiconductors such as TiO₂, ZnS and CdS can also be used as photocatalysts in the synthesis of organic compounds. Some potentially useful preparative reactions include oxidations, reductions, cyclodimerizations, isomerizations and photoaddition reactions.

Furthermore, it should be mentioned that photocatalytic processes with the aid of TiO₂ can be used for environmental purification [1]. This is due to the fact that the oxidation potential of TiO₂ (3.0 V) is considerably higher than that of more conventional oxidizing agents such as chlorine (1.36 V) and ozone (2.07 V). Due to its chemical inertness and non-toxicity TiO₂ is compatible with many types of practical catalytic systems. Many photodegradation reactions of noxious, malodorous chemicals, oil on water etc. have been reported.

► Exercises for Chapter 11

Exercise 11.1

Explain why photocatalysts based on TiO₂ have limited efficiency for splitting water into hydrogen.

Exercise 11.2

To create a good catalyst with high photo-catalytic activity the major criterion is a well designed bandgap. List other questions which should come in mind.

Exercise 11.3

- Name the most popular H₂ and O₂ co-catalysts for semiconductor-sensitised water cleavage photosystems.
- Describe briefly the function of the co-catalysts.

Exercise 11.4

Name sacrificial electron acceptors (A) and electron donors (D) which can increase the efficiency of photocatalysts in water splitting.

Exercise 11.5

Which photosensitiser can absorb visible light?

Exercise 11.6

Why can TiO₂ be used as photocatalyst for environmental purification processes?

12

Phase-Transfer Catalysis

12.1

Definition [1, 2]

Phase-transfer catalysts accelerate reactions of two immiscible reactants. Phase-transfer catalysis (PTC) is useful primarily for performing reaction between anions (and certain neutral molecules such as H_2O_2 and transition metal complexes such as RhCl_3) and organic substrates. PTC is needed because many anions (in the form of their salts, such as NaCN) and neutral compounds are soluble in water and not in organic solvents, whereas the organic reactants are not usually soluble in water. The catalyst acts as a shuttling agent by extracting the anion or neutral compound from the aqueous or solid phase into the organic reaction phase (or interfacial region) where the anion or neutral compound can freely react with the organic reactant already located in the organic phase.

Reactivity is further enhanced, sometimes by orders of magnitude, because once the anion or neutral compound is in the organic phase, it has very little hydration or solvation associated with it, thereby greatly reducing the energy of activation.

PTC is not likely to be involved in the manufacture of large tonnage heavy organic chemicals but is an unusual and elegant catalytic technique that is energy sparing and gives high yields at low-residence times under mild conditions. It is therefore typical of the methods that will be attractive in the future.

12.2

Catalysts for PTC [1]

Suitable catalysts for PTC are those which have a highly lipophilic cation (i.e. have strong affinity for an organic solvent). Catalysts used most extensively are quaternary ammonium or phosphonium salts (quats). Examples are:

- Tetra-*n*-butylammonium bromide (TBAB)
- Triethylbenzylammonium chloride (TEBA)
- Methyltriocetylammmonium chloride (Aliquat 336 or Adogen 464); $\text{PhCH}_2\text{NEt}_3\text{Cl}$ (TEBA, TEBAC)
- Cetyltrimethylammmonium bromide (“cetrimide”) for basic PTC

Neutral complexing agents for organic cations, e.g. crown ethers, polyethylene glycols (PEGs), cryptands, etc., are also suitable catalysts. Open chain PEGs (e.g. PEG 400) are the least expensive catalysts and may be preferable to quats in some processes. Crown ethers and cryptands (neutral, oligodentate metal ligands of spherical shape with macrooligocyclic framework that usually contain N bridgehead atoms and oligo(ethylene glycol) ether units) can solubilize organic and inorganic alkali metal salts even in nonpolar organic solvents; they form a complex with the cation (Fig. 12-1), and thus act as an “organic mask”.

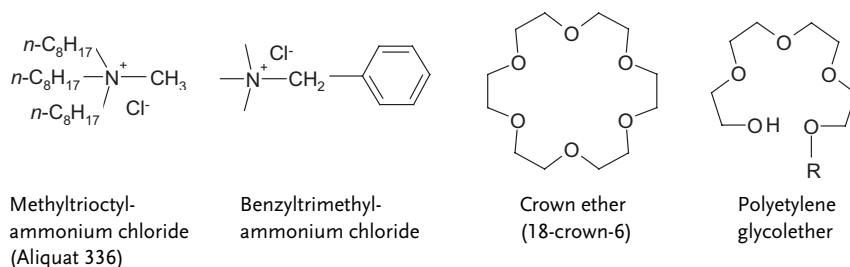


Fig. 12-1 Structures of phase-transfer catalysts

Although crown ethers were often found to be very effective catalysts, they have only found limited commercial application because of their high cost (10 to 100 times that of quats) and perceived toxicity. Cryptands are even more expensive than crown ethers.

Most commonly used organic solvents in liquid/liquid PTC are toluene and other hydrocarbons, chlorobenzene, and in the lab – chlorinated solvents such as CH_2Cl_2 and CHCl_3 . For solid/liquid PTC the more polar acetonitrile and even DMF are employed, too.

Some newer variants of PTC are:

- Triphase catalysts (in which the catalyst is anchored to a polymer for ease of removal)
- Inverse PTC: extraction of cations for electrophilic reactions by large lipophilic catalyst anions
- Extraction of uncharged species into organic media by onium salts. These include transition metal salts (complex formation with, e.g. CuX , PdCl_2), and acids, H_2O_2 and amines which form weakly hydrogen-bonded complexes with quats

12.3

Mechanism and Benefits of PTC [5, 7]

Since the catalyst is often a quaternary ammonium salt (e.g. tetrabutyl ammonium, $[\text{C}_4\text{H}_9]_4\text{N}^+$), also called the “quat” and symbolized by Q^+ , the ion pair Q^+X^- (X^- being the anion to be reacted) is a much looser ion pair than say Na^+X^- . This

looseness of the ion pair is a key reason for enhanced reactivity, which will ultimately lead to increased productivity (reduced cycle time) in commercial processes. At the end of the reaction, an anionic leaving group is usually generated. This anionic leaving group is conveniently brought to the aqueous (or solid) phase by the shuttling catalyst, thus facilitating the separation of the waste material from the product. This mechanism is called the „extraction mechanism“ of PTC and is shown in Figure 12-2.

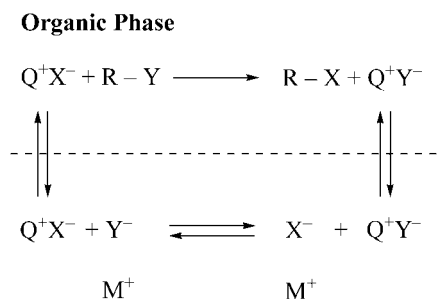


Fig. 12-2 The extraction mechanism of phase-transfer catalysis [5]

Due to process improvements, some benefits have been realized through phase-transfer catalysts, which can

- Increase productivity: increase yield, reduce cycle time, reduce or consolidate unit operations, increase reactor volume efficiency
- Improve environmental performance: eliminate, reduce or replace solvent, reduce non-product output
- Increase quality: improve selectivity, reduce variability
- Enhance safety: control exothermic reactions, use less hazardous raw materials
- Reduce other manufacturing costs: eliminate workup unit operations, use alternate less expensive or easier to handle raw materials

Especially in the manufacture of fine chemicals no catalytic method has made such an impact as PTC.

12.4

PTC Reactions [2, 7]

PTC technology is used in a wide variety of applications. PTC reactions under *neutral* conditions include

- Substitutions with many ions
- Reductions
- Oxidations (e. g. with MnO_4^- , CrO_4^- , OCl^-)
- Epoxidation

- Carbonylation
- Transition metal co-catalysis

More widely applicable are *base-catalyzed* phase-transfer reactions using aqueous concentrated or solid NaOH, KOH, K₂CO₃, NaH, etc. These include

- Alkylations
- Isomerizations
- Addition reactions
- Condensations
- Eliminations
- Hydrolyses
- Nucleophilic aromatic substitutions
- Carbene reactions etc.

New interesting applications have been in the epoxidation of difficult olefin compounds, side-chain chlorination of substituted toluenes, diazotization, polymer manufacturing and modification, and in organometallic and analytical chemistry.

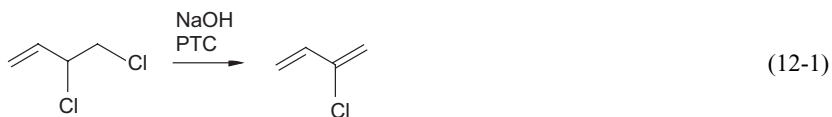
12.5

Selected Industrial Processes with PTC [6–8]

There are hundreds of commercial applications of phase-transfer catalysis and they were commercialized due to the competitive advantages which they truly provide. Following is only a selection of industrial processes using PTC.

1. Continuous Dehydrohalogenation to Produce the Large Scale Monomer Chloroprene [1]

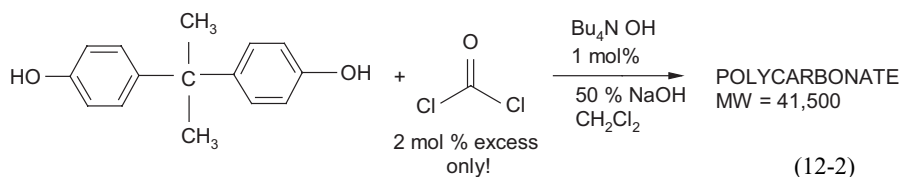
Dehydrohalogenation of 3,4-dichloro-1-butene with NaOH and the PTC cocoalkyl benzyl bis [β -hydroxypropyl]ammonium chloride can be carried out in a reactor cascade of 3–8 stirred vessels (Eq. 12-1):



There can be achieved: productivity ~16 t/hr, yield up to 99.2% and NaOH usage only 0.8 mole % excess.

2. Polycarbonate Manufacture with Phosgene [7]

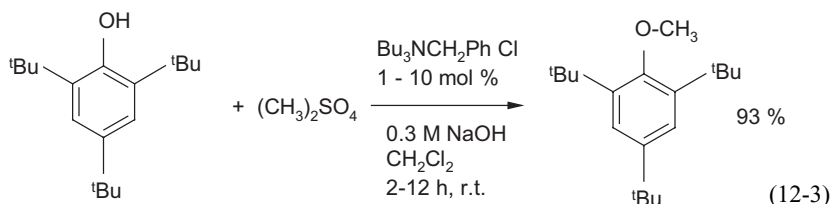
This process allows an outstanding reduction of excess hazardous high volume raw material such as phosgene (Eq. 12-2):



Achieved: Great improvement in safety and environmental contamination can be achieved by reducing the phosgene excess by 94%. PTC provides 200 times less hydrolysis of phosgene/chloroformate than traditional catalysis.

3. Etherification (*O*-alkylation) [4]

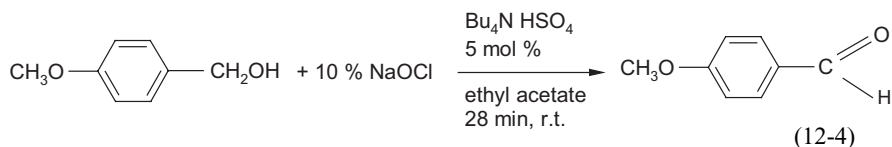
A special Williamson ether synthesis can be carried out as follows (Eq. 12-3):



PTC usually provides the best Williamson ether synthesis. This reaction achieves:

- High-yield etherification
- No need for excess pre-formed alkoxide
- Usually short cycle time and easy workup
- Non-dry mild reaction conditions

4. Aldehydes by Oxidation of Alcohols with Hypochlorite (Eq. 12-4)



This achieves a reaction with

- A high yield in short reaction time at room temperature
- An inexpensive oxidizing agent/no transition metal with high selectivity (vs. over-oxidation)

5. Carbonylation [6]

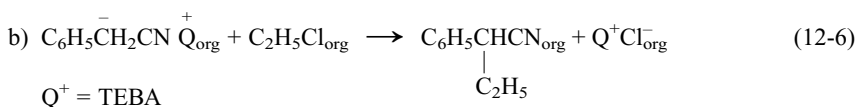
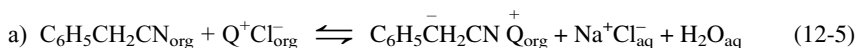
Phase-transfer catalysis offers a variety of conceptual and practical advantages. Among these advantages unique to PTC are the ability of quats to transfer the anionic forms of metal carbonyls in the organic phase, in which CO is about 20 times

more soluble than in water, which further leads to less hydrolysis of CO to formate and esters to acids.

For example, malonic esters can be made by PTC carbonylation of ethyl chloroacetate at 1 bar CO at 25 °C in the presence of cobalt carbonyl. Ni(CN)₂ was used for the PTC double carbonylation of alkynols, using PEG-400 as the phase-transfer catalyst, LaCl₃ as an additional co-catalyst, toluene as the solvent, and 0.5 M NaOH as the optimum base concentration. Yields of ene-dicarboxylic acids were up to 97%.

6. 2-Phenylbutyronitrile by Alkylation [3, 8]

An industrial process for the production of 2-phenylbutyronitrile consists of stirring phenylacetoneitrile and an alkylating agent, preferably alkyl chloride, with aqueous 50% NaOH solution and a PTC benzyltriethylammonium chloride (TEBA). This very efficient synthesis proceeds according to Equations 12-5 and 12-6:



The system in which the alkylation occurs is heterogeneous, consisting of two strictly immiscible liquid phases. The PTC process replaced old technology which used sodium amide in toluene.

The new process is carried out by stirring neat phenylacetoneitrile (no solvent) with about 1% molar TEBA, and concentrated aqueous NaOH while gaseous ethyl chloride is introduced to the mixture. The reaction proceeds quickly with a moderate exothermic effect, so the reaction vessel is cooled to keep the temperature at 15–20 °C. The ethyl chloride is consumed nearly quantitatively, allowing the reaction to be stopped when the proper amount of ethyl chloride is absorbed. Subsequently, the mixture is diluted with a small amount of water, the organic phase separated, and the organic washed with acidified water (to remove the catalyst) and purified by distillation under reduced pressure.

Thanks to the high selectivity and higher yield of the product of higher purity, the actual yield of the desired 2-phenylbutyronitrile is around 85–90% as compared to 65–68% in the process using sodium amide. In addition to those advantages, the catalytic process offers many other benefits: significant economic advantage in cost savings of the starting materials, ease of operating the process and increased safety measures. The catalytic process does not require the use of an organic solvent; therefore, the amount of product obtained from the unit volume of the vessel is 3–4 times larger. The traditional process required that first sodium amide was reacted with phenylacetoneitrile and then ethyl bromide was added. Since both of these reactions were strongly exothermic, all operations were much more time consuming. Thus the catalytic process requires much less time for the batch completion [3].

What we have seen from these examples is, that phase-transfer catalysis delivers high productivity, enhanced environmental performance, improved safety, better quality and increased plant operability in commercial manufacturing processes for organic chemicals in many of reaction categories. Enormous opportunity exists right now to increase corporate profits and process performance by retrofitting existing non-PTC processes with PTC and by developing new processes using PTC.

► Exercises for Chapter 12

Exercise 12.1

Describe the molecular structure of phase-transfer catalysts.

Exercise 12.2

What are the major benefits of PTC?

Exercise 12.3

How can the effect of PTC be explained in carbonylation reactions?

Exercise 12.4

Describe the action of crown ethers as PTC.

Exercise 12.5

Explain the main limiting factor for the application of PTC, the lack of stability at higher temperatures, particularly under highly basic conditions.

13

Planning, Development, and Testing of Catalysts

13.1

Stages of Catalyst Development [T40]

The development of a catalyst up to industrial application involves three stages:

- The research stage
- Intensive testing in the laboratory and on the pilot-plant scale
- The industrial stage

In the research stage, the first step is to formulate the problem. This involves gathering information about market requirements and estimating the value that a particular catalyst system could have at some time in the future.

Next the concept must be described in chemical terms so that it can be seen whether the project is technically and economically feasible. Estimates must be made whether a profitable yield and selectivity can be achieved, and the raw material supply and future demand for the product must be guaranteed. Only when the results of these estimations are satisfactory can the actual catalyst planning begin.

If several selective catalysts are initially available, then their suitability and lifetime are intensively investigated in a test reactor known as a pilot plant. The final step is then erection and startup of the industrial plant. Before the actual production in the industrial plant begins, detailed tests are carried out so that any teething problems can be identified right at the beginning and eliminated.

Figure 13-1 shows schematically the cost and time frame for a catalyst development in industry.

For catalysts produced on the pilot-plant scale other catalyst properties are in the foreground than in the screening on laboratory level. For example, catalyst lifetime, mechanical and thermal stability, poison resistance, etc. Also, activation and regeneration procedures are investigated in this stage. Small pilot test units (100–1000 mL catalyst volume) are in operation using predominantly industrial feed stocks. Pilot-plant reactors also generate data regarding mass and heat transfer, important for the process and reactor design.

The time required for the development of a new or an improved catalyst including the trial plant production is quite different. For a substantial improvement of existing

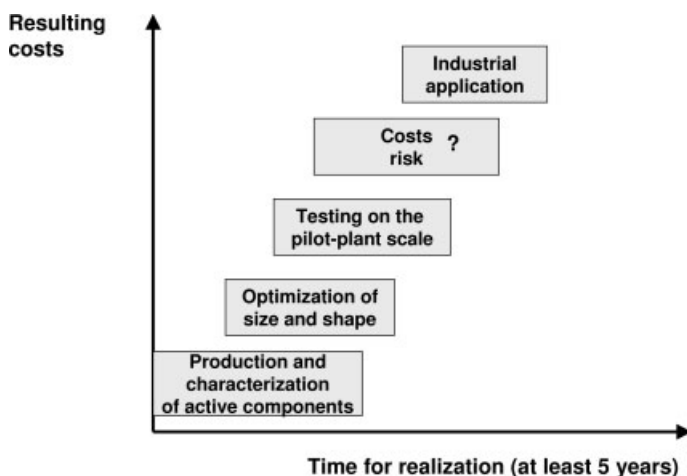


Fig 13-1 Main steps in catalyst development

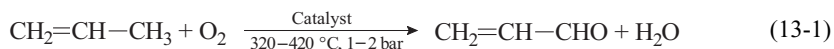
catalysts, one can estimate an average of 2 years, if the production line exists or has to be only partially revamped. The costs for such improvements are about 0.5–1.5 million US \$. In the case of new catalysts the development times are in the range of 3–5 years, sometimes even longer. The cost average can be estimated to be 2–3 million US \$, sometimes even more.

The development of an industrial catalyst must also take other parameters into account such as support materials and the type of reactor in which the catalyst will be used. Thus the choice of catalyst depends on many factors, as shown in Scheme 13-1.

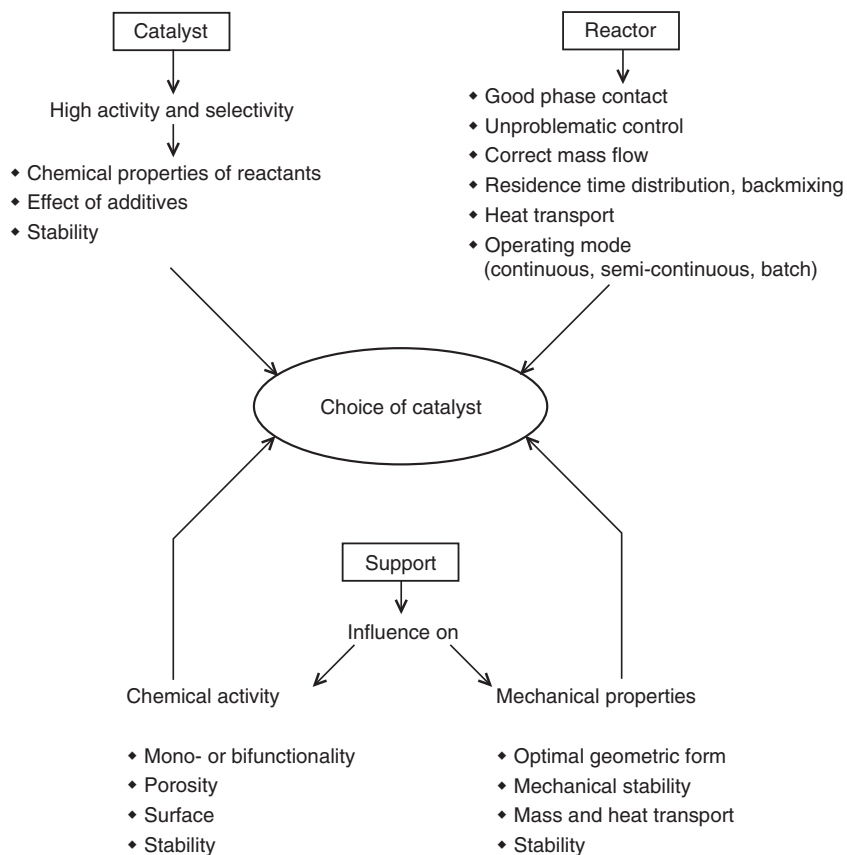
With regard to the morphology of the catalyst, a distinction is made between microeffects and macroeffects. Microeffects include the crystallinity, surface properties, and porosity, while examples of macroeffects include particle size and stability. Macroeffects are often not adequately taken into account, although mechanical destruction is one of the most common reasons for changing industrial catalysts.

Although microeffects and macroeffects have their own characteristics, they often act closely together. This is demonstrated by the example of Al_2O_3 , in which variation of the crystallite size and controlled phase transition by means of heat treatment have a major effect on the wear resistance and compressive strength of the material. Interactions between the active component and the support material are discussed in detail in Section 5.4. Chapter 14 deals with the influence of the reactor type on the choice of catalyst.

An example of a successful catalyst development is the production of acrolein by oxidation of propene with air (Eq. 13-1)



The first acrolein plant with a bismuth/molybdenum oxide catalyst was brought on stream by Degussa in 1967. Catalyst development concentrated on the optimiza-



Scheme 13-1 Target quantities and influences on the choice of catalyst [T40]

tion of the active phase and the shape of the catalyst. In decades of development work, the selectivity of the catalyst was ever further increased, and the acrolein yield increased from 40 to 80 % (Table 13-1).

The use of various promoters increased the activity of the catalyst to such an extent that the operating temperature for the formation of acrolein could be lowered from 450–500 to 300–330 °C. In this way the catalyst lifetime was extended to several years.

This example shows just how complex the composition of modern catalysts is, and that the manner in which the catalyst is produced can have a decisive influence on its effectiveness.

Table 13-1 Development of a catalyst for the oxidation of propene to acrolein [7]

| | 1967 | 1972 | 1982 | 1988 |
|----------------------|----------------------------------|--|---|---|
| Form | tablet | extrudate | shell catalyst | extrudate |
| Chemical composition | Bi, Mo, Fe, P, Ni, Co, Sm oxides | Bi, Mo, Fe, P, Ni, Co, W, Si, K oxides | Bi, Mo, Fe, P, Ni, Co, Sm, K, Al, Si oxides | Bi, Mo, Fe, P, Ni, Co, Sm, K, Al, Si oxides |
| Acrolein yield | 40 % | 70 % | 76 % | >80 % |

13.2

An Example of Catalyst Planning: Conversion of Olefins to Aromatics

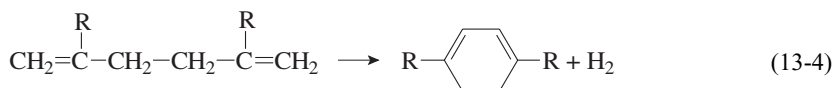
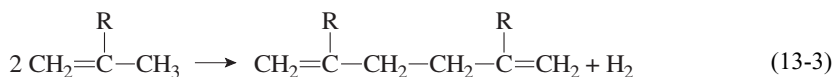
In this section we shall discuss an example that is described in detail in the literature [29, T40]. An attempt was made to develop a catalytic process for the production of aromatics from olefins by means of an oxidative dehydroaromatization reaction.

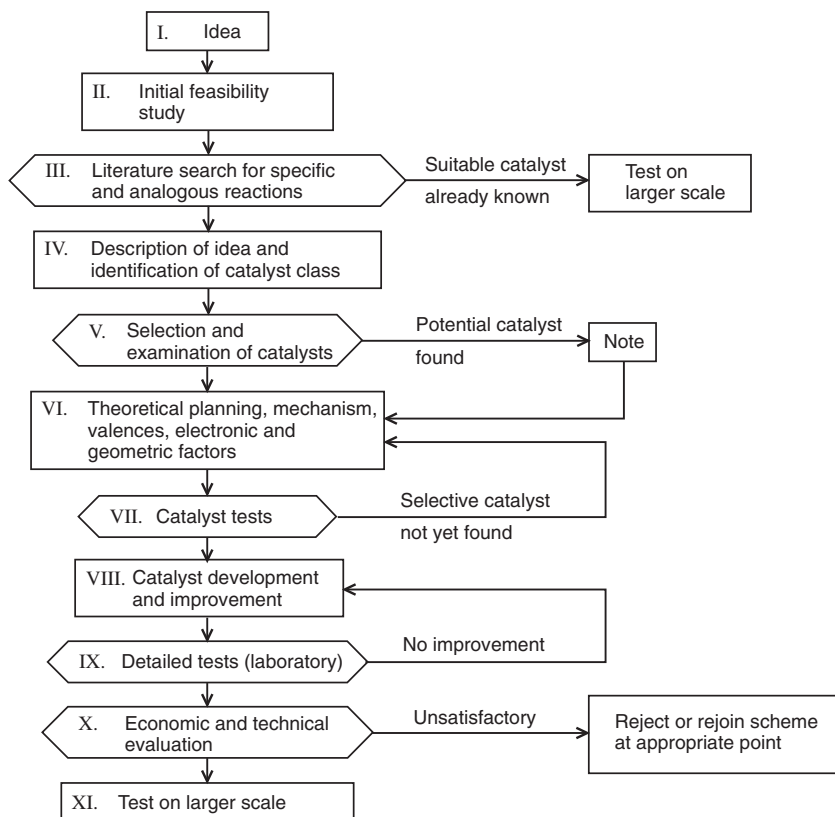
The desired reaction can be formulated as shown in Equation 13-2.



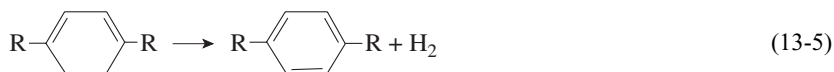
This equation can be regarded as the idea behind the process. The route from this idea to a satisfactorily operating catalytic process is shown in Scheme 13-2. The idea is followed by an initial feasibility study (step II). This involved carrying out simple thermodynamic calculations, which showed that conversion of propene to benzene is at least theoretically possible. The next step is a thorough literature search in which one attempts to find out whether this particular reaction or an analogous reaction has already been carried out. In our example, all that was found was the suggestion that the reaction proceeds more selectively in the presence of oxygen.

Step IV is the formulation of the idea and identification of the catalyst class. For this, the probable course of the reaction must be formulated (Eqs. 13-3 to 13-5).





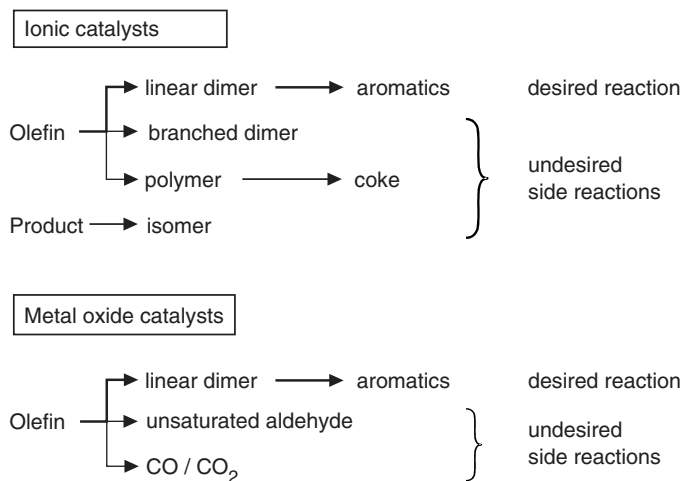
Scheme 13-2 Catalyst planning procedure



According to Equation (13-3), two olefin molecules form a diene, which undergoes cyclization in the next step (Eq. 13-4). The final conversion of the cyclohexadiene system to an aromatic compound (Eq. 13-5) is, like the other two steps a dehydrogenation reaction. Suitable catalysts for these reactions could be the ionic and the metal oxide catalysts. The possible side reactions of both classes are summarized in Scheme 13-3.

The key disadvantage of ionic catalysis is that a carbenium ion is formed as intermediate product and leads to the formation of the undesired branched dimers and high-molecular polymers. Thus only the metal oxides remain as potential catalysts.

Some tests were carried out with some metal oxides already used in other catalytic reactions, including the oxides of Pt, Cr, Mo, Th, and Co. The results, however, were unsatisfactory. Therefore, a search was made for a new metal oxide catalyst by using an exact theoretical plan. Thus, we are at the next step of the process, in



Scheme 13-3 Possible catalyst systems and their disadvantages

which the mechanism, oxidation states, and electronic and geometric factors are investigated. Two conclusions were drawn (Scheme 13-4):

- 1) Under the influence of oxygen, the olefin forms a π -allyl intermediate, which adds to the metal ion.
- 2) An electron is transferred from this intermediate to the metal center. Since the desired dimer is formed from two molecules that are bound to the same metal ion, the catalyst must be capable of accepting two electrons.

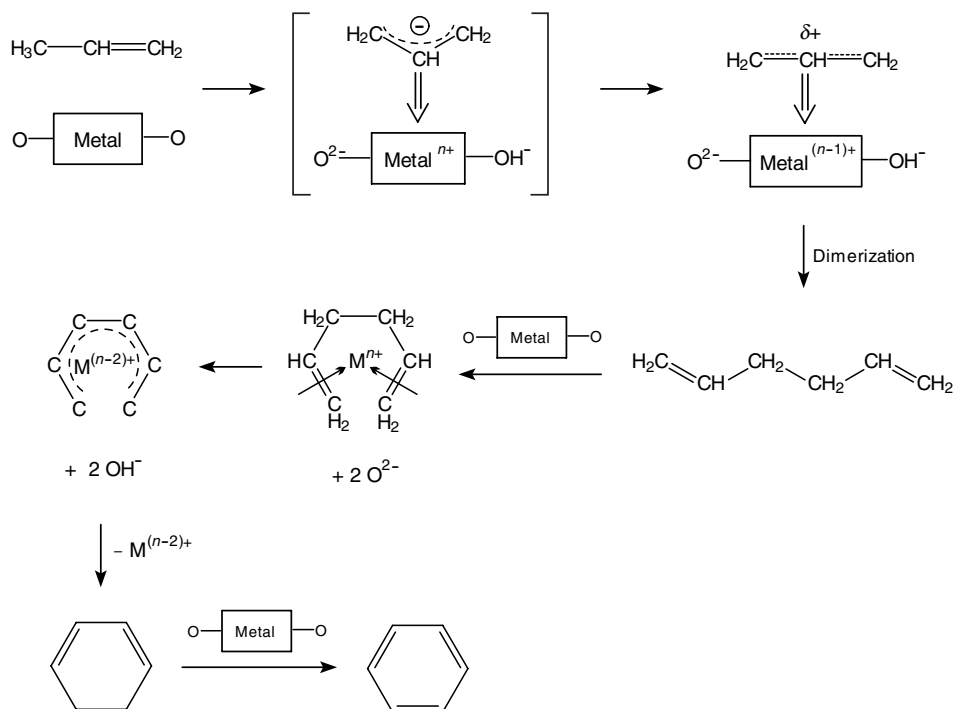
A search was now made for metal oxides that can adsorb olefins in the oxidized state and whose oxidation states differ by two units. These include thallium, lead, indium, and bismuth. Since the oxides of bismuth and lead are of low thermal stability, attention was focussed on the oxides of thallium and indium.

Let us return to the flow sheet of Scheme 13-2. In step VI we made a preliminary choice of catalyst by using theoretical considerations. However, since experiments are the only sure method for testing the mechanistic hypothesis, the next step is catalyst testing.

These tests showed that thallium is also unsuitable for this reaction because the reduced form of the oxide is lost from the reactor due to its volatility. Hence, only the highly selective indium(I)/indium(III) oxide remained as the catalyst of choice.

Let us briefly examine the entire catalyst planning process once again (Scheme 13-5). The ionic catalysts proved to be unfavorable since they gave large amounts of branched products. Since the proven metal oxide catalysts also had many disadvantages, a completely new catalyst was sought. This search led to metal oxides of Groups 13–15, whereby indium oxide proved to be highly selective. Nevertheless, this oxide also has disadvantages, especially the formation of the side products CO_2 and acrolein.

Let us return to our general Scheme 13-2. The next step is improving the catalyst. In our case this means limiting the oxidation to CO_2 and acrolein (step VIII). At-

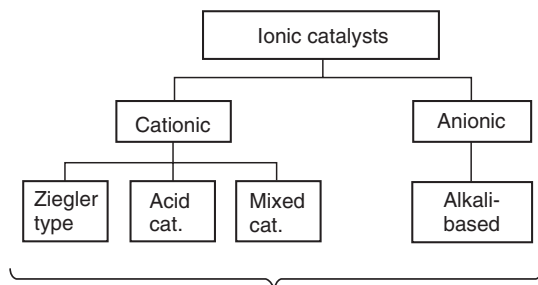


Scheme 13-4 Mechanism of olefin dimerization and cyclization

tempts were made to achieve this by manufacturing a catalyst with optimal pore structure and surface properties.

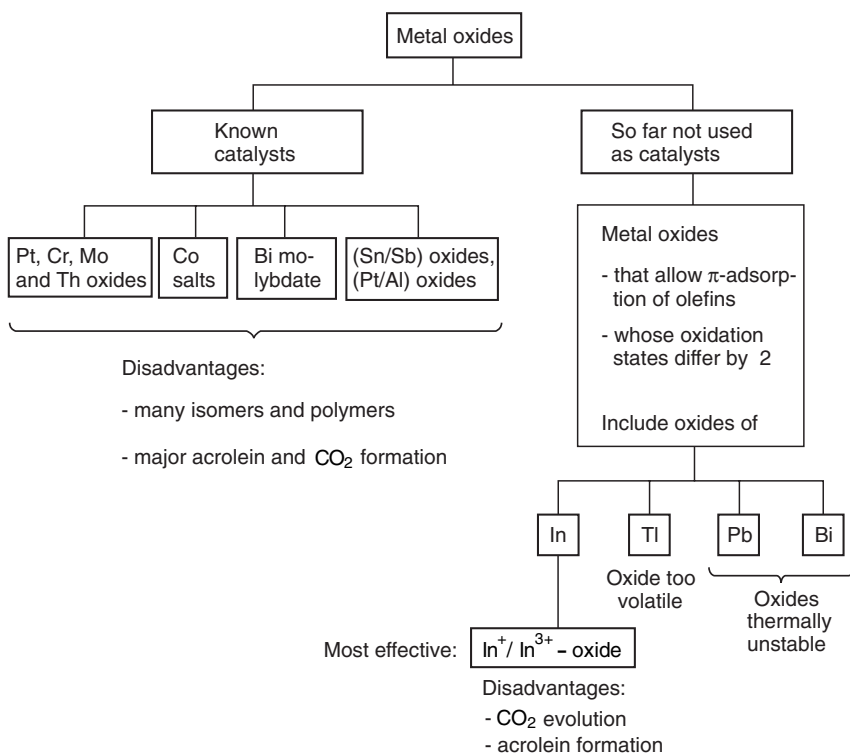
The formation of CO_2 requires the most oxygen of all products. Assuming that the majority of the oxygen is adsorbed on the catalyst, additives that hinder oxygen adsorption should lead to formation of less CO_2 . Since the oxygen can form peroxo species, additives such as Ca and Ba, which promote peroxide formation, should be avoided. Since oxygen acts as an electron acceptor, electronegative catalyst additives should counteract the adsorption of oxygen. Such an effect has been observed with bismuth phosphate, which is a more selective catalyst than bismuth oxide.

On the other hand, it can be expected that radical-like allyl ligands will dimerize rather than react with oxygen. Thus, electrons should be removed from the adsorption centers. Dopants that facilitate this electron transfer should have a positive effect. Such an additive is Bi_2O_3 , with which the indium oxide was doped. The pore structure of the support material could also have an influence on the over-oxidation. Small pores would promote further oxidation by restricting diffusion. Hence supports with large pores should be best. Many of these suggestions were tested, but, as is often the case in heterogeneous catalysis, conflicting results were obtained. Since the entire process was not very interesting from an economic viewpoint, we will end the discussion here.



Disadvantages:

- branched products
- higher polymers
- coke residues



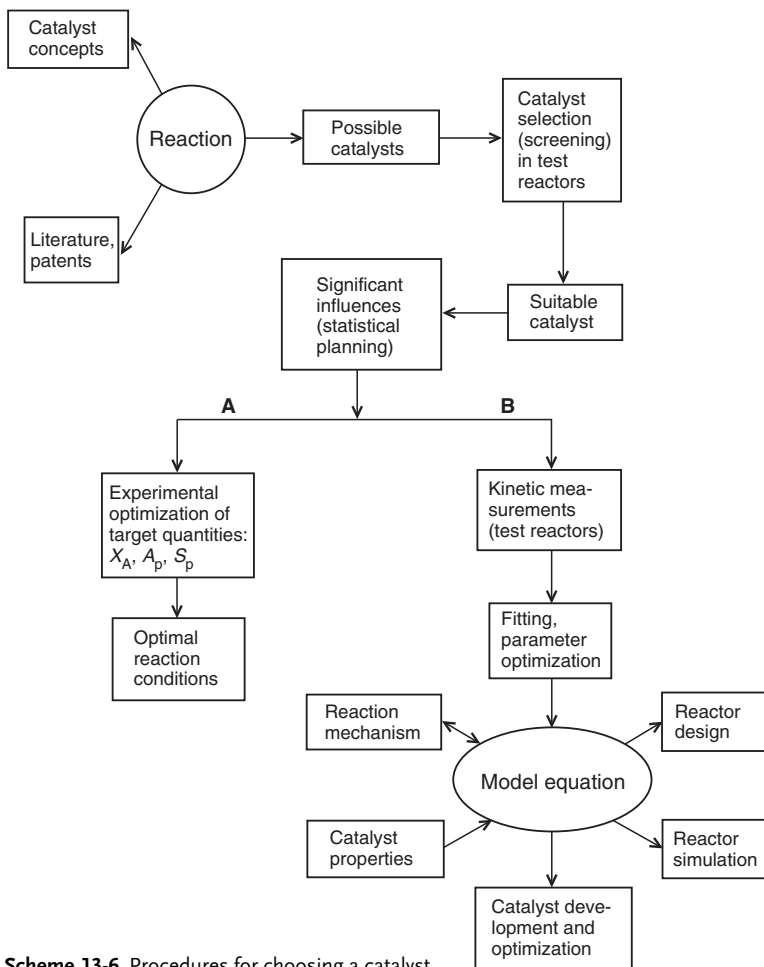
Scheme 13-5 Catalyst planning for the oxidative dehydroaromatization of olefins (Eqs. 13-3 to 13-5)

To summarize: a suitable catalyst was found by means of mechanistic reasoning, and it was shown that planned research can lead to a satisfactory solution within a relatively short time and with minimum effort.

When the detailed tests are complete, an economic and technical evaluation is carried out (Scheme 13-2, step X). Only when this is satisfactory is a process tested on an industrial scale.

13.3 Selection and Testing of Catalysts in Practice

To shorten the laborious process of purely empirical catalyst selection, which sometimes involves hundreds of tests, today use is made of the various catalyst concepts



Scheme 13-6 Procedures for choosing a catalyst

and statistical methods for test planning [25, T40]. The individual steps of such a procedure are shown in Scheme 13-6. This scheme, with its many steps, clearly shows the efforts involved in finding an optimal catalyst and optimal reaction conditions for the desired reacton.

Scheme 13-6 shows two routes, which differ in the amount of knowledge gained. The more pragmatic procedure **A** dispenses with extensive kinetic measurements and aims at direct optimization of the process, whereas in the detailed procedure **B**, modelling and analysis of the catalytic process provide the foundation for reactor design and simulation. In this chapter we shall discuss both possibilities schematically in order to provide chemical engineers with support in the complex field of catalyst development [27].

13.3.1

Catalyst Screening

A catalytic reaction represents a complex problem that is influenced by numerous factors. In order to find a suitable catalyst or solvent for a particular reaction, screening tests are carried out. This means keeping several reaction conditions constant while only one parameter is varied. The procedure is briefly summarized in Table 13-2 [1].

Table 13-2 Catalyst screening

| Measurement method | Advantages | Disadvantages |
|---|--|---|
| Conversion under standardized experimental conditions | Rapid predictions due to simple measurement and evaluation procedure | Low reliability due to arbitrary choice of conditions |

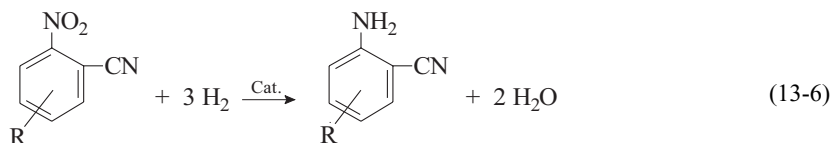
Screening tests do not allow any absolute predictions about the activity or applicability of a catalyst. Instead they provide measurements that can be compared with one another. Therefore, it is important that parameters, once chosen, are applied to all screening experiments.

Catalyst screening provides a comparison of several catalysts with respect to the desired target parameter. Nonsystematic influences can also be investigated in the course of the screening process, for example:

- Dependence of the reaction on solvent
- Effect of adding reagents and cocatalysts
- Influence of catalyst pretreatment
- Estimation of catalyst lifetime

Let us now examine the screening procedure for the example of a catalytic hydrogenation [13, 30].

In the catalytic hydrogenation of substituted 2-nitrobenzotrile, the cyano group is also attacked under normal reaction conditions, and several side products are obtained besides the desired product 2-aminobenzotrile (Eq. 13-6).



Side products: amide, diamine, dimer of the nitro compound.

Table 13-3 lists catalyst systems described in the literature for the hydrogenation of similar nitro compounds.

Table 13-3 Hydrogenation of substituted 2-cyanonitro compounds [30]

| Catalyst system | Amine yield [%] (reaction time) |
|------------------------------------|---------------------------------|
| SnCl ₂ /HCl in DMF | 67 |
| Fe/HCl in methanol | 78 |
| Fe/glacial acetic acid, 2-propanol | 88 |
| Raney Ni, 2-propanol | 91 (24 h) |
| Pd/BaSO ₄ , dioxane | 79 (3 h) |

None of the known examples met the requirements for high yields at short reaction times with environmentally friendly reagents. Therefore, various supported noble metal catalysts and solvents were tested under the same reaction conditions in a catalyst screening program.

It is known that the hydrogenation activity of supported Pd catalysts is the least affected by different substituents and changes in the reaction conditions. In suspension, aromatic nitro compounds are generally hydrogenated in the temperature range 50–150 °C at pressures of 1–25 bar and with catalyst concentrations of 0.1–1 %. In the screening tests the following reaction conditions were kept constant: pressure, temperature, catalyst concentration, starting material concentration, and stirring speed. The results are summarized in Tables 13-4 and 13-5.

Table 13-4 Catalyst screening in the hydrogenation of substituted 2-nitrobenzonitrile

| Experiment | Catalyst | 2-Aminobenzonitrile yield [%] |
|------------|----------------------|--|
| 1 | Pd/C (1) | 87.2 |
| 2 | Pd/C (2) | 85.2 |
| 3 | Pd/C (3) | 90.0 (incl. 10% dimer as intermediate product) |
| 4 | Pd/BaSO ₄ | 84.1 |
| 5 | Pt/C | 34.1 |
| 6 | Raney Ni | 6.3 |
| 7 | Rh/C | 19.7 |

Constant reaction conditions: 5 mL stirred autoclave, 0.1 g starting material, 1.0 mL ethanol, 25 °C, 1 bar H₂ pressure, 20 mg catalyst, 120 min reaction time, stirring speed 700 rpm, catalysts 1–3: commercial 5% Pd/activated carbon catalysts.

Table 13-5 Solvent screening in the hydrogenation of substituted 2-nitrobenzotrile

| Experiment | Solvent | 2-Aminobenzotrile yield [%] |
|------------|---------------------------------|-----------------------------|
| 1 | dioxane | 60 |
| 2 | methanol | 59 |
| 3 | acetic acid | 33 |
| 4 | ethanol | 90 |
| 5 | <i>tert</i> -butyl methyl ether | 74 |
| 6 | toluene | 53 |
| 7 | ethyl acetate | 24 |
| 8 | dichloromethane | 75 |
| 9 | hexane | 33 |
| 10 | acetic anhydride | 21 |
| 11 | isopropanol | 72 |
| 12 | DMF | 77 |

Reaction conditions: Table 13-4.

The best catalyst proved to be the supported Pd catalyst (3) since the dimer can be regarded as an intermediate product. This catalyst was then used for the subsequent solvent tests (Table 13-5).

In all screening tests it is important that stirring be carried out with a high rate of over 600 rpm to ensure that the reactions proceed under kinetic control.

Ethanol proved to be the best solvent and was used for subsequent tests. The successful screening program was followed by reactor optimization with a special testing plan (see Section 13.3.3).

13.3.2

Catalyst Test Reactors and Kinetic Modeling [27, 28]

Heterogeneously catalyzed gas-phase reactions play a very important role in industrial chemistry. Therefore, this chapter deals with how kinetic data are obtained for such reactions.

Kinetic Modeling

The kinetics of catalytic reactions can be explored using any type of reactor with known contacting pattern. The only prerequisite to observe is to apply the correct performance equation. Usually the extent of conversion of gas passing in steady flow through a batch or solids is measured. In turn we discuss the experimental devices:

- Differential (flow) reactor
- Integral (plug flow) reactor
- Mixed flow reactor (recycle reactor)

A batch reactor for both gas and solid can also be used.

Differential Reactor

We have a differential flow reactor on the premises that the rate is constant at all points within the reactor. The rate of reaction can be determined as a function of either concentration or partial pressure of the reactants. Since rates are concentration-dependent this assumption can only be made for extremely small conversions or for shallow small reactors.

As a result, the reactant concentration through the reactor is essentially constant and approximately equal to the inlet concentration. Thus, the reactor is considered to be gradientless, the reaction rate is considered spatially uniform within the bed, and the reactor operates in an isothermal manner. A typical arrangement is shown in Figure 13-2.

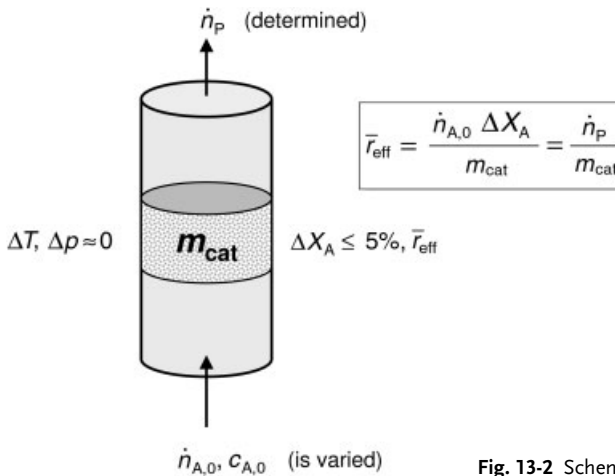


Fig. 13-2 Scheme of a differential reactor

In some cases sampling and analyses of the product stream may be difficult for small conversions in multicomponent systems. During kinetic measurements the flow rate through the catalyst bed is monitored, as are the entering and exiting concentrations. Therefore, if the weight of catalyst m_{cat} is known, the rate of reaction per unit mass of catalyst, r'_A , can be calculated. Since the differential reactor is assumed to be gradientless, the design equation will be similar to the CSTR design equation.

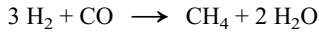
For each run in a differential reactor the performance Equation 13-7 becomes

$$-r'_A = \frac{\dot{n}_{A,0} \Delta X_A}{m_{\text{cat}}} = \frac{\dot{n}_P}{m_{\text{cat}}} \quad (13-7)$$

Thus each run gives directly a value for the rate at the average concentration in the reactor, and a series of runs gives a set of rate-concentration data which can then be analyzed for a rate equation. The following example illustrates the suggested procedure.

Example: Differential reactor

The formation of methane from carbon monoxide and hydrogen using a nickel catalyst was studied in a differential reactor. The reaction



was carried out at 260 °C. The partial pressures of H₂ and CO were determined at the entrance to the reactor, and the methane concentration was measured at the reactor exit.

| Run | p_{CO} (bar) | p_{H_2} (bar) | $c_{\text{CH}_4} \cdot 10^4$ (mol/L) |
|-----|-----------------------|------------------------|--------------------------------------|
| 1 | 1.0 | 1.0 | 2.44 |
| 2 | 1.8 | 1.0 | 4.40 |
| 3 | 4.08 | 1.0 | 10.0 |
| 4 | 1.0 | 0.1 | 1.65 |
| 5 | 1.0 | 0.5 | 2.47 |
| 6 | 1.0 | 4.0 | 1.75 |

The exit volumetric flow rate from a differential packed bed containing 10 g of catalyst was maintained at 300 L/min for each run.

Theoretical considerations predict that if the rate-determining step in the overall reaction is the reaction between atomic hydrogen adsorbed on the nickel surface and CO in the gas phase, then the rate law will be in the form

$$r'_{\text{CH}_4} = \frac{ap_{\text{CO}}p_{\text{H}_2}^{1/2}}{1 + bp_{\text{H}_2}}$$

- Relate the rate of reaction to the exit methane concentration.
- Verify the assumption of the rate law by determination of the parameter a and b employing nonlinear regression.

Solution:

- The rate can be written in terms of the volumetric flow rate and the concentration of methane. Since \dot{V}_0 , c_{CH_4} and m_{cat} are known for each run, we can calculate the rate of reaction (Eq. 13-7). For run 1:

$$r'_{\text{CH}_4} = \frac{\dot{n}_{\text{CH}_4}}{m_{\text{cat}}} = \frac{\dot{V}_0 c_{\text{CH}_4}}{m_{\text{cat}}} = \frac{300 \cdot 2.44 \cdot 10^{-4}}{10} = 7.32 \cdot 10^{-3} \text{ mol min}^{-1} \text{ g}^{-1} \quad (\text{run 1})$$

The rate for runs 2 through 6 can be calculated in a similar manner:

$$r_2 = 0.0132 \quad r_3 = 0.030 \quad r_4 = 0.00495 \quad r_5 = 0.00742 \quad r_6 = 0.00525$$

b) With POLYMATH the rate law can be determined as follows:

Differential Reactor
Nonlinear regression (L-M)

Model: $r = a \cdot p_{\text{CO}} \cdot p_{\text{H}_2}^{5e-1} / (1 + b \cdot p_{\text{H}_2})$

| <u>Variable</u> | <u>Ini guess</u> | <u>Value</u> | <u>95% confidence</u> |
|-----------------|------------------|--------------|-----------------------|
| a | 1, | 0,0180768 | 3,728E-04 |
| b | 1, | 1,4602939 | 0,051166 |

Nonlinear regression settings
Max # iterations = 64

Precision

$R^2 = 0,9999879$
 $R^2_{\text{adj}} = 0,9999849$
Rmsd = 1,245E-05
Variance = 1,394E-09

Rate law:

$$r'_{\text{CH}_4} = \frac{1.81 \cdot 10^{-2} p_{\text{CO}} p_{\text{H}_2}^{1/2}}{1 + 1.46 p_{\text{H}_2}}$$

In principle the kinetics of an industrial process can be measured on the laboratory scale or in a pilot plant. Apart from the small amounts of material involved, on the laboratory scale the test conditions can be chosen such that chemical and transport phenomena (microkinetic and macrokinetic effects), which are equally important in an industrial process, can be investigated in isolation [T26].

The two types of laboratory reactor shown in Figure 13-3 have proved to be the most suitable for reaction engineering investigations on heterogeneously catalyzed gas-phase reactions [27].

The concentration-controlled, gradientless differential circulating reactor is best suited for kinetic measurements. Such modern laboratory reactors are now of major importance. They allow kinetic data to be measured and evaluated practically free of distortion by heat- and mass-transport effects [17]. Depending on the material flow, a distinction is made between reactors with outer and inner circulation. Evaluation of the kinetic measurements is straightforward because the simple algebraic balance equation for a stirred tank reactor (Eq. 13-8) can be applied (prerequisite: high recycle ratio R). In practice it is found that recycle ratios of $R = 10-25$ are sufficient to achieve practically ideal stirred tank behavior [8].

$$-r'_A = \frac{\dot{n}_{A,0} - \dot{n}_A}{m_{\text{cat.}}} = \frac{\dot{n}_{A,0} X_A}{m_{\text{cat.}}} \quad (13-8)$$

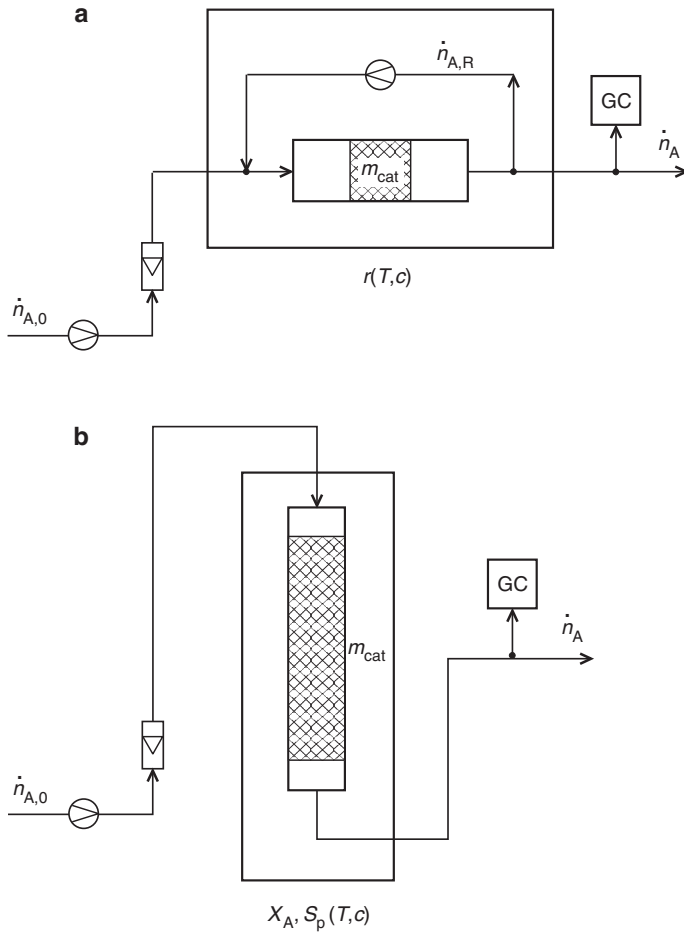


Fig. 13-3 Catalyst test reactors

(a) Gradientless reactor
(differential circulating reactor)

(b) Laboratory or pilot
integral reactor

Information: r and kinetic parameters
differential values measured
under transport-free conditions

r_{eff}
integral measures of activity (X_A)
and selectivity (S_p)
behavior over the lifetime of the catalyst

Evaluation: algebraic equation

differential equation

Behavior: like a continuous stirred tank
approximately isothermal

like a flow tube
temperature profile

Before a series of tests is carried out for a particular reaction, the suitability of the differential circulating reactor for kinetic investigations should be proven. The following should be tested:

- The gradient-free operation of the reactor: no influence of the rate of rotation of the reactor drive or the gas-delivery system on the reaction rate
- Exclusion of pore diffusion: tests with different catalyst particle sizes and pressures
- Ideal stirred tank behavior: residence time measurements, e. g., by step-injection tracer experiments
- Influence of so-called blank test reactions, e. g., reactor-wall catalysis above ca. 450 °C

A very simple variant of the differential circulating reactor is the so-called jet loop reactor shown schematically in Figure 13-4. Combined with online analysis of the product stream, the apparatus can be used to investigate commercially available or specially manufactured heterogeneous catalysts for gas-phase reactions (Fig. 13-5). After passing through a nozzle, the gas (e. g., CO/H₂ in methanol synthesis) flows through the inner tube and carries recycle gas with it in the direction of flow shown in the figure. On the catalyst bed, which consists of about two layers of pellets (ca. 25 g), the synthesis gas is converted into methanol in accordance with the thermodynamic equilibrium. A gas stream is removed from the reactor in an amount corresponding to the feed stream and analyzed by GC. Typical results are exemplified by the gas chromatograms shown in Figure 13-6.

A commercial CuO-based methanol catalyst was preformed with synthesis gas (Fig. 13-6a). After a short time, CO₂ and H₂O are found in the gas mixture as a result of catalyst reduction. Above ca. 200 °C methanol is formed, and eventually the stationary equilibrium with ca. 20 % methanol at 220 °C is reached (Fig. 13-6b).

Such a reactor, designed for temperatures up to 500 °C and pressures up to 400 bar, was used for exact kinetic modeling of methanol synthesis [26].

Reaction Conditions:

12 g Cu catalyst, cylindrical pellets,

diameter = height = 5 mm

225–265 °C, 20–80 bar;

Feed stream 7–25 % CO

1–15 % CO₂

60–90 % H₂

Throughput 0.2–1.2 m³/h

Recycle ratio $R \geq 30$

$r_{\text{CH}_3\text{OH}} = 0.01\text{--}0.09 \text{ kmol}(\text{kg cat.})^{-1} \text{ h}^{-1}$

Langmuir–Hinshelwood kinetics were determined, and the rate-determining step is reduction of the intermediate formaldehyde (Eqs. 13-9 and 13-10).



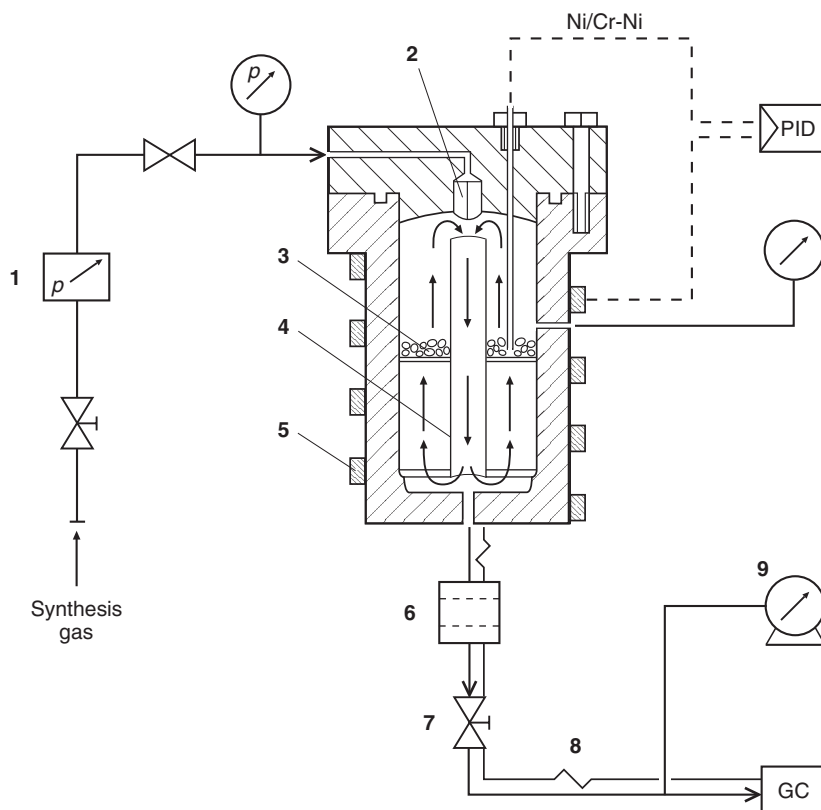


Fig. 13-4 Jet loop reactor for catalyst investigations (high-pressure laboratory, FH Mannheim, Germany)

- 1) Thermal mass flow controller (up to 200 bar); 2) Nozzle, interchangeable;
- 3) Catalyst pellets on wire mesh; 4) Central tube; 5) Heating band 500 W;
- 6) Microfilter; 7) Precision feed valve; 8) Supplementary heating; 9) Gas meter

Another versatile catalyst test reactor for the investigation of multiphase reactions is shown in Figure 13-7. In such reactors, rotational velocities in excess of 750 rpm ensure very good mass transfer between the catalyst, the gas bubbles, and the liquid, and an internal circulation is generated in the reactor [4].

Numerous kinetic studies with such reactors have been reported in the literature, including:

- Hydrodesulfurization of model substances such as dibenzothiophene [20]
- Hydrogenation of olefins
- Dehydrocyclization reactions

The fewest experimental problems are caused by the integral reactor due to its simple construction and straightforward operation. It consists of a flow tube, 20–50 cm in length and ca. 2 cm in diameter, filled with catalyst. The conversion achieved in such reactors is high and can readily be determined by comparing the



Fig. 13-5 Jet loop reactor (high-pressure laboratory, FH Mannheim, Germany)

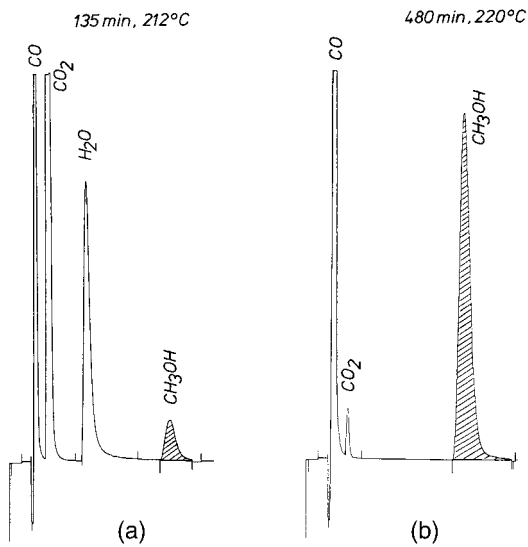


Fig. 13-6 Gas chromatogram of methanol synthesis in the jet loop reactor
Reaction conditions: CO/H₂ = 1/2, 40 bar, 25 g cat., $\dot{V}_0 = 500$ mL/min,
nozzle diameter 0.1 mm



Fig. 13-7 Industrial catalyst test center (Süd-Chemie AG, Heufeld, Germany)

initial and final concentrations of a reactant. A test series is carried out with variation of the values of the catalyst mass m_{cat} or the feed flow rate $\dot{n}_{A,0}$, thus covering a wide range of conversions.

The favored method is to evaluate the data with a differential form of the design equation of the tubular reactor (Eq. 13-11).

$$-r'_A = \frac{dX_A}{d(m_{\text{cat.}}/\dot{n}_{A,0})} \quad (13-11)$$

The rate r'_A can be obtained directly from the individual measurements by graphical differentiation (Fig. 13-8). The slope of the tangent of the conversion–time factor curve corresponds to the momentary reaction rate under the given test conditions.

The disadvantage of the integral reactor is that it can not be operated isothermally and that the measured overall conversion is generally the result of a complex interplay between transport phenomena and chemical reaction. Hence the integral reactor is mainly used for comparative catalyst studies and lifetime tests. Its advantages are:

- Rapid, empirical, and practice-relevant process development
- Conclusions about catalyst activity from changes in temperature and concentration profiles
- Catalyst deactivation can be followed
- Relatively simple scale-up

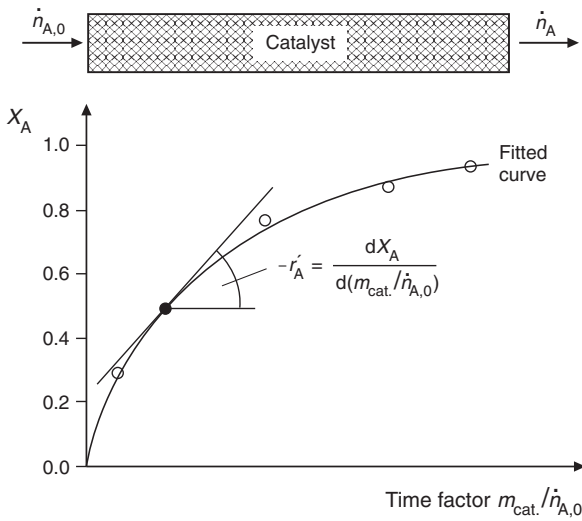


Fig. 13-8 Evaluation of the data from an integral reactor

In reaction engineering investigations it is generally not sufficient to draw conclusions about the activity and selectivity of a catalyst on the basis of conversion and yield. Transport limitations and hence the structure of the individual catalyst particles (shell catalyst/bulk catalyst, molded catalyst/extruded catalyst, etc.) must also be taken into account. The determination of the parameters and the selection of models for the quantitative kinetic description of the catalyst should be followed by the simulation of industrial reactors in order to obtain more information on the practical suitability of the chosen catalyst.

Example: Integral reactor

The following kinetic data on the reaction $A \rightarrow R$ are obtained in an experimental packed bed reactor using various amounts of catalyst and a fixed feed rate $\dot{n}_{A,0} = 10 \text{ mol/h}$. The initial concentration is $c_{A,0} = 2 \text{ mol/L}$.

| m_{cat} (g) | 1 | 2 | 3 | 4 | 5 | 6 | 7 |
|----------------------|-------|-------|-------|-------|-------|-------|-------|
| X_A | 0.116 | 0.203 | 0.272 | 0.330 | 0.370 | 0.408 | 0.440 |

Find the reaction rate equation $r = k c_A^n$, using the differential method of analysis.

Solution:

Equation 13-11

$$r = \frac{dX_A}{d(m_{\text{cat}}/\dot{n}_{A,0})} \quad (13-11)$$

shows that the rate of reaction is given by the slope of the X_A versus $m_{\text{cat}}/\dot{n}_{A,0}$ (time-factor TF) curve. A method to determine r is to fit the conversion X_A to a polynomial in time-factor TF and then to differentiate the resulting polynomial. Choosing a third-order polynomial

$$X_A = a_0 + a_1 TF + a_2 TF^2 + a_3 TF^3$$

we use the POLYMATH software to express conversion as a function of TF to obtain the parameters

$$a_0 = 6.97 \cdot 10^{-4}$$

$$a_1 = 1.268$$

$$a_2 = -1.404$$

$$a_3 = 0.699$$

A plot of X_A versus TF and the corresponding third-order polynomial fit is shown in Figure 13-9.

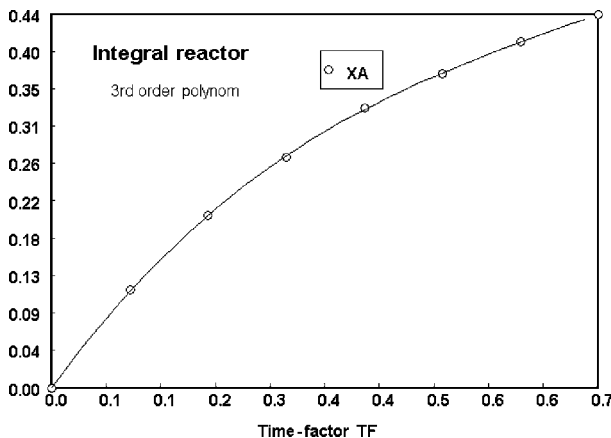


Fig. 13-9 Polynomial fit of X_A vs. TF (example integral reactor)

Differentiating the polynomial expression yields

$$\begin{aligned} \frac{dX_A}{dTF} &= a_1 + 2a_2 TF + 3a_3 TF^2 \\ &= 1.268 - 2 \cdot 1.404 \cdot TF + 3 \cdot 0.699 \cdot TF^2 \end{aligned}$$

To find the derivative at various TF -values we substitute the appropriate TF into the differential equation to arrive the new data set in Table 13-6. The c_A values can be calculated from $c_A = c_{A,0}(1 - X_A)$.

The results are shown in Table 13-6.

Table 13-6 Processed data from example

| Run | m_{cat} (g) | c_A (mol/L) | $\frac{m_{\text{cat}}}{n_{A,0}} = TF$ (g h mol ⁻¹) | X_A | $r = \frac{dX_A}{dTF}$ (mol g ⁻¹ h ⁻¹) |
|-----|----------------------|---------------|---|-------|--|
| 0 | 0 | 2.0 | 0 | 0 | 1.268 |
| 1 | 1 | 1.768 | 0.1 | 0.116 | 1.008 |
| 2 | 2 | 1.594 | 0.2 | 0.203 | 0.790 |
| 3 | 3 | 1.456 | 0.3 | 0.272 | 0.614 |
| 4 | 4 | 1.340 | 0.4 | 0.330 | 0.480 |
| 5 | 5 | 1.260 | 0.5 | 0.370 | 0.388 |
| 6 | 6 | 1.184 | 0.6 | 0.408 | 0.338 |
| 7 | 7 | 1.120 | 0.7 | 0.440 | 0.330 |

With the POLYMATH nonlinear regression program the rate law with the parameter k and n can be determined.

Integral Reactor

Nonlinear regression (L-M)

Model: $r = k \cdot c_A^n$

| <u>Variable</u> | <u>Ini guess</u> | <u>Value</u> | <u>95 % confidence</u> |
|-----------------|------------------|--------------|------------------------|
| k | 0, 3 | 0, 2428941 | 9, 855E-05 |
| n | 2, | 2, 4234404 | 7, 232E-04 |

Nonlinear regression settings

Max # iterations = 64

Precision

$R^2 = 0,9915899$

$R^2_{\text{adj}} = 0,9901882$

Rmsd = 0,0104325

Variance = 0,0011609

The rate law is $r = 0.243c_A^{2.42}$.

13.3.3

Statistical Test Planning and Optimization [6, 21]

Statistical test planning is an effective aid to recognizing significant quantities that influence chemical reactions. A systematic process for searching for suitable catalysts and optimizing them is especially helpful in the case of catalytic reactions, with their numerous test parameters.

In this chapter we shall largely dispense with the mathematical basis of statistical test planning and we will illustrate the method with the aid of some simple practical examples.

13.3.3.1 Factorial Test Plans

A 2^n factorial design is the simplest complete test plan for investigating the influence of n variables on the test result.

Definitions:

Variable: independent quantity of arbitrary magnitude, assumed to have an influence on the test result

Levels: settings of the parameters, e. g., temperature as reaction parameter 30 and 60 °C

Designation of the variables:

- variable at the lower level
- + variable at the higher level
- (1) all variables at the lower level
- a variable A at higher level, all other variables at lower level
- A, B variables (effects)
- AB, AC interaction effects

A factorial design with three variables and two levels would lead to a test plan with eight experiments (Table 13-7). In a three-dimensional depiction, these eight tests occupy the corners of a cube (Fig. 13-10).

Table 13-7 2^3 factorial design (eight experiments, three factors)

| Experiment designation | A | B | C |
|------------------------|---|---|---|
| (1) | – | – | – |
| a | + | – | – |
| b | – | + | – |
| ab | + | + | – |
| c | – | – | + |
| ac | + | – | + |
| bc | – | + | + |
| abc | + | + | + |

Factorial designs should be preferentially used when:

- The effect of many variables in a limited area has to be tested rapidly
- The interaction effects between several variables are unknown
- Initial tests for the selection of variables are to be carried out
- Several target quantities have to be simultaneously distinguished

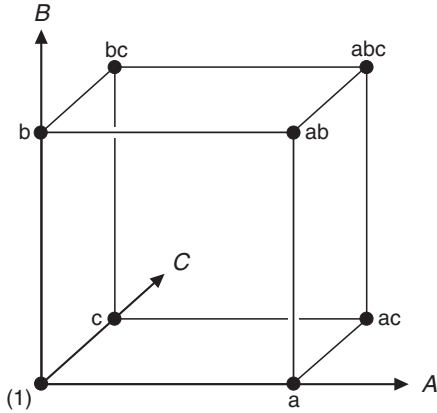


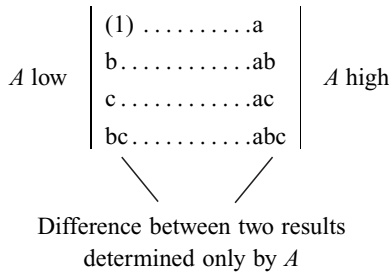
Fig. 13-10 2^3 factorial design with designation of the experiments

Evaluation of 2^n Factorial Designs:

The following questions have to be answered:

- 1) Which variables have an influence on the target quantity?
- 2) Which variables interact with one another?

1) Four pairs of results are influenced only by the variable A :



The effects of the variables are expressed relative to the mean value of all the measurements and half of the difference between levels, for example:

$$A = 1/8 [(a - 1) + (ab - b) + (ac - c) + (abc - bc)]$$

The values calculated in this way allow the effects to be compared with one another. However, whether an effect is measurable depends on the scatter of the tests (significance tests).

2) A distinction is made between twofold and multifold interactions. For example, the interaction AB is defined as the difference in effect A with B high and effect A with B low; hence:

$$AB = 1/8 [(ab - b) + (abc - bc) - (a - 1 + ac - c)]$$

All effects and interactions can be calculated rapidly by using the Yates scheme [25]. The tests are arranged in the standard order. Then the first and second, third and fourth, etc., values are added together to give the top half of column (1). Now the first value is subtracted from the second, the third from the fourth, and so on, to give the bottom half of column (1).

The calculation is continued until n columns are obtained (i.e., equal to the number of variables). The last column gives the “total” and 2^n times the effects and interactions. The “total” is the 2^n -fold mean test result that is theoretically obtained under average test conditions.

The procedure will now be explained for the example of oxo synthesis. Conjugated dienes are converted into mono- and dialdehydes by phosphine-modified rhodium catalysts [12]. The target quantity, in this case the extent of dialdehyde formation, depends mainly on the three reaction parameters temperature (A), cocatalyst ratio (B), and total pressure (C). A 2^3 factorial design was carried out (Table 13-8). The evaluation of the test results by the Yates scheme is shown in Table 13-9.

Table 13-8 2^3 factorial design for oxo synthesis

| Factors | Levels | | | | | | | |
|----------------------|--------|-----|-----|-----|-----|-----|-----|-----|
| Temp. [°C] A | 90 | | | | 120 | | | |
| Cocatalyst ratio B | 6 | | 30 | | 6 | | 30 | |
| Pressure [bar] C | 100 | 150 | 100 | 150 | 100 | 150 | 100 | 150 |
| Experiment | (1) | c | b | bc | a | ac | ab | abc |

Table 13-9 Evaluation of the 2^3 factorial design

| Experiment | Dialdehyde yield [%] | | | | Effect or interaction | Meaning |
|------------|----------------------|------|------|------|-----------------------|---------|
| | | (1) | (2) | (3) | | |
| (1) | 5.6 | 8.5 | 21.1 | 49.5 | 6.2 | Total |
| a | 2.9 | 12.6 | 28.4 | -1.7 | -0.21 | A |
| b | 6.0 | 12.9 | -2.3 | 6.7 | 0.84 | B |
| ab | 6.6 | 15.5 | 0.6 | 3.3 | 0.41 | AB |
| c | 6.3 | -2.7 | 4.1 | 7.3 | 0.91 | C |
| ac | 6.6 | 0.6 | 2.6 | 2.9 | 0.36 | AC |
| bc | 7.6 | 0.3 | 3.3 | -1.5 | -0.19 | BC |
| abc | 7.9 | 0.3 | 0 | -3.3 | -0.41 | ABC |

Interpretation of the Results:

The average value of the yield is 6.2% and is theoretically attained under average reaction conditions, that is

Reaction temperature: 105 °C
 Cocatalyst ratio: 18
 Pressure: 125 bar

Effect $A = -0.21$ means that the yield decreases by 0.21 % when the reaction temperature is raised by 15 °C, and so on.

The predictions are valid only for the measurement range, but it has to be questioned whether the smallest effects are at all meaningful. In the laboratory the effects are assessed in terms of the experimental scatter or the precision of the instrumentation. An effect must differ significantly from the experimental scatter. Test results are assessed by carrying out significance tests.

Terms:

a) Experimental error variance s^2 : a measure of the scatter

$$s^2 = \frac{1}{n-1} \sum_{i=1}^n (x_i - \bar{x})^2 = \frac{\text{Sum of squares}}{\text{Degrees of freedom}} \quad (13-12)$$

$$\bar{x} = \text{mean value} = \frac{1}{n} \sum_{i=1}^n x_i \quad (13-13)$$

b) Sample standard deviation s : has the same dimensions as the measured quantity

$$s = \sqrt{s^2}$$

c) Sample: a randomly selected part of the total number of measurements.

d) Normal distribution: the fact that the results of a measurement are scattered around a mean value is well known. If the number of times a particular value occurs within a certain interval is plotted, then the distribution shown in Figure 13-11 is obtained.

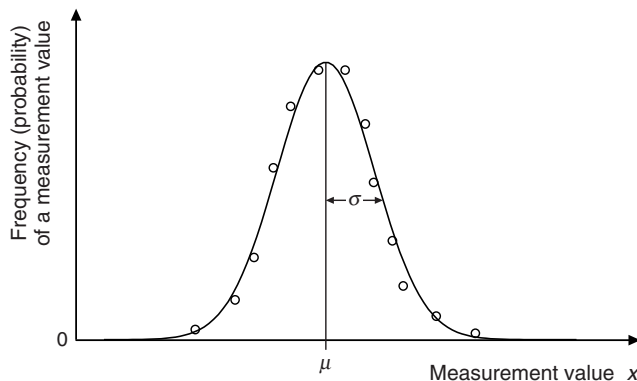


Fig. 13-11 Gaussian or normal distribution

Dividing the actual frequencies by the total number of measurements of the sample gives the relative frequency distribution. If the relative probability distribution is calculated by using the total number of measurements, the probability distribution is obtained (normal or Gaussian distribution; Eq. 13-14).

$$N(\mu, \sigma) = \frac{1}{\sigma\sqrt{2\pi}} e^{-(x-\mu)^2/2\sigma^2} \quad (13-14)$$

The normal distribution has a mean value μ and a variance σ^2 . The sample average \bar{x} and the sample variance s^2 are estimates for μ and σ^2 of the total number of measurements, which have no systematic errors.

The frequency, i.e., probability, with which the measurements occur at a given distance from the mean value have been tabulated. Such tables are used to determine whether experimental results support a hypothesis [3, 21].

Let us now check the significance of the results of our factorial design (Table 13-10). The standard deviation is known from earlier investigations to be $\sigma = 0.92$.

The variance of the effects is calculated from the variance of the measurements by means of the error-propagation law (Eq. 13-15).

$$Var_{\text{Eff}} = \frac{1}{2^n} \sigma^2 \quad (13-15)$$

From Equation 13-15 we obtain:

$$\sigma_{\text{Eff}} = \sqrt{1/8} \cdot \sigma = 0.32$$

Step 1: H_0 : the effects A, B, \dots belong to a normal distribution with $\mu = 0$ and $\sigma = 0.32$

Step 2: chosen level of confidence = 95 % (5 % level of risk)

Step 3: test quantity $z = \frac{\text{Eff} - \mu}{\sigma_{\text{Eff}}} = \frac{\text{Eff} - 0}{0.32}$

Step 4: significance number $c = 2$ (from Gaussian distribution table; two-sided statistical decision)

Result: only the effects B and C are significant (see Table 13-10).

Table 13-10 Significance test on the results of the factorial design

| Effects | $z = \frac{\text{effect}}{0.32}$ | $z > c$ |
|---------------|----------------------------------|------------------|
| $A = -0.21$ | 0.66 | no |
| $B = 0.84$ | 2.6 | yes, significant |
| $AB = 0.41$ | 1.3 | no |
| $C = 0.91$ | 2.9 | yes, significant |
| $AC = 0.36$ | 1.1 | no |
| $BC = -0.19$ | 0.59 | no |
| $ABC = -0.41$ | 1.3 | no |

13.3.3.2 Plackett–Burman Plan [14, 22]

The Plackett–Burman plan, which is based on statistics and combinatorial analysis, allows $N - 1$ effects of variables to be determined simultaneously in N tests. In this highly simplified test plan, only the main effects can be determined numerically; at the same time, error estimation is performed by means of a blank variable. Interactions between the variables can not be determined. A test matrix for seven variables is shown in Table 13-11.

Table 13-11 Plackett–Burman test plan with seven factors

| Exp. no. | A | B | C | D | E | F | G |
|----------|---|---|---|---|---|---|---|
| 1 | + | + | + | – | + | – | – |
| 2 | + | + | – | + | – | – | + |
| 3 | + | – | + | – | – | + | + |
| 4 | – | + | – | – | + | + | + |
| 5 | + | – | – | + | + | + | – |
| 6 | – | – | + | + | + | – | + |
| 7 | – | + | + | + | – | + | – |
| 8 | – | – | – | – | – | – | – |

To calculate the effects the measurements are added or subtracted with the signs listed in the columns, and the sum is divided by four.

The blank effects should be zero. Usually the blank effects are regarded as the experimental error and are used to test the significance of the main effects. This is done by performing a t -test: the mean sum of squares of the blank effects is calculated as the variance (Eq. 13-16).

$$s^2 = \frac{\Sigma \text{effects}^2 \text{ of the blank variables}}{\text{sum of blank variables}} \quad (13-16)$$

The variance of an effect is determined by calculating the test quantity $t = \text{effect}/s$.

An example is the identification of the significant reaction parameters in the bis-hydroformylation of 1,3-pentadiene (Table 13-12). The results of the hydroformylation experiments are summarized in Table 13-13. The results were evaluated by the method described above (Table 13-14).

The blank variable G also exhibited an effect and therefore could not be used for estimating the standard deviation. The reason for this is probably that the highly simplified test plan did not take any interaction effects into account. Hence the standard deviation of $s = 0.9$ known from other test series was used for the significance test (t -test):

t -values (from statistics tables)

| | |
|-----|------------|
| 99% | $t = 63.7$ |
| 95% | $t = 12.7$ |
| 90% | $t = 6.3$ |

Table 13-12 Experimental parameters and reactions conditions

| Variables | Levels | |
|---|--------|---------|
| | - | + |
| (A) Temperature [°C] | 100 | 120 |
| (B) Total pressure [bar] | 100 | 150 |
| (C) CO content synthesis gas [%] | 30 | 70 |
| (D) Catalyst quantity [HRh(CO)(PPh ₃) ₃] [mg] | 50 | 200 |
| (E) Solvent | ether | benzene |
| (F) Solvent quantity [mL] | 20 | 50 |
| (G) Blank variable | - | - |

10.2 g 1,3-pentadiene (0.15 mol), 1 g PPh₃, 150 mL rocking autoclave

Table 13-13 Plackett–Burman plan for the hydroformylation of 1,3-pentadiene

| Experiment | Reaction time [h] | Yield [%] | |
|------------|-------------------|---------------|----------------------------------|
| | | Monoaldehydes | Dialdehydes (target quantity) |
| 1 | 18 | 53.3 | 8.4 |
| 2 | 3 | 43.2 | 23.4 |
| 3 | 22 | 43.8 | 6.5 |
| 4 | 11 | 48.3 | 23.1 |
| 5 | 6 | 51.6 | 6.8 |
| 6 | 7 | 36.6 | 2.5 |
| 7 | 9 | 63.3 | 12.9 |
| 8 | 13 | 49.6 | 4.0 |

Table 13-14 Evaluation of the experimental matrix (target quantity: dialdehyde yield)

| | A | B | C | D | E | F | G |
|------------------------|------|------|-------|------|------|------|------|
| Column total | 2.6 | 48.0 | -27.0 | 3.60 | -6.0 | 11.0 | 23.4 |
| Effects ($\Sigma/4$) | 0.65 | 12.0 | -6.8 | 0.9 | -1.5 | 2.8 | 5.9 |
| $t = \text{Effects}/s$ | 0.7 | 13.3 | -7.6 | 1.0 | -1.7 | 3.1 | - |

Only the variables *B* (total pressure) and *C* (CO content of synthesis gas), with degrees of confidence of 95 and 90 %, respectively, are significant.

13.3.3.3 Experimental Optimization by the Simplex Method [16, 24, 25]

This simple search method allows multidimensional optimization to be carried out experimentally; the functional dependence of the target function on the individual parameters need not be known. The value of the target function (e. g., the yield of a

product) is determined experimentally and is the criterium for deciding whether further search steps should be carried out or the procedure ended after successful optimization.

Procedure of the Simplex Method

At the start of the search ($n + 1$) points (i. e., in two-dimensional space, three points) are fixed so that they form the corners of a regular simplex. In the example of Figure 13-12, this is an equilateral triangle. The value of the function is then determined for each of these points, and the search is then begun according to the following rules:

- 1) Determination of the target quantity at the corners of the simplex; ($n + 1$) experiments
- 2) Selection of the "worst" corner $\vec{x}^{(<)}$
- 3) Generation of a new corner $\vec{x}_{n+<}$ by reflection of the triangle about the side opposite to the worst corner
- 4) Determination of the target quantity y in the new corner
- 5) Replace the result of the worst corner by y
- 6) If y is worse than all other results, go to point 7, otherwise point 2
- 7) Selection of the second worst corner as $\vec{x}^{(<)}$, then go to point 3
- 8) The procedure is terminated when the target quantity can no longer be improved

$$\vec{x}_{n+2} = \frac{2}{n} \sum_{i=1}^{n+1} \vec{x}_i - \left(1 + \frac{2}{n}\right) \vec{x}^{(1)} \quad \text{for the first reflected point} \quad (13-17)$$

$$\vec{x}_{n+k+1} = \left(1 + \frac{2}{n}\right) \vec{x}_{n+k} - \left(1 + \frac{2}{n}\right) \vec{x}^{(k)} + \vec{x}^{(k-1)} \quad \text{for the } k\text{th reflected point hfill} \quad (13-18)$$

\vec{x} = positional vector of the simplex corners

n = dimension of the factor space (number of variables to be investigated)

$\vec{x}^{(n)}$ = corner with the worst result

An example is the experimental optimization of the bis-hydroformylation of 2,4-hexadiene [12]. In the bis-hydroformylation of the diene with the catalyst $[\text{HRh}(\text{CO})(\text{PPH}_3)_3]$ under the usual reaction conditions, the highest yield of dialdehyde was 54 %. A systematic simplex search with several significant parameters was carried out with the aim of improving this result. The three variables reaction temperature, total pressure, and H_2 content of the synthesis gas were chosen, and the search was begun with an unsymmetrical tetrahedron. The calculated points and the experimental results are listed in Table 13-15.

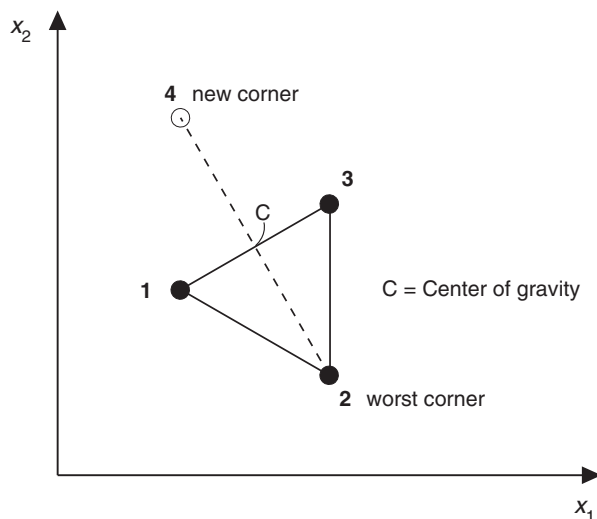


Fig. 13-12 Simplex method with two variables

Table 13-15 Bis-hydroformylation of 2,4-hexadiene: experimental optimization by the simplex method

| Experiment | T [°C] | $P_{\text{tot.}}$ [bar] | H_2 [%] | Dialdehyde yield [%] | Notes |
|------------|-------------|----------------------------|--------------|-------------------------|---------------------|
| 1 | 100 | 130 | 50 | 51.4 ^{a)} | |
| 2 | 110 | 130 | 50 | 52.4 ^{b)} | |
| 3 | 107 | 130 | 54 | 55.5 ^{c)} | |
| 4 | 105 | 150 | 52 | 57.4 | |
| 5 | 114 | 143 | 55 | 58.0 | 1st reflected point |
| 6 | 107 | 152 | 58.3 | 58.7 | 2nd reflected point |
| 7 | 110 | 166.6 | 57.2 | 60.2 | Optimum |
| 8 | 115.3 | 157.7 | 62.7 | 59.0 | |

a) Worst corner of 1st simplex. b) Worst corner of 2nd simplex. c) Worst corner of 3rd simplex.

Reaction Conditions

8.2 g diene (0.1 mol), 80 mL benzene, 25 mg Rh_2O_3 (0.1 mmol), 1 g PPh_3 (co-catalyst); rocking autoclave.

When experiment 8 gave a worse result, the optimization process was terminated. It remains an open question whether with this catalyst system the yield of dialdehyde could be further increased by using higher pressures, other solvents, or more favorable reactor types (e.g., continuous operation).

Transferring these optimum experimental conditions to other dienes is not possible since the experimental parameters presumably depend on other factors such as the structure of the diene and substituents.

13.3.3.4 Statistical Test Planning with a Computer Program

Statistical test planning can be carried out advantageously by expert systems which design the test plan, evaluate the results, and optimize the process in a single logically constructed sequence. An example is the program APO (Analysis Process Optimization) [30].

The program

- prepares test plans on the basis of a given working hypothesis
- evaluates and assesses the experimental results
- calculates optimal parameter settings
- analyzes weaknesses in the model and systematic errors in the conduction of the process
- analyzes the influence of many parameters on the target quantities

APO presents the results in tabular and graphical form and provides detailed hints for the further development and improvement of the working hypothesis.

To develop a test plan the program only requires information on the independent variables. After input of the variables (experimental parameters) and their levels, the program calculates those points in a multidimensional space that provide the best predictions in a subsequent modeling process. The input levels of a variable determine the range of values, which should have been determined in preliminary investigations and catalyst screening. In general at least 3–5 levels per variable should be chosen. The maximum number of experiments is limited to 80 for nine independent variables.

As an example of the application of the program, we shall use the previously discussed example of the selective hydrogenation of a substituted *o*-cyano aromatic nitro compound with a supported Pd catalyst (see Section 13.3.1).

For hydrogenation in suspension, the following seven influencing quantities are of importance: temperature, pressure (H_2 partial pressure), type and quantity of catalyst, starting material concentration, stirring speed, and solvent.

On the basis of preliminary investigations, four of the seven variables were kept constant: starting material concentration (5%), stirring speed (710 rpm, kinetic region), the catalyst (5% Pd/activated carbon), and the solvent (ethanol). For the remaining three variables, the following ranges of values were chosen, whereby the reaction engineering conditions were also taken into account:

- Temperature: 0–80 °C, five levels
- Pressure (H_2 partial pressure): 1–40 bar, five levels
- Catalyst quantity (relative to starting material): 1–20%, four levels

The input menu of the program APO was then filled in as presented in Table 13-16.

The program checks that the generated test plan fulfills certain mathematical criteria (e.g., correlations, homogeneity) and provides comments.

Table 13-17 lists the distributions of the experimental combinations in the entire variable space and the corresponding experimental results (percentage amine yields). The experiments and the experimental results can also be plotted on the surfaces of the four geometric bodies depicted in Figure 13-13.

Table 13-16 Input menu for producing the test plan

| Details of the statistical test plan | Selection |
|---|-----------|
| (a) Special features of the model | none |
| (b) Take second-order effects into account | yes |
| (c) Number and names of independent variables | 3 |
| (d) Number of levels of the independent variables | 5/5/4 |
| (e) Number of restrictions | 0 |
| (f) Generation of restrictions | – |
| (g) Desired number of experiments | 15 |
| (h) Rating of edge zones | 3 |
| (i) Number of given experiments | 0 |
| (j) Number of randomly generated experiments | 0 |
| (k) Calculate test plan | |

Table 13-17 Hydrogenation of substituted *o*-cyanonitrobenzene: test plan and modeling by APO [13]

| Exp. | Reaction conditions | | | | Amine yield [%] | | |
|------|---------------------|-------------------------------|---------------------------------|------------|-----------------|-----------------------------|-----------|
| | Temp. [°C] | H ₂ pressure [bar] | Cat.-quantity [%] ^{a)} | Time [min] | Experiment | Calculated by APO 1st model | 2nd model |
| 1 | 0 | 1 | 1 | 128 | 5.3 | 7.4 | 5.4 |
| 2 | 80 | 40 | 20 | 13 | 5.9 | 5.4 | 4.9 |
| 3 | 50 | 5 | 5 | 62 | 84.9 | 80.9 | 82.4 |
| 4 | 10 | 25 | 10 | 59 | 95.6 | 97.3 | 98.7 |
| 5 | 25 | 10 | 20 | 22 | 79.1 | 73.3 | 79.6 |
| 6 | 80 | 40 | 1 | 231 | 34.1 | 35.8 | 34.4 |
| 7 | 0 | 25 | 10 | 87 | 92.2 | 98.1 | 94.1 |
| 8 | 50 | 1 | 5 | 137 | 85.6 | 82.1 | 85.4 |
| 9 | 25 | 5 | 20 | 36 | 81.7 | 78.8 | 82.5 |
| 10 | 10 | 10 | 10 | 86 | 93.2 | 95.4 | 91.4 |
| 11 | 0 | 40 | 5 | 396 | 87.6 | 85.9 | 87.4 |
| 12 | 80 | 1 | 1 | 205 | 54.6 | 57.8 | 52.4 |
| 13 | 50 | 5 | 20 | 46 | 74.3 | 81.9 | 72.5 |
| 14 | 10 | 25 | 5 | 141 | 79.8 | 74.3 | 72.1 |
| 15 | 25 | 10 | 1 | 387 | 29.2 | 28.7 | 36.0 |
| 16 | 80 | 1 | 11,4 | 44 | 88.0 | 126.0 | 92.1 |
| 17 | 7 | 40 | 14,0 | 35 | 96.5 | 118.8 | 119.0 |

a) Relative to mass of starting material.

Exp. 1 – 15: test plan according to APO; Exp. 16 and 17: optimization.

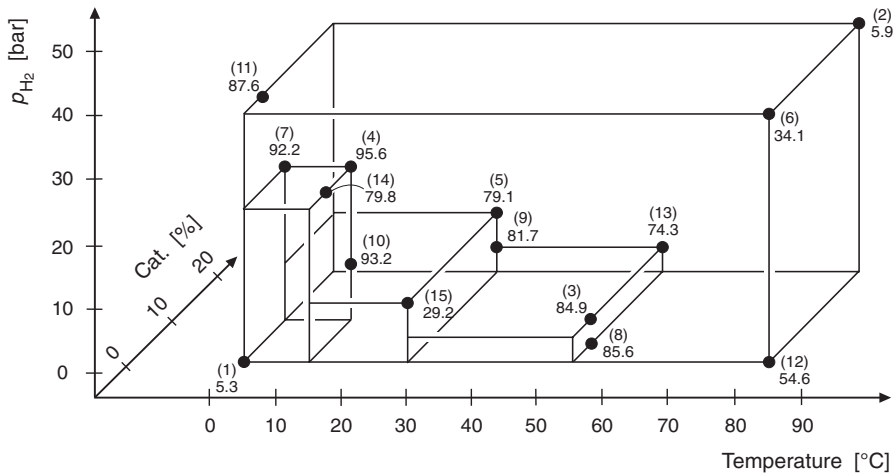


Fig. 13-13 Representation of the experiments and the results in the variable space

On closer inspection it can be seen that each plane of these geometric bodies is defined by at least three points. In the appropriate system correlation, these 15 experimental settings can cover the entire variable space for a parameter optimization procedure. The quasiorthogonal planning method ensures that various optimality criteria (e.g., edge-zone weighting) are taken into account.

The results of the hydrogenation experiments in the APO test plan and the values calculated from model equations are listed in Table 13-17, experiments 1–15. These results were then used for calculation and analysis of a model. APO provides a detailed commentary on the model analysis with the following statements:

- Standard error for the target quantity product: 5.25
- Error variance: 16.63 % of the total variance of the target quantity
- Degree of determination: 98.42 % (independence of all coefficients of the model equation)
- Normal distribution of the residuals: 70 % probability
- Temperature: considerable error fluctuations in the variable
- Hydrogen partial pressure: neither systematic errors nor weaknesses in the model
- Catalyst: weakness in the model, which, however, is superimposed by considerably inhomogeneous variances

One should not attach too much importance to the not unexpected criticism regarding the variable temperature, since the maintainance of the levels in the highly exothermic reaction in an autoclave can sometimes be problematic. The model weakness catalyst may be due to inhomogeneous distribution in the autoclave.

Next a model analysis was carried with the aim of determining the optimum experimental parameters from the model-space representation. In order to rapidly obtain an overview, the isoline representation was chosen. Here contour lines are used to depict the calculated product yield as a function of the corresponding combina-

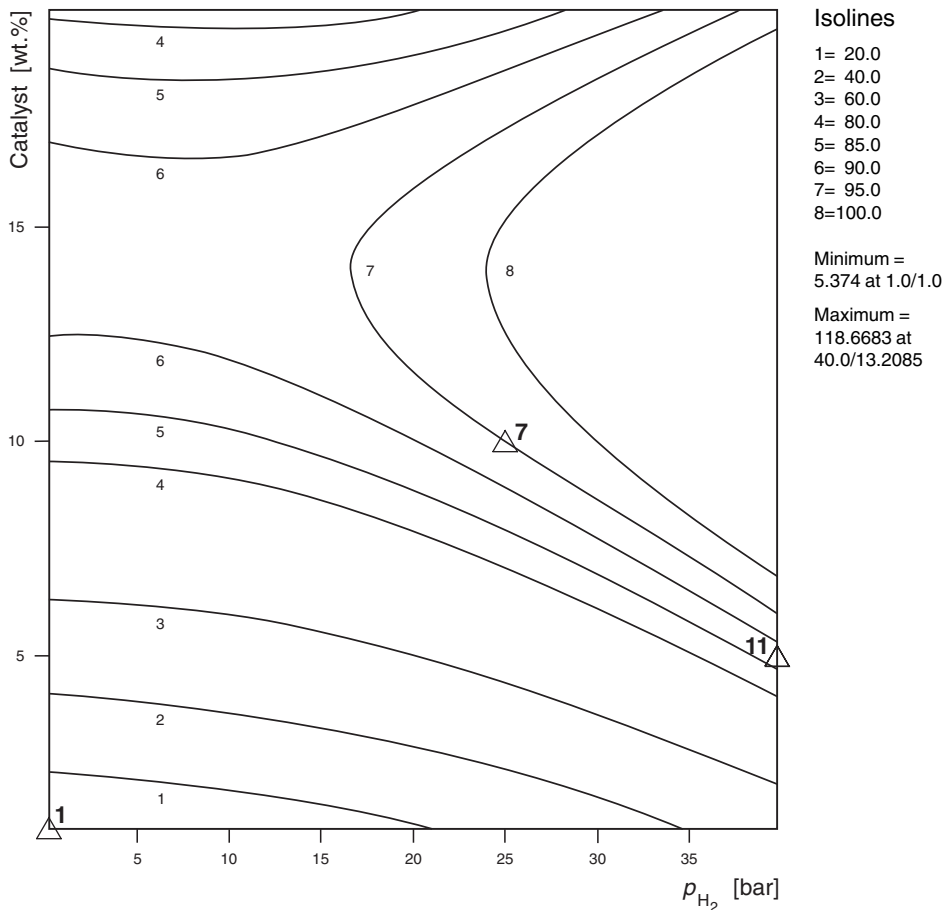


Fig. 13-14 Contour line depiction of the target quantity product at 0 °C (2nd APO model)

tion of adjustable parameters (e. g., pressure and catalyst quantity) with one constant quantity (temperature); see Figure 13-14. The program calculates the coordinates of the extreme values of the target parameters, i. e., the optimum.

Numerous isoline diagrams revealed that the optimum experimental conditions are low temperature (<20 °C), 10–14 % catalyst, and high pressure (>25 bar). There is also a secondary local maximum at low pressure (1 bar) and higher temperature (80 °C). Simultaneous optimization by model-space analysis gave the experimental settings: 80 °C, 1 bar H₂ partial pressure, 11.4 % catalyst.

However, in the experiment with these settings, only 88 % yield was determined, i. e., the optimum was not attained (experiment 16). In order to make use of this data, the result was added to the previous 15 experiments as a given experiment. Repeating the model analysis now led to an improvement in the model. As can be seen from Table 13-17, the values of the target parameters calculated from the second

model equation describe the experimental results more exactly. The percentage effects of the variables after the extension of the test plan were as follows:

| | |
|--------------------------|-----------------|
| Temperature: | $X(1) = 20.3\%$ |
| H ₂ pressure: | $X(2) = 22.8\%$ |
| Catalyst quantity: | $X(3) = 56.8\%$ |

The variables temperature and pressure have almost the same weighting in the calculation of the target quantity. The repeated simultaneous optimization gave the following optimal settings: 7.0°C, 40.0 bar H₂ partial pressure, 14.0 % catalyst. For these parameters APO calculated a target quantity value of 119 (no upper limit). The experiment (no. 17) gave a reproducible amine yield of 96.5 %. The optimization procedure was ended with this very good result. The clear improvement in the mathematical model resulting from the additional empirical value can also be seen in the isoline diagram at 0°C (Fig. 13-14). All investigated results lie within the ranges calculated with the model equations.

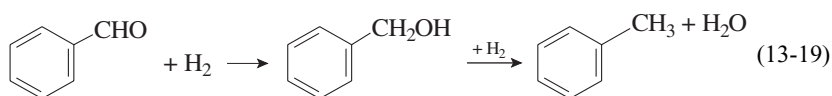
It would seem logical to use such programs in the field of heterogeneous catalysis in particular. Numerous influencing quantities can be taken into account without knowledge of the generally complex kinetics. Experimental optimization on the basis of statistical modeling replaces the usual intuitive approach and leads to the goal with a minimum of effort. However, this does not mean that the experience and creativity of the experts can be dispensed with.

13.3.4

Kinetic Modeling and Simulation [5, 18]

This chapter describes how a catalytic reaction can be modeled on the basis of kinetic measurements and how the resulting model equations can be used in reactor simulation and design (see also Scheme 13-6). This detailed analysis of the catalytic behavior requires a major measurement and data-evaluation effort and is rarely carried out in industrial practice.

We shall discuss the process for the example of the hydrogenation of benzaldehyde in various reactors [15]. The heterogeneously catalyzed hydrogenation of benzaldehyde is a model reaction for the hydrogenation of aromatic aldehydes. The main reactions are shown in Equation 13-19.



Supported Pd/C catalysts, Raney nickel, and nickel boride are good catalysts for the hydrogenation of benzaldehyde. By measuring the take up of hydrogen in a batch reactor, it was found that the reaction is zero order in the reactants benzaldehyde and hydrogen at pressures above 3 bar and aldehyde concentrations in excess of 1 mol/L. With the catalyst 3 % Pd/C a reaction rate of $1.6 \times 10^{-2} \text{ mol g}^{-1} \text{ min}^{-1}$ was measured at 22°C and was independent of the solvent [2].

Other authors carried out measurements with Raney nickel at 70 °C and 6 bar and found that the reaction rate was strongly dependent on the reactant/catalyst ratio, the following range being given:

$$r = 1.7 \times 10^{-4} \text{ to } 1.3 \times 10^{-3} \text{ mol g}^{-1} \text{ min}^{-1}$$

No statements were made about the selectivity of product formation. In a more recent study kinetic measurements were made in a suspension process carried out in an autoclave operating in the batch mode, and the results were used for the simulation of a trickle-bed reactor [15].

The kinetic study was carried out under the following reaction conditions:

| | |
|---|--|
| Raney nickel (Engelhard): | 68% Ni, specific surface area 130 m ² /g, pellet density 1.72 g/cm ³ , porosity 0.67, particle size range 35–70 μm |
| Catalyst concentration: | 25–50 kg/m ³ |
| Temperature: | 343–373 K |
| Pressure: | 1.7–11.2 bar |
| 300 mL stirred autoclave, batch operation | |

Figure 13-15 shows the typical course of a hydrogenation reaction.

The benzaldehyde concentration is plotted as a function of reaction time. Above 1.5 mol/L there is a linear dependence that apparently reflects zero reaction order with respect to the aldehyde. At lower concentrations the reaction is apparently first order. The kinetic data were only determined in the region of zero reaction order at

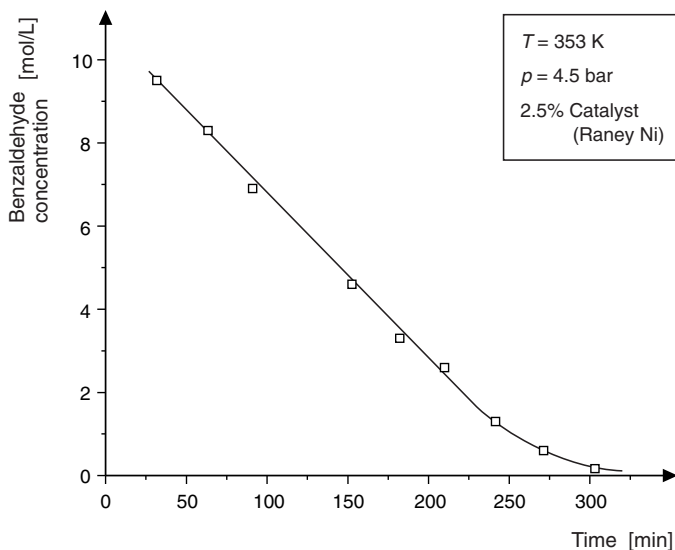


Fig. 13-15 Kinetic study of the hydrogenation of benzaldehyde in a stirred autoclave operating in suspension mode [15] (with permission of Elsevier, Amsterdam)

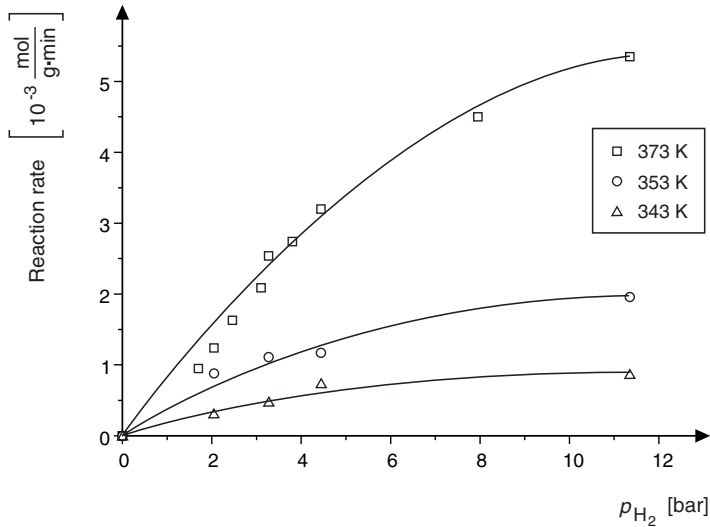


Fig. 13-16 Hydrogenation of benzaldehyde in a stirred autoclave: dependence of reaction rate on H_2 pressure [15] (with permission of Elsevier, Amsterdam)

a stirrer speed of about 2000 rpm. Measurements with stirring speeds in the range 1200–2000 rpm gave constant reaction rates, which means that gas–liquid mass transfer is negligible.

A linear relationship was also found between the reaction rate and the catalyst concentration. Numerous measurements with smaller catalyst particle sizes (10 μm) gave comparable reaction rates. This means that mass transfer within the particle also plays no role in the reaction. An activation energy of the hydrogenation reaction of 55.4 kJ/mol (4.5 bar, 2.5 % catalyst) was measured.

The influence of the hydrogen concentration on the reaction rate was investigated at various hydrogen pressures (Fig. 13-16).

Furthermore, it was found that the benzyl alcohol formed in the reaction has no influence on the reaction rate. From all the experimental results, a Langmuir–Hinshelwood model was deduced, with a rate-determining influence of the surface reaction according to Equation 13-20.

$$r = \frac{kK_{\text{B}}c_{\text{B}}K_{\text{H}}p_{\text{H}}}{1 + K_{\text{B}}c_{\text{B}}(1 + \sqrt{K_{\text{H}}p_{\text{H}}})^2} \quad (13-20)$$

c_{B} = benzaldehyde concentration

p_{H} = hydrogen partial pressure

$K_{\text{B}}, K_{\text{H}}$ = adsorption constants of benzaldehyde and hydrogen

In the investigated range, K_{B} is on the order of 1 L/mol, and this results in a reaction order of zero at high benzaldehyde concentrations (Eq. 13-21).

$$r = k \frac{K_H p_H}{(1 + \sqrt{K_H p_H})^2} = k_0 \quad (13-21)$$

This model was used to analyze the reaction rate data (Fig. 13-16). The following temperature dependences were found for k and K_H :

$$k = 2.18 \times 10^8 \exp(-10000/T) \text{ kmol kg}^{-1} \text{ s}^{-1}$$

$$K_H = 1.85 \times 10^{-10} \exp(5500/T) \text{ kPa}^{-1}$$

As expected, k increases with increasing temperature while K_H decreases. The conditions of the trickle-bed reactor study are summarized in the following:

- Discontinuously operated trickle-bed reactor with recycle, 1 inch diameter
- Liquid flow rate: 0.004 m/s
- Gas flow rate: 0.004–0.008 m/s
- Temperature: 353–373 °C
- Pressure: 2.2–5.8 bar
- 170 g catalyst and 1 L liquid

The limiting factor in this reactor is the hydrogen, and this must be taken into account in all mass-transfer resistances. Hydrogen transfer from the gas into the liquid, onto the surface of the pellet, and into the interior of the pellet is the same provided the pellet is completely wetted. The total process can then be described by Equation 13-22 [11].

$$k_L a_L (p_H/H - c_{H,L}) = k_S a_S (c_{H,L} - c_{H,S}) = \eta \frac{k K_H H c_{H,S}}{(1 + \sqrt{K_H H c_{H,S}})^2} = r_0 \quad (13-22)$$

$c_{H,L}$ = H₂ concentration in the liquid

$c_{H,S}$ = H₂ concentration on the outer catalyst particle surface

H = Henry's constant

$k_L a_L$ = gas–liquid mass-transfer coefficient

$k_S a_S$ = liquid–solid mass-transfer coefficient

η = catalyst effectiveness factor (function of the Thiele modulus)

Details of the calculation can be found in the literature [15, 23].

For the calculation of r_0 the effective diffusion coefficient D_{eff} is required (Eq. 13-23).

$$D_{\text{eff}} = \frac{\varepsilon_p D_H}{\tau} \quad (13-23)$$

ε_p = pellet porosity

D_H = diffusion coefficient of hydrogen

τ = tortuosity factor

Table 13-18 compares the reaction rates measured in the trickle-bed reactor with those predicted by the model calculation. The predicted values are in good agreement with the experimental data. The effectiveness factor of the catalyst is very low,

Table 13-18 Hydrogenation of benzaldehyde in a trickle-bed reactor: measured values and model calculations [15]

| T [K] | [kPa] | $-\Delta c/\Delta t$ [kmol m ⁻³ s ⁻¹] | | η calculated |
|------------|-------|--|----------------------|----------------------|
| | | measured | calculated | |
| 353 | 360 | 7.8×10^{-2} | 8.2×10^{-2} | 0.042 |
| | 580 | 1.3×10^{-1} | 1.1×10^{-1} | 0.041 |
| 373 | 220 | 8.8×10^{-2} | 9.0×10^{-2} | 0.043 |
| | 360 | 1.5×10^{-1} | 1.4×10^{-1} | 0.041 |
| | 580 | 2.5×10^{-1} | 2.2×10^{-1} | 0.040 |

Parameter values:

$$k_L a_L = 0.12 \text{ s}^{-1}, k_S a_S = 0.70 \text{ s}^{-1}, D_H = 8 \times 10^{-9} \text{ m}^2/\text{s}, \tau = 3, H = 2.3 \times 10^4 \text{ kPa kmol}^{-1} \text{ m}^3$$

and this means that transport resistance in the pores is highly significant. As expected, gas–liquid transport resistance is also very important, but liquid–solid transport resistance is negligible.

The most important result is that the reaction is about 50 times faster in suspension than in the trickle-bed reactor. Therefore, at such high reaction rates the suspension reactor is preferred, although gas–liquid mass transfer and separation of the catalyst can cause problems.

Thus, benzaldehyde hydrogenation was tested under practice-relevant conditions in a catalyst test reactor of simple design, and parameter studies were carried out. The construction of the laboratory plant is shown schematically in Figure 13-17. Since we are dealing with an integral reactor, in spite of the relatively small amount of catalyst in the trickle-bed reactor, only comparative measurements were carried out.

Continuous hydrogenation of benzaldehyde in the solvents hexane and isopropanol:

- Reactor: Catatest plant (VINCI technologies, Fachhochschule Mannheim)
- Substrate concentration: 10 % benzaldehyde
- Throughput: 0.125 L/h benzaldehyde solution
- Reaction conditions:
 - 25 bar, molar ratio H₂/aldehyde = 40/1 (isopropanol)
 - 15 bar, molar ratio H₂/aldehyde = 20/1 (hexane)
- Catalyst: 13.6 g of 0.3 % Pd/Al₂O₃ (HO-22, BASF)

The Catatest plant allows the reaction parameters pressure, temperature, and liquid and gas feed to be varied over wide ranges; Figure 13-18 shows just a few results. The reaction products in both test series were benzyl alcohol and toluene. Considerable influence of the solvent and the temperature on the product distribution and the conversion were found.

In the polar solvent isopropanol, benzyl alcohol is predominantly formed at low temperatures, and the amount of toluene formed increases continuously with increasing temperature. In contrast, in the nonpolar solvent hexane, toluene is the predominant final product of the hydrogenation, in spite of the small excess of hydrogen and the low pressure. Between 120 and 130 °C the selectivity with respect to

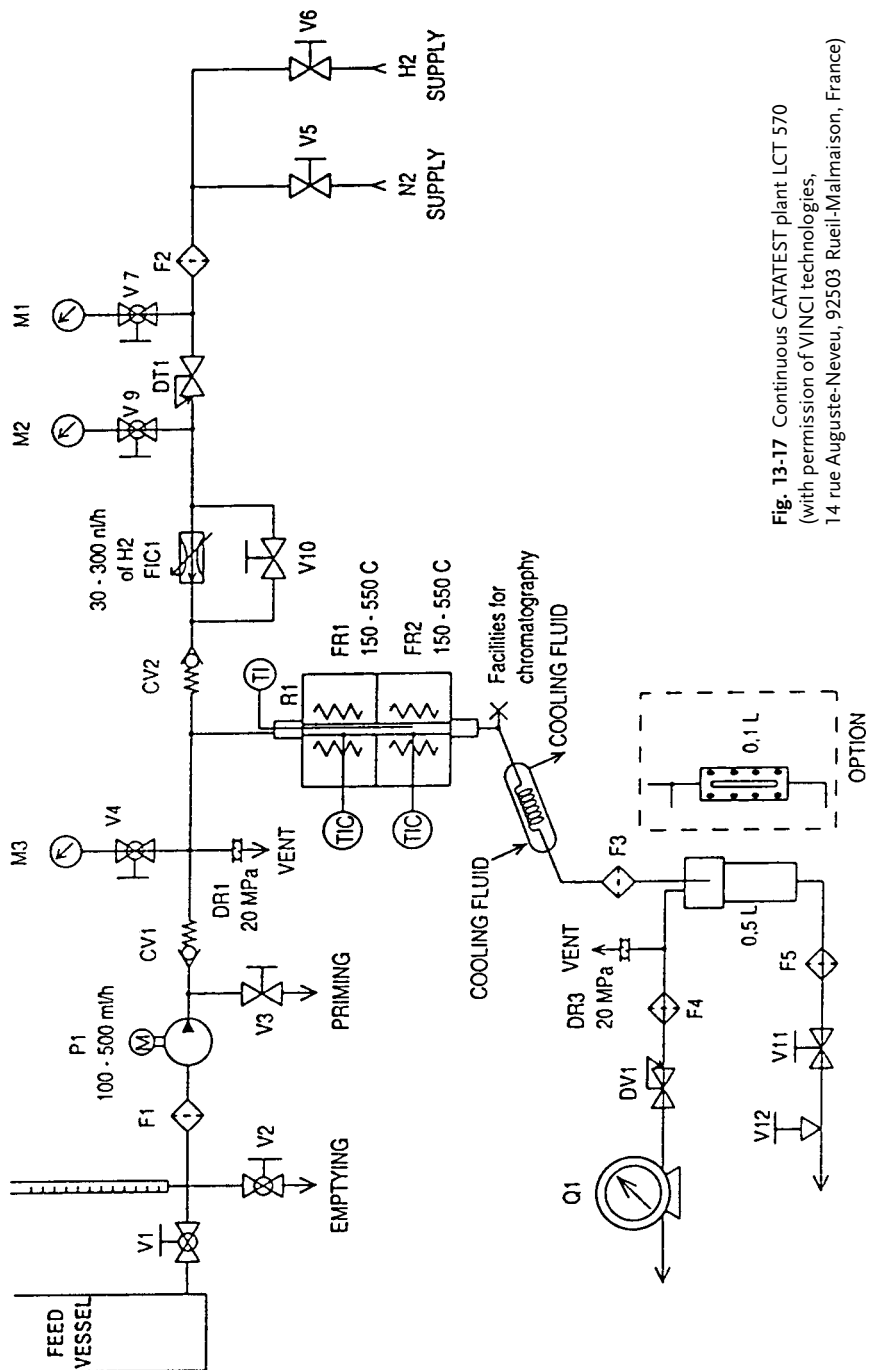


Fig. 13-17 Continuous CATATEST plant LCT 570 (with permission of VINCI technologies, 14, rue Auguste-Neveu, 92503 Rueil-Malmaison, France)

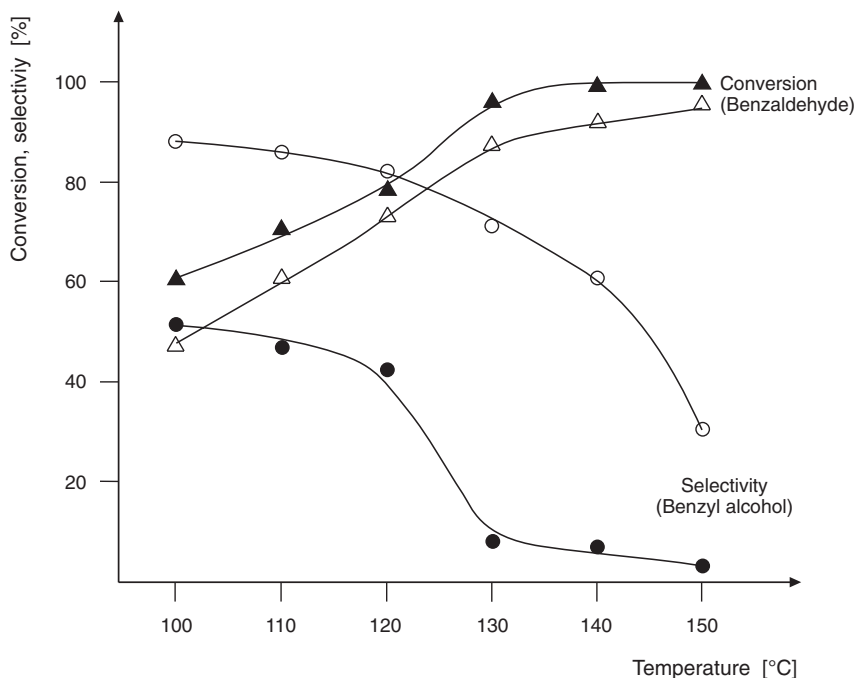


Fig. 13-18 Continuous hydrogenation of benzaldehyde: influence of temperature and solvent on conversion and selectivity

△ ○ Isopropanol, $p = 25$ bar, $H_2/\text{aldehyde} = 40/1$

▲ ● Hexane, $p = 15$ bar, $H_2/\text{aldehyde} = 20/1$

benzyl alcohol decreases drastically, and at 150 °C in hexane, exclusively toluene is obtained with quantitative conversion (Fig. 13-18).

Another practical example is the modeling of a trickle-bed reactor [11, 23]. The reaction investigated was the high-pressure hydrogenation of a lactone to a diol on a Cu–Zn mixed oxide catalyst [19].

Initially the kinetics were investigated in a stirred autoclave in order to develop a microkinetic model. Also of interest were the fluid-dynamic conditions and the axial dispersion (residence-time behavior). Here we shall only deal with the measured residence-time distributions.

As can be seen from Figure 13-19, the residence-time distributions of the trickle-bed reactor, as determined by pulse injection, showed that considerable backmixing takes place in the reactor. As expected, this decreases with increasing liquid feed. The external holdup was calculated from the residence-time curves.

A simulation was carried out to determine to what extent the conversion in the reactor is influenced by:

- The microkinetics
- Liquid feed and holdup
- Mass transfer: film diffusion of hydrogen and of the substrate

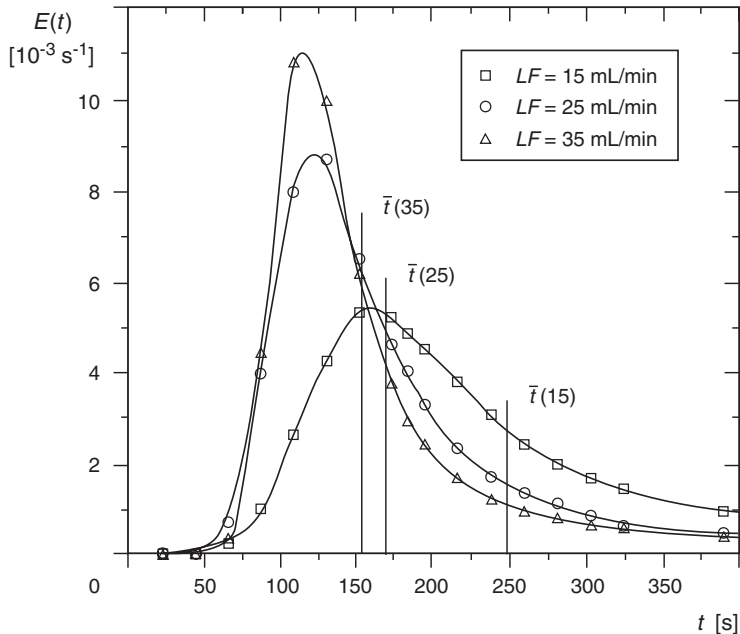


Fig. 13-19 Residence-time spectra in a trickle-bed reactor as a function of liquid flow (LF) [19]. Reactor length 1 m, diameter, 25.4 mm, Cu/Zn mixed oxide catalyst (tablets 6×3 mm), liquid phase *tert*-butanol, gas flow 10 L/min, 100 bar H_2 pressure, 25 °C

The ideal plug-flow model has to be corrected when applied to a trickle-bed reactor, since the conversion in the reactor is not determined by the reaction rate per unit mass but by a corrected value relative to the void volume in the reactor that is occupied by liquid.

The application of the reaction rate from the suspension reactor would only be justified if the catalyst in the fixed bed were as completely wetted by liquid as in the stirred autoclave. A semi-empirical model was used to estimate the conversion (Eq. 13-24)

$$\frac{dc}{dz} = -r(H_{ex}/LF)\rho_K A \quad (13-24)$$

LF = liquid feed, mL/min

H_{ex} = external holdup

$\rho_{cat.}$ = pellet density of the catalyst

A = cross-sectional area of the reactor

z = tube length (independent variable)

The ratio H_{ex}/LF is the effective mean residence time of the liquid in the reactor.

The reaction rate is determined by three simultaneous processes:

- 1) Diffusion of the substrate molecules to the catalyst surface

$$-r = k_S a_S (c_{S,L} - c_{S,S}) \quad (13-25)$$

k_S = liquid–solid mass-transfer coefficient, m/s

a_S = specific surface area, m²/kg

$c_{S,L}$ = substrate concentration in the liquid

$c_{S,S}$ = substrate concentration on the catalyst surface

- 2) Diffusion of hydrogen from the gas phase to the catalyst

$$-r = k_{\text{tot}} a_S (c_{H,L} - c_{H,S}) \quad (13-26)$$

k_{tot} = total transfer coefficient for H₂

$c_{H,L}$ = the equilibrium concentration of hydrogen in the liquid phase corresponding to a given H₂ partial pressure. It is related to the gas-phase concentration by the modified Henry's law (Eq. 13-28)

$$c_{H,G} = H_m c_{H,L} \quad (13-27)$$

H_m = modified Henry constant

- 3) Surface reaction (microkinetics). A five-parameter Langmuir–Hinshelwood model proved to be best suited for describing the kinetics (Eq. 13-28). The criteria were:

- Surface reaction is rate-determining
- Selective adsorption
- Adsorption and desorption equilibrium attained
- Molecular adsorption

$$-r = \frac{k [K_H K_S c_{H,S} c_{S,S} - c_{D,S} / (K_D K_R)]}{(1 + K_S c_{S,S} + c_{D,S} / K_D)(1 + K_H c_{H,S})} \quad (13-28)$$

k = rate constant of the reaction

K_H = adsorption constant of hydrogen

K_S = adsorption constant of the substrate

K_D = desorption constant of the diol (product)

K_R = equilibrium constant of the reaction

To calculate the diol concentration, the simplifying assumption of selective hydrogenation was made (Eq. 13-29).

$$c_{D,S} = c_{S,0} X \quad (13-29)$$

Since r is contained in two nonlinear expressions, a global equation for the kinetics can not be derived. The equations can, however, be solved simultaneously by dynamic modeling with the program ISIM [18]. The corresponding ISIM program is shown in Figure 13-20.

All calculations were made for a reactor operating at 200 bar and 150°C under the assumption of isothermal conditions, since the adiabatic temperature difference under the given concentration conditions was only a few degrees and the reactor was operated in a polytropic mode. The target quantity was the conversion, which was calculated as a function of various reactor parameters. Some results of the simulation are described in the following.

```

1 constant kgas = 0.588      : Transport coefficient substrate
2 constant kh = 0.04        : Transport coefficient hydrogen
3 constant k = 0.017713     : Rate constant
4 constant Kh = 0.411495   : Adsorption constant hydrogen
5 constant Ks = 55.3381    : Adsorption constant substrate
6 constant Kd = 0.073762   : Desorption constant product
7 constant Kr = 3.74371    : Equilibrium constant of the reaction
8 constant Dk = 2.56      : Catalyst density
9 constant A = 5.06        : Cross-sectional area of reactor
10 constant LF = 10        : Liquid feed in mL/min
11 constant Hex = 0.2      : External holdup
12 :
13 cint = 1
14 tfin = 100
15 ca = 0.12382           : Initial concentration substrate
16 chO = 0.960           : Equilibrium concentration H2 in the
17                       : Liquid phase at 150° and 200 bar
18 :
19 DO 1 LF = 10,15,5
20 Reset
21 1 sim
22 :
23 initial
24 c = ca
25 cs = 0
26 zfin = tfin
27 :
28 dynamic
29 Hex = 3.9065E-02 + 1.4157E-02*LF - 3.25E-04*LF*LF
30 ch = chO + (r/kgas)
31 cs = c + (r/kgas)
32 cd = ca*U/100
33 N = (1 + Ks*cs + cd/Kd)*(1 + Kh*ch)
34 r = -k*(Kh*Ks*ch*cs - cd/(Kd*Kr))/N
35 c' = r*Dk*(A/LF)*Hex
36 U = 100*(1 - (c/ca))
37 z = t
38 prepare z, U, r, cs, cd, ch
39 output z, U, r

```

Fig. 13-20 ISIM program for the simulation of a trickle-bed reactor for the high-pressure hydrogenation of a lactone [19]

Influence of Liquid Feed and Holdup

In these simulation runs, the liquid feed LF was varied between 10 and 25 mL/min (Fig. 13-21). The substrate concentration was 5 %, and the dimensions of the reactor in the program correspond to those of the test reactor.

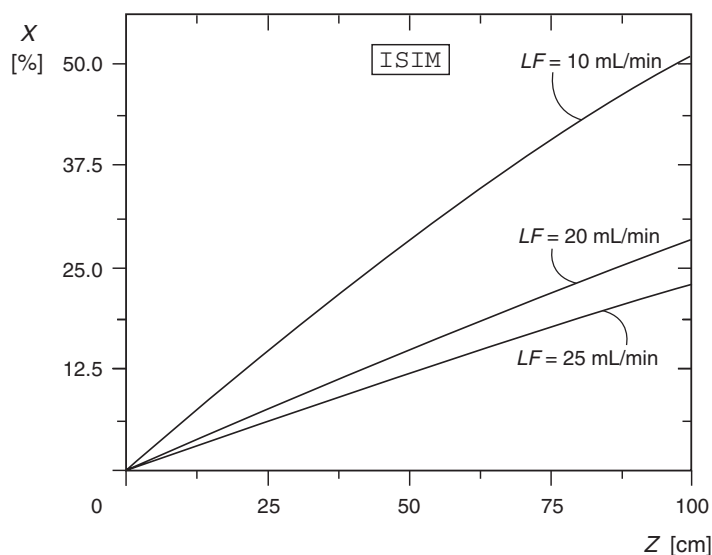


Fig. 13-21 Lactone hydrogenation in a trickle-bed reactor: conversion profiles as a function of liquid flow at constant liquid holdup [19]

In the first simulation (model **A**) the liquid holdup was regarded as a constant (relative to $LF = 10$ mL/min). In a second calculation (model **B**), the external holdup was input as a function of the liquid feed. From the residence time measurements in the trickle-bed reactor, the correlation of Equation 13-30 was obtained.

$$H_{\text{ex}} = 3,91 \exp(-2) + 1.42 \exp(-2LF) - 3.25 \exp(-4LF^2) \quad (13-30)$$

This equation was used as input for the DYNAMIC part of the program. The conversion profiles were then calculated by simulation (Fig. 13-22).

Table 13-19 lists the results of both simulations and the experimentally determined conversions. The results obtained by model **B** with variable holdup agree quite well with the experimental data.

Influence of the Reactor Length

This calculation was intended to show how the conversion changes in the same reactor with increasing tube length and various liquid feeds (Fig. 13-23). As Figure 13-23 shows, tube lengths in the range of about 2–3 m give satisfactory yields.

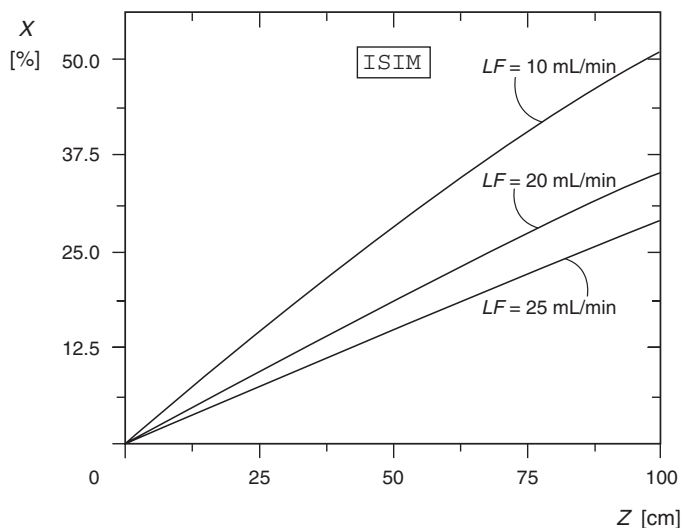


Fig. 13-22 Lactone hydrogenation in a trickle-bed reactor: conversion profiles taking into account the external liquid holdup [19]

Table 13-19 Measured and calculated conversion in the trickle-bed reactor; influence of the external holdup

| Liquid feed LF [mL/min] | Conversion [%] | | |
|----------------------------|----------------|---|--|
| | Experimental | Simulation A ($H_{\text{ex}} = \text{const.}$) | Simulation B ($H_{\text{ex}} = f(\text{LF})$) |
| 10 | 49.3 | 50.6 | 50.6 |
| 15 | 42.3 | 36.5 | 42.7 |
| 20 | 33.9 | 28.4 | 35.8 |
| 25 | 28.0 | 23.2 | 29.1 |
| 30 | 22.5 | 19.6 | 22.5 |

Constant reaction conditions:
 $p_{\text{H}_2} = 200 \text{ bar}$, $150 \text{ }^\circ\text{C}$, Cu/Zn mixed oxide catalyst

Influence of Mass Transfer

The calculated mass-transfer coefficients used in the program show that the transport resistance for hydrogen is higher than that for the substrate. Therefore, in the following simulation calculations, a high value and a much lower, but nevertheless realistic value of the global mass-transfer coefficient were introduced into Equation 13-26. The aim was to find out whether the reaction rate is mainly determined by mass transfer or by the surface reaction. As can be seen from Figures 13-24 and 13-25, the process is essentially determined by the intrinsic kinetics.

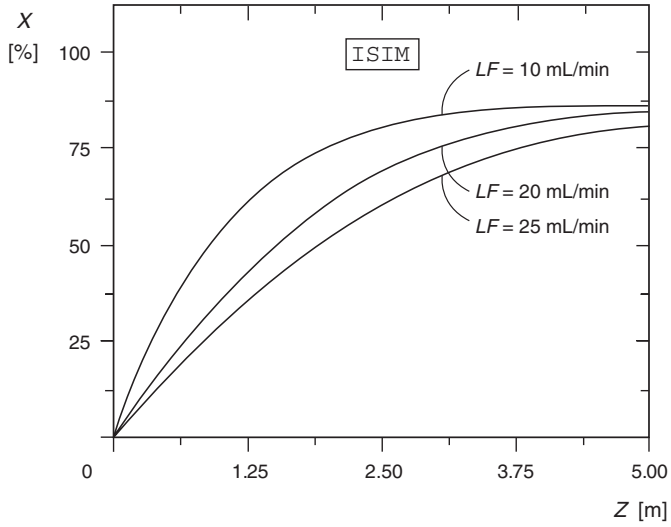


Fig. 13-23 Lactone hydrogenation in a trickle-bed reactor: conversion profiles as a function of liquid flow and reactor length [19]

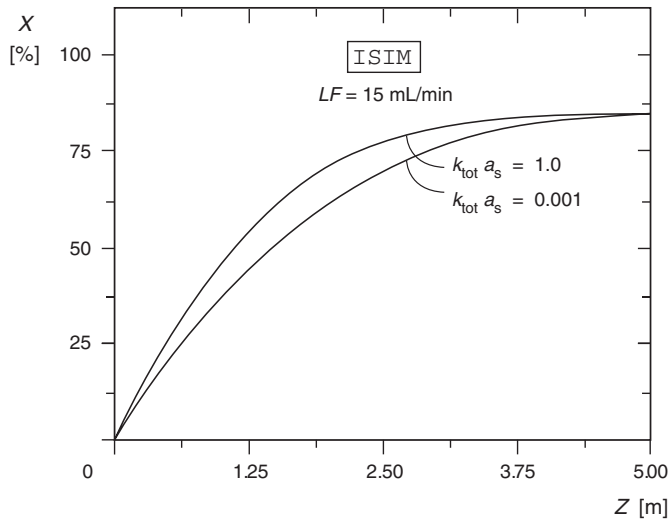


Fig. 13-24 Lactone hydrogenation in a trickle-bed reactor: conversion profiles as a function of the global mass-transfer coefficient of hydrogen [19]

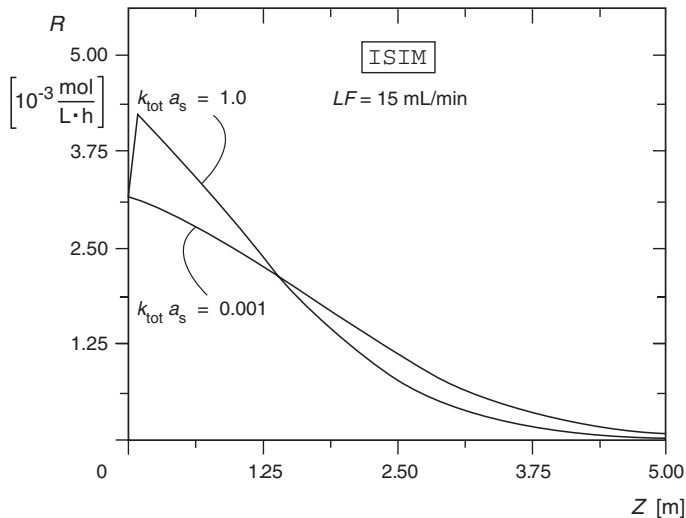


Fig. 13-25 Lactone hydrogenation in a trickle-bed reactor: reaction rate profiles as a function of mass transfer [19]

An assumed value of $k_{\text{tot}}a_s = 0.001$ corresponds to about one-tenth of the true value in the lactone hydrogenation, and would hence correspond to an extremely high mass-transfer limitation. Figure 13-25 shows that for low mass-transfer limitation ($k_{\text{tot}}a_s = 1.0$) the reaction rate increases in the entry region of the reactor. This is because rapid diffusion of the hydrogen increases its concentration on the catalyst surface up to saturation. The associated high consumption of substrate leads to a steep gradient of the curve, whereby at a reactor length of ca. 1.3 m, the substrate supply becomes limiting, and the reaction rate even drops below the curve with higher hydrogen-transport limitation. The results suggest that for an initial estimate of the conversion, the relationships for substrate diffusion and hydrogen transport from the gas phase can be neglected.

The simulation results show that in addition to precise microkinetics, knowledge of the fluid dynamics, especially the liquid holdup, is an essential prerequisite for modeling a trickle-bed reactor. The advantage of a simulation program is not so much the calculation of the conversion for a concrete situation; rather, it is the splitting of a complex problem into individual steps, which allows parameter studies to be carried out [10].

13.3.5

Modeling and Simulation with POLYMATH

There are some software packages (i.e. ODE solvers, regression etc.) available to solve problems from reaction engineering and other areas. POLYMATH is an extremely user-friendly software package which makes modeling easy for the education of chemical engineers and chemists. POLYMATH is used to numerically solve

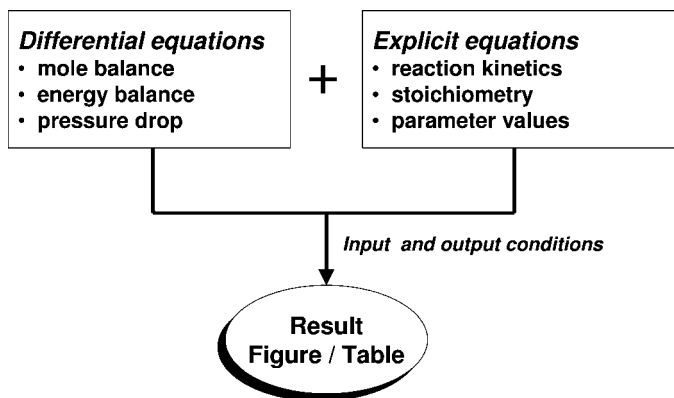


Fig. 13-26 Reactor modeling

coupled differential equations simultaneously or to find kinetic parameters in rate expressions by regression. Using an identified model the influence of various reaction parameters on the overall process can be simulated easily.

Therefore, we use POLYMATH to solve some examples in this textbook. With POLYMATH one simply enters all equations and the corresponding parameter values into the computer with the initial (rather, boundary) conditions and they are solved and displayed on the screen. It is usually easier to leave the mole balances, rate laws, and concentrations as separate equations rather than combining them into a single equation to obtain an analytical solution of the problem. The basic procedure for reactor modeling and simulation is shown in Figure 13-26.

POLYMATH can also be easily applied for regression of rate data (linear, polynomial, nonlinear regression). All one has to do is to type the experimental values in the computer, specify the model, enter the initial guesses of the parameters, and then push the computer button, and the best estimates of the parameter values along with 95% confidence limits appear. The application of POLYMATH is described in some textbooks with many examples taken from practice [31–33].

13.3.6

Catalyst Discovery via High-Throughput Experimentation [34, 35]

The methods of combinatorial chemistry which were developed to speed the synthesis and discovery of pharmaceutical active compounds, have recently been adapted for catalyst development. Techniques are applied that quickly generate a vast collection of compounds that might be catalytically active, a so-called library of catalysts.

High-throughput experimentation combines advanced miniaturized, automated and parallel experimental methods together with computational techniques to provide a faster and more efficient route to better, cheaper and more environmentally friendly products and processes. High-throughput experimentation increases the rate of materials discovery and development up to 1000-fold. However, there must also be developed techniques for

- Analysing
- Data management and interpretation of the experiments
- Methods for rapid catalyst preparation and catalyst screening
- Automation and
- Robotics

With increasing demand for shorter time to market, including shorter development times in the laboratory and pilot plant stage, such tools need be available for an accelerated development of catalytic processes.

In practice it has been proven useful to define two stages in high-throughput screening of catalysts. Table 13-20 lists the distinctive features of the two different stages.

Table 13-20 Stage I and Stage II technologies for high-throughput experimentation [34]

| | Features | Analytical techniques employed |
|----------|--|---|
| Stage I | Maximum sample throughput Reduced information (–/0/+) Analysis of target compounds Used for new discoveries | <i>Parallel and quasi-parallel techniques</i> IR thermography Photoacoustic deflection Adsorption techniques <i>Sequential techniques</i> Mass spectrometry MS |
| Stage II | Approaching real conditions Existing system knowledge Detailed analysis of compounds Used for continuous improvements | <i>Parallel techniques</i> – <i>Sequential techniques</i> Gas chromatography GC GC/MS Multidimensional GC |

Stage I experiments are carried out in microchemical reactor systems [34]. Figure 13-27 shows a routinely employed 384-fold single bead reactor.

As a size comparison, this reactor type is approximately half the size of a credit card. The features of the microchemical reactor system can be described as follows:

- Very dense arrangement (60 cat/cm²)
- „Single bead“ catalysts and new micro-scale testing
- Continuous flow and stationary experimental conditions
- Employs simple synthesis methods for the catalysts (e.g. wet impregnation)
- Adaption of several analytical techniques

Today parallel reactor systems for rapid catalyst testing under real process conditions are state-of-the-art. An example of an integrated system is the 48-parallel high-throughput reactor, which can be applied to discover and to optimize new heterogeneous catalysts. It provides continuous flow of the reactants through separate

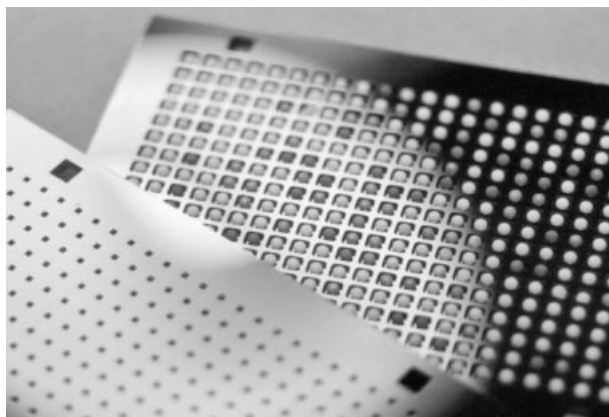


Fig. 13-27 384-fold single bead reactor employed at hte AG, Heidelberg, Germany

parallel reactor liners ensuring uniform temperature and uniform flow distribution together with fast sequential online analysis [36]. Figure 13-28 shows a special stage-II parallel high pressure reactor system, developed at hte AG Heidelberg.

Many refinery processes operate in the mid- to high-pressure regime and in a number of cases reactions will either be run in three phases or even produce liquid products from gaseous educts. In this cases a phase separation is necessary in order to analyze separately the gaseous and liquid components. These requirements need a suitable reactor configuration.



Fig. 13-28 Stage-II parallel high pressure reactor system (hte AG, Heidelberg, Germany)

The features of the stage-II reactor, which can be employed for hydrogenations, oxidations, polymerizations etc. shown in Figure 13-28 include

- On-line process automation
- $T_{\max} = 200\text{ }^{\circ}\text{C}$, $p_{\max} = 200\text{ bar}$
- Variable volumes (60–150 mL)
- Gas- and liquid dosing (inert)

The high-throughput experimentation techniques can be applied in all sectors of industrially relevant catalysis: oil and gas conversion, basic and intermediate chemicals, specialty and fine chemicals, environmental catalysis, polymerization and pharmaceuticals.

The first independent company established to exploit combinatorial chemistry and high-throughput experimentation for developing commercially useful catalysts was Symyx Technologies, CA, founded in 1994. Other high-throughput experimentation companies have since been established for developing new catalytic materials including Avantium in Holland, hte AG in Germany, and Torial in the United States. It becomes clear that high-throughput experimentation has kept the promise of becoming an important additional tool for catalysis research in academia and industry.

► Exercises for Chapter 13

Exercise 13.1

Decide whether the following statements are true (t) or false (f). A differential circulating reactor:

- Should be operated with a low recycle ratio
- Has a residence time spectrum like a plug flow reactor
- Has a residence time spectrum like a continuous stirred tank
- Exhibits temperature and pressure gradients
- Provides a product stream with high conversion

Exercise 13.2

A batch hydrogenation depends on three parameters. Set up a test matrix for a 2^3 factorial design with the following conditions:

| Variables | Levels | |
|------------------------------------|--------|------|
| Reaction time [min] | 30 | 45 |
| Temperature [$^{\circ}\text{C}$] | 50 | 80 |
| Cat. concentration [%] | 0.25 | 0.40 |

Exercise 13.3

The influence of reaction time, temperature, and catalyst concentration on the yield of a chemical reaction was investigated in a 2^3 factorial design. The following table lists the eight experiments that were carried out together with the yields achieved:

| Experiment | A [min] | B [°C] | C [%] | Yield [%] |
|------------|---------|--------|-------|-----------|
| (1) | 20 | 55 | 0.1 | 15 |
| a | 30 | 55 | 0.1 | 18 |
| b | 20 | 65 | 0.1 | 20 |
| ab | 30 | 65 | 0.1 | 26 |
| c | 20 | 55 | 0.2 | 11 |
| ac | 30 | 55 | 0.2 | 29 |
| bc | 20 | 65 | 0.2 | 23 |
| abc | 30 | 65 | 0.2 | 33 |

- a) Calculate the effects and their interactions.
How can the result be interpreted?
- b) The standard deviation of the target quantity is known from earlier tests: $\sigma = 4.2$.
Which effects and interactions are significant (confidence level 95 %, $c = 2.0$)?

Exercise 13.4

In a hydrogenation process operated in suspension mode, the influence of five variables on the yield of product was of interest. The five variables and their levels were:

| Variable | Low level (-) | High level (+) |
|--|------------------|-------------------|
| A Temperature [°C] | -18 | 0 |
| B Starting material conc. [%] | 5.0 | 10.0 |
| C Cat. conc. [%] | 0.2 | 0.4 |
| D Purity of solvent | tech. | chem. pure |
| E Blank variable | - | - |
| F Stirring speed [min^{-1}] | 100 | 500 |
| G Blank variable | - | - |

The experiments were carried out according to a Plackett–Burman plan. The results are summarized in the following matrix:

| Experiment | A Temp. | B St. M. | C Cat. | D Solv. | E – | F Stirrer | G – | Product yield |
|------------|------------|-------------|-----------|------------|--------|--------------|--------|------------------|
| 1 | + | + | + | – | + | – | – | 0.315 |
| 2 | + | + | – | + | – | – | + | 0.336 |
| 3 | + | – | + | – | – | + | + | 0.330 |
| 4 | – | + | – | – | + | + | + | 0.464 |
| 5 | + | – | – | + | + | + | – | 0.322 |
| 6 | – | – | + | + | + | – | + | 0.507 |
| 7 | – | + | + | + | – | + | – | 0.482 |
| 8 | – | – | – | – | – | – | – | 0.463 |

Determine the significance of the effects by performing a t -test. The number of degrees of freedom corresponds to the number of blind variables, in this case $n = 2$.

| Probability | Two-sided test |
|-------------|----------------|
| 80 % | $t = 1.89$ |
| 95 % | 4.30 |
| 99 % | 9.9 |

Exercise 13.5

In an experimental optimization by the simplex method, the yield of a process was determined as a function of two variables x_1 and x_2 . The following table shows the results of the initial simplex with three experiments:

| Experiment | x_1 | x_2 | Yield [%] |
|-------------------|-------|-------|-----------|
| 1 | 37 | 21.0 | 40.0 |
| 2 | 39 | 21.0 | 41.0 |
| 3 \vec{x}_{n+1} | 38 | 22.8 | 41.4 |

- Calculate the coordinates of the next optimization experiment 4.
- Experiment 4 led to a considerably improved yield of 42.4 %. Under which reaction conditions should the fifth experiment be performed?

14 Catalysis Reactors

The selection and design of a catalysis reactor depends on the type of process and fundamental process variables such as residence time, temperature, pressure, mass transfer between different phases, the properties of the reactants, and the available catalysts [16].

The prerequisites for successful reactor design are the coupling of the actual microkinetics of the reaction with the mass and energy transfer and the determination of fluid-dynamic influences such as backmixing, residence time distribution, etc. The factors that influence the modeling of a reactor are summarized in Figure 14-1 [11].

The choice and calculation of the reactor for a specific chemical reaction involves solving the following problems, on the basis of theoretical knowledge or by more empirical considerations:

- Choice of the reactor type according to the flow behavior of the fluid
- Heat removal

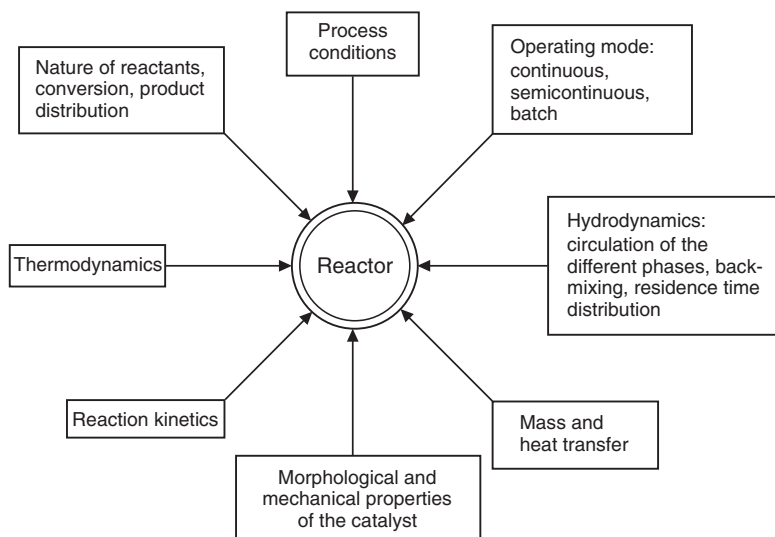


Fig. 14-1 Influences on the design of catalysis reactors

- Heat and mass transfer
- Fluid dynamics

Catalysis reactors can be classified according to their phase conditions. The most important industrial reactor types are two-phase reactors for the system gas/solid and three-phase reactors for the system gas/solid/liquid [13, 15].

Understanding the fundamental reactor types requires knowledge of the design equations of reaction engineering, which will be treated in short form here. Details can be found in text books dealing with chemical reaction engineering [6, T26].

Catalytic gas-phase reactions are generally carried out in continuous fixed-bed reactors, which in the ideal case operate without backmixing. The model reactor is the ideal plug flow reactor, the design equation of which is derived from the mass-balance equation. As we have already learnt, in heterogeneous catalysis the effective reaction rate is usually expressed relative to the catalyst mass m_{cat} , which gives Equation (14-1). The left side of this equation is known as the time factor; the quotient is proportional to the residence time on the catalyst.

$$\frac{m_{\text{cat}}}{\dot{n}_{A,0}} = \int_0^{X_A} \frac{dX_A}{r_{\text{eff}}} \quad (14-1)$$

m_{cat} = catalyst mass, kg

$\dot{n}_{A,0}$ = feed rate of starting material A

X_A = conversion of A

The differential form of the design equation for a heterogeneous catalyzed reaction in a fixed-bed reactor can be described by Equation 14-2:

$$\frac{dX_A}{dm_{\text{cat}}} = \frac{r_{\text{eff}}}{\dot{n}_{A,0}} \quad (14-2)$$

In an ideal tube with plug flow profile, the reaction rate is not constant; it varies in the direction of flow. Therefore, a pronounced temperature profile develops along the length of the reactor. Because the mathematical expression for r_{eff} is often complex, the integral in Equation (14-1) must generally be solved numerically. The feed rate $\dot{n}_{A,0}$ can be determined from the known production capacity of the reactor. Thus, Equation 14-1 allows the catalyst mass and therefore the reactor volume to be calculated from the target quantity conversion and the kinetics. This shows the fundamental importance of kinetics in reaction engineering.

The counterpart of the ideal plug flow reactor is the ideal continuous stirred-tank reactor with complete backmixing of the reaction mass. Because of the ideal mixing, the reaction rate is constant, and a simple design equation is obtained for the catalysis reactor (Eq. 14-3).

$$\frac{m_{\text{cat}}}{\dot{n}_{A,0}} = \frac{X_A}{r_{\text{eff}}} \quad (14-3)$$

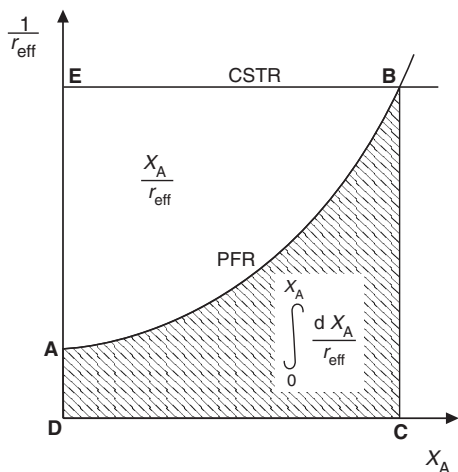


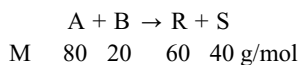
Fig. 14-2 Comparison of a continuous stirred tank reactor (CSTR) with a plug flow reactor (PFR)

The graphical depiction of the two design equations in Figure 14-2 clearly shows the advantages of the tubular reactor compared to the stirred tank. By plotting $1/r_{\text{eff}}$ against X_A , the time factor can be obtained as the area under the curve for the tubular reactor or the corresponding straight line of the continuous stirred tank. While the catalyst mass or reactor volume is proportional to the area under the curve ABCD for the plug flow reactor, the much larger rectangular area BCDE applies for the continuous stirred tank. In the majority of cases of simple reactions, the stirred tank requires a larger reactor volume than the tubular reactor, and the ratio becomes increasingly unfavorable with increasing conversion. Thus, the degree of backmixing is a decisive quantity in the design of catalysis reactors. However, the continuous stirred tank has the advantage that it can be operated isothermally, and in contrast to the tubular reactor there is no temperature profile in the homogeneous reaction space.

Example 1

Reactor calculation: comparison of a fixed-bed reactor with a continuous stirred tank reactor (CSTR)

The gas-phase reaction is to be carried out isothermally according to the equation



A and B are to be fed in stoichiometric proportions to the reactor. The rate law for the reaction follows a Langmuir-Hinshelwood mechanism,

$$r_{\text{eff}} = \frac{k_1 p_A p_B}{1 + K_2 p_A + K_3 p_R} \quad (\text{kmol h}^{-1} \text{ kg}^{-1})$$

The reactor is operated at 2 bar and 300 °C, there is required an output of 10 t R/day. The rate law parameters are

$$\begin{aligned}k_1 &= 0.595 \text{ kmol h}^{-1} \text{ kg}^{-1} \text{ bar}^{-2} \\K_2 &= 4.46 \text{ bar}^{-1} \\K_3 &= 41.65 \text{ bar}^{-1}\end{aligned}$$

- Determine the catalyst weight for a conversion of 80% in a packed-bed reactor.
- Also determine the CSTR catalyst weight necessary to achieve the same conversion as in the packed-bed reactor.

Solution:

- For a fixed-bed reactor, we can use the design Equation 14-2 for a heterogeneous catalyzed reaction:

$$\frac{dX_A}{dm_{\text{cat}}} = \frac{r_{\text{eff}}}{\dot{n}_{A,0}} \quad (14-2)$$

Our first step is to express the partial pressures p_A , p_B , and p_R as a function of X , combine the partial pressures with the rate law r as a function of conversion, and carry out the integration of the fixed-bed equation.

Considering the mole balance we obtain

| Reactant | n_i (mol) | x_i | $p_i = x_i P = x_i \cdot 2$ |
|----------|--------------|-----------------|-----------------------------|
| A | $1-X$ | $x_A = (1-X)/2$ | $p_A = 1-X$ |
| B | $1-X$ | $x_B = (1-X)/2$ | $p_B = 1-X$ |
| R | X | $x_R = X/2$ | $p_R = X$ |
| S | X | $x_S = X/2$ | $p_S = X$ |
| | $\Sigma = 2$ | | |

Note that P designates the total pressure.

Substituting the partial pressures in the rate law gives

$$r(X) = \frac{k_1(1-X)^2}{1 + K_2(1-X) + K_3X} = \frac{0.595(1-X)^2}{1 + 4.46(1-X) + 41.65X}$$

The molar flow rate $\dot{n}_{A,0}$ can be obtained from

$$\dot{n}_{A,0} = \frac{\dot{n}_P}{X_A} = \frac{10.000}{24 \cdot 60 \cdot 0.80} = 8.67 \text{ kmolA/h}$$

The design Equation 14-2 and the rate law $r(X)$ are now combined and solved using an ordinary differential equation solver ODE. The POLYMATH-program and the result is shown as follows:

POLYMATH Program:

Differential equations as entered by the user

$$[1] \quad d(m)/d(U) = Na0/r$$

Explicit equations as entered by the user

$$[1] \quad k3 = 41.65$$

$$[2] \quad Na0 = 8.67$$

$$[3] \quad k1 = 0.595$$

$$[4] \quad k2 = 4.46$$

$$[5] \quad r = (k1*(1-U)^2)/(1+k2*(1-U)+k3*U)$$

$$m_{\text{cat}} = 1614 \text{ kg}$$

b) For the ideal CSTR, the design equation based on mass of catalyst is

$$\frac{m_{\text{cat}}}{\dot{n}_{A,0}} = \frac{X_A}{r_{\text{eff}}} \quad (14-3)$$

At $X = 0.80$ we have

$$r = \frac{0.595(1 - 0.8)^2}{1 + 4.46(1 - 0.8) + 41.65 \cdot 0.8} = 6.76 \cdot 10^{-4} \text{ kmol h}^{-1} \text{ kg}^{-1}$$

$$m_{\text{cat}} = \frac{\dot{n}_{A,0} X_A}{r} = \frac{8.67 \cdot 0.8}{6.76 \cdot 10^{-4}}$$

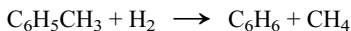
$$m_{\text{cat}} = 10.260 \text{ kg}$$

Note that the resulting catalyst mass in a CSTR would be very large at the given high conversion.

Example 2

Reactor Calculation: Hydrodealkylation

The hydrodealkylation of toluene is to be carried out in a packed-bed reactor. The molar feed of toluene to the reactor is 50 mol/min and the reactor is operated at 40 bar and 640 °C. The feed consists of 30% toluene, 45% hydrogen, and 25% inerts. Hydrogen is used in excess to help prevent coking.



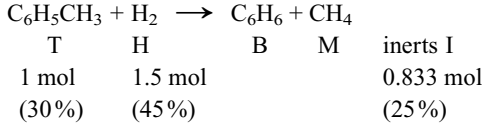
The rate law is

$$r_{\text{eff}} = \frac{8.7 \cdot 10^{-4} p_T p_H}{1 + 1.39 p_B + 1.083 p_T} \quad (\text{mol toluene kg}^{-1} \text{ min}^{-1})$$

Plot the conversion and the partial pressures of toluene, hydrogen, and benzene as a function of catalyst weight.

Solution:

From the mole balance and stoichiometric relations of all reactants including the inerts we obtain



When the conversion is obtained the mole balance becomes

| Reactant | mol n_i | x_i | $p_i = x_i P$ |
|----------|---------------|----------------|--------------------------|
| T | $1-X$ | $(1-X)/3.33$ | $40(1-X)/3.33 = 12(1-X)$ |
| H | $1.5-X$ | $(1.5-X)/3.33$ | $12(1.5-X)$ |
| B | X | $X/3.33$ | $12X$ |
| H | X | $X/3.33$ | $12X$ |
| I | 0.833 | | |
| | $\Sigma 3.33$ | | |

Now we can express all partial pressures as a function of the conversion X and we are able to write the POLYMATH program for the ODE solver as follows:

Hydrodealkylation

Differential equations as entered by the user

$$[1] \quad d(X)/d(m) = rT/nT0$$

Explicit equations as entered by the user

$$[1] \quad pB = 12 * X$$

$$[2] \quad pT = 12 * (1 - X)$$

$$[3] \quad pH = 12 * (15e - 1 - X)$$

$$[4] \quad nT0 = 50$$

$$[5] \quad rT = 87e - 5 * pT * pH / (1 + 139e - 2 * pB + 1038e - 3 * pT)$$

We set our final catalyst weight at 10000 kg and carry out the calculation. Figure 14-3 shows the conversion as a function of catalyst weight.

With 10000 kg of catalyst there can be achieved a conversion of 78.5%. Profiles of the partial pressures of reactants are shown in Figure 14-4.

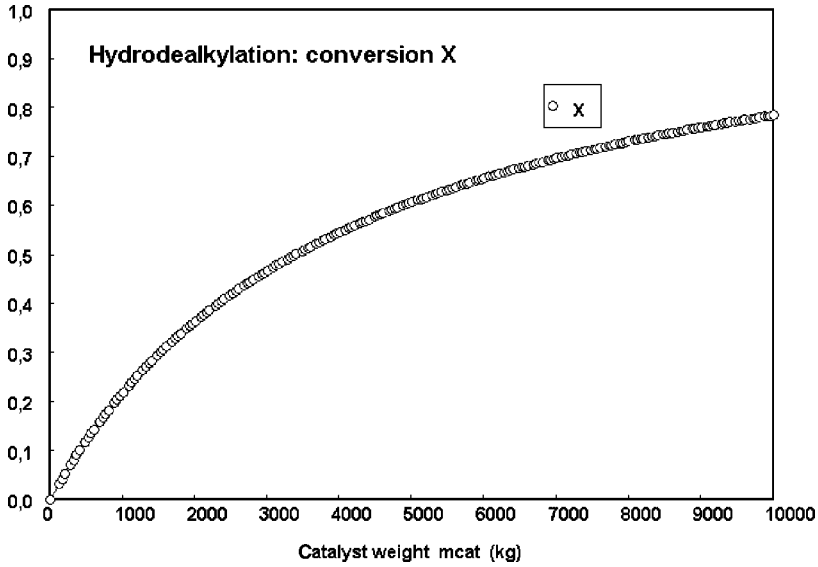


Fig. 14-3 Conversion down the packed bed

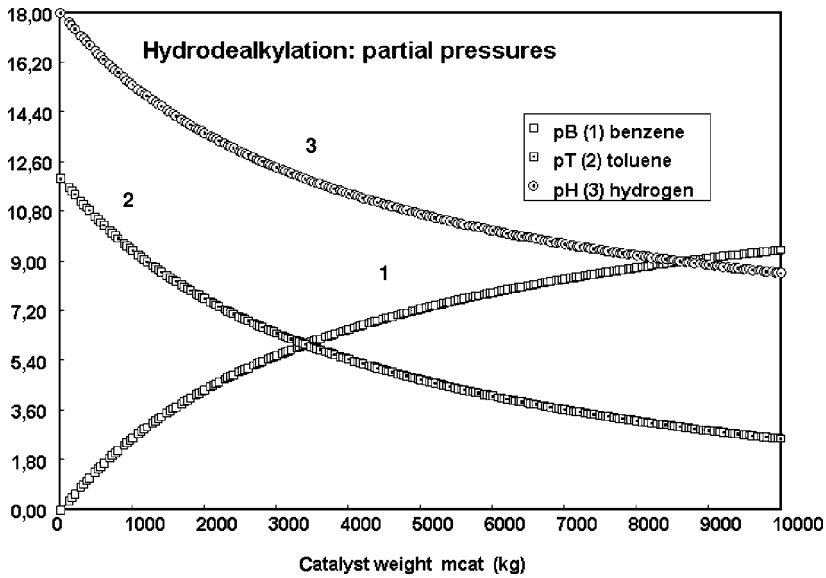


Fig. 14-4 Partial pressure ratio profiles

14.1

Two-Phase Reactors [13, 15]

Gas-phase reactions in the presence of solid catalysts have numerous technical advantages. They can generally be carried out continuously at low to medium pressure. In comparison to liquid-phase processes, they usually require higher reaction temperatures and therefore thermally stable starting materials, products, and catalysts. For this reason, the selectivity of gas-phase processes is often lower than that of liquid-phase processes.

Of major importance in this type of reaction is a large surface area of the solid. Depending on the nature of the solid (particle size, porosity, etc.), the required residence time, the mass-flow mode, and the heat transfer, a wide range of different reactors are used (Fig. 14-5).

The most important factors to be considered in the design of such reactors are:

- 1) Residence-time distribution: influence on conversion and selectivity.
- 2) Temperature control: maintenance of temperature limits, axially and radially; minimum temperature difference between reaction medium and catalyst surface, as well as within the catalyst particle.
- 3) Catalyst lifetime and catalyst regeneration.
- 4) Pressure drop as a function of catalyst shape and gas velocity.

The most widely used types of reactor for heterogeneously catalyzed reactions in the chemical and petrochemical industries are fixed-bed and fluidized-bed reactors [T26]. The most important reactors for heterogeneously catalyzed reactions are the fixed-bed reactors. They can be classified according to the manner in which the temperature is controlled into reactors with adiabatic reaction control, reactors with autothermal reaction control, and those with reaction control by removal or supply of heat in the reactor. Some of the well-known reactor designs are discussed below.

Single-Bed Reactor

The single-bed reactor is the simplest catalysis reactor. It is completely filled with catalyst and is mainly used for thermally neutral and autothermal gas reactions. Owing to its design, the pressure drop is high, and the residence-time distribution has a major influence on the selectivity and conversion of the reaction. Of particular importance is the maintenance of temperature limits, both axially and radially, as heat removal is naturally poor. An advantage is the ease of catalyst regeneration.

Process Examples:

- Isomerization of light gasoline: 400–500 °C, 20–40 bar H₂ pressure, Pt/Al₂O₃ catalyst.
- Catalytic reforming of solvent naphtha: cascade of 3–5 single-bed reactors, 450–550 °C, 20–25 bar H₂ pressure, Cr₂O₃/Al₂O₃/K₂O catalyst.
- Hydrocracking of heavy hydrocarbons: 400–500 °C, 20–60 bar H₂ pressure, oxidic or sulfidic hydrogenation catalysts (Mo/W, Co/W) on acidic supports.

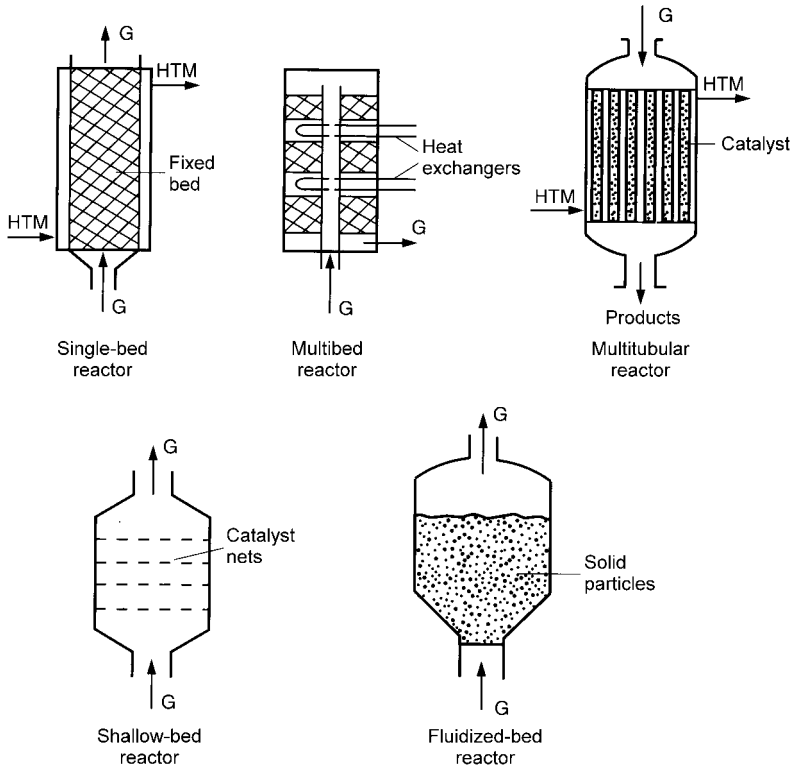


Fig. 14-5 Examples of important gas–solid reactors [T26]

Multibed Reactor

This type of reactor contains several separate, adiabatically operated catalyst beds, allowing defined temperature control. Several methods of cooling are possible: internal or external heat exchangers or direct cooling by introduction of cold gas (quench reactor). The multibed reactor is particularly suitable for high production capacities.

Process Examples:

- Ammonia synthesis: several adiabatically operated catalyst layers with interstage cooling, 400–500 °C, 200–300 bar, iron oxide catalyst.
- Methanol synthesis by the high-pressure process: CO/H₂, 350–400 °C, 200–300 bar, Zn/Cr oxide catalyst, quench reactor.
- Contact process: oxidation of SO₂ to SO₃, 450–500 °C, V₂O₅ catalyst, external heat exchanger.

Multitubular Reactors

In these reactors the catalyst is located in a bundle of thin tubes (diameter: 1.5–6 cm), around which the heat-transfer medium (boiling liquid, high-pressure water, salt melt) flows, giving intensive heat exchange. Multitubular reactors with up to 20 000 or more parallel tubes are used preferentially for strongly endo- or exothermic reactions. The high flow rate in the tubes leads to a relatively uniform residence time, so that the reactors can be modeled as almost ideal tubes. Due to the nonadiabatic process control, a characteristic axial temperature gradient becomes established. The radial temperature profile in the catalyst bed must also be taken into account. Owing to the design of the reactor, changing the catalyst is a laborious process that can be carried out at most twice per year.

Process Examples:

- Low-pressure methanol synthesis: 260–280 °C, 45–55 bar, Cu/ZnO catalysts.
- Oxidation of ethylene to ethylene oxide: 200–250 °C, supported silver catalyst.
- Hydrogenation of benzene to cyclohexane: 250 °C, 35 bar H₂, Ni catalysts.
- Dehydrogenation of ethylbenzene to styrene: 500–600 °C, endothermic, Fe₃O₄ catalysts.

Shallow-Bed Reactors

In these reactors the catalyst is present in the reactor in the form of a thin packed bed or metal net. They are used for reactions with very short residence times and mostly for autothermally operated, heterogeneously catalyzed gas reactions at high temperatures.

Process Examples:

- Dehydrogenation of methanol to formaldehyde: methanol, air and steam are passed over a 5–10 cm high bed of silver crystals.
- Combustion of ammonia to form nitrous gases (Ostwald nitric acid process): cold air and ammonia are introduced, with an excess of air such that the heat of reaction is consumed in heating the initial mixture; 900 °C, Pt/Rh nets.
- Ammoxidation of methane (Andrussow process for the production of HCN): methane, ammonia, and air are passed over a Pt or Pt/Rh net at 800–1000 °C.

Fluidized-Bed Reactors

In a fluidized-bed reactor, finely divided catalyst particles of diameter 0.01–1 mm are held in suspension by flowing gas. This widely used technique allows large volumes of solid to be handled in a continuous process. The factors for the formation of the fluidized state are the gas velocity and the diameter of the particles. Large-scale industrial reactors are operated with fine-grained catalysts and high gas velocities to give a large solid–gas exchange area and high throughput.

The thorough mixing of the solid leads to effective gas–solid heat exchange with an excellent heat-transfer characteristic and hence a uniform temperature distribution in the reaction space. Heat-transfer coefficients are typically $100\text{--}400\text{ kJ m}^{-2}\text{h}^{-1}\text{K}^{-1}$ and for small particles can be as high as $800\text{ kJ m}^{-2}\text{h}^{-1}\text{K}^{-1}$. For fine particles and at high reaction rates, circulating fluidized-bed reactors with separation and recycling of the solid are particularly suitable.

To give a conversion comparable to that of a fixed-bed reactor, a fluidized-bed reactor must be considerably larger. Disadvantages are the broad residence-time distribution of the gas, which favors side reactions; attrition of the catalyst particles; and the difficult scale-up and modeling of this type of reactor.

Process Examples:

- Ammoxidation of propene to acrylonitrile (SOHIO process): a mixture of propene, ammonia, and air reacts on a Bi/Mo oxide catalyst; $400\text{--}500^\circ\text{C}$, $0.3\text{--}2$ bar, high gas throughput, small catalyst particles (mean particle diameter ca. $50\ \mu\text{m}$); the high heat of reaction is removed by cooling coils incorporated in the fluidized bed.
- Oxidation of naphthalene or *o*-xylene to phthalic anhydride: The liquid starting material is injected into the fluidized bed, which has a temperature of $350\text{--}380^\circ\text{C}$; large excess of air, $\text{V}_2\text{O}_5/\text{silica}$ gel catalyst, low gas throughput, catalyst particle diameter of up to $300\ \mu\text{m}$.
- Catalytic cracking of kerosene or vacuum distillate to produce gasoline: capacities up to 3×10^6 t/a, $450\text{--}550^\circ\text{C}$, aluminosilicate catalysts.

14.2

Three-Phase Reactors [7, 12]

The reaction of gases, liquids, and dissolved reactants on solid catalysts requires intensive mixing to ensure fast mass transfer from the gas phase to the liquid phase and from the liquid phase to the catalyst surface. Three-phase reactions between gaseous and liquid reactants and solid catalysts are often encountered in industrial chemistry. Figure 14-6 shows a stirred-tank-reactor cascade for the development of catalytic processes. A well-known example is the hydrogenation of a liquid on a noble metal catalyst. Conducting the process in the liquid phase has advantages and disadvantages, which we will briefly discuss.

The generally low reaction temperatures allow the production of heat-sensitive compounds and the use of thermally less stable but particularly active or selective catalysts such as:

- Solid–liquid phase (SLP) catalysts
- Ion-exchange catalysts
- Immobilized transition metal complex catalysts

Liquid-phase processes generally give higher space–time yields than gas-phase processes. The higher heat capacity and thermal conductivity of liquids leads to bet-

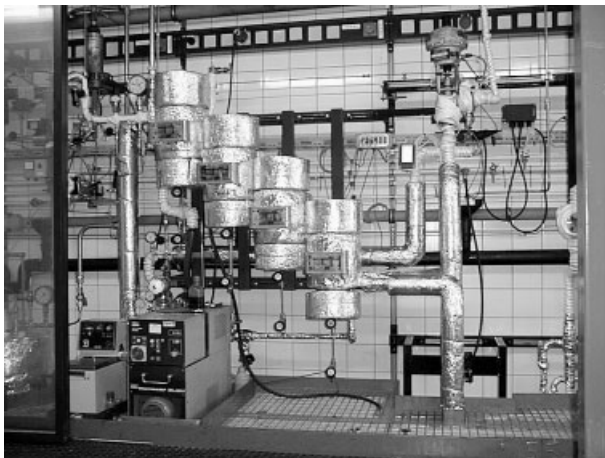


Fig. 14-6 Miniplant unit for the development of catalytical processes in three-phase reactions (Degussa AG, Marl, Germany)

ter heat transfer in the catalyst layer and in the heat exchangers. Heat can be removed very effectively by evaporative cooling. With liquids, the reactivity can be influenced by, for example, suppressing secondary reactions in the liquid phase and by modification of the active centers of the catalyst.

Disadvantages of liquid-phase processes are:

- Separation and purification of the product streams is laborious
- Separation of suspended catalyst from the reaction products is often difficult
- Mass transfer is hindered by the liquid phase, and the necessary intensive mixing of the material streams requires mechanically stable catalysts and supports and often high pressures

Depending on the arrangement of the catalyst, three-phase reactors can be classified as:

- Fixed-bed reactors with a stationary catalyst packing
- Suspension reactors, in which the catalyst is finely dispersed in the liquid (Fig. 14-7)

14.2.1

Fixed-Bed Reactors

Fixed-bed reactors contain a bed of catalyst pellets (diameter 3–50 mm). The catalyst lifetime in these reactors is greater than three months. The best known design is the trickle-bed reactor [8, 10].

In a trickle-bed reactor the liquid flows downwards through a packed catalyst bed, while the gas can flow cocurrently or countercurrently to the liquid. The gas phase, which is present in excess, is the continuous phase. In the cocurrent trickle-bed reactor (Fig. 14-8), the gas/liquid mixture leaving the bottom of the reactor is sepa-

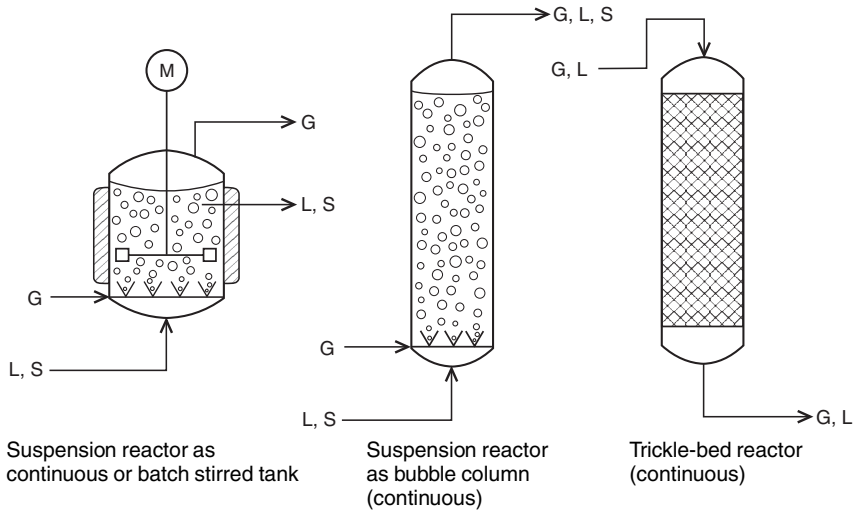


Fig. 14-7 Three-phase reactors

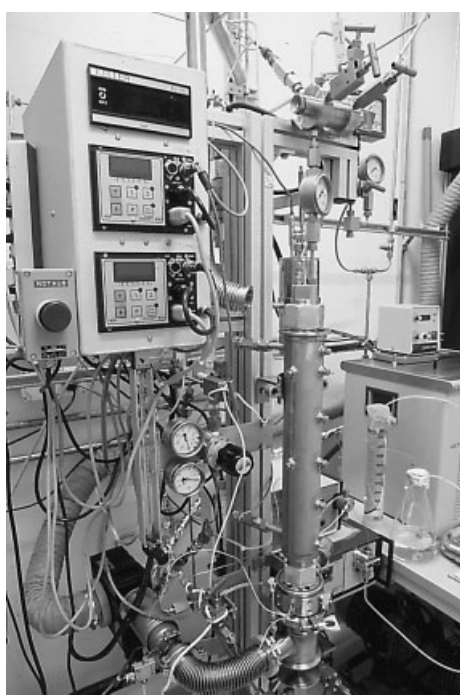


Fig. 14-8 Pilot plant with 0.2 L trickle-bed reactor (Hoffmann-La Roche, Kaiseraugst, Switzerland)

rated, and the gas is recycled. The advantages of this type of reactor are the good residence-time behavior of the liquid and gas streams and the possibility of operating with high liquid flows. In the simplest case the flow of the liquid phase can be described as plug flow (ideal tube). Backmixing is not a problem provided the catalyst bed is sufficiently long (at least 1 m).

Average values for the liquid flow are $10\text{--}30\text{ m}^3\text{ m}^{-2}\text{ h}^{-1}$, and for the gas flow $300\text{--}1000\text{ m}^3\text{ m}^{-2}\text{ h}^{-1}$. Solid–liquid separation is not necessary. Disadvantages are the poor heat removal and the occurrence of hot spots with potential instabilities. However, since the reactors are generally operated adiabatically, the relatively poor heat removal is not necessarily a problem.

Stream formation in large-diameter reactors and wall channeling in small-diameter reactors can lower reactor performance. Often the catalyst is not fully exploited owing to incomplete wetting by the liquid and low mass-transfer rates together with low residence times within the catalyst pellets.

Trickle-bed reactors are widely used in petrochemical hydrogenation processes and in the production of basic products. They are being used increasingly for the manufacture of fine chemicals.

Process Examples [14, T26]:

- Petrochemistry: desulfurization, hydrocracking, refining of crude oil products (e. g., hydrogenative refining of tar fractions from low-temperature carbonization), $300\text{--}350\text{ }^\circ\text{C}$, 220 bar, NiS/WS₂/Al₂O₃ catalysts).
- Synthesis of butynediol from acetylene and formaldehyde: reactor height 18 m, diameter 1.5 m, $100\text{ }^\circ\text{C}$, 3 bar, copper acetylide catalyst, introduction of cold acetylene at various points in the reactor.
- Selective hydrogenation (cold hydrogenation) of acetylene and allene contained in C₄ fractions: up to $50\text{ }^\circ\text{C}$, 5–20 bar, supported Pd catalysts.
- Hydrogenation of aldehydes and ketones to alcohols: $100\text{--}150\text{ }^\circ\text{C}$, up to 30 bar, Ni, Pd, Pt catalysts.
- Hydrogenation of butynediol, adiponitrile, and fatty acid esters.
- Reduction of adiponitrile to hexamethylenediamine: $100\text{--}200\text{ }^\circ\text{C}$, 200–400 bar, Co or Ni on Al₂O₃.
- Fine chemicals: hydrogenation of quinones, sugars, lactones, substituted aromatic compounds.

Small trickle-bed reactors, operated in batch mode by recycling the liquid phase, are also used, for example, for the hydrogenation of trifluoroacetic acid [11].

14.2.2

Suspension Reactors [2, 4]

In suspension reactors, gas and catalyst particles are distributed in a relatively large volume of liquid. Catalyst concentrations are typically less than 3 % with particle sizes of less than 0.2 mm. In general, the reactants (L and G) are introduced into the lower part of the reactor together with the catalyst (S), which is suspended in the

liquid. In the upper part of the reactor, the unconsumed gas is separated or removed together with the liquid product (L) and the suspended catalyst (S). In this system, the liquid is the continuous phase, in which the gas is dispersed as bubbles. Suspension reactors behave largely as gas–liquid systems, and little energy is required for suspension.

Suspension reactors can be regarded as isothermal with a behavior that approximates that of an ideal stirred tank. The reactors are followed by a phase-separation unit in which the liquid is separated from the catalyst and the gas. The gas and the catalyst can be partially recycled.

The advantage of suspension reactors is the effective exploitation of the catalyst, which is completely wetted by the liquid. Because of the small particle size, diffusion processes within the catalyst play no role, and owing to the good temperature control, local overheating can not occur. This type of reactor is particularly suitable for rapidly deactivated catalysts since rapid catalyst replacement is possible.

Disadvantages are potential problems in separating the catalyst and the risk of fractionation and sedimentation of the catalyst in the reactor. Since the residence-time behavior is similar to that of a continuous ideal stirred tank, lower conversions are attained compared to a fixed-bed reactor. A comparison of the two most important three-phase reactors — the trickle-bed reactor and the suspension reactor — is given in Table 14-1.

The majority of suspension reactors are stirred tanks and bubble columns (see Fig. 14-7). Other industrially important variants of the suspension reactor are the loop and Buss (jet) loop reactors, which achieve better exploitation of the catalyst by recirculating it in a loop (Fig. 14-9).

Three-phase bubble columns are operated with the liquid flowing cocurrently with the rising gas. They are used when the mass-transfer resistance lies on the liquid side and the reaction is relatively slow. The gas is introduced at the bottom of the reactor through perforated plates or sintered disks, and the reactors often incorporate sieve trays. Without internals the liquid is almost ideally mixed at high gas velocities, and this results in good heat transfer. The residence-time distribution of the gas and the liquid corresponds approximately to that of a cascade of stirred-tank reactors. The advantages of bubble columns are the simple, inexpensive design and their versatility. Reaction volumes of up to several cubic meters are possible. Bubble columns with internal circulation are also used (loop and air-lift reactors).

In *loop reactors*, the liquid is completely mixed in a relatively small reactor, which gives good heat removal.

In the *Buss loop reactor*, the liquid with the suspended catalyst form a jet that entrains the gas, finely dividing it. The high flow rates lead to intensive turbulence and a high interfacial area between the small gas bubbles and the suspension. An external heat exchanger in the loop allows isothermal operation and very effective removal of the heat of reaction from the system, even with highly exothermic reactions. However, Buss loop reactors can only be operated in a discontinuous mode and require special, highly abrasion resistant catalysts.

Table 14-1 Comparison of trickle-bed and suspension reactors

| Characteristic | Trickle-bed reactor | Suspension reactor |
|---------------------------------------|------------------------------------|---|
| Process mode | continuous | mostly batch |
| Degree of automation | high | low |
| Conditions (temperature, pressure) | moderate | mild |
| Temperature | depends on position | uniform |
| Pressure drop | high | low |
| Reactor performance | high | moderate |
| Plant size | easily extended by tube bundles | limited |
| Selectivity | low | high |
| Liquid content | low | high |
| Residence time behavior | | |
| – liquid | ideal plug flow reactor | ideal stirred tank – plug flow reactor with axial dispersion |
| – gas | ideal plug flow reactor | plug flow reactor with axial dispersion |
| Catalyst effectiveness factor | very low | ca. 1 |
| Catalyst performance | low | high |
| Heat usage | unfavorable | favorable |
| Applicability | limited (selectivity) | universal |
| Particular suitability | high liquid feeds | in case of rapid catalyst deactivation |

Process Examples:

- Liquid-phase hydrogenation of chlorinated aromatic nitro compounds; for example, conversion of *p*-chloronitrobenzene to *p*-chloroaniline in a stirred tank with a powder catalyst (Ni/SiO₂ or Pd on activated carbon).
- Continuous hydrogenation of fats in a chamber reactor (several stirred chambers one above the other), narrow residence-time spectrum is an advantage, 150–200 °C, 5–15 bar.
- Hydrogenation of benzene to cyclohexane in a bubble column: 200–225 °C, ca. 50 bar, Raney nickel (10–100 μm), removal of heat of reaction from the suspension in an external circuit. Cyclohexane is removed as a gas.
- Hydrogenation of fatty esters to fatty alcohols in a bubble column.
- Hydrogenation of fats and fatty acids in a tank reactor with a turbine stirrer (110–120 rpm); H₂ is introduced through a distributor at the bottom, 150–200 °C, up to 30 bar, Ni/Cu catalysts.

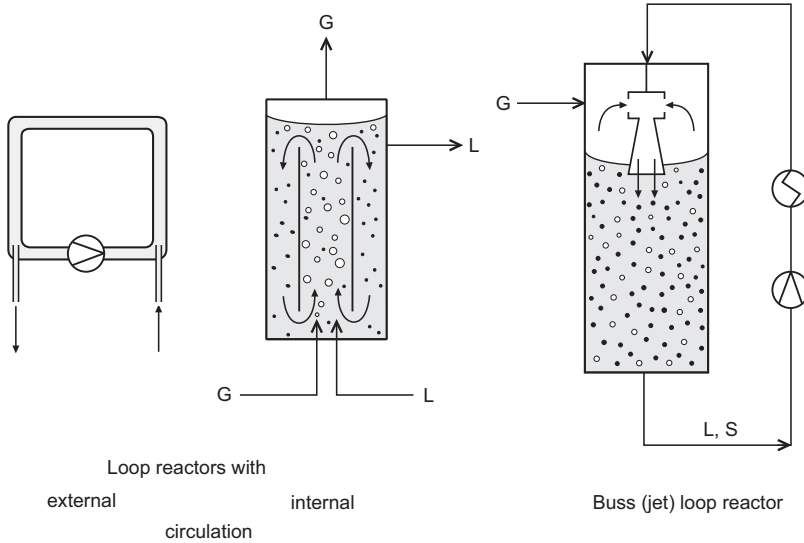


Fig. 14-9 Variants of the suspension reactor

- Hydrogenation of oil in a Buss loop reactor.
- Hydrogenation of 2-ethylanthraquinone to 2-ethylanthraquinol: bubble column with parallel chambers, suspended catalyst.

The choice of the “right” reactor for a given catalytic reaction can often not be answered unambiguously, as shown, for example, by the fact that different technologies compete in the high-pressure hydrogenation of adiponitrile in the presence of ammonia (Table 14-2) [11].

In new plants for the hydrogenation of fine chemicals there is currently a trend to use Buss loop reactors rather than conventional stirred tanks. Today, trickle-bed reactors are generally preferred to suspension reactors for hydrogenation processes.

Table 14-2 Various technologies for the hydrogenation of adiponitrile [11]

| Company | Reactor | Temperature control |
|----------------|---|---|
| BASF | trickle bed | cooling and partial recycling of liquid phase |
| Phillips | suspension loop reactor | |
| DuPont | sump reactor (liquid and gas are passed cocurrent from below into catalyst fixed bed) | several catalyst beds with intermediate cooling |
| ICI | fixed bed | cooling of recycled off-gas |
| Vickers–Zimmer | multitubular reactor with downward cocurrent operation | evaporative cooling with inert solvents |

The examples of the hydrogenation of glucose to sorbitol and of esters to alcohols demonstrate the dilemma of reactor choice. Formerly, suspension reactors with Raney nickel or copper chromite catalysts were used, but today trickle-bed reactors with novel noble metal catalysts are preferred. The following advantages are claimed for the trickle-bed reactors:

- No loss of metal; higher product quality (no contamination)
- Fewer side reactions in the liquid phase due to the lower liquid holdup

The major disadvantage is the risk of poor temperature control owing to the occurrence of hot spots in the catalyst bed. Examples of this are:

- Benzene is formed as a side product in the hydrogenation of cyclohexene
- In the hydrogenation of benzoic acid, decarboxylation of the cyclohexane carboxylic acid product can occur. Therefore, a cascade of stirred-tank reactors is preferred here

The catalyst form is also decisively influenced by the chosen reactor type. It has been found experimentally that at particle sizes below 0.1 mm pore diffusion is rarely limiting, whereas at particle sizes above 5 mm, pore diffusion is always dominant. This is the reason why shell catalysts are advantageously used in trickle-bed reactors. The diffusion limitation need not always result from the transport of the gas in the pores; it can also be due to the substrate. Such effects are found with long-chain organic molecules, for example:

- Hydrogenation of linoleic esters (C_{18}): a shell catalyst with Pd on activated carbon is recommended
- Hydrogenation of C_{12} – C_{22} nitriles: a large-pore catalyst based on Ni/MgO/SiO₂ is recommended [11]

These few examples show how the complexity of three-phase processes greatly complicate reactor modeling and scale-up. The engineer responsible for reactor design must be familiar with reaction engineering and should also work in close cooperation with the synthetic chemist and the catalyst expert.

14.3

Reactors for Homogeneously Catalyzed Reactions [3, 5]

Homogeneously catalyzed reactions with dissolved transition metal complexes are generally carried out in the usual two-phase reactors for gas–liquid systems. The standard reactor is the batch or continuous stirred tank. Since diffusion problems are rarely encountered in homogeneous catalysis, the reaction engineering is much simpler than for heterogeneously catalyzed reactions.

Efficient mixing of the two phases is important as this determines the exchange surface area between the gas and the liquid. Modern stirred tanks (Fig. 14-10) are often equipped with gasifying stirrers, in which the gas is drawn in at the top of the drive shaft and then finely dispersed by the stirrer blades.



Fig. 14-10 0.5 L stirred autoclave reactor in a high-pressure cell (FH Mannheim, Germany)

Since we have already become familiar with the most important reactors for gas–liquid reactions, we will restrict ourselves here to a few examples of processes in special reactors.

Bubble-column Reactors:

- Homogeneously catalyzed air oxidation of hydrocarbons (e. g., of toluene to benzoic acid): 130–150 °C, 1–10 bar, Mn or Co salts as catalyst.
- Oxidation of *p*-xylene to terephthalic acid with Co/Mn salts and bromide at 100–180 °C and 1–10 bar.
- Oxidation of ethylene to acetaldehyde (Wacker process): 100–120 °C, 1–10 bar, PdCl₂/CuCl₂ catalyst.
- Oxo synthesis: reaction of ethylene with synthesis gas to form propanal, 100–150 °C, 200–300 bar, propanol solvent, [HCo(CO)₄] catalyst.

Loop Reactors:

- Oxo synthesis.
- Carbonylation of methanol with CO to produce acetic acid, 150 °C, 200–300 bar, CoI₂ catalyst (Rh catalysts preferred nowadays).

Stirred Tanks:

- Hydroformylation of olefins with Co or Rh catalysts.
- Low-pressure hydroformylation of propene to butanals with water-soluble Rh phosphine complexes (Rhône-Poulenc/Ruhrchemie process): 50–150 °C, 10–100 bar, 10–100 ppm Rh.
- Polymerization of ethylene with $\text{TiCl}_4/\text{Al}(\text{C}_2\text{H}_5)_3$ at 70–160 °C and 2–25 bar.

► **Exercises for Chapter 14****Exercise 14.1**

The design equation for a catalysis reactor is:

$$\frac{m_{\text{cat}}}{\dot{n}_{\text{A},0}} = \int_0^{X_{\text{A}}} \frac{dX_{\text{A}}}{r_{\text{eff}}}$$

- a) To which quantity is the left side of the equation proportional?
- b) Prepare a graphical depiction of the integral.
- c) To which ideal reactor does the catalysis reactor correspond?
- d) What is meant by the term effective reaction rate?

Exercise 14.2

The driving force of a reaction is much smaller in a reactor with backmixing than in a reactor without backmixing. Why?

Exercise 14.3

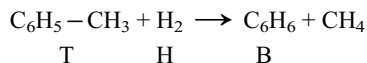
The kinetics of a second-order heterogeneously catalyzed gas-phase reaction of the type $\text{A} \rightarrow \text{R}$ is investigated in a differential circulating reactor. Under isothermal conditions with a reactor feed stream of $\dot{V}_0 = 1 \text{ L/h}$ and $c_{\text{A},0} = 2 \text{ mol/L}$ and a catalyst quantity of 3 g, an outlet concentration of $c_{\text{A}} = 0.5 \text{ mol/L}$ was obtained.

- a) Calculate the rate constant for the reaction.
- b) What quantity of catalyst would be required in an integral reactor (ideal plug flow reactor), in which a conversion of 80% is to be achieved for a feed stream of 1000 L/h with a concentration of $c_{\text{A},0} = 1 \text{ mol/L}$?
- c) The same reaction is carried out in a reactor with complete backmixing. What quantity of catalyst is required (conditions as in b).

Discuss the result.

Exercise 14.4

The catalytic dealkylation of toluene is carried out over a bifunctional catalyst at 660 °C and 30 bar:



The reaction follows a rate law of the Langmuir–Hinshelwood type:

$$r = \frac{kK_{\text{T}}p_{\text{T}}p_{\text{H}}}{1 + K_{\text{T}}p_{\text{T}} + K_{\text{B}}p_{\text{B}}}$$

At 660 °C:

$$k = 0.202 \text{ mol kg}^{-1} \text{ bar}^{-1} \text{ h}^{-1}$$

$$K_{\text{T}} = 0.9 \text{ bar}^{-1}$$

$$K_{\text{B}} = 1.0 \text{ bar}^{-1}$$

The molar ratio of toluene ($M = 92$) to hydrogen in the initial mixture is 1/10. Calculate the catalyst mass for a reactor handling 2000 t/a toluene with 60 % conversion (1 year = 8000 operating hours).

Exercise 14.5

Name industrial processes that are carried out in the following reactors (one per reactor):

- Single-bed reactor
- Tubular reactor
- Multibed reactor
- Shallow-bed reactor
- Fluidized-bed reactor

Exercise 14.6

In the oxidation of methane to formaldehyde, CO_2 is the main side product. At the reaction temperatures required to oxidize methane, formaldehyde is unstable and is easily oxidized to CO_2 . Since both reactions are exothermic, the catalyst temperature rises, and this favors further oxidation and catalyst sintering.

Which recommendations can be made for the choice of catalyst and reactor?

- High porosity
- Low porosity
- High thermal conductivity
- Low thermal conductivity
- Tubular reactor
- Fluidized-bed reactor

- Shallow-bed reactor
- Single-bed reactor

Exercise 14.7

Compare trickle-bed and suspension reactors according to the following criteria:

- Temperature distribution
- Selectivity
- Residence-time behavior of the liquid
- Catalyst particle diameter
- Catalyst effectiveness factor
- Catalyst performance

Exercise 14.8

Phthalonitrile is produced industrially from *o*-xylene and NH_3/O_2 .

- a) What type of reaction is involved?
- b) What type of reactor can be recommended for the process?

Exercise 14.9

In the hydrogenation of α -methylstyrene, varying degrees of catalyst effectiveness factors η were found:

- A) Supported $\text{Pd}/\text{Al}_2\text{O}_3$ catalyst with 0.03 mm particle diameter in a suspension reactor: $\eta = 1$.
- B) The same supported catalyst with 8.25 mm particle diameter in a trickle-bed reactor: $\eta = 0.007$.

Explain this dramatic difference.

15

Economic Importance of Catalysts

The modern industrialized world would be inconceivable without catalysts. There is no other technical principle which combines economic and ecological values as closely as catalysis. The development of chemical products in advanced, industrialized societies will only be technically, economically and ecologically possible by means of specific catalysts. Examples include the specific production of stereochemically pure pharmaceuticals, the construction of tailored polymer materials, the reduction of pollutants from manufacturing plants and combustions systems (e.g. power stations, motor vehicles). Another major topic for the 21st century, the production, storage, and conversion of energy, will also be promoted by catalysts [4].

Thus, catalysis is the No. 1 technology in chemical industry:

- > 95% of all products (volume) are synthesised by means of catalysis
- > 70% of all products (processes) are synthesised by means of catalysis
- > 80% of the added value in chemical industry is based on catalysis
- ~ 20% of the world economy depends directly or indirectly on catalysis

Approximately 80% of all catalytic processes require heterogeneous catalysts, 15% homogeneous catalysts and 5% biocatalysts [3]. The total commercial value of all catalysts worldwide is over 12 billion EUR. In crude oil refining processes the catalysts costs amount to only about 0.1% of the product value, and for petrochemicals this value is about 0.22%.

Since the special properties of the catalysts decisively influence the economics of a process, their true economic importance is considerably higher than their „market value“. The value of the products that are produced with catalysts is ~ 500 billion EUR p.a. Also market estimates vary widely – for example, there are no figures available for the considerable internal consumption of the chemical industry – the key importance of industrial catalysts can be recognized from the above data. In this chapter we shall treat the catalysts according to their area of use.

The traditional area in which catalysts have been used for over 100 years is the chemical industry. For example, the contact process for the production of sulfuric acid was introduced as early as 1880. In the 1920s and 1930s catalysts for crude oil processing came on the market, initially in the USA and later in Europe, mainly after World War II. Environmental catalysts became of importance from 1970 on-

wards. They can be divided into automobile and industrial catalysts, the latter being those that purify off-gases from power stations and industrial plants. The environmental catalysts are not part of any wealth-creating process; instead, they contribute to protection of the environment and thus to a generally higher standard of living. Therefore, their importance can scarcely be expressed in monetary terms.

Thus the catalyst market can be divided into four main areas:

- Environmental catalysts (industrial and automobile environmental catalysts)
- Chemistry catalysts
- Petroleum refining catalysts
- Polymerization catalysts

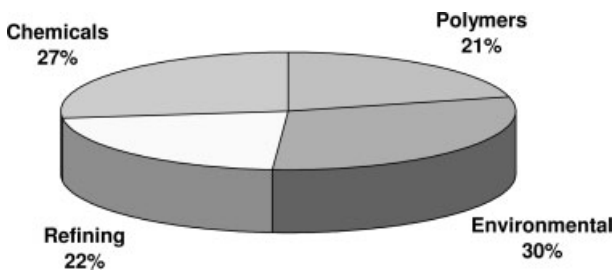


Fig. 15-1 Worldwide catalyst market according to application [1]

Figure 15-1 shows the market distribution for the different catalyst areas.

The average annual growth rate for catalysts during the period 1995–2005 has been 4%, and the greatest growth has been ascertained in North America and Europe. Therefore, the development of high performance and conceptually innovative catalytic processes is crucial for catalysis industry sector. Additionally, it is the key for a sustainable future for Europe.

Catalysts are relatively expensive and are truly specialty chemicals. They are typically more expensive than the bulk pharmaceutical aspirin (~2 EUR/kg) and about the same price as vitamin C (~6–8 EUR/kg). Tonnages are also of the same order of magnitude as for pharmaceuticals.

Approximately 24–28 wt.-% of the produced catalysts have been sold to the chemical industry and 38–42 wt.-% to petrochemical companies including refineries. 28–32 wt.-% of solid catalysts were spent in environmental protection and only 3–5 wt.-% in the production of pharmaceuticals [2].

Petroleum refining catalysts on average are the cheapest and cost about one-half as much per kg as chemicals catalysts. They are dominated by the cheap acid catalysts used for alkylation, which account for 90% per weight but only about 30% per value in this sector. The new solid acid catalysts and especially the high active zeolite catalysts used for cracking processes are more expensive and account for about one-tenth of the tonnage but about 40% of sales value. The other petroleum refining catalysts (i. e. for hydrotreating, hydrocracking, reforming, and isomerization) are of less significance [4].

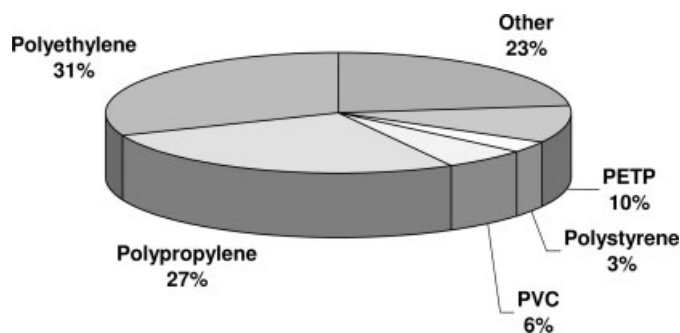


Fig. 15-2 Global market for polymerization catalysts, 2000 (2020.5 million US \$) [4]

Figure 15-2 shows the global market for polymerization catalysts, the main sectors are for polyethylene and polypropylene manufacture.

Materials that promote polymerization may be divided into true catalysts such as metal complexes, metal oxides, and anionic and cationic catalysts and initiators, which appear as end groups in the final polymer. It seems to be clear that the most expensive polymerization catalysts are the single-site metallocene catalysts. Sales has grown from 1 million US \$ in 1994 to 100 million US \$ in 2000. Ziegler catalysts used for polypropylene and polyethylene, and the dibutyl tin and special basic catalysts for polyurethanes are also expensive.

The main group in chemical catalysts is general organic synthesis. It includes catalysts for esterification, hydrolysis, alkylation (dominated by cumene and ethylbenzene), and halogenation. A special class of this area are oxidation catalysts. About one-half of this market by value is the silver catalyst for ethylene oxide. Relatively cheap catalysts are those for the oxychlorination of ethylene, they make up one-third by weight but only 5% by value.

Other expensive oxidation catalysts are the manganese and cobalt salts in acetic acid plus bromine promoter for oxidation of *p*-toluic acid to terephthalic acid.

The final category of chemical synthesis catalysts is the iron-based catalysts for ammonia and the copper- or chromium-based catalysts for methanol synthesis. The cost is relatively low but the tonnage for ammonia alone is about one-fifth of total catalysts for chemicals.

The main hydrogenation catalysts are:

1. Raney nickel for margarine and related processes.
2. Nickel and to a lesser extent Pd or Pt for hydrogenation of benzene to cyclohexane.
3. Silver gauze for dehydrogenation or oxidative dehydrogenation of methanol to formaldehyde.
4. Co and Rh catalysts for the oxo process.

The main dehydrogenation process is the conversion of ethylbenzene to styrene (iron-based catalyst).

The catalysts for automobile emission control are based on precious metals such as platinum, palladium, and rhodium. These are almost an order of magnitude more expensive than the chemical catalysts, and the tonnage is correspondingly smaller. Automobile catalysts are generally honeycomb supports doped with Pt or Pd. For the denitrogenation of power station flue gases by the SCR process, the honeycomb catalysts mainly used are made of V_2O_5 , WO_3 , MoO_3 , and TiO_2 . Market data for industrial catalysts only reflect the cost of the catalysts, which account for only about 10% of the cost of a complete off-gas purification plant. During the last few years there has been a precipitous drop in palladium consumption due to its partly replacement by platinum in dental alloys and automobile emission catalysts [4].

The environmental and the polymerization area are seen as the growth market for catalysts, while petroleum refining catalysts are expected to be static.

At present more than 15 international companies are producing about 100 fundamental types of solid catalysts. Besides these types, numerous special catalysts exist tailored for certain processes or plants and so-called custom catalysts [2].

Some catalyst producers are given below:

- Engelhard Corp. (inclusive Harshaw Catalyst)
- Syntex (ICI Catalysts and ICI Catalco)
- Davison Chemicals and Grace
- SÜD-CHEMIE Catalyst Group (inclusive UCI, Houdry, Prototec/USA, NGC, CCIFE/Japan, UCIL/India, AFCAT and SYNCAT/South Africa)
- UOP and Katalytiks
- Shell and Criterion Catalysts inclusive Zeolyst International
- Johnson Matthey
- Caldicat
- Degussa
- BASF
- Haldor Topsoe
- Nippon Shokubai
- Nikki Chemicals

In this chapter we have seen that catalysts play an essential role in industry, not only in economic terms but also in reducing pollution of the environment.

16 Future Development of Catalysis

16.1 Homogeneous Catalysis [2, 11]

Nowadays the broad spectrum of catalytic processes would be inconceivable without homogeneous transition metal catalysis, the importance of which can be expected to grow in future [2].

The driving force for the introduction of new processes are economic considerations, which are largely influenced by the production costs of the product and product quality. The optimal exploitation of raw materials, energy saving, and the environmental friendliness of processes will still take precedence in future. Selectivity is becoming more and more the decisive factor in industrial processes, mainly as a result of increasing purity demands, for example, in polymer chemistry and in the pharmaceutical sector. Higher selectivity means that better use is made of raw materials and therefore lower formation of side products, which must be removed in expensive separation processes or pollute the environment.

There is a need for correlation of structure, dynamical rearrangements, transition states and reaction intermediates of enzyme, heterogeneous and homogeneous catalytic systems through investigations of the same reactions under similar experimental conditions.

For example, correlations exist between metalloenzyme and heterogeneous transition metal catalytic processes in the areas of alkane hydroxylation and dehydrogenation, olefin epoxidation, and nitrogen fixation, despite the fact that heterogeneous catalysts typically operate under high temperature and sometimes high pressure conditions, while enzymes catalyze similar transformations under ambient conditions.

Potentially acting between these extremes are synthetic metal complexes that mimic the metalloenzyme active sites and catalyze reactions under relatively mild conditions.

New strategies of catalyst synthesis must be developed to establish molecular control over the structure, location and promoter distribution of catalysts. Molecular characterization of the working catalysts can provide the crucial experimental information on structural details and can lead to identification of elementary reaction steps [3].

It is apparent that in future, new transition metal catalysts with new ligands, newly discovered reactions, and improvements to existing processes will be introduced into

industry [2, 7]. Energy and raw materials politics will presumably increasingly determine the future direction of development of industrial organic chemistry. Only a few aspects can be discussed here. Homogeneous catalysis has by no means reached the limits of its potential, but is of course not easy to depart from the well-trodden paths of known technologies.

In the case of basic chemicals the chances for new catalytic processes are small, but they are better for higher value chemicals such as fine and specialty chemicals. Pharmaceuticals and agrochemicals are two areas where homogeneous catalysts have advantages. Complex molecules can often be synthesized in single-step one-pot reactions with the aid of transition metals. This sector has many potential points of overlap with biotechnology, especially enzyme catalysis [5].

Especially noteworthy is the field of asymmetric catalysis. Asymmetric catalytic reactions with transition metal complexes are used advantageously for hydrogenation, cyclization, codimerization, alkylation, epoxidation, hydroformylation, hydroesterification, hydrosilylation, hydrocyanation, and isomerization. In many cases, even higher regio- and stereoselectivities are required. Fundamental investigations of the mechanism of chirality transfer are also of interest. New chiral ligands that are suitable for catalytic processes are needed.

A major disadvantage of homogeneous catalysis up to now has been that in general olefins can effectively be activated but not alkanes. If it becomes possible to carry out the CH activation of alkanes in homogeneously catalyzed reactions, this would open up cheap new routes to many industrial chemicals. Research in this direction has been carried out for many years, a major target being the exploitation of methane or lower alkanes in catalytic processes. Interesting stoichiometric and also catalytic CH activation reactions have been discovered. The key reaction is the cleavage of the C–H bond with insertion of a metal center. Numerous interesting reactions are then possible, mainly giving oxygen-containing compounds such as alcohols, aldehydes, and carboxylic acids (Fig. 16-1) [7]. Another desirable reaction is the direct oxidation of methane to methanol.

Another area that is still of interest is the long-known synthesis gas chemistry, for example, conversion to C₂–C₄ olefins or C₁ and C₂ oxygen compounds such as methyl formate and acetic acid.

Methanol is also an important starting material for further syntheses. Interesting new routes could be based on reactions such as carbonylation, reductive carbonylation, and oxidative carbonylation. Another example is the homologization of methanol to ethanol via acetaldehyde.

A further area of major future potential is CO₂ chemistry. The chemical exploitation of the huge quantities of CO₂ that are released into the atmosphere is of great interest. Although many CO₂ complexes of transition metals and model reactions are already known, so far none has been introduced into industry. The main reactions investigated up to now are the reaction of CO₂ with alcohols and olefins to give esters and lactones and the reduction of CO₂ to CO.

Of particular interest in the long term are catalytic processes on the basis of water and air, operated with solar energy. These include the reduction of atmospheric nitrogen to ammonia or hydrazine, the activation of oxygen for use in fuel cells, and

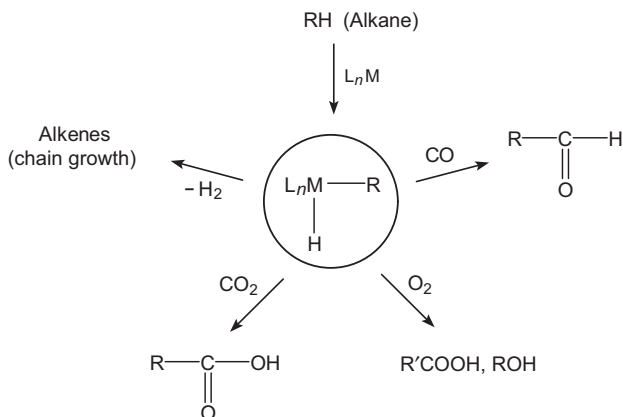


Fig. 16-1 CH activation of alkanes [7] L_nM = catalyst (M = metal, L = ligand)

the photochemical cleavage of water to give oxygen and hydrogen. Interesting approaches involve carbonyl catalysts and clusters.

Since only 12 metals have been used as homogeneous catalysts in industrial reactions up to now, a broad-based study of the less well investigated metals (e.g., the lanthanides) is called for [7].

Changing the phase in which a homogeneous catalyst is used also has major development potential. An example is multiphase catalysis, in which the catalyst is dissolved in a solvent in which the substrate or the product is insoluble. The catalyst and product solution can then be separated by a simple phase-separation process. In particular, water-soluble catalysts for use in two-phase processes have very good future prospects. The heterogenization of homogeneous catalysts is another area where improvements are necessary and possible.

These few examples show that although homogeneous transition metal catalysis has achieved remarkable success in the last few years, there is still a very large potential for further development, both in fundamental research and in industrial application.

16.2

Heterogeneous Catalysis [9, 12]

Heterogeneous catalysts are among those products that will continue to exhibit development potential for the next few decades. One reason for this is that scientific knowledge about the individual steps and mechanisms of heterogeneously catalyzed reactions is still incomplete. Another is the increasing necessity to produce chemicals in an economic and environmentally friendly manner. Modern methods for the investigation of surfaces are particularly helpful in the search for new catalysts and the improvement of existing catalysts, and they make a more systematic catalyst research possible [4].

There is a demand in modern in-situ techniques for catalyst investigation such as

- In-situ techniques for chemical analysis of catalyst surfaces with atomic resolution under actual operating conditions; there is achieved time resolution that is shorter than turnover times
- Techniques for rapid evaluation of both catalyst structure and adsorbate structure under reaction conditions; the dynamic rearrangement of the catalytically active surface should be correlated with catalytic performance in practice
- Predictive techniques for guiding and accelerating the development of catalysts for specific applications [3]

Two main areas of future catalyst development can be expected:

- Improvement of existing processes: increasing the yield and selectivity, energy savings in the production processes
- Development of new processes: use of other raw materials with the aid of new catalysts

Although a decline in research activity in the field of heterogeneous catalysis was predicted in recent years, this in fact did not happen. Instead, stricter environmental requirements and the general trend towards milder reaction conditions have meant that heterogeneous catalysis has increased in importance [5]. This is demonstrated by many examples, including:

- Better removal of harmful impurities from raw materials and intermediates
- Development of processes low in off-gases and wastewater, including those for fine chemicals
- Reducing the number of process steps by activation of simpler raw materials (e. g., alkanes)
- Replacement of expensive and less widely available catalyst components (e. g., Pt by other metals or metal oxides)

Here we will discuss some trends and perspectives of heterogeneous catalysis by means of a few examples [6].

In the beginning, the development of a new product or process is slow until a certain state of knowledge is reached, after which rapid growth is observed. The process is adopted in many sites, tested and developed further. Finally, the development process or the growth in knowledge proceeds slowly, and a state of saturation or maturity is reached (Fig. 16-2).

This S-shaped development cycle applies both to the production of chemicals (especially basic chemicals) and catalyst development. If further progress is to be made, then new routes must be explored before existing technologies reach their limits. Process development often proceeds in technological leaps and bounds, as has been seen in many areas of chemistry/catalysis in the past. Often the decisive improvement to the process is only possible with the aid of catalysts:

- Methanol synthesis: replacement of high-pressure processes by medium- and low-pressure processes

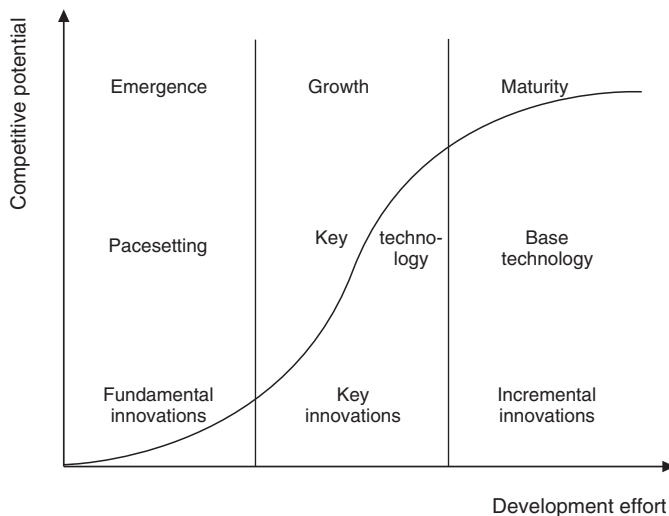


Fig. 16-2 Development cycle of a product or process

- Oxo synthesis: replacement of Co by Rh catalysts
- Direct oxidation of ethylene to ethylene oxide with supported silver catalysts

Which possibilities can be expected in the future?

16.2.1

Use of Other, Cheaper Raw Materials

Raw material costs decisively influence the total manufacturing costs of many chemical products; a contribution of 70 % by the raw materials is not unusual. Thus the use of less highly refined raw materials is desirable. Therefore, efforts are being made worldwide to produce valuable chemicals from lower alkanes such as methane, ethane, propane, and butane instead of the olefins that are currently used.

Natural gas, the main component of which is methane, is of particular interest as a raw material. Currently, methane is converted to synthesis gas by steam reforming. This route involves high energy costs since a highly endothermic reaction is involved. A promising reaction is the oxidative coupling of methane to give ethane (Eq. 16-1) or ethylene, preferably with alkali or alkaline earth metal catalysts. The reaction temperatures of over 600 °C are still a disadvantage.



Another possibility is the partial oxidation of methane to oxygen-containing compounds (methanol, higher alcohols, aldehydes) or synthesis gas and dehydrogenative coupling to give aromatic compounds.

The activation of higher alkanes is also being intensively investigated. An example is the oxidative dehydrogenation of ethane, propane, and isobutane to the corre-

sponding alkenes and oligomeric products. Economically favorable processes would be the direct oxidation of propane to acrylic acid or of isobutane to methacrylic acid.

Other good prospects are offered by C_1 chemistry, especially that of methanol, the price of which has continuously fallen and is now only about twice that of ethylene. A major challenge for catalyst research is the oxidative coupling of methanol to produce ethylene glycol.

Catalytic oxidations of hydrocarbons have relatively low selectivities. Reactions with interesting perspectives are the direct oxidation of propylene to propylene oxide, of benzene to phenol, and of propane to isopropanol and acetone.

Another challenge for the future is the exploitation of new raw materials and energy sources. New poison-resistant catalysts will be required in a few decades in order to economically process heavy crude oils, tar sands, and oil shales. Coal gasification and liquefaction will regain importance. Even if hydrogen technology and high-temperature reactions with solar energy are introduced, other chemical problems will only be solvable with the aid of catalysts [10].

Other examples for a better utilization of alternative and renewable feedstocks are:

- Development of catalysts for depolymerizing mixed polymers
- Development of catalysts for the selective synthesis of chemicals from CO and CO_2
- Development of catalysts for the conversion of cellulose and carbohydrates to chemicals
- Improve existing processes by reducing the levels of CO_2 produced as a byproduct

16.2.2

Catalysts for Energy Generation

Conventional combustion processes generally proceed at high temperatures and lead to formation of undesired nitrous oxides. Combustion catalysts are intended to achieve fast total combustion of the fuel at lower temperatures. Catalytic combustion of methane in a gas turbine has already been developed by a company in Japan, where a research society for catalytic combustion has also been established. However, the complex metal oxide catalysts do not yet have sufficient temperature stability and resistance to catalyst poisons.

Fuel cells with improved catalysts would allow the most efficient use of fossil fuels for the direct generation of electricity. There is major interest in the electrochemical reaction of synthesis gas or, better still, methane. It would be desirable to simultaneously generate energy and to produce valuable oxidation products in a fuel cell. Another interesting fuel is methanol, but technical realization has so far been unsuccessful because of the associated high activation energies.

Emission control is of the greatest importance in energy generation, and new high-performance catalysts play a key role here. For example, new catalysts that can decompose nitrous oxides into N_2 and O_2 would be of interest because the use of

ammonia in the SCR process could then be dispensed with. A start has already been made in this direction: in Japan it was found that [Cu]-ZSM-5 zeolites are highly active and stable catalysts for the dissociation of NO [8].

16.2.3

Better Strategies for Catalyst Development

Up to now there has been no general theory for the description and prediction of heterogeneous catalytic processes. The reason is the complexities of real systems, which consist of numerous components, including structure and dispersion stabilizers, dopants, additives for increased selectivity, and many others. Therefore, there is great need for research on the behavior of catalyst surfaces that consist of several components [4]. The fundamental knowledge required, for example, to improve the selectivity of catalysts is also lacking.

Studies of reaction intermediates and transition states, that are carried out at low pressures using model systems, should be correlated with studies of reaction intermediates during catalytic reactions. Interesting areas for investigations are the catalytic conversion of chiral molecules and high temperature, short residence time processes involving free radicals that include pyrolysis and catalytic combustion.

New strategies of catalyst synthesis must be developed to establish molecular control over the structure, location and promoter distribution of catalysts to achieve high selectivity. These include single molecular precursors, and synthesis of microporous framework around nanoparticles of uniform particle size. The combination of precisely designed and uniform nanoparticle catalysts with highly ordered supports giving the optimum combination of activity, selectivity and throughput is achievable.

A key current limitation in the discovery of new zeolites is the lack of fundamental understanding of the zeolite nucleation and crystallization process. Therefore, correlations between structure-directing templates and the resulting zeolite material have to be achieved [3].

The structure–activity relationships of catalysts, i. e., the connections between the production parameters, the structure, and the catalytic properties of solids are generally elucidated by empirical means. Catalyst development usually starts from a working hypothesis that is based on a semi-empirical model of the course of the reaction. However, it would be a mistake to assume that targeted design of catalysts can be achieved by means of modern surface analysis techniques and computer calculations alone.

A successful catalyst development strategy must take the chemical and physical conditions into account, from the outer shape of the catalyst to the pore structure to the active center, and from the chemical composition to the various crystalline phases to the influence of promoters. The reactor type must also be included in an overall view of the process [10].

Mechanistic concepts of the microscopic interaction between catalyst and substrate are becoming increasingly refined, and the possibilities have by no means been exhausted, so that advances are still to be expected. Here we can only discuss a few recent trends.

The principle technologies recommended for catalyst research and development are:

New catalyst design:

- Combined experimental mechanistic understanding, and improved computational modeling of catalytic processes.
- Computer aided, nanostructural fabrication of active sites producing economically viable catalyst structures

High-throughput synthesis and testing of catalysts (see Section 13.3.6):

- Identification of high-throughput methods for synthesizing catalysts
- Development of high-throughput analytical techniques for evaluating catalyst performance
- Development of reaction protocols for rapid screening of large numbers of catalyst simultaneously at elevated pressure [13]

Shaped catalyst bodies with optimized geometries (e.g., wagonwheels, honeycombs) offer lower resistance to gas flow and lower the pressure loss in reactors. The mechanical and thermal stability of catalysts and supports is being improved. New support materials such as magnesite, silicon carbide, and zircon ($ZrSiO_4$) ceramics with modified pore structures offer new possibilities. Meso- and macropores can be incorporated into solids to accelerate transport processes, and the question of porosity will increasingly be the subject of interest.

Higher starting material purities are being achieved by the use of guard catalysts that remove catalyst poisons such as sulfur and halogen compounds, metals, and organic impurities. Here the zeolites have advantages over conventional adsorbents such as activated carbons [8].

The search for new selectivity promoters will be improved, and more and more unusual elements such as Sc, Y, Ga, Hf, and Ta will be used. The zeolites have major potential, and it is expected that especially the pentasils and the metal-doped zeolites will achieve wider application in organic syntheses. The industrial application of aluminosilicates and sheet silicates is also imminent.

Another promising class of compounds are the heteropolyacids. Depending on the reaction conditions, they can act according to three basic mechanisms: as normal surface catalysts, with involvement of the entire volume, or as pseudo-liquid phase catalysts. They have so far mainly been used in Japan for hydrogenation/dehydrogenation, selective oxidation, and acid/base reactions.

Other catalysts for acid/base reactions will also increase in importance, for example, acid modification of support materials (B/Al_2O_3 , Zr/TiO_2 , W/ZrO_2) and superacids, combinations of metal sulfates on metal oxides, such as $FeSO_4$ on Fe_2O_3 and $ZrSO_4$ on ZrO_2 or TiO_2 [8].

Colloids and amorphous metals and alloys are further interesting nontraditional catalysts, but there are difficulties in manufacturing them reproducibly. Other development possibilities are represented by transition metal compounds such as Mo and W carbides

and nitrides, which are already being tested as potential replacements for the noble metal platinum [5]. Special areas that will develop rapidly are biocatalysis, enzyme catalysis, photocatalysis, and electrocatalysis, to name but a few.

New types of reactor, such as the membrane reactor, will in future be applied to additional areas of application. Already today this type of reactor is being used not only for homogeneous catalysis, but also for selective hydrogenation. Selective oxidation reactions in a membrane reactor appear promising.

Some important directions of catalyst development are described in the „Vision 2020 Catalysis Report“ of the American Chemical Society (ACS) and other joint associations [13]. Recommendations for the most significant areas of application of catalyst technology in which improvements in homogeneous or heterogeneous catalyzed processes are as follows. Generally, these processes should focus on lowering energy requirements via higher selectivity, more moderate temperature or pressure, and a reduced number of unit operations:

- Selective oxidation
- Alkane activation
- Alkylation
- Olefin polymerization
- Selective synthesis, such as stereo- and regioselective
- Byproduct and waste minimization
- Alternative and renewable feedstocks

In the near future one can expect the following general trends in the catalyst development [9]:

- Catalyst preparation, characterization and testing that includes robotic and computer-programmed instruments
- Broader application of multipurpose microreactors and various in-situ methods to characterize catalyst surfaces closer to industrial conditions
- Scientific catalyst design as an inseparable part of catalyst development to make the development procedure more rational and effective
- General programs for computer scaling-up of micro- or bench-scale reactor data to demonstration plant unit
- Development of catalysts possessing optimal shape designed by process engineering
- Further development of heat-resistant materials for catalytic combustion in power generation
- Development of catalysts for processes converting renewable materials
- Further development of materials suitable for catalytic membranes and fuel cells
- Development of catalysts to make processes with zero waste and 100% selectivity possible

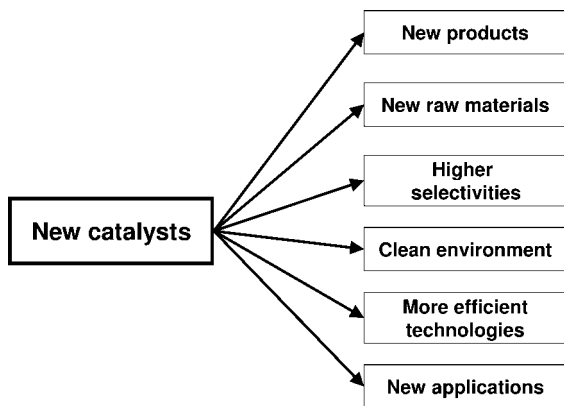


Fig. 16-3 New catalysts – a key innovation in the future

Figure 16-3 summarizes the main features of expected catalyst development.

However, we have to consider that technological developments are not predictable. Generally they are not the result of a logically designed development program, often they are surprise discoveries. But it is safe to say that catalysis will remain one of the most important areas of research in academia and technology.

Solutions to the Exercises

Chapter 1

Exercise 1.1

- Homogeneous catalysis: all reactants and the catalyst (NO) are gaseous.
- Heterogeneous catalysis: three phases.
- Homogeneous catalysis in aqueous solution.

Exercise 1.2

| | Heterogeneous catalysts | Homogeneous catalysts |
|---------------------|-------------------------------|---|
| Active centers | only surface atoms | all metal atoms |
| Concentration | high | low |
| Diffusion problems | yes, mass transfer controlled | mostly none; kinetically controlled reactions |
| Modifiability | low | high |
| Catalyst separation | simple | laborious |

Exercise 1.3

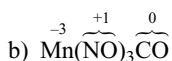
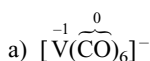
- Severe reaction conditions and high temperatures are possible
- Wide applicability
- High thermal stability of the catalyst
- Catalyst recycling unnecessary or simple

Exercise 1.4

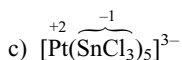
- a) Activity: quantitative measure for the comparison of catalysts
 Selectivity: the fraction of the starting material that is converted to the desired product
- b) – Reaction rate as a function of concentration under constant conditions
 – Measurement of the activation energy
 – Achievable yield per unit time and reaction space (space–time yield)

Exercise 1.5

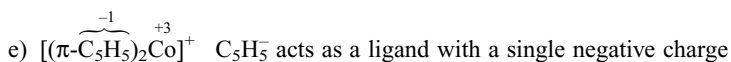
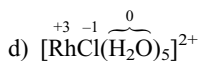
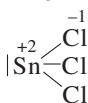
| | Homogeneous catalysis | Heterogeneous catalysis |
|------------------------------|-----------------------|---------------------------------------|
| Activation of H ₂ | oxidative addition | dissociative chemisorption |
| Activation of olefin | π complex formation | π complex formation (surface complex) |

Chapter 2**Exercise 2.1**

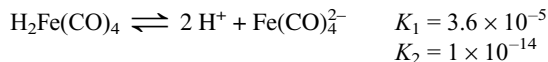
In metal carbonyl nitrosyls, the NO ligand is present as the nitrosyl cation NO⁺



SnCl₃⁻ is an anionic π complex ligand with a single negative charge



- f) $\overset{+1}{\text{H}_2}\overset{-2}{\text{Fe}}\overset{0}{\text{(CO)}_4}$ iron carbonyl dihydride is a strong acid and therefore a hydric compound:



The metal center has a formal negative oxidation state

- g) $[\overset{-0.5}{\text{Ni}}_4\overset{0}{\text{(CO)}_9}]^{2-}$

- h) $\overset{0}{\text{Fe}}\overset{0}{\text{(CO)}_3}\overset{0}{\text{(SbCl}_3)_2}$ | SbCl_3 is a neutral π -acidic ligand

- i) $\overset{+0.5}{\text{O}_2}\overset{+5}{\text{Pt}}\overset{-1}{\text{F}_6}$ The $[\text{PtF}_6]^-$ ion stabilizes the dioxygenyl cation

- j) $\overset{-1}{\text{H}}\overset{+1}{\text{Rh}}\overset{0}{\text{(CO)}}\overset{0}{\text{(PPh}_3)_3}$ Hydrido compound with neutral π -acidic ligands

Exercise 2.2

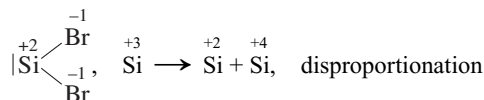
- a) $\text{Pt}^{2+} \rightarrow \text{Pt}^{4+}$, oxidative addition of HCl.
- b) α -Elimination, permethyltungsten gives a carbene structure.
- c) $\text{Co}^{3+} \rightarrow \text{Co}^+$, neutral trimethylphosphite ligands, reductive elimination of H_2 .
- d) Redox reaction:
- $$[(\pi\text{-C}_5\text{H}_5)\overset{-1}{\text{W}}\overset{0}{\text{(CO)}_3}] \overset{+1}{\text{Na}} + \overset{+1}{\text{C}}\overset{-1}{\text{H}_3}\text{I} \rightarrow (\pi\text{-C}_5\text{H}_5)\overset{-1}{\text{W}}\overset{+2}{\text{(CO)}_3}\overset{0}{\text{C}}\overset{-1}{\text{H}_3} + \text{NaI}$$
- e) $\text{Ir}^+ \rightarrow \text{Ir}^{3+}$, variant of oxidative addition (addition of oxonium salts).
- f) Mn retains the oxidation state +1, formation of an olefin π complex with displacement of a CO ligand (coordination number remains unchanged).
- g) $\text{Mo}^0 \rightarrow \text{Mo}^{2+}$, the π -allyl group acts as a ligand with a single negative charge. A π -olefin complex is converted into a π -allyl complex; special case of an oxidative addition reaction.
- h) The hydridorhenium compound acts as a metal base and forms a Lewis acid/Lewis base complex with BF_3 .

Exercise 2.3

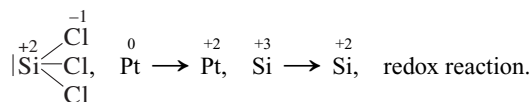
- a) $\overset{+2}{\text{Co}} \rightarrow \overset{0}{\text{Co}}, \overset{0}{\text{H}} \rightarrow \overset{+1}{\text{H}}$, redox reaction.
- b) $\overset{-2}{\text{Fe}}(\overset{0}{\text{CO}})_2(\overset{+1}{\text{NO}})_2 \rightarrow [\overset{-1}{\text{Fe}}(\overset{-1}{\text{NO}})_2]_2, \overset{-2}{\text{Fe}} \rightarrow \overset{-1}{\text{Fe}}, \overset{0}{\text{I}} \rightarrow \overset{-1}{\text{I}}$, redox reaction.
- c) $\overset{-1}{\text{CH}_3}\overset{+2}{\text{Pt}}(\overset{-1}{\text{PPh}_3})_2, \overset{0}{\text{Pt}} \rightarrow \overset{+2}{\text{Pt}}$ oxidative addition of an alkyl halide to a d^{10} platinum complex with simultaneous loss of a PPh_3 ligand.
- d) $[\overset{+1}{\text{Mn}}(\text{CO})_6]^+ [\overset{+3}{\text{AlCl}_4}]^-$ ligand substitution; oxidation states remain unchanged. Removal of chloride ligands by the chloride acceptor AlCl_3 . CO enters the resulting empty coordination site under pressure to give salts of the hexacarbonyl cation.
- e) Platinum retains the oxidation state +2, $\overset{-2}{\text{N}}(\text{in } \text{N}_2\text{H}_4) \rightarrow \overset{0}{\text{N}} + \overset{-3}{\text{N}}$, disproportionation.

Exercise 2.4

- a) $\overset{0}{\text{W}}(\overset{0}{\text{CO}})_6 + \overset{+3}{\text{Si}}\overset{-1}{\text{Br}}_6 \rightarrow \overset{0}{\text{W}}(\overset{0}{\text{CO}})_5\overset{0}{\text{SiBr}}_2 + \overset{+4}{\text{Si}}\overset{-1}{\text{Br}}_4 + \text{CO}$
 In complexes the neutral SiBr_2 group has a silene structure:



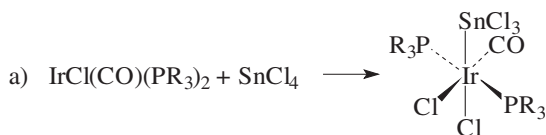
- b) $\overset{0}{\text{Pt}}(\overset{0}{\text{PPh}_3})_4 + \overset{+3}{\text{Si}}\overset{-1}{\text{Cl}}_6 \rightarrow \overset{+2}{\text{Pt}}(\overset{0}{\text{PPh}_3})_2(\overset{-1}{\text{SiCl}_3})_2 + 2 \text{PPh}_3$
 The SiCl_3 group acts as an anionic complex ligand



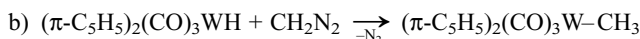
- c) $\overset{0}{\text{Fe}} \rightarrow \overset{0}{\text{Fe}}$, nucleophilic substitution of a CO ligand.

Exercise 2.5

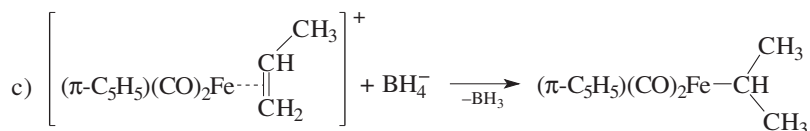
- a) Rh retains the oxidation state +3; insertion of ethylene into a transition metal-hydride bond with formation of a σ -alkyl complex.
- b) Rh retains the oxidation state +1; formation of a π -olefin complex and simultaneous displacement of a PPh_3 ligand.

Exercise 2.6

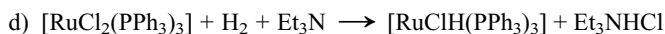
Oxidative addition of a metal halide to an Ir complex; $d^8 \longrightarrow d^6$, $\text{Ir}^{+1} \longrightarrow \text{Ir}^{+3}$; SnCl_4 is formally cleaved into the two anionic groups Cl^- and SnCl_3^- .



Insertion of carbene CH_2 (from diazomethane) into a metal–hydride bond gives a methyl complex.



Nucleophilic attack of hydride on a cationic olefin complex gives a σ -alkyl complex. Fe retains the oxidation state +2.



Ru retains the oxidation state +2; heterolytic addition of H_2 ; the tertiary amine is a strong base that traps the protons and thus supports the reaction.

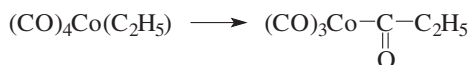
Exercise 2.7

- Oxidative addition: addition of small covalent molecules to a transition metal in a low oxidation state with an increase of the oxidation state of the central atom by two units (Eq. 2-31)
- Requirement: coordinatively unsaturated compounds
- Reverse: reductive elimination

Exercise 2.8

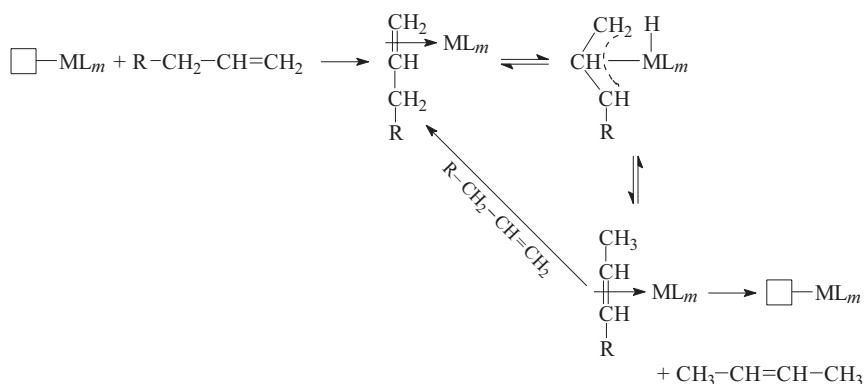
Insertion of a molecule in a transition metal–X bond ($X = \text{H}, \text{C}, \text{N}, \text{O}, \text{Cl}, \text{metal}$) without changing the formal oxidation state of the metal (Eq. 2-55).

Example: CO insertion into a cobalt carbonyl complex to give an acyl complex.



Exercise 2.9

Formation of an ethylene π complex is followed by an insertion reaction to give the alkyl complex $[\text{CH}_3\text{CH}_2\text{Pt}(\text{SnCl}_3)(\text{CO})(\text{PPh}_3)]$.

Exercise 2.10

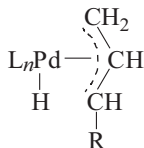
Complexation of the alkene is followed by an H abstraction to give a labile π -allyl hydride and then a rearrangement with allyl insertion into the M–H bond.

Exercise 2.11

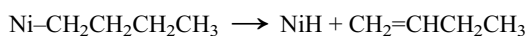
- Electrons flow from the metal into the antibonding σ orbital of hydrogen, weakening the bond. Two *cis* M–H bonds can be formed by oxidative addition if two vacant coordination sites are present on the metal center.
- Heterolysis of H_2 by removal of H^+ in the presence of strong bases.

Exercise 2.12

β -Hydride elimination with formation of a π -allyl complex:

**Exercise 2.13**

β -Hydride elimination takes place:

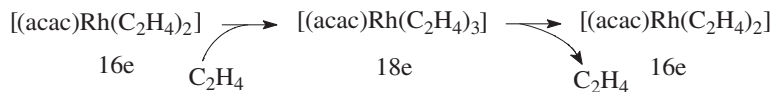


Exercise 2.14

The addition of PPh_3 lowers the equilibrium concentration of $[\text{RhCl}(\text{PPh}_3)_2(\text{solvent})]$.

Exercise 2.15

The *acac* complex can react by an associative mechanism, but this route is blocked for the 18-electron complex $[\text{CpRh}(\text{C}_2\text{H}_4)]$.

**Exercise 2.16**

- a) A $\overset{+1}{\text{Rh}}$ 16 e
 B $\overset{+1}{\text{Rh}}$ 16 e
 C $\overset{+3}{\text{Rh}}$ 18 e

b) Only complex C is coordinatively saturated.

Exercise 2.17

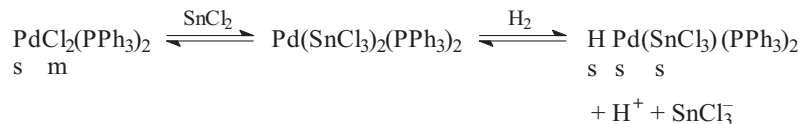
- a) Oxidative addition of H_2 to a square-planar Rh^{I} complex, $d^8 \rightarrow d^6$, formation of an octahedral Rh^{III} dihydrido complex.
 b) Dissociation of a phosphine ligand gives an empty coordination site on the transition metal Rh^{3+} .
 c) Formation of a π complex with ethylene, Rh^{3+} .
 d) *cis*-Insertion reaction of the ethylene ligand into the rhodium–hydride bond with formation of a σ -alkyl complex, Rh^{3+} .
 e) Irreversible reductive elimination of ethane, $\text{Rh}^{3+} \rightarrow \text{Rh}^{1+}$.
 f) A phosphine ligand coordinates to the coordinatively unsaturated Rh^{I} complex.

Exercise 2.18

In the complexes $[\text{PtX}_4]^{2-}$, Pt^{2+} acts as a soft acid according to the HSAB concept. The ligands X^- become increasingly soft in the given sequence, and the combination soft/soft gives more stable compounds.

Exercise 2.19

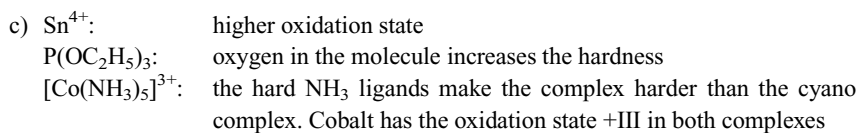
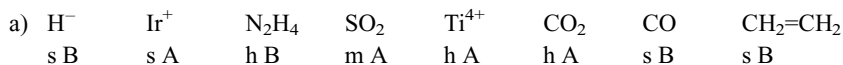
The cocatalyst SnCl_2 supports the formation of hydrides, and the SnCl_3^- ligands inhibit the reduction of Pd^{II} to the metal. The symbiosis of the two very soft ligands H^- and SnCl_3^- leads to highly active, stable catalysts:



(s = soft, m = medium hard)

Exercise 2.20

Bases containing the elements P, As, Sb, Se, and Te are soft compounds according to the HSAB concept and therefore form stable complexes with the soft transition metals and thus deactivate the catalysts. The hard oxygen and nitrogen bases hardly react with the transition metals due to the hard/soft dissymmetry.

Exercise 2.21**Exercise 2.22**

- a) $[\text{Ni}(\text{CO})_4]$: terminal CO groups in a neutral complex
 $[\text{Mn}(\text{CO})_6]^+$: in metal carbonyl cations, the positive charge on the metal center increases the CO frequency
 $[\text{V}(\text{CO})_6]^-$: in metal carbonyl anions, the CO ligand has to accept more negative charge from the metal, and the CO bands are therefore at lower wavenumbers than in neutral complexes
- b) Replacing the phenyl groups by electronegative chloro groups, which are capable of backbonding, increases the CO stretching frequency

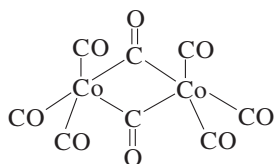
Exercise 2.23

The CO stretching frequency is an indication of the metal basicity of carbonyl complexes. It increases with decreasing electron density on the metal, i. e., when the metal acts as base.

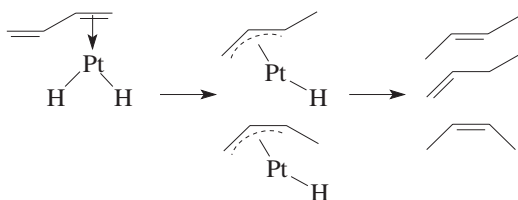
Exercise 2.24

A) Metal–metal bond with terminal CO ligands $(\text{CO})_4\text{Co}-\text{Co}(\text{CO})_4$

B) Bridging CO ligands:

**Chapter 3****Exercise 3.1**

H addition to the conjugated diene gives a π -allyl complex, via which the subsequent isomerization/hydrogenation of the diene takes place:

**Exercise 3.2**

Oxo synthesis converts 1-hexene to heptanal and 2-methylhexanal, which are separated by distillation.

Exercise 3.3

- 1) Wacker–Hoechst process: oxidation of ethylene to acetaldehyde with Pd/Cu catalysts followed by oxidation to acetic acid.
- 2) Methanol carbonylation with rhodium iodide catalysts gives acetic acid directly.

Exercise 3.4

- 1) Oxidative addition of HCl to an Rh^I complex gives the active hydrido rhodium(III) catalyst **A**.
- 2) Coordination of butadiene to the catalyst followed by insertion of the diene into the Rh–H bond to give the *syn*- π -crotyl complex **B**.
- 3) Coordination of ethylene and subsequent insertion into the terminal Rh–C bond to the precursor **C** of the desired diene.
- 4) Coordination of butadiene to complex **D**, elimination of *trans*-1,4-hexadiene, and regeneration of the π -allyl complex **B**.

Exercise 3.5

The metal ion is alkylated, and ethylene is activated by coordination to the transition metal. Since the metal is present in a relatively high oxidation state, nucleophilic attack of the alkyl group on the neighboring alkene is favored, and a *cis* insertion reaction occurs. This process continues until chain termination occurs.

Exercise 3.6

Many active centers with different structures are present on the surfaces of solids; therefore, the selectivity is low. In homogeneous catalysis there is only one active species, and the ligands can readily be modified.

Exercise 3.7

Enantioselective syntheses are carried out with the help of chiral auxiliaries that are not incorporated in the target molecule but are either lost or recycled. The most attractive variant of this approach is of course enantioselective chemical catalysis, where the expensive chiral auxiliary is used in catalytic amounts.

Exercise 3.8

Enantiomeric excess e.e. is the surplus of one enantiomer (*R* or *S*) over the other in a mixture of the racemate (*R* + *S*):

$$\%e.e. = \frac{R - S}{R + S} \times 100 = [\%R - \%S] = \text{optical yield}$$

Exercise 3.9

They are transition metal complexes, often of rhodium or ruthenium.

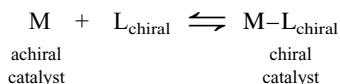
1. The transition metal binds a chiral ligand to give a chiral catalyst.
2. The catalyst simultaneously binds H₂ and the substrate.
3. The hydrogen can be added in two ways to the double bond in the substrate to give different enantiomers.
4. The chiral product is released.

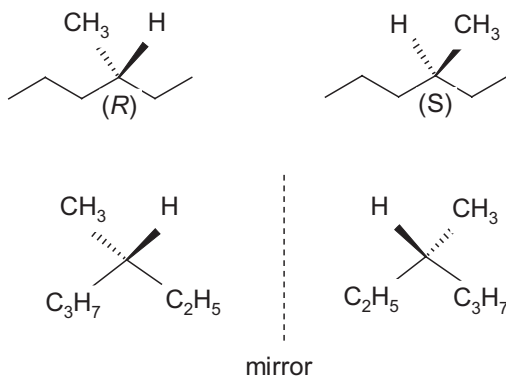
Exercise 3.10

The biological activity of two enantiomers can differ considerably. The desired biological activity is usually associated with only one of the two stereoisomers of a chiral compound.

Exercise 3.11

An important prerequisite for high enantioselectivity is that coordination of a chiral ligand to the metal ion results in a substantial rate acceleration. Thus, if the metal–chiral ligand complex rapidly exchanges its ligands in solution, then high enantioselectivities will be observed only when M–L is a much more active catalyst than M:



Exercise 3.12**Exercise 3.13**

The table shows how the catalyst was developed over time. The TON here is defined as the number of moles of product produced by 1 mole of catalyst. Because of the expense of the catalyst the TON should be more than 50 000.

| Change made | TON |
|--|---------|
| Initial catalyst | 100 |
| Substrate treated | 1000 |
| Removal of impurity | 8000 |
| Altered catalyst, 2 moles of BINAP bound to the Rh, can be re-used with 10% loss | 80 000 |
| Recovery of the Rh and BINAP from the reaction mixture with only 2.5% loss | 400 000 |

The efficiency now compares well with many enzyme-catalyzed processes.

Chapter 4

Exercise 4.1

| | Enzyme catalysis | Homogeneous/ heterogeneous catalysis |
|-------------------------------------|---|---|
| Activity | TOF very high | much lower |
| Selectivity | very high enantio- and regioselectivity | generally lower |
| Stability | stable only under mild conditions | much higher |
| Sensitivity to reaction environment | high sensitivity (pH, solvent) | minute |
| Cost | high | lower |

Exercise 4.2

| Immobilized enzymes | Whole cells |
|-------------------------|------------------------|
| Heterogeneous catalysis | multi-step reactions |
| One-step reactions | no cofactor problems |
| Simple product recovery | long catalyst lifetime |
| Enzyme engineering | metabolic engineering |

Exercise 4.3

The interpretation follows from the limiting case of Equation 4-8. Consider the limiting case of a high reactant concentration which is so high that the catalytic sites are saturated and $[S] \gg K_M$. Then, the rate equation reduces to $r_{\max} = k_{\text{cat}}[E]_{\text{tot}}$ and k_{cat} is recognized as a first-order rate constant. If the rate were written per enzyme molecule rather than per unit volume, then the reaction would be of zero order, and k_{cat} would be the rate at saturation (the maximum number of reactant molecules converted per catalytic site per unit time); this is the definition of the turnover frequency.

Exercise 4.4

To write the equation in a more familiar form, numerator and denominator are divided by K_M , and $1/K_M$ is defined as K_R :

$$r = \frac{k_{\text{cat}} K_R [S][E]_{\text{tot}}}{1 + K_R [S]}$$

This equation now has the form of a Langmuir–Hinshelwood equation, except that the rate is shown to be proportional to the concentration of enzyme. If the rate were written per enzyme molecule, the form would be identical to the Langmuir–Hinshelwood form, with k_{cat} equal to the rate constant and $K_R (= 1/K_M)$ equal to the equilibrium constant for the binding of the reactant to the enzyme. The sequence of steps is then



where ES is the reactant–enzyme complex and P is the product, and the second step is rate determining. K_M is identified as the equilibrium constant for dissociation of the reactant–enzyme complex.

It is no surprise that the Langmuir–Hinshelwood and Michaelis–Menten equations are equivalent; the assumptions underlying them are equivalent. Each is based on the assumption that reactant first bonds to uniform catalytic sites (which can be saturated) and then reacts.

Exercise 4.5

Cofactors may assist with catalysis. These are small organic molecules which can interact with the substrate. Sometimes bound metal atoms play either a structural or a catalytic role.

Exercise 4.6

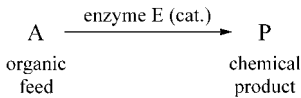
The key point here is that it is the difference in energy between the ES complex and the transition state (the activation energy for the forward reaction) that counts. Tight binding of a substrate corresponds to an ES complex that is very stable (low energy). That makes it harder to get from there up to the transition state, so the activation energy is effectively increased. That slows down the reaction. Tight binding of the transition state, on the other hand, makes it more stable (lower energy) and so it is easier to get there starting from the ES complex. So, the activation energy is effectively decreased and that increases the rate of the reaction.

Exercise 4.7

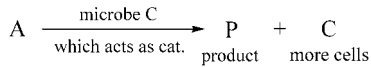
In competitive inhibition, an inhibitor is adsorbed on the same type of site as the substrate. The resulting inhibitor–enzyme complex is inactive. In uncompetitive inhibition the inhibitor attaches itself to the enzyme–substrate complex, rendering it inactive.

Exercise 4.8

Enzyme fermentations can be represented by



Microbial fermentation can be represented by



The key distinction between these two types of fermentation is that in enzyme fermentation the catalytic agent, the enzyme, does not reproduce itself, but acts as an ordinary catalyst, while in microbial fermentation the catalytic agent, the cell or microbe, reproduces itself. Within the cells it is the enzyme which catalyzes the reaction, just as in enzyme fermentation; however, in reproducing itself the cell manufactures its own enzyme.

Chapter 5**Exercise 5.1**

Equation (5-7) is transformed into a linear equation.

$$\theta_A = \frac{K_A p_A}{1 + K_A p_A} \quad \text{and} \quad \theta_A = \frac{V}{V_\infty}$$

V_∞ = volume at complete coverage

$$\frac{V}{V_\infty} = \frac{K_A p_A}{1 + K_A p_A}$$

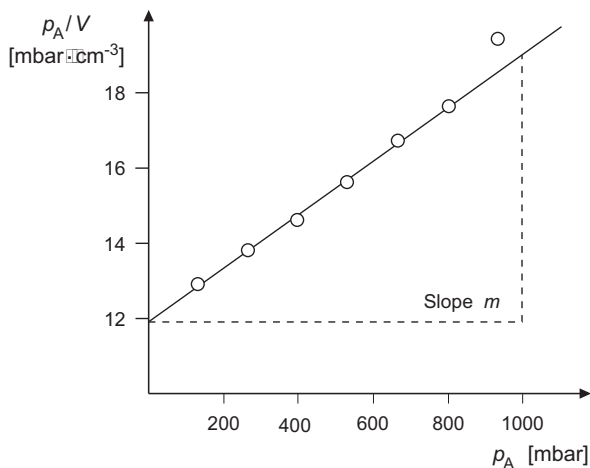
rearrangement gives

$$\frac{1}{V_\infty K_A} + \frac{p_A}{V_\infty} = \frac{p_A}{V}$$

Thus, plotting p_A/V against p_A gives a straight line with slope $1/V_\infty$ and an intersection with the axis of $1/K_A V_\infty$. The following values can be calculated from the experimental measurements:

| | | | | | | | |
|--------------|------|------|------|------|------|------|------|
| p_A (mbar) | 133 | 267 | 400 | 533 | 667 | 800 | 933 |
| p_A/V | 12.9 | 13.8 | 14.6 | 15.6 | 16.7 | 17.6 | 19.4 |

The calculated values are displayed in the following figure. At high loadings, a straight line is no longer obtained.



Langmuir isotherm for Exercise 5.1

$$\text{Slope } m = \frac{18.95 - 11.9}{1000} = 0.0071$$

$$V_\infty = 1/m = 141.8 \text{ cm}^3$$

At $p = 0$ we obtain for the ordinate intersection

$$\frac{p_A}{V} = 11.9$$

$$\frac{1}{V_\infty K_A} = 11.9$$

$$K_A = \frac{1}{141.8 \times 11.9} = 5.9 \times 10^{-4} \text{ mbar}^{-1}$$

Exercise 5.2

According to Eq. 5-8

$$-\frac{dp_A}{dt} = k \theta_A = \frac{k K_A p_A}{1 + K_A p_A} \quad p_A = \text{partial pressure of phosphine}$$

For $K_A p_A \ll 1$

$$-\frac{dp_A}{dt} = k K_A p_A$$

and the reaction is thus first order.

For $K_A p_A \gg 1$ in contrast

$$-\frac{dp_A}{dt} = k$$

i. e., the reaction is zero order.

Exercise 5.3

a) Eley–Rideal mechanism: only one partner (hydrogen) is adsorbed and reacts with the other starting material (CO_2) from the gas phase.

$$\text{b) } r_{\text{eff}} = \frac{\text{kinetic term} \times \text{driving force}}{(\text{chemisorption term})^n} \quad (5-16)$$

Exercise 5.4

The kinetic expression

$$r = \frac{k K_{\text{IB}} c_{\text{IB}}^2}{1 + K_{\text{IB}} c_{\text{IB}}}$$

describes the findings in the simplest form.

Adsorbed isobutene forms a solvated carbenium ion, which reacts with a molecule from the gas phase. This Eley–Rideal mechanism is often observed for solid acids.

Exercise 5.5

The two components compete for the catalytically active sites. The nitrogen compounds are more strongly adsorbed than the sulfur compounds and displace them from the active surface sites. This explains the low reaction rate of the sulfur compounds in the presence of nitrogen compounds.

The higher reactivity of the nitrogen compounds in the mixture indicates that they occupy the majority of the catalytic centers and hinder the reaction of the sulfur compounds by blocking the adsorption sites,

The results are indicative of Langmuir adsorption on an ideal surface. If the organo-nitrogen compounds are the only strongly adsorbed species, then as a first approximation the rate of hydrodesulfurization r_{HDS} can be described by the equation

$$r_{\text{HDS}} = \frac{k K_S p_S K_{\text{H}_2} p_{\text{H}_2}}{1 + K_S p_S + K_N p_N} \quad \text{where } K_N p_N \gg (1 + K_S p_S)$$

Exercise 5.6

- 1) Dissociative adsorption of oxygen.
- 2) Eley–Rideal step in which gaseous SO_2 reacts with adsorbed oxygen to give SO_3 .

Exercise 5.7

Chemisorption, surface reaction, desorption.

Exercise 5.8

$$r'_{\text{CH}_4} = N_{\text{CH}_4} D \frac{1}{M_{\text{Ru}}} \cdot \frac{\% \text{ Ru}}{100} \quad (\text{cf. Section 1.2})$$

N is the number of molecules that react at an active surface atom under the given conditions, that is, reacting molecules per atom of catalyst or moles per mole of catalyst. Therefore, for 1 g of catalyst (metal + support), we obtain:

$$r'_{\text{CH}_4} = \frac{0.160 \text{ mol}}{\text{mol Ru s}} \cdot 0.42 \cdot \frac{1 \text{ mol Ru}}{101.1 \text{ g}} \cdot 0.005$$

$$r'_{\text{CH}_4} = 3.32 \times 10^{-6} \text{ mol s}^{-1} \text{ g cat.}^{-1}$$

Exercise 5.9

| | Chemisorption | Physisorption |
|------------------------|---|---|
| Cause | covalent or electrostatic forces, electron transfer | van der Waals forces, no electron transfer |
| Adsorption heat | high $\sim \Delta H_R$ 80–600 kJ/mol usually exothermic | low \sim heat of melting \sim 10 kJ/mol always exothermic |
| Temperature range | generally high | low |
| No. of adsorbed layers | monolayer | multiple layers |

Exercise 5.10

- Dissociative chemisorption of a saturated hydrocarbon, abstraction of H, alkyl complex formation.
- Associative chemisorption through the electron lone pair, double alkyl complex.
- Dissociative chemisorption, H abstraction, π -allyl complex formation.

Exercise 5.11

- Fe: At the process temperature, CO is completely dissociated, and the concentration of CH₂ groups is therefore high. The formation of higher hydrocarbons is favored.
- Ni: CO dissociation is more difficult, so that the concentration of CH₂ is lower. Hydrogenation with formation of methane dominates.
- W, Mo: Poor Fischer–Tropsch catalysts; the metal carbides are probably too stable to readily undergo hydrogenation.
- Pt: platinum group metals are not Fischer–Tropsch catalysts.

Exercise 5.12

Titanium nitride is too stable.

Exercise 5.13

CO is strongly chemisorbed and blocks the sites for hydrogen.

Exercise 5.14

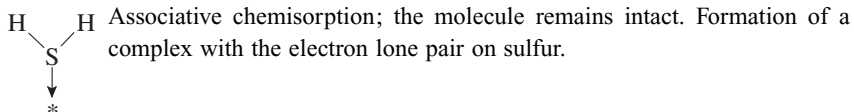
The catalyst is porous; pore diffusion resistance lowers the activation energy by a factor of 2.

Exercise 5.15

There are two different adsorption sites, one of which forms a single metal–CO bond, while at the other, the CO molecule dissociates into the atoms C and O, which are individually adsorbed.

Exercise 5.16

- Lewis acid complex with the base NH_3 .
- Carbonyl complex, linear.
- Carbonyl complex, bridging, two centers.
- Dissociative chemisorption of H_2 .
- Dissociative chemisorption of ethane, formation of a σ -alkyl and a hydride bond.
- Dissociative chemisorption of H_2 on ZnO , heterolytic.
- π -Olefin complex.
- Ethylene as double π -alkyl complex, associatively bound.

Exercise 5.17**Exercise 5.18**

- | | |
|--------------------|---|
| Cube surface | A |
| Octahedron surface | C |
| Prism surface | B |
- Each surface has a particular catalytic activity. The most densely occupied surfaces (especially fcc) are often the most active.
Steps and kinks on the surface have a major influence on the catalytic activity.

Exercise 5.19

- a) (1 1 0) b) (2 3 0) c) (0 1 0)

Exercise 5.20

- Miller indices: position of the crystal/atomic planes in the coordinate system.
- Diagonal (1 1 1) surface is normally of higher activity because it is more densely occupied.

Exercise 5.21

The reaction is structure-insensitive.

Exercise 5.22

To maximize the surface area.

Exercise 5.23

| | | | | | | |
|----|---|-----|----------------|-----|-----|----------|
| Pd | Al ₂ O ₃ | ZnO | Alumosilicates | MgO | CoO | Zeolites |
| – | I, at high temperature <i>n</i> -type semiconductor, A | S | A, I | I | S | A |

Exercise 5.24

- p*-type semiconductor
- Cationic chemisorption: $\text{CO} \rightarrow \text{CO}^+ + \text{e}^-$
- p*-type doping; increased conductivity

Exercise 5.25

| | | | | | |
|-----------------|-------------------|-----------------|------------------|--------------------------------|-----|
| VO ₂ | Cu ₂ O | WO ₃ | MnO ₂ | Nb ₂ O ₅ | CoO |
| p | p | n | n | n | p |

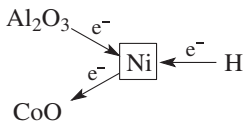
Exercise 5.26

Donor reaction: the donor is SO₂.

Exercise 5.27

Ni on CoO (c) ↑ catalytic activity
 Ni (a)
 Ni on Al₂O₃ (b)

Flow of electrons from the substrate through the metal to the support is most favorable for the donor reaction of the hydrogen (“rectifier effect”).



Exercise 5.28

In the donor reaction $\text{H} \rightarrow \text{H}^+ + \text{e}^-$ electrons are donated to the catalyst.

MnO is a semiconductor which readily takes up electrons. The *p*-type conductivity is enhanced by Li^+ .

Exercise 5.29

The catalyst should function as an electron acceptor or have acidic properties. It should also have a low porosity so that total oxidation of the maleic anhydride is prevented by mass transfer resistance. Vanadium phosphorus oxide complexes in which several V oxidation states are combined are used; mean specific surface area $20 \text{ m}^2/\text{g}$.

Exercise 5.30

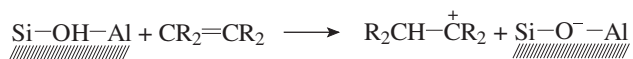
- Al_2O_3 has OH groups on the surface that act as Brønsted acid centers and has Lewis acid centers as electron acceptors (see Fig. 5-32).
- $\text{SiO}_2/\text{Al}_2\text{O}_3 > \text{SiO}_2 \gg \gamma\text{-Al}_2\text{O}_3 > \text{MgAl}_2\text{O}_4 > \text{MgO}$.

Exercise 5.31

An additional proton is necessary for charge compensation when Si^{4+} is replaced by Al^{3+} in the lattice.

Exercise 5.32

Titration with bases; poisoning with N bases such as NH_3 , pyridine, quinoline; IR spectroscopic investigations on catalysts with adsorbed pyridine.

Exercise 5.33

A C=C bond is protonated by a Brønsted acid center on the surface to give a carbocation that initiates the polymerization.

Exercise 5.34

Electronic interactions; reduced support species on the metal surface; phase formation at interfacial surfaces.

Exercise 5.35

Specific surface area, pore volume, pore structure.

Exercise 5.36

SMSI = strong metal–support interaction.

Exercise 5.37

Activity, selectivity, and stability.

Exercise 5.38

Acidic cracking centers are neutralized by bases; potassium lowers the coking tendency of Al_2O_3 supports.

Exercise 5.39

Decreasing productivity; lower selectivity.

Exercise 5.40

Measurement of the decreasing catalyst activity as a function of time.

Exercise 5.41

Activity losses due to phase changes to oxides with smaller surface area or due to thermal sintering.

Exercise 5.42

Under certain circumstances, formation of highly toxic $[\text{Ni}(\text{CO})_4]$ could occur.

Exercise 5.43

$\text{F} < \text{Cl} < \text{Br} < \text{I}$

Softer halides form stronger bonds with the soft transition metals.

Exercise 5.44

- a) Rapid coking
- b) Continuously

Exercise 5.45

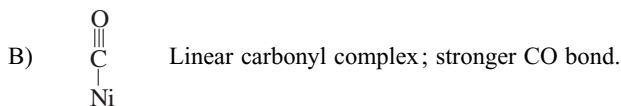
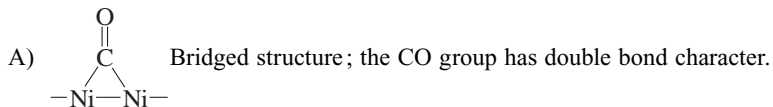
- A) IR reflection spectroscopy
- B) Temperature-controlled desorption
- C) BET method
- D) SIMS
- E) ESCA, ESR
- F) X-ray structure analysis
- G) Scanning electron microscopy

Exercise 5.46

Number of active surface atoms per gram of catalyst. Degree of dispersion.

Exercise 5.47

At 200 °C surface-bound water is released, and Al^{3+} -bound OH groups remain on the surface. These form hydrogen bonds with pyridine (1540 cm^{-1}). Partial dehydration of the OH groups gives O^{2-} and free Al^{3+} , which forms a Lewis acid–base complex with pyridine (1465 cm^{-1}).

Exercise 5.48**Exercise 5.49**

Dissociative adsorption: $\text{CO}_2 \longrightarrow \text{CO} + \frac{1}{2} \text{O}_2$.

Exercise 5.50

The C=C double bond of ethylene is weakened by π complexation to Pd, and the IR frequency is therefore lower.

Exercise 5.51

LEED = low-energy electron diffraction.

A surface method that uses low-energy electrons to provide diffraction patterns for the upper atomic layers. Can detect surface structures and the occupation of the surface by adsorbed molecules (adsorption complexes).

Exercise 5.52

TPR, for integration of the H₂ consumption signal.

Exercise 5.53

TPD: the interaction of probe molecules such as ammonia or pyridine with zeolites can be determined.

Chapter 6**Exercise 6.1**

Active surface area; pore structure; mechanical strength.

Exercise 6.2

- Pore structure and surface of the catalyst can be controlled.
- Catalysts can be tailor-made with respect to mass-transfer effects.
- More economic, since the content of expensive active components is often low.
- The distribution and crystallite size of the active components can generally be varied over a wide range.
- Multiple impregnation is possible.

Exercise 6.3

Activated carbon, silicagel, Al₂O₃

Exercise 6.4

- Nonporous, low surface area supports.
- Porous supports with wide pores: silicates, α -Al₂O₃, SiC, ZrO₂, graphite.

Exercise 6.5

Diffusion-controlled reactions; fast reactions.

Exercise 6.6

- a) Because they have smooth, nonporous surfaces.
- b) Washcoat.

Exercise 6.7

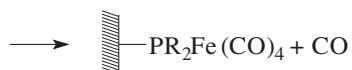
- a) Short transport or diffusion paths; pore structure independent of the support; improved heat transfer in the catalyst layer; low coking.
- b) Generally α -Al₂O₃ spheres; low specific surface area ($< 1 \text{ m}^2/\text{g}$).

Exercise 6.8

In mononuclear complexes, only one metal center is present, and C–C coupling is not possible.

Exercise 6.9

The steric and electronic properties of the coordinated metal atoms or ions can be better controlled than in conventional heterogeneous catalysts.

Exercise 6.10

Bonding of the metal to the phosphine ligand in a ligand-exchange reaction.

Exercise 6.11

Low mechanical stability; poor heat-transfer properties; low thermal stability (150 °C max.).

Exercise 6.12

A solution of an organometallic complex in a high-boiling solvent is applied to a porous inorganic support. The diffusion-controlled reaction takes place in the solvent film.

Chapter 7

Exercise 7.1

- a) Aluminosilicates with ordered crystalline networks of composed interlinked AlO_4^- and SiO_4 tetrahedra and a channel structure containing water molecules and mobile, exchangeable alkali metal ions.
- b) Number and strength of the acid centers; isomorphic substitution; metal doping.

Exercise 7.2

- a) Reactant shape selectivity in the cracking of octanes: the linear alkane fits in the pores and is cleaved. The branched alkane does not enter the pores and therefore does not react. A mixture of various alkanes and alkenes is formed.
- b) Product shape selectivity in the alkylation of toluene with ethylene: Only the slim *p*-ethyltoluene molecule can escape from the pores. The *ortho* isomer is too bulky and remains in the pores.

Exercise 7.3

- Wide range of variability
- Shape selectivity
- High thermal stability
- Strongly acidic zeolites
- Incorporation of many metals
- Bifunctionality (acid/metal)

Exercise 7.4

The zeolite catalyst leads to a shape-selective hydrogenation, in which the strongly branched starting material does not fit in the pores and is hardly hydrogenated. There is no steric hindrance with the conventional catalyst.

Exercise 7.5

Shape selectivity can occur when the starting materials, products, or transition state of a reaction have dimensions similar to those of the zeolite pores.

Exercise 7.6

Shape-selective reaction of methanol with ZSM-5 catalysts. Hydrocarbons that exceed the ideal size for gasoline are retained in the zeolite pores until they have been catalytically shortened enough to escape. The product spectrum of this process is far more favorable than that of the Fischer–Tropsch process.

Exercise 7.7

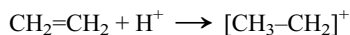
Exchange of the alkali metal ions in the channels with ammonium ions followed by heating to 500–600 °C, which leads to cleavage of ammonia and leaves behind protons.

Exercise 7.8

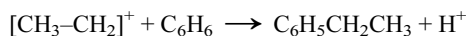
With narrow-pore acidic zeolites in the H form. The trimethylamine fraction can be lowered to less than 1 % as a result of shape selectivity.

Exercise 7.9

a) The acid form of ZSM-5 is sufficiently strong to form carbocations:



The carbocation can attack benzene. Deprotonation of the product then gives ethylbenzene:



b) No, because there are no acid centers.

Exercise 7.10

The rate equation corresponds to the Eley–Rideal mechanism. The equation can be written as

$$r = k\theta_{\text{O}}c_{\text{T}}$$

where θ_{O} is the degree of coverage of the active centers by the olefin. The equation thus applies to the rate-determining step of the reaction of the adsorbed carbenium ion with toluene in the pore volume of the zeolite.

Exercise 7.11

AlPO_4 molecular sieves do not have ion-exchange properties.

Exercise 7.12

By dealumination with reagents such as SiCl_4 : Al is removed from the lattice as AlCl_3 ; hydrothermal treatment with steam at 600–900 °C.

Chapter 8**Exercise 8.1**

- | | | | |
|---------|---------|------|----------|
| 1. G | 4. J | 7. I | 10. C, D |
| 2. G, H | 5. K | 8. A | 11. A |
| 3. E | 6. B, L | 9. D | 12. F |

Exercise 8.2

C (B)

Exercise 8.3

- Liquid phase: low temperature, high concentration of starting materials, higher conversion, better heat transfer
- Disadvantages: higher pressure, slower mass transfer
- Gas phase: mild, fewer side products, but higher energy demand

Exercise 8.4

- Hydroformylation of propene to butanals (oxo synthesis); distillative separation.
- Aldol condensation of *n*-butanal to 2-ethylhexenal.
- Hydrogenation of the unsaturated aldehyde to 2-ethylhexanol.

Exercise 8.5

- a)
 - A. Dissociative chemisorption of H_2 ; π -olefin complex of propenol.
 - B. Hydrogenation to the σ -alkyl complex.
 - C. Complete reduction of the alkyl complex; desorption of the alcohol from the catalyst surface.
 - D. Abstraction of H from the OH group of the alkyl complex; rearrangement.
 - E. π -Complexation of the aldehyde; hydride complex.
 - F. Desorption of the aldehyde; H remains dissociatively bound on the surface.
- b) Isomerization of an α,β -unsaturated alcohol (enol) to an aldehyde.

Exercise 8.6

- CO insertion into the metal hydride complex **A** to give the formyl complex **B**.
- Hydrogenation of the formyl complex to the σ -alkyl complex **C**.
- CO insertion to give the acyl complex **D**.
- Hydrogenation of the acyl complex and water cleavage to give the ethyl complex **E**.
- CO insertion reaction followed by reduction; chain growth; longer chain alkyl complex **F**.
- Hydrogenative cleavage of the alkyl complex **F** to give the alkane **G** and the metal hydride complex **A**.

Exercise 8.7

1. Dissociative chemisorption of propene; π -allyl complex of Mo.
2. Nucleophilic attack by Mo lattice oxygen; insertion to give the σ -allyl complex.
3. Elimination (desorption) of acrolein; reduction to the dihydroxy complex.
4. Reoxidation by take up of oxygen from the gas phase; dehydration; formation of oxide ions; diffusion to the vacant lattice sites.

Exercise 8.8

1. Dissociative chemisorption of the aldehyde; aldehyde oxygen atom migrates to the vacant anion site; reduction of the metal; formation of OH^- by H abstraction from the aldehyde.
2. Intermediate state; coupling of the aldehyde carbon to two lattice oxide ions.
3. Oxidation of the intermediate state with two lattice oxygen atoms and take up of a hydrogen atom from lattice hydroxide to give the carboxylic acid; further reduction of the metal; formation of two vacant anion sites in the lattice.
4. Reoxidation of the lattice by atmospheric oxygen; the metal provides electrons for the formation of oxide anions, which are incorporated in the lattice.

Exercise 8.9

Fine chemicals are generally complex, multifunctional molecules, which means that chemo-, regio-, and stereoselectivity are important considerations. Such complex molecules usually have high boiling points and limited thermal stability, thus necessitating reaction in the liquid phase at moderate temperatures. Furthermore, processing tends to be multipurpose and batch-wise. This means that not only raw materials costs but also simplicity of operation and multipurpose character of the installations are important economic considerations.

Exercise 8.10

Chemoselectivity: competition between different functional groups in a molecule.

Regioselectivity: e. g. *ortho* versus *para* substitution in aromatic rings.

Stereoselectivity: enantioselectivity and diastereoselectivity.

Exercise 8.11

Oxidation: instead of KMnO_4 , MnO_2 , $\text{K}_2\text{CrO}_4 - \text{O}_2$, H_2O_2 , organic peroxides, e. g. *tert*-butyl hydroperoxide (often catalyzed reactions).

Hydrogenation: instead of $\text{Fe}/\text{HCl} - \text{H}_2 + \text{catalyst}$.

Acid–base catalysis: instead of AlCl_3 , H_2SO_4 – acidic zeolites such as zeolite H-beta.

Exercise 8.12

Starting from *p*-isobutylacetophenone, the classical route involves a further five steps with substantial inorganic salt formation, while the alternative requires only two steps, one of which is a catalytic hydrogenation. The other step involves catalytic carbonylation. Both of these catalytic steps are 100% atom selective, and no waste is produced.

Chapter 9**Exercise 9.1**

Electrode reactions can be accelerated by structural or chemical modification of the electrode surface and by additives to the electrolyte.

Exercise 9.2

In addition to the total concentration of the adsorbed atoms, the individual properties of the electrode surface, its local crystallographic orientation, its morphology and the presence and concentrations of defects in the lattice structure also take effect.

Exercise 9.3

- Lower kinetic barrier for splitting of hydrogen molecules
- Mild reaction conditions (temperature, pressure)
- Control of the amount of chemisorbed hydrogen by the current density or potential
- Sometimes the adsorption of poisons can be diminished owing to the cathodic potential to the catalyst.

Exercise 9.4

Low-overpotential electrodes such as Pt, Ni, C, Fe.

Exercise 9.5

This is an example of an indirect electroorganic synthesis process with the aid of Ce^{4+} ions as an electric charge carrier. The resulting Ce^{3+} ions must be electrochemically regenerated in a separate electrochemical reactor.

Exercise 9.6

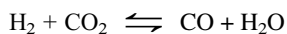
The cathodic reaction. The reduction of oxygen is a complex electrochemical process with two parallel pathways (direct four-electron pathway and the peroxide pathway).

Exercise 9.7

- CO is formed during the oxidation of methanol; CO can block the surface of the catalyst and hinder any further reaction
- Methanol crossover through the polymer electrolyte to the cathode causes the formation of a mixed potential
- Generally lower electrochemical activity.

Exercise 9.8

A reverse shift reaction parallel to the reactions already mentioned takes place:



Exercise 9.9

At low temperature the PEMFC can be contaminated by CO, which acts as a severe catalyst poison. The SOFC as well as the MCFC are high-temperature fuel cells. Under these conditions CO cannot be adsorbed at the surface; it can even be used as fuel.

Chapter 10**Exercise 10.1**

The three-way catalyst enables the removal of the three pollutants CO, NO_x, and hydrocarbons.

Exercise 10.2

Pt, Pd for the oxidation of CO and hydrocarbons.
Rh, Pd for the reduction of NO.

Exercise 10.3

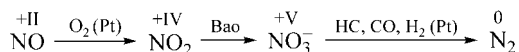
Exhaust gases are a complex mixture of many compounds, but three components predominate:

- CO from partially reacted hydrocarbons
- Volatile organic compounds (VOCs) from partially reacted hydrocarbons
- Oxides of nitrogen (NO_x) from reactions between atmospheric nitrogen and oxygen.

Exercise 10.4

Under lean-burn conditions the fuel efficiency is substantially higher due to the excess of oxygen. But the NO_x reduction is extremely difficult.

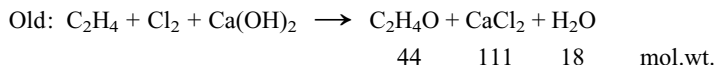
The NO_x can be removed with the NO_x storage-reduction (NSR) catalyst, based on a two-step process. In this process the engine switches periodically between a long lean-burn stage and a very short fuel-rich stage. The NSR catalyst combines the oxidation activity of Pt with an NO_x storage compound based on BaO.

Exercise 10.5**Exercise 10.6**

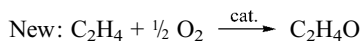
- a) SCR process for denitrification of flue gases; important environmental process for power stations.
- b) TiO_2
 WO_3/MoO_3
 V_2O_5
 $300\text{--}400^\circ\text{C}$

Exercise 10.7

GHSV and pressure drop.

Exercise 10.8

$$\text{atom efficiency} = \frac{44 \times 100}{173} = 25\%$$



$$\text{atom efficiency} = 100\%$$

Exercise 10.9

The E factor describes the amount of waste generated per kg of product. Fine chemicals and specialties have the highest E factors.

Exercise 10.10

- Increased selectivity and reactivity
- High *para* selectivity due to shape selectivity of the zeolite
- Azeotropic removal of water formed during the reaction regenerates the active acid sites on the catalyst, permitting re-use of the solid acid catalyst
- High space time yields
- Simple separation of catalyst from reaction mixture.

Exercise 10.11

Ionic liquids offer:

- Fewer regulatory concerns, reduced worker exposure to vapors, safer to handle
- Low replenishment and waste disposal cost
- Lower cost of product isolation
- Safer operation (nonvolatile/nonflammable)
- Environmental friendliness
- Controlled reaction selectivity
- Ease of product separation.

Chapter 11**Exercise 11.1**

The quantum yields for hydrogen evolution are very low (typically 2–3%), because sunlight contains little UV.

Exercise 11.2

- How does water adsorb on the catalyst?
- How does water dissociate?
- Is the use of co-catalyst necessary?
- How does this co-catalyst work?
- Where are the electrons and holes generated?
- How does the electron flow proceed from catalyst to reagents?

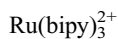
Exercise 11.3

- a) H₂ catalyst: Pt
O₂ catalyst: RuO₂
- b) The co-catalysts
- Act as traps for photogenerated electrons
 - Reduce the overall probability of electron–hole recombination
 - Increase the overall efficiency of the photosystem.

Exercise 11.4

Acceptors: Fe³⁺, Ag⁺, [PtCl₆]²⁻

Donors: EDTA, methanol, glucose, isopropanol, triethanolamine

Exercise 11.5**Exercise 11.6**

The high oxidation potential of TiO_2 (3.0 V) is even higher than that of conventional oxidizing agents such as chlorine and ozone.

Chapter 12**Exercise 12.1**

The phase-transfer agent is Q^+ , which is a highly lipophilic cation (one having a strong affinity for an organic solvent), such as tetraalkylammonium or a tetraalkylphosphonium ion, or a complexing agent like a crown ether.

Exercise 12.2

- High productivity
- Enhanced environmental performance
- Improved safety
- Better quality
- Economic advantage in cost savings of the starting materials
- Reduction of other manufacturing costs (work-up unit operations).

Exercise 12.3

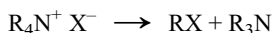
Phase-transfer catalysts have the ability to transfer the anionic forms of metal carbonyls in the organic phase, in which CO is much more soluble than in water. Thus, the hydrolysis of CO to formate and esters to acids can be reduced.

Exercise 12.4

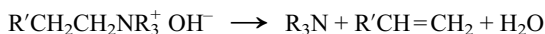
Crown ethers can solubilize organic and inorganic alkali metal salts even in non-polar organic solvents. They form a complex with the cation and thus act as an “organic mask”.

Exercise 12.5

In general, the stability of a phase-transfer catalyst is a function of cation structure, presence of anions, type of solvent, concentration, and temperature. Degradation of catalysts under PTC conditions may occur. For instance, ammonium and phosphonium salts may be subject to decomposition by internal displacement (usually at temperatures of 100–200 °C):



In the presence of strong bases, decomposition by Hofmann degradation can occur:



Relatively cheap polyethylene glycols (of molecular weights 400 and 600) have proved very useful in some cases, because they are stable up to about 200 °C.

Chapter 13**Exercise 13.1**

In the given sequence: f, f, t, f, t.

Exercise 13.2

Reaction time (min) **A**

Temperature (°C) **B**

Catalyst concentration (%) **C**

Experiment

| 30 | | | | 45 | | | |
|------|-----|------|-----|------|-----|------|-----|
| 50 | | 80 | | 50 | | 80 | |
| 0.25 | 0.4 | 0.25 | 0.4 | 0.25 | 0.4 | 0.25 | 0.4 |

(1) c b bc a ac ab abc

Exercise 13.3

a) Effects and interactions:

$$\text{A} = 4.6 \quad \text{B} = 3.6 \quad \text{AB} = -0.6 \quad \text{C} = 2.1 \quad \text{AC} = 2.4 \quad \text{BC} = 0.4 \quad \text{ABC} = -1.4$$

The mean yield of 21.88% is theoretically obtained for an experiment with average experimental conditions:

| | |
|------------------------|--------|
| Reaction time | 25 min |
| Temperature | 60 °C |
| Catalyst concentration | 0.15% |

Effect A means that the yield increases by 4.6% when the reaction time is increased by 5 min, i. e., the yield increases at a rate of 0.92%/min. In the same way, improvements of 0.73 %/°C and 42.6%/ % cat. can be calculated.

b) From Equation (13-14) we obtain

$$\sigma_{\text{Eff}} = \sqrt{1/8} \cdot 4.2 = 1.49$$

$$\text{Test quantity } z = \frac{\text{Effect}}{\sigma_{\text{Eff}}} = \frac{\text{Effect}}{1.49}$$

and therefore:

| Effects | $z = \frac{\text{Effects}}{1.49}$ | $z > c?$ |
|------------|-----------------------------------|----------|
| A = 4.6 | 3.09 | yes |
| B = 3.6 | 2.42 | yes |
| AB = -0.6 | 0.40 | no |
| C = 2.1 | 1.41 | no |
| AC = 2.4 | 1.61 | no |
| BC = 0.4 | 0.27 | no |
| ABC = -1.4 | 0.94 | no |

Result: The yield depends only on the reaction time and temperature, and not on the catalyst quantity, provided it is at least 0.1%.

Exercise 13.4

Result of the Plackett–Burman matrix:

| | A | B | C | D | E (-) | F | G (-) | Yield |
|------------|--------|--------|-------|-------|----------|--------|----------|----------|
| Σ | -0.613 | -0.025 | 0.049 | 0.075 | -0.003 | -0.023 | 0.055 | 3.219/8 |
| $\Sigma/4$ | -0.153 | -0.006 | 0.012 | 0.019 | -0.0008 | -0.006 | 0.014 | = 0.4024 |

From Equation (13-15) we obtain

$$s^2 = \frac{0.0008^2 + 0.014^2}{2} = 9.85 \times 10^{-5}$$

$$\text{Standard deviation } s = \sqrt{s^2} = 0.0097$$

Determination of the significance of the effects by a t -test:

$$\text{Test quantity } t = \frac{\text{Effect}}{\text{Standard deviation } s}$$

We obtain

$$\text{Effect A (temperature)} = -0.153/0.0097 = -15.74$$

$$\text{Effect D (solvent)} = 0.019/0.0097 = 1.93$$

Comparison with the values in the t -test table shows: only effect A is highly significant; D is only significant to 80 % and hence practically unconfirmed. The other effects are meaningless.

Exercise 13.5

Experiment 1 represents the worst corner.

a) From Equation (13-16) we obtain

$$\vec{x}_{n+2} = \frac{2}{2} 114 - \left(1 + \frac{2}{2}\right) 37 \rightarrow x_1 = 40$$

$$\vec{x}_{n+2} = \frac{2}{2} 64.8 - \left(1 + \frac{2}{2}\right) 21 \rightarrow x_2 = 22.8$$

b) From Equation (13-17) we obtain

$$\begin{aligned} \text{for } x_1: \quad \vec{x}_{n+2+1} &= \left(1 + \frac{2}{2}\right) 40 - \left(1 + \frac{2}{2}\right) 39 + 37 \\ &= 80 - 78 + 37 = 39 \end{aligned}$$

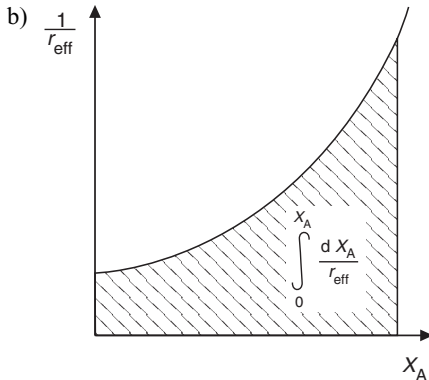
$$\begin{aligned} \text{for } x_2: \quad \vec{x}_{n+2+1} &= \left(1 + \frac{2}{2}\right) 22.8 - \left(1 + \frac{2}{2}\right) 21 + 21 \\ &= 45.6 - 42 + 21 = 24.6 \end{aligned}$$

Coordinates of 5th experiment: $x_1 = 39$, $x_2 = 24.6$.

Chapter 14

Exercise 14.1

a) Catalyst residence time.



c) Ideal tubular reactor.

d) Besides temperature and concentration, r_{eff} also depends on macrokinetic factors (e. g., mass transport).

Exercise 14.2

Constant reaction rate, on average lower than in a tubular reactor, in which the highest reaction rate is reached at the beginning and then declines towards the end of the reactor.

Exercise 14.3

a) From Equation (13-7) we obtain:

$$-r'_A = \frac{\dot{n}_{A,0} - \dot{n}_A}{m_{\text{cat}}} \quad \dot{n} = c \cdot \dot{V}$$

$$-r'_A = \frac{(c_{A,0} - c_A) \dot{V}_0}{m_{\text{cat}}} = \frac{(2 - 0.5) \cdot 1}{3} = 0.50 \text{ mol h}^{-1} \text{ g cat}^{-1}$$

$$-r'_A = k c_A^2$$

$$k = \frac{-r'_A}{c_A^2} = \frac{0.50}{0.5^2} = 2.00 \text{ L}^2 \text{ h}^{-1} \text{ g cat}^{-1} \text{ mol}^{-1}$$

b) From Equation (14-1)

$$\frac{m_{\text{cat}}}{\dot{n}_{A,0}} = \int_0^{X_A} \frac{dX_A}{-r'_A} \quad -r'_A = k c_{A,0}^2 (1 - X_A)^2$$

Introducing the kinetic expression as a function of conversion

$$\frac{m_{\text{cat}}}{\dot{n}_{A,0}} = \int_0^{X_A} \frac{dX_A}{k c_{A,0}^2 (1 - X_A)^2}$$

Rearrangement and integration gives:

$$\frac{m_{\text{cat}} k c_{A,0}^2}{c_{A,0} \dot{V}_0} = \frac{X_A}{1 - X_A}$$

$$m_{\text{cat}} = \frac{X_A \dot{V}_0}{(1 - X_A) k c_{A,0}} = \frac{0.8 \times 1000}{0.2 \times 2.00 \times 1} = 2000 \text{ g} = 2 \text{ kg}$$

c) Equation (14-3) applies; introducing the kinetic equation gives:

$$\frac{m_{\text{cat}}}{\dot{n}_{A,0}} = \frac{X_A}{-r'_A} \quad -r'_A = k c_{A,0}^2 (1 - X_A)^2 \quad \dot{n}_{A,0} = c_{A,0} \dot{V}_0$$

$$\frac{m_{\text{cat}}}{c_{A,0} \dot{V}_0} = \frac{X_A}{k c_{A,0}^2 (1 - X_A)^2}$$

$$m_{\text{cat}} = \frac{X_A \dot{V}_0}{k c_{A,0} (1 - X_A)^2} = \frac{0.8 \times 1000}{2.00 \times 1 \times 0.2^2} = 10\,000 \text{ g} = 10 \text{ kg}$$

For a simple irreversible reaction, the ideal tubular reactor is always advantageous due to freedom from backmixing. Especially at high throughputs, backmixing has a strongly negative effect on the required reaction volume or catalyst mass.

Exercise 14.4

1. The partial pressures in the kinetic equation have to be expressed as functions of the conversion, and this achieved by means of a material balance. After conversion X :

| Substance | n_i | x_i | $p_i = x_i P = x_i \cdot 30$ (bar) |
|---------------|----------|---------------------|------------------------------------|
| T | $1 - X$ | $\frac{1 - X}{11}$ | $p_T = \frac{(1 - X) 30}{11}$ |
| H | $10 - X$ | $\frac{10 - X}{11}$ | $p_H = \frac{(10 - X) 30}{11}$ |
| B | X | $\frac{X}{11}$ | $p_B = \frac{X \cdot 30}{11}$ |
| M | X | $\frac{X}{11}$ | $p_M = \frac{X \cdot 30}{11}$ |
| $\Sigma = 11$ | | | |

2. r is expressed as a function of conversion:

$$r = \frac{k \cdot 0.9 (1 - X) 30 \cdot (10 - X) 30}{11 \cdot 11 \left(1 + 0.9 \frac{(1 - X) 30}{11} + 1.0 \frac{X \cdot 30}{11} \right)}$$

$$\frac{1}{r} = \frac{1 + 2.454 (1 - X) + 2.727 X}{0.00135 (1 - X) (10 - X)}$$

3. The design equation (14-1) applies:

$$\frac{m_{\text{cat}}}{\dot{n}_{A,0}} = \int_0^X \frac{dX}{r} = A$$

By numerical integration using the Simpson rule, we obtain

| X | $1/r$ (kg h kmol ⁻¹) |
|-----|----------------------------------|
| 0 | 255.8 |
| 0.1 | 289.4 |
| 0.2 | 331.5 |
| 0.3 | 385.7 |
| 0.4 | 458.2 |
| 0.5 | 559.9 |
| 0.6 | 712.7 |

$$A = \frac{0.6}{3 \times 6} (255.8 + 4 \times 289.4 + 2 \times 331.5 + 4 \times 385.7 + 2 \times 458.2 + 4 \times 559.9 + 712.7)$$

$$A = 249.6 \text{ kg h kmol}^{-1}$$

4. Calculation of the feed

$$\dot{n}_{A,0} = \frac{2000 \times 1000}{8000 \times 92} = 2.72 \text{ kmol toluene h}^{-1}$$

5. Calculation of the catalyst mass

$$m_{\text{cat}} = \dot{n}_{A,0} \cdot A = 2.72 \times 249.6 = 678.3 \text{ kg}$$

Exercise 14.5

| | |
|------------------------|--|
| Single-bed reactor: | isomerization of light gasoline |
| Tubular reactor: | methanol synthesis (low-pressure process) |
| Multibed reactor: | contact process (oxidation of SO ₂ to SO ₃) |
| Shallow-bed reactor: | combustion of ammonia to nitrous gases (Ostwald process) |
| Fluidized-bed reactor: | ammoxidation of propene to acrylonitrile |

Exercise 14.6

The formaldehyde formed should be removed as quickly as possible from the active catalyst. The temperature in the catalyst bed should be as low as possible, and the temperature profile should be uniform.

This requires a catalyst with low porosity and high thermal conductivity.

A shallow-bed reactor is used.

Exercise 14.7

| | Trickle-bed reactor | Suspension reactor |
|-----------------------------------|-------------------------|----------------------|
| Temperature distribution | profile | uniform |
| Selectivity | low | high |
| Residence time behavior of liquid | ideal plug flow reactor | ideal stirred tank |
| Catalyst diameter | large, mm | small, μm |
| Catalyst effectiveness factor | $\ll 1$ | ≈ 1 |
| Catalyst performance | low | high |

Exercise 14.8

- a) Ammoxidation of a methyl aromatic compound with an allylic double bond.
- b) Fluidized-bed reactor (cf. SOHIO process).

Exercise 14.9

- A) The microkinetics are decisive. There is no limitation by pore diffusion.
- B) For the trickle-bed reactor, larger catalyst pellets must be used. This case lies in the region of pore-diffusion inhibition, which distorts the kinetics and allows only a very low degree of exploitation of the catalyst.

References

Textbooks and Reference Books on Homogeneous Catalysis [T]

- [T1] Buddrus, J. (1980): Grundlagen der organischen Chemie (Kap. 15: „Metallorganische Verbindungen“), de Gruyter, Berlin.
- [T2] Collman, J.P., Hegedus, L.S. (1980): Principles and Applications of Organotransition Metal Chemistry, University Science Books, Mill Valley, Calif. (USA).
- [T3] Davies, S.G. (1982): Organotransition Metal Application to Organic Synthesis, Pergamon Press.
- [T4] Elschenbroich, Ch., Salzer, A. (1989): Organometallics, 2. Aufl., VCH, Weinheim.
- [T5] Falbe, J. (Ed.) (1980): New Syntheses with Carbon Monoxide, Springer-Verlag, Berlin–Heidelberg–New York.
- [T6] Huheey, J.E. (1993): Inorganic Chemistry, 4th ed, Harper Collins College Publishers.
- [T7] Keim, W. (Ed.) (1983): Catalysis in C₁-Chemistry, D. Reidel Publ. Comp., Dordrecht.
- [T8] Jones, W.H. (1980): Catalysis in Organic Synthesis, Academic Press, London.
- [T9] Kirk-Othmer (1992): Encyclopedia of Chemical Technology, J. Wiley, New York. (Vol. 5, 324: „Homogeneous Catalysis“).
- [T10] Kochi, J.K. (1978): Organometallic Mechanisms and Catalysis, Academic Press, London.
- [T11] Masters, C. (1981): Homogeneous Transition-metal Catalysis – a gentle art, Chapman and Hall, London–New York.
- [T12] Nakamura, A., Tsutsui, M. (1980): Principles and Applications of Homogeneous Catalysis, J. Wiley, New York.
- [T13] Negishi, E.I. (1980): Organometallics in Organic Syntheses, J. Wiley, New York.
- [T14] Parshall, G.W. (1980): Homogeneous Catalysis, J. Wiley, New York.
- [T15] Pearson, A.J. (1985): Metallo-Organic Chemistry, J. Wiley, New York.
- [T16] Pracejus, H. (1977): Koordinationschemische Katalyse organischer Reaktionen, Theodor Steinkopff, Dresden.
- [T17] Sheldon, R.A. (1983): Chemicals from Synthesis Gas, Serie Catalysis by Metal Complexes, D. Reidel Publ. Comp., Dordrecht.
- [T18] Shriver, D.F., Adkins, P.W., Langford, C.H. (1994): Inorganic Chemistry, 2nd ed. Oxford University Press.

Textbooks, Reference Books and Brochures on Heterogeneous Catalysis [T]

- [T19] Atkins, P.W. (1994): Physical Chemistry, 5th ed, Oxford University Press.
- [T20] Bond, G.C. (1987): Homogeneous Catalysis – Principles and Applications, Oxford Science Publ., Clarendon Press, Oxford. (Short introduction to heterogeneous catalysis).

- [T21] Bremer, H., Wendlandt, K.P. (1978): *Heterogene Katalyse – Eine Einführung*, Akademie-Verlag, Berlin.
- [T22] Campbell, I.M. (1988): *Catalysis of Surfaces*, Chapman and Hall, London–New York.
- [T23] Fonds der Chemischen Industrie (1985): *Katalyse*, Folienserie, Frankfurt/M.
- [T24] Gates, B.C. (1992): *Catalytic Chemistry*, J. Wiley, New York. (Textbook on catalysis, fundamentals and applications).
- [T25] Gates, B.C., Katzer, J.R., Schuit, G.C.A. (1979): *Chemistry of Catalytic Processes*, Mc Graw Hill, New York.
- [T26] Hagen, J. (1992): *Chemische Reaktionstechnik – Eine Einführung mit Übungen*, VCH, Weinheim.
- [T27] Hauffe, K. (Ed.) (1976): *Katalyse*, de Gruyter, Berlin. (Selected Chapters on homogeneous, heterogeneous, and enzymatic catalysis of simple reactions).
- [T28] Hegedus, L. (Ed.) (1987): *Catalyst Design – Progress and Perspectives*, J. Wiley, New York.
- [T29] Hughes, R. (1984): *Deactivation of Catalysts*, Academic Press, London.
- [T30] Jaffe, J., Pissmen, L.M. (1975): *Heterogene Katalyse*, Akademie-Verlag, Berlin.
- [T31] Kirk-Othmer (1993): *Encyclopedia of Chemical Technology*, Vol 5, 340. (Heterogeneous Catalysis)
- [T32] Kripylo, P., Wendlandt, K.P., Vogt, P. (1993): *Heterogene Katalyse in der chemischen Technik*, Dt. Verlag für Grundstoffindustrie, Leipzig–Stuttgart. (Chemistry and technology of the production of catalysts, and Chemistry and technology of heterogeneously catalyzed reactions).
- [T33] Le Page, J.F. (1987): *Applied Heterogeneous Catalysis – Design, Manufacture, use of solid catalysts*, technip, Paris.
- [T34] Muchlenow, I.P. (1976): *Technologie der Katalysatoren*, VEB Dt. Verlag für Grundstoffindustrie, Leipzig.
- [T35] Richardson, J.T. (1989): *Principles of Catalyst Development*. Plenum Press, New York–London.
- [T36] Römpps Chemie-Lexikon (1983). Francksche Verlagsbuchhandlung, Stuttgart.
- [T37] Satterfield, C.N. (1980): *Heterogeneous Catalysis in Practice*, Mc Graw Hill, New York.
- [T38] Schlosser, E.G. (1972): *Heterogene Katalyse*, Verlag Chemie, Weinheim.
- [T39] Shriver, D.F., Atkins, P.W., Langford, C.H. (1994): *Inorganic Chemistry*, 2nd ed. Oxford University Press.
- [T40] Trimm, D.L. (1980): *Design of Industrial Catalysts*, Elsevier, Amsterdam.
- [T41] Ullmann's Encyclopedia of Industrial Chemistry, 5. Aufl. (1985). VCH, Weinheim. (Vol. A 5, 340; Heterogeneous Catalysis).
- [T42] Wedler, G. (1970): *Adsorption – Eine Einführung in die Physisorption und Chemisorption*, Verlag Chemie, Weinheim.
- [T43] Wedler, G. (1982): *Lehrbuch der Physikalischen Chemie*, Verlag Chemie, Weinheim.
- [T44] White, M.G. (1990): *Heterogeneous Catalysis*, Prentice Hall, Englewood Cliffs, New Jersey. (Physisorption, Chemisorption).
- [T45] *Katalyse* (1994): *Topics in Chemistry. Heterogene Katalysatoren*. BASF AG Ludwigshafen. (Brochure with some reviews on heterogeneous catalysis of industrial relevance).
- [T46] Ertl, G., Knözinger, H., Weitkamp, J. (Eds.) (1997): *Handbook of Heterogeneous Catalysis*. VCH, Weinheim.

Chapter 1

- [1] Baltes, J., Cornils, B., Frohning, C.D. (1975): *Chem. Ing. Tech.* **47** (12), 522.
- [2] Emig, G. (1987): *Chemie in unserer Zeit* **21** (4), 128.
- [3] Falbe, J., Bahrman, H. (1981): *Chemie in unserer Zeit* **15** (2), 37.
- [4] Folienserie des Fonds der Chemischen Industrie, Nr. 19 (1985): *Katalyse*.

- [5] Godfrey, J.A., Searles, R.A. (1981): *Chemie-Technik* **10** (12), 1271.
- [6] Hagen, J. (1992): *Chemische Reaktionstechnik – Eine Einführung mit Übungen*, VCH, Weinheim.
- [7] Mroß, W.D. (1985): *Umschau* **1985** (7), 423.
- [8] Riekert, L. (1981): *Chem. Ing. Tech.* **53** (12), 950.
- [9] Süß-Fink, G. (1988): *Nachr. Chem. Tech. Lab.* **36** (10), 1110.
- [10] Ugo, R. (1969): *Chim. Ind. (Milano)* **51** (12), 1319.

Chapter 2

- [1] Berke, H., Hoffmann, R. (1978): *J. Am. Chem. Soc.* **100**, 7224.
- [2] Brown, S., Bellus, P.A. (1978): *Inorg. Chem.* **17**, 3726.
- [3] Calderazzo, F. (1977): *Angew. Chem.* **89**, 305.
- [4] Collman, J.P. et al. (1978): *J. Am. Chem. Soc.* **100**, 4766.
- [5] Hagen, J. (1977): *Chemie für Labor und Betrieb* **28** (4), 125.
- [6] Hagen, J., Tschirner, E.G., Fink, G., Lorenz, R. (1985): *Chemiker-Ztg.* **109**, 3.
- [7] Hagen, J. (1985): *Chemiker-Ztg.* **109** (2), 63 (Teil I). *Chemiker Ztg.* **109** (6), 203 (Teil II).
- [8] Hagen, J. (1987): *Der Innovationsberater (DIB)*, 2/87, 1883. Rudolf Haufe Verlag, Freiburg.
- [9] Hagen, J. (1988): *Chemie für Labor und Betrieb*, **39** (12), 605.
- [10] Halpern, J. (1970): *Acc. Chem. Res.* **3**, 386.
- [11] Henrici-Olivé, G., Olivé, S. (1971): *Angew. Chem.* **83** (4), 121.
- [12] Herrmann, W.A. (1988): *Kontakte (Darmstadt)* **1988** (1), 3.
- [13] Klein, H.F. (1980): *Angew. Chem.* **92**, 362.
- [14] Pearson, R.G. (1977): *Chem. Brit.* **3**, 103; (1963): *J. Am. Chem. Soc.* **85**, 3533; (1966): *Science* **151**, 172.
- [15] Shriver, D.F. (1970): *Acc. Chem. Res.* **3**, 231.
- [16] Shriver, D.F. (1983): *Chem. Brit.* **1983** (6), 482; (1981): *Am. Chem. Soc. Symp. Ser.* **152**, 1.
- [17] Stille, J.K., Lau, K.S.Y. (1977): *Acc. Chem. Res.* **10**, 434.
- [18] Taube, R. (1975): *Z. Chem.* **15** (11), 426.
- [19] Tolman, C.A. (1972): *Chem. Soc. Rev.* **1**, 337.
- [20] Tolman, C.A. (1977): *Chem. Rev.* **77**, 313.
- [21] Ugo, R. (1969): *Chim. Ind. (Milano)* **51** (12), 1319.

Chapter 3

- [1] Bach, H., Bahrmann, H., Gick, W., Konkol, W., Wiebus, E. (1987): *Chem. Ing. Tech.* **59** (11), 882.
- [2] Brunner, H. (1980): *Chemie in unserer Zeit* **14** (6), 177.
- [3] Casey, C.P. (Ed.) (1986): *J. Chem. Educ.* **63**, 188.
- [4] Cornils, B., Herrmann, W.A., Kohlpaintner, C.W. (1993): *Nachr. Chem. Tech. Lab.* **41** (5), 544.
- [5] Falbe, J., Bahrmann, H. (1984): *Chemie in unserer Zeit*, **15** (2), 37. Falbe, J., Bahrmann, H. (1984): *J. Chem. Educ.* **61**, 961.
- [6] Halpern, J. (1981): *Inorg. Chem. Acta*, **50**, 11.
- [7] Herrmann, W.A. (1991): *Kontakte (Darmstadt)*, **1991** (3), 29.
- [8] Keim, W. (1984): *Chem. Ind. XXXVI*, 397.
- [9] Keim, W., in Graziani, M., Giongo, M. (Ed.) (1984): *Fundamental Research in Homogeneous Catalysis* **4**, 131. Plenum Press, New York.
- [10] Keim, W. (1984): *Chemisch Magazine* Juli 1984, 417.
- [11] Keim, W. (1984): *Chem. Ing. Tech.* **56** (11), 850.

- [12] Parshall, G.W. (1978): *J. Mol. Catal.* **4**, 243.
- [13] Parshall, G.W. (1987): *Organometallics* **6**, 687.
- [14] Russell, J.H. (1988): *Chemie-Technik* **17** (6), 148.
- [15] Sheldon, R.A., Kochi, J.K. (1981): *Metal-Catalyzed Oxidations of Organic Compounds*, Academic Press, New York.
- [16] Waller, J.F. (1985): *J. Mol. Catal.* **31**, 123.
- [17] Weissermel, K., Arpe, H.-J. (1998): *Industrielle Organische Chemie*, 5. Aufl., Wiley-VCH, Weinheim.
- [18] Blaser, H.U., Spindler, F., Studer, M. (2001): *Enantioselective Catalysis in Fine Chemicals Production. Applied Catalysis A: General* **221**, 119.
- [19] Cornils, B., Herrmann, W.A., Schlögl, R., Wong, C.H. (Ed.) (2000): *Catalysis from A to Z*. Wiley-VCH, Weinheim.
- [20] Cornils, B., Herrmann, W.A. (Eds.) (1996): *Applied homogeneous catalysis with organometallic compounds*, Vols. 1 and 2, VCH Weinheim.
- [21] Cybulski, A., Moulijn, J.A., Sharma, M.M., Sheldon, R.A. (2001): *Fine Chemicals Manufacture – Technology and Engineering*. Elsevier, Amsterdam.
- [22] Whyman, R. (2001): *Applied Organometallic Chemistry and Catalysis*. Oxford Chemistry Primers 96.
- [23] <http://www.uyseg.org/catalysis/asymmetric/asymm2.htm>
- [24] <http://www.organic-chemistry.org/namedreactions/suzuki-coupling.shtm>
- [25] <http://www.uyseg.org/catalysis/polyethene/poly7.htm>

Chapter 4

- [1] Bommarius, A.S., Riebel, B.R. (2004): *Biocatalysis – Fundamentals and Applications*. Wiley-VCH, Weinheim.
- [2] Chorkendorff, I., Niemantsverdriet, J.W. (2003): *Concepts of modern Catalysis and Kinetics*, Wiley-VCH, Weinheim.
- [3] Fogler, H.S. (1999): *Elements of Chemical Reaction Engineering*, 3rd ed., Prentice Hall PTR, New Jersey.
- [4] Van Santen, R.A., van Leeuwen, P.W.N.M., Moulijn, J.A., Averill, B.A. (Ed.) (1999): *Catalysis – an integrated Approach*, 2nd ed., Elsevier.
- [5] <http://www.uyseg.org/catalysis/principles/>

Chapter 5

- [1] Beeck, O. (1945): *Rev. Modern Physics* **17**, 61.
- [2] Boudart, M., Djéga-Mariadassou, G. (1984): *Kinetics of Heterogeneous Catalytic Reactions*. Princeton Univ. Press, Princeton New Jersey.
- [3] Bradley, S.A., Gattuso, M.J., Bertolacini, R.J. (1989): *Characterization and Catalyst Development*. ACS Symp. Ser. **411**, 2.
- [4] Bradshaw, A.M., Hoffmann, F.M. (1978): *Surf. Sci.* **72**, 513.
- [5] Coughlin, R.W. (1967): *Classifying catalysts, some broad principles*. *Ind. Eng. Chem.* **59** (9), 45.
- [6] Delmon, B., Froment, G. (1980): *Catalyst Deactivation*. Elsevier, Amsterdam.
- [7] Dirksen, F. (1983): *Chemie-Technik* **12** (6), 36.
- [8] Emig, G. (1987): *Chemie in unserer Zeit* **21**, 128.
- [9] Erbudak, M. (1991): *Swiss.Chem.* **13** (11), 63.
- [10] Ertl, G. (1990): *Angew. Chem.* **102**, 1258.
- [11] Friend, C.M., Stein, J., Muetterties, E.L. (1981): *J. Am. Chem. Soc.* **103**, 767.

- [12] Höldeich, W., Mroß, W.D., Gallei, E. (1985): Arab. J. Sci. Eng. **10** (4), 407.
- [13] Hsiu-Wei, C., White, J.M., Ekerdt, J.G. (1986): J. Catalysis **99**, 293.
- [14] Huder, K. (1991): Chem. Ing. Tech. **63** (4), 376.
- [15] Jakubith, M. (1991): Chemische Verfahrenstechnik. VCH, Weinheim.
- [16] Klabunde, K.J., Fazlul Hoq, M., Mousah, F., Matsuhashi, H. (1987): Metal Oxides and their physico-chemical properties in Catalysis and Synthesis. In: Preparative Chemistry using supported reagents. Academic Press, London.
- [17] Kung, H.H. (1989): Transition metal oxides. In: Surface chemistry and Catalysis. Elsevier, Amsterdam.
- [18] Lamber, R., Jaeger, N., Schulz-Ekloff, G. (1991): Chem. Ing. Tech. **63** (7), 681.
- [19] Levsen, K. (1976): Chemie in unserer Zeit **10**, 48.
- [20] Lintz, H.G. (1992): Chemie in unserer Zeit **26**, 111.
- [21] Maier, W.F. (1989): Chem. Industrie 12/89, 52.
- [22] Maier, W.F. (1989): Einfluß der Katalysatorstruktur auf Aktivität und Selektivität von Hydrierreaktionen. In: Dechema-Monographien, Bd. **118**, 243.
- [23] Maier, W.F. (1989): Angew. Chem. **101**, 135.
- [24] Moulijn, J.A., Tarfaoui, A., Kepteijn, F. (1991): Catal. Today **11** (1), 1.
- [25] Mroß, W.D., Kronenbitter, J. (1982): Chem. Ing. Tech. **54** (1), 33.
- [26] Mroß, W.D. (1984): Ber. Bunsenges. Phys. Chem. **88**, 1042.
- [27] Neddermeyer, H. (1992): Chemie in unserer Zeit **26**, 18.
- [28] Niemantsverdriet, J.W. (1993): Spectroscopy in Catalysis. VCH, Weinheim.
- [29] Noerskov, J.K. (1991): Prog. Surf. Sci. **38** (2), 103.
- [30] Polanyi, M., Horiuti, J. (1934): Trans. Faraday Soc. **30**, 1164.
- [31] Pulm, H. (1991): GIT Fachz. Lab. 9/91, 969.
- [32] Schäfer, H. (1977): Chemiker-Ztg. **101** (7/8), 325.
- [33] Schwankner, R.J., Eiswirth, M. (1985): Umschau **85**, 471.
- [34] Schwankner, R.J. (1989): Praxis d. Naturwiss.-Chemie 1/38, 2.
- [35] Stone, F.S. (1990): J. Mol. Cat. **59**, 147.
- [36] Suib, S.L. (1993): Selectivity in Catalysis. In: ACS Symp. Ser. **517**, 1.
- [37] Vannice, M.A. (1990): J. Mol. Cat. **59**, 165.
- [38] Vannice, M.A. (1975): J. Catal. **37**, 449.
- [39] van Santen, R.A. (1991): Surf. Sci. 251/252, 6.
- [40] Mansour, A.E. et al. (1989): Angew. Chem. **101** (Nr. 3), 360.
- [41] Dodgson, I., Johnson Matthey, U.K. (1998): Proc. 2nd NICE Workshop on Catalysis in Fine Chemicals Production, march 9/10 1998, Louvain-la-Neuve, Belgium.
- [42] Raab, C.G. et al., in „Heterogeneous Catalysis and Fine Chemicals III“. M. Guisnet et al. (Eds.), Elsevier 1993, 211.
- [43] Cybulski, A., Moulijn, J.A., Sharma, M.M., Sheldon, R.A. (2001): Fine Chemicals Manufacture – Technology and Engineering. Elsevier, Amsterdam.
- [44] Cornils, B., Herrmann, W.A., Schlögl, R., Wong, C.H. (Ed.) (2000): Catalysis from A to Z. Wiley-VCH, Weinheim.
- [45] Chorkendorff, I., Niemantsverdriet, J.W. (2003): Concepts of modern Catalysis and Kinetics, Wiley-VCH, Weinheim.

Chapter 6

- [1] Delmon, B. et al. (Ed.) (1979): Preparation of Catalysts. Elsevier, Amsterdam.
- [2] Emig, G. (1977): Chem. Ing. Tech. **49**, 865.
- [3] Griebbs, H.R. (1977): Chemtech Aug. 1977, 512.
- [4] Gubicza, L., Ujhidy, A., Exner, H. (1988): Chemische Industrie 7/88, 48.
- [5] Hartley, F.R. (1985): Supported Metal Complexes. D. Reidel Publ. Comp., Dordrecht.

- [6] Hesse, D., Redondo de Beloqui, M.S. (1989): Einfluß der Porenstruktur auf das Umsatzverhalten von Supported Liquid-Phase-Katalysatoren. In: Dechema-Monographien, Bd. 118, 305. VCH, Weinheim.
- [7] Higginson, G.W. (1974): Chem. Eng. **81** (20), 98.
- [8] Hölderich, W., Schwarzmann, M., Mroß, W.D. (1986): Erzmetall **39** (6), 293.
- [9] Kotter, M., Riekert, L. (1982): Chem. Eng. Fundam. Vol. **2** (1), 19.
- [10] Kotter, M. (1983): Chem. Ing. Tech. **55**, 179.
- [11] Luft, G. (1991): Chem. Ing. Tech. **63** (7), 659.
- [12] Mroß, W.D. (1985): Jahrbuch 1985 der „Braunschweigische Wissenschaftliche Gesellschaft“, 101.
- [13] Panster, P. (1992): Chemie in Labor und Biotechnik **43**, 16.
- [14] Schneider, P., Emig, G., Hofmann, H. (1985): Chem. Ing. Tech. **57**, 728.
- [15] Scholten, J.J.F. (1985): J. Mol. Cat. **33**, 119.
- [16] Schuit, G.C.A., Gates, B.C. (1983): Chemtech Sept. 1983, 556.

Chapter 7

- [1] Chen, N.Y., Garwood, W.E., Dwyer, F.G. (1989): Shape Selective Catalysis in Industrial Applications. Chemical Industries, A Series of Reference Books and Textbooks, Bd. 36. Marcel Dekker, New York, Basel.
- [2] Dyer, A. (1988): An Introduction to Molecular Sieves. J. Wiley, New York.
- [3] Hölderich, W., Gallei, E. (1985): Ger. Chem. Eng. **8**, 337.
- [4] Hölderich, W., Hesse, M., Näumann, F. (1988): Angew. Chem. **100**, 232.
- [5] Karge, H.G., Weitkamp, J. (Hrsg.) (1984): Zeolites as Catalysts, Sorbents and Detergent Builders. Elsevier, Amsterdam.
- [6] Kerr, G.T. (1989): Spektrum d. Wissenschaft **1989** (9), 94.
- [7] Tißler, A., Müller, U., Unger, K. (1988): Nachr. Chem. Tech. Lab. **36** (6), 624.
- [8] Unger, K., Kanz-Reuschel, B., Brenner, A., Wallau, M., Spichtinger, R. (1992): Labor 2000 (1992), 179.
- [9] Vedrine, J.C. (1982): Physical Methods for the Characterization of Non-Metal Catalysts. In: Surface Properties and Catalysis by Non-Metals. NATO ASI Series, 123. C.D. Reidel Publ. Comp., Dordrecht.

Chapter 8

- [1] Anderson, J.B.F., Griffin, K.G., Richards, R.E. (1989): Chemie-Technik **18** (5), 40.
- [2] Augustine, R.L. (1985): Catalytic Hydrogenation. Marcel Dekker, New York.
- [3] Blaser, H.U., Indolese, A., Schnyder, A. (2000): Applied homogeneous catalysis by organometallic complexes. Current Science **78** (11), 1336.
- [4] Bommarius, A., Drauz, K.H., Eils, S., Kirchhoff, J., Schwarm, M. CHIMICA OGGI/ Chemistry Today, Oct. 2000, 12.
- [5] Bröcker, F.J., Kaempfer, K. (1975): Chem. Ing. Tech. **47** (12), 513.
- [6] Cervený, L. (Ed.) (1986): Catalytic Hydrogenation. Elsevier, Amsterdam.
- [7] Cybulski, A., Moulijn, J.A., Sharma, M.M., Sheldon, R.A. (2001): Fine Chemicals Manufacture – Technology and Engineering. Elsevier, Amsterdam.
- [8] Emig, G. (1977): Chem. Ing. Tech. **49** (11), 865.
- [9] Emig, G. (1987): Chemie in unserer Zeit **21** (4), 128.
- [10] Engler, B.H. (1991): Chem. Ing. Tech. **63** (4), 298.
- [11] Ertl, G. (1990): Angew. Chem. **102**, 1258.
- [12] Fink, K. et al. (1992): Chem. Ing. Tech. **64** (5), 416.

- [13] Godfrey, J.A., Searles, R.A. (1981): *ChemieTechnik* **10** (12), 1271.
- [14] Guisnet et al. (Ed.)(1991): *Heterogeneous Catalysis and Fine Chemicals II*. Elsevier, Amsterdam.
- [15] Herrmann, W.A. (1991): *Metallorganische Chemie in der industriellen Katalyse: Reaktionen, Prozesse, Produkte. Teil 1: Kontakte (Darmstadt) 1991* (1), 22. Teil 2: Kontakte (Darmstadt) **1991** (3), 29.
- [16] Hölderich, W., Schwarzmann, M., Mroß, W.D. (1986): *Erzmetall* **39** (6), 292.
- [17] Kanzler, W., Schedler, J., Thalhammer, H. (1986): *Chemische Industrie* 12/86, 1188.
- [18] Kotowski, W., Bekier, H. (1992): *Chem. Tech.* **44** (5), 163.
- [19] Mroß, W.D. (1985): *Umschau* **1985** (7), 423.
- [20] Mücke, M. (1975): *Chem. Lab. Betr.* **26** (1), 10.
- [21] Schmidt, K.H. (1984): *Katalysatoren für chemische Großsynthesen. Teil I: Chem. Ind. Okt. 1984*, 572. Teil II: *Chem. Ind. Nov. 1984*, 716.
- [22] Sheldon, R.A., *Fine chemicals by catalytic oxidation. CHEMTECH SEPT. 1991*, 566.
- [23] Sleight, A.W., Linn, W.J., Aykan, K. (1978): *Chemtech April 1978*, 235.

Chapter 9

- [1] Acres, G.J.K. et al. (1997): *Electrocatalysts for fuel cells. Cat. Today* **38**, 393.
- [2] Carrette, L., Friedrich, K.A., Stimming, U. (2001): *Fuel Cells – Fundamentals and Applications. Fuel Cells 2001* (1), 5.
- [3] Cornils, B., Herrmann, W.A., Schlögl, R., Wong, C.H. (Ed.) (2000): *Catalysis from A to Z*. Wiley-VCH, Weinheim.
- [4] Dubé, P. et al. (2003): *J. Appl. Electrochemistry* **33**, 541.
- [5] Gerischer, H., Vielstich, W. *Electrocatalysis* (1997): in: Ertl, G., Knözinger, H., Weitkamp, J. (Eds.) *Handbook of Heterogeneous Catalysis*, 1325. VCH, Weinheim.
- [6] Horányi, G. (1994): *Heterogeneous catalysis and electrocatalysis. Cat. Today* **19**, 285.
- [7] Langer, S.H., Card, J.C., Foral, M.J. (1986): *Electrogenerative and related processes. Pure & Appl. Chem.* **58** (6), 895.
- [8] Lipkowski, J., Ross, P.H. (Eds.) (1998): *Electrocatalysis*. Wiley-VCH, Inc.
- [9] *Ullmanns' Encyclopedia of Industrial Chemistry*, 6th Ed, Vol. 11, 428. Technical Electrocatalysis.
- [10] Vielstich, W., Iwasita, T. *Fuel Cells* (1997): In: Ertl, G., Knözinger, H., Weitkamp, J. (Eds.) *Handbook of Heterogeneous Catalysis*, 2090. VCH, Weinheim.
- [11] <http://www.menegaldo.free.fr/sciencinfuze/fc/examples.htm>

Chapter 10

- [1] Anastas, P.T., Kirchhoff, M.M., Williamson, T.C. *Applied Catalysis A: General* **221** (2001), 3.
- [2] Bosteels, D., Searles, R.A. *Exhaust Emission Catalyst Technology. Platinum Metals Rev.* 2002, **46**, (1), 27.
- [3] Chorkendorff, I., Niemantsverdriet, J.W. (2003): *Concepts of modern Catalysis and Kinetics*, Wiley-VCH, Weinheim.
- [4] Clark, J.H.: *Catalysis for green chemistry. Pure Appl. Chem.*, Vol. 73 (1), 103 (2001).
- [5] Cornils, B., Herrmann, W.A., Schlögl, R., Wong, C.H. (Ed.) (2000): *Catalysis from A to Z*. Wiley-VCH, Weinheim.
- [6] Eissen, M., Hungerbühler, K., Dirks, S., Metzger, J. *Green Chemistry April 2003*, G 25.
- [7] Engler, B. H. (1991): *Chem. Ing. Tech.* **63** (4) 298.
- [8] Fink, K. et al. (1992): *Chem. Ing. Tech.* **64** (5), 416.
- [9] Lancaster, M. (2002): *Green Chemistry – An Introductory Text*. Royal Soc. of Chemistry, Cambridge.
- [10] Ritter, S.K. (2002): *Green Chemistry Progress Report. Chemical & Eng. News* **80** (47), 19.

- [11] Anon. (1988/89): Thermische oder katalytische Abluftreinigung? *Chemie–Umwelt–Technik* **29**.
- [12] Weisweiler, W. (1989): Umweltfreundliche Entstickungskatalysatoren. In: *Dechema-Monographien*, Bd. **118**, 81.
- [13] Weisweiler, W., *Chemie-Ing. Techn.* **72** (51), 441 (2000).

Chapter 11

- [1] Fujishima, A., Rao, T.N. *Pure & Appl. Chem.* **70**, (11), 2177.
- [2] Kisch, H., Macyk, W. (2002): *Nachrichten aus der Chemie* **50** (Okt. 2002), 1078.
- [3] Mills, A., Lee, S.K. (2003): *Platinum Metals Rev.* 2003 (**47**), (1), 2.
- [4] Serpone, N., Emeline, A.V. (2002): Suggested Terms and Definitions in Photocatalysis and Radiocatalysis. *Int. Journal of Photoenergy* **4** (2002), 91.
- [5] Thomas, J.M., Thomas, W.J. (1997): *Principles and Practice of Heterogeneous Catalysis*, Wiley-VCH, Weinheim.
- [6] Zou, Z., Ye, J., Arakawa, H. (2003): Photocatalytic splitting into H₂ and/or O₂ under UV and visible light irradiation with a semiconductor photocatalyst. *Int. Journal of Hydrogen Energy* **28**, 663.
- [7] <http://www.edu.chem.tue.nl/6KM11>: Fundamentals of Photocatalytic Water Splitting by visible Light (TU Eindhoven)

Chapter 12

- [1] Cornils, B., Herrmann, W.A., Schlögl, R., Wong, C.H. (Ed.) (2000): *Catalysis from A to Z*. Wiley-VCH, Weinheim.
- [2] Dehmlow, Dehmlow (1993): *Phase Transfer Catalysis*, 3rd Ed., VCH, Weinheim.
- [3] Makosza, M., Fedorynski, M. (1998): Alkylation of phenylacetonitrile. *The Sachem Phase Transfer Catalysis Review*, Sachem Inc. 1998, Issue 3, 2.
- [4] McKillop, A., Fiaud, J., Hug, R. (1974): *Tetrahedron* **30**, 1379.
- [5] Starks, C. (1971): *J. Amer. Chem. Soc.* **93**, 195.
- [6] Starks, C., Liotta, C., Halpern, M. (1994): *Phase-Transfer Catalysis: Fundamentals, Applications and Industrial Perspectives*. Chapman & Hall, New York.
- [7] <http://www.phasetransfer.com/overview.htm>
- [8] <http://www.sacheminc.com/catalysts/ptc/phases/Phases03.pdf>

Chapter 13

- [1] Agar, D., Bever, P.M., Wenert, D. (1988): *Chem. Ing. Tech.* **60** (9), 712.
- [2] Baltzly, R. (1976): *J. Org. Chem.* **41** (6), 920.
- [3] Bandermann, F. (1972): *Statistische Methoden beim Planen und Auswerten von Versuchen*. In: *Ullmanns Enzyklopädie der technischen Chemie*, Bd. 1, 4. Aufl., 294. VCH, Weinheim.
- [4] Berty, J.M. (1983): *Appl. Ind. Catalysis* **1**, 41.
- [5] Carlson, R. (1992): *Design and optimization in organic synthesis*. Elsevier, Amsterdam.
- [6] Davis, L. (1992): *Chemistry and Industry* **1992**, 634.
- [7] Deller, K. (1990): *Chemische Prod.* 1/2/90, 44.
- [8] Dreyer, D., Luft, G. (1982): *Chem. Tech. (Heidelberg)* **11** (8), 1061.
- [9] Emig, G. (1977): *Chem. Ing. Tech.* **49** (11), 865.
- [10] Greger, M., Gutsche, B., Jeromin, L. (1992): *Chem. Ing. Tech.* **64** (3), 253.

- [11] Gut, G. (1982): *Swiss Chem.* **4**, 17.
- [12] Hagen, J. (1975): Diss. RWTH Aachen.
- [13] Hagen, J., Roessler, F., Zwick, T. (1993): *Chemie-Technik* 7/93, 76.
- [14] Heidel, K. (1973): *Fette, Seifen, Anstrichmittel* **75**, 233.
- [15] Herskowitz, M. (1991): Hydrogenation of Benzaldehyde to Benzylalcohol in a slurry and fixed-bed reactor. In: M. Guisnet et al. (Hrsg.). *Heterogeneous Catalysis and Fine Chemicals II*, 105. Elsevier, Amsterdam.
- [16] Hoffmann, U., Hofmann, H. (1971): *Einführung in die Optimierung*. Verlag Chemie, Weinheim.
- [17] Hofmann, H. (1975): *Chimia* **29** (4), 159.
- [18] Ingham, J., Dunn, I.J., Heinzle, E., Prenosil, J.E. (1994): *Chemical Engineering Dynamics – Modelling with PC Simulation*. VCH, Weinheim.
- [19] Kromm, K. (1994): *Dipl.-Arbeit FH Mannheim – Hochschule für Technik und Gestaltung*.
- [20] Mahoney, J.A., Robinson, K.K., Myers, E.C. (1978): *Chemtech Dec.* 1978, 758.
- [21] Petersen, H. (1992): *Grundlagen der Statistik und der statistischen Versuchsplanung*. ecomed, Landsberg.
- [22] Plackett, R.L., Burman, J.P. (1946): *Biometrika* **33**, 305.
- [23] Ramachandran, P.A., Chaudhari, R.V. (1980): *Chem. Eng. Dec.* 1, 74.
- [24] Reh, E. (1992): *GIT Fachz. Lab.* **5**, 552.
- [25] Retzlaff, G., Rust, G., Waibel, J. (1978): *Statistische Versuchsplanung*. Verlag Chemie, Weinheim.
- [26] Schermuly, O., Luft, G. (1978): *Ger. Chem. Eng.* **1**, 222.
- [27] Schneider, P., Emig, G., Hofmann, H. (1985): *Chem. Ing. Tech.* **57** (9), 728.
- [28] Tarham, M.O. (1983): *Catalytic Reactor Design*. Mc Graw Hill, New York.
- [29] Trimm, D.L. (1973): *Chemistry and Industry*, 3. Nov. **1973**, 1012.
- [30] Zwick, T. (1992): *Dipl.-Arbeit FH Mannheim – Hochschule für Technik und Gestaltung*.
- [31] Cutlip, M.B., Shacham, M. (1999): *Problem Solving in Chemical Engineering with Numerical Methods*. Prentice Hall, Upper Saddle River, New Jersey.
- [32] Fogler, H.S. (1999): *Elements of Chemical Reaction Engineering*, 3rd Ed., Prentice-Hall, Upper Saddle River, New Jersey.
- [33] Hagen, J. (2004) *Chemiereaktoren – Auslegung und Simulation*. Wiley-VCH, Weinheim.
- [34] Hagemeyer, A., Strasser, P., Volpe, A.F., Jr. (Eds.) (2004): *High-Throughput Screening in Chemical Catalysis*. Wiley-VCH, Weinheim.
- [35] Wittcoff, H.A., Reuben, B.G., Plotkin, J.S. (2004): *Industrial Organic Chemistry*. Wiley-Interscience, New Jersey.
- [36] Brochure hte AG Heidelberg: Our expertise – your innovation. www.hte-company.de

Chapter 14

- [1] Agar, D.W., Ruppel, W. (1988) *Chem. Ing. Tech.* **60** (10), 731.
- [2] Alper, E., Wichtendahl, B., Deckwer, W.D. (1980): *Chem. Eng. Sci.* **35**, 217.
- [3] Concordia, J.J. (1990): *Chem. Eng. Prog.* **86** (3), 50.
- [4] Deckwer, W.D., Alper, E. (1980): *Chem. Ing. Tech.* **52**, 219.
- [5] Falbe, J. (Hrsg.) (1978): *Katalysatoren, Tenside und Mineralöladditive*. G. Thieme, Stuttgart.
- [6] Fogler, H.S. (1992): *Elements of Chemical Reaction Engineering*, 2nd Ed., Prentice Hall, New Jersey.
- [7] Gianetto, A., Silveston, P. (Eds.) (1986): *Multiphase chemical reactors*. Hemisphere, Washington.
- [8] Gianetto, A., Specchia, V. (1992): *Chem. Eng. Sci.* **47** (13, 14), 3197.
- [9] Greger, M., Gutsche, B., Jeromin, L. (1992): *Chem. Ing. Tech.* **64** (3), 253.
- [10] Herskowitz, M., Smith, J.M. (1983): *AIChE J.* **29**, 1.

- [11] Jenck, J.F. (1991): Gas-liquid-solid reactors for hydrogenation in fine chemicals synthesis. In: M. Guisnet et al. (Ed.): *Heterogeneous Catalysis and Fine Chemicals II*, Elsevier, Amsterdam.
- [12] Ramachandran, A., Chaudhari, R.V. (1980): *Three-phase Catalytic Reactors*. Gordon and Breach, New York.
- [13] Tarham, M.O. (1983): *Catalytic Reactor Design*. Mc Graw Hill, New York.
- [14] Trambouze, P. (1981): *Chem. Ing. Tech.* **53** (5), 344.
- [15] Trambouze, P., Van Landeghem, H., Wauquier, J.P. (1988): *Chemical reactors – design/engineering/operation*. Editions Technip, Paris.
- [16] Weiss, S. et al. (Hrsg.) (1987): *Verfahrenstechnische Berechnungsmethoden, Teil 5: Chemische Reaktoren, Ausrüstungen und ihre Berechnung*. VCH, Weinheim.

Chapter 15

- [1] Frost and Sullivan (2004): *Advanced Catalysts – Global Overview of Technological Developments*, D 282.
- [2] Kochloefl, K. (2001): Development of Industrial Solid Catalysts. *Chem. Eng. Technol.* **24**, 229.
- [3] Weitkamp, J., Gläser, R. (2004): Katalyse. In: Winnacker and Küchler, *Chemische Technik – Prozesse und Produkte*. Wiley-VCH, Weinheim.
- [4] Wittcoff, H. A., Reuben, B. G., Plotkin, J. S. (2004): *Industrial Organic Chemicals*, 2nd Ed., Wiley-Interscience, New Jersey.

Chapter 16

- [1] Asche, W. (1993): *Chemische Ind.* 11/93, 40.
- [2] Cornils, B., Herrmann, W.A. (Eds.) (1996): *Applied homogeneous catalysis with organometallic compounds*, Vols. 1 and 2, VCH Weinheim.
- [3] Anon. (2001): Future directions of catalysis science – Workshop. *Catalysis Letters* **76** (3–4), 111.
- [4] Gallei, E.F., Neuman, H.P. (1994): *Chem. Ing. Tech.* **66** (7), 924.
- [5] Grünert, W., Völker, J. (1992): *Chem. Technik* **44** (11/12), 395.
- [6] Haber, J., Herzog, K. (1994): Heterogene Katalyse. Trends und Perspektiven. In: *Topics in Chemistry. Heterogene Katalysatoren*. BASF AG, Ludwigshafen.
- [7] Keim, W. (1984): *Chemisch Magazine Juli 1984*, 417.
- [8] Kochloefl, K. (1989): *Chem. Ind.* 8/89, 41.
- [9] Kochloefl, K. (2001): Development of Industrial Solid Catalysts. *Chem. Eng. Technol.* **24**, 229.
- [10] Kral, H. (1989): *Chem. Ind.* 8/89, 44.
- [11] Whyman, R. (2001): *Applied Organometallic Chemistry and Catalysis*. Oxford Chemistry Primers 96.
- [12] Wittcoff, H.A., Reuben, B.G., Plotkin, J.S. (2004): *Industrial Organic Chemicals*, 2nd Ed., Wiley-Interscience, New Jersey.
- [13] Vision 2020 Catalysis Report, ACS et al. <http://www.ccrhq.org/vision/index/roadmaps/catrep.html>.

Subject Index

a

- π acceptor 35
- σ -acceptor 20
- acceptor reactions 144f.
- acetaldehyde 44, 49f., 67f., 305
- acetic acid 61, 65f.
 - anhydride 61
- acetonitrile 140f.
- acetophenone 283f.
- acetyl iodide 49, 65
- acid hard 35
- acid/base
 - catalysis 143, 291
 - catalysts 143, 170
 - concept 169
 - interaction 171
 - reactions 21
- acrolein 273f., 280, 348ff.
 - synthesis 228
- acrylamide 92f.
- acrylonitrile 274ff.
- activated carbon 184
- activation 14, 224
 - energy 5, 103, 116f., 130, 204, 385
- active center 5, 7, 11f., 104, 108, 131
- active sites 85, 195, 245, 456
- activity 179ff., 440
- acyl complex 31, 41, 49
- acyl metal complex 31
- adiponitrile 50
- Adkins catalyst 225
- adsorbate 212f.
- adsorption 99, 102, 114, 117f., 210, 212, 456
 - competitive 138, 216, 252
 - cooperative 138
 - enthalpy 118, 303
 - equilibria 104
 - heterolytic 161
 - hydrogen 299
 - mixed 106, 110
 - multipoint 131
 - oxygen 161, 299
 - pyridine 251
 - single-point 131
 - two-point 137
- afterburning process 322f.
- agglomeration 216
- alcohol dehydrogenase (ADH) 86
- aldehydes 56
- aldol condensation 236, 325f.
- Aldox process 236f.
- Aliquat 336, 340
- alkaline fuel cell (AFC) 308, 310
- alkoxy carbonyl complexes 35
- alkoxy complexes 33
- alkyl complex 30
- alkylation 263
 - benzene 248
 - 2-phenylbutyronitrile 344
 - toluene 247
- alkylidene complex 34
- alloys 149f.
 - bimetallic 148
 - copper–nickel 148f.
- η^3 -allyl complex 26
- π -allyl complex 36, 39, 48, 444, 447
- π -allyl radical 121
- σ -allyl radical 121
- aluminium oxide 170, 173
- aluminiumphosphate (AlPO₄) 253
- aluminosilicates 169, 172, 179, 239, 465
- amidocarbonylation 290
- amino acids 337
- aminoacylase process 95
- 2-aminobenzonitrile 356ff.
- ammonia
 - combustion 412
 - desorption 213
 - oxidation 204

- ammonia synthesis 137f., 190f., 262, 266, 268, 411
 – mechanism 267
 ammoxidation 263, 274ff., 482
 – methane 412
 – propene 413
 Analysis Process Optimization (APO) 379ff.
 Andrussov process 412
 anode 305
 – reaction 307
 arene complex 36
 aromatics 350
 aromatization
 – alkanes 190
 – *n*-alkenes 168
 Arrhenius equation 5
 Arrhenius law 100
 aspartame 94f.
 asymmetric catalysis 75ff.
 asymmetric epoxidation 79f.
 atom efficiency 283f., 289f., 472
 Auger electron spectroscopy (AES) 218f.
 autoclave 11, 39, 55, 242
 automobile exhaust control 265
 automotive exhaust catalysis 317
 Avantium, NL 400
- b**
- Bacillus proteolicus/thermoproteolyticus* 94
 backbonding 18, 21
 π backbonding 35, 50
 backmixing 404f., 416, 422
 Balandin 127, 131
 band model 145, 150, 155
 bandgap 337
 – energy (E_{bg}) 331f.
 BaO 321
 base
 – hard 35f.
 – soft 33, 36
 BASF 216f., 223, 229f., 266, 270, 272, 287, 289, 306, 329, 419
 BASF process 65
 σ basicity 28, 32
 π basicity 28
 benzyltriethylammonium chloride (TEBA) 344
 benzyltrimethylammonium chloride 340
 BET equation 210
 BET surface area 207, 209, 211
 bifunctional activation 37
 bifunctional mechanism 306
 bimetallic catalysts 151ff.
 BINAP 79
 (S)-BINAP 76, 78
 biocatalysis 83ff.
 biocatalysts 9f., 83ff.
 biochemistry 84
 bioreaction engineering 84
 bishydroxylation 305
 bismuth molybdate catalysts 280
 Boltzmann factor 156
 π bonding 21
 Boots process 293
 boric acid 69
 BP Amoco 66
 Brønsted acid 26, 122, 217, 252
 Brønsted acid centers 173, 249, 319, 460
 Brønsted acidity 172, 249
 Brønsted centers 170f., 251
 Brønsted equation 171
 bubble column 417ff.
 – reactors 68
 Buss loop reactor 417, 419
 butadiene
 – coupling 81
 – cyclooligomerization 21, 29
 1-butanol 62
 1-butene 47
 1-butyl-3-methylimidazolium-tetrafluoroborate 328
 butynediol synthesis 416
 by-products 282
- c**
- C₁ chemistry 434
 C₂ symmetry 76
 α -cage 240
 β -cage 240
 calcinations 224, 226
 capillary condensation 209f.
 carbene 32, 34
 carbon dioxide 271
 carbon monoxide 311f.
 carbonyl complex 23, 34f., 54, 458, 462
 carbonylation 48, 51, 53f., 61, 289, 343ff.
 – 1-decene 55
 – methanol 28, 49, 54, 421
 carboxylation 32
 carboxylic acids 49
 catalase 88
 catalysis
 – asymmetric 75
 – definition 1
 – enantioselective 448
 – enzyme 451

- fuel cell 307
- hard 42
- heterogeneous 431
- history 2f.
- homogeneous 15 ff.
- ligand-accelerated 82
- multiphase 431
- reactors 403 ff.
- shape-selective 201, 239 ff., 259
- soft 42
- catalyst
 - acidic 169 ff.
 - acidity 4f., 175
 - activity 9, 125
 - additive 353
 - Ag/Al₂O₃ 218
 - aluminosilicate 174
 - anchored 233
 - automobile 428
 - asymmetric 430
 - basic 169 ff., 176 f.
 - bifunctional 253 f., 262
 - bimetallic 151 ff.
 - bimetallic Ru/Sn 286
 - binary oxide 167 f.
 - bismuth molybdate 273
 - bismuth/molybdenum oxide 348
 - bleeding 13
 - bulk 224, 238
 - classification 9, 144
 - characterization 52
 - chemistry 426
 - chiral 75, 449
 - choice 349
 - combustion 434
 - commercial value 425
 - concepts 40
 - Co/phosphine 63
 - cracking 172, 217, 243
 - deactivation 9, 195 ff., 201, 204, 206 f.
 - dehydrogenation 201
 - design 436
 - development 347 ff., 435 ff.
 - economic importance 425
 - egg-shell 226 f.
 - egg-yolk 226 f.
 - energy generation 434
 - enantioselective 75
 - environmental 426
 - ethylene oxide 228
 - future development 429 ff.
 - grafted 235
 - heterogeneous 10, 439 f.
 - homogeneous 9 f., 231 ff., 429 ff., 439
 - honeycomb 188, 222 f., 238, 319, 428
 - highly dispersed supported metal 235
 - hydrodesulfurization 193
 - hydrogen 336
 - hydrogenation 427
 - immobilized 9
 - immobilized homogeneous 231
 - immobilized molybdenum oxide 234
 - impregnated 224, 228
 - indium(i)/indium(iii) oxide 352, 354
 - industrial 179
 - inhibitors 198
 - innovation 438
 - iron 192
 - ionic 352, 354
 - lifetime 9
 - loading 228
 - losses 204
 - market 426
 - mass 6, 107, 366, 404, 423
 - metal cluster 13
 - metal oxide 273 f.
 - metallocene 427
 - metal oxide 166, 352, 354
 - methanation 192
 - modification 12
 - monolith 238
 - morphology 348
 - NiO 165
 - noble metal 225
 - organometallic 15
 - oxidation 44, 169, 217, 288, 427
 - oxygen 336
 - Pd 290 f.
 - performance 6, 179 f.
 - petroleum refining 426
 - planning 350 ff.
 - platinum/graphite 216
 - platinum shell 228
 - poison 52, 194, 198 f., 311
 - poisoning 319
 - polymerization 426 f.
 - precipitated 224
 - producers 428
 - production 223 ff.
 - Pt 314
 - Pt/Al₂O₃ 203
 - recycling 12, 231
 - redox 301, 304, 306
 - regeneration 68, 196, 202, 206
 - Re/Pt 202
 - rhodium 232
 - Rh/phosphine 63
 - screening 356

- separation 12
- shapes 223
- sheet 319
- shell 224, 238
- ship in a bottle 292
- silica-supported chromium 277
- silver 190, 219
- single site 73 f., 427
- SLP 236, 238
- soft 47 f.
- solid–liquid phase (SLP) 413
- SSP 235
- stability 9
- sulfided Ni 194
- support 180 ff.
- supported 9, 168, 180 ff.
- – liquid phase (SLPC) 232
- – metal 217, 226
- – Ag 289
- – Ni/SiO₂ 269
- – nickel 184
- – Pd 357
- – Pt 187
- – Rh 189
- supported solid phase (SSPC) 232
- surface 140 f., 217
- *tert*-phosphine-modified 58
- test reactor 358 ff.
- testing 355 ff.
- transition metal 11, 429
- triphase 340
- vinyl chloride 228
- weight 406, 408
- Ziegler 427
- Ziegler-Natta 73
- catalyst–substrate interactions 203
- catalytic afterburning 264 ff., 322 ff., 329
- – plant 324
- catalytic cracking 206, 256, 413
- catalytic cycle 1 f., 41
- catalytic oxidation, CO 138 f.
- catalytic reforming 264, 411
- CATATEST plant 286, 388
- cathode 305
- reaction 307
- Cativa process 66
- C–C-linkage 289
- cell voltage 307
- cetyltrimethylammonium bromide 339
- CH activation 430
- alkanes 431
- chalcone 325
- characterization
- chemical 214
- physical 208
- charge carriers 296
- C–H coupling 30
- chemical reaction engineering 404
- chemicals
- bulk 266, 282
- commodity 282
- fine 281 f.
- inorganic 261
- organic 261, 263
- speciality 282
- chemisorption 5, 100, 102 ff., 115 ff., 119 f., 171, 195, 211 f., 215, 222, 457
- ammonia 172
- associative 119, 186, 220, 457 f.
- CO 122 f., 160
- dissociative 13, 106, 119, 121, 186, 212, 457, 468
- enthalpies 127
- ethylene 217
- heat of 103
- heterolytic 122
- HCl 172
- hydrogen 127
- molecular 119, 121
- olefins 174
- chemoselectivity 469
- chirality 79
- chlorohydrin 329
- chloroprene 342
- cinnamaldehyde 279
- citral 289
- citronellal 61
- Clariant 291
- Claus process 262
- cleavage
- heptanes 246
- CO bands 58
- CO complex 124, 140
- CO conversion 225, 162
- CO insertion 468
- C–O stretching frequency 37, 58, 192, 222
- CO₂ chemistry 430
- cobalt catalyst 55, 62
- cobalt complex 335
- cobalt naphthenate 69
- co-catalysts 58, 62, 333, 338, 473
- coenzymes 86
- cofactor 84, 86, 97, 452
- regeneration 86
- coke formation 173 f., 184, 201

coking 197, 201 f.
 complex
 – bridged 122
 – chromium 236
 – diamagnetic 40
 – formation 19, 23 f.
 – linear 122
 – olefin 18
 – organometallic 15
 – π -acceptor 21
 – π -allyl 21
 – σ -allyl 21
 – titanium 236
 π complex 17
 concepts
 – Brønsted 21
 – Lewis 21
 conduction band (CB) 145, 155 ff., 331, 336
 conductivity 144, 157 ff.
 conductors 144
 cone angle 17
 confidence level 374, 376
 constraint index CI 245 f.
 contact process 411
 continuous stirred tank reactor (CSTR) 404 ff., 420 f.
 conversion 6, 404, 409
 coordination number 15 f., 18
 copper 337
 copper catalyst 54, 67, 148
 – supported 186
 cordierite 318, 322
 cost index CI 325
 cracking 264
 – alkanes 251
 – hexenes 247
 – reactions 175
 cross coupling 70, 291
 crown ethers 340, 345, 474
 cryptands 340
 current density 295, 300, 302
 cyclic voltammetry 299
 cyclization 327
 – olefin 353
 cyclobutadiene irontricarbonyl 20
 1,5,9-Cyclododecatriene nickel 20
 cyclohexane hydroperoxide 70
 cyclohexanol 69, 303
 cyclohexanone 69
 cyclohexene, hydrogenation 7
 1,5-cyclooctadiene 30
 cyclooctatetraene irontricarbonyl 20

d

Davis 253
 deactivation 1, 195 f.
 – process 196
 – rate 204
 dealkylation
 – cumene 249
 – toluene 422
 1-decene 73
 decomposition 33 f.
 – ethanol 166 f.
 – N_2O 164 f.
 – NO 320 f.
 Degussa, Marl 95 f., 225, 229, 234 f., 256, 286 f., 348, 413 f.
 dehydration
 – butanol 246
 – ethanol 166 f., 173
 dehydrogenation 263
 – butanes 168
 – cyclohexane 132, 148 f., 184
 – cyclohexanone 184
 – ethylbenzene 225, 412
 – methanol 412
 dehydrohalogenation 342
 – alkyl halides 176
 dehydroxylation 176
 – alcohols 176
 – Al_2O_3 170
 demetallation 202
 demethylation 264
 DENOX process 318
 deposits 201
 DESONOX process 265
 desorption 99
 – isotherm 209
 – temperature-programmed (TPD) 212, 214
 desulfurization 319
 detergents 71
 dewaxing 254, 256
 diastereometric complexes 77 f.
 Diels-Adler reaction 326
 diene complex 36
 Diesel engine 320
 differential reactor 358 ff.
 diffusion 99, 391
 dimerization
 – ethylene 39, 46
 – olefin 45, 61, 353
 dimethoxylation 306
 dimethyl ether 185, 248
 (S,S)-DIOP 76

- DIPAMP 76, 78
 direct electrochemical reactions 300
 direct methanol fuel cell (DMFC) 308, 313, 315
 (+)-disparlure 79
 dispersion 10, 115, 183 f., 212, 215
 disproportionation 247 f., 264
 – *m*-xylene 248
 – toluene 247
 dissociation 16
 – CO 192
 – heterolytic 160
 – N₂ 191 f.
 distribution
 – Gaussian 373
 – normal 373 f.
 – relative frequency 374
 donor reaction 144 f., 148, 164
 donors 166
 π donors 28
 σ donors 22 ff., 27, 35
 σ-donor strength 57 f.
 doping 178
 drying 224, 226 f.
 DSM 94, 236
 DUPHOS 76
 DuPont 309, 419
- e**
 E factor 325 f., 329, 472
 effective diffusion coefficient 386
 effective reaction rate 100 f., 107 f.
 effectiveness factor 386, 424
 effectivity 12
 σ effect 31
 effects 370 ff., 375, 401 f., 475
 electric forces 296
 electrocatalysis 295 ff.
 electrocatalyst 307, 310 f.
 – Pt/Ru 312
 electrocatalytic hydrogenation 302 f.
 electrocatalytic oxidation 304
 – methanol 306
 electrocatalytic process 302
 electrochemical addition 305
 electrochemistry 295 ff.
 electrode
 – kinetics 295 f.
 – passivation 301
 – potential 296, 304
 – redox reactions 296
 – surface 295 f., 298
 electrolyses 301, 305
 electrolyte 295 f.
 – polymer 303
 electrolytes 309
 electron acceptor 334 f., 338
 electron donor 333 f., 338
 16/18-electron rule 17, 40
 electron spectroscopy for chemical analysis (ESCA) 217
 electronegativity 163
 electronic effect 151, 153, 183 f., 186, 191
 electronic factor 142 ff.
 electrophilic attack 35, 37
 electrophilic ligand addition 155
 electrophilicity 155
 Eley–Rideal mechanism 111 ff., 138, 455, 466
 elimination 32
 – β-hydride 444
 – reaction 30
 β elimination 33 f.
 enantiometric excess 78, 82, 449
 enantioselective isomerization 78
 enantioselectivity 75, 83 f., 449
 Enichem 288
 ensemble effect 153, 190
 entropy 118, 120
 environmental catalysis 317 ff.
 environmental protection 2, 264 f.
 enzyme 83 ff., 9 f.
 – immobilized 92, 451
 – membrane reactor 95 f.
 enzyme-substrate complex 85
 epoxidation 44
 – asymmetric 79 f.
 equation
 – algebraic 362
 – design 422
 – differential 362, 366, 397, 404, 407 f.
 – explicit 397
 equilibrium constant 16
 earthalkali metal oxides 177
 erionite 245
 error variance 373, 381
 ESCA spectrum 218
 ESR spectroscopy 172
 etherification 343
 ethylation
 – benzene 252
 – phenol 252
 ethylene glycol 13
 ethylene oxide 190, 219 f., 412
 2-ethylhexanol 62, 236 f., 279
 ethylidyne complex 121

exchange current density 295 ff.
 exhaust gases 328
 extraction 340

f

factorial design 370 ff., 400, 476
 factorial test plans 370 ff.
 Faraday constant 307
 fatty acid 270
 – – methyl esters 270
 fatty alcohols 270
 faujasite 249
 feed rate 404
 fermentations
 – enzyme 453
 – microbial 453
 Fermi level 145 f., 148, 157, 165
 film diffusion 100 f.
 fine chemical synthesis 285
 fine chemicals 281 ff., 416, 468
 fine chemistry technologies 283
 Fischer–Tropsch catalysts 457
 Fischer–Tropsch synthesis 8, 37, 130,
 259, 279
 flue gas purification 264 f.
 formaldehyde 323, 423
 formic acid decomposition 124 f., 137
 four-electron pathway 312 f.
 Freundlich equation 104
 Friedel–Crafts-acylation 291 f.
 fuel cell system 306, 308, 311
 fuel cells 434, 470 f.
 fuel-rich stage 321
 furan 306

g

gas chromatogram 363, 365
 gas hourly space velocity (GHSV) 324
 gas purification 322
 geometrical effects 123
 Gibb's free energy 118, 120
 glycerol 270
 glycidol 61
 green chemistry 283, 317, 324 ff., 329

h

Haber–Bosch process 266
 Hammett acidity function 171
 hard dissymmetry 19, 33
 hard–soft dissymmetry 43, 46 f., 49
 heat exchange 413
 heat of adsorption 102 f., 118, 160
 heat of desorption 127
 heat of formation 125, 127

heat transfer 404, 414
 heat-transfer coefficient 413
 Heck coupling 290
 Henkel 270
 Henry constant, modified 391
 Henry's constant 386
 Henry's law 391
 herbicide 96
 heterogeneous catalysis 99 ff., 295
 – characterization 207 ff.
 – energetic aspects 116
 – mechanism 102, 109
 – reaction steps 99 f.
 – steric effects 131
 heterogenization 231
 heterolytic addition 19
 heterolytic cleavage 122, 176
 heterolytic process 60
 heterolytic reactions 143
 heteropolyacids 288, 436
 1-hexene 73
 hexachloroplatinic acid 228
 1,4-hexadiene 81
 Heyrovsky reaction 297
 high-density polyethylene (HDPE) 276
 high-dust configuration 319
 high-pressure IR 54 ff.
 high-throughput experimentation 397, 400,
 436
 high-throughput screening 398
 H-mordenite 252
 Hoechst process 293
 Hoffmann La Roche 415, 290
 Hofmann degradation 475
 holdup 389
 – external 390, 394
 – liquid 393 f., 396, 420
 homolytic addition 28
 homolytic process 60
 homolytic reaction 143
 Horiuti 127
 HSAB concept 18 f., 32, 35 f., 42, 45, 49 ff.,
 445 f.
 hte AG, Heidelberg 389 f.
 hte Shell higher olefin process (SHOP) 12
 hydride complexes 128 f.
 hydride elimination 13
 β -hydride elimination 33, 45, 68
 hydrocarbons 322
 hydrocarboxylation 49
 hydrocracking 254, 256, 264, 411
 hydrocyanation 50, 60 f.
 hydrodealkylation 407 ff.
 hydrodesulfurization 126, 214, 264

- hydroformylation 28, 41 f., 48, 54 f., 57, 61 f., 375 ff., 422
 - propene 63 f., 236
 - hydrogen 311
 - activation 19, 25
 - catalysts 334
 - electrode reaction 296
 - peroxide 288, 298, 313
 - hydrogenation 14, 31, 45, 47, 61, 126 f., 183, 263, 267 f., 285, 379, 416
 - acetone 187 f.
 - acetylene 129
 - adiponitrile 419
 - alkene 128
 - alkynes 194
 - asymmetric 59, 77
 - benzene 412, 418
 - benzaldehyde 303, 383 ff.
 - *n*-butyraldehyde 155
 - C₁₂–C₂₂ nitriles 420
 - chemoselective 286
 - chloronitrobenzene 183
 - CO 146, 185 f.
 - cobalt-catalyzed 57
 - crotonaldehyde 152, 155, 188
 - cyclic ketone 327
 - cyclohexanone 303 f.
 - dienes 48
 - electrochemical 315
 - 2-ethylanthraquinone 419
 - ethyl acetate 151 f.
 - ethylene 135, 137, 142, 147 f., 176
 - fats 269 f., 418
 - fatty acids 418
 - fatty esters 418
 - gas-phase 279
 - high pressure 286
 - lactone 389
 - linoleic esters 420
 - liquid-phase 279
 - pilot plant 287
 - 1-propen-1-ol 279
 - shape selective 254 f.
 - soya oil 269
 - substituted *o*-cyanonitrobenzene 380
 - substituted 2-nitrobenzonitrile 356 f.
 - substituted pyridine 153 f.
 - hydrogenolysis 41, 126, 148 f.
 - ethane 184
 - hydrolases 85
 - hydroperoxide 44, 69
 - hydrotalcite clays 292
 - hydrovinylation, styrene 328
 - hydroxylation 96 f.
 - phenol 288
 - 4-hydroxyphenoxypropionic acid 96
 - hypochlorite 343
 - H-ZSM-5 213, 246, 248, 250
- i*
- ibuprofen 289, 292 f.
 - ICI 270, 419
 - IFP 328
 - immobilization 231
 - impregnation 225 f.
 - incipient wetness impregnation 226 f.
 - indenoxyde 61
 - indirect electrochemical reactions 300
 - indium catalyst 327
 - induced-fit model 85
 - industrial gases 262
 - industrial plant 347
 - industrial process 59 ff., 261
 - infrared spectroscopy 52 f., 171
 - inhibition 199, 207
 - competitive 90, 98, 453
 - noncompetitive 90
 - uncompetitive 90, 98, 453
 - inhibitor 90, 194, 197
 - insertion
 - acetylene 31
 - alkene 41
 - CO 31 f., 41
 - ethylene 50
 - reaction 30, 39
 - in-situ spectroscopy 52 f.
 - in-situ techniques 432
 - insulators 143 f., 169
 - integral reactor 358
 - interactions 371 f., 401, 475
 - ion exchange membrane 305
 - ion scattering spectroscopy (ISS) 219 f.
 - ionic liquids 327, 329, 473
 - room temperature 327
 - ionization potential 163, 165
 - IR spectroscopy 124, 128, 140, 217, 251
 - IR spectrum 222
 - iridium catalyst 66 f.
 - iron catalysts 137
 - ISIM program 391 f.
 - isomerases 85
 - isomerization 60 f., 175, 264, 411
 - acid-catalyzed 253 f.
 - butene 176
 - double-bond 45, 71
 - olefin 34, 39, 46

- xylene 256
 - isomorphic substitution 248, 288
 - isophorone diamine 286
 - isopropanol 187f.
 - isotopic labeling 53
- j**
- Jacobsen complex 80
 - Jacobsen epoxidation 80
 - jet loop reactor 363 ff.
- k**
- Kelvin equation 209
 - key reactions 40f.
 - kinetic diameter 245
 - kinetic measurements 55
 - kinetic modeling 358 ff., 383 ff.
 - kinetic term 108
 - kinetics 87 ff.
 - heterogeneous catalysis 102
- l**
- lambda-probe 317
 - L-amino acid 95f.
 - Langmuir adsorption 204
 - Langmuir equation 104, 209f.
 - Langmuir isotherm 105, 112, 454
 - Langmuir–Hinshelwood equation 450
 - Langmuir–Hinshelwood kinetics 187, 363
 - Langmuir–Hinshelwood mechanism 88, 109, 111, 139, 166, 385, 405
 - lattice 167
 - defects 133
 - oxygen 174, 319
 - planes 142
 - type 132
 - lazabemide 290
 - L-dopa 59
 - lean-burning conditions 317f., 321, 329
 - lean-burning engines 320
 - Lewis acid 22, 32, 217, 251
 - – catalyst 326
 - – centers 23, 36f., 173f., 291, 460
 - Lewis bases 19
 - Lewis centers 151, 170f.
 - ligands 15 ff., 85, 440f.
 - π -acceptor 27, 30
 - allyl 21
 - anionic 19
 - basicity 57
 - bidentate 75f.
 - chiral 75f., 305, 449
 - coordination 16, 34
 - dissociation 26
 - effects 17, 55
 - electron-donating 29
 - electron-donor 23
 - exchange 19
 - exchange reactions 38
 - hard 50
 - ionic 15
 - multidentate 232
 - neutral 15
 - nucleophilic 32
 - nucleophilicity 18
 - olefin 19
 - optically active phosphine 77
 - phosphine 15 ff., 22
 - phosphite 15f.
 - polarization 37
 - soft 45
 - η^1 24
 - η^2 24
 - π ligands 35
 - Lindlar's catalyst 194
 - Lineweaver-Burk plot 89, 91f.
 - liquid feed 390, 393
 - liquid holdup 393
 - LLDPE 74
 - L-Menthol 78
 - L-methionine 95
 - \ln^+/\ln^{3+} -oxide 352, 354
 - lock and key model 85f.
 - low-density polyethylene (LDPE) 276
 - low-dust configuration 319
 - low-energy electron diffraction (LEED) 136, 138, 140, 215f., 463
 - Lurgi process 270
 - lyases 85
- m**
- M Forming process 246
 - macroeffects 348
 - macrokinetics 107, 115
 - magnesium oxide 176f.
 - maltol 306
 - Markownikow addition 45f.
 - Mars–van Krevelen mechanism 163
 - mass index 325f.
 - mass transfer 389, 396, 404, 414
 - coefficient 394f.
 - limitation 396
 - liquid–solid 391
 - total 391
 - mean value 374
 - mechanism
 - S_N2 18
 - mediator 301, 305

- mercury porosimetry 208f., 211
- metachlor 61
- metal alkyl mechanism 45f.
- metal allyl mechanism 45
- metal base 23
- metal basicity 22f., 27f.
- metal catalysts 125f., 199
- metal complexes 31
- metal dispersion 141
- metal distribution 229
- metal formates 125
- metal oxides 123, 159, 164, 300
- metallocene catalysis 73f.
- metals 117f., 145f., 150f.
 - hard 21
 - modification 154
 - soft 20f.
- metathesis 34, 60f., 71
- methanation 204
- methane 360
- methanization (SNG) 262
- methanol 430
 - carbonylation 65f.
 - catalyst 271
 - electrooxidation 306
 - oxidation 313f.
 - plant 271f.
 - synthesis 168, 190, 192, 270ff., 363, 365, 412f.
 - – mechanism 270ff.
 - to gasoline process (MTG) 248, 256
 - to olefin process (MTO) 256
- methyl iodide 49, 65
- 3-methylhexane 82
- methylaluminoxanes (MAO) 73f.
- methylation, toluene 247
- methyltrioctylammonium chloride 339f.
- Michaelis–Menten equations 97, 452
- Michaelis–Menten expression 88f.
- Michaelis–Menten parameters 90
- microbiology 84
- microeffects 348
- microkinetics 100, 102, 107, 115
- microporous materials 209
- Miller indices 133, 142, 458
- Mittasch 270
- mixed oxides 144
- Mobil Oil Corporation 243, 247
- Mobil–Badger process 256
- modeling 396
- mole balance 408
- molecular biology 84
- molecular sieve 245
- molten carbonate fuel cell (MCFC) 308, 310
- molybdenum 123
- Monsanto process 49, 65f.
- Monsanto-L-Dopa Process 77
- morphology 208
- MTG process 259
- multiplet theory 131
- multiple-tube reactors 270
- multi-step process 284
- n**
- Nafion H 326
- Nafion-membranes 309
- naphtha reforming 203
- Natta 277
- Ni catalysts 124, 136f.
- nickel complex 16, 20
 - – catalysts 72
- nickel oxide/hydroxide 304
- nickel tetracarbonyl 204
- nicotinamide adenine dinucleotide (NAD) 86
- nitrile hydratase 93
- NMR spectroscopy 53
- nonpoisons 199
- nonstoichiometric oxides 157f.
- Norton 256
- No_x removal 317f.
- No_x storage-reduction catalyst (NSR) 320f., 471
- nucleophiles 35
- nucleophilic attack 30, 34f., 44, 50
- nucleophilic ligand addition 155
- nucleophilicity 155
- o**
- 1-octene 73
- octyl-4-methoxycinnamate 290
- olefin reactions 263
- olefin–metal bonding 20
- α -olefins 71f.
- oligomerization 264
 - isobutene 114
 - ethylene 71f.
 - olefin 45, 61
- optimization 376, 402, 477
- organoboronic acid 70
- organopolysiloxane catalysts 234f.
- Ostwald 1
- Ostwald process 10, 204, 412
- o-tolyl-benzonitrile 291
- Otto engine 320
- overpotential 300ff.

- overvoltage 301 ff.
 oxad reaction 13
 oxidation 61, 263, 288
 – alcohols 305, 343
 – ammonia 164
 – benzene 164
 – benzaldehyde 280
 – *n*-butane 178
 – cells 305
 – CO 165 f., 317
 – cyclohexane 69
 – ethylene 67, 190, 421
 – H₂ 164
 – hydrocarbons 60, 317, 421
 – mechanism 163
 – methane 423, 433
 – α -phenylethanol 283
 – phthalic anhydride 413
 – potential 338
 – propene 164, 348, 350
 – *p*-xylene 421
 – reactions 162 f.
 – state 15, 19, 23 f., 28 f., 35, 37 f., 40, 43, 185, 440, 442 f.
 oxidative addition 13, 24 ff., 39, 41, 43, 57, 70, 441 ff., 445
 oxidative coupling 29 f.
 – methane 177, 433
 oxidative dehydroaromatization 350 ff.
 oxidative dimerization 164
 oxide catalysts 123
 oxides
 – acidity 174
 – mixed 175
 oxidoreductase 85
 oxirane process 45
 oxo alcohols 63
 oxo synthesis 62, 372, 421, 445
 oxychlorination 263
 oxygen
 – electrode reaction 298
 – lattice 163
- p**
- palladium 68
 – catalyst 67, 70, 129, 183, 303
 partial pressure 110, 112, 406, 408 f.
 Pauling 145, 147 f.
 Pd catalysts 138
 – supported 185
 peptide synthesis, enzymatic 94
 percentage d character 147 f., 150
 perovskites 322
 peroxide pathway 312 f.
 phase changes 203
 phase transfer catalysis (PTC) 339 ff., 475 f.
 – benefits 340 f.
 – extraction mechanism 341
 – industrial processes 342 ff.
 – inverse 340
 pheromone 79
 Phillips 277, 419
 – catalysts 277
 – triolefin process 60
 phosgene 342 f.
 phosphine decomposition 114
 phosphoric acid fuel cell (PAFC) 308
 photocatalysis 331 ff.
 photocatalysts 338
 photodegradation 338
 photoelectrons 218
 photoelectrosynthesis 337
 photo-Kolbe reaction 338
 photooxidation 337
 photosensitizer 331, 336
 physisorption 102 f., 115, 119, 212, 457
 pilot plant 347 f., 415
 Plackett–Burman plan 375 f., 402, 476
 platinum catalysts 303
 plug flow reactor (PFR) 404 f.
p-methoxyacetophenone 292
 poisoning 190, 197
 – effect 199
 – irreversible 199
 – metals 199
 – reversible 199
 – semiconductor oxides 200
 – solid acids 200
 – supported palladium catalysts 200
 – surface 215
 Polanyi 127
 pollutants 322 ff.
 polycarbonate 342 f.
 polyethylene 73
 polyethylene glycol (PEG) 340, 475
 POLYMATH 361, 368 f., 396 f., 406 ff.
 – program 91
 polymerization 60 f., 175
 – ethylene 81 f., 278
 – olefin 34, 45, 73, 174, 276
 polynomial 368
 polystyrene 233
 pore diffusion 99 ff., 228, 420
 pore distribution 208
 pore profiles 227
 pore size distributions 209
 pore structure 353
 porosity 208

- porphyrins 202
- potential diagram 119f.
- power law 107, 205
- precipitation 224, 226
- promoter 153, 189ff., 195, 204, 306
 - alkali metal 219
 - Al_2O_3 190
 - catalyst-poison-resistant 190
 - cesium 190
 - Co 194
 - electronic 190
 - examples 191
 - iodide 49
 - K_2CO_3 193
 - K_2SO_4 193
 - potassium 191f.
 - potassium aluminumsilicate 193
 - Ru 314
 - structure 189
 - textural 190
 - transition metal oxides 193
- propene, epoxidation 45
- proton exchange membrane fuel cell (PEMFC) 308ff.
- Pt catalysts 139, 152, 311
- Pt/Ru alloy 306
- Pt/Sn catalysts 153

- q**
- quaternary ammonium salt (quat) 339f.
- quench reactors 271

- r**
- racemate 78
- radical process 70
- radical reactions 69
- Raney nickel 384
- rate coefficient 108
- rate constant 295
- rate equation 110
- rate law 360f.
- rate-determining step 110
- raw materials 433
- reaction
 - acid–base 43
 - anodic 311, 315
 - carbonylation 13, 31
 - cathodic 312, 315
 - C–C coupling 29
 - CH activation 430
 - donor 459f.
 - electrochemical 295f.
 - electrode 296, 469
 - enzyme-catalyzed 85, 87
 - gas-phase 404
 - gas–solid 410
 - homogeneously catalyzed 420
 - insertion 445
 - key 13, 16
 - kinetics 107
 - ligand 35
 - ligand-exchange 18
 - ligand-substitution 18
 - rate 4f., 107, 110, 126
 - redox 296, 301
 - selective oxidation 230
 - sequential 8
 - structure sensitive 134ff., 203
 - temperature-programmed 214
- reactor
 - autoclave 421
 - batch 6
 - bubble-column 421
 - calculation 405, 407, 478ff.
 - differential 363, 400, 422
 - fixed-bed 12, 404ff., 411, 414
 - fluidized-bed 274, 411f.
 - gradientless 359, 361f.
 - high pressure 399
 - integral 362, 364, 366ff., 387
 - loop 417, 419, 421
 - membrane 437
 - modeling 397
 - multi-bed 411
 - multitubular 412
 - packed bed 367
 - parallel 8
 - recycle 358
 - shallow-bed 412, 481
 - single bed 398, 411
 - stirred tank 361
 - suspension 415ff., 424, 482
 - three-phase 413
 - trickle-bed 384, 386f., 389, 392, 414ff., 418, 420, 424, 482
 - two-phase 404, 410ff., 420
- recrystallization 204
- recycle ratio 361
- redispersion 204
- redox catalysts 143
- redox couples 301
- redox initiator 70
- redox mechanism 43
- redox potentials 333
- redox reaction 24, 442
- reduction
 - CO 317
 - electrocatalytic 298

- oxygen 312
 - temperature-programmed (TPR) 214f.
 - reductive amination 286f.
 - reductive elimination 24ff., 43, 47, 441, 445
 - refinery process 262, 264
 - reforming 254
 - methane 188f.
 - processes 202
 - regeneration 181, 195
 - regioselectivity 84, 469
 - regression 91, 397
 - nonlinear 360f., 369
 - Reppe 60
 - alcohol synthesis 48
 - residence-time distribution 389f., 417
 - resistance term 108
 - reversible hydrogen electrode (RHE) 299
 - Rh/Sn-catalysts 151f.
 - rhodium catalysts 62, 64f.
 - supported 185f.
 - rhodium recycling 66
 - Rhodococcus rhodochrous 93
 - Rhône-Poulenc 284, 291
 - ring distribution 229
 - Roelen 60f., 62
 - Rosenmund reaction 201
 - Ru/Os reforming catalysts 150
 - Ruhrchemie 62, 64
 - Ruhrchemie/Rhône Poulenc process 12, 64f.
 - ruthenium 306
 - complexes 335
- s**
- salene 80
 - salicylaldehyde 80
 - sample 373
 - Schiff bases 80
 - Schulz–Flory distribution 71
 - SCR process 204, 256, 434, 472
 - secondary ion mass spectrometry (SIMS) 219
 - segregation 215
 - selective catalytic reduction (SCR) 204, 318, 320
 - selective oxidation, propene 272ff.
 - selective toluene disproportionation 247
 - selectivity 1, 8, 179ff., 284, 429, 440
 - product 244, 247
 - reactant 244f.
 - restricted transition state 244, 247
 - shape 242ff.
 - selectoforming process 243, 245
 - semiconductor, 143f., 155ff., 331ff.
 - chemisorption 160
 - excitation energies 156
 - *i*- (intrinsic) 156
 - oxides 160, 162, 167f.
 - – nonstoichiometric 159
 - *n*-type 156, 158, 160f., 184, 459
 - *p*-type 156, 158, 160f., 459
 - sulfides 160
 - shape selectivity 465f.
 - shaping 224
 - Sharpless 79, 305
 - epoxidation 80
 - Shell hydroformylation process 58
 - Shell process 63
 - SHOP process 60, 71f.
 - silicalite 253
 - significance 477
 - test 374
 - silanol groups 249
 - silica 173
 - silicate 250
 - silicoaluminiumphosphate (SAPO) 253
 - simplex method 376ff., 402, 477
 - simulation 383ff., 392f., 396f.
 - single-crystal 132f., 135, 216, 221, 243
 - sintering 197, 203ff., 215
 - size distribution 215
 - Smidt 67
 - SMSI effects 187ff.
 - S-Naproxen 78
 - sodalite cage 240
 - soft dissymmetry 19, 33
 - SOHIO process 273f., 276, 413, 482
 - solar energy 333
 - solid oxide fuel cell (SOFC) 308, 310
 - space velocity 6
 - space–time yield 6
 - specific pore volume 209
 - specific surface area 107, 181f., 211
 - stability 179f.
 - standard deviation 373
 - statistical test planning 369ff.
 - steam reformer 308
 - steam reforming 262, 316
 - steric effects 136
 - stereoselectivity 469
 - strong metal–support interaction (SMSI) 183
 - structure 132
 - body-centered cubic 132
 - face-centered cubic 132
 - hexagonal close packing 132
 - substrate 85ff., 143, 301

- concentration 88, 90
 - control 88
 - succinic dialdehyde 306
 - Süd-Chemie 366
 - Sumitomo 292
 - superacids 170, 250
 - superbases 170, 292
 - supercritical carbon dioxide 326 ff.
 - supercritical CO₂ 327 f.
 - support 123, 141, 153, 168, 211, 463
 - Al₂O₃ 225
 - effects 168
 - inorganic 234
 - monolithic 264
 - organic polymer 233
 - TiO₂ 204
 - V₂O₅ 204
 - supported catalysts 180
 - surface acidity 170
 - surface 207
 - analysis 208, 214
 - area 103, 463
 - complexes 131
 - coverage 104 ff., 110, 126, 192
 - physics 221
 - titration 212
 - sustainable development 283
 - Suzuki coupling 70, 291
 - sweetener 94
 - Symyx Technologies 400
 - synthesis gas 13, 188, 271, 363, 430
 - reactions 8
- t**
- Tafel equation 295
 - Tafel slope 295
 - Takasago process 78, 82
 - Tanabe Seiyaku process 95
 - temperature-programmed desorption (TPD) 212 f.
 - temperature-programmed oxidation (TPO) 214
 - temperature-programmed sulfidation (TPS) 213
 - templates 242
 - tert.*-butyl hydroperoxide 45, 79
 - tetra-*n*-butylammonium bromide (TBAB) 339
 - texture 195, 208
 - thermolysin 94
 - Thiele modulus 386
 - three-way catalyst 317 f., 328, 471
 - time factor 367 f., 404 f.
 - tin modifier 306
 - Tischchenko reaction 177
 - titania 332 ff.
 - anatase 332 ff.
 - electrode 337
 - rutile 332 f.
 - titanium dioxide 331
 - titanium (IV) silicalite (TS-1) 288
 - Tolman 16 f., 29, 40 f.
 - Torial, USA 400
 - tortuosity factor 386
 - Toyo Soda process 94
 - Toyota 321
 - TPPTS 64
 - trans* effect 18, 50
 - transferases 85
 - transition metal 117 f., 128, 146
 - catalysts 15, 59
 - complexes 16 ff., 58
 - hydrides 23
 - oxides 319
 - transition state 116 ff., 121
 - transmetalation 71
 - transmission electron microscopy 215
 - transport resistance 387
 - triethylbenzylammonium chloride (TEBA) 339
 - triphenylphosphine 57, 62, 233, 236
 - t*-test 375, 402, 477
 - turnover frequency (TOF) 7, 75, 88, 97
 - turnover number (TON) 5, 7, 75, 83, 134, 187, 450
 - two-phase technology 12, 64
- u**
- Ugo 42
 - Union carbide 62
 - UV light 332
- v**
- valence band (VB) 145, 155 ff., 331, 336
 - valence electrons 40, 42
 - van der Waals forces 102 f.
 - variable 370 f., 376, 379, 383
 - blank 375
 - variance 374
 - Vickers-Zimmer 419
 - VINCI technologies 286, 387 f.
 - vinyl acetate 69
 - 4-vinylcyclohexene 30
 - volatile organic compound (VOC) 317, 322
 - volcano curve 297, 300
 - volcano plot 125 f., 137, 146
 - Volmer reaction 297

voltammetry 298

VPI-5 253

w

Wacker process 49, 67 f., 254, 421, 448

washcoat 188, 318, 322

water

– cleavage 338

– photocatalytic oxidation 325, 333

– photocleavage 336

– photooxidation 334

– photoreduction 333 f.

water-gas shift equilibrium 270

Wilkinson's catalyst 17, 40, 47, 51, 77

Williamson ether synthesis 343

work function 145 f., 157

x

XPS 216

y

Yates scheme 372

z

zeolite A 240

zeolite H-beta 291 f.

zeolites 201, 235 f., 239 ff., 465 f.

– acid/base properties 250

– acidity 247

– applications 255

– catalytic properties 243

– cation-exchanged 249

– crystallization 242

– Cu 320

– dealumination 242, 250

– deammonization 248 f.

– detergents 255

– general formula 239

– hydrothermal treatment 250

– isomorphic substitution 252

– metal-doped 253

– modification 252

– molar ratio M 239

– organic syntheses 257

– pentasil 241 f.

– [Pd^{II}][Cu^{II}] 254

– pore size 245

– production 242

– [Rh] 254

– [Ru] 254

– Si/Al ratio 249 f.

– structures 242

– TS1 242

– Y (faujasite) 240 f., 248

Ziegler catalysts 81, 276

zirconium catalysts 73

ZnO 271

ZSM-5 242, 248, 253, 255, 259